TREATISE ON MATERIALS SCIENCE AND TECHNOLOGY

VOLUME 9

CERAMIC FABRICATION PROCESSES

EDITED BY
FRANKLIN F. Y. WANG
Department of Materials Science
State University of New York
at Stony Brook
Stony Brook, New York

1976

ACADEMIC PRESS New York San Francisco London
A Subsidiary of Harcourt Brace Jovanovich, Publishers

ACADEMIC PRESS, INC.
111 Fifth Avenue, New York, New York 10003

United Kingdom Edition published by
ACADEMIC PRESS, INC. (LONDON) LTD.
24/28 Oval Road, London NW1

LIBRARY OF CONGRESS CATALOG CARD NUMBER: 77-182672

ISBN 0-12-341809-7

PRINTED IN THE UNITED STATES OF AMERICA

List of Contributors

Numbers in parentheses indicate the pages on which the authors' contributions begin.

G. F. AUSTIN (135), Zircoa, Solon, Ohio

PAUL F. BECHER (217), U. S. Naval Research Laboratory, Washington, D.C.

R. J. BROOK (331), Department of Ceramics, The University of Leeds, Leeds, United Kingdom

ROBERT E. COWAN (153), Los Alamos Scientific Laboratory, University of California, Los Alamos, New Mexico

C. GRESKOVICH (15), General Electric Corporate Research and Development, Metallurgy and Ceramics Laboratory, Schenectady, New York

KEDAR P. GUPTA (305), Monsanto Company, St. Peters, Missouri

R. NATHAN KATZ (35,241), Army Materials and Mechanics Research Center, Watertown, Massachusetts

CHANDRA P. KHATTAK (295), Brookhaven National Laboratory, Upton, New York

Y. S. KIM (51), Bell Telephone Laboratories, Incorporated, Allentown, Pennsylvania

M. H. LEIPOLD (95), Jet Propulsion Laboratory, California Institute of Technology, Pasadena, California

E. M. LENOE (241), Army Materials and Mechanics Research Center, Watertown, Massachusetts

W. C. LO (265), Bell Telephone Laboratories, Incorporated, Allentown, Pennsylvania

G. D. MCTAGGART (135), Zedmark, Inc., Valencia, Pennsylvania

J. L. PENTECOST (1), Department of Ceramic Engineering, Georgia Institute of Technology, Atlanta, Georgia

JAMES S. REED (71), New York State College of Ceramics at Alfred University, Alfred, New York

THOMAS REYNOLDS III (199), Ferroxcube Corporation, Saugerties, New York

ROBERT B. RUNK (71), Engineering Research Center, Western Electric Co., Princeton, New Jersey

MINORU TOMOZAWA (227), Materials Division, Rensselaer Polytechnic Institute, Troy, New York

J. C. WILLIAMS (173), Bell Laboratories, Inc., Murray Hill, New Jersey

Foreword

The essence of materials science and technology is the close relationship between the processing of materials and their properties. In recent years, the strict requirements for the designs and applications of materials have produced a corresponding demand upon the processing of materials. The results have been very dramatic. We can now produce materials in such variety as was not possible only a few years ago. Due to the proprietary nature of the information about the material processing, there is a scarcity of published literature on this topic.

This volume is intended to be an introductory text for any engineer who wishes to produce technical ceramics. It can also be used as a ceramic processing textbook for junior or senior undergraduate engineering students, provided that the lecturer will supply supplementary information. The volume is designed to provide sufficient information for anyone to proceed with the processing. It also provides a wide range of literature references for anyone who wishes to study the topics more thoroughly. The general tone of the volume emphasizes practical modern techniques. Theories are introduced only if they aid in the understanding of processing parameters. Usually, the preference for a specific processing method is very subjective. The volume seeks to provide a more balanced introduction to the various competing methods. A more detailed comparison of these methods will have to be left to future volumes. This volume is limited to the processing of technical ceramics such as high alumina electrical ceramics, titanate–zirconate capacitors, ferrite magnetics, and oxide ceramics such as magnesia, zirconia, and others. In addition, carbides are also included for discussion. This limitation allows the volume to be contained within a reasonable size. Obviously, future volumes will have to be initiated to cover all the omissions here.

There are 17 articles in this volume. The first four are devoted to various aspects of ceramic powder preparations and characteristics. The first article gives a brief introduction to the modern practices in powder preparation processes. Professor Pentecost draws on his vast industrial experience and provides a treatment of powder preparation processes

rather than a glossary of preparation processes of various substances. Many of the processes are already in common industrial use, but they are not much discussed in technical literature, except in patent literature. The second paper discusses milling processes in greater detail. Dr. Greskovich emphasizes the particle reduction (or comminution) aspect of the milling operation. He discusses the sintered microstructures from powders which were prepared under different milling conditions. His comparison of powder characteristics as prepared by ball milling and jet milling demonstrates clearly the effect of processing techniques on powders.

In the third article, Dr. Katz provides a comprehensive survey of measuring methods which can be used to characterize various aspects of powders. As Dr. Katz states so aptly, "the characterization of ceramic powders can be extremely time consuming and expensive task. It is therefore important to limit the characterization program to those features of the powder which will result in a reproducible end product." In the fourth paper, Dr. Kim discusses the effects of ceramic powder characteristics on the control of the properties of sintered electronic ceramics. This is an area where much work needs to be done. Dr. Kim has done an admirable job in pointing out the relationships between the powder features and the properties of sintered products. There are many overlapping topics in each of the four chapters of this section. This practice is continued throughout the volume to emphasize the underlying relationships among the articles.

The next group of five articles covers the forming process. It is in this section that the processes are limited specifically to the technical ceramics. Processes themselves are applicable to other types of ceramics, but the discussions here are intentionally limited to technical ceramics. The fifth article is on dry pressing. Professor Reed and Dr. Runk introduce the variables of the dry pressing process, and discuss compaction behavior and die wall effects. Dry pressing is the most widely used process in making technical ceramics. This paper gives many valuable pointers to the process. Increasingly, however, hot pressing is becoming the process to prepare especially highly refractory ceramics or carbides. Dr. Leipold discusses hot pressing in the sixth article, using magnesium oxide and tantalum carbide as case histories. Because the selection of equipment features is extremely important in hot pressing, Dr. Leipold discusses such features extensively, both in the case of uniaxial and isostatic hot pressing. It is obvious from this article that the simultaneous applications of heat and pressure result in a very complex process. In the seventh paper, Dr. Austin and Dr. McTaggart state that, "Isostatic pressing is a well-established method of forming that has not yet begun to reach its potential in the ceramic industry. As mold design technology improves and press manufacturers learn how to construct smaller units with higher capacities, the use of isostatic pressing in the ceramic industry will accelerate." In contrast to the above three pressing operations, the next two

articles on forming cover the casting processes. The eighth article is on slip casting. As such, it is relatively more traditional. Mr. Cowan briefly introduces the general theories of slip casting and slips. He then discusses several novel casting processes and the case histories of slip casting oxides. The ninth paper discusses a special casting method, namely, the doctor-blade process. This is a method particularly suited for preparing thin sheets of ceramics. Mr. Williams draws on his extensive experience in this process and gives us a very comprehensive discussion. He introduces many hitherto unpublished results which are invaluable to the understanding of the doctor-blade process. He also discusses the firing of cast tape and the surface finishes and microstructure. In these areas, he provides links between this article and later articles (the tenth and fourteenth). In this section (the fifth through ninth articles), the forming processes treated are limited to pressing and casting. There are many other forming processes which are not mentioned in this volume. Pressing and casting constitute, however, the processes used in the majority of cases.

The next three articles cover firing and finishing processes. In the tenth article, Dr. Reynolds discusses various factors which must be considered during the firing process of the electronic ceramics. He uses titanates and ferrites as examples. They demonstrate the close interrelationships among the pre-firing processes and the firing process. In the eleventh paper, Dr. Becher discusses machining and surface finishing of ceramics, which include grinding, mechanical polishing, and nonabrasive finishing. He deals also with the effect of surface finishing on properties. Professor Tomozawa, in the twelfth article, on surface treatments, introduces the topics of chemical strengthening and surface coating. These two types of surface treatment are more successful in the glass systems, although their applications to ceramic systems are increasing. Of course, the traditional glaze is a surface coating. Professor Tomozawa provides some important insights into the mechanisms of chemical and mechanical strengthening through surface treatment. This is an area which has great potential in ceramic processing.

The group of articles on testing methods cover only two topics which are of paramount importance to technical ceramics. They are mechanical behaviors (thirteenth article) and surface texture (fourteenth article). Obviously, other properties, such as magnetic, dielectric, electrical, piezoelectric, and thermal, are also very important. Space limitations prevent their inclusion in this volume. Mechanical testing establishes the soundness of the ceramic product. As such, it is a "must" test for all products, regardless of the end use. Surface texture is currently a special requirement for the ceramic substrates which are used in microelectronics. The degree of sophistication for the surface texture testing and the intimate relationship between the control of surface texture and the processing warrant its inclusion. It is predictable that future demands on other types of technical ceramics will also require the product to meet surface texture specifications.

In the thirteenth chapter, Drs. Lenoe and Katz present a wide range of mechanical behaviors for consideration. Their inclusion is required by the modern usages of ceramic materials. It is no longer sufficient to consider only the tensile strength as representative of the mechanical properties of the ceramic material. The limited space here prevents a thorough discussion of the effects of processing on the mechanical behaviors. It is a topic which is the essence of ceramic science. It deserves a special volume of its own.

Dr. Lo provides a comprehensive treatment of the methods of measuring surface texture in the fourteenth article. In addition, the figures in his chapter provide clear demonstrations as to what quantity each measurement is actually measuring. It will doubtless be a great aid for practitioners of these methods.

In the last three articles, attention is given to special processing methods. In the fifteenth article, Dr. Khattak gives a brief description of crystal growth methods. He provides many valuable current literature references on this subject, which obviate discussion in any greater detail. In the sixteenth paper, Dr. Gupta introduces the topic of controlled solidification in ceramic eutectic systems, still in its infancy. Dr. Gupta introduces the subject with the aid of results in metallic systems. This method is basically a ceramic analog to the metallic casting method. It will be a very important processing method for ceramics in the years to come. In the final article, Professor Brook provides a detailed discussion of controlled grain growth. Control of microstructure is discussed in all the articles of this volume. Professor Brook examines the kinetics of grain growth, and demonstrates the applications of theoretical expressions to the kinetic studies of grain growth. He provides insights into the control and avoidance of grain growth through processing. It is the ultimate goal of ceramic processing to be able to control microstructure according to property specification. This volume shows its readers how to begin to achieve this goal. Much progress has yet to be made.

It is the fondest hope of this editor that this volume can serve not only as a desktop reference book on ceramic fabrication processes but also as a key to further insights and understanding of these processes.

The contributors have tried to achieve a balance between a broad survey of each topic and the detailed description of each process. The volume is not designed to be a handbook, but, rather, a practical introductory text. The Editor claims all responsibility for any faults or shortcomings. He wishes to acknowledge gratefully the able assistance of Miss Mary-Faith Hughes and Miss Jeanne Carleton. He is, as always, greatly sustained by his wife, whose understanding enabled him to complete this volume.

FRANKLIN F. Y. WANG

Preface

Materials limitations are often the major deterrents to the achievement of new technological advances. In modern engineering systems, materials scientists and engineers must continually strive to develop materials which can withstand extreme conditions of environment and maintain their required properties. In the last decade we have seen the emergence of new types of materials, literally designed and processed with a specific use in mind. Many of these materials and the advanced techniques which were developed to produce them, came directly or indirectly from basic scientific research.

Clearly, the relationship between utility and fundamental materials science no longer needs justification. This is exemplified in such areas as composite materials, high-strength alloys, electronic materials, and advanced fabricating and processing techniques. It is this association between the science and technology of materials on which we intend to focus in this treatise.

The topics to be covered in *Treatise on Materials Science and Technology* will include the fundamental properties and characterization of materials, ranging from simple solids to complex heterophase systems. The *Treatise* is aimed at the professional scientist and engineer, as well as at graduate students in materials science and associated fields.

The Editor would like to express his sincere appreciation to the members of the Editorial Advisory Board who have given so generously of their time and advice.

H. HERMAN

Contents of Previous Volumes

Powder Preparation Processes

J. L. PENTECOST

Department of Ceramic Engineering
Georgia Institute of Technology
Atlanta, Georgia

I. Introduction

For the purpose of definition, fine oxide powders will be used to include particles 1 μm in diameter and below. This diameter may be an equivalent spherical diameter, calculated from surface area measurements or from electron microscopic examination. This infers surface areas of greater than 1 m^2/gm for spherical particles since $D = 6/A\rho$, where D is diameter in microns, A the surface area in m^2/gm and ρ is density in gm/cm^3.

Large quantities of powders with such surface area and particle size are in commercial manufacture. Carbon blacks, silica, and titania are produced in hundreds of thousands of tons per year in the United States. Unfortunately

each material has unique requirements for economical production, and frequently, the particle's morphology or trace anion or cation impurities that are unique to a manufacturing process influence the utilization or properties of the final product. The purpose of this chapter is to describe some of the processes that have been used on the laboratory, pilot process, or production level to produce fine particles. The emphasis has been placed on oxides for ceramic-type application; however, other materials have been discussed where unique or interesting processes were involved.

Conceptually, fine particles may be produced by size-reduction processes such as grinding or atomization and by growth processes such as precipitation, decomposition, etc. For convenience in covering these diverse methods, groupings have been made of similar techniques.

II. Size Reduction Processes

Ideally, if materials of the desired composition, single phase, and the desired crystal structure could be readily reduced to submicron size by a single grinding process, many complex and varied chemical preparation processes would be unnecessary. Grinding, attrition, impacting and other size reduction processes (such as atomization of the liquid, which is not covered in this discussion) have the attraction that a wide variety of materials may be prepared in fine particles by essentially the same technique. Unfortunately no widely useful, highly efficient, grinding method is available to produce large quantities of particles in the submicron range. Several classical and recently developed techniques deserve mention for this purpose and many conventional milling techniques will produce particles in the range of 0.1 to 1 μm in laboratory and industrial processing (Quatinetz *et al.*, 1963).

A. Grinding and Attrition Processes

For particles in the range below 10 μm, grinding processes are notably inefficient. This inefficiency is due primarily to the tendency of small particles to reagglomerate under grinding pressure (Meloy, 1970), but the large surface area of the fine particles and the inability to concentrate the crushing energy on a small number of particles at a time probably contributes significantly to the inefficiency.

Ball and rod mills are widely used for particles size reduction (Farrant and North, 1957). A wide variety of media are used for the balls or rods; the preferable materials are dense, hard materials of high specific gravity. Alumina, steel, zirconia, and mullite are among the most common, though

natural silica pebbles and other specialized media such as cemented carbides may be used for application where low contamination or nondeleterious contamination is desired.

The principal differences between rod and ball media lie in the grinding action. For rods, the large particles are ground somewhat more efficiently, resulting in a narrow range of particle sizes. Ball media tend to grind all size particles similarly, hence a wider distribution of sizes (Farrant and North, 1957).

The rotational speed of a ball or rod mill is critical, and varies inversely with the square root of the diameter. At the optimum speed, media cascade continuously, generally in a contacting mass of impacting and abrading media. Too slow a speed results in slower grinding and increased wear on the cylindrical side. Too fast a speed causes the media at the top of the charge to be propelled in an arc falling on the lower balls and causing increased ball wear or even chipping. For small (laboratory size) mills the diameter of the media also affect the optimum speed of rotation. The relationship between speed and grinding action has been investigated for many materials (Farrant and North, 1957).

To speed up a ball mill's action, vibration may be used rather than rotation to provide the grinding action. Since many more impacts per second can be generated, grinding in a vibratory mill is up to an order of magnitude faster than conventional rotational ball mills. A medium similar to that used for rotating mills is also used in vibratory mills.

B. Grinding Additives

Since agglomeration results in a slowed grinding and limits the efficiency of grinding to fine sizes, minor organic additives are sometimes used to reduce agglomeration. A number of studies have been performed by the cement industry and organic materials such as acetamine, acetylurea furfuryl alcohol, tetrahydofurfuryl alcohol, furan, tiophene, and tetrahydrofurfurylamine, have been found effective in reducing grinding time. Typical additions are 0.1 % or less (Serafin, 1969a–d, 1970). For dry grinding alumina, 0.6 % addition of triethanolamine has been shown to reduce grinding time 20–30 % in the 1–5 μm particle size range.

C. Fluid Energy and Shear Mills

A number of mill designs in which the particles are impacted in a fluid (either liquid or gas) are in use. Some of these designs use high shear in a thin film or liquid (such as the Morehouse mill). Others use opposing or proximate jets of particles entrained in a working fluid. A design (Doyle and Becker,

1969) in large scale use for grinding pigments and other fine particle materials such as silica gels is a fluid energy mill in which tangential jets inject a high pressure gas (entraining the solid material) which expands rapidly, causing particle–particle impacts at high velocity (Fig. 1). The grinding efficiency is high even below 10 μm and contamination is minimal since most collisions occur in the gas stream rather than against the wall of the mill.

In all fluid energy mills, the particle recovery is a problem since very fine particulates are difficult to collect. Large volumes of gases must be handled, cyclones are inefficient for micron size particles and filters clog rapidly. High pressure steam or compressed air are typical working fluids for this type of milling, and with high pressure steam, very fine oxide particles may tend to hydrate unless removed from the gas stream rapidly.

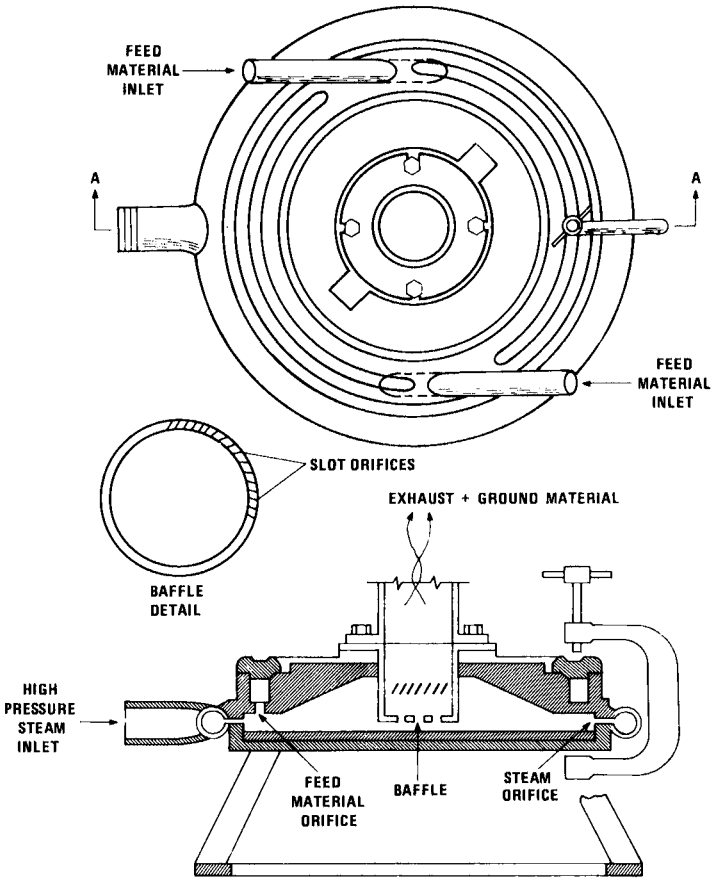

Fig. 1. Fluid Energy Mill for decomposing nitrates. Typical 800°C steam is used as the energy source. (Courtesy W. R. Grace & Co.)

D. Attrition Mills

A recent development in milling to submicron sizes (Sadler *et al.*, 1975; Stanley *et al.*, 1973a,b) is an attrition mill design consisting of a stationary cage and a moveable cage of vertical bars rotated in a liquid containing the solid to be ground (Fig. 2). The solid material usually consists of two size fractions: a coarse fraction that is the grinding medium and a fine fraction that is to be ground. After grinding, the desired particles are physically and/or chemically separated from the coarse fraction. Remarkable size reductions are reported (Sadler *et al.*, 1975) although most measurements have been in surface area rather than on actual particle size. Surface areas equal to 0.1 μm equivalent spherical particles were achieved in 2 hr of attrition milling compared to 30 hr for vibratory milling, while conventional ball milling had only reached 4 μm particle size in 30 hr. In such intensive grinding in water, some hydration of the surface of oxide particles might be expected, though the performance of the particles in packing and sintering is similar to other submicron powders. One advantage of this technique, or any attrition technique, is the ability to produce submicron particles of compositions difficult to prepare by other techniques. ZrO_2, Al_2O_3, SiO_2 and other materials have been ground successfully to submicron size in a few hours of grinding (Stanley *et al.*, 1973a,b). Little information is available on the range of particle sizes obtained by attrition milling. Since sand-size coarse medium is used for grinding, some particles considerably larger than the calculated spherical diameters could be present in the fine-size fraction. The problem of contamination must also be considered. In grinding silica and silicon carbide, as much as 20–30% of the media was ground to -325 mesh size and appeared in the fine fraction after initial separation by screening.

The attrition mill offers an efficient means of size reduction in the submicron range, and where the grinding media contamination can be tolerated or removed, this technique offers substantial advantages, in both laboratory and production sizes, over other types of ball or vibratory milling.

E. Characteristics of "Ground" Particulates

When particles are subjected to grinding, very high stresses (hundreds of MN/m^2) are generated at the particle surfaces. Under such stress, plastic flow occurs and highly strained particles result. The higher energy content of milled powders is easily demonstrated in the sintering activity of submicron oxides after only 2 hr of dry ball milling. The X-ray patterns of such powders also reveal lattice distortions, amorphous layers, and structural transformations.

"Grinding" techniques, though usually inefficient in *size* reduction, should not be overlooked as a means of easily modifying the characteristics of powder prepared chemically or by other techniques.

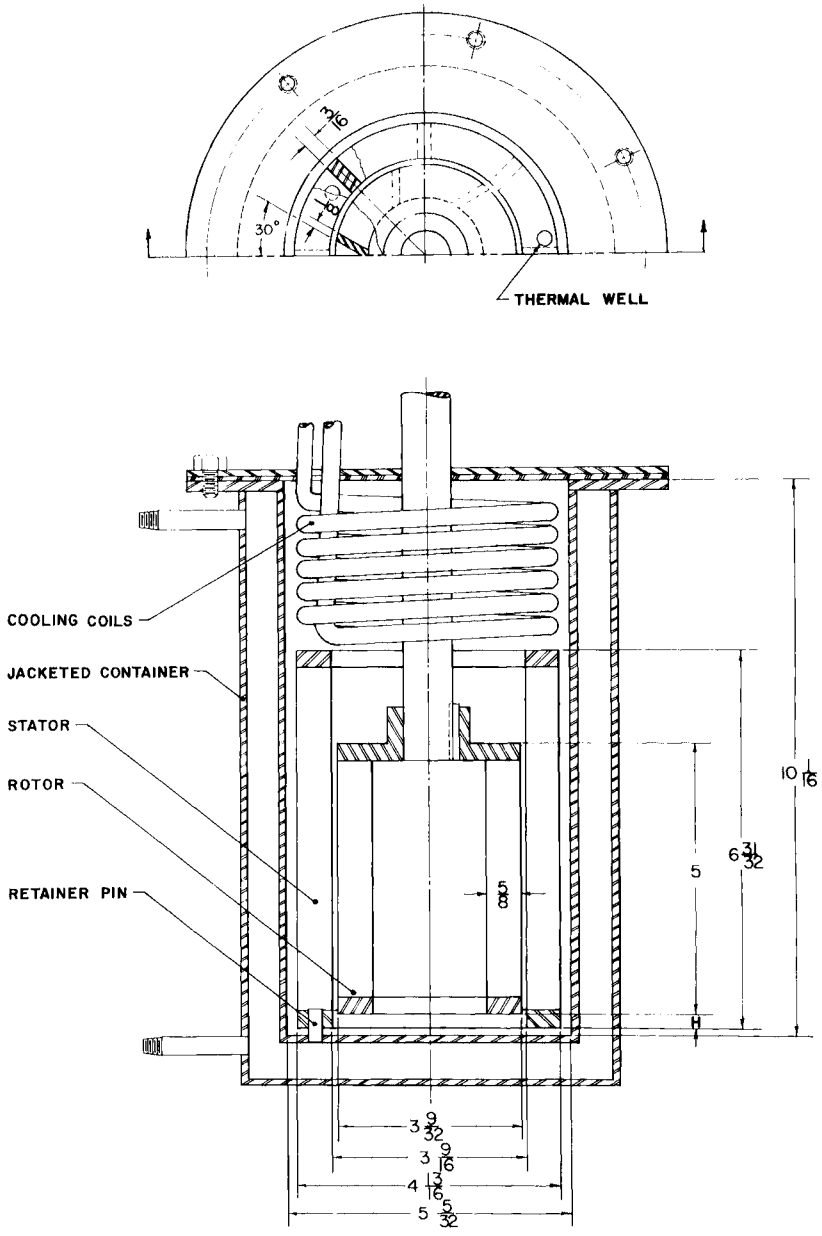

Fig. 2. Internal details of a 5 inch attrition mill. (Courtesy U.S. Bureau of Mines, Tuscaloosa, Alabama.)

III. Particle Growth Processes

A. Decomposition Process

Decomposition of a chemical precursor that yields the desired oxide or other compound must actually be classified as a crystallization or construction process rather than a decomposition. The desired particulate is actually constructed from the debris of decomposition, and thus a growth process results.

Several requirements must be met if a decomposition is to yield submicron particles. First, the crystal structure of the desired particulate must be quite different from that of its precursor. If not, the morphology of the particulates may strongly resemble the original precursor morphology from which it is constructed. For convenience, it is also desirable that the precursor not melt or segregate below the decomposition temperature so that large surface areas and permeable masses of uniform composition can be maintained during decomposition. And finally, the most desirable decomposition is one that yields the desired solid plus gaseous products that can be handled without severe hazard or atmospheric contamination.

Sulfates, nitrates, oxalates, hydroxides, carbonates, and many other salts have been used as precursor materials. Each has its advantages and problems. Rather than reviewing these details, which can usually be found in referenced literature, emphasis will be placed in the following discussion on specific equipment and techniques which use decomposition techniques for growth of the desired particulates.

B. Preparing Complex Compositions

One of the difficulties in preparing fine ceramics is the difficulty in achieving homogeneity at the individual grain level. Consider for a moment, the grain size desired in many finished compositions—3 to 10 μm. To start with -325 mesh raw materials, which may have 40 μm size grains present, requires diffusion paths of several grain diameters, even if perfect mixing could be achieved before forming and firing (Serafin, 1969d).

Chemical preparation of complex compositions has been the approach frequently used. All desired metal ions are prepared in a solution and co-precipitated as hydroxide, oxalate, etc. Subsequent calcination and re-grinding usually provide a uniform chemical composition of fine size (0.1–0.5 μm). Co-precipitation appears to be an excellent approach and has been used effectively; however, careful study reveals potential sources of inhomogeneity in batching. Few compounds precipitate at exactly the same pH or concentration, hence precipitations must be performed during inten-

sive mixing to ensure that selective precipitation does not occur. Continuous, stoichiometric, and intensive mixing techniques must be used for successful co-precipitation on laboratory or plant scale (Vanik and McKinney, 1971).

An alternative to co-precipitation is co-crystallization of complex salts that contain the desired ions. This has been reported for magnesium aluminum sulfate to form a precursor of magnesium aluminate spinel (Palmour and Dokuzoguz, 1970). Other systems are practical (Rigterink, 1972) although more difficult to achieve in practice than solution techniques. When co-crystallized salts or salt hydrates are considered, the temperature program for dehydrating or decomposing must also be considered. Since salt hydrates lose water in distinct steps, it is possible to mix or un-mix certain salts if the melting and dehydrating temperatures are not similar for each salt. An example of this effect is the decomposition of mixtures of $Cu(NO_3)_2$ hydrate and $Ni(NO_3)_2$ hydrate. By selection of the dehydrating temperature and calcination schedule, the copper oxide can be coated on nickle oxide particles, or nickle oxide coated on copper oxide particles, depending on the complex phase relationships between the two salt hydrates, the temperature, and the composition of the liquid phase.

Sol–gel techniques have been reported in detail for preparation of uranium, zirconium, thorium and several other oxides (Rigterink, 1972; Vanik and McKinney, 1971; Rundell *et al.*, 1970). The particles in these sols are only a few tens to a few hundred angstroms in size and solids concentration is usually low, but mixing of sols has resulted in controlled stoichiometry of complex oxide mixtures. Silicates and glass compositions are particularly attractive for this preparation approach. One of the problems associated with this approach is the low solids concentration. Often 10% solids (90% water) will form a rigid gel which must be dewatered and resists all attempts to filter, filter press, or handle as a conventional precipitate. The solid, when dried, is sometimes of extremely low bulk density and must be compacted or pelletized before further ceramic processing.

C. Decomposition of Organometallic Compounds

Mazdiyasni *et al.* (1965, 1967, 1969) have demonstrated the utility of several types of organometallic compounds for producing high purity single and mixed oxides. Generally the alkoxides (alcoholates) are preferred with isopropoxides, butoxides, and amyloxides commonly used. These compounds decompose typically

$$Zn(OR_4) \xrightarrow[\text{inert gas}]{\Delta} ZrO_2 + 2\,ROH + \text{olefin}$$

The compounds may also be oxidized

$$Ba(OCH_3)_2 + Ti(OC_4H_9)_4 + 22\,O_2 \longrightarrow BaTiO_3 + 18\,CO_2 + 21\,H_2O$$

A hydrolysis to yield hydroxides may also be achieved with steam. Zirconia, yttria, barium titanate, alumina, and other oxides and oxide mixtures have been prepared in high purities, and the sintering activity of these oxide powders appears to equal or exceed that exhibited by powders derived from other processes. Transparent and translucent ceramics have been prepared from powders of this origin (Mazdiyasni *et al.*, 1967).

The cost of preparing large quantities of powders by this synthesis technique appears reasonable; however, the precautions required in processing volatile, flammable, and often pyrophoric organometallic compounds has discouraged many investigators. When pyrolyzed, the resulting oxide powder sometimes retains a small carbon or hydrocarbon residue that might be undesirable for hydrogen firing or hot pressing; however, this is normally removed when sintered in air.

These organometallic compounds may also be used as the basis for pyrolysis, hydrolysis, or vapor phase reactions in which the oxide is deposited as a dense coating.

D. Special Equipment for Decomposition of Salts and Compounds

Recently a high temperature fluid energy mill has been constructed embodying the essential grinding features of ordinary fluid energy mills, but designed to operate at temperatures up to 800° to 900°C (Duecker and Glemza, 1972; Levy and Vanik, 1970; Levy *et al.*, 1973). The mill is constructed of a high temperature alloy and the source of fluid powder is superheated steam or air (400°–800°C). The entire assembly thus can operate at a red heat and above the decomposition temperature for many sulfates, nitrates, hydroxides, and oxylates. In addition to providing a method of "grinding" particles, this type of mill can also simultaneously provide energy for the thermal decomposition of salts or compounds (Fig. 2).

For the production of high purity compositions of mixed oxides, the feed to a fluid energy mill (FEM) may be mixed hydroxide slurries, mixed salt solutions, molten salt mixtures, or even solid compounds. The resulting particles of oxides are so minute that difficulty is experienced in separating them from the large volume of hot gases that entrain them. A yield of over 80 % of the material is considered good collection efficiency. Some recombination of oxides and hot gases also occurs and the resulting powders from FEM rarely show less than 15 % volatiles. The surface area of these particles is quite high and average particle size may range below 500 Å. To be useful for ceramic processing, this precursor powder must then be calcined to grow the particles to the desired size.

The appearance of the precursor particles after FEM is one of thin bubbles or sections of hollow spheres as though the salt or compound decomposed was literally exploded into tiny, thin-wall bubbles, many of which are fractured before collection. As this material is calcined, the thin-wall "bubble" material coalesces into solid, dense, and more equiaxed particles.

Fluid energy milling has been used to produce alumina, magnesium aluminate spinel, barium titanate, lead zirconate titanate, zirconia, and other oxides in high purity (less than 300 ppm impurities) and particle sizes 0.1–0.3 μm of well crystallized, single phase material (Duecker and Glemza, 1972; Levy and Vanik, 1970; Levy, 1973; Levy *et al.*, 1973; Rettew *et al.*, 1972; Sanchez *et al.*, 1971). In addition the technique is sufficiently flexible to produce intimately doped oxides, stabilized zirconia, and other mixed oxides of ceramic interest while maintaining the same particle sizes and purities. Essentially the FEM uses its configuration to supply the decomposition energy so rapidly and to remove the decomposition products so quickly that further growth, sintering, or agglomerating of the particles is prevented.

A similar technique for preparation of complex, fine-particle, technical ceramic compositions (principally ferrites and garnets) has been used by Bomar *et al.* (1974). A special spray dryer operating at temperatures sufficiently high to perform decomposition and dehydration is used. The results achieved were similar to fluid energy milling, although the lower temperatures limited the number of compounds that could be utilized as starting materials.

For such decomposition processing as FEM or "spray calcining," nitrates provide a good starting compound. A wide variety of soluble nitrates are available, and nitrate hydrates melt at low temperatures and can be used as molten salt feed. The nitrates decompose cleanly and at low temperatures and the decomposition products can be scrubbed or catalytically cleaned from the exhaust stream.

IV. Cryochemical or Freeze Drying

The use of a freeze-drying technique for producing fine oxide particles has received intensive investigation (Johnson and Schnettler, 1970; Rigterink, 1968, 1972). The technique has proved versatile, and cost projections for large scale operation are promising. The technique is basically a salt decomposition process where droplets of salt solutions containing the desired metal ions are rapidly frozen. The freezing process produces spheres of frozen solution approximately 0.1–0.5 mm in diameter.

To obtain the final oxide, the frozen spheres are dried by a combination of vacuum and gentle heating so that all ice is sublimed and the sphere is not melted. The resulting porous spheres are an anhydrous sulfate (or other salt) and conventional calcining techniques are used to remove the sulfate and grow the oxide particles to the desired size.

Several advantages of this process are evident. (1) Many complex compositions can be readily prepared as solutions of soluble salts. (2) Little segregation occurs in freezing so that the intimate mixing of a solution is approximated in the frozen droplet. (3) Anhydrous salts can be readily produced in the freeze-drying operations. This eliminates the problems attendant with the melting of hydrated salts at temperatures far below their decomposition temperature. (4) The porous spheres are readily calcined

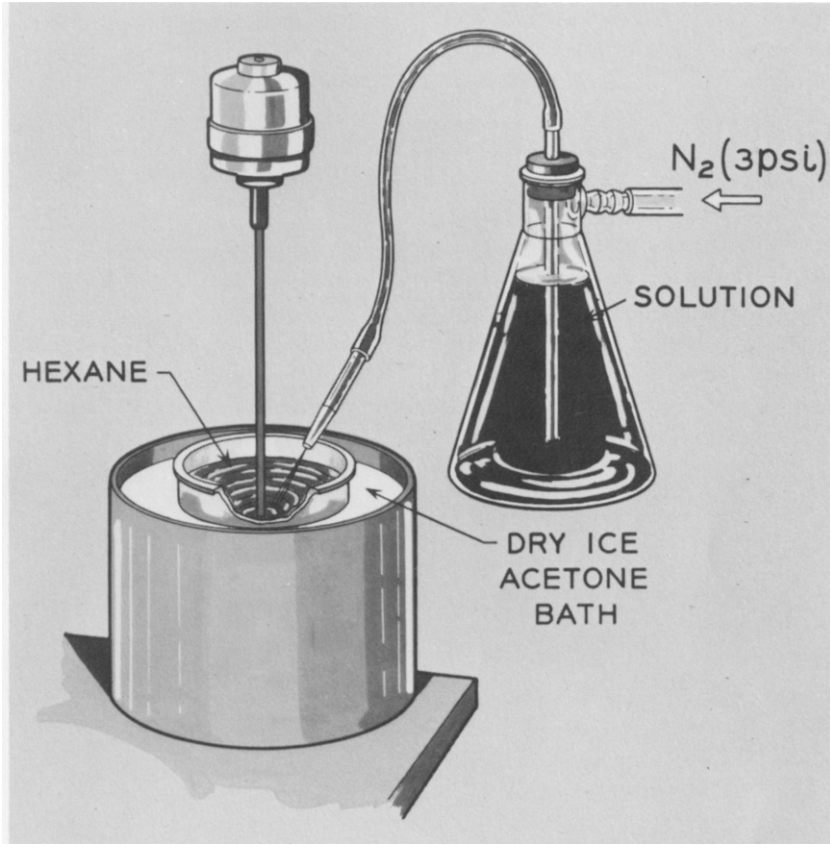

Fig. 3. Laboratory method of freezing droplets of solution.

to the oxide because gases can escape from individual spheres and the entire bed of spheres is quite permeable. (5) A highly reactive or sinterable powder is produced with crystallite size from 0.1 to 0.5 μm. For laboratory use, the cryochemical process is easily adapted to production of a few hundred grams of an oxide composition. Simple dry ice–acetone freezing can be used with laboratory glassware as shown in Fig. 3. For freeze drying, glassware can also be used to form a cooled, evacuated flask with a suitable condenser in the vacuum line (Fig. 4).

Some of the problems experienced with this approach are the difficulty in finding suitable soluble salts and the incompatibility of two different soluble salts (e.g., $FeSO_4$ and barium acetate to form insoluble $BaSO_4$ when preparing barium ferrite (Rigterink, 1968). Laboratory freeze-drying equipment is readily available but is not a common fixture in most ceramic processing facilities. Some salt solutions also require quite low temperatures for freezing. The low temperature limitation of some commercial freeze dryers may thus prevent their use with some salts.

Slurries of hydroxides or gels could be used as feed for the cryochemical process; however, some of the advantages of intimate mixing might be lost with slurry techniques.

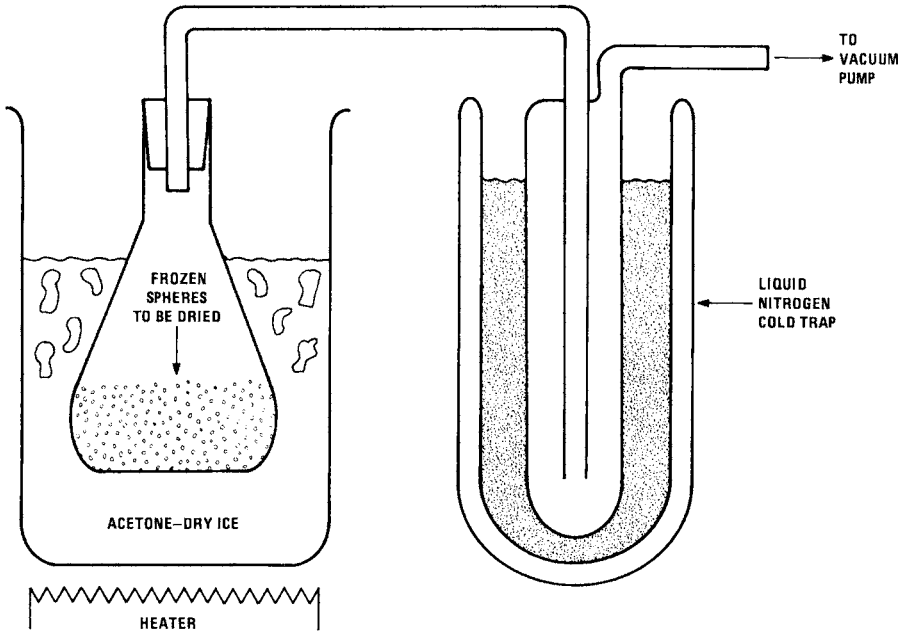

Fig. 4. Laboratory freeze drying scheme. Spheres are slowly warmed *in vacuo* without melting.

V. Vapor Phase and Vaporization Processes

Vaporization of most oxides requires substantial energy input and hence is rarely economical or attractive as a production technique. The very rapid condensation that is possible with most oxides vaporized at high temperatures results from high supersaturation plus rapid nucleation and often yields very small particles of oxide. Since plasma of up to 20,000°K is readily generated either by dc or rf techniques, these very high temperatures may be used to vaporize and condense material into fine particulates. The details of the techniques vary widely (Everest *et al.*, 1971; Veale, 1972) but oxides, elements, carbides, mixed oxides, and mixed carbides have been prepared in particle sizes well below 0.1 μm.

Lower temperature vapor phase reactions involving organometallics have been mentioned previously, but vaporization of halide compounds and reactions in the vapor phase have also been used to produce many oxides and carbides (Everest *et al.*, 1971; Veale, 1972). The commerical production of some silica materials, TiO_2, and carbon blacks are also examples of vapor phase reactions involving halides and hydrocarbons, respectively.

VI. Summary

A wide variety of powder production processes are available that yield particles less than 1.0 μm in diameter. Unfortunately, the wide differences in the chemical and physical nature of oxides, carbides, elements, etc., preclude the use of any single process for preparation of all powders. Several newer techniques, such as attrition milling, fluid energy milling/decomposition, and continuous co-precipitation offer economical ways to prepare both laboratory scale and small production level amounts of a variety of pure or mixed oxide materials. The utility of such fine-size powders has been readily demonstrated in the laboratory and in limited commercial applications. These powders promise greatly improved ceramics and unique new processing technology; the current limitation to further exploitation is simply the commercial availability of many of these fine size materials at reasonable costs.

References

Bomar, S. H., Logan, K. V., and Rodique, G. F. (1971). "Application of High Velocity and High Pressure Fabrication Methods Using Powder Metal for the Production of Missile Components," Final Technical Report, Contract No. DAA H03-69-C-0334, Report No. QL-TR-

71-1, Manufacturing Methods and Technology Project AM CMS 4297.03.2993. Army Missile Command Redstone Arsenal, Alabama.

Bomar, S. H., Jong, B. W., and Logan, K. V. (1974). "A Manufacturing Methods and Technology Study Covering Manufacturing Techniques for Ferrites and Garnets Used in Phased Array Radar," Final Technical Report, Contract No. DAAH01-72-C-0888, Manufacturing Methods and Technology Project AMCMS 4297.03.2993. Georgia Institute of Technology, Atlanta.

Doyle, C. E., and Becker, D. L. (1969). U.S. Patent 3,425,633.

Duecker, H. C., and Glemza, R. (1972). U.S. Patent 3,672,831.

Everest, D. A., Sayce, I. G., and Selton, B. (1971). *J. Mater. Sci.* **6**, 218–224.

Farrant, J. C., and North, R. (1957). *In* "Chemical Engineering Practice" (H. W. Cremer and T. Davis, eds.), Vol. 3. Butterworth, London.

Johnson, D. W., and Schnettler, F. J. (1970). *J. Amer. Ceram. Soc.* **53**, 440–444.

Levy, N., Jr. (1973). U.S. Patent 3,708,438.

Levy, N., Jr., and Vanik, M. C. (1970). U.S. Patent 3,514,252.

Levy, N., Jr., Wirth, D. G., Jr., and Rettew, R. R. (1973). U.S. Patent 3,725,094.

Mazdiyasni, K. S., Lynch, C. T., and Smith, J. S. (1965). *J. Amer. Ceram. Soc.* **48**, 372–375.

Mazdiyasni, K. S., Lynch, C. T., and Smith, J. S., II. (1967). *J. Amer. Ceram. Soc.* **50**, 532–537.

Mazdiyasni, K. S., Dolloff, R. T., and Smith, J. S., II. (1969). *J. Amer. Ceram. Soc.* **52**, 523–526.

Meloy, T. P. (1970). *In* "Ultrafine Grain Ceramics" (J. J. Burke, N. L. Reed, and V. Weiss, eds.). Syracuse Univ. Press, Syracuse, New York.

Palmour, H., III, and Dokuzoguz, H. Z. (1970). U.S. Patent 3,544,266.

Quatinetz, M., Schafer, R. J., and Smeal, C. R. (1963). *In* "Ultrafine Particles" (W. E. Kuhn *et al.*, eds.). Wiley, New York.

Rettew, R. R., Wirth, D. G., and Levy, N. W., Jr. (1972). U.S. Patent 3,655,330.

Rigterink, M. D. (1968). *J. Can. Ceram. Soc.* **37**, 56–60.

Rigterink, M. D. (1972) *Amer. Ceram. Soc., Bull.* **51**, 158–161.

Rundell, C. A., Kwedar, J. A., and Duecker, H. C. (1970). U.S Patent 3, 533, 738.

Sadler, L. Y., Stanley, D. A., and Brooks, D. R. (1975). *Powder Technol.* **12**, 19–28.

Sanchez, M. G., Levy, N., Jr., and Rettew, R. R. (1971). U.S. Patent 3,577,487.

Serafin, F. G. (1969a). U.S. Patent 3,420,687.

Serafin, F. G. (1969b). U.S. Patent 3,442,673.

Serafin, F. G. (1969c). U.S. Patent 3,443,975.

Serafin, F. G. (1969d). U.S. Patent 3,459,570.

Serafin, F. G. (1970). U.S. Patent 3,492,138.

Stanley, D. A., Sadler, L. Y., III, Brooks, D. R., and Schwartz, M. A. (1973a). "Attrition Milling of Ceramic Oxides." Bureau of Mines, U.S. Dept. of Interior, Tuscaloosa Metallurgy Research Laboratory, Tuscaloosa, Alabama.

Stanley, D. A., Sadler, L. Y., III, and Brooks, D. R. (1973b). *Proc. Int. Conf. Particle Technol., 1st, 1973.*

Sterne, J. H., III, and Stratton, C. L. (1968). *Amer. Ceram. Soc., Bull.* **47**, 298–301.

Vanik, M. C., and McKinney, R. W. (1971). U.S. Patent 3,586,635.

Veale, C. R. (1972). "Fine Powders-Preparation Properties and Uses." Wiley (Halsted), New York.

Milling

C. GRESKOVICH

General Electric Corporate Research and Development
Metallurgy and Ceramics Laboratory
Schenectady, New York

I. Introduction

Milling, which may be defined as particle size reduction by means of mechanical forces, often plays an essential role in the processing of fine, chemically homogeneous powders that give rise to new or improved material properties. Several examples may be mentioned. Highly dense, translucent Al_2O_3 may be successfully obtained with enhanced optical and microstructural perfection by using dry ball-milling or vibratory milling approaches (Wolkodoff and Weaver, 1968; Klingler *et al.*, 1971). Dry ball-milling is a necessary step in the fabrication of polycrystalline ceramic lasers composed of 89 mole % Y_2O_3 + 10 % ThO_2 + 1 % Nd_2O_3 (Greskovich and Chernoch, 1973). A wet ball-milling operation is a necessary step in producing acceptable powders for synthesis of sintered PLZT (Pb, La) (Zr, Ti)O_3] and barium ferrite ($BaFe_{12}O_{19}$) ceramics (Haertling, 1970; Arendt, 1973). The PLZT materials have important electrooptic applications such as optical shutters, filters, and information display, whereas $BaFe_{12}O_{19}$, on the other hand, finds use as a permanent magnet material in sound reproducing and recording devices. Finally, fluid energy milling is found to be a useful treatment for Co_5Sm powders that give rise to the most powerful permanent magnets currently known (Benz and Martin, 1972) and for (Y, Gd)$_3$ (Fe, Al)$_5O_{12}$

garnet powder used for phase shifters in radar systems (C. Greskovich, unpublished research, 1973).

The physical and chemical characteristics of a powder are largely responsible for the physical and chemical properties of the final product synthesized from that powder. In the last 15 years great emphasis has been placed on the preparation of micron to submicron sized powders in order to produce highly dense, small grain size ceramic materials of homogeneous composition by a sintering or hot pressing approach. [By sintering we mean a heat treatment process by which compacted powders are transformed into a strong, dense polycrystalline mass, while hot pressing refers to the same but with the application of an external pressure ($\sim$ 5000 psi) during heat treatment.] Broad experience in sintering and solid-state reaction technologies shows that the densification rate as well as the rate of solid-state reaction of multicomponent powders depend markedly on the average particle size in such a way that the finer the average particle size the higher the sintering and chemical reaction rates for most ceramic materials. The milling or comminution of powders is frequently necessary to obtain chemically uniform, finely divided powders with a desirable particle size distribution and with little or no aggregation of particles. As a result of the need for finer and finer ceramic powders, most of this chapter on milling will pertain to fine grinding methods. This is not meant to imply that coarse particles have no place in ceramic technology for, on the contrary, such particles are important for the control of shrinkage in several types of refractories and the control of microstructure in other ceramic bodies.

In this paper on milling we will cover a brief review of some of the theoretical concepts of comminution and mention some of the types of milling equipment. Detailed discussion will concern two types of fine grinders or pulverizers, one being the conventional ball mill and the other being a newly developed fluid energy (jet) mill. Particular attention will be focused on the preparation of several special or newly developed ceramics with attractive and exceptional physical properties for novel applications. Some of the topics of discussion will concern grinding mechanisms operating during milling as well as problems associated with aggregation, dispersion of chemical constituents in the powder, and contamination from wear of grinding media and mill walls.

II. Comminution Theory

There are several proposed laws of comminution. Von Rittinger (1867) proposed that the energy spent in milling is proportional to the new surface formed:

$$E = C_1 (1/D_2 - 1/D_1) \tag{1}$$

where E is the energy spent per unit volume; C_1, a constant; D_1, the initial particle size; and D_2, the final particle size after size reduction.

Kick (1885) applied the classical theory of elasticity and strength to the grinding process. He stated that a critical stress is required for fracture and that the same energy is required to break up a large particle into an infinite number of smaller particles step at a time. Kick's relation may be expressed as

$$E = C_2 \log (D_1/D_2) \tag{2}$$

where C_2 is a constant and D_1/D_2 is the particle size reduction ratio.

Another of the classical laws is that of Bond (1952) which states that the total work useful in particle breakage is essentially inversely proportional to the square root of the diameter of the product particles. Bond's mathematical expression is actually empirical since it was formulated on laboratory tests.

$$E = C_3 (1/D_2^{1/2} - 1/D_1^{1/2}) \tag{3}$$

where C_3 is a constant.

Because of the many oversimplifications and assumptions used to derive the above formulas, the practical use of these "laws" are employed qualitatively. Empirical observations reveal that Rittinger's law is often qualitatively applicable to the reduction of coarse particles, whereas Kick's hypothesis can be applied to the fine grinding of particles. There are, however, several objections to the use of these laws. First, there is usually a big discrepancy between the energy spent in milling and the surface energy of the newly formed surfaces. Theoretical grinding efficiencies are usually low, of the order of 1 %, with most kinetic energy converted into heat. Second, it is very doubtful that large particles have the same critical stress for fracture as small particles. A third objection is that it is obviously very difficult to disintegrate large uniform particles into smaller particles of uniform size. This is implied in the above-mentioned concepts of milling since the effects of particle size distribution in the feed or product material are not directly taken into consideration.

Several attempts have been made to improve these theories. Charles (1957) suggested that at least two independent numbers are necessary to characterize a specific particle size distribution resulting from comminution. He derived the following generalized energy-size reduction relationship:

$$E = Ak^{(1-n)} \tag{4}$$

where k is the size modulus (a constant) for a given particle size distribution, and constants A and n relate to particular grinding or crushing conditions. Holmes (1957) has reported energy equations similar to Eq. (4).

Schuhmann (1960) presented a generalized derivation for a complex comminution process that included the summation of various types of comminution events occurring in the fine sizes of the comminution product. He found that the energy consumption in comminution could be described by

$$E = Ak^{-\alpha} \tag{5}$$

where α is the particle size distribution modulus and the reciprocal of A is a measure of the grindability (the volume of comminuted material finer than unit size produced per unit of energy expended"). Both Eqs. (4) and (5) were developed using an empirical power law–size distribution equation (Schuhmann, 1940) that represents to a large extent the fine sizes of the comminution product. The exponents α and n are related by $\alpha - n + 1 = 0$.

In the last 15 years considerable effort has been aimed at developing theoretical models capable of predicting the particle size distribution that develops when an individual, homogeneously brittle solid undergoes a single fracture process. On the basis of the Griffith theory (Griffith, 1920) of brittle strength, Gilvarry (1961) formulated a model for fragmentation in which he envisioned that particle fracture proceeds mainly by the activation of internal volume, facial and edge flaws that are distributed independently of each other. A major result of his investigation is that the size distribution predicted reduces to the frequently used empirical distribution functions determined by Schuhmann (1940) and Rosin and Rammler (1933) for the process of comminution. From this finding it was concluded that the predominant mechanism causing fragmentation is the activation of edge flaws. Meloy (1963) presented a model based on the concept that at the time of fracture the crack density at any point within the solid is proportional to the peak energy. The size distribution function obtained could fit experimental data with reasonable accuracy. In a more recent work Meloy (1970) reviewed some of the current theories of comminution and discussed many of the serious problems associated with the "flaw" and "crack density" models. Finally, Rose (1971) proposed that an adequate theory of comminution should consider and explain not only the distribution of particle sizes of the material formed but also the distribution of strengths of a given particle size and how the strength changes with particle size. The application of his mathematical treatment to ball-milling experiments showed that calculated results are in rough agreement with practice.

In summary, the development of an adequate unified theory of milling from first principles appeals to be extremely difficult. There are a variety of complex comminution events occurring that depend greatly on the nature of the material and the type of milling device employed. It is most reasonable, then, to make use of empirical observations and relations which, if carefully interpreted in the light of modern theories of comminution, can give a better understanding of the milling process and perhaps lead to a rational theoretical treatment. Finally, this brief review on comminution theory is not intended to be an exhaustive literature survey of the subject matter but only to serve the purpose of exposing the inexperienced reader to some of the difficulties in developing an adequate theory of comminution.

III. Some Types of Milling Equipment

There is a variety of crushing and grinding equipment employed for size reduction of raw materials selected for the fabrication of many ceramics. Some of the comminution processes for coarse crushing and intermediate grinding are gyratory-, jaw- and roll-crushing, hammer milling, wet pan, and dry pan operations. Such milling operations reduce the size of feed material from the centimeter–meter range to sizes in the millimeter–centimeter range. The types of mechanical forces that may be operating on the feed material during comminution by using the above milling devices are those of tension, compression, shear, and impact. Some insight on the choice of milling equipment for laboratory use can be made by knowing the hardness, feed size, and the particle size-reduction ratio desired. On a commercial scale, the economics of the milling process plays a dominant role in the selection of equipment. In many cases manufacturers of such equipment will make preliminary crushing or grinding tests on a given starting material and will sometimes make recommendations.

The types of mills used for fine grinding processes in the ceramic industry include vibratory mills, centrifugal mills, colloid mills, ball mills, and fluid energy mills. The primary cause of grinding action in each case is considered to be high frequency vibration (vibratory mill), impact (centrifugal mill), intense shear (colloid mill), tumbling and friction (ball mill), and particle collision grinding (fluid energy mill). These fine grinders or pulverizers comminute materials which are a fraction of a millimeter in size or less to sizes generally below 100 μm(microns). A practical lower particle size limit or grinding limit of 0.1 to 1 μm appears to exist for most milling operations using fine grinders, and in this case the nature of the fracture process is very important. Important factors needed to be taken into consideration for the

selection of a fine grinding mill are the physical and chemical nature of the material to be ground, the grinding rate, the rate of contamination from mill wear, and the particle size distribution desired. For example, a fluid energy mill can efficiently break up hard materials such as Al_2O_3 with little or no contamination but ball-milling the same material may lead to lower grinding rates, higher contamination rates, and a broader particle size distribution. If the starting or feed material consists of two or more phases with different densities and a homogeneous distribution of phases is required, ball-milling or vibratory-milling, for example, may be the preferred milling technique over fluid energy-milling because there is a tendency toward phase and particle segregation by air classification in the fluid energy mill. Since ball-milling is a common fine grinding technique found in nearly all ceramic laboratories and since fluid energy-grinding mills are becoming popular because of their ability to produce micron size powder particles with control of particle size distribution and contamination, we will discuss these two methods of fine grinding in greater detail.

A. Ball Mills in the Laboratory

For laboratory use the name "jar mill" is often used interchangeably with "ball mill." We will adopt the use of the latter name for convenience. Furthermore, the expressions "pebble milling" and "ball milling" are sometimes mutually substituted for each other. Again, we shall employ the expression "ball milling" to signify the use of any type of grinding medium in these conventional laboratory mills.

1. Construction

The common laboratory ball mill ranges in volume from about a pint to several gallons in capacity and is usually cylindrically shaped with a length that may be either larger or smaller than the diameter. Materials generally used as mill liners are vulcanized rubber, polyurethane, high density alumina, porcelain, tungsten carbide, stainless steel, and others. The choice of mill lining depends on the wear rate of the lining, the type of contamination that can be tolerated, and the efficiency of milling. From the point of view of impurities alone, the best selection of mill liners is one that has the same composition as that of the material to be ground. In some of these mills lifters bars can be bolted or welded into place to suppress slippage of the media during grinding. However, slippage can be usually avoided by rotating the mill cylinder on conventional variable-speed, motor-driven friction rolls at 60 to 70 % of the critical speed. Here, the critical speed is defined as that speed at which the grinding media begin to centrifuge in the absence of any

powder or liquid charge inside the mill and can be calculated (in rpm) as the ratio $54.2/\sqrt{r}$, where r is the mill radius in feet.

There are different kinds of grinding media commercially available in the form of balls or cylinders for use in ball mills. Selection of a grinding media appropriate for a given milling experiment depends primarily on the media's composition, hardness, toughness, and bulk density. The bulk density of the grinding medium is considered to be an important factor in determining the milling rate of a powder. Some types of grinding media commerically available and their approximate bulk density in grams per cubic centimeter are porcelain balls (2.3), Al_2O_3 balls (3.6), ZrO_2 cylinders (5.4), steel balls (7.7), and tungsten carbide balls (14.8). The use of high-density grinding media provides greater impact during the tumbling action and consequently gives rise to faster grinding rates. The rate of grinding may also be increased by employing smaller diameter balls of high-density grinding media because of the greater number of contacts per unit volume acting to impose mechanical forces on the powder particles.

2. Charging the Mill

Ball mills are generally filled with grinding media to approximately 50 % of their total volume. The powder charge is usually 25 % of the total mill volume for dry ball-milling and is generally 30 to 40 % of the total volume for wet ball-milling operations. These conditions normally permit good grinding efficiences. A grinding aid, such as stearic acid or oleic acid, is usually added in small percentages ($\sim$ 1 wt %) to powders undergoing dry milling in order to enhance the grinding efficiency. This additive minimizes the packing or caking of powder on the grinding media and mill wall as the concentration of fines increases during milling. Such grinding aids are also frequently beneficial as compaction aids during the subsequent pressing of the powder if a sintering route is to be followed.

In the case of wet ball-milling, a solid charge is ground while suspended in a liquid medium (vehicle), which for most practical purposes is usually alcohol, acetone, or water. The type of liquid used depends to a great extent on its inertness toward chemical reactivity with the mill lining, grinding media, and powder charge. Enough liquid should be added to the powder charge to make a creamy slurry or suspension of optimum viscosity. The milling of suspensions having high viscosity often gives rise to low grinding rates while that of suspensions with high fluidity usually leads to high levels of contamination from wear of the mill lining and grinding media. A common procedure in wet milling practice is to add a dispersing aid in amounts up to 1 wt % which inhibits particle flocculation in the suspension and permits further particle size reduction. Some dispersing aids commonly used are sodium silicate and tetrasodium pyrophosphate.

3. *Stages of Ball-Milling*

There are several reasons why one may select ball-milling as a powder-treatment step. The primary purpose for ball-milling, of course, is to reduce the size of individual particles and powder aggregates. In addition one may wish to eliminate or reduce particle segregation and preferred orientation effects in a single-phase starting powder. In multicomponent powder batches it is usually desirable to disperse the various chemical constituents by thoroughly mixing in a ball mill. Although all of these reasons for ball-milling are important, we shall direct our attention only to the fundamental comminution process during ball-milling.

The physical process of ball-milling can be considered to consist of the following stages (Harwood *et al.*, 1965; Matkin, 1973):

1. Marked reduction in the size of aggregates by light milling;
2. Fracture of individual particles and the formation of defects and changes within the particles during longer milling;
3. Re-agglomeration at prolonged periods of milling.

Most ceramic powders having an average particle size in the micron range or less generally contain a small fraction of aggregates or agglomerates. Here the definitions of an aggregate and an agglomerate are a group of particles held together by strong and weak interparticle forces, respectively (Irani and Callis, 1963). The formation of aggregates frequently results from a calcination treatment that promotes sufficient diffusion of matter into the neck regions between individual particles and creates strong interparticle bonds. A typical photomicrograph of aggregates found in a ThO_2-doped Y_2O_3 powder prepared by a wet chemical approach followed by calcination at 850°C for 4 hr is shown in Fig. 1A (Greskovich and Woods, 1973). These aggregates are about 10 to 15 μm in size and contain platelike particles whose edge lengths are 1 to 3 μm. After dry ball-milling this powder for 6 hr, the aggregates are broken down (Fig. 1B) into smaller, equiaxed soft agglomerates that have a favorable response to the subsequent forming and sintering processes. Some of the sources of agglomeration during milling are the adherence of newly formed surfaces, adherence of particles caused by the presence of a dry-milling aid or moisture in the milling atmosphere, and bonding at interparticle interfaces caused by localized temperature rises due to friction. It is also evident that all three stages of milling have occurred in Fig. 1B. In addition to the breakdown of aggregates and the reagglomeration of very fine particles, individual particles have been fractured to sizes of the order of 0.1 μm.

Aggregates in a processed powder can affect the development of the microstructure during sintering or hot-pressing and can influence the final

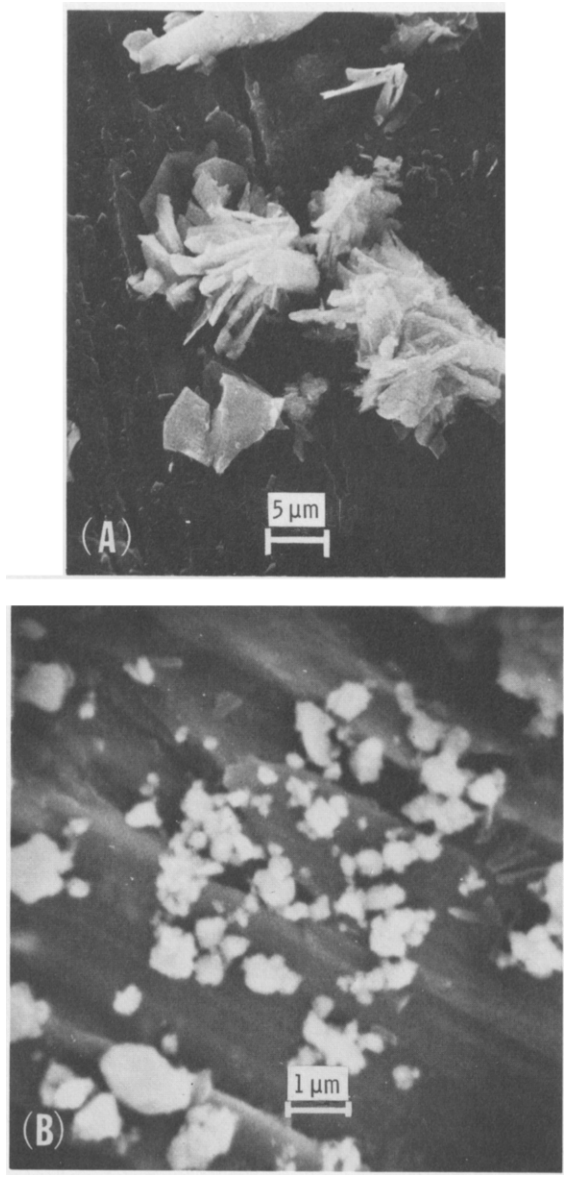

Fig. 1. Typical scanning electron micrograph of (A) powder aggregates in ThO_2-doped Y_2O_3 powder calcined at 850°C for 4 hr and (B) powder particles and agglomerates in dry ball-milled, calcined powder (Greskovich and Woods, 1973).

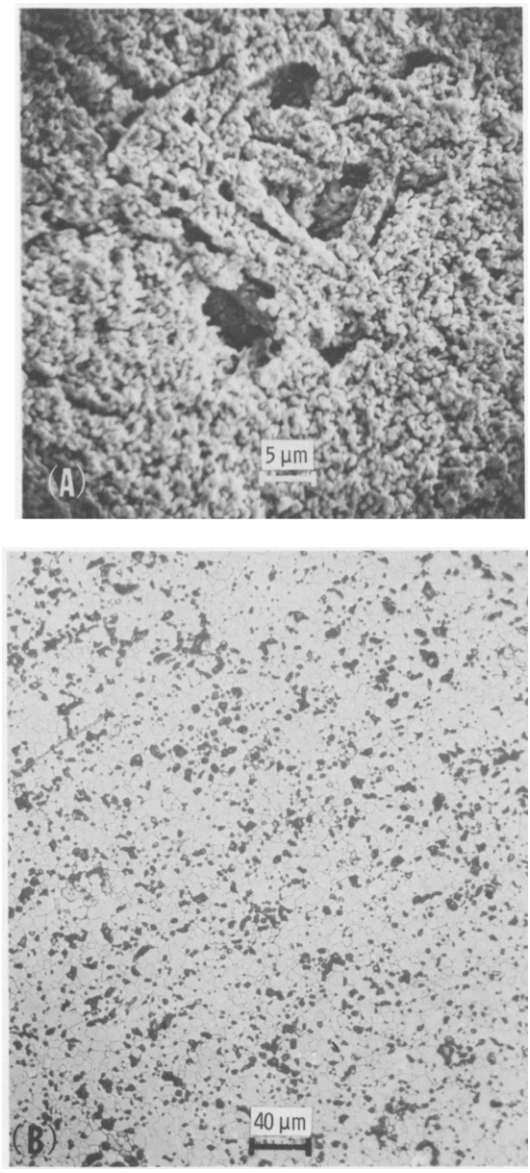

Fig. 2. (A) Scanning electron micrograph of polished section of an Al_2O_3 compact which was lightly pressed (4000 psi) and sintered to about 6% shrinkage at 1270°C. (B) A polished and chemically etched section of the same Al_2O_3 compact sintered at 1700°C for 3 hr (Greskovich, 1972).

properties (Vasilos and Rhodes, 1968; Niesz *et al.*, 1972). A scanning electron micrograph of a polished surface of a Al_2O_3 powder compact lightly pressed and sintered at a low temperature is given in Fig. 2A (Greskovich, 1972). Both dense and porous regions caused by the presence of aggregates in the pressed compact can be observed in the microstructure. The Al_2O_3 aggregates are composed of chains of oblong-shaped particles whose long dimension is about 0.5 μm. After further sintering at higher temperatures, the microstructure (Fig. 2B) formed is again characterized by regions that are more porous than others. The large pores comprising the regions of high porosity appear to result from the bridging of powder aggregates in the pressed compact and are extremely difficult to eliminate by sintering processes. Such pores have large light scattering cross sections and increase the optical attenuation coefficient of polycrystalline, translucent Al_2O_3. These low density inhomogeneities are believed to be deleterious to the production of high surface quality Al_2O_3 substrates for integrated electronic circuits (Sundahl and Berrin, 1972).

There are several changes which can occur during stage 2 of milling. In the ball-milling of fine BeO powder, for example, there is not only a gradual decrease in the average particle size, but also a decrease in the range of particle sizes (Denton *et al.*, 1969). The size distribution becomes narrower with increasing milling time because there is a conversion of larger particles into finer particles with a corresponding decrease in the upper size limit. In addition to actual comminution events, plastic and elastic deformation can arise within individual particles. For example, residual strains of the order of 0.1 % have been measured by X-ray line broadening of milled powders of Al_2O_3 (Lewis and Lindley, 1966; Wheeler and Lewis, 1969). Finally prolonged milling is known to cause phase transformation in lead oxide powder (Senna and Kuno, 1971). In fact, phase changes can also take place when a powder such as calcite is ground with a mortar and pestle (Burns and Bredig, 1956). These observations on structural changes in powders undergoing grinding at room temperature suggest that high pressures and/or elevated temperatures may be responsible for these effects.

4. Contamination Problems

The contamination of powders during the milling operation is a serious problem in many cases. With other things being equal, the amount of contamination increases monotonically with increasing milling time. The sintering or hot pressing behavior of high purity powders can depend markedly on the amount and kind of contamination picked up during milling. During the milling of contaminant-sensitive materials, the wear rates of the grinding media and mill lining are of primary importance. Some control of wear rates, however, can be achieved not only by proper selection of grinding media and

mill lining, but also by optimization of the concentration of particles in suspension and by careful selection of the starting material, if this is possible. For example, alumina linings generally have greater abrasion resistance than porcelain linings, and zirconia media has lower wear rates as compared to some types of alumina grinding media. Wet ball-milling is conveniently carried out at relatively high powder concentrations to minimize mill wear but not too high a concentration to reduce grinding efficiency and dispersion of the various chemical components. Finally, if a mechanically weak or friable starting material is selected for use instead of a strong, coarse material, efficient break up of particle can be expected to occur with little contamination.

Several examples of modern ceramic materials can be cited in which impurity pickup can affect the sintering and grain growth rates, the appearance or disappearance of a solid second phase in the microstructure, and the final properties. Translucent Al_2O_3 bodies made from ball-milled powder sometimes contain "white spots" which can be characterized as porous, coarse-grain centers having diameters as large as several millimeters and which are typically associated with SiO_2 impurity (Francis *et al.*, 1972). It was reasonably well demonstrated that the SiO_2 can originate from abrasion of the Al_2O_3 mill lining and grinding media, which contain high levels of SiO_2. Improved optical transmission can be anticipated by milling with 99 + % Al_2O_3 ball mills to reduce the SiO_2 contamination associated white spots in the sintered product.

A particular example of the importance of impurities is illustrated in the processing of high purity ThO_2-doped Y_2O_3 powder used for the production of single phase, transparent sintered material that has potential applications as infrared windows and domes, laser hosts, lenses, and gem stones. This powder is dry ball-milled in the presence of 1 wt % stearic acid in a rubber-lined mill containing ThO_2-doped Y_2O_3 cylinders as the grinding media (Greskovich and Woods, 1973). A typical microstructure (Fig. 3) formed by sintering compacts made from the milled powder at high temperatures shows that a highly reflecting, solid second phase is located at grain boundaries and grain intersections. A scanning electron microscope equipped with a solid-state X-ray detector revealed that the second-phase particles are sulfur-rich. This finding strongly suggested that the source of sulfur was the rubber lining of the mill. A standard combustion test used to detect sulfur did indeed show that the rubber lining contained about 2 % sulfur. Therefore, it was concluded that during milling rubber particles abrade off of the mill lining, mix into the fine (0.1 μm) powder batch, and subsequently give rise to sulfur-rich inclusions formed in the sintered material. The elimination of sulfur is essential for the fabrication of single-phase Y_2O_3 base ceramics with high optical quality. Single-phase material can be produced by using a sulfur-free mill liner such as polyurethane, for example, or by

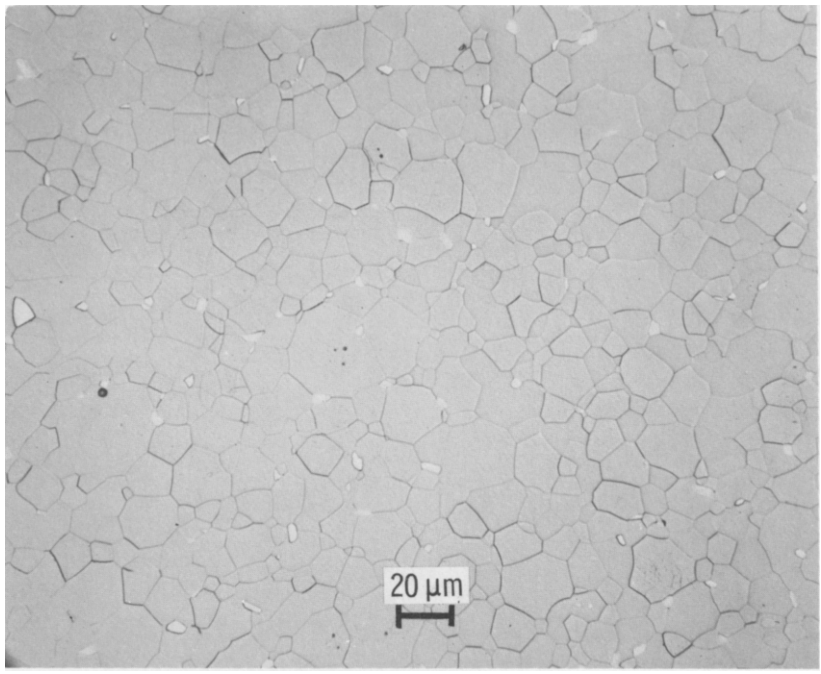

Fig. 3. Solid second-phase particles present in a microstructure of ThO_2-doped Y_2O_3 ceramic sintered at 2000°C for 2 hr.

using high sintering temperatures and long sintering times to remove sulfur from the specimen by diffusional processes.

A final example of the criticality of mill wear is given by the author's experience with the wet ball-milling of $(Y, Gd)_3(Fe, Al)_5O_{12}$ powder used to produce sintered magnetic phase shifters for radar systems. These sintered magnets require a dense, single-phase microstructure so that low magnetic losses will result. The development of single-phase microstructure is difficult because after the mixing and calcination of the various oxide components, the calcined material is wet ground in alcohol for 4 hr in a stainless steel mill to increase the chemical diffusion and sintering rates. Although the milling treatment is very effective, it introduces excess iron into the powder. If the compositional limits are very narrow for the sintered product phase, as the case is here, the excess iron creates an iron-rich second phase in the microstructure. This iron-rich second phase, which appears quite similar to the second phase particles shown in Fig. 3, can be eliminated by starting initally with an iron-deficient powder to compensate for the iron pick-up from the stainless steel balls and mill lining. However, this method is difficult to control

from a practical point of view. Furthermore, the pickup of chromium and nickel from the stainless steel may have adverse effects on some of the magnetic properties. The use of hardened steel balls and stainless steel lifters does appear to help reduce overall contamination during milling. If such a powder requires a milling treatment in a stainless steel ball mill, then excess iron and other soluble impurities may be removed from the processed powder by methods of acid leaching.

B. Fluid Energy (Jet) Milling

Fluid energy mills, more commonly called jet mills, have attracted considerable interest and investigation in both process industry and the laboratory during the last 15 years because this type of milling device has the significant advantage of producing fine powders with control of particle size and distribution while maintaining purity. These mills function by making use of jets to achieve high velocities of particles that fracture by self-attrition upon impact and then pass through a classifying system. Both hard and soft materials can be pulverized down to micron-to-submicron particles in jet mills operated usually with compressed air. Superheated steam, nitrogen, carbon dioxide, water, and slurries are other types of fluids that can be employed. The capacity of these mills can range from grams to thousands of pounds per hour with effective particle size reduction.

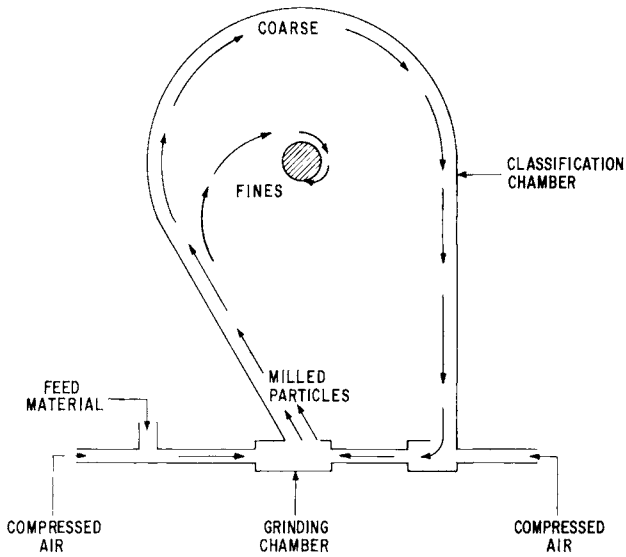

Fig. 4. Schematic representation of the essential features of a Trost-type fluid energy mill.

The relatively simple operation of a Trost jet mill can be discussed here as an example (Rockwell and Gitter, 1964). The essential features of this type of mill are schematically shown in Fig. 4. A vibratory hopper feeds a solid material to be ground into a stream of compressed air that is expanded through two diametrically opposed jets. The solid particles are accelerated to very high (sonic) velocities where particle fracture takes place on impact or collision in a grinding chamber. Mori (1962) demonstrated that particles may undergo impact grinding and, perhaps, surface grinding. It was pointed out that the rate of grinding appears to be proportional to the jet pressure and the cross-sectional area of the jet opening. The maximum stress created by an assumed elastic collision of the particles is proportional to the 2/5 power of the particle velocity and independent of the particle size (Rumpf, 1960). After self-attrition of the feed particles, the product particles travel in rectilinear paths through an upstack channel at reduced velocities and are carried tangentially into a flat, shallow, circular classifying chamber. Particles with a high surface-to-mass ratio spiral through a central exhaust opening leading to a collector system, whereas those with a low ratio continue to travel along the periphery of the classifying chamber and are reaccelerated by the second of the two jets to collide with new feed material on a continuous basis. The synthesis of particles with controlled size and distribution is accomplished by the nature and size of the feed material, feed rate, design and alignment of the jets, design of classifying chamber, and the fluid pressure, temperature, and volume (Rockwell and Gitter, 1964).

The jet-milling method of fine grinding produces a finished powder with essentially no contamination. There are two primary reasons for this achievement. The first is that the jet mill operates with no moving parts. The second is that appropriate liner components such as polyurethane or hard ceramic materials can be selected for use. If a small amount of polyurethane particles is picked up during jet milling, these particles can be burned out of the milled powder by a subsequent oxidizing treatment at elevated temperatures either before or during the sintering of the compacted powder.

Jet-milling can influence the particle size distribution of a powder and, consequently, the structural development of the sintered material made from that powder. The calcined powder used for making magnetic garnets of composition $(Y, Gd)_3(Fe, Al)_5O_{12}$ (Fig. 5A) consists of aggregates as large 400 μm in size and contains a small amount of incompletely reacted secondary phases detected by X-ray diffraction techniques (C. Greskovich, unpublished research, 1973). After passing the calcined powder through the jet mill, aggregate size reduction occurs as is shown in Fig. 5B. Because of the narrow composition limits of the garnet phase with respect to iron content, jet-milling produces powder with aggregate and particle size reduction without iron contamination. In Fig. 6 Coulter Counter particle size analyses plotted in

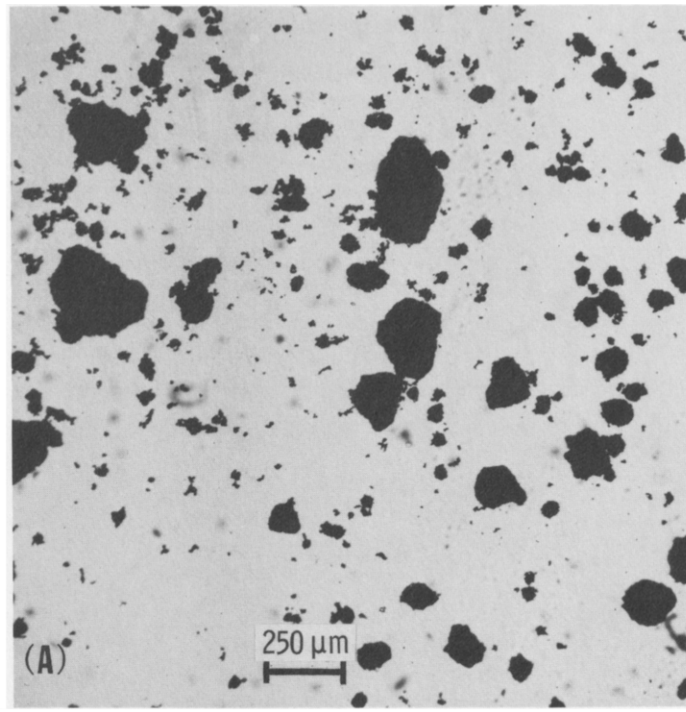
(A)
250 µm

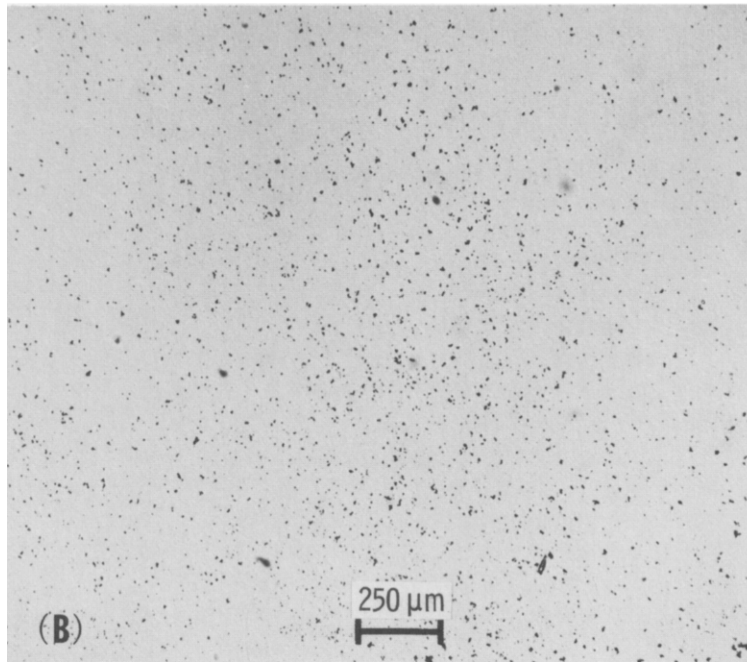
(B)
250 µm

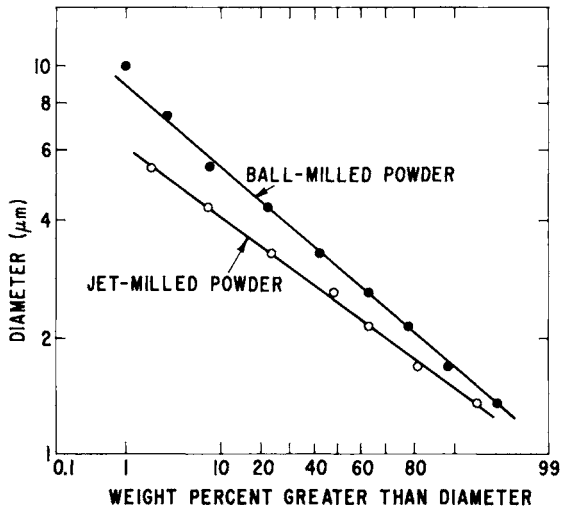

Fig. 6. Particle size distribution of ball-milled and jet-milled powders of $(Y, Gd)_3(Fe, Al)_5O_{12}$.

the form of cumulative percentages versus equivalent spherical diameter, are shown for jet-milled and ball-milled calcined powder. Note that the jet-milled powder has a narrower particle size distribution over the particle size range (1–6 μm) detected with the Coulter Counter. Furthermore, the average particle size of the jet-milled powder is smaller than that of the ball-milled powder because the entire curve for jet-milled powder lies below that for ball-milled powder. The linear behavior of the Coulter Counter curves represented in Fig. 6 indicates that the powder particles follow a log–normal distribution.

The ability to generate a uniform microstructure of sintered $(Y,Gd)_3(Fe, Al)_5O_{12}$ powder produced by the jet-milling approach depends to a large extent on the nature of the calcined powder used as feed material. If the calcined powder is not single-phase, then microstructures derived from jet-milled powder can exhibit a nonuniform distribution of solid second phase as shown in Fig. 7A. (Dark spots in this photomicrograph are closed pores.) This "clumping" of solid second phase is not observed in sintered material made from ball-milled calcined powder. This suggests, therefore, that during the jet-milling of calcined powder containing secondary phases, particle size and density differences between the secondary and the major (garnet) phases promote different rates of particle classification. This effect leads to differences in composition in the jet-milled powder that gives rise to non-

◀ **Fig. 5.** Transmitted-light photomicrograph of (A) aggregates in unmilled calcined powder of $(Y, Gd)_3(Fe, Al)_5O_{12}$ and (B) particles of jet-milled calcined powder.

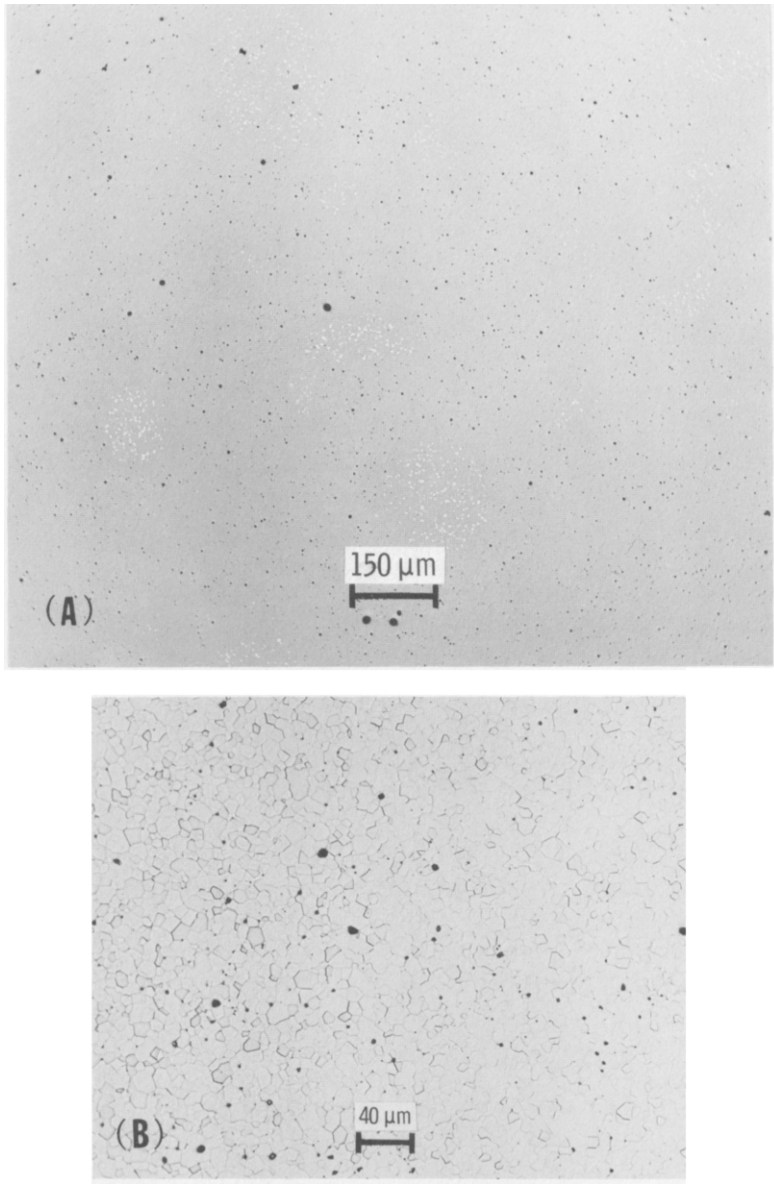

Fig. 7. (A) Nonuniform distribution of second phase particles in sintered $(Y, Gd)_3(Fe, Al)_5O_{12}$ made from jet-milled powder. (B) Uniform, single-phase microstructure synthesized from jet-milled powder, chemically etched.

uniform microstructures in the sintered product. Sintered material can exhibit a uniform single-phase microstructure if virtually single-phase calcined powder is fed into the jet mill. An illustration of this type of microstructure is shown in Fig. 7B, which contains uniformly equiaxed grains, no solid second phase, and a small fraction of closed pores located primarily on grain boundaries.

References

Arendt, R. H. (1973). *J. Appl. Phys.* **44**, 3300–3305.
Benz, M. G., and Martin, D. L. (1972). *J. Appl. Phys.* **43**, 3165–3170.
Bond, F. C. (1952). *Trans. AIME* **193**, 484–494.
Burns, J. H., and Bredig, M. A. (1956). *J. Chem. Phys.* **25**, 1281.
Charles, R. J. (1957). *Trans. AIME* **208**, 80–88
Denton, I. E., Matkin, D. I., and Hill, N. A. (1969). *Proc. Brit. Ceram. Soc.* **12**, 33–39.
Francis, T. L., MacZura, G., Marhanka, J. E., and Parker, H. J. (1972). *Amer. Ceram. Soc., Bull.* **51**, 535–538.
Gilvarry, J. J. (1961). *J. Appl. Phys.* **32**, 391–399.
Greskovich, C. (1972). *Phys. Sintering* **4**, 33–46.
Greskovich, C., and Chernoch, J. P. (1973). *J. Appl. Phys.* **44**, 4599–4606.
Greskovich, C., and Woods, K. N. (1973). *Amer. Ceram. Soc., Bull.* **52**, 473–478.
Griffith, A. A. (1920). *Phil. Trans. Roy. Soc. London, Ser. A* **221**, 163–198.
Haertling, G. H. (1970). *Amer. Ceram. Soc., Bull.* **49**, 564–567.
Harwood, N. G., MacDonald, G. I., and Middel, V. J. (1965). *Proc. Brit. Ceram. Soc.* **3**, 49–66.
Holmes, J. A. (1957). *Trans. Inst. Chem. Eng.* **35**, 125–156.
Irani, R. R., and Callis, C. F. (1963). "Particle Size: Measurement, Interpretation, and Application." Wiley, New York.
Kick, F. (1885). "Das Gesetz der proportionalen Widerstande und seine Anwendung." Leipzig.
Klinger, E. A., Dawihl, W., and Dorre, E. (1971). U.S. Patent 27,083.
Lewis, D., and Lindley, M. W. (1966). *J. Amer. Ceram. Soc.* **49**, 49–50.
Matkin, D. I. (1973). *Trans. Brit. Ceram. Soc.* **72**, 57–61.
Meloy, T. P. (1963). *Trans. AIME* **226**, 447–448.
Meloy, T. P. (1970). *In* "Fine Grain Ceramics" (J. J. Burke, N. L. Reed, and V. Weiss, eds.), pp. 17–37. Syracuse Univ. Press, Syracuse, New York.
Mori, Y. (1962). "Symposium Zerkleinern," pp. 515–530. Verlag Chemie, Weinheim.
Niez, D. E., Bennett, R. B., and Snyder, M. J. (1972). *Amer. Ceram. Soc., Bull.* **51**, 677–680.
Rockwell, P. M., and Gitter, A. J. (1964). *66th Ann. Meet. Amer. Ceram. Soc.*
Rose, H. E. (1971). *Euro. Symp. Size Reduct., 3rd*, pp. 57–87.
Rosin, P., and Rammler, E. (1933). *J. Inst. Fuel* **7**, 29–35.
Rumpf, H. (1960). *Chem.-Ing.-Tech.* **32**, 129–135.
Schuhmann, R. (1940). *AIME, Tech. Publ.* **1189**.
Schuhmann, R. (1960). *Trans. AIME* **217**, 22–25.
Senna, M., and Kuno, H. (1971). *J. Amer. Ceram. Soc.* **54**, 259–262.
Sundahl, R. C., and Berrin, L. (1972). *Nat. Bur. Stand. (U.S.), Spec. Publ.* **348**, 271–291.
Vasilos, T., and Rhodes, W. (1968). *In* "Fine Grain Ceramics" (J. J. Burke, N. L. Reed, and V. Weiss, eds.), pp. 137–172. Syracuse Univ. Press, Syracuse, New York.
von Rittinger, P. R. (1867). "Lehrbuch der Aufbereitungskunde." Ernst & Korn, Berlin.
Wheeler, E. J., and Lewis, D. (1969). *J. Mater. Sci.* **4**, 681–691.
Wolkodoff, V. E., and Weaver, R. E. (1968). U.S. Patent 3,377,176.

Characterization of Ceramic Powders

R. NATHAN KATZ

Army Materials and Mechanics Research Center
Watertown, Massachusetts

I. Introduction

Virtually all ceramics, including those formed by melt processes, depend upon particulate precursors. The dependence of the end product's properties on the nature of the precursor powder has been amply demonstrated for the mechanical, optical, and electrical properties of ceramics (Arendt *et al.*, 1974). Therefore, in order to maintain or modify the desired properties of a given ceramic material, it is necessary to have as detailed as possible a characterization of the starting powders.

This chapter will deal with the methods used in the characterization of ceramic powders. It will attempt to give a comprehensive, but not exhaustive,

survey of characterization techniques in the areas of greatest practical importance. Greater detail can be obtained from several recent reviews of characterization in general (National Materials Advisory Board, 1967), and the characterization of ceramic and ultrafine powders in particular (Burke *et al.*, 1970; Stover, 1967; Hench and Gould, 1971; Veale, 1972). An excellent example of the application of many characterization techniques discussed below to the evaluation of alumina powders has recently appeared in the literature (Berrin *et al.*, 1972; Johnson *et al.*, 1972). One aspect of characterization upon which the reliability of all subsequent measurements depend (namely, sampling) will not be treated in this chapter.

II. Chemical and Crystallographic Characterization

Whether one is characterizing a batch of powder as a first step in a research program, or as a routine quality control step in production, the first question to be answered is: "Is this powder the material it is purported to be?" Given a batch of powder, we must determine the following.

a. What are the composition, impurities (cation and anion), and possible deviation from stoichiometry?
b. If made by solid state reaction, is it fully reacted? Are there unreacted phases? (i.e., in spinel prepared from MgO and Al_2O_3 the chemistry, impurity content, and stoichiometry could indicate no problem, but the powders may never have reacted to form the spinel).
c. Does it contain spurious phases introduced by milling, attrition, or sheer happenstance? If so, how much?

This portion of the chapter will introduce some of the standard methods used to identify the elemental and crystallographic character of the powder.

A. Chemical Characterization

1. Wet Chemistry

Wet chemistry is one of the standard methods of analytical chemistry. However, it is less utilized by ceramists, as compared to other methods of chemical analysis primarily because of the basic inertness and refractoriness of ceramic compounds. These properties make it extremely difficult to put ceramic powders into solution, which is necessary for wet analysis. Ceramics must generally be fused with alkaline or acidic compounds then dissolved in acid prior to wet analysis. In such cases, the preparation and analysis of the compounds and acids utilized can become more important (and presumably

more time consuming) than the analysis of the original samples, especially in the parts per million range, as has been pointed out by Bradley *et al.* (1972). A recent example of wet analysis is the photometric method devised for the determination of iron, titanium, aluminum, silicon, and nickel in boron carbide by Czyrklis and Ferraro (1971). They fused boron carbide powder in sodium carbonate and dissolved the melt in diluted hydrochloric acid for analysis. On a weight percent basis their results were accurate to the first decimal place for iron and titanium and to the second decimal place for the other impurities. A thorough search of *Chemical Abstracts* will usually uncover methods for the more common ceramic materials.

2. X-Ray Fluorescence Spectrometry

This technique is simpler and faster than wet chemistry for the analysis of both major and trace elements in ceramic powders, and since it is nondestructive it leaves the powder available for further characterization by other techniques. Experimental details of the method are given in several standard texts (Liebhafsky *et al.*, 1960; Cullity, 1956). Basically, one excites the sample to be examined with a primary high energy beam of X rays which causes it to emit secondary or fluorescent radiation. Appropriate detection apparatus, records the characteristic X-ray lines as a function of the Bragg angle. From Bragg's Law

$$n\lambda = 2d \sin \theta \tag{1}$$

The wavelength λ for each line in the fluorescent spectra can be calculated, since for a given spectrometer both the d spacing of the analyzing crystal, and the Bragg angle θ are known. Wavelength, atomic number, and spectral series (K, L, M, N lines) can be related by Mosely's law (Barrett, 1952); thus, one can identify each observed wavelength with a particular element. The technique will, in practice, detect all elements heavier than sodium (wavelengths less than 10 Å) (National Materials Advisory Board 1967). The lower level sensitivity of this method is about 20–200 parts per million (ppm) dependent on atomic number and specimen nature (particle size and interelement interactions). Given proper calibration standards, the technique can be quite accurate and extremely fast; therefore, it is used in industrial quality control in the cement, clay, and glass industries (Stover, 1967).

3. Emission Spectroscopy

Since ceramic materials are generally nonconductors and insoluble, dc arc excitation is most commonly utilized for cation analysis (Bradley *et al.*, 1972). The spectral lines of the light emitted as the sample is vaporized in the arc are separated by means of prisms or optical gratings and recorded on a

photographic plate for analysis, relative to a known standard for calibration. For many cations this technique can routinely detect concentrations in the 1 to 10 ppm range.

4. Mass Spectroscopy

This technique can detect all elements in a sample with a sensitivity well below 1 ppm (National Materials Advisory Board, 1967). It has been utilized by Leipold and co-workers (Leipold and Blosser, 1970) to detect anion impurities such as H, OH, C, N, F, P, S, and Cl with reliable results at less than the 10 ppm level. To utilize this technique on ceramics, however, special specimen preparation is required. The powders, if nonconducting, must be mixed with a conductor to provide a spark source, and bakeout of the specimen in the mass spectrometer source at modest temperatures is often required to reduce surface contamination.

5. Neutron Activation Analysis

Neutron activation analysis consists of exposing the sample to an intense neutron source for various times during which the elements to be measured are converted to radioactive isotopes. These radioactive isotopes can be detected by suitable apparatus and the amount and type of isotopes can be related back to the amount and type of element in the sample. Although only a limited number of elements may be measured at a time, the technique is nondestructive.

This technique is particularly well suited for anion analysis and has recently been used by Priest *et al.* (1973) to determine O_2 at the level of 0.30 % in silicon nitride. In this case, oxygen is converted into a nitrogen isotope, ^{16}N, which is radioactive and can be measured. One source of error or limitation of the technique is that sometimes the impurity to be detected and the host substance will both produce the same isotope. This, for example, would happen if one desired to measure trace amounts of oxygen in calcium fluoride by the activation technique. Both the oxygen impurity and the host fluoride would yield the radioactive isotope, ^{16}N, and an accurate determination of oxygen would be very difficult or impossible.

6. Nondispersive X-Ray Analysis

Nondispersive X-ray analysis (NDX) has recently emerged as a powerful technique for obtaining elemental analysis (Frankel and Woldseth, 1973). When coupled with a scanning electron microscope one can obtain analysis from particles approximately 1 μm in diameter or larger quite easily. Thus, one can simultaneously obtain information about the size, size distribution, shape, phase distribution, and chemical analysis of discrete particles in a powder. Properly used, the results of the NDX technique compare favorably

with those from atomic absorption techniques. The principal limitations are (1) lack of/or poor detection of light elements; (2) limited resolving power (for example, in NDX analysis of silicon nitride the Al peak is frequently observed as a perturbation on the Si peak); and (3) relatively long counting times.

B. Crystallographic Characterization

1. X-Ray Diffraction

Since most of the compounds which ceramists routinely work with have crystal structures that have already been determined by crystallographers, this section assumes that all of the phases in the powder under investigation have been indexed in the Powder Diffraction File (Joint Committee on Powder Diffraction Standards, 1973). If one encounters a phase or phases not identifiable by the techniques described below or in standard references (Cullity, 1956; Barrett and Massalski, 1966), the investigator should seek the advice of a trained crystallographer rather than try to make his own crystal structure determination.

The identification of the crystalline phases in a powder depends upon the knowledge of only two types of information: (a) the interplanar distances of the diffracting planes (h, k, l) known as the d spacings [see Eq. (1)], and (b) the relative intensity for each measured d spacing. There are two methods of obtaining this information: X-ray camera techniques, principally the Debye–Scherrer method, which records a series of lines of varying intensity and position of a strip of film; and diffractometer techniques, which record a series of diffraction peaks on a recorder strip chart. Both techniques depend upon Bragg's law [Eq. (1)], which relates the wavelength of the incident X rays (which is known) and the angle of incidence between the diffracting planes, and the incident beam of X rays (which is measured from the position of lines on the film or peaks on the diffractometer chart), to the spacing of the diffracting planes, d (h, k, l) (which is the unknown in the relationship). For each d spacing measured, one assigns a relative intensity, using a photodensitometer for the film or the area under the peak on the diffractometer trace. Then with a list of d spacings and relative intensities, one takes the eight most intense reflections (d values) in order of their intensity and consults the powder diffraction file index, which lists crystalline materials with respect to the eight most intense reflections. The investigator may obtain one or several possible compounds from this index. He then uses the index to identify the catalog number for the complete diffraction pattern for the compounds and uses all of the d spacing and intensity information to make a final determination. This system is used in reverse as often as in the way described above. For example, one usually knows that he is working with, for example, MgO

powder; therefore, he goes to the file and obtains the diffraction pattern for MgO and then compares this with the pattern he has obtained. In this manner spurious phases or major deviations from stoichiometry (or even the presence of impurities and crystal lattice defects) can be elucidated by the presence of new peaks or by shifts in *d* spacing.

In practice the diffraction patterns of several phases must be separated, for example, Gazza and Messier (1972) have recently used various techniques

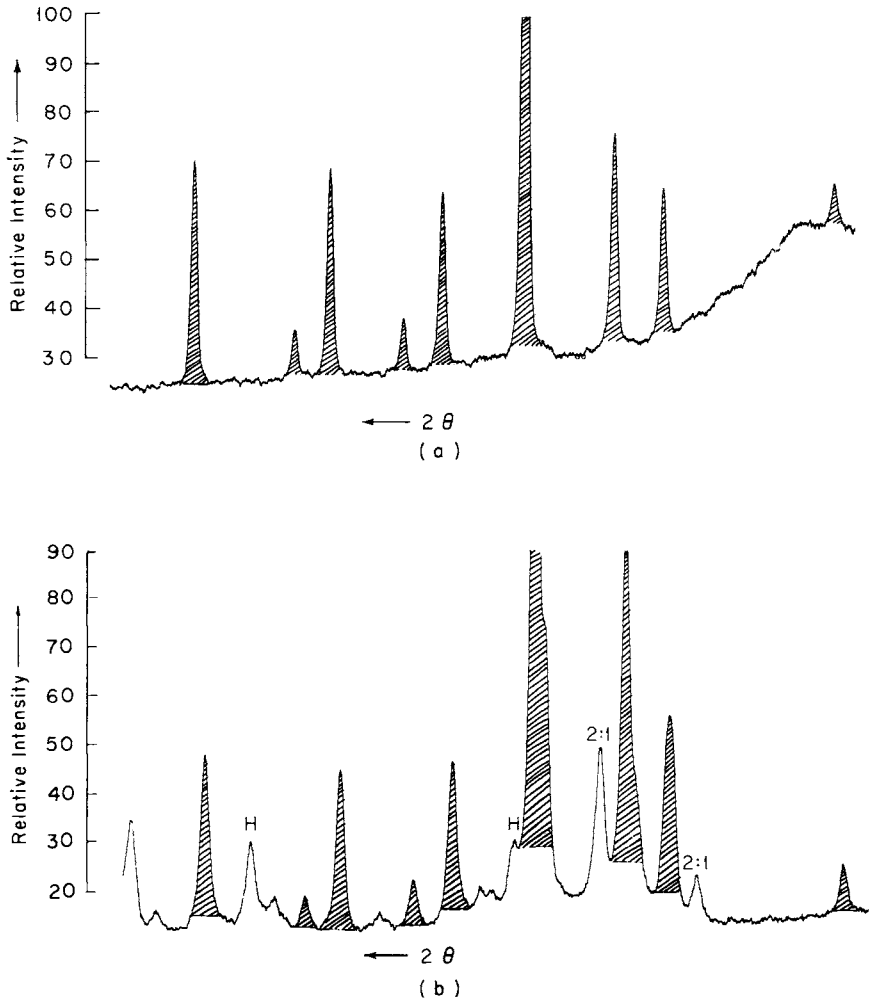

Fig. 1. X-Ray diffraction patterns of YAG. (a) Pure YAG. (b) YAG containing extraneous phases.

involving the co-precipitation of $Y_3Al_5O_{12}$ (YAG) from aqueous solution. The diffraction pattern of pure YAG powder made by one co-precipitation process is shown in Fig. 1a. Figure 1b resulted from a different co-precipitation technique, in addition to YAG, $YAlO_3$(H), and $Y_4Al_2O_9$ (2:1) were observed. Confronted with the powder pattern in Fig. 1b, and no other information, the difficulty of determining which phases were present and correctly identifying them is clear. Thankfully, by coupling chemical analysis, phase diagram data, or processing information with X-ray diffraction one usually has some idea of where to start the hunt.

The lack of a diffraction pattern or broad low angle scattering peaks indicates the presence of amorphous (glassy) phases. Unfortunately, unless one is prepared to undertake a lengthy research study, little other information is readily obtainalbe for characterization purposes from such patterns. Small percentages of glass in mixed crystalline and glass materials cannot generally be detected.

X-Ray diffraction, like all X-ray characterization techniques, is nondestructive, although in glass or ionic crystals, high intensity X rays may induce electronic defects known as color centers, which can affect electrical and optical properties.

2. Electron Diffraction

When a beam of high energy electrons are elastically scattered by the positive potential field of the atomic nucleus, diffraction results. The coherent, elastically scattered electrons diffracted from a representative volume of material produce its characteristic diffraction pattern analogous to an X-ray pattern. Following Tufts (1971) one can derive an equation to relate the d spacing to the constants of the electron microscope from Bragg's law

$$d_{hkl} = \lambda L/r \tag{2}$$

where L = specimen to film distance, λ = electron wavelength, r = radius of the diffraction ring (or spot) pattern. λL is called the diffraction constant of the electron microscope and each microscope must be calibrated to determine λL for each lens setting and electron energy used (Hirsh *et al.*, 1965). This is usually provided as a set of curves with the microscope.

Using such a relationship, the pattern obtained from a single unknown impurity particle of approximately 0.1 μm diameter in pyrolytic graphite was indexed by the author. The pattern (d spacings checked against the Powder Diffraction File) indicated that the particle was either rhombohedral boron or B_4C. By virtue of having had processing information and thermodynamic data available, it was concluded the pattern resulted from B_4C (Katz and Gazzara, 1968). This indicates again the interrelationship between character-

ization techniques and other information often required to come to a firm conclusion. Usually data obtained from only one method of characterization are insufficient to produce a result in which the investigator can have confidence.

3. Optical Microscopy

Optical microscopy, the oldest of microscopic techniques, is still one of the most valuable (Frechette, 1971; Hartshorne and Stuart, 1970; Delly, 1973). Light microscopes are limited to useful magnifications of a maximum of 1000–3000 ×, thus the optical microscope can only be used to obtain information on particles larger than about 0.5 μm. Using transmitted light, one can measure the index of refraction n of a transparent particle by immersing it in liquids of known n. When the particle disappears its n is determined. This one measurement can often identify a mineral (ceramic) phase. If a powder that consists of fairly coarse particles has several minor phases present, X-ray identification may be facilitated by physically separating the phases under the microscope with a wet toothpick or other "advanced" analytical tool. It is this ability for the observer to be in a tangible rather than merely an instrumental relationship to the material being studied which makes optical microscopy indispensable. Using the transmitted light, polarizing microscope, a trained mineralogist can often determine the crystal system to which a particle belongs. To do this he will utilize light extinction behavior, retardation, birefringence, idiomorphic crystal forms which the particles may show, and observed cleavage behavior. Such information is often extremely helpful in subsequent X-ray or electron diffraction studies. In any powder characterization, one of the first procedures should be to examine the powder optically.

III. Characterization of Powder Morphology

After the chemical and crystallographic identity of a powder, the next most important information concerning its character is morphology. For purposes of this chapter, morphology means size, size distribution, shape, surface area, and other parameters that may help to define how a powder will flow, pack, react, and yield the microstructure of the finished ceramic body. Since the driving force for converting a mass of discrete powder particles into a solid body is the reduction of surface energy, it is obvious that the shape and surface area of the particles define the thermodynamics of densification. However, since interparticle bonding and pore and grain boundary migration, which determine final microstructure and properties, depend upon mass transport

at particle surfaces, the morphology of the particles will also determine the kinetics of densification. As will be seen below, the measurement of the morphological characteristics of particles and powders is generally carried out by indirect methods based on assumptions that may often yield quite different results on the same powders (Johnson *et al.*, 1972). These apparent inconsistencies are due to the underlying assumptions associated with each technique. Therefore, this section will tend to emphasize the assumptions implicit in the various techniques rather than how they are actually carried out. The latter information is readily available (see Reference list at the end of the chapter and manufacturers' instruction manuals). The crystallite size distribution within a powder may vary considerably from the particle size distribution of the powder and may change dramatically during powder processing. This subject will not be covered here but has been recently reviewed by Oel (1969).

The various techniques for determining particle size and size distribution yield useful results only over certain size ranges, although many techniques overlap in size range coverage. Table I presents the principal techniques to be discussed and their size range coverage. Also presented is the physical basis for the technique, which most often measures one characteristic and then deduces a size parameter from the changes in this characteristic. Determination of shape is generally the result of direct methods of observation.

TABLE I

RANGE OF COMMON PARTICLE SIZING TECHNIQUES

Technique	Size range	Physical basis of technique	Reference
Screening and sieving technique	> 25 to < 38 μm (-400 mesh) (Special sieves are now available that go down to 0.44 μm)	Ability of smallest particle cross section to pass through a square opening	Gaudin (1939) ASTM (1969)
Sedimentation technique	~ 100 to > 0.05 μm	Equivalent Stokes diameter	Lankard and Niesz (1971)
Electrolyte conductivity change (Coulter Counter)	> 0.8 μm	Volume of electrolyte displaced	Veale (1972)
Microscopy			
Optical	0.5 to several microns	Projected area observed	Gaudin (1939)
Scanning electron (SEM)	~ 0.02 to several microns	Projected area observed	—
Electron microscope	0.001 to 5 μm	Projected area observed	Lankard and Niesz (1971)

A. Screening and Sieving Techniques

Screening is an old, standard technique for obtaining particle size separations and measuring particle size distributions. Since in screening we measure the ability of a particle to pass through a square opening of fixed size in a wire mesh, screening gives an approximate measure of the minimum projected diagonal of the particle. The minimum projected diagonal of the particle is determined approximately by the two smallest dimensions of the parallelepiped enclosing the particle. Within reasonable limits the height of the particle is not involved in the sizing of the particle. It should now be apparent why different techniques of particle size measurement can give very different results. A spherical particle and a platelet can have the same minimum projected diagonal and yet have very different volumes and surface areas, but they will both yield the same mesh value.

Although automatic screening equipment (for example, the RO-TAP machine) is available, screening -400 mesh or smaller powders, wet or dry, can be extremely tedious.

Screen analysis data may be presented as either cumulative percent versus size or percent in an individual size distribution versus size; in both cases the axis may be linear or logarithmic. More details are available in the standard references (Gaudin, 1939; Orr and Dallavalle, 1959; American Society for Testing and Materials, 1969; Lankard and Niesz, 1971) and in literature available from sieve manufacturers.

B. Sedimentation Techniques

The sedimentation technique is based upon the Stokes equation for the rate of free fall of a sphere in a fluid under laminar flow conditions. Since almost no powder is truly spherical, what is actually derived is an equivalent Stokes diameter of a sphere having the same settling characteristics as the particles being measured. Obviously, the less the particle resembles a sphere, the less the "equivalent Stokes diameter" relates to the true shape or size of the powder.

The Stokes equation is

$$d = \left[\frac{18\eta v}{(\rho - \rho_f)g}\right]^{1/2} \tag{3}$$

where d = Stokes diameter, v = rate of fall, ρ = particle density, ρ_f = fluid density, η = fluid viscosity, and g = gravitational constant. If the particles are small enough (submicron), they may not settle in accordance with the above equation due to convection, Brownian motion, and lack of true laminar

flow. In this size range, centrifugal settling is used and the Stokes equation becomes

$$d = \left[\frac{18\eta \ln x/x_0}{(\rho - \rho_f) w^2 t}\right]^{1/2} \tag{4}$$

where t = time, w = angular velocity, x = distance of particle diameter d from the axis of rotation, x_0 = radius of rotation of the particle at time = 0, and all other symbols as defined above.

Ultracentrifuging coupled with advanced optical techniques permits measurement of particles as small as 25μm equivalent Stokes diameter (Veale, 1971). New methods coupling sedimentation with the transmission of a finely collimated X-ray beam through the suspension can automatically yield cumulative distributions of equivalent Stokes diameters in the 50 to 0.2 μm range (Oliver *et al.*, 1970/1971).

If the fluid in the sedimentation technique is changed from water to air, the technique is commonly referred to as air classification. The same equations hold in either medium, but of course settling velocities are much greater in air than water (Norton, 1952).

C. Electrolytic Conductivity

This technique is more familiarly referred to by the commercial name of one of the instruments utilizing it—namely, the Coulter Counter method. In this method, particles well dispersed in an electrolyte, pass through a narrow orifice which has electrodes on either side. As a particle passes through, it changes the resistance of the electrolyte. This change in resistance is converted into a change in voltage. By setting various threshold voltages and changing orifice size, one can obtain the particle size distribution. It is important to note that unless the dispersion of the powder in the electrolyte is very high, the assumption of one particle in the orifice at a time is not valid. It should not be surprising that because of this assumption, the method generally errs in the direction of undercounting fine particles and overcounting large ones. This method measures particle volume; thus it may not correspond to sieve analysis, for example. Several recent reviews and papers based on this method are available (Allen, 1967; Wanless, 1968).

D. Microscopic Techniques

The various microscopic techniques such as optical, scanning electron, and electron microscopes can all provide information as to the particle size and size distributions, but more importantly they yield the most direct

information of the characteristic referred to as particle shape. The shape of each particle in a powder will be somewhat different than the shape of its companion particles. However, in a given powder, most particles will tend to be essentially spherical, dendritic, fragmented, or some other shape. The difficulties in quantitizing shape, as well as a variety of shape descriptions, have been discussed by Hausner (1967).

Particle size distributions for optical and electron microscope images are obtained using standard analytic procedures of quantitative metallography to obtain the distribution corrected for the random projected area of particles shown on photos or TV display images. Several recent articles (Crowl, 1967; Collins, 1967; Fisher, 1967) discuss the experimental procedures and sources of error in several of these techniques.

E. Surface Area

The surface area of a powder is important both as a characteristic of the powder size and as an indication of the activity of a powder in reactions such as encountered in sintering. Generally, surface area measurements are preformed by gas adsorbtion following the method of Brunauer *et al.* (1938) (the BET method), although other methods such as liquid-phase sorption, fluid flow, and various thermal methods have been used (Orr and Dallavalle, 1959). Gas adsorption techniques determine the volume of gas necessary to coat the powder with a monolayer of adsorbed gas, and from the molecular diameter the surface area of the powder is calculated. The advantage of the BET method is that multilayer rather than monolayer adsorption is considered and thus it yields a more realistic value.

The surface measured will include fissures and pores that are connected to the surface; thus, when combined with other methods of particle size determination, and assuming a given particle geometry, information on the amount of surface-connected porosity in the powder can be inferred. Usually the gas used is nitrogen, but krypton or other gases may also be used. Since the explanation of the use of the BET isotherm is rather lengthy, the reader is referred to Orr and Dallavalle (1959) or Veale (1972).

F. Other Methods

Other methods are available for particle sizing although much less frequently used than the above. They include electrostatic precipitation, sonic analysis (for measuring airborne particulates), diffusion battery (air- or gas-borne particles with an upper size limit of 0.2 μm), adhesion, and light scattering (Orr and Dallavalle, 1959). X-Ray diffraction broadening often measures the polycrystalline nature of the particles rather than the particle

size and thus while commonly encountered as a characterization technique, this method should always be checked by some other measurement.

IV. Bulk Properties

A. Powder Flow and Packing

Since powder consolidation processes such as sintering depend upon the way a powder flows and packs to fill a die, some method of assessing the rheological behavior of powders is necessary. Several of these have been discussed by Stover (1967) and Berrin *et al.* (1972). Some of the more widely used parameters are the Hausner ratio, which is generally thought to relate to the frictional forces to move a mass of powder, and the compaction ratio, which gives a measure of how well a powder can be densified by cold pressing. The Hausner ratio is the ratio of tap density to apparent density, where the apparent density is just the powder bulk density, and the tap density is the powder density after the powder container is tapped a given number of times. The compaction ratio is the ratio of pressed density to apparent density, where the pressed density is determined at the compaction pressure of interest in the process.

B. Thermal Response of Powders

The thermal response of powders can be utilized to measure powder activity, adsorbed species on the powder, phase transformation or volatilization tendencies of the powder. Generally, differential thermal analysis (DTA) or thermogravimetric analysis (TGA) is used. Stover (1967) has reviewed the use of these techniques in powder characterization. One of the prime uses of these techniques is to monitor the calcination of powders prior to sintering to assure that various batches of powder will exhibit similar sintering kinetics. Messier and Gazza (1972) have recently utilized the TGA method to study the thermal decomposition of complex nitrates used as precursers in the formation of $Y_3Al_5O_{12}$ (YAG) and $MgAl_2O_4$ (spinel) powders. Stoichiometry was dependent upon proper thermal control of the nitrate decomposition process.

C. Agglomerates

At various stages in powder production and handling, but most usually during calcining, agglomerates will form in the powder. An agglomerate is an aggregation of smaller particles held together by relatively weak forces.

Although one usually takes care to remove agglomerates (by screening, classification, milling, etc.) from the powder during various stages of treatment, they may reform during storage (for even brief times) with generally deleterious effects on the density and strength of the ceramic body made from the powder. For high performance ceramic manufacture, it is important to eliminate all agglomerates, since they are often found to be the source of fracture initiation in the densified body. Where some agglomerates must be tolerated in the powder, the compaction behavior of the powder has been shown to be a function of the agglomerate strength (Lankard and Niesz, 1971).

V. Summary

The characterization of ceramic powders can be an extremely time-consuming and expensive task. It is therefore important to limit the characterization program to those features of the powder that will result in a reproducible end product. Since "a reproducible product" will depend on the perspective of the user as related to his requirements, what will be an adequate characterization program will vary greatly between one user and another. However, some generalizations can be made. (1) The synthesizer or manufacturer of a powder will probably need to do more characterization on the powder (to maintain its total quality) than will most users of the powder. (2) Even when minimal characterization is required, the reliance upon one technique for characterizing a given feature can lead to trouble. Therefore, several methods should be employed to cross-check results. (3) When one is reporting on a powder, the minimum information to be provided should be (a) chemistry and technique utilized, (b) phase analysis and how obtained, and (c) average particle size, and size distribution and how obtained. The fact that such information is often lacking in the literature is an indication of the critical need for an increased awareness of the importance of powder characterization.

References

Allen, T. (1967). *In* "Particle Size Analysis," pp. 110–127. *Soc. Anal. Chem.*, London.

American Society for Testing and Materials. (1969). "Manual of Test Sieving Methods," STP447. *Amer. Soc. Test Mater.*, Philadelphia, Pennsylvania.

Arendt, R. H., Charles, R. J., Greskovich, C., and Palm, J. A. (1974). "Characterization of Materials in Research—Ceramics and Polymers." Syracuse Univ. Press., Syracuse, New York.

Barrett, C. S. (1952). "Structure of Metals." McGraw-Hill, New York.

Barrett, C. S., and Massalski, T. B. (1966). "Structure of Metals." McGraw-Hill, New York.
Berrin, L., Johnson, D. W., and Nitti, D. J. (1972). *Ceram. Bull.* **51**, 840–844.
Bradley, N. J., Cooper, B. S., and Hobbs, D. J. (1972). "Modern Oxide Materials." Academic Press, New York.
Brunauer, S., Emmett, P. H., and Teller, E. (1938). *J. Amer. Chem. Soc.* **60**, 309–319.
Burke, J. J., Reed, N. L., and Weiss, V., eds. (1970). "Ultrafine-Grained Ceramics." Syracuse Univ. Press, Syracuse, New York.
Collins, G. F. (1967). *In* "Particle Size Analysis," pp. 65–76. *Soc. Anal. Chem.*, London.
Crowl, V. T. (1967). *In* "Particle Size Analysis," pp. 36–44. *Soc. Anal. Chem.*, London.
Cullity, B. D. (1956). "Elements of X-Ray Diffraction." Addison-Wesley, Reading, Massachusetts.
Czyrklis, W. R., and Ferraro, T. A. (1971). AMMRC PTR 71-1 AD No. 731 477.
Delly, J. G. (1973). *Ind. Res.*, 44–46.
Fisher, C. (1967). *In* "Particle Size Analysis," pp. 77–94. *Soc. Anal. Chem.*, London.
Frankel, R., and Woldseth, R. (1973). *Res./Develop.* 38–42.
Frechette, V. D. (1971). *In* "Characterization of Ceramics," pp. 257–271. Dekker, New York.
Gaudin, M. A. (1939). "Principles of Mineral Dressing." McGraw-Hill, New York.
Gazza, G. and Messier, D. R. (1972). U.S. Patent 3,681,011.
Hartshorne, N. H., and Stuart, A. (1970). "Crystals and the Polarizing Microscope." Amer. Elsevier, New York.
Hausner, H. H. (1967). *In* "Particle Size Analysis," pp. 20–28. *Soc. Anal. Chem.*, London.
Hench, L. L., and Gould, R. W. (1971). "Characterization of Ceramics." Dekker, New York.
Hirsh, P. B., Howie, A., Nicholson, R. B., Pashley, D. W., and Whalen, M. J. (1965). Plenum, New York.
Johnson, W. D., Nitti, D. J., and Berrin, L. (1972). *Ceram. Bull.* **51**, 896–899.
Joint Committee on Powder Diffraction Standards. (1973). "Powder Diffraction File." Swarthmore, Pennsylvania.
Katz, R. N., and Gazzara, C. P. (1968). *J. Mater. Sci.* **3**, 61–69.
Lankard, D. R., and Niesz, D. E. (1971). *In* "Characterization of Ceramics," pp. 349–370. Dekker, New York.
Leipold, M. H., and Blosser, E. R. (1970). *In* "Ultrafine-Grained Ceramics," (J. J. Burke, N. L. Reed, and V. Weiss, eds.), pp. 99–107. Syracuse Univ. Press, Syracuse, New York.
Liebhafsky, H. A., Pfeiffer, H. G., and Zemany, P. D. (1960). "X-Ray Absorbtion and Emission in Analytical Chemistry." Wiley, New York.
Messier, D. R., and Gazza, G. E. (1972). *Ceram. Bull.* **51**, 692–697.
National Materials Advisory Board. (1967). "Characterization of Materials," NMAB Report MAB 229-M. *Nat. Acad. Sci.—Nat. Acad. Eng.*, Washington, D.C.
Norton, F. N. (1952). "Elements of Ceramics." Addison-Wesley, Reading, Massachusetts.
Oel, H. J. (1969). *Mater. Sci. Res.* **4**, 249–272.
Oliver, J. P., Hickin, G. K., and Orr, C. (1970/1971). *Powder Technol.* **4**, 257–263.
Orr, C., Jr., and Dallavalle, J. M. (1959). "Fine Particle Measurement." Macmillian, New York.
Priest, H. F., Burns, F. C., Priest, G. L., and Skarr, E. C. (1973). *J. Amer. Ceram. Soc.* **7**, 395.
Stover, E. R. (1967). "Critical Survey of Characterization of Particulate Ceramic Raw Materials," AFML TR67-56. Air Force Mater. Lab.
Tufts, C. F. (1971). *In* "Characterization of Ceramics," pp. 177–218. Dekker, New York.
Veale, C. R. (1972). "Fine Powders—Preparation, Properties and Uses." Wiley, New York.
Wanless, L. (1968). *Trans. Brit. Ceram. Soc.* **67**, 29–48.

Effects of Powder Characteristics

Y. S. KIM

Bell Telephone Laboratories, Incorporated
Allentown, Pennsylvania

I. Introduction

During the last two decades significant strides have been made by modern science and technology in developing new and useful electronic materials (Kingery, 1960; Bratschun *et al.*, 1971; Buessem, 1965; Whittemore, 1969). These materials are of tremendous economical and technical importance today. Electronic Industries Associates (1973) has forecasted that the total sales of electronics will gross up to $\$33 \times 10^9$ for 1973. *Ceramic Age* (1973) estimates that electronic ceramic sales will reach $\$1.4 \times 10^9$ in 1973. It is clear that the use of ceramics in electronics is already significant and will expand in the future since the properties of ceramics will be essential for many applications.

Examples of the types of electronic ceramics that assume very important roles in today's device technologies are ferrites used in switching (Greifer,

1969), transformer (Snelling, 1969), and microwave (Lax, 1962; Thourel, 1964) applications; hard ferrites (Gordon, 1956; Jonker *et al.*, 1956–1957); ferroelectric materials (Jaffe *et al.*, 1971) with piezoelectric properties, high dielectric constants (Roup, 1958), and high Q's; Yamaguchi and Takahashi, 1970); and ceramic substrates (Fehlner and Halaby, 1967; Heil, 1967), mainly alumina and berylia for microelectronic hybrid circuits. These electronic ceramics play an important role in today's industrial technology. It is important that materials be economically produced and of high quality with very precisely controlled properties.

To produce a ceramic body that possesses a specific set of physical, chemical, and electromagnetic properties requires that well controlled and characterized raw materials be uniformly blended and heat treated to produce a ceramic powder. This powder is formed into a specific shape and the formed "green" part is sintered at a high temperature to yield the ceramic body.

The characteristics of the sintered ceramic body depend to a high degree on the characteristics of the starting raw materials as well as the characteristics of the ceramic powders produced from these raw materials. Important properties of ceramic powders used to prepare piece parts or as raw materials are chemical composition; particle shape, size, and particle size distribution; agglomerate shape and size; and size distribution as well as particle and agglomerate hardness.

It is noted that both particle and agglomerate characteristics are important. The particle is an individual or discrete unit, usually in the micron or even submicron size range. Because the individual particles in most ceramic powders are small, they have a very high surface area and usually a high surface free energy. To reduce this surface free energy the particles tend to agglomerate. The agglomerate, a cluster of individual particles, can have a very dominant influence on the properties of a powder.

Figure 1 illustrates the points discussed above. Powder *properties* have a strong influence on the *characteristics* of ceramic powders as they are *processed* to form a ceramic part. The powder properties that are considered to have the most significant effects on powder characteristics are (1) chemical composition, (2) particle shape and size distribution, (3) agglomerate shape and size distribution, (4) particle hardness, and (5) agglomerate hardness. These properties all have an influence on powder characteristics and the effects of each of the above factors are interdependent. The powder characteristics that can affect the behavior of ceramic powders at each stage in a process sequence are (i) surface area, (ii) surface free energy, (iii) bulk density, and (iv) flow characteristics (powder rheology). Each of these parameters has effects, which again are not mutually exclusive, on the raw materials and on the way these materials react when they are intimately blended and heat treated or calcined to form a ceramic powder. Again, the

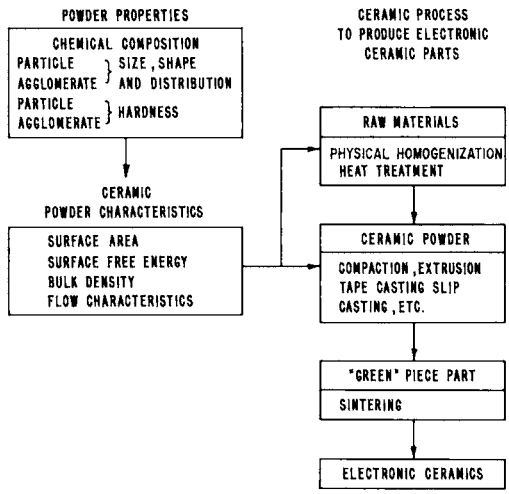

Fig. 1. Properties of ceramic powder and their influence on processing and final properties of electronic ceramics.

above parameters affect the way the powder behaves when it is formed into a piece part and the manner in which the piece part sinters to form the final ceramic body.

It is the purpose of this chapter to discuss ceramic powders in terms of their properties and characteristics and the effect these characteristics have on a material as it is processed to form a ceramic body. The chapter is divided into four sections: I. Introduction; II. Powder Properties and Characteristics; III. Effects of Powder Characteristics on Composition, Ball Milling, Calcining, Pressing and Sintering; and IV. Summary.

II. Powder Properties and Characteristics

A. Chemical Composition

Ceramic powders are synthesized from one or more starting raw materials, and the raw materials themselves have a strong influence on powder characteristics. Chemically, a ceramic powder consists of one or more chemical compounds. These compounds are usually oxides, although other compounds such as nitrides and carbides are also important in many ceramic compositions. Chemically, a ceramic composition can be divided into major components and minor components. Examples are given in the following table for two cases: ferrites and piezoelectric compounds.

	Ferrite	Piezoelectric compound
Major compounds in the ceramic powder before heat treatment	Fe_2O_3, MnO, NiO ZnO, MgO, Li_2O	PbO, ZrO_2, TiO_2
Minor compounds in the ceramic powder before heat treatment	CaO, SiO_2, Al_2O_3	SiO_2, Al_2O_3, Fe_2O_3

The major components are normally intentionally compounded from raw materials that can be any one of several forms such as oxide, carbonate, oxalate, nitrate, etc. The minor compounds can be intentionally incorporated into a mixture, but often the minor compounds are contaminants that are unintentionally added during the ceramic processing. Particle attrition techniques such as ball-milling are often a source of such contamination. Impurities in the raw materials represent another source of contamination. It is, thus, important for the ceramicist to consider the entire ceramic process when formulating a powder composition, for minor elements in a given composition can have a very strong influence on ceramic powders themselves (Nelson *et al.*, 1959; Takahashi, 1971) as well as the finished ceramic (Atkins and Fulrath, 1969; Johnson, 1967).

As an example it was found that contamination (Kim, 1973; Webster *et al.*, 1965) of silica (SiO_2) and alumina (Al_2O_3) that occurred during ball-milling with mullite balls of a piezoelectric lead zirconate titanate (PZT) resulted in an unusable powder because a sintered part prepared from this material was heterogenous, had a second phase, and a low density. A micrograph of the sintered PZT with the second phase is shown in Fig. 2.

B. Particle Size, Shape, and Distribution

Ceramics materials are commonly prepared either by mixing and comminution of bulk material or by solution techniques such as precipitation (Ayers, 1941; Penniman and Zoph, 1921; Plews, 1938), freeze drying (Kim, 1971a, Schnettler *et al.*, 1968), and liquid drying (Miller and Kim, 1973). In general, particles prepared by the solution techniques, especially precipitation methods, are found to have a size distribution that fits a log-normal distribution. Powders prepared by comminution are frequently described by the Gaudin (1926), Schuhmann (1940), and Rosin–Rammler (1933) laws.

Particle size, shape, and distribution affect behavior of raw materials when they are physically mixed together by ball-milling or other techniques and when the mixture is reacted at high temperature to form a desired compound or mixture of compounds. It is known that particle size and shape are

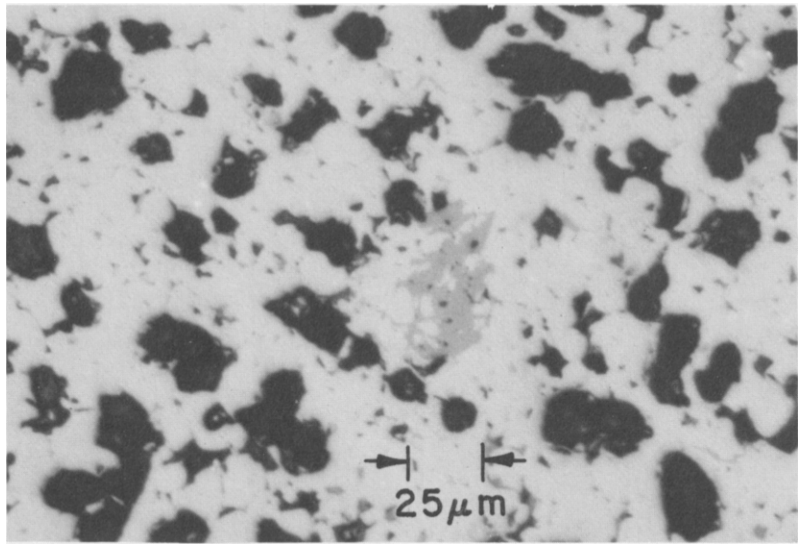

Fig. 2. A second phase (contaminated) in the microstructure of lead zirconate titanate (PZT) composition.

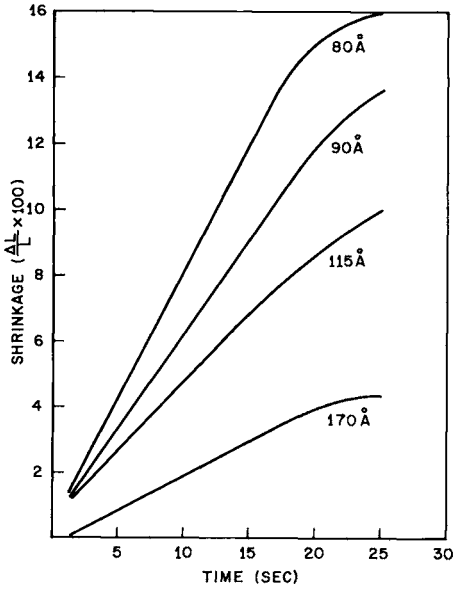

Fig. 3. Shrinkage at 700°C of titanate (TiO_2) compacted bodies with four particle sizes as a function of sintering time. From Vergnon *et al.* (1973).

related to other physical and chemical properties of a material. For instance, the particle size of a material determines its effective surface area, which can have a significant effect on powder reactivity (Bratton, 1969; Economos, 1955; Hasegawa and Sato, 1967; Gallagher *et al.*, 1972, 1973).

In Fig. 3 an example is presented that shows the effect of particle size on the reactivity of TiO_2 powder in terms of the sintering kinetics of this powder (Vergnon *et al.*, 1973). It is noted that there are numerous articles in the literature (Coulter, 1953; DeHoff and Rhimes, 1968; Hillard, 1962; Lamar, 1952; Oatley *et al.*, 1965; Stover, 1967) on the techniques employed to characterize ceramic powders for the variables discussed in this text.

C. Agglomerate Shape and Size

In the present text, an agglomerate is defined to be an assemblage of discrete particles that can be separated without breaking the individual particles. Ceramic parts are usually fabricated from pressing powder containing a certain size, distribution, and shape of agglomerates. The pressing powder usually contains organic binders to hold agglomerates together and cause agglomerates to adhere to one another. The usage and effect of binders on agglomerating of powders are discussed by Fisher and Potter (1955), Kapur and Fuerstenau (1967), Levine (1969), and Pincus and Shipley (1969). The presence of discrete agglomerates that cannot be broken down during piece part formation by pressing, extrusion, etc. (Francis and MacZura, 1972; Kim and Berrin, 1970), can have a strong influence on the density of the pressed part and sintered part (Pincus and Shipley, 1969). In practice, agglomerate shape and size are examined by scanning electron microscope (SEM) and sieve analysis, respectively (DeHoff, 1971; Kaye and Jackson, 1967).

D. Particle and Agglomerate Hardness

The hardness of particles and agglomerates of particles in a powder affects the ability to comminute the particles and homogenize the powder. Niesz *et al.* (1972) have done an extensive study on strength characterization of powder aggregates. Perhaps the most important influence of hardness is its effect on contamination. For example, ball-milling of hard materials such as garnet or alumina can lead to significant abrasion of the ball mill and balls. Thus, contamination (pickup) is a severe problem in the processing of refractory electronic materials, and techniques must be developed to compensate for this contamination (Blockman and Mattiesen, 1970, 1971).

E. Specific Surface Area

The specific surface area is one of the more important parameters used to characterize powders. The specific area (m^2/gm) offers information on the

combined effects of several other related parameters such as particle size, shape, size distribution, surface texture, and open porosity within a crystallite or agglomerate. Among several techniques employed to measure specific surface area of powders, the Brunauer, Emmett, and Teller (BET) method of determining monolayer coverage from an adsorption isotherm has been utilized extensively to measure the specific surface areas of ceramic powders (Brunauer *et al.*, 1938).

F. Surface Energy

The surface energy (γ) can be thought of as the reversible work required to form a unit area of a new surface by cleavage at constant temperature and pressure (Adamson, 1967). The adsorption of impurities reduces γ. If γ is considered as a manifestation of the energy required to break the bonds between atoms from one atomic layer and the next, then some of the energy can be recovered if adsorbates bond to the surface atoms whose valence requirements are unsatisfied (Somorjai, 1972; Lindford, 1973). Adsorbates can have a significant influence on powder behavior, and some of these effects will be discussed below.

The surface energy includes energy caused by lattice strain, surface segregation of ions normally at random in the bulk, and distortion in the electric fields of atoms on the surface itself (Weyl, 1953). An enhancement of "activity," for example, results from the presence of a surface that contains structural imperfections.

It is known that a powder with high reactivity is produced by calcining mixtures of carbonates, oxalates, hydroxides, etc., at a temperature just above the decomposition temperature of the constituents. This is because of the highly defective nature of the decomposition products, as mentioned above. Such a powder will tend to adsorb impurities such as water vapor in order to reduce its specific surface energy, and this can result in a powder with poor rheological properties. Thus, an optimum powder for a given process is not necessarily the most "reactive" powder.

It is difficult to measure surface energy routinely, but it can be measured with special care by the microcalorimeter technique (Taylor and Hockey, 1966).

G. Density

Density is a fundamental property, and there are several ways to measure the relative density of a powder. These are tap density, bulk density, and apparent density. The tap density of a powder is measured by pouring into a container calibrated for volume and tapping the container for a set time period with a given force and tap frequency. The tap density would then be the ratio of powder weight to volume after the powder has been compacted by a given

tapping action (Marshall, 1961). Bulk density would be a special case of the tap density. It is a measure of the ratio of powder weight to volume before any compaction by tapping. Apparent density is a measure of the basic granule density which includes the material volume and volume of trapped pores. It is measured by either a sedimentation technique (Heywood, 1961) or, more commonly, by a fluid immersion technique (American Society for Testing and Materials, 1967). The powder density is an indirect measure of the degree of sintering reaction (compound formation) that takes place when a powder mixture is reacted during calcining (Yamaguchi, 1968). It is also related to the amount of particle growth and hardness of agglomerates (Mazdiyasni and Brown, 1971; Tokue *et al.*, 1968).

In any controlled ceramic process, the control and understanding of powder density is essential, because the physical and chemical characteristics that affect powder density will influence the manner in which the powder reacts and behaves during subsequent processing steps.

H. Rheology

The rheological behavior of a ceramic powder system is affected by particle and agglomerate size, shape, agglomerate preparation technique (spray drying, granulating, etc.), and the nature of the binders employed. The latter factor can have a dominant effect on powder rheology. Some of these factors are described in more detail in the following section.

The rheological behavior of powders has been studied in detail by many workers (Brown, 1961; Neumann, 1953; Westman and Hugill, 1930). In practice powder flow properties are characterized by measuring the flow rate of a specific quantity of powder through a standard cone (Brown and Hawksley, 1947). Attempts have been made to correlate these measurements with other parameters (Fisher and Potter, 1955) such as green density and physical texture of a pressed part.

III. Effect of Powder Characteristics on Composition, Ball-Milling, Calcining, and Sintering

It would be ideal if a chain of events could be described from raw material to finished product with a complete description of each event that would allow a quantitative evaluation and understanding of an entire ceramic process. In practice, the interaction of the materials during a ceramic process is so complex that a totally quantitative description of all events and their interpretations is not possible. However, in order to approach an understanding

of a ceramic process it is necessary to obtain quantitative values for each possible variable and to assign limits to the numerical variations that are permissible. To understand the role of powders in ceramic processes it is necessary to attach meaningful numbers to the factors previously enumerated.

A raw material is the starting point of the procedure that produces a ceramic powder and ultimately an electronic ceramic. Composition and particle size, shape, and hardness affect properties and behavior of a raw material. These powder characteristics usually have a wide range of variations depending upon the preparation techniques of the manufacturer. It is generally good practice for the user to obtain a complete analysis on those parameters outlined above, on at least a sampling basis, in order to insure reproducibility of the raw material characteristics. For example, alumina powder prepared by the Bayer process (Gitzen, 1970) will behave differently from alumina prepared by non-Bayer techniques.

Recently developed solution techniques such as freeze drying, coprecipitation (Akashi *et al.*, 1970; Cholyi and Novasodova, 1970; Gallagher *et al.*, 1969) and liquid drying offer considerably different powder characteristics from that of the powders prepared by other, more standard methods.

Once the systematic characterization of the raw materials has been performed and the results are satisfactory, a process moves on to batch formulation, mixing, calcining, and ball-milling. This conventional ceramic process is widely utilized in preparing small and large quantities of material that contain single and multiconstituents. The formulated batch powder is subjected to a mixing procedure to obtain physical uniformity. Not only must major constituents be uniformly and intimately mixed, but minor constituents must also be uniformly incorporated into the batch. Some examples of minor additives are CaO, SiO_2, and TiO_2, which are additions to ferrite compositions (Akashi, 1966; Kim, 1964; Stijnties and Klerk, 1971), MgO additions to Al_2O_3 (Kim and Monforte, 1971), ThO_2 addition to Y_2O_3 (Greskovich and Woods, 1973; Jorgensen and Anderson, 1967), and SiO_2, Al_2O_3 and La_2O_3 to PZT compositions (Haertling and Land, 1971; Kim, 1973).

The powder and agglomerate characteristics of the raw materials play a very important role. If the particles are too large or if the particles tend to form dense agglomerates, uniform and intimate mixing is difficult or impossible. Also, if the particles are hard (abrasive), there can be significant contamination during the mixing process, for example, during ball-milling. These interacting factors will then have a dominant effect on the kinetics of compound formation during the calcining.

Calcining temperature and atmosphere have a very strong influence on the characteristics of a powder. The higher the temperature the greater the degree of reaction. However, if the calcine temperature is too high, significant sintering can take place during calcining, and the sintered agglomerates will

be difficult to break. These agglomerates can have a dramatic effect on the microstructure of a sintered part (Kim, 1965; Magee *et al.*, 1971). If the calcine temperature is too low, the reaction kinetics can be very slow and the resultant powder is not homogeneous.

One additional factor, mentioned previously, has an important influence on powder characteristics and is worth repeating here. If the calcining temperature is such that raw materials such as carbonates, nitrates, etc., are just decomposed and compound formation is just initiated but not completed, then the resulting calcined powder can have a very high free energy due to the small particle size and highly defective nature of the newly formed compounds. It is the author's experience (Kim, 1971b,c) that this state is to be avoided since these powders adsorb water and other ambient species and exhibit very poor rheological and pressing characteristics. Many workers (Buckner and Wilcox, 1972; Swallow and Jordan, 1964) have found that a specific calcining temperature and time produces an optimum degree of reaction. Below and above this critical temperature subsequent processing conditions are difficult to optimize.

Figure 4 shows an example of a ferrite (spinel) formation during calcination of Fe_2O_3, $MnCO_3$, and $MgCO_3$ to produce the spinel phase. Quantitative measurement of the spinel content of the powder is by X-ray diffraction analysis (Kim, 1965; Klug, 1953). This type of relationship has been used as a process control tool in manufacturing of various ferrites (Jong and Ownby, 1973; Kedesdy and Katz, 1953; Kedesdy and Tauber, 1957). The characteristics of each of the calcined powders shown in Fig. 4 is different and will affect ball-milling and subsequent operations.

In usual ceramic practice, the ball-milling operation is used in processing

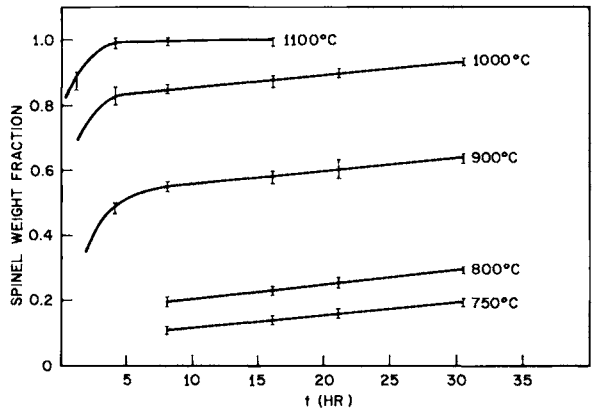

Fig. 4. MgMn ferrite (spinel) formation as a function of temperature and time.

ceramic materials to homogenize powders, reduce particle size, and break up agglomerates. Ball-milling is an efficient and economical process compared to most other available particle attrition and mixing processes. However, special attention is required in the processing of electronic ceramics by the ball-milling process. In this operation mixing, packing, and grinding of the powders take place depending upon the type of powders and type of milling (wet or dry) (Hart and Hudson, 1964; Takei, 1958). To control the ball-milling operation the degree of contamination (pickup) from the milling media and rate of size reduction are important parameters (Brown, 1964).

It is evident that one must select proper milling media and establish optimum milling conditions for each given powder. Information on the selection of the milling media and the optimization of milling conditions is available from ball-milling manufactures (U.S. Stoneware Inc., 1971; Coors Porcelain Co., 1971) and other investigators (Vydrik, 1959; Yamaguchi, 1968).

It has been observed that the particle size usually decreases and the amount of contamination increases as the milling time is increased for a given material. In Fig. 5, an example is presented (Chol, 1971) in which there is linear increase in the surface area of MnZn ferrite particle as a function of increasing milling time for two different millings. For some cases, long milling time results in excessive pickup and is detrimental to final properties. Often, discontinuous grain growth (Chol, 1971) can result in ferrites if too much iron is picked up from a mill. The degree of contamination that occurs during milling of a yttrium aluminum iron garnet composition can be seen in Fig. 6 (Kim, 1967). Since stoichiometry of garnets has a dominant effect on properties, control of milling pick up is essential (Cohen and Chegwidden, 1966). Similar trends are also observed for milling of MgMn ferrite composition (Kim, 1965).

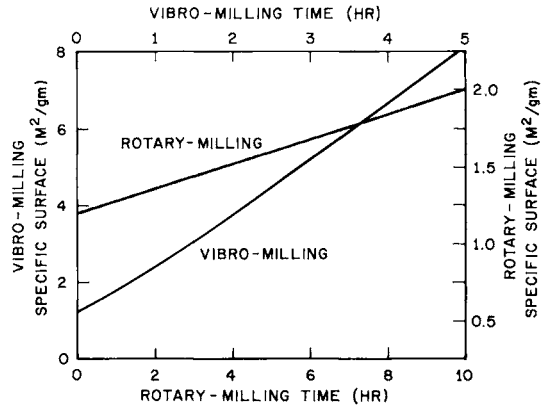

Fig. 5. Specific surface of MnZn ferrite as a function of milling time. From Chol (1971).

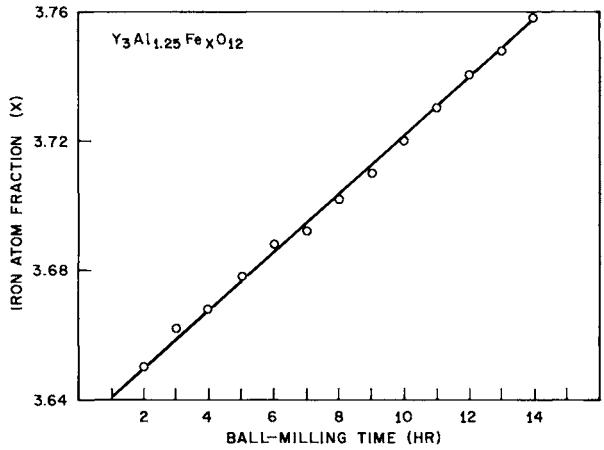

Fig. 6. Iron pickup in yttrium aluminum iron garnet as a function of ball-milling time.

As far as the selection of ball-milling materials is concerned, high density and high purity alumina and zirconia milling media are commonly used in processing alumina substrates and PZT material, respectively. On the other hand, high carbon steel or tungsten carbide milling media are used almost exclusively in processing ferrite products. For special cases where only minimal contamination is tolerable polyethylene or rubber lined milling jars are frequently used. It is also desirable to employ a milling media whose composition is identical to the material to be milled or that adds one of the constituents of the mix, e.g., iron balls to mill ferrite.

In addition to the more common wet ball-milling, dry ball-milling is also used in processing particular powders. Such powders can have different characteristics than the conventionally prepared powders, with respect to particle size, shape, and bulk density (Hart and Hudson, 1964). Dry milling action can increase the bulk density of a powder and improve its flowability. Since dry milling a powder can usually be accomplished in a short period of time, contamination is minimized.

After either dry or wet ball-milling, the resultant materials should be evaluated for particle size, distribution, shape, and degree of contamination. The characterized ball-milled powders then proceed to pressing powder preparation. The pressing powder is an assembledge of agglomerates that can be prepared by several techniques: (1) spray-drying (Helsing, 1969; Motyl, 1963; Takenaka *et al.*, 1971), (2) granulating and (3) screening, with or without organic binders. Of these techniques, spray-drying is commonly used in processing small and large batches of ceramic materials. Discussion of the details of spray-drying is beyond the scope of this article. However,

details of the spray-drying procedure are available in the literature (Rasmussen, 1930).

The spray dried powders are evaluated for agglomerate size, size distribution, shape, bulk density (or tap density), and flowability. A comparison of

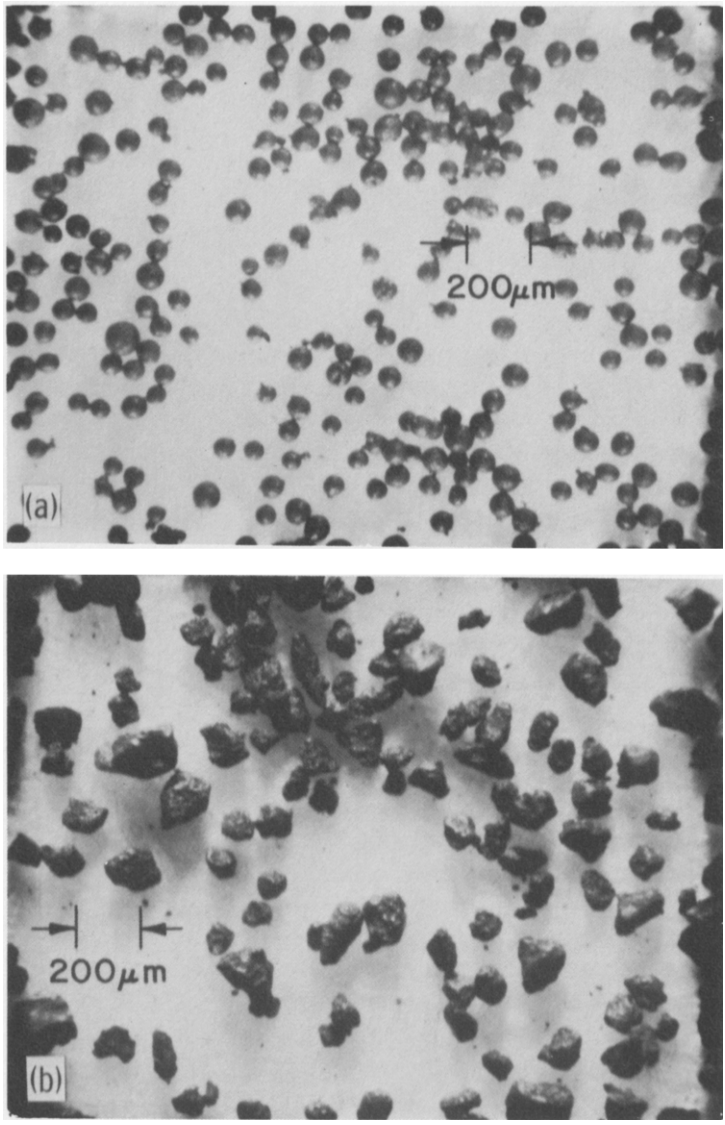

Fig. 7. Ferrite sheet pressing powders. (a) Spray dried powder; (b) nonspray dried powder.

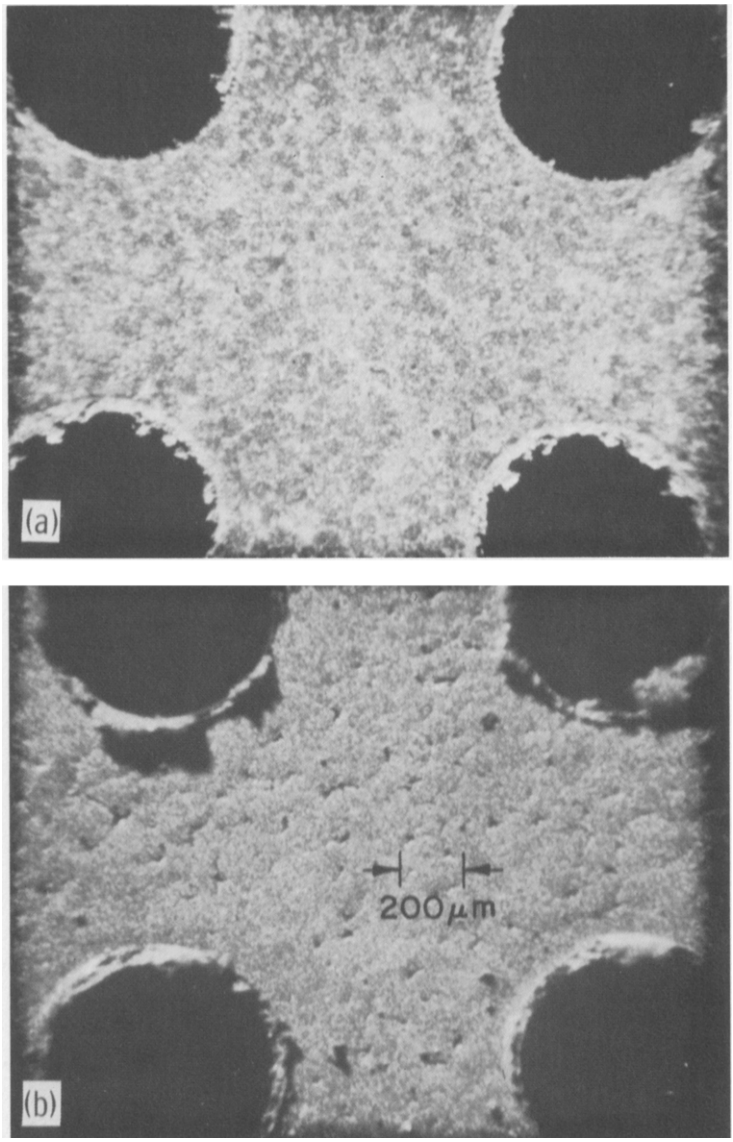

Fig. 8. Surface texture of the green ferrite sheets. (a) Pressed from spray dried powder; (b) pressed from nonspray dried powder.

pressing powders prepared by spray-drying and granulation are shown, respectively, in Fig. 7. The spray dried powders have a spherical shape. The agglomerates are soft enough to be readily crushed upon pressing. On the other hand, the granulated agglomerates are irregular in shape having a wide range of sizes. These agglomerates are usually harder than those of the spray dried powder. These differences would affect pressing condition and texture of the pressed parts, accordingly. This is illustrated in Fig. 8, which compares pressed sheets of ferrite that have been pressed from spray dried and agglomerated materials, respectively.

Recently, an important parameter for characterizing the shape, size, distribution, and particle density has been developed and is called the "Hausner index." This is defined as the ratio of the tap density d_t to apparent density d_a. Details can be found in Hausner (1967). The two density factors are important powder characteristics; each can be influenced by factors such as particle shape, size, and distribution. High friction between particles should result in low apparent density. Values of d_t/d_a have been shown to increase with increasing irregularity of powder grain shape and with higher specific surface area of powders (James, 1972). It is evident that the Hauser index can be useful as a process control guide. In ferrite processing, this index is frequently used to control the calcining, ball-milling, and press powder agglomeration. Using tap density as a guide for pressing, it has been observed that a linear relationship exists between tap density of a powder and linear shrinkage of a pressed piece part (Berry *et al.*, 1959; Tokue *et al.*, 1968).

In addition to the control of agglomerate size, distribution, and shape, one must prepare the agglomerates so that they possess good flow or rheological properties. Such properties permit a uniform transmission of pressure throughout the entire body during pressing and allow enough deformation of an agglomerate during pressing to produce a uniformly pressed, high density part. Characteristics of a pressing powder that one strives for are listed below (Stover, 1967).

1. Spherically shaped agglomerates that easily flow over one another to uniformly fill a die
2. Controlled agglomerate porosity and pore distribution for optimum space filling by constituent particles when the agglomerates are crushed
3. Uniform particle surface texture and composition
4. Uniform distribution of forming aids that control the yield stress and coefficient of friction during particle rearrangement when agglomerates are crushed
5. Random mixing of phases within agglomerates and uniformity of composition between agglomerates.

The chemistry of a mixture obviously has a dominant effect on the sintering of the mixed powder. Many references can be found on the effect of composition, temperature, time, and atmosphere on the sintering of electronic ceramics, and the reader is referred to the literature (Johnson, 1967; Stuijts, 1973; Vergnon *et al.*, 1973; Wilder and Fitzimmers, 1965) for details on specific type of ceramics. Recently Coble (1973) has extensively discussed the effects of the powder characteristics on sintering behavior of ceramic materials.

IV. Summary

The characterization and control of the physical and chemical properties of ceramic powders is essential if specially tailored electronic ceramics are to be produced from these powders. The characteristics of a sintered ceramic part depend to a very high degree on the characteristics of starting raw materials as well as the ceramic powders prepared from these raw materials.

Powder properties that are considered to have the most significant effect on powder characteristics are chemical composition, particle shape, size distribution, agglomerate shape, size distribution, particle hardness, and agglomerate hardness. The effect of these properties on the characteristics of a ceramic powder are interdependent. Powder characteristics that can affect the behavior of a ceramic powder at each stage in a process sequence are surface area, surface free energy, bulk density, and powder rheology.

The interaction of raw materials during ceramic powder preparation and the reaction of ceramic powder during the process sequence that leads to fabrication of a ceramic body are very complex. It is not possible today to gain a totally quantitative understanding of an entire ceramic processes. It is, nevertheless, critical to characterize at least qualitatively each of the variables associated with a ceramic process to gain overall process and material control. Characterization of the above-listed properties of a ceramic powder is certainly a necessary step toward a controlled ceramic process.

Once the chemistry system of a material is defined, the chemical composition of the raw materials must be carefully evaluated. Any constituents that are added to the powder during processing, either intentionally or via contamination, must also be carefully considered. The effect of mixing particle and agglomerate attrition procedures and forming aids must be evaluated in terms of their respective effects on particle and agglomerate size distribution and hardness. These latter parameters will have a very strong effect on subsequent behavior of the ceramic powder.

Heat treatment (calcining) of a mixed powder will affect all the enumerated

characteristics, and the temperature and atmosphere are to be evaluated in terms of their effects on the powder. Net powder reactivity is, to a large degree, controlled by this step. For a given set of desired end properties in a ceramic part, there is an optimum reactivity that must be "built" into the powder. Finally the characteristics of a processed powder, including powder rheology, will affect the uniformity and physical texture of a pressed part. The reactions and degree of densification that occur upon sintering, then, are to a large degree controlled by the built in properties of the prepared pressing powder.

With the increasingly important technical and related economic impact and role of ceramics in our present and future society there will be even greater emphasis placed on fabrication of newer and better controlled ceramics. The characterization and control of ceramic powders that is required to synthesize and produce these newer materials encompasses a field of study that has not been fully exploited. Much work remains in this area before we can begin to approach a goal of well-understood and controlled ceramic processes.

ACKNOWLEDGMENTS

The author wishes to extend his gratitude to H. M. Cohen for encouragement and critical review of this manuscript. Thanks are due to P. K. Gallagher and D. W. Johnson, Jr., for valuable comments.

References

Adamson, A. W. (1967). "Physical Chemistry of Surfaces." Wiley (Interscience), New York.
Akashi, T. (1966). *NEC Res. Develop.* **8**, 89–106.
Akashi, T., Sugano, I., Okuda, T., and Tsuji, T. (1970). *NEC Res. Develop.* **19**, 89–93.
American Society for Testing and Materials. (1967). Fluid Immersion Tech., Part 13, C 20–46 (1961), 8–10. *Amer. Soc. Test Mater.*, Philadelphia, Pennsylvania.
Atkins, R. B., and Fulrath, R. M. (1969). Research Report UCRL-18795, AEC Contract No. W-7405-ENG-48. University of California, Berkeley.
Ayers, J. W. (1941) U.S. Patent 2,255,607.
Berry, T. F., Allen, W. C., and Hassett, W. A. (1959). *Amer. Ceram. Soc., Bull.* **38**, 393–400.
Blockman, F. G., and Mattiesen, K. E. (1970). *J. Amer. Ceram. Soc.* **53**, 517–520.
Blockman, F. G., and Mattiesen, K. E. (1971). *J. Amer. Ceram. Soc.* **54**, 180–183.
Bratschun, W. R., Mountvala, A. J., and Pincus, A. G. (1971). *NASA Spec. Publ.* **NASA SP-5097**.
Bratton, R. J. (1969). *Amer. Ceram. Soc., Bull.* **45**, 825.
Brown, C. S. (1964). *Proc. Brit. Ceram. Soc.* **2**, 55–72.
Brown, R. L. (1961) *SCI (Soc. Chem. Ind., London) Monogr.* **4**.
Brown, R. L., and Hawksley, P. G. W. (1947). *Fuel* **26**, 159.
Brunauer, S., Emmett, P. H., and Teller, E. T. (1938). *J. Amer. Chem. Soc.* **60**, 309.
Buckner, D. A., and Wilcox, P. D. (1972). *Amer. Ceram. Soc., Bull.* **51**, 219–222.
Buessem, W. R. (1965). *Miner. Ind. Bull. (Penn. State Univ. Spec. Publ.)* **36**, 1–4.
Ceramic Age. (1973). **89**, No. 1, 9–13.
Chol, G. R. (1971). *J. Amer. Ceram. Soc.* **54**, 34–39.

Cholyi, V. P., and Novasodova, E. B. (1970). *Inorg. Mat.* (in English) **6**, 1902–1906.
Coble, R. L. (1973). *J. Amer. Ceram. Soc.* **56**, 461–466.
Cohen, H. M., and Chegwidden, R. A. (1966). *J. Appl. Phys.* **37**, 1081–1082.
Coors Porcelain Co. Technical Bull. (1971). New AB-9. Ceramic Grinding Media.
Coulter, W. H. (1953). U.S. Patent 2,656,508.
DeHoff, R. T. (1971). *In* "Quantitative Steology, Characterization of Ceramics" (L. L. Heach and R. W. Gould, eds.), pp. 529–553. Dekker, New York.
DeHoff, R. T., and Rhines, F. N. (1968). "Quantitative Microscopy." McGraw-Hill, New York.
Economos, G. (1955). *J. Amer. Ceram. Soc.* **38**, 241–244.
Electronic Industries Associates. (1973). *Electron. News* **18**, No. 904, 1.
Fehlner, F. P., and Halaby, S. A. (1967). *Electron. Package Prod.* **5**, 13–18.
Fisher, J. R., and Potter, J. F. (1955). *Amer. Ceram. Soc., Bull.* **34**, 177–181.
Francis, T. L., and MacZura, G. (1972). *Amer. Ceram. Soc., Bull.* **51**, 535–538.
Gallagher, P. K., and Johnson, D. W., Jr. (1972). *J. Amer. Ceram. Soc.* **55**, 232–233.
Gallagher, P. K., O'Bryan, H. M., Schrey, F., and Monforte, F. R. (1969). *Amer. Ceram. Soc., Bull.* **48**, 1053-1059.
Gallagher, P. K., Johnson, D. W., Jr., Schrey, F., and Nitti, D. J. (1973). *Amer. Ceram. Soc., Bull.* **52**, 842–849.
Gaudin, A. M. (1926). *Trans. Amer. Inst. Chem. Eng.* **73**, 253.
Gitzen, W. H., ed. (1970). "Alumina as a Ceramic Material," *Amer. Ceram. Soc.*, Columbus, Ohio.
Gordon, I. (1956). *Amer. Ceram. Soc., Bull.* **38**, 393–400.
Greifer, A. P. (1969). *IEEE Trans. Magn.* **5**, 774–811.
Greskovich, C., and Woods, K. N. (1973). *Amer. Ceram. Soc., Bull.* **52**, 473–478.
Haertling, G. H., and Land, C. E. (1971). *J. Amer. Ceram. Soc.* **54**, 1–11.
Hart, L. D., and Hudson, L. K. (1964). *Amer. Ceram. Soc., Bull.* **43**, 13–17.
Hasegawa, K., and Sato, I. (1967). *J. Appl. Phys. (Tokyo)* **38**, 4707–4713.
Hausner, H. H. (1967). *J. Powder Met.* **3**, 7–13.
Heil, S. D. (1967). *Proc. Int. Symp. Hybrid Microelectron.*, pp. 44–48.
Helsing, H. J. (1969). *Powder Met. Int.* **2**, 62–65.
Heywood, H. (1961). *Powder Met.* **7**, 1–28.
Hilliard, J. E. (1962). *Trans. AIME* **224**, 906–917.
Jaffe, B., Cook, W. R., Jr., and Jaffe, H. (1971). "Piezoelectric Ceramics." Academic Press, New York.
James, P. J. (1972). *Powder Met. Int.* **4**, 193–198.
Johnson, D. L. (1967). *In* "Sintering and Related Phenomena"(G. C. Kuczynski, ed.), pp. 269–274. Gordon & Breach, New York.
Jong, B. W., and Ownby, P. D. (1973). *Bull. Amer. Ceram. Soc.* **52**, 526–528.
Jonker, G. H., Wijn, H. P. S., and Brown, P. W. (1956–1957). *Philips Tech. Rev.* **18**, 145.
Jorgensen, P. J., and Anderson, R. G. (1967). *J. Amer. Ceram. Soc.* **50**, 553–558.
Kapur, P. C., and Fuerstenau, D. W. (1967). *J. Amer. Ceram. Soc.* **50**, 14–18.
Kaye, B. H., and Jackson, M. R. (1967). *Powder Technol.* **1**, 43–50.
Kedesdy, H., and Katz, G. (1953). *Ceram. Age* **62**, 29–34.
Kedesdy, H., and Tauber, A. (1957). *J. Metals* **9**, 1140–1148.
Kim. Y. S. (1964). *Pap., 66th Ann. Meet. Amer. Ceram. Soc.* Pap. No. 18-L-64, p. 281.
Kim. Y. S. (1965). *Pap., Electron. Div. Fall Meet. Amer. Ceram. Soc.* Pap. No. 24-E-65F, p. 727.
Kim, Y. S. (1967). *Anal. Chem.* **39**, 664–666.
Kim, Y. S. (1971a). *J. Korean Ceram. Soc.* **7**, 15–32.
Kim, Y. S. (1971b). *Pap., 73rd Annu. Meet. Amer. Ceram. Soc.* Pap. No. 2-JI-71, p. 461.
Kim, Y. S. (1971c). *In* "Ferrites" (Y. Hoshino, S. Iida, and M. Sugimoto, eds.), pp. 438–440. University Park, Tokyo.

Kim, Y. S. (1973). *Pap., 75th Annu. Meet. Amer. Ceram. Soc.* Pap. No. 4-E-73, p. 368.
Kim, Y. S., and Berrin, L. (1970). *Pap., 73rd Annu. Meet. Amer. Ceram. Soc.* Pap. No. 8-E-70, p. 412.
Kim, Y. S., and Monforte, F. R. (1971). *Amer. Ceram. Soc., Bull,* **50**, 532–535.
Kingery, W. D. (1960). "Introduction to Ceramics." Wiley, New York.
Klug, H. P. (1953). *Anal. Chem.* **5**, 704–708.
Lamar, R. S. (1952). *Amer. Ceram. Soc., Bull.* **31**, 283–288.
Lax, B. (1962). "Microwave Ferrite and Ferrimagnetism." McGraw-Hill, New York.
Levine, S. L. (1969). *Amer. Ceram. Soc., Bull.* **48**, 230–231.
Lindford, R. G. (1973). *Solid State Surface Sci.* **2**, 3–143.
Magee, J. H., Morton, V., Fisher, R. D., and Lowe, I. J. (1971). *In* "Ferrites" (Y. Hoshino, S. Iida, and M. Sugimoto, eds.), pp. 217–220. University Park, Tokyo.
Marshall, P. R. (1961). *Powder Met.* **7**, 29–43.
Mazdiyasni, K. S., and Brown, L. M. (1971). *J. Amer. Ceram. Soc.* **54**, 479–483.
Miller, T. J., and Kim, Y. S. (1973). *Pap., Electron. Div. Fall Meet. Amer. Ceram. Soc.* Pap. No. 27-E-73, p. 632.
Motyl, E. J. (1963). *West. Elec. Eng.* **7**, 2–10.
Nelson, K. E., and Cook, R. L. (1959). *Ceram. Age* **10**, 499–500.
Niesz, D. E., Bennett, R. B., and Snyder, M. J. (1972). *Amer. Ceram. Soc., Bull.* **51**, 677–680.
Neumann, B. S. (1953). *In* "Flow Properties of Disperse Systems" (J. J. Hermans, ed.), pp. 382-422. Wiley (Interscience), New York.
Oatley, C. W., Nixon, W. C., and Pease, R. F. W. (1965). *Advan. Electron. Electron Phys.* **21**, 181–247.
Penniman, R., and Zoph, N. (1921). U.S. Patent 1,368,748.
Pincus, A. G., and Shipley, L. E. (1969). *Ceram. Ind.* **92**, 106–109 and 146.
Plews, G. (1938). U.S. Patent 2,111,727.
Rasmussen, E. H. (1930). *Amer. Ceram. Soc., Bull.* **39**, 732–734.
Rosin, P., and Rammler, E. (1933). *J. Inst. Fuel* **7**, 25.
Roup, R. R. (1958). *J. Amer. Ceram. Soc.* **41**, 499–501.
Schnettler, F. J., Monforte, F. R., and Rhodes, W. W. (1968). *Sci. Ceram.* **4**, 79–90.
Schuhmann, R. (1940). *AIME, Tech. Publ.* **1189**.
Snelling, E. C. (1969). "Soft Ferrite." CRC Press, Cleveland, Ohio.
Somorjai, G. A. (1972). "Principles of Surface Chemistry." Prentice-Hall, Englewood Cliffs, New Jersey.
Stijnties, T. G. W., and Klerk, J. (1971). *In* "Ferrites" (Y. Hoshino, S. Iida, and M. Sugimoto, eds.), pp. 191–198. University Park, Tokyo.
Stover, E. R., ed. (1967). Air Force Tech. Report, AFML-TR-67-56: AD 816014.
Stuijts, A. L. (1973). *In* "Sintering and Related Phenomena" (G. C. Kuczynski, ed.), Vol. 6, pp. 331–350. Plenum, New York.
Swallow, D., and Jordan, A. K. (1964). *Proc. Brit. Ceram. Soc.* **2**, 80–117.
Takahashi, M. (1971). *Jap. J. Appl. Phys.* **10**, 643–651.
Takei, T. (1958). *J. Jap. Soc. Powder Powder Met.* **5**, 80.
Takenaka, H., Kawashima, Y., Yoneyama, T., and Matsuda, K. (1971). *Chem. Pharm., Bull.* **19**, 1234–1244.
Taylor, J. A. G., and Hockey, J. A. (1966). *J. Phys. Chem.* **70**, 2169–2172.
Thourel, L. (1964). "The Use of Ferrites at Microwave Frequencies." Pergamon, Oxford.
Tokue, T., Ishino, K., and Makino, M. (1968). *J. Jap. Soc. Powder Powder Met.* **15**, 168–172.
U.S. Stoneware Inc., Technical Bull. (1971). JM-290R. Grinding Media.
Vergnon, P., Aster, M., and Teichner, S. J. (1973). *In* "Sintering and Related Phenomena" (G. C. Kuczynski, ed.), Vol. 6, pp. 301–310. Plenum, New York.
Vydrik, G. A. (1959). *Steklo Keram.* **16**, 35–39.

Webster, A. H., Weston, T. B., and Craig, R. R. (1965). *J. Can. Ceram. Soc.* **34**, 121–129.
Westman, A. E. R., and Hugill, H. R. (1930). *J. Amer. Ceram. Soc.* **13**, 767.
Weyl, W. A. (1953). *In* "Structure and Properties of Solid Surface" (R. Gomer and C. S. Smith, eds.), pp. 147–184. Univ. of Chicago Press, Chicago, Illinois.
Whittemore, O. J. (1969). "Electronic Ceramics." *Amer. Ceram. Soc.* Columbus, Ohio.
Wilder, D. R., and Fitzsimmers, E. S. (1965). *J. Amer. Ceram. Soc.* **38**, 66–71.
Yamaguchi, F., and Takahashi, M. (1970). *J. Phys. Soc. Jap.* **28**, 313–315.
Yamaguchi, T. (1968). *J. Jap. Soc. Powder Powder Met.* **15**, 43–47 and 135–139.

Dry Pressing

JAMES S. REED

New York State College of Ceramics
at Alfred University, Alfred, New York

and

ROBERT B. RUNK

Engineering Research Center
Western Electric Co.
Princeton, New Jersey

I. Introduction

The fabrication of polycrystalline technical ceramics generally involves the consolidation and shaping of a fine powder, followed by a sintering process to achieve the requisite fired microstructure and properties. The most popular method for achieving these steps in the manufacturing of refractory and electronic technical ceramic components, from computer memory cores to structural refractories, is dry pressing. Dry pressing may be defined as the simultaneous uniaxial compaction and shaping of a granular powder with

small amounts of water and/or organic binders during confined compression in a die. The extensive practice of dry pressing stems from the inherent ability to form rapidly a wide variety of shapes with close tolerances and controlled compact character using highly mechanized and automated equipment. For example, steatites, aluminas, titanates, and ferrites have been dry pressed in sizes ranging from a few mils to several inches in linear dimensions at rates up to 5000 parts per minute on smaller parts. The forte of dry pressing is the manufacture of small parts with surface relief in the pressing directions. Sheets of ceramic with high aspect ratios, less than a few hundred mils thick, are now conventionally formed by continuous tape casting; and for shapes with one greatly elongated dimension or with two- or three-dimensional surface relief, other fabrication methods such as extrusion and slip casting can be competitive. The discussion here is restricted to one-dimensional pressing; two- and three-dimensional pressing are discussed in another article in this volume, by Austin and McTaggart, on isostatic pressing.

II. Process Variables

A. Press Parameters

A sequence of intermittent steps is involved in dry pressing a ceramic component (Fig. 1). Feeding is typically synchronized with a drop in the bottom piston followed by a compression step and then ejection of the piece. For soft powders the die materials are typically abrasion-resistant hardened steels with a high Young's modulus of elasticity. For longer wear or abrasive powders, special steel, borided steel, or metal carbide tooling is employed. Pressures range up to several tens of thousands of psi; punch speeds are of the order of a fraction to a few seconds. Functional variables which must be considered in the press design are: (1) design of die set (geometry, materials, gap between movable and fixed components); (2) powder feed mechanism and driving force for filling; (3) flow and compaction properties of powder (control of powder character); (4) temperature and atmosphere of feed powder and die; (5) punch pressure and/or displacement program and dwell time; and (6) ejection program. Accordingly, the press must be equipped to provide the requisite actions with sufficient precision to ensure reproducible compact character and geometry. Several distinct modes of compaction as outlined in Table I are possible. In the simplest mode (Fig. 2A) for an uncomplicated part, the die remains in a fixed position and the die cavity is filled as the bottom punch is lowered to a preset depth. During pressing the die and bottom punch remain fixed while the top punch is dis-

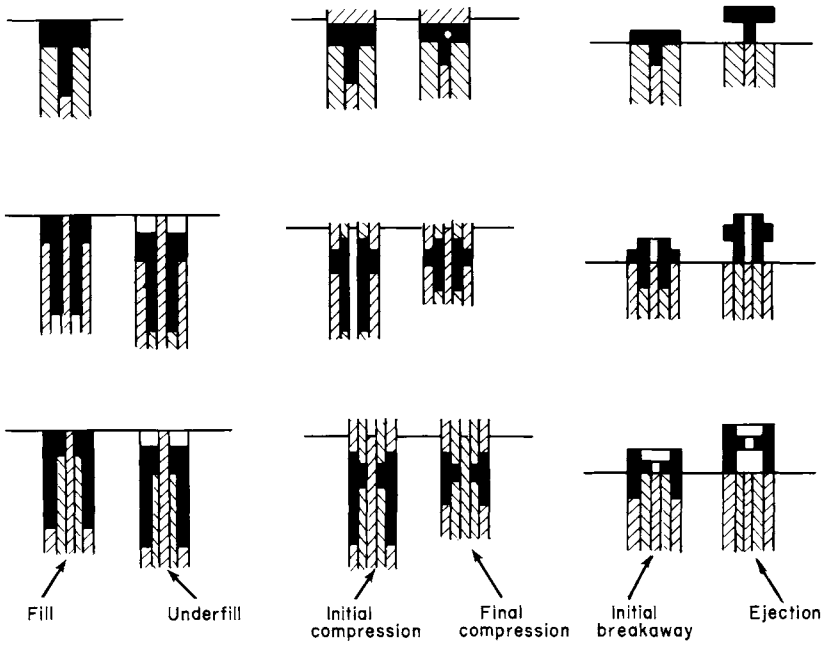

Fig. 1. Sequence of dry pressing a ceramic component. (Reprinted from "Ceramic Fabrication Processes," by W. D. Kingery by permission of the MIT Press, Cambridge, Mass.)

placed downward with a predetermined applied force. After a dwell time the top punch rises, followed by the ejection of the part by the bottom punch. The cycle is then repeated. For a more complicated part, such as a ferrite cup core, it has been found advantageous to employ a spring hold-down device

TABLE I

DRY PRESSING MODES

Type	Top punch	Die	Bottom punch	
			Pressing	Ejection
Single action	Moves	Fixed	Fixed	Moves
Double action	Moves	Fixed	Moves	Moves
Floating die	Moves	Moves	Fixed	Moves
Multiple motion	Simple or composite		Composite	
	Moves	Fixed	Moves[a]	Moves
Floating die, multiple motion	Simple or composite		Composite	
	Moves	Moves	Moves[a]	Moves

[a] Lowest level component may be stationary.

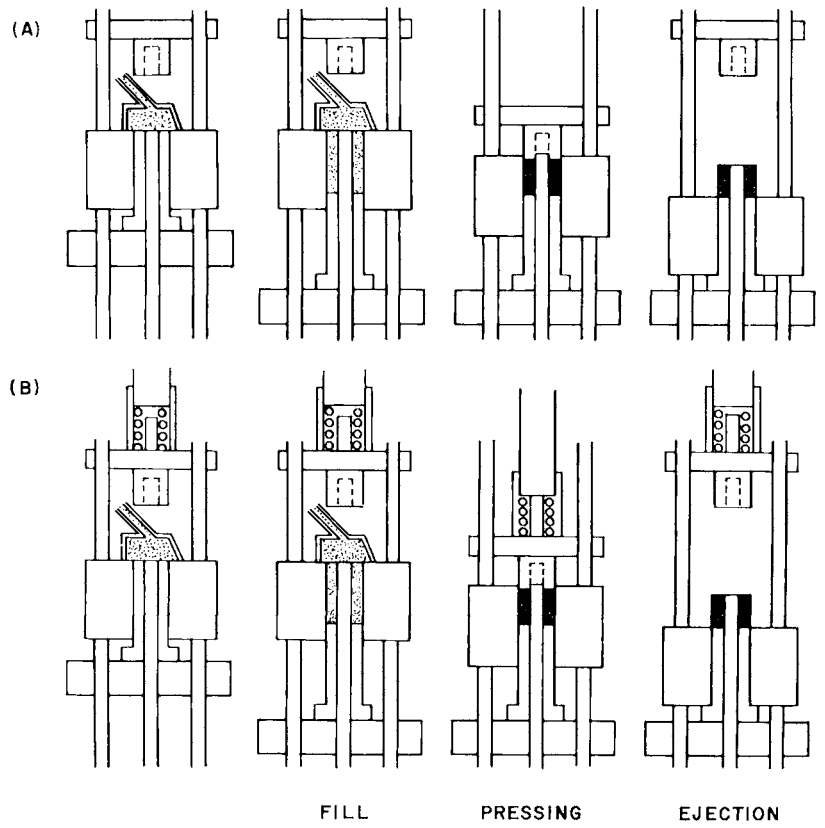

Fig. 2. Die filling, compression, and ejection: (A) simplest mode, (B) with spring hold-down device.

on the top punch to hold the pressed part between the punches during the ejection cycle (Fig. 2B). In all cases, one of the most critical steps in dry pressing is filling the die uniformly. This becomes even more difficult with finer particles because of increased particle-to-particle contact and the entrapment of air. In the two cases just mentioned a more uniform powder fill is achieved by a suction created when the bottom piston moves down relative to the die supporting the filling shoe; suction filling is absolutely necessary for the uniform filling of deep slender cavities in composite punches (Winterberg, 1969). The pressure on the punches may be induced hydraulically or mechanically. Multistation systems incorporate a number of tool sets mounted on a rotary table; filling, pressing, and ejection occur simultaneously as the tools move around the unit. Programmed stops for the punch motion may be set at a fixed displacement or a fixed pressure. Figure 3 shows a typical compaction program.

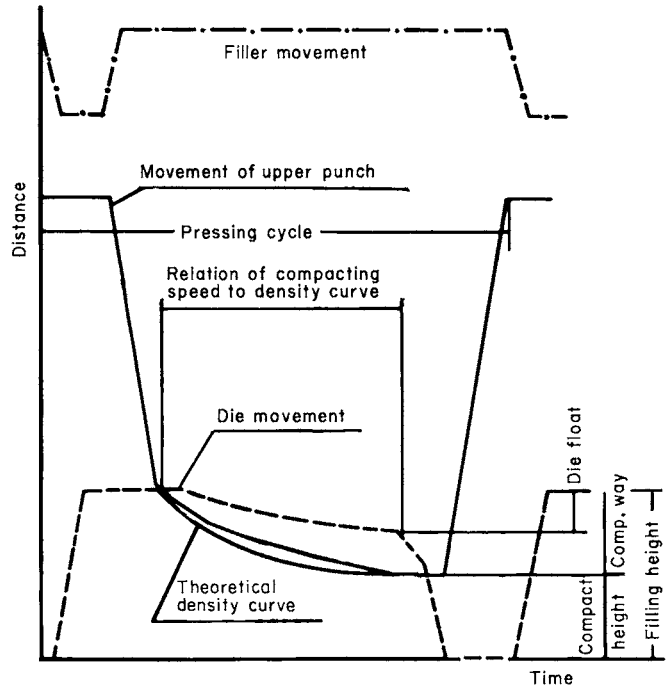

Fig. 3. Compaction program. (After Winterberg, 1969.)

Control of compact tolerances to better than ± 1 % in weight, ± 0.001 inch in thickness, and ± 0.0002 inch in parallelism are advertised capabilities for modern single-action presses. Production rates range from < 1 per minute to somewhat greater than 300 per minute for single-action presses and can go as high as 5000 per minute for high-speed rotary presses (Hirschhorn, 1969). Die set life is reported to range up to several hundred thousand pieces (Thurnauer, 1958). Advertised press specifications for a modern hydraulic 12-ton press are presented in Table II.

B. Powder Characteristics

As mentioned above, uniform mold filling is one of the most critical dry pressing parameters. This requires a powder that has uniform flow characteristics or a powder that exhibits good "pourability." Flow rates of powders can be measured and monitored using the American Society of Testing Materials (ASTM) Designation B213-48, standard method which measures the flow rate (cubic centimeters per minute) through a funnel orifice. Generally, coarser particles tend to flow more uniformly than finer ones and an ideal granular size distribution is one between about 16 and 80 mesh. As little as

TABLE II

SPECIFICATIONS FOR A 12-TON HYDRAULIC COMPACTING PRESS[a]

	Minimum	Maximum
Ram force-pressing		
Upper ram	1.0 ton	12.5 ton
Lower main ram	0.2	12.9
Lower auxiliary ram	02.	2.8
Ram force-withdrawal		
Upper ram	0.7	8.0
Lower main ram	0.7	8.2
Lower auxiliary ram	0.2	2.8
Powder fill depth		3 in.
Cycle rate		47 strokes/min
Operating pressure	250 psi	3000 psi
Cycling pressure	250	500
Upper ram speed-down (unloaded)		10.2 in./sec
(loaded)		1.5
Upper ram speed-up		16.4
Lower ram speed-up (unloaded)		10.2
(loaded)		1.5
Lower ram speed-down		16.4
Upper ram stroke		4 in.

[a] Model HC-12, Hydramet American Inc., Royal Oak, Michigan.

10 % finer material can impede the free pouring characteristics of the powder. Detailed discussions of ideal particle size distributions and particle packing arrangements have been treated elsewhere (e.g., Kingery, 1958). However, it is often necessary to dry press ceramic parts from powders with a finer mean particle size such as some ferrite powders (Motyl, 1963), highly reactive alumina powders (Berrin *et al.*, 1972; Bruch, 1967), and many other powders produced by precipitation, plasma spraying, and cryogenic techniques. For such materials it is first necessary to granulate or aggregate the fine particles into larger agglomerates to increase their flowability. Three granulation techniques include (1) compaction followed by crushing and screening, (2) ball-milling and screening, (3) and spray drying. In each case a binder is often added during the granulation process. While not absolute, the three techniques are usually applied for small, intermediate, and large quantities of powders respectively.

Bruch (1967) has applied the compaction technique to Linde A* alumina, which possesses a mean particle size of 0.3 μm as received. The alumina,

*Crystal Products Division, Union Carbide Corporation, San Diego, California.

mixed with 0.25 wt % $MgCO_3$, was placed in rubber bags, double isostatically pressed at 1000 to 16,000 psi, with an intermediate crushing step. The material was then loosely broken up by hand and passed through a set of screens with mesh sizes between 16 and 100 mesh.

Ball-milling has been successfully employed for granulating co-precipitated manganese zinc ferrite powders with an initial mean particle size of 0.2 μm. The powder was ball milled for two hours with 42 wt % water, 0.5 wt % polyvinyl alcohol (binder), 0.3 wt % gum arabic (deflocculant), and 3.3 wt % zinc stearate (lubricant). The slurry was then dried and granulated powder passed through screens with sizes between 80 and 200 mesh.

Spray drying has also been an instrumental step in the successful dry pressing operation of large quantities of ferrite powder (Motyl, 1963). In the spray dryer, aqueous ferrite slurries (containing the required binder,

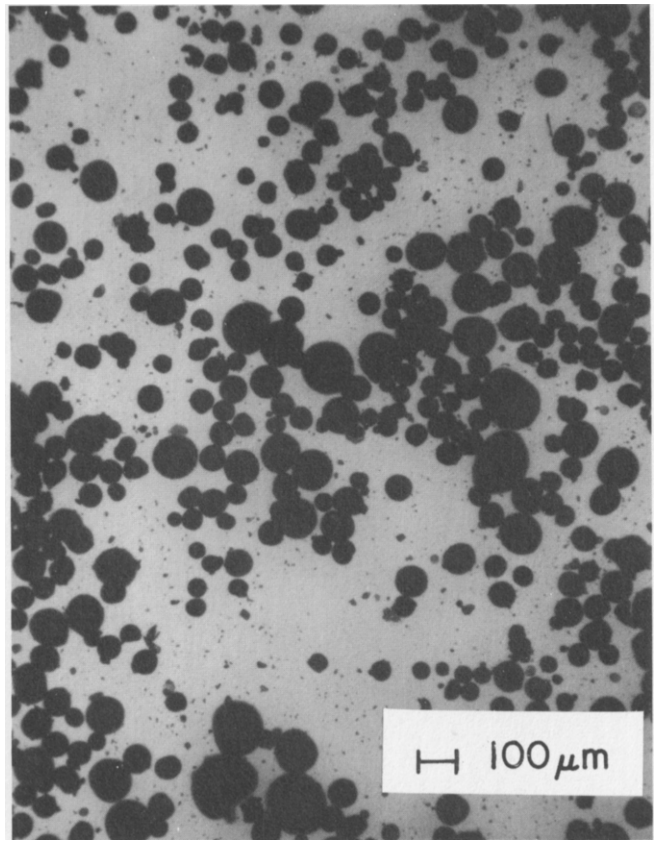

Fig. 4. A typical spray dried ferrite powder.

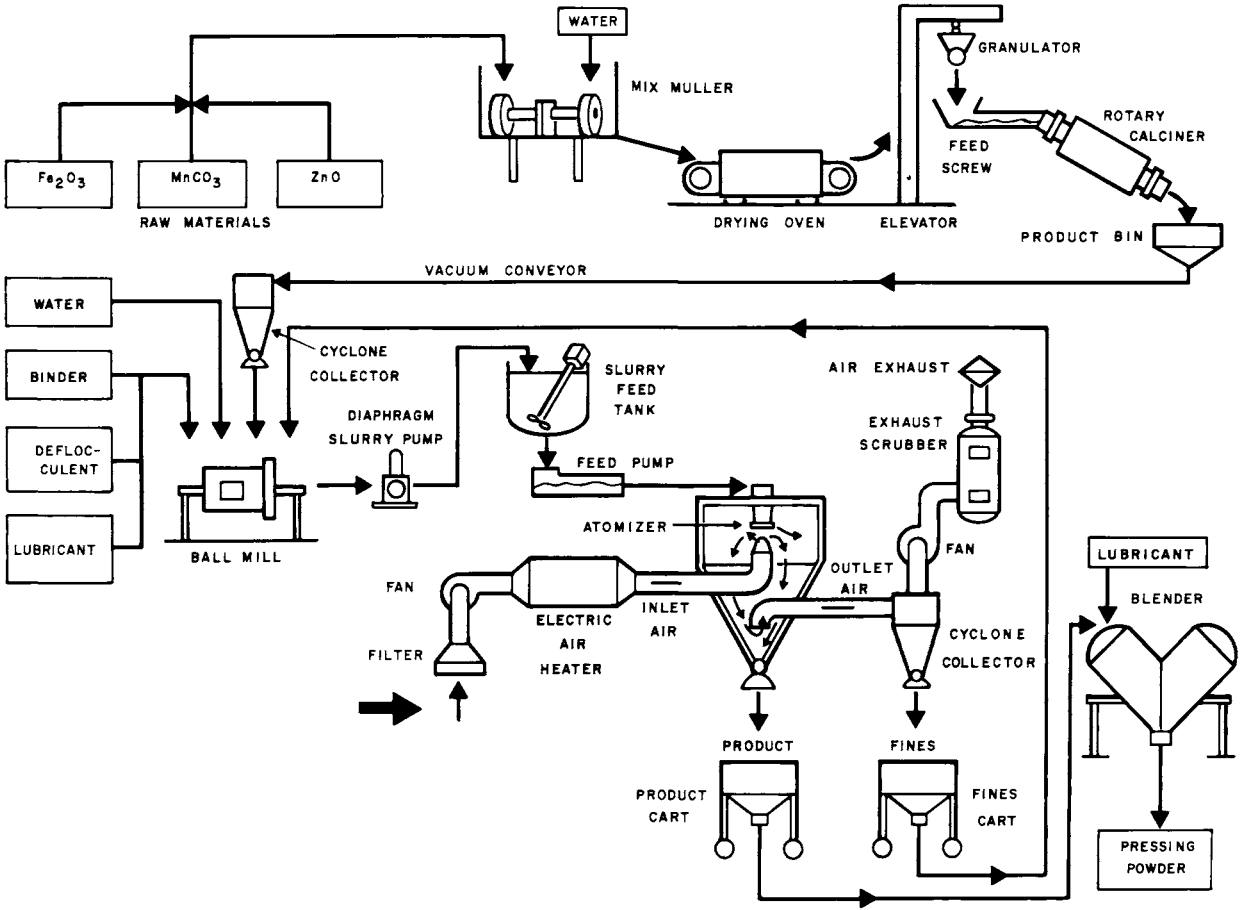

Fig. 5. Flow diagram for the spray drying of a ferrite powder. (After Motyl, 1963.)

lubricants, and deflocculants) are atomized into small droplets and sprayed into a turbulent, heated air stream. During the process the water evaporates, leaving behind a dried, narrow size distribution of submillimeter, roughly spherical, agglomerates. A typical spray dried ferrite powder is shown in Fig. 4. Spray drying also permits close automatic control over the final moisture, binder, and lubricant content to within $< \pm 0.5\ \%$ (Helsing, 1969). By controlling all the parameters of the process (Fig. 5) one can precisely control the powder characteristics insuring consistantly good flow properties.

C. Binders

The selection and application of organic or inorganic binders can be classified as the second most critical factor in the dry pressing process. Under the term "binders" is loosely collected all pressing aids such as binders, lubricants, plasticizers, and deflocculants. For the functions of such additives to ceramic powders see Table III (Pincus and Shipley, 1969). The ideal binder or combination of additives will improve flowability, reduce abrasion, improve bonding strength, increase internal lubrication, and aid external or die-wall lubrication. These attributes in effect contribute to the overall formability and increase the level and uniformity of the final pressed or green density of the ceramic part. Such an ideal binder system also "burns off" during the initial stages of the firing or sintering cycle without deleterious

TABLE III

Functions of Additives to Ceramic Batches[a]

Additive	Function
Binder	Green strength
Lubricant	Mold release, interparticulate sliding
Plasticizer	Rheological aids, improving flexibility of binder films, allowing plastic deformation of granules
Deflocculant	pH control, particle-surface charge control, dispersion
Wetting agent	Lowering surface tension of liquid
Water retention agent	Preventing squeezing-out of water during pressure application
Antistatic agent	Charge control
Antifoaming agent or foam stabilizer	Preventing foam or strengthening wanted foams
Chelating or sequestering agent	Inactivating undesirable ions
Fungicide and bactericide	Stabilizing against degradation with aging

[a] After Pincus and Shipley (1969).

effects such as interfering with pore removal, leaving behind noncombustible residues, reacting with desirable components of the ceramic body, or volatilizing at such a great rate as to bloat the ceramic body. It is also desirable for the effluents from such a burn-off cycle to be either innocuous or treatable in a fashion acceptable to current safety standards.

Table IV (Pincus and Shipley, 1969) lists a large number of organic and inorganic additives used for dry pressing ceramic parts. The selection of a binder system for a particular ceramic powder from such a vast list, unfortunately, still remains a matter of accumulated experience. Although some attempts have been made to characterize some of the controlling factors (Hoffman, 1972; Levine, 1969; Cowan and Ehart, 1966; Pincus and Shipley, 1969) such as the characteristics of the ceramic powder, the individual additives in the binder system and the interaction between the additives as well as between them and the surface of the ceramic particles, the task is an exceedingly difficult one.

TABLE IV

MATERIALS USED FOR BINDERS[a]

Organics	Inorganics
Starches	Water
Dextrins	Clays
Gums	Bentonites
	Magnesium aluminum silicates
Flours	Soluble silicates
Casein	Organic silicates
Gelatins	Colloidal silica
Albumins	Phosphates
Proteins	Borophosphates
Lignins	Aluminates
Celluloses	Colloidal alumina
Bitumens	
Rubbers	
Resins	
Natural	
Synthetic	
Alginates	
Chlorinated hydrocarbons	
Waxes	
Paraffin	
Microcrystalline	
Synthetic alcohols, esters, and glycols	
Hydrogenated oils	

[a] After Pincus and Shipley (1969).

TABLE V

BINDER SYSTEMS FOR SOME CURRENT CERAMIC DRY PRESSED PRODUCTS

	Binders	Plasticizers	Lubricants
Ferrite core	Polyvinyl alcohol	Gum arabic	Zinc stearate
Steatite insulator	Microcrystalline wax	—	Magnesium stearate
Alumina sparkplug	Low oil content Microcrystalline wax Emulsion	1:1 Potassium hydroxide: tannic acid	Wax emulsion also provides lubrication
Alumina, magnesia or magnesia-chrome refractory brick	Ca- or Na-Lignosulfonate	—	Stearic acid

The best lubricants in practice are those with polar groups, and for oxide powders oleic acid, stearic acid, zinc stearate, alcohols, and waxes are commonly added in minor amounts. Table V shows successful binder systems for the dry pressing of four ceramic powders currently in common practice.

III. Compaction Behavior

A. TRANSMISSION OF STRESS IN POWDER COMPACTS

During compaction the dispersed powder becomes a cohesive unit, the porosity decreases, single crystal or aggregated particles fracture, and the number of interparticle contacts and degree of particle interlocking increases. The force applied by the moving punch is transmitted through the compact via interaction forces at particle contacts. An unbalanced system of normal and shear (frictional) stresses at contacts (see Fig. 6) can lead to particle deformation and sliding and multiple particle rearrangements. The reaction forces of neighboring particles in contact restrict sliding and translation. A detailed description of the rearrangement motions for a number of particles in a powder would be nearly impossible; multiple particle sliding and rearrangement can lead to the collapse of lower porosity groups surrounding larger pores, decreasing the average porosity and the volume fraction of coarse pores. Greater displacements of particles in line with the applied pressure are expected, but lateral displacements can also be expected, especially initially, due to the random blocking of neighboring particles and the random availability of nearby pores. As the applied force increases, contact

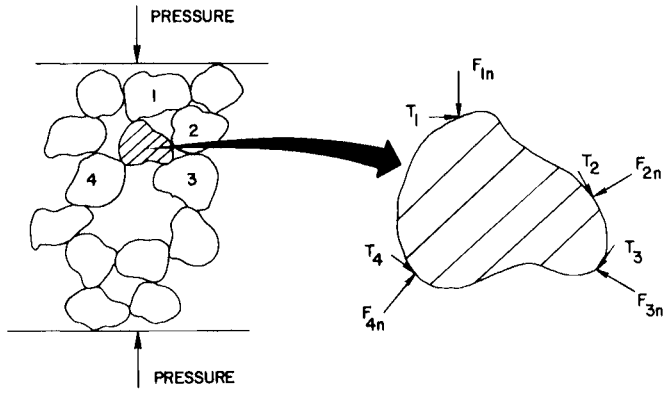

Fig. 6. Forces acting on a particle during compaction.

stresses increase and therewith both normal and frictional forces are increased. Frictional restraining forces would be expected to vary widely from contact to contact in real compacts, and restraints at particular contact points would critically restrict sliding. Because of the sum of the contact areas is only a small fraction (as little as 10^{-4}) of the total cross section of the powder, the contact stresses can cause elastic deformation and perhaps plastic flow or fracture at local contacts for relatively low applied pressures. The increase in the number of contacts per unit volume and a greater deformation at contacts would tend to diminish the stress multiplication at the contact points. Particle characteristics and/or adsorbed monolayers of surfactants, which would reduce the coefficient of friction between particles, would act to reduce the tangential restraining forces for a given normal force.

B. Stages in Compaction

Detailed studies of the particle mechanics and microstructural changes are quite limited. The general change in bulk porosity on compaction is illustrated in Fig. 7. Compaction behavior is conveniently considered in four stages distinguished in terms of a range of pressure and predominant mode of densification.

1. Particle Sliding and Rearrangement without Fracture

The initial compaction is characterized by irreversible flow at applied pressures less than 100 psi for fine powders containing weakly agglomerated particles. Powder porosities on filling range typically between 0.8 to 0.95 for a bulky powder feed and between 0.6 and 0.75 for spray dried "granulated"

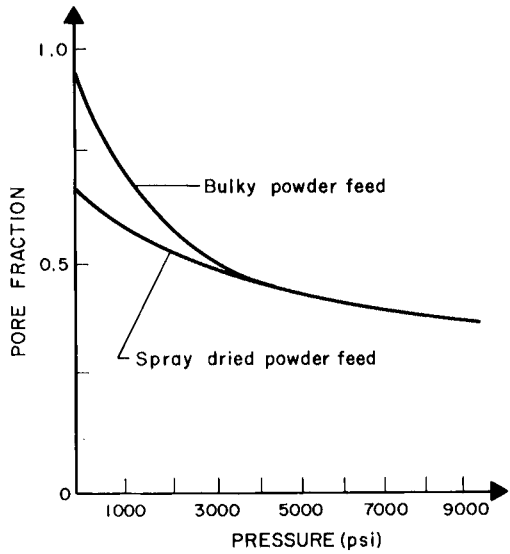

Fig. 7. Variation of compact porosity with punch pressure on dry pressing.

feed. Punch travel in this stage ranges between $\frac{1}{4}$ and $\frac{1}{2}$ of the total, depending on the porosity of the feed material. The escape of gas between the die and the punch causes "flashing" of the powder there, and compression of air in the pore phase can occur if the strain rate is high.

The evolution of the microstructure of the compact is quite different for granulated powders than for bulky powders. The particle packing in the granules and the cohesive strength of the granules can be quite important in controlling the pore structure and the degree of preferred orientation of particles at this stage in the compact.

2. Onset of Local Deformation and Fracturing of Particles at Points of Contact

Micron size particles have approximately 1 contact/particle pair and several points of contact per particle. With a continued increase in applied pressure, more intimate particle configurations are formed that can collapse only if local fractures occur at points of concentrated stress. In this stage the grain size/particle size, intergranular strength (particle is aggregate of crystallites), particle size and shape, and the modulus of elasticity (hardness) of the particle phase are quite important. Densification results for this stage typically exhibit a linear relationship between relative density and log pressure followed by a second linear dependence of density on log pressure but of greater slope (Fig. 8). The critical stress corresponding to the change

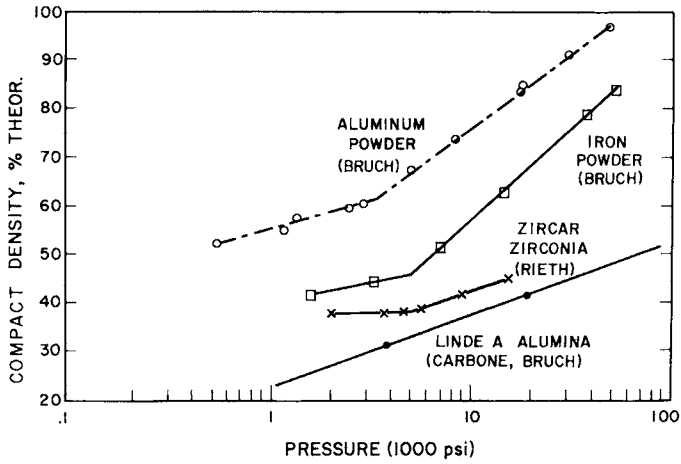

Fig. 8. Variation of relative compact density with log pressure.

in slope is interpreted (Bruch, 1967; Niesz *et al.*, 1972) as a qualitative index of the fracture stress of the particle (aggregate) leading to continued sliding and rearrangement; compaction studies appear to indicate the presence and relative strength of aggregates in powders. Compaction slopes for applied pressures exceeeding the critical pressure are similar for specimens of the same material phase with different powder character, whereas the initial compaction density is very sensitive to the powder character. Incremental fragments are observed to be a fraction of the size of the parent particles (Turba, 1965; Leiser and Whittemore, 1970). Powders with acicular particles typically exhibit higher compact porosities, and the compaction-pressure diagram for these powders may show two critical stress levels demarcating changes in the slope of density/log pressure (Leiser and Whittemore, 1970). Several compaction studies (Bruch, 1967; Lawrence, 1970) indicate that relative densities at an equivalent applied pressure are lower for powders containing particles with a higher Young's modulus of elasticity and Moh's hardness.

The increase in compact density with an increase in applied pressure is achieved principally from the elimination of the larger pores on particle rearrangement (Fig. 9); minor reductions in the volume of small pores are also observed (Carbone, 1973). The elimination of pores comparable to or larger than the particle size are of great importance in realizing maximal densities during "normal" sintering (Bruch, 1967; Kingery and François, 1967). Higher compact densities also reduce firing shrinkage and provide efficiencies in the sintering time or temperature.

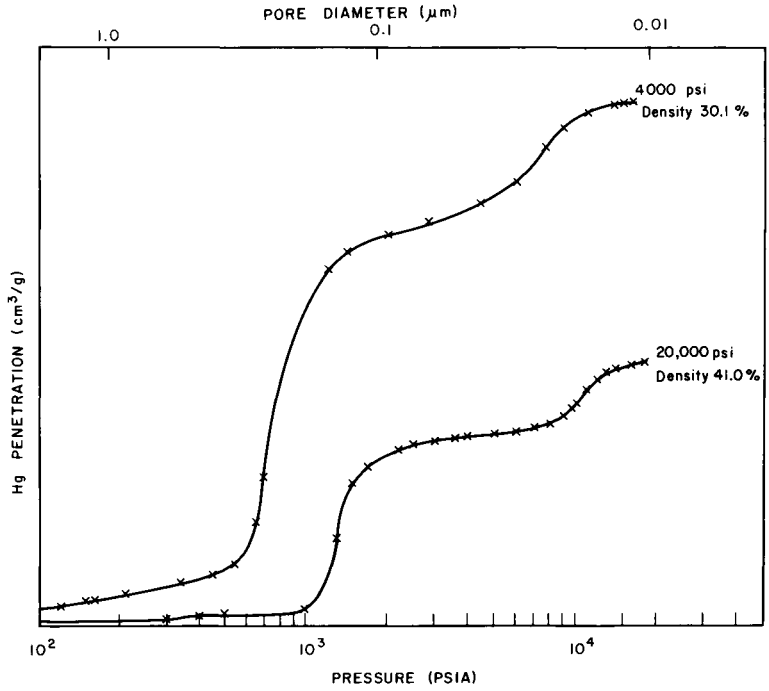

Fig. 9. Pore size distribution in compacts of Linde A® alumina (specimen density, pressing pressure indicated).

Adsorbed lubricants and binders as discussed in the preceding section can reduce interparticle frictional forces and improve compact strength if they are not easily extruded from interfacial regions. Bruch (1967) reported that additions of various lubricants up to 20 % did not aid in the compaction of submicron alumina powders. However, much empirical evidence suggests that minor additions of admixed lubricant first increase the density a few percent, but a relative maximum is quickly attained above which no further improvement is realized. Powder metallurgy compaction results (Winterberg, 1969) indicate that the optimum addition of lubricant correlates extremely well with the ratio of the die wall friction area/pressing area and the principal role of the lubricant is in reducing die wall friction (see Section IV below).

The affect of CO_2, O_2, N_2, H_2, and H_2O gaseous adsorbates on the compaction behavior of alumina powders has been examined and found to be insignificant on densification; in the presence of H_2O vapor, however, hard noncohesive granules are formed and the compaction is very unsatisfactory (Sturgis and Nelson, 1969).

3. Elastic Compression

In the range of pressure between 10,000 and 30,000 psi, the rate of particle fracturing and rearrangement drops significantly and the elastic strain energy density in the compact rises at an increasing rate. Relatively ductile particles such as KBr exhibit plastic flow in regions of concentrated stress and on compaction the slope of relative density/log pressure is much larger than those for typical ceramic powders. KBr specimens are routinely pressed to approximately theoretical density in evacuated dies at approximately 80,000 psi for specimens in IR spectroscopy. Differential elastic moduli for the powder and admixed phases and elastic anisotropy of "brittle" powder particles will cause inhomogeneous strain gradients with increasing applied pressure. These elastic strains are largely reversible and can lead to complications in controlling compact defects. The dry pressing novice quickly recognizes that the use of pressures in excess of some practical limit $\approx$ 30,000 psi for typical ceramics greatly maximizes the difficulty in realizing satisfactory compacts and increases die wear at an accelerated rate.

4. Ejection

On ejecting the pieces from the die, residual elastic strains are relieved (Poisson effect) and the dimensions of the piece increase as much as 1/2 %. Pore pressures are also relieved on ejection and entrapped gases must be vented slowly if the permeability of the compact is low. Lubricants can effectively drop ejection pressures from several thousand to several hundred psi. Since the compact is relatively weak in tension, relatively small stresses can cause fracture of the compact on ejection (see Fig. 2).

IV. Die Wall Effects on Compaction

A. Critical Compact Depth/Diameter Concept

Frictional forces between the compact and the die wall lead to characteristic stress gradients and density gradients in the compact. It is observed for single action compaction, using a particular die set and powder, that there is a critical compact depth below which no significant densification occurs. An insight into the significance of the die wall friction can be gained from the following approximate model (Fig. 10). The relation between the axial stress (P_a) and radial stress (P_R) on compression of an isotropic solid is

$$P_R = [\mu/(1 - \mu)]P_a \tag{1}$$

where μ is Poisson's ratio.

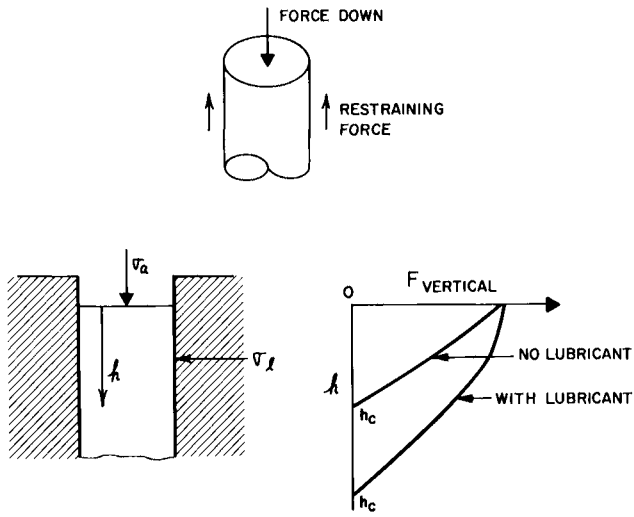

Fig. 10. Friction effects on compaction.

Assuming the compact to be an elastic solid, axial strain at a depth h_c can occur only if the restraining force at the die wall is exceeded by the normal force,

$$\begin{gathered} \text{force down} > \text{restraining force} \\ P_a(\pi/4)\ (\text{diameter})^2 > \pi\ (\text{diameter})\ h_c f P_R \end{gathered} \tag{2}$$

where f is the coefficient of friction at die wall.

$$P_a(\pi/4)\ (\text{diameter})^2 > \pi\ (\text{diameter})\ h_c f\ (\mu/1 - \mu)\ P_a \tag{3}$$

$$h_c < \text{diameter}/4f(\mu/1 - \mu)$$

$$h_c < \text{diameter for } f\ (\mu/1 - \mu) = 0.25$$

In practice $h_c \ll$ diameter for a uniform compaction.

B. Flow Gradients in Confined Compression

Flow gradients during compaction have been studied by introducing markers such as thin horizontal or vertical layers of a powder of differing color but similar compaction behavior on filling the die, and by introducing easily deformed lead grids in the die before filling and compaction which have a relatively high X-ray cross-section (Stuijts and Oudemans, 1965).

The powder flow is largely vertical but some horizontal flow has also been observed; the relative axial displacement decreases at points away from the moving punch; and greater axial flow is observed in the center than at regions close to the die wall.

C. Pressure Gradients on Compaction

The die wall friction that restricts flow on compaction causes pressure gradients and therefore density gradients throughout the compact. The assessment of the pressure fields is complicated in that the pressure sensor cannot interfere with the compaction process if reliable results are desired. External measurements have involved measuring punch pressures and die distortion for various die geometries (Duwez and Zwell, 1949; Huffine and Bonilla, 1962; Shank and Wulff, 1949; Spenser *et al.*, 1950; Walker, 1923). Direct methods include measurements of microhardness and density (Kuczynski and Zaplatnskyj, 1956; Unckel, 1945), the deformation of lead pellets dispersed in the compact (Kamm, 1947, 1948), and electrical readout of implanted electrical resistance gauges (Train, 1957). General pressure variations in a compact for single action pressing with die wall lubrication are illustrated in Fig. 11 for the pressing of magnesium carbonate (Train, 1957). The detailed form of the pressure fields depends on the compact geometry and die wall friction (Kuczynski and Zaplatnskyj, 1956).

On initial compaction, the maximum pressure occurs at the edges of the compact just below the flash at the punch–die interface and the applied pressure is directed diagonally into the depth of the compact. At some intermediate range of pressure (stage 2 compaction) the maximum pressure is still located at the top edges but a region of pressure lower than that along adjacent diagonals appears just below the center of the punch. Ulti-

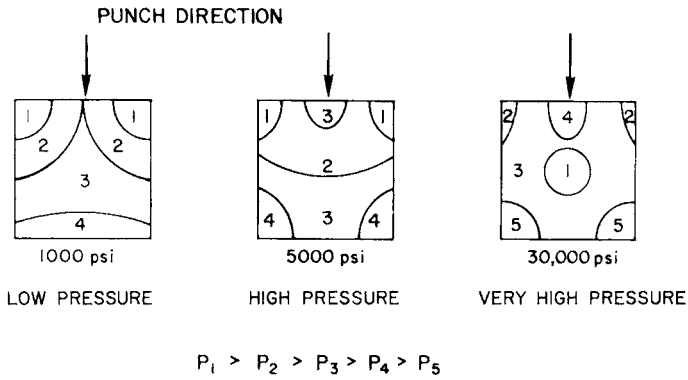

Fig. 11. Pressure variations in single action pressing of a cylindrical compact.

mately on approaching stage 3 compaction the maximum pressure appears at a depth below the center of the punch and the edges and region adjacent to the center of the punch are relatively lower. The effect of lubrication is to reduce the pressure gradients, effectively increasing the pressure near the bottom of the compact and reducing compaction density variations. The resolution of forces in the compact is often referred to as the Y-thrust. For the same compact geometry, it is clear that double action pressing and a floating die act to reduce pressure gradients.

V. Control of Defects in Compacts

Tensile strengths (diametral compression) of alumina compacts containing 1 wt % polyethylene glycol binder are reported to range from 400 psi on compaction at 30,000 psi to 800 psi on compaction at 60,000 psi (Claussen and Jahn, 1970). Fracture strength of powder metal compacts may be as much as one order of magnitude higher. In metal compacts the plastic flow of the metal particles contributes significantly to the strength, but in compacts of brittle powders mechanical interlocking of particles and short range attractions between molecular groups of absorbed polymer binders contributes the strength. The compact must have adequate strength to survive ejection intact and for handling prior to sintering. Thin cross sections, edges, and low density compacts are especially susceptible to fracture in handling. The dry pressing novice quickly learns that particular binders work better for particular compositions and an optimum proportion obtains for each powder and method of preparation.

The most common defect in dry pressing compacts is the laminations that appear on ejection. These are commonly perpendicular to the direction of punch travel and may not become apparent until the piece is handled or sintered. Pores with cusps at pore–particle junctions and pores associated with a lamination between "unbonded" particles are especially effective as stress multipliers. The interaction of stress fields active on ejection and the stress multipliers can lead to fracture planes in the relatively weak, brittle compact. Stress fields effective in the compact on ejection can arise for the following reasons.

1. Relaxation of elastic energies introduced in stage 3 compaction; the resolution of the stresses can be very nonuniform if density gradients are quite significant as at compact edges.
2. Stresses at the surface of the compact due to the frictional restraint of the die wall; during ejection, the unejected portion is more restrained and the center portion of the compact can expand at a greater rate than

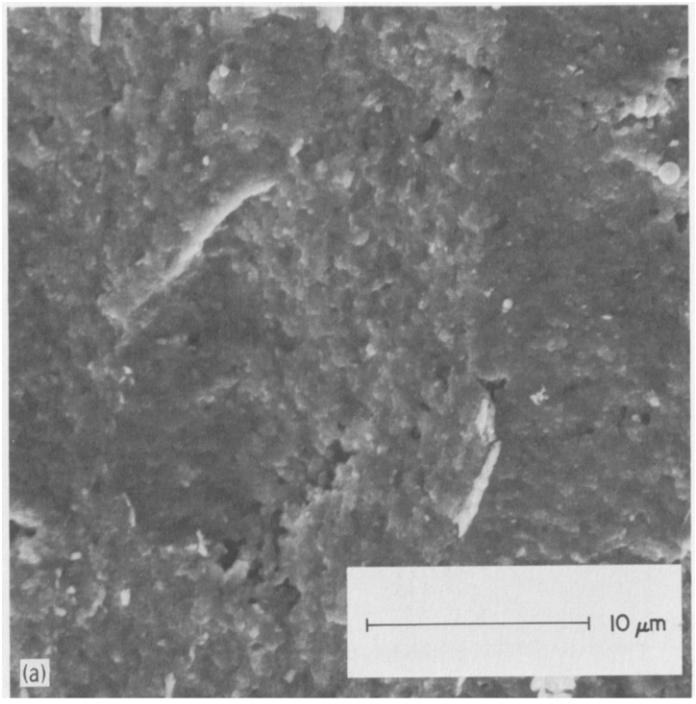
10 μm
(a)

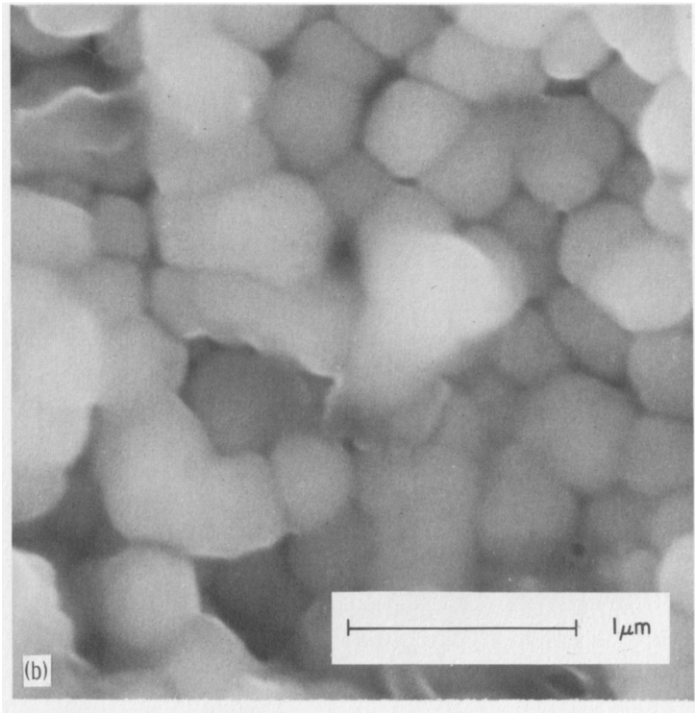
1μm
(b)

the near-surface region adjacent to the die wall (Long and Alderton, 1960).

3. Stresses imposed on the compact on recovery of elastic energy stored in the die during ejection (Long, 1963).

Laminations are minimized by improving the fracture strength of the compact and reducing the pressing pressures required. This is accomplished by improving powder characteristics, fill density, and die wall lubrication, and/or changing the die design and introducing a more effective binder system.

Cracks in the compact may also occur on ejection due to the escape of compressed gas in pores. It is reported (Long and Alderton, 1960) that very little gas escapes during the later compaction stages in metal powder compaction, and for each compact a threshold pressure must be exceeded to initiate cracks. Their studies indicated that the tendency for the formation of cracks increased for more rapid pressing to higher pressures in larger compacts. Characteristics that decrease the permeability of the compact, such as high volume fractions of polymer phases and smaller pore sizes, would also be expected to increase the tendency for gas pressure cracks.

High compact densities and minimal density gradients are usually preferred characteristics for ease in sintering to achieve the requisite fired microstructure. These characteristics are favored by using higher pressure, slower rates of pressure build-up and longer dwell times, higher densities of feed powder, use of lubricants, lower depth/diameter ratios, double action compaction, a floating die, and uniform fill depths for composite punch assemblies.

It has been observed that in the use of ultrafine powders (particle size $< 0.1\ \mu m$) for their high sintering activity, the compact fabrication becomes more difficult. Sintered compacts of these ultrafine powders often exhibit a very fine mottled appearance; inspection of the mottled regions indicates that their basis is coarse residual pores presumably remnants of nonuniform packing of aggregates (Bruch, 1967; Rieth, 1973; Berrin *et al.*, 1973). For an example, see Fig. 12. For these fine-grained microstructures the pores are of the optimum size for maximum scattering of visible light. Since the number of contacts per unit volume varies with $(\text{particle size})^{-3}$, compacts of ultrafine powders have high densities of points of restraint and many particles are very often aggregates of smaller grains. Complete breakdown of all aggregates is extremely difficult. The mottled texture can be eliminated by pressing at higher pressures (Bruch, 1967) and pressing with a higher moisture content (Rieth, 1973). Pressure gradients appear to be more severe in the ultrafine

◀ **Fig. 12.** Scanning electron micrographs of compacts of Zircar® zirconia: (a) clusters of coarse pores > 10 times grain size, (b) random pores < 5 times grain size.

powder compacts (Rieth, 1973) and die sticking is more of a problem (Rieth, 1973; Bruch, 1967). On die-sticking, a small spherical segment is often pulled away from the compact, as might be expected for the pressure field in stage 2 compaction. Die-sticking can be minimized by using very highly polished dies of a material with higher Young's modulus (Bruch, 1967).

VI. Simplified Pressing Program

A simplified dry pressing program usually comprises the pressing of a simple shape such as a disk or preferably a shape more similar to the desired part. The powder, mixed with the chosen binder system, is examined for its flowability and granulated if necessary. Several parts are then pressed at a series of pressures from low pressures, producing compacts with just enough strength to remain whole, to high pressures, producing compacts which just begin to laminate.

The relationship between the applied pressure and the green density of the compacts is measured roughly from their weights and geometric volumes. In most cases the conditions a. chosen that produce parts with the highest green density without laminations or other compaction defects, since these conditions achieve the highest fired density during sintering. However, there are other sintering phenomena to consider, such as the attainment of certain microstructural characteristics. Therefore, any pressing program should be coordinated with the desired firing or sintering schedule.

When the optimized pressing and firing schedules are achieved, the final dry press tooling necessary to obtain the exact dimensional tolerances can be specified from the firing shrinkages. As discussed earlier, more complicated shapes would require a more rigorous pressing program.

References

Berrin, L., Johnson, D. W., Jr., and Nitti, D. J. (1972). *Amer. Ceram. Soc., Bull.* **51**, 840–844 and 896–900.

Bruch, C. A. (1967). *Ceram. Age* 44–53.

Carbone, T. (1973). Progress Report. M.S. Thesis, Alfred University, Alfred New York.

Claussen, N., and Jahn, J. (1970). *Powder Met. Int.* **2**, 87–90.

Cowan, R. E., and Ehart, E. P. (1966). *Amer. Ceram. Soc., Bull.* **45**, 535–538.

Duwez, P., and Zwell, L. (1949). *J. Metals* **1**, 137–144.

Helsing, H. J. (1969). *Powder Met. Int.* **1**, 62–65.

Hirschhorn, J. S. (1969). "Introduction to Powder Metallurgy." *Amer. Powder Met. Inst,* New York.

Hoffman, E. R. (1972). *Amer. Ceram. Soc., Bull.* **51**, 240–242.

Huffine, C. L., and Bonilla, C. F. (1962). *AIChEJ* **8**, 490–493.

Kamm, R. (1947). *Trans. AIME* **171**, 439–456.

Kamm, R. (1948). *Trans. AIME* **180**, 694–706.
Kingery, W. D. (1958). *In* "Ceramic Fabrication Processes" (W. D. Kingery, ed.), pp. 55–61. Wiley, New York.
Kingery, W. D., and François, B. (1967). *In* "Sintering and Related Phenomena" (G. C. Kuczynski *et al.*, eds.), p. 471. Gordon & Breach, New York.
Kucyznski, G. C., and Zaplatnskyj, I. (1956). *J. Metals* **8**, 215.
Lawrence P. (1970). *J. Mater. Sci.* **5**, 663–668.
Leiser, D. B., and Whittemore, O. J., Jr. (1970). *Amer. Ceram. Soc., Bull.* **49**, 714–717.
Levine, S. L. (1969). *Amer. Ceram. Soc., Bull.* **48**, 230–231.
Long, W. M. (1963). *In* "Special Ceramics 1962" (P. Popper, ed.), p. 327. Academic Press, New York.
Long, W. M., and Alderton, J. R. (1920). *Powder Met.* **6**, 52–72.
Motyl, E. J. (1963). *West. Elec. Eng.* **7**, 3–11.
Niesz, D. E., Bennet, R. B., and Snyder, M. J. (1972). *Amer. Ceram. Soc., Bull.* **51**, 677–680.
Pincus, A. G., and Shipley, L. E. (1969). *Ceram. Ind.* **92**, 106–109 and 146.
Rieth, P. (1973). M.S. Thesis, Alfred University, Alfred, New York.
Shank, M. E., and Wulff, J. (1949). *Trans. AIME* **185**, 561–570.
Spencer, R. S., Gelware, G. D., and Wiley, R. M. (1950). *J. Appl. Phys.* **21**, 527–531.
Stuijts, A. L., and Oudemans, G. J. (1965). *In* "Fabrication Science," pp. 81–99. *Brit. Ceram. Soc.* Stoke-on-Trent, England.
Sturgis, D. H., and Nelson, J. A. (1969). *J. Amer. Ceram. Soc.* **52**, 286.
Thurnauer, H. (1958). *In* "Ceramic Fabrication Processes" (W. D. Kingery, ed.), pp. 62–70. MIT Press, Cambridge, Massachusetts.
Train, D. (1957). *Trans. Inst. Chem. Eng.* **35**, 258–266.
Turba, E. (1965). *In* "Fabrication Science," pp. 101–115. *Brit. Ceram. Soc.*, Stoke-on-Trent, England.
Unckel, H. (1945) *Arch. Eisenhuttenw.* **18**, 161–167.
Walker, E. E. (1923). *Trans. Faraday Soc.* **19**, 73–82.
Waye, B. E. (1964). *J. Brit. Ceram. Soc.* **1**, 387–384.
Winterberg, F. (1969). *Powder Met. Int.* **1**, 29–32.

Hot Pressing

M. H. LEIPOLD

Jet Propulsion Laboratory
California Institute of Technology
Pasadena, California

I. Introduction

The term "hot pressing" as a fabrication procedure describes the enhancement of densification by coincident application of external pressure with temperature. This pressure serves to augment the normal driving force for densification (reduction of internal surface area). The increased rates of

densification may permit practical firing times while the temperature is much lower than normally required. Hot pressing is accomplished by placing a loose powder or a compacted preform in a suitable chamber and applying pressure from one or more directions while the entire system is held at an elevated temperature. After densification (by means of one or more physical mechanisms), the part is cooled, the pressure released, and a finished form removed.

The selection of hot pressing as a desirable procedure is usually based on the need for very stringent microstructural control in addition to the requirement of high density. In many cases, hot-pressing is selected as a means of varying the microstructure over a wide range while attempting to maintain uniform starting materials and thermal history. In contrast to this rather broad, flexible control of microstructure, hot pressing is, in general, expensive, time consuming, and rather limited in the variety of shapes that can be processed.

A particularly important microstructural feature that may be controlled by hot pressing is grain size. Ceramics produced by other methods normally exhibit grain sizes of 20 μm or greater, and it is only with the use of grain growth inhibiting additives that grain sizes of less than 10 μm can be produced in high density compacts. However, with hot pressing, grain sizes of a micron or less and in some cases, less than 0.1 μm are achievable. In addition, conventionally sintered single phase ceramics can normally be considered to be in a reasonable state of physical equilibrium and chemical homogeneity while hot pressed ceramics in general are not.

A number of specialized procedures including linear, isostatic, pseudoisostatic for hot pressing are in use. Linear hot pressing is by far the most common and is usually accomplished by placing the powder in a suitable cylindrical cavity and applying pressure by means of rams, which provide force in one direction. The selection of materials, powders, and conditions for this technique will be extensively discussed here. In addition to this procedure, the other forms of hot pressing will also be presented but to a more limited extent.

In an attempt to provide applications of the principles described here adequately, two examples will be presented. To relate the selection of appropriate hot pressing procedures most conveniently, each section will first present the selection principles and then indicate the use of those principles with the two examples.

The two materials that will be described are magnesium oxide and tantalum carbide. The first of these, magnesium oxide, is a typical oxide ceramic, widely used as a research material, and has commercial application in refractories and in optics. The material being fabricated in this case was to be a high density, high purity, fine grained specimen to be used in studies of mechanical properties. The selection of hot pressing was based on the require-

ments of high density and fine grain sizes. The desire to retain high purity eliminated the possibility of using grain growth inhibition methods. Further, since the application was research, the high cost associated with hot pressing was not critical. One characteristic of magnesium oxide that would influence its behavior during hot pressing is its high stoichiometry, and thus solid state processes such as diffusion would be little influenced by reactions with the environment. However, the oxide is highly susceptible to reactions with the atmosphere (CO_2, H_2O) and is known to be somewhat volatile especially in conjunction with these atmospheric contaminants.

The second example involves the preparation of fine-grained tantalum carbide specimens for a variety of physical and mechanical property measurements. Again, a desire to control grain size, density, and purity dictated the initial choice of hot pressing as a fabrication procedure. This carbide is typical of the refractory metal carbides and exhibits wide variations in stoichiometry. Hence, its solid state processes could be expected to vary widely with changes in atmosphere, initial particle composition, and contamination.

II. Uniaxial Hot Pressing

Uniaxial pressing is by far the most commonly used form of hot pressing and has been developed to where it has found significant commercial application as well as applications in research and development (see Fig. 1a,b). The system for linear pressing can be quite simple and straightforward; however, systems tend to be more complex with increasing temperatures, pressures, and material reactivities.

The use of linear pressing introduces severe limitations to available specimen geometries since only right parallelepiped sections can be accommodated. Further, pressing becomes increasingly difficult as the height L of the section increases with respect to its perimeter (usually diameter D (of a cylindrical section). When L/D is less than 1, difficulties are few (Dombravo *et al.*, 1963), but as L/D increases to between 1 and 3, problems with die wall friction, ram motion, and pressure distribution becomes substantial. L/D of greater than 3 can be accomplished with only the most refined and highly developed techniques. In lieu of such long sections hot press welding of two previously pressed compacts can prove effective.

In this section the various materials, equipment, and procedures for producing linear hot pressings will be presented. In many cases they are not unique to linear hot pressing but are presented here because this is the most common form of pressing.

Fig. 1. (a) Hot pressed B_4C body armor plate. Courtesy Norton Co., Worcester, Massachusetts. (b) Hot pressed transparent polycrystalline MgO 0.25 inches thick. Courtesy AVCO Systems Division, Wilmington, Massachusetts.

A. Equipment

The equipment required to conduct uniaxial hot pressing varies widely from the simple units consisting of a furnace contained in a small press to more complex highly instrumented facilities (see Fig. 2). Some used in research are capable of monitoring and precisely controlling the time, temperature, pressure, and environment, while large units used commercially are capable of applying loads of several hundred tons to compact extremely large specimens (see Fig. 2b). The first requirements in the selection of development of an appropriate facility are the approximate temperatures and pressures. Most uniaxial hot pressing is done in the range of 2000–25,000 psi and this, along with the specimen cross-sectional area, dictates the press capacity. Limited efforts have explored pressures above this (Kalish and Clougherty, 1969a,b; Vasilos and Spriggs, 1965). Control requirements on the pressure are not stringent, with 10 % variations in pressure during compac-

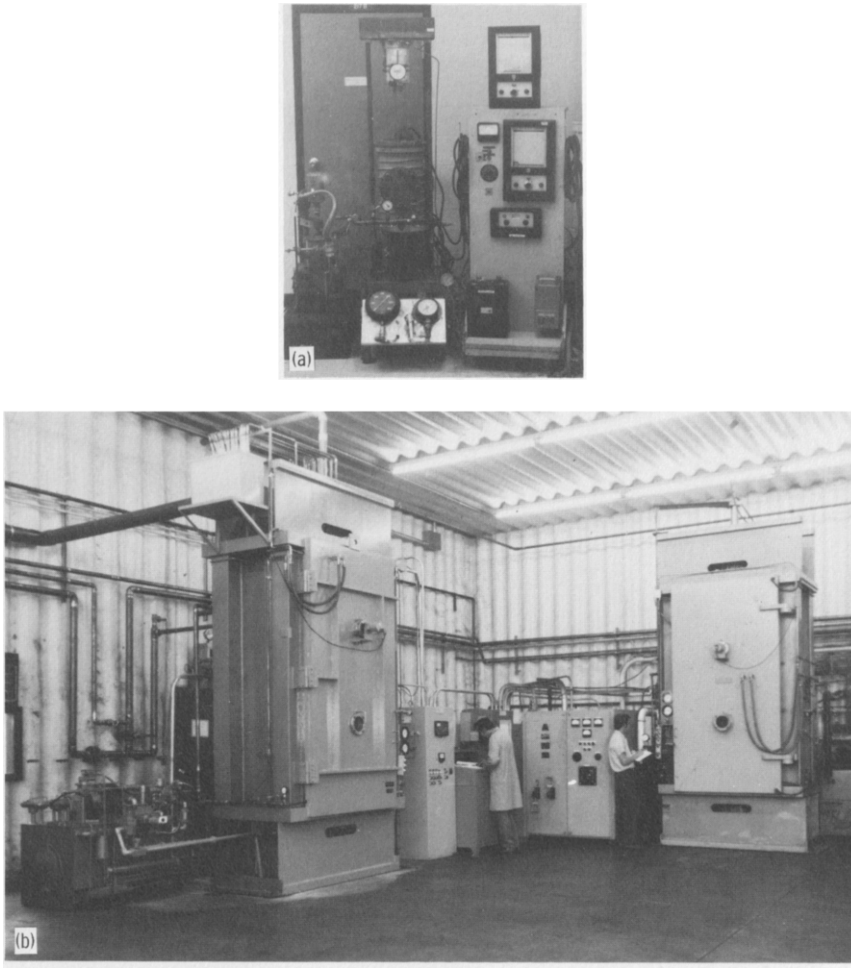

Fig. 2. (a) Research hot press; 1200°C, 14,000 lb, controlled atmosphere, heating and cooling rates, size = 3/4 in. diameter × 2 in. high. (b) Industrial hot press; 3000°C, 400,000 lb, carbon atmosphere, size = 20 in. diameter × 36 in. high. Courtesy Boride Products, Inc., Traverse City, Michigan.

tion being entirely satisfactory. Only when studies are being made of the compaction process itself is closer control desirable. Simple hydraulic systems are the most widely used, and a typical system is outlined in Fig. 3. The use of the air–oil intensifier rather than a hydraulic pump offers the advantage of quiet operation and convenient control. The regulator on the air supply permits convenient setting of the maximum desired pressure, and the throttle

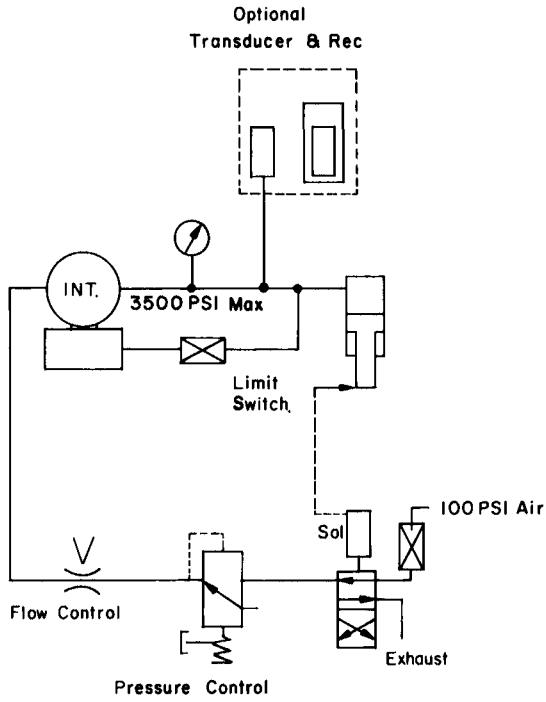

Fig. 3. Typical hydraulic system for hot press.

valve controls the rate of ram travel. The limit switch, set slightly beyond expected ram travel, may be used to detect rapid motion following a die or ram failure and to shut off and exhaust the supply air to the intensifier, thus stopping the system. Measurement of applied load to the hot pressing may, of course, be easily obtained by including the optional pressure transducer and recorder. In most situations, however, this type of record is not required.

The second primary variable in hot pressing is the required temperature. This is dictated primarily by the physical properties of the powder being pressed. These properties will be discussed more thoroughly in Section II, 2, b. Also of importance is the environment required either for a particular powder being pressed or for the die, punch, and heater materials being used. The latter often introduces environmental requirements such as nonoxidizing conditions which are not required for the powder.

As an initial guideline, the pressing temperature can be taken as one-half the absolute melting point T_m of the material being pressed (or one-half the lowest eutectic in multiphase systems). This approximation, of course, can be refined with more detailed analysis. In some cases, the required temperature is as high as 0.6 T_m. Having thus arrived at an approximate figure for

required temperature, the furnace design consistent with this temperature can be made.

The heating method is usually either conventional resistance wire or induction, although direct resistance heating through conductive rams and powder charge has been employed (Vasilos and Spriggs, 1965). The choice between resistance and inductive heating is largely a matter of convenience and equipment availability, and inductive coupling has found extensive use with graphite systems.

The materials of construction depend primarily on the temperature range of operation. The lower temperatures (up to 1200°C) can be achieved by conventional chrome–nickel–iron or nickel–chrome–iron–aluminum alloys. Even when nonoxidizing conditions are required in the heating chamber, the required oxidation of the heating elements can be achieved by a preliminary heating in air. For temperatures above 1200°C, silicon carbide (to 1600°C), refractory metal (to 2800°C), or graphite (to 3000°C) heaters have found use. Platinum base systems can be used but are expensive to replace if a pressing component should fail and damage the furnace. In all cases the furnace and heater design should be kept as simple and inexpensive as possible. The mass of the hot pressing die considerably reduces the temperature gradient experienced by the compact. Sophisticated approaches to controlling the temperature distributions are not required, except in the case of unusually long (greater than 3 to 1) L/D configurations (Hausner, 1958). The heater should be kept close to the die to improve heat transfer and reduce energy loss. This, coupled with the likelihood of brittle or semi-brittle failure in the die or rams, not infrequently damages the heating system. Over-design of the strength of die and ram components is, of course, helpful but is often not sufficient.

Temperature control in the hot pressing chamber can be normally obtained by conventional means. Control systems capable of approximately $\pm 1\ \%$ precision are entirely suitable since the mass of the hot pressing die serves to reduce fluctuations in the compact. It should be emphasized, however, that the temperature experienced by the compact may be considerably less than that indicated by the heating element. With furnaces of the order of 3–8 in. in diameter, temperature differences of 50°–75°C or higher may easily occur. It is recommended that a calibration check be made using a thermocouple buried within a compact during a dummy run.

It is frequently desirable to include a temperature programming system as part of the temperature control function. Control of the rate of temperature change is often as critical as control of its absolute value. It is important in control and maintenance of the appropriate environment in the pressing chamber, in the thermomechanical compaction properties of the compact, and in the life of the ram and dye components. These are discussed in greater

detail in later sections. Requirements for programming vary from simple linear control to quite sophisticated requirements (Section II, 2, e).

A process variable that is frequently measured during uniaxial pressing is the amount of compaction or ram travel. Although measurement of this variable is not required in routine operation, it is frequently very useful for trouble shooting, evaluation, and improvement of the process. Measurement of the total compaction (as a function of time) may be easily made by a simple linear potentiometer attached externally to the pressure ram. Because of its simplicity and usefulness, it is recommended for all but the most routine operations. The other equipment requirements are highly variable and vary from essentially nothing to sophisticated powder processing facilities for toxic, radioactive, and reactive materials.

For the hot pressing of very fine grain magnesium oxide, the press shown in Fig. 2a was ultimately developed. Initial consideration of the temperature requirements (one-half the absolute melting point = 1280°C) and a desire for an extremely fine grain size (suggesting minimum pressing temperatures) indicated that conventional iron base heaters would be suitable. These also introduce no environment requirements of their own. Commercial performed semicircle heaters were used because of their low cost and ease of replacement.* Temperature control was achieved with strip-chart proportioning controller, and programing was incorporated by attaching a reversible clock drive motor to the control point mechanism. This drive motor was energized through a percent-on timer allowing maximum temperature to be obtained in periods ranging from 1 to 20 hours. Power input to the furnace was proportioned through a magnetic amplifier and saturable reactor.

The nominal requirement for hot pressing, based on a 2 cm diameter specimen size, would range up to 10,000 pounds and since it was desirable to use maximum pressures to achieve the minimum grain size a 7-ton pressure ram was selected. The system is shown in Fig. 2(a). A linear transducer was included to monitor the ram position on a strip chart.

The development of the system for hot pressing tantalum carbide was developed in anticipation of specimen sizes of up to 1 3/4 in. diameter and pressures up to approximately 10,000 psi. A 20,000 pound capacity was selected as being minimum suitable. A furnace chamber approximately 6 in. diameter was then dictated.

Taking the temperature requirement of one-half the absolute melting point (1850°C), a graphite or refractory metal heating system was indicated and since the densification of tantalum carbide was anticipated to be variable because of possible stoichiometry changes, maximum operating temperatures of approximately 2200°–2300°C were selected to allow for possible variation.

* KSP Lindberg Division Sola Basic Industries, Watertown, Wisconsin.

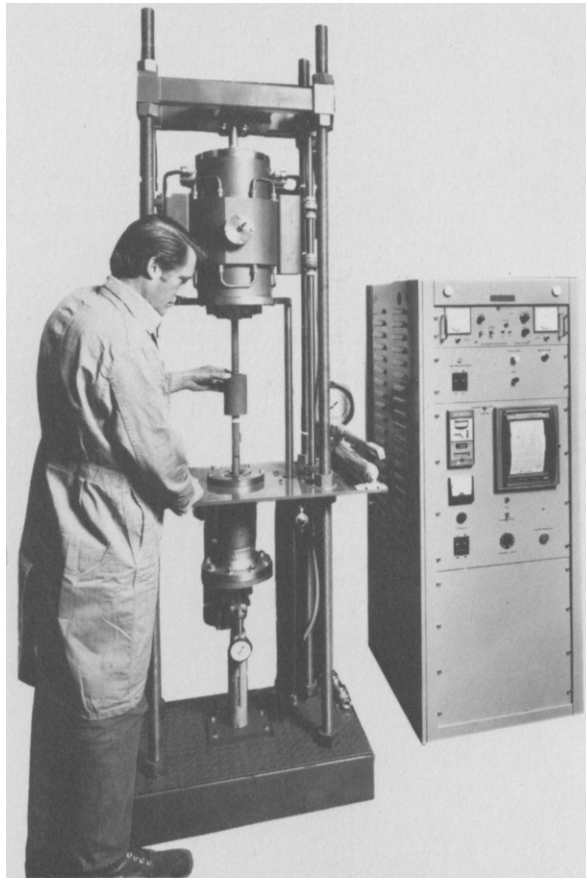

Fig. 4. Commercially available hot press; 2500°C, 20,000 lb, 10^{-5} torr vacuum, heating and cooling rates, size = 3 in. diameter × 3 in. long. Courtesy Astro Industries, Santa Barbara, California.

The chamber heater material was graphite, with the lower cost of graphite systems as the primary consideration. The general compatibility of carbides with carbon materials was a consideration although stoichiometry changes could be produced in the carbide by interaction with the graphite system.

The detailed design and construction of the system was handled commercially with a three phase star configuration graphite heater energized through 3 single-phase silicon control rectifier systems. Linear ramp control of heating and cooling rates was again included as previously described.

The design of a system at these power levels and especially involving high

vacuum operations would perhaps prove difficult for most materials investigators. Unless considerable expertise were available, effort should be directed toward obtaining a complete package unit from a reputable manufacturer. That approach was used here and the completed unit is shown in Fig. 4.

B. Selection of Starting Powder

The choice of starting material that is to be compacted by hot pressing is extremely wide. A decision must be made first as to whether the compositions of the starting material and final product will be essentially the same or whether the starting and end point compositions will differ with decomposition or interactions occurring. Since the basis for selection differs considerably with these two methods, they will be discussed separately.

When the starting and ending phase structures are the same, the densification occurs by normal sintering mechanism, and the details of the initial particle configuration are critical. Most conventional theories (Section II, 2, d) suggest fine particles, since this reduces the average distance each atom must move for densification. However, the use and handling of ultrafine particles introduces a number of difficulties; often they are reactive, even pyrophoric in case of nonoxides, and the large surface area contributes adsorbed contamination resulting in significant impurity levels in the final compact (Nielsen and Leipold, 1966). For these reasons powder particle sizes in the range of 0.1–1 μm are probably the most effective.

The problem of surface contamination has been amply demonstrated (Rice, 1969b). Others have been made to reduce the effects of particle surface contamination by appropriate washing prior to hot pressing. Isopropyl alcohol has been reported (Rossi and Fulrath, 1965) to be beneficial as well as absolute ethanol (Leipold and Nielsen, 1966). The mechanism of such improved densification remains unclear.

Although factors of particle size distribution and particle geometry undoubtedly play a role in the attainment of final hot press characteristics, little information is available on systematic experimental studies of their effects. In part this lack stems from the inability to systematically vary these characteristics while holding other material characteristics constant.

The purity and homogeneity of the starting powder are critical both to its final characteristics and to its behavior during hot pressing. Because hot pressing is accomplished at temperatures at which atomic motion is rather limited, the initial homogeneity in the starting powders tends to remain. Figure 5 shows a calcium agglomerate in hot press magnesium oxide. The source of this particle is not known and the total calcium concentration in the bulk magnesium oxide is of the order of 200 parts per million.

Another variable in hot pressing related to the chemistry of the starting and

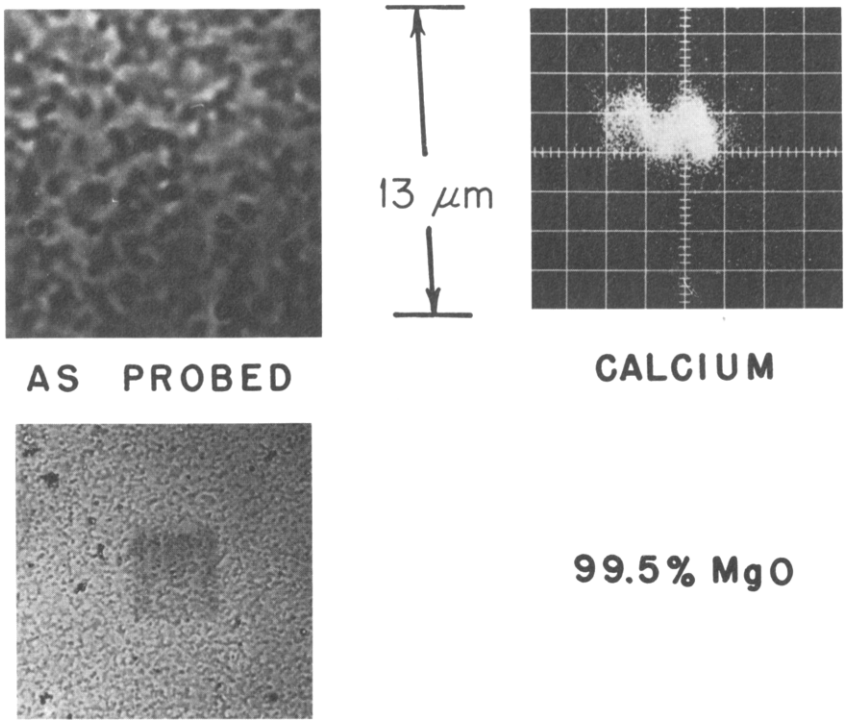

Fig. 5. Ca agglomerate in hot-pressed MgO. From Leipold (1966).

finished compact is the stoichiometry. Control of this material characteristic is especially important since it frequently controls the particular densification mechanism. An excellent example of the results of this kind of effect may be seen with tantalum carbide in which up to one fourth of the carbon atoms may be missing. Results of this effect on the density under comparable high pressing conditions is shown in Fig. 6. These variations in stoichiometry may be nonhomogeneously distributed within the powder. This effect is shown in Fig. 7. Control of these chemical parameters both as to bulk and distribution is exceedingly difficult but is necessary to the hot pressing technique. Only when starting powder character is closely controlled, or at least maintained constant by uniform processing, can repetitive successful hot pressing be made.

The selection of starting material is considerably altered when this material is to undergo considerable reaction during the densification process. This procedure, generally described as reactive hot pressing is typified by the

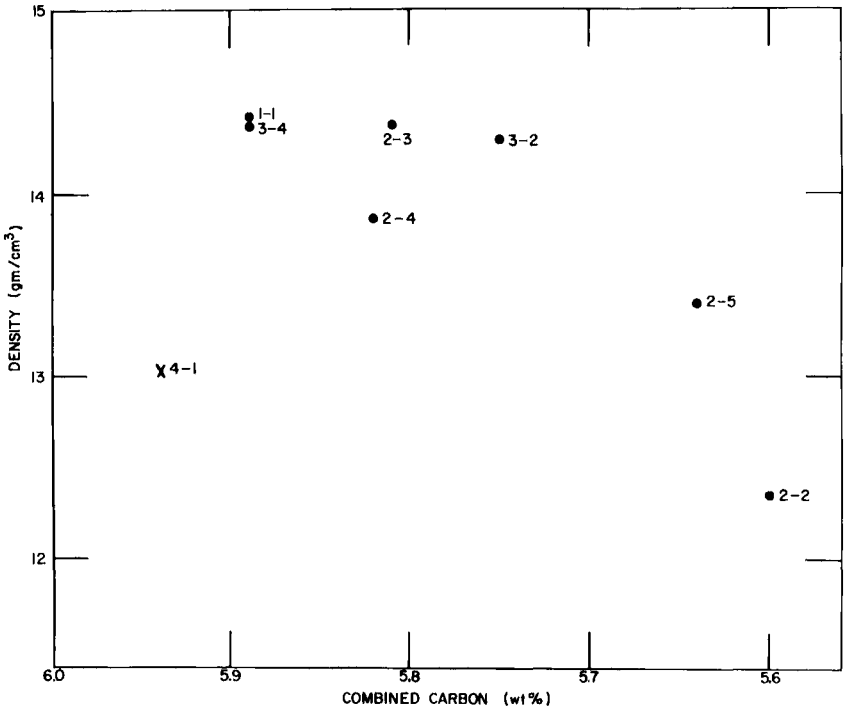

Fig. 6. Density versus carbon content for TaC_{1-x} after hot pressing at 1865 ± 50°C, 6500 psi for 1 hr. TaC = 6.20 wt% C. Numbers represent different manufacturing lots of powder. From Leipold and Becher (1970).

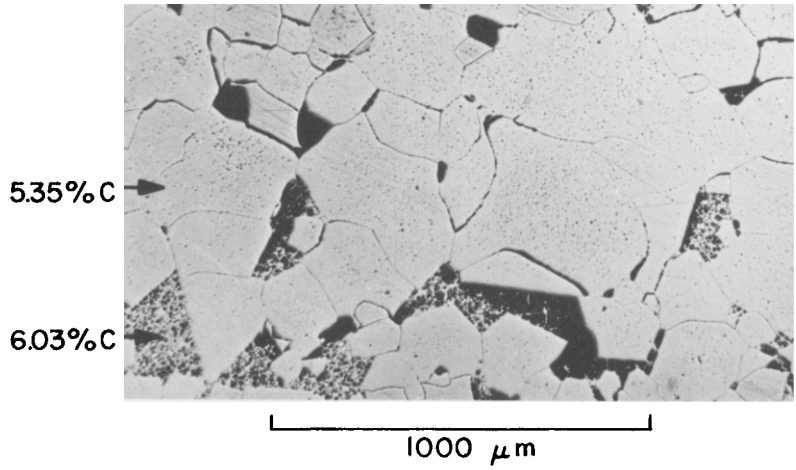

Fig. 7. Hot pressed TaC shows variations in carbon content as determined by electron beam microprobe. Pressing conditions were 1915°C at 6500 psi for 1 hr, density = 99.7%.

reaction of one or more components ZrC + TaC → (Zr, Ta)C solid solution (Shigetomo, 1970) or decomposition of a compound to provide a reactive solid phase and a volatile phase (Zisner, 1967) ($Mg(OH)_2 \rightarrow MgO + H_2O$). In such cases enhancement of densification rates is proposed by means of compounds existing in activated states. However, in the former case, the problem of homogenization of the final phase structure is often difficult. Fine particle size, very thorough mixing, freeze drying (Gazza, 1972), or co-precipitation (Okamoto *et al.*, 1969) are often useful. The attainment of homogeneity often requires either more extensive heating during the pressing or by postpressing heat treatment. This can negate the higher reaction rates achieved during the activated pressing. However, convenience in obtaining unreacted starting materials can justify use of this method.

With hot pressing employing decomposition reactions, homogeniety is not a problem, but other problems occur with extraction of the volatile decomposition products. The environment within the die chamber has very little relationship to that within the furnace chamber. Hence, considerable pressures of volatile impurities may be maintained, especially with nonporous dies such as alumina or refractory metals.

Further, the nature of these volatile species (OH, CO_2, S, NO_3) respond poorly to chemical analyses in these hot pressed refractory materials and their presence is often overlooked. When this problem of volatile constituent removal can be minimized by use of porous dies (graphite), slow heating rates, then the approach may prove superior. Although the chemical nature of the starting compound is critical, its physical nature is not and although minor variations in response undoubtedly occur, selection may be based on cost, purity, and availability.

There have been reports (Chaklader and McKenzie, 1966) of enhanced densification at the temperature of a phase transformation

$$ZrO_{2mono} \rightleftarrows > ZrO_{2tetr}.$$

However, the existence of such a transformation at an appropriate temperature cannot be controlled in fabrication of a particular system and the magnitude of the enhancement is not well documented.

The attainment of high density during hot pressing can be augmented by the use of hot pressing additives. For example, a powerful means of improving the hot pressing response of MgO is through the addition of small amounts (approximately 1 %) of lithium fluoride. Table I shows some comparative results for magnesium oxide pressed with various halide additions. The MgF_2 data are included for comparison; it is not considered an aid. Again, the decision to use such additives must be given careful consideration. Of primary importance is the effect on the desired application of the additive remaining

TABLE I

DENSIFICATION OF MgO BY HOT PRESSING

Additive	Die type	Temp (°C)	Pressure (ksi)	Time (min)	Density (g/cm^3)	Reference
2 % LiF	Graphite	970	4	10	3.56	Rice (1969b)
2 % NaF	Graphite	1040	4	10	3.53	Rice (1969b)
None	Graphite	1315	5	15	3.56	Rice (1969b)
None	Al_2O_3	1000	15	30	3.55	Leipold and Kapadia (1973)
1 % MgF_2	Al_2O_3	1050	15	30	3.35	Leipold and Kapadia (1973)

in the final compact. The quantity of lithium fluoride remaining in magnesium oxide after pressing can be reduced by appropriate heat treatment (Rice, 1969a). The remaining additive does affect behavior, but the mechanism of such affect is unclear.

In contrast, nickel and cobalt hot pressing additives to refractory carbides are not easily removed and would deteriorate high temperature behavior. However, in their major application of room-temperature hardness, no serious losses are noted. Second, there are no universal hot pressing aids and while the halides have been often useful with many oxides and metals with the refractory carbides, selection of the appropriate additive and the required amount, particularly with the fabrication of a new material, can be a research

TABLE II

DENSIFICATION AIDS FOR HOT PRESSING

Matrix	Aid	Reference
MgO	1–3 wt % LiF, NaF	Rice, 1969; Benecke *et al.*, 1967; Carnall and Hatch, 1967 Rice, 1971
CaO	1–3 wt % LiF, NaF	Rice, 1969b
Al_2O_3	1–2 wt % LiF	Rice, 1969b
ThO_2	10–25 at % F	Stuart *et al.*, 1972
BeO	0.5 % Li_2O	Hendricks, 1970
UC, TaC	1–20 % U, Co	Stoops, 1969
TaC, TiC, WC, ZiC	1–1000 % Fe, Ni, Co, Mn	Kose *et al.*, 1967
Si_3N_4	1–3 wt % MgO	Deeley *et al.*, 1961
ZrB_2 TiB_2	1–10 % Ni, Cr	Kinoshita, 1967 Hamano *et al.*, 1966

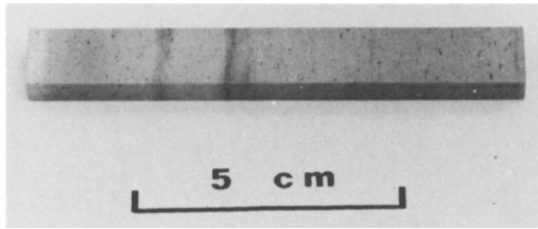

Fig. 8. Rectangular bar slice from Al_2O_3 cylinder originally 4 cm diameter × 10 cm long. Black bands and spots result from carbon contamination but are *not* visible in microstructure. Density = 3.98 gm/cm^2.

task in itself. Table II lists several successfully developed hot pressing aids which may aid a potential user.

The method of placement of the powder within the die can involve simply pouring loose powder into the cavity and applying nominal ram pressure (~ 1000 psi) to hold the charge in place. This method encounters difficulty with fine powders whose cold pressed density may be only 20–30 %, where to produce a 1 in. long specimen, a 5–6 in. long die would be required and large ram travel (with friction) would be encountered. Further, if graphite dies are being used, and the ram must be removed to add more powder charge, dusting of graphite will occur, leaving a carbon-rich line (black in the case of oxides). The effect of such a region is unclear (see Fig. 8).

More efficient powder charging can be obtained by pre-pressing the powder at room temperature to high pressures (~ 50,000 ksi) either in a high strength die or isostatically. Care must be taken, however, to prevent excess pressure to the preform during heating to hot pressing temperature. Any fractures in the compact tend to remain as low density regions in the final densified part (see Fig. 9).

The magnesium oxide powders hot pressed in these examples are extensively described elsewhere (Leipold and Neilson, 1966). They consisted of (1) a commercial powder, nominally 0.1 μm in diameter and approximately 99.5 % pure, and (2) specially prepared high purity (99.95 %) powder prepared from decomposition of hydromagnesite. The latter was available in a range of particle sizes controlled by the decomposition temperature. In general, however, approximately 0.1 μm appears to be optimum. Densification of both powders could be enhanced by alcohol wash; however, the high purity powder could be pressed to theoretical density (4 μm grain size) at 900°C and 10 kpsi while the less pure material required 1100°C (0.3 μm grain size). The difference in behavior was generally related to purity differences but not to specific concentrations. The powders were isostatically prepressed

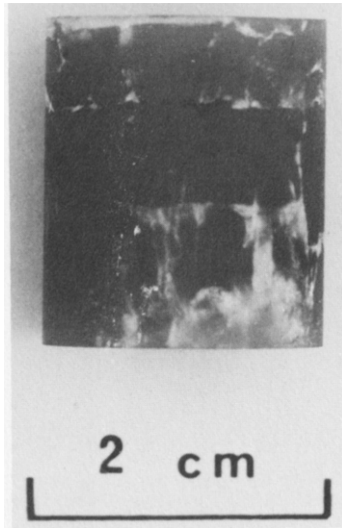

Fig. 9. Preform fractures in hot pressed translucent MgO. Fractures are visible in microstructure as low density regions.

at 75 ksi and machined to fit the dies. Prepressing was required to obtain greater than 3 cm finished length.

With the tantalum carbide, all materials were commercial and detailed results are available (Leipold and Becher, 1970) and ranged in size from 0.01 to 1 μm for various sources and lots. Although the size was important in behavior, even greater variations existed for powders nominally the same. The results demonstrate the susceptibility of the hot pressing technique to variations in detailed powder chemistry in that full density was obtained at 1600°C with a specific batch of powder, while a second batch of powder of the same nominal specification did not yield full density at temperatures as high as 2100°C (see Fig. 10a,b). The variability was in part explained by powder stoichiometry (see also Fig. 6) with other unexplained factors remaining. Here the powder was merely cold compacted in place at 2000 psi.

C. Ram and Die Materials

The selection of the proper ram and die materials for hot pressing applications is perhaps the most critical part of the system design. A number of features must be considered: (1) reactivity between the die and powder to be pressed, (2) mechanical properties—creep strength, ultimate strength, and mode of failure, (3) thermal expansion as compared to the densified compact,

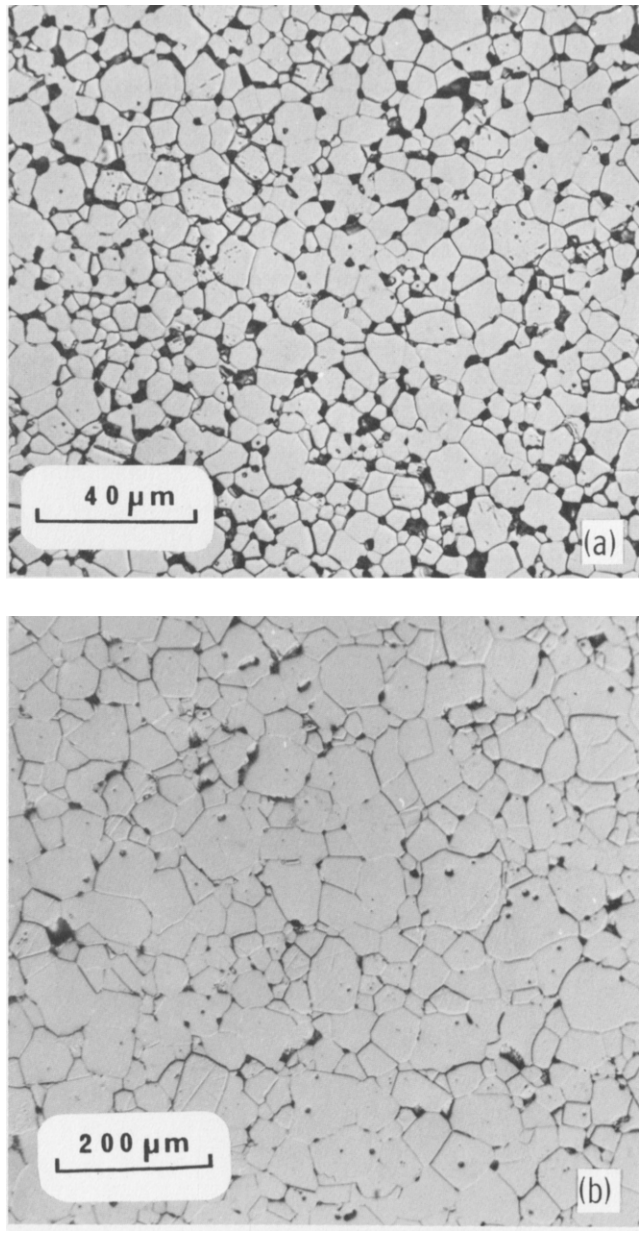

Fig. 10. TaC of nominally the same composition and nature showing porosity and grain size differences after hot pressing. From Leipold and Becher (1970).

and (4) cost, life, and ease of machining. The materials from which hot pressing dies and rams can be made are theoretically infinite and each of these properties could be discussed in terms of potential materials. However, the number of materials that have found practical application in hot pressing is much more limited, and it is more convenient to discuss these materials in turn with respect to their individual advantages and disadvantages.

The materials that have found wide usage in hot pressing are carbon (various forms), refractory metals, ceramics, super alloys, and composites of these.

Undoubtedly the most widely used material for hot pressing rams and dies is graphite. Major advantages of graphite are its ease of machining and its low cost; however, some of new forms are somewhat more expensive. The properties of graphite in hot pressing, however, are mixed. The low coefficient of thermal expansion eliminates the problem of compact cracking during the cooling cycle and greatly simplifies its removal from the die. Resistance to creep is excellent to at least 2500°C and tensile and compressive strengths are such that die pressures of the order of 5000 psi are attainable with conventional graphites and up to 15,000 psi with more sophisticated and expensive types (Wise and Trask, 1971). At temperatures below approximately 1200°C the strength of conventional graphites are inferior to other types of dies, and higher pressures (up to 25,000 psi) are available with other die materials.

A major drawback to graphite-based hot pressing systems is the reactivity

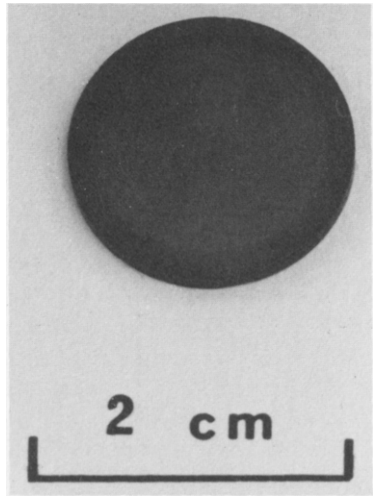

Fig. 11. ZrC hot pressing showing carbon rich zone at periphery after pressing in graphite die at 1700°C and 5000 psi.

of the graphite with many ceramics. Even with reasonably compatible materials such as carbides, changes in the compact stoichiometry can be introduced by the graphite. Figure 11 shows a carbon rich zone in dense ZrC pressed in graphite. Similar stoichiometry changes can be encountered with oxides especially troublesome in materials with which defect structure control is required as for electronic applications. More severe reaction can occur, such as complete reduction of the oxide ($NiO + C \rightarrow Ni + CO$). Other advantages of graphite are its self-lubricating surface, preventing sticking and galling, and its long life.

In general, graphite should be considered the first choice for hot pressing dies and rams with other materials being substituted when graphite is deemed unsatisfactory.

Refractory metal dies such as tungsten, molybdenum, tantalum and niobium would at first glance appear to be advantageous die and ram materials. Their strengths are reasonable in the 1000°–2000°C region and they are reasonably available and machinable, but they are costly. However, two very serious limitations exist with these materials — their reactivity and their ease of deformation. The first of these is especially serious with oxides and less so but still significant with carbides and nitrides. The low resistance to mechanical deformation presents problems not primarily because of bulk deformation but through galling. Small particles of the densified compact frequently lodge between the ram and die, and after cooling and removal of the ram, serious scoring of the components occur, rendering them useless. For this reason, if other considerations should suggest use of refractory metal dies, it is strongly recommended that the composite type described later be considered. The most promising refractory metal die consists of TZM* molybdenum die coated with a $MoSi_2$ or B† surface layer. The $MoSi_2$ was developed for oxidation resistance; however, in this case, it is primarily advantageous through improved surface hardness and elimination of galling. However, occasional difficulties with internal spalling of the coatings may be encountered.

A variety of super alloys such as Rene 41,‡ Udimet 700,§ Inconel X‖ can be used for hot pressing ceramics. However, the majority of these alloys exhibit excessive creep rate and are prone to stress rupture failure at temperatures above approximately 900°C and stressed 10,000–15,000 psi. Consequently their usefulness is limited to ceramics that can be densified at temperatures less than this. In addition two other serious shortcomings exist. These

* Hitemco, Hicksville, New York.

† Materials Development Corporation, Medford, Massachusetts.

‡ Various manufacturers.

§ Special Metals, Allegheny Ludlum, New Hartford, New York.

‖ International Nickel Company, Huntington, West Virginia.

dies are highly susceptible to galling from the abrasive ceramic materials so damage to die and ram surfaces is frequently encountered. In addition, most of these alloys exhibit thermal expansion in the range of 14 to 18 $\times$ 10^{-6}/°C, higher than many ceramic materials. Consequently a densified compact must be hot ejected from the die. If not, it will be crushed or be impossible to remove upon cooling to room temperature. Such hot ejection can be accomplished but is extremely inconvenient. Some ferrous alloys are available (ferritic structure) that have expansions of the order of 10 to 12 $\times$ 10^{-6}/°C and are usable with some ceramic materials, however, the high temperatures strength of these alloys generally become inadequate above 600°–700°C. In summary, these iron–cobalt–nickel base alloys can be useful in hot pressing lower melting materials at lower temperatures, provided that the thermal expansion of the ceramic is sufficiently high. They can be particularly useful with halides. At these lower temperatures, problems with reactivity are generally less severe and further the superalloy does not require environmental protection at the temperatures.

Ceramic dies that find extensive use in hot pressing are silicon carbide and aluminum oxide. The aluminum oxide offers useable strength to approximately 1200°C, its thermal expansion is compatible with most oxides, and its reactivity, surface hardness, and resistance to creep are entirely suitable. However, the primary difficulty is with brittle failure even at temperatures as high as 1200°C. This is especially true with pressures above 10,000 psi where these dies are normally used. The brittle failure problem is especially difficult since nondestructive methods are not presently available to predict behavior. Consequently, with any specific lot of alumina dies that have been machined and processed identically, observed behavior varies widely. Several dies may give lives of 20–50 runs while numerous others will fail upon the first loading. Not infrequently, failure in a ceramic die is accompanied by destruction of heating elements and other interior portions of the hot press. Further, the machining of alumina dies requires availability of diamond grinding equipment and operators skilled in handling ceramics. The cost of an individual die also becomes substantial when the high probability of die failure is considered.

Silicon carbide is quite comparable to alumina in its general behavior except that the maximum use of temperature is of the order of 1400°C. Only high density direct-bonded silicon carbide should be used, at present a substantially more expensive material. In other ways silicon carbide is quite comparable to alumina in terms of its expansion, lack of reactivity of environmental requirements, machining, etc. In addition, silicon nitride would appear to hold potential as a ceramic die and ram material; however, at this writing its use as such has not been reported.

Serious problems with brittle failure of the ceramic components are sub-

stantially reduced when their use is limited to rams. Here the stresses are compressive and failure probability is considerably reduced. Consequently, serious consideration should be given to the use of ceramic rams even when another material is selected for die use. The ceramics, when used as rams, offer long life, resistance to creep, low reactivity, and freedom from environmental protection requirements. Some difficulty is occasionally encountered with sticking between the oxide rams and specimens when compared to the use of graphite rams (see Section II, f). Alumina is generally preferable to silicon carbide because of lower costs.

As is apparent in the foregoing discussion of die materials, the choice of an individual material often involves a tradeoff: failure probability versus abrasion resistance, thermal expansion versus reactivity. There have been successful attempts at optimization of these tradeoffs through the use of composite systems involving, for example, one material to provide strength and another to provide reduced wear and reactivity. The most successful of the systems has been the use of molybdenum jackets surrounding an alumina liner. The liner provides a surface in contact with compact exhibiting low reactivity and high surface hardness. Strength is provided by the molybdenum jacket. Precise sizing of the jacket and liner is required to assure that the

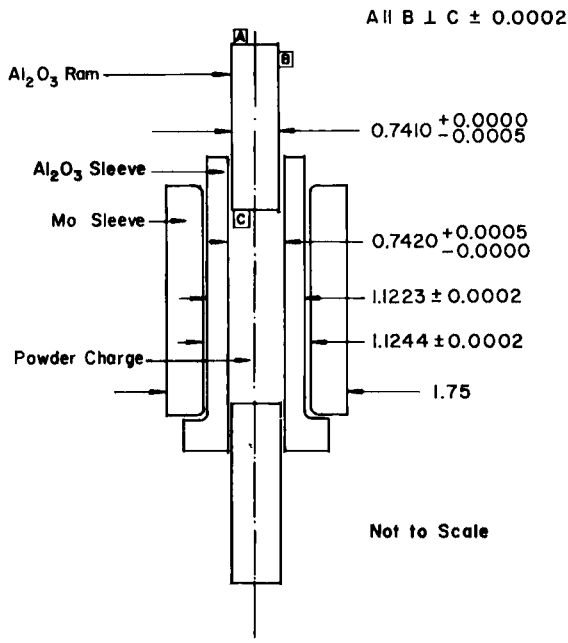

Fig 12. Composite die for hot pressing.

molybdenum supports the stress at use temperatures. An example is shown in Fig. 12. With this configuration liner integrity is not required and liners can be used long after they have failed through brittleness by simply reassembling parts within the jacket. Catastrophic failure is thus eliminated and failure normally occurs by creep rupture in the jacket. However, a system of this type has been successful for more than 50 runs at 15,000 psi and temperatures in the 900°–1100°C region.

The stress distribution between the liner and jacket depends upon the temperature of use, and of course, zero stress in the liner is theoretically obtainable only at a single temperature; however, experience has shown that use of a given system over a temperature of at least 200°C is entirely adequate.

If this type of composite system is to be employed in an oxidizing atmosphere, protective coating ($MoSi_2$) of the molybdenum is again required for oxidation resistance. While the cost of such a die configuration is high, its life and predictable behavior offer considerable advantage when graphite cannot be used because of environmental or pressure requirements.

The design of hot pressing dies is essentially a thick-walled cylinder process with the maximum die stress calculated (Flügge, 1962)

$$\sigma_m = \frac{p_i(R_i^2 + R_o^2) - 2p_o R_o^2}{(R_o^2 - R_i^2)} \tag{1}$$

where σ_m is maximum internal fiber stress, p_i is internal hydrostatic pressure, p_o is external hydrostatic pressure ($= 0$ for unsupported die), and R_i, R_o are internal and external radii.

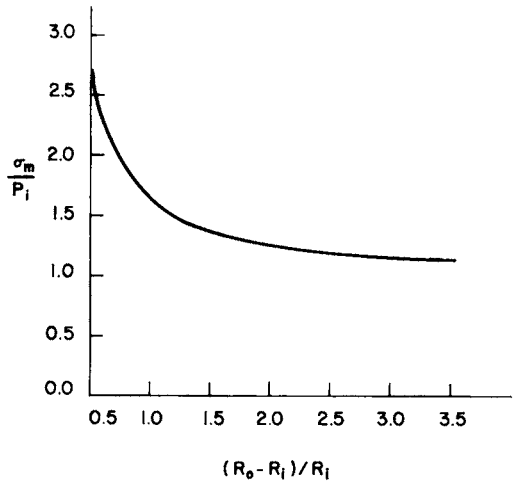

Fig. 13. Maximum stress versus wall thickness for thick-walled cylindrical die.

Figure 13 shows the effect of increasing wall thickness on this interior stress, and it may be seen that little is gained with wall thickness greater than twice internal radius. With metals the stress level will normally be limited by creep or creep-rupture failure, while fracture stress is a limitation for aluminum oxide, silicon carbide, and graphite at all but the highest temperatures. Because of improvements constantly being made in the high temperature behavior materials, it is not possible to provide strength limitations for future designs. However, Table III does indicate reasonable value strength and other properties of materials suitable for hot pressing components consistent with present technology. It must be emphasized that, in the case of nonmetals, the strength value is strongly dependent on its source and character. Properties much different could be obtained.

TABLE III

NOMINAL PROPERTIES OF DIE AND RAM MATERIALS AT NOTED TEMPERATURES

Material	Condition	Thermal expansion ($°C^{-1}$)	Modules of elasticity (mpsi)	Tensile fracture strength (kpsi)	Compressive strength (kpsi)	Creep rupture strength (kpsi)
Al_2O_3 (RT) $\rho > 99\ \%$	$Al_2O_3 > 99\ \%$	9.0	52	30–50	> 300	[a]
SiC (RT) $\rho > 99\ \%$		3.9	~ 65	~ 40	> 200	[a]
Mo (TZM) (1000°C)	stress relieved	4.9	34	80	[a]	28
Udimet 700 (1000°C)	solution treated and aged	16.5	20.6	40	[a]	~ 10
Rene 41 (1000°C)		16.8	20	50(925°)	[a]	10
422M (700°C)		10.4		40	[a]	9
Graphite (conv.)	RT $\rho = 1.7$	2–4	1–2	~ 4[b]	~ 10[b]	[a]
Graphite (fine grained)[c]	RT $\rho = 1.86$	8.82		10[b]	21[b]	[a]
Graphite composite[d]	RT $\rho = 1.34$	1.5–2.5	~ 3	15–20[b]	[a]	[a]

[a] Not normal failure mode.

[b] Normally increases with increasing temperature.

[c] POCO Graphite Inc., P.O. Box 2121, Decatur, Texas 76234.

[d] Carborundum Co., P.O. Box 577, Niagara Falls, New York 14302.

Die–ram clearances should be based on the particle size of the powder being compacted, the types of dies and rams, and the amount of motion anticipated during compaction. With fine particles and where extensive ram travel is anticipated, tolerances as small as 0.001 minimum to 0.002 maximum should be used. This is especially true with ceramic dies. With graphite, somewhat larger tolerances are suitable (0.002–0.005 for small pressings and up to 0.010 for parts several inches in diameter). With coarse material in the die cavity, as in the pseudo-isostatic pressing procedure, 0.010–0.050 clearances are reasonable.

Another factor requiring precise dimensional control is the parallelism of the ram ends. This is especially true with ceramic rams where the alignment in the load column must be kept within 0.0001–0.0002 per inch of diameter, or failure of the rams will be frequently encountered. With graphite, having a lower elastic modulus and being less susceptible to an immediate brittle failure, this requirement is much less stringent (0.0005 to 0.001 per inch of diameter). It is, of course, necessary to ascertain that loading system itself closes with comparable parallelism.

The die designs for the two case histories considered here are shown in Figs. 12 and 14. The graphite system used for tantalum carbide is typical of the simple frequently encountered graphite types. In contrast, the alumina–molybdenum system used for the magnesium oxide is perhaps the most complicated in terms of design that presently finds use; however, it is extremely effective when the higher pressing pressures are required (see Fig. 12).

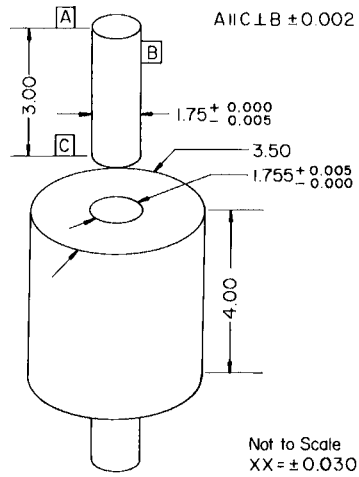

Fig. 14. Graphite die for hot pressing carbides to temperatures of 2500°C and pressures of 9000 psi. Punches are high strength fine grained graphite. Die is conventional. See Table III.

D. Selection of Environment

The appropriate environment in which to conduct the given hot pressing is frequently limited by the die materials and furnace element rather than by the ceramic being processed. The environment is controlled solely by the ceramic with preparation of materials in which the defect structure is critical, as for electronic materials (see also Section II,4 a). In contrast, many oxides—alumina, beryllia, magnesia—are pressed in graphite systems in reducing atmospheres. Here the environment is dictated completely by the requirements of the graphite. In other situations, as with carbides, the carbon environment is generally compatible with the material, although changes in stoichiometry can be introduced.

Major reactions between the ceramic powders being processed and some portions of the environment can occur at these temperatures. For example, zirconium carbide hot pressed in graphite dies and rams reacts with a nitrogen atmosphere to form a zirconium carbide nitride solid solution with the rejection of excess carbon into a graphite second phase (Leipold and Nielsen, 1964).

The nature of the atmosphere within the die cavity can also be considerably different from that within the chamber surrounding it. In an extreme case with alumina dies and rams having a 0.001 in. clearance, a back pressure within the die cavity developed sufficient to reverse the motion against the 15,000 psi external pressure. The die assembly at the time was in a 10 μm vacuum. To reduce the levels of such entrapped gases, the seal between the die and ram can frequently be broken by momentarily releasing the external load to allow small motion between the die and ram. The breaking of the seal is usually accompanied by a pressure rise in the vacuum chamber. Methods involving channels along the die and ram surfaces have been suggested to reduce this problem (Lawless, 1972).

The concentrations and pressures of the entrapped gases within a confined compact can produce phases that are normally encountered. The existence of brucite (Leipold and Nielsen, 1968) at temperatures of 700°C and kaolinite at 800°C are examples (Scott and Carruthers, 1969). Both can be explained by the assumption of high pressures of water vapor within the hot pressing cavity.

Difficulties with gas pressures within the die cavity are considerably reduced when more porous dies such as graphite are used. However, it can by no means be assumed that levels are negligible. The removal of gas atoms from a porous compact has been shown to be slow (Anderson *et al.*, 1965).

The selection of environment for these examples was straightforward. Magnesium oxide, being rather insensitive to environment, can be pressed in O_2, air, argon, or in a mechanical pump vacuum. Results are similar, with

the exception of final specimen color for the MgO of 99.5 % purity. The specimens pressed to high density in air or O_2 are pink in color while those in vacuum or argon are colorless to gray. The reason for the difference is not known but is believed to be related to defect chemistry of the impurities. Higher purity MgO (99.95 %) is white in all environments.

When the tantalum carbide is pressed in graphite, the use of a nonoxidizing atmosphere is mandatory. Dual mode operation was finally selected, with a vacuum ($\sim 10^{-5}$ torr) employed to provide minimum contamination at lower temperatures, and with inert gas (He, Ar) introduced above 2000°C to suppress graphite volatilization.

E. Selection of Pressing Parameters

The primary parameters to be considered in obtaining sound hot pressings are time, temperature, and pressure. As is true with most complex kinetic processes, optimum values can seldom be uniquely or simply defined. Recently, there have been attempts (Palmour and Johnson, 1967) to optimize the selection of these variables, particularly time and temperature, based on the control of rate of densification. This approach appears to hold promise, but at this writing has had only limited application and considerably complicates the requirements for rate of temperature control.

When one attempts to predict theoretically the hot pressing behavior of any ceramic, one can become quickly emersed in innumerable theories of densification, mechanisms, and activation energies. Although diffusion (Coble and Ellis, 1963; Rossi and Fulrath, 1965) as a limiting mechanism is probably the most universally accepted concept, plastic (McClelland, 1961) and viscous deformation (Murray *et al.*, 1958), particle rearrangement (Felten, 1961), fracturing (Williams and Morris, 1967), and others are not without their proponents. Even considering only diffusion, the question of type (surface, grain boundary, volume) and rate-limiting species (cation versus anion) is not easily resolved. An excellent summary of the correlation of theoretical and experimental behavior during hot pressing of a number of materials is available (Vasilos and Spriggs, 1966). A correction to the theoretical analysis subsequent to that study has been made (Paladino and Coble, 1963) with some improvement in agreement; however, prediction of experimental conditions from theory to within an order of magnitude would be excellent analytically but totally unsatisfactory experimentally. For materials in which the defect structure is more complex, such as those developing nonstoichiometry, the situation worsens considerably since changes in such structure during hot pressing are to be expected. Figure 15 shows the comparison of measured diffusivity and diffusivity calculated from densification rates for various tantalum carbides using a widely accepted model for hot

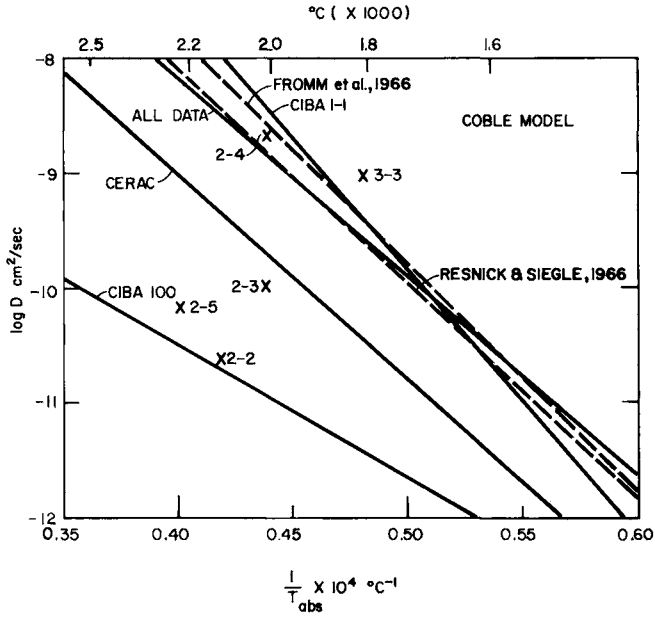

Fig. 15. Diffusivity calculated from densification rates and Coble model versus temperature. "X" represents individual batches of powder, solid lines least square fits to larger batches (Leipold and Becher, 1970). Dashed lines are reported direct diffusion data.

pressing. Although the average behavior of all kinds of TaC indicates agreement with the model, individual sources do not, and attempts to calculate pressing conditions for them are in error by many hundreds of degrees.

Since the purpose here is on selection rather than to give explanation, an extensive theoretical discussion of hot pressing mechanisms will not be included. Rather, guidelines will be given in which reasonable initial predictions of parameters and rates may be made (see also the compilation of literature references in Table IV). These may then be revised consistent with initial results with further empirical suggestions of the interactions of the time, temperature, pressure parameters. It must be emphasized again, however, that different sources of powder and indeed different lots from the same source can be expected to behave differently. Consequently, information in the literature can only be considered as a guideline.

As was stated previously, the temperature for hot pressing is generally approximately one-half the absolute melting point, and this would be a recommended starting point when sintering aides are not being used. Slightly higher temperatures are frequently required for the more difficult to sinter, highly covalently bonded compounds (BN, Si_3N_4, SiC, etc.). The rate of attainment of this maximum temperature is most frequently limited by other

TABLE IV

HOT PRESSING CERAMICS

Material	Reference
Review, oxides	Poluboyarinov and Shal'nov, 1963; Spriggs *et al.*, 1963
Al_2O_3	Mangsen *et al.*, 1960; Rankin *et al.*, 1971 (+ Mo); Chaklader and McKenzie, 1966 (with clay)
$3Al_2O_3$ $2S_1O_2$ (Mullite)	Mazdiyasni and Brown, 1972
HfO_2 (7 M% Y_2O_3)	Brown and Mazdiyasni, 1970
BeO	Carniglia *et al.*, 1964; Kodaira and Koizumei, 1971; Moorthy *et al.*, 1967; Amato *et al.*, 1967
CaO	Rice, 1969
CiO_2	Nakayama *et al.*, 1966
$LiAl_5O_8$	Gazza, 1972
MgO	Hanna, 1970; Zizner, 1967; Ramakrishnan, 1968; Sheets and Duckworth, 1968; Leipold and Nielsen, 1966
SiO_2	Vasilos, 1960
$MgAl^2O^4$	Hummler and Palmour, 1968; Budnikov and Kharitonov, 1967
TiO_2	Egerton and Thompson, 1972; Roy and Parsons, 1969
ThO_2	Kulkarni and Moorthy, 1965
VO_2	Amato *et al.*, 1966; Van Asbroeck *et al.*, 1967
Y_2O_3	Dutta and Gazza, 1969
ZnO	Dutta and Spriggs, 1969
ZrO_2	Kainarskü *et al.*, 1967; Chaklader and Baker, 1965; Amato *et al.*, 1967
Ferroelectrics	Haertling, 1963; Levett, 1963; Haertling, 1970; Jaeger and Egerton, 1962
Ferrites	Suemune, 1971
Cement	Roy *et al.*, 1972
BN	Kusnetsova and Poluboyarinov, 1966
Berylides	Mannas and Smith, 1962
KCl	Anderson *et al.*, 1973
UF_4	Barnes and Murray, 1958
LiF	Neuroth and Warnach, 1969
MgF_2	Buckner *et al.*, 1962
SiC	Dombravo *et al.*, 1963
(Ta, Hf, Zr) C	Fischer, 1964; Matsuo *et al.*, 1970; Leipold and Becher, 1970
(Zr, Hf, Ti) B_2	Toibana and Hashimoto, 1967; Kalish and Clougherty, 1969 ; Kinoshita, 1969 (LaB_6); Kinoshita *et al.*, 1970 ($MoSi_2$)
SiB_6	Dutta and Gazza, 1973

than the material being fabricated. Thermal shock to ceramic dies and heating elements, or power requirements usually dictate a minimum of one to several hours to maximum temperature. If pressings are being conducted in vacuum, the ability to maintain desired vacuum levels against out-gassing can limit maximum heating rates. The time at maximum temperature during a pressing generally is in the range of ten minutes to several hours with shorter times being preferable, both economically and for maintenance of fine grain size. Initially the recommended procedure is to continue a pressing until the rate of densification approaches zero ($< 0.1\ \% \Delta L/L$ per minute). The required time and final product can then be used to indicate desirable changes in temperature for additional pressings.

The procedure for application of pressure during the hot pressing is probably the least agreed upon feature of hot pressing. Procedures range from applications of full pressure at room temperature to maintenance of essentially zero pressure until full temperature is reached. The former is advantageous with respect to maximizing sintering enhancement but poor with respect to removal of entrapped gases. The latter, of course, reverses this situation. The proper procedure for any situation is so strongly dependent upon particle characteristics, particle pretreatment, and details of the pressing condition that no detailed recommendations can be made. With ceramic dies having small clearances and powders likely to desorb gases, such as oxides, a recommended starting procedure is application of a third maximum pressure until about half the anticipated pressing temperature is reached. Pressure should then be increased linearly achieving maximum pressure before maximum temperature. Where gas entrapment is less of a problem, as for example with a carbide in a graphite die, pressure approaching maximum may be applied at room temperature. At the completion of the pressing, pressure may be rapidly removed from the pressed compact. There is no evidence that maintaining this pressure during cooling has any significant effect on the final compact.

Temperature–pressure–time curves for the carbide and oxide system described here are given in Fig. 16a,b. These were developed after several prior runs. Note the differences in results for the two lots of carbide powder of the same nominal specification.

F. Special Operations

This section will consider a number of special procedures which are needed occasionally for satisfactory hot pressing. These include lubricants, parting agents or separators, hot ejection, special powder handling procedures, etc.

The use of parting agents or separators is probably the most frequently encountered special operation. Here, thin foils (0.005–.010 in.) are placed

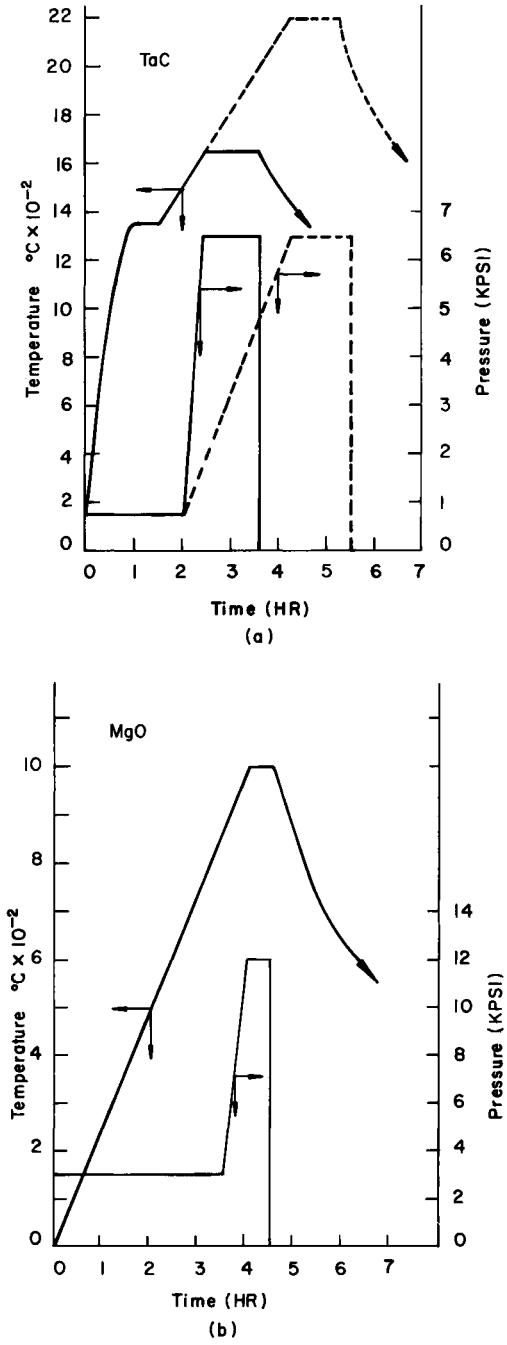

Fig. 16. Typical temperature–time and pressure–time cycles for hot pressing MgO and TaC.

between the ram ends and the powder to prevent reaction and/or sticking. The refractory metals such as molybdenum, tantalum, or tungsten are frequently used when pressing nitrides, borides, sulfides in graphite dies. This substantially reduces the area in contact with the carbon, especially when the length-to-diameter ratio is small. Sticking is occasionally encountered with oxide rams when pressing other oxides. Here either solid separators such as refractory metals or graphite foil may be used or coarse grained oxide particles ($-60 + 100$ mesh) may be placed between the ram and a cold-pressed compact. Separators are also useful for pressing a number of materials at one time (Clark, 1971).

The tendency of the densified compact stick to the ram can also be reduced by hot ejection (Spriggs *et al.*, 1963). The process of hot ejection is also effective in removing compacts whose expansion is the same as or greater than die, since normal thermal contraction will not free the part from the die. The process of hot ejection is most easily accomplished by removing the upper portion of the load system and upper ram and replacing it with a hollow refractory sleeve into which compact is then pressed. It is normally accomplished at temperatures in the 300°–800°C range.

Die wall lubricants in hot pressing has not found significant use, except for graphite dies and rams, which could be considered self-lubricating. Interparticle lubrication is sometimes considered to be a contribution of hot pressing aids and is discussed in Section II, B, 2,b).

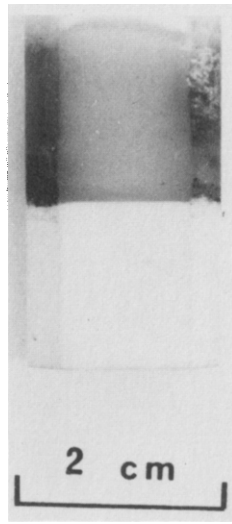

Fig. 17. Diffusion-bonded joint between cold pressed and sintered 95% dense MgO and hot press 99.9% dense MgO.

In the carbide examples presented here no special operations were used. With the magnesium oxide, however, special parting agents and adhesion enhancement were used. Parting agents took the form of $-60+100$ mesh fused MgO grains in layers 1–2 grains thick between the ram and the prepressed compact.

Occasionally it is desirable to promote rather than reduce adhesion between the hot pressed compacts and its adjoining rams. Such a situation is encountered in producing long ($L/D \approx 5:1$) MgO blanks for dogbone tensile specimens. Since the ends of the blank are to form the grip material, it is not necessary for it to be microstructure controlled. Consequently, short MgO rams ($L/D = 1$) were cleaned on one end by etching in phosphoric acid and placed in contact with the preformed MgO powder compact (with about 0.010 in. loose powder at the interface) in the hot pressing die. After hot pressing the ends were diffusion bonded to the densified compact. For this application, the joints were not in a region of maximum stress and were quite satisfactory. A hot press welded joint between 95 % dense cold-pressed and sintered MgO and 99.9 % translucent MgO is shown in Fig. 17.

G. Product

The removal of a densified compact from a hot pressing die does not necessarily complete its fabrication processing. Certainly a variety of machining and special treatments exist that lie beyond the scope of this discussion, for example, the polarization of a magnetic ceramic. However, a number of postpressing treatments do exist that lie within the realm of normal processing. These include resintering and homogenization, removal of hot pressing aides, reduction of entrapped gas, etc. As was stated earlier, a ceramic compact after being hot pressed cannot be considered to be in a state of chemical or structural equilibrium and the approach toward such equilibrium can often produce dramatic changes in the structure and properties of the body.

The removal of hot pressing aides by a postpressing heat treatment is fairly common and effective with alkali halides in MgO. Heat treatments in the range of 1000°–1300°C have been shown to be effective in reducing although not eliminating the quantities of these and similar additives (Rice, 1971),

A resintering accompanied by grain growth can produce improved homogenization. A hot pressed welded specimen of NiO with greater L/D than normally practical was produced (Nielsen and Leipold, 1966) with accompanying grain growth.

The removal of gases can be accomplished by a post-hot pressing anneal, however, because of the high density normally achieved during hot pressing, such removal must normally be by diffusion rather than by permeation and consequently, long times are required. The use of the higher temperatures

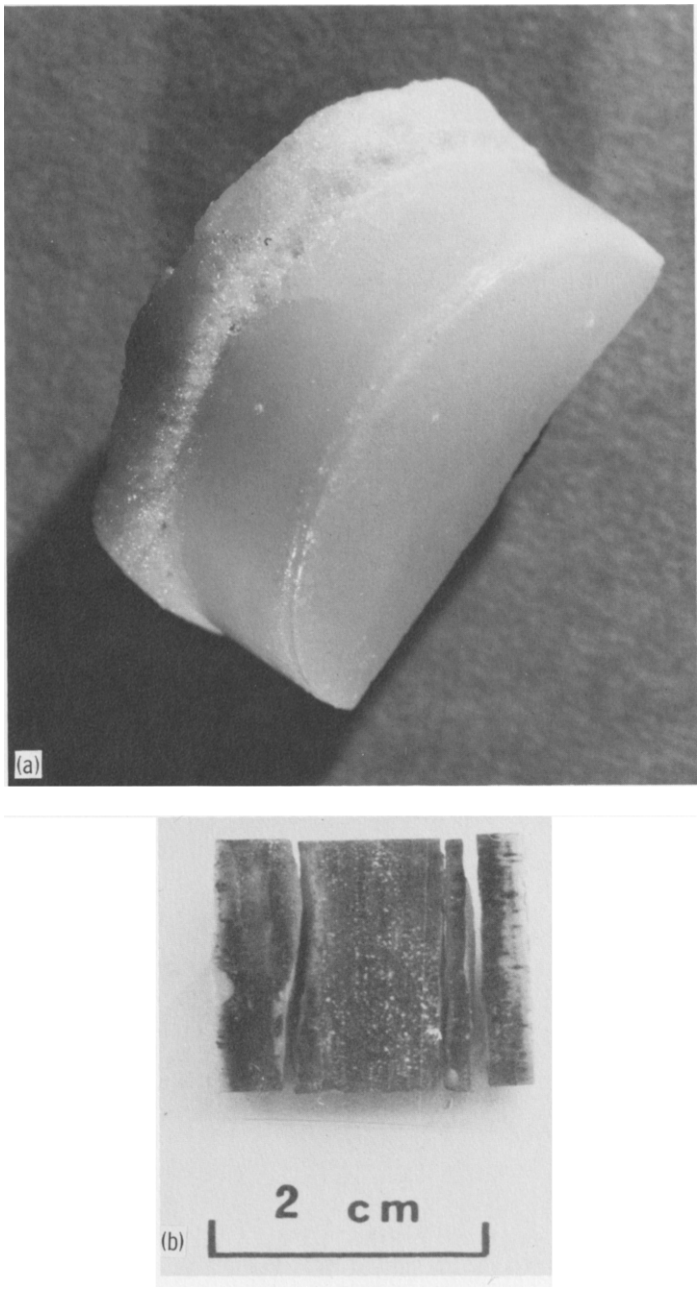

Fig. 18. Hot pressed MgO shows degradation during post pressing heat treatment. (a) Indicates softening and bloating, (b) indicates gas pressure and fracturing.

frequently produces bloating or increased tendency for fracture due to the pressure of the entrapped gases (Rice, 1969b). Figure 18a shows a two-part specimen of MgO having different impurity levels, hot press welded together, and reheated to 2200°C. The severe bloating at the less pure end is indicative of internal pressures and lack of specimen cohesiveness. In this case, the volatile species are probably vapors of low melting oxides rather than normal gases. Figure 18b shows an MgO specimen that delaminated as a result of internal gas pressure.

III. Hot Isostatic Pressing

The term isostatic pressing is used synomously with hydrostatic pressing, and with it, pressure is applied to the powder from three directions rather than only one as in linear pressing. As with cold isostatic pressing the powder must be contained in some kind of a deformable enclosure. Here, however, it is usually a metal can. The can is then placed in a high pressure autoclave containing a furnace and the pressure medium is a gas rather than a liquid medium (Hodge, 1965). The primary advantages in isostatic pressing as compared to uniaxial pressing are more uniform pressure distribution throughout the compact yielding more uniform properties, slightly greater flexibility in shape, and a greater range and ratio of available dimensions. Long thin rods, for example, can be pressed, although in some cases difficulties are encountered in maintaining their straightness. The disadvantages of hot isostatic pressing are considerable capital expenditure in equipment, more complex and expensive processing of each specimen, extreme difficulty in desorbing gases from the powder particle surfaces, inability to monitor compaction behavior during processing, and lack of precise dimensional control in any one direction (control of the cross section is possible in uniaxial pressing).

Many of the requirements and procedures for hot isostatic pressing are quite similar to those for uniaxial pressing and consequently considerably less extensive coverage is required here. In most cases, reference can be made back to sections on uniaxial pressing.

A. Equipment

Without the assistance of experienced experts, design and construction of a hot isostatic press is beyond the capacity of research organizations and probably beyond that of most industrial operations. Consequently, if hot isostatic pressing is to be done, equipment must be purchased from a reliable

manufacturer or the service obtained on a contract basis. Equipment and services are presently available in sizes to several cubic feet, temperatures to 2500°C and pressures to 50,000 psi (Hodge, 1965). The maximum temperature, pressure, and size are not available in a single unit, however.

B. Selection of Starting Powder

The primary characteristics of the powder for hot isostatic pressing are the same as for uniaxial pressing. However, considerably greater emphasis must be placed on the role of adsorbed gases on the powders. Because the powder is entirely sealed within its container during hot isostatic pressing, there is no possibility of removal of any gaseous impurities.

C. Selection of Container Materials

The container materials comparable to the die materials must be selected on the basis of mechanical properties and reactivity. The reactivity now includes both the lack of reaction with the compacted powder and easy removal (usually by solution) after compaction. The mechanical requirements are simply a low flow stress compared to the hydrostatic stress at the temperature of compaction. Ferrous alloys, either mild steel or stainless steel, are usually used up to approximately 1100°–1200°C and refractory metals at temperatures above this. The thermal expansion of the container is not usually considered in this application. The other container factors such as the cost are usually secondary in its selection. Welding is usually used to close the tube after being filled with the loose or precompacted powder. A vacuum stem is included for removing entrapped gas.

D. Selection of Environment

The environment surrounding the powder within the container should ideally be a high vacuum to eliminate back pressures from any adsorbed or entrapped gases within it. However, the extremely fine particles used to maximize densification rates are extremely difficult to desorb because of both the chemical affinity of the surface for gas molecules and the difficulty in removing gas atoms from within the porous compact. Magnesium oxide in a hot isostatic container that had been desorbed at 200°C for 24 hr by mechanical pump vacuum still indicated approximately 10 % $Mg(OH)_2$ after hot isostatic pressing. Higher degasing temperature would tend to reduce particle reactivity. This problem of gas entrapment is a significant one in the hot isostatic pressing of ceramics with reactive surfaces such as oxides (Leipold and Nielsen, 1968). Completely satisfactory solutions are apparently not presently available.

E. Selection of Pressing Parameters

The mechanisms that control densification during hot isostatic pressing are essentially identical to those in uniaxial pressing and the behavior is quite comparable. The improved pressure distribution increases the efficiency of the process slightly so that temperatures and/or times might be reduced slightly (5 to 10 %) during hot isostatic pressing. Reference to the previous section on selection of parameters should be made.

F. Other Requirements

The use of parting agents, separators, lubricants, etc., in theory are the same for hot isostatic pressing as for uniaxial pressing. However, their use is much more limited. The use of a separating agent between the container and a compact is apparently the only application of these special requirements.

G. Product Evaluation

Again, no special considerations are necessary for hot isostatically pressed material and reference to previous sections should be made.

IV. Other Hot Pressing Methods

Included here will be a number of rather unusual and little-used methods of hot fabricating ceramics that may find use in special situations. Because of their limited applicability and because they are similar in most cases to previously described methods, only very brief descriptions will be given.

A. Pseudo-isostatic Pressing

This method of hot pressing is shown in Fig. 7. The transfer medium can be sand (Levey and Smith, 1968), graphite (Lange and Terwilliger, 1973), powdered ZrO_2 (Haertling, 1963), (Brandmayr *et al.*, 1961), or a molten glass (Barbaras, 1970; Havel, 1969; Kodaira *et al.*, 1972). The method is capable of retaining a considerable amount of the detail in the original compact and an example of the finished part is shown in Fig. 19. In general, the part is often presintered to reduce penetration of the pressure transfer medium. There is a considerable difference in the before-to-after compression ratio in the directions parallel and perpendicular to ram motion, but proper design of the initial compact can substantially reduce this effect. Extensive experimental and analytical evaluation of this technique are not available and its use would probably involve considerable process development time.

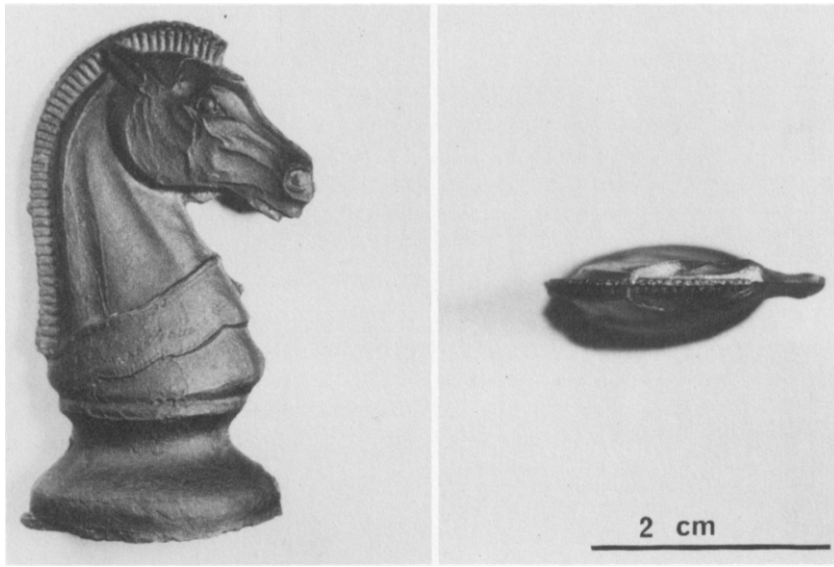

Fig. 19. Pseudo-isostatic pressed piece of SiC (+ 1 wt% Al_2O_3) with density > 99%. (Base was initially cylindrical.) From Lange and Terwilliger (1973).

B. Continuous Hot Pressing

This method of hot pressing is not truly continuous, in that a ram is repeatedly removed, additional powder charge introduced, compacted, moved downward through the die, and the cycle repeated (Oudemans, 1969). Compacted material is slowly and continuously removed from the lower portion of the die at lower temperatures. The method is similar in concept to continuous casting of metals except that in that case additional material is continuously added.

The quality of a continuously hot pressed part is, of course, contingent upon a sound interface between a previously compacted section and a new powder charge. With ceramic dies, interfacial problems are minimal. However, when the ram and die material are made of graphite a carbon-containing zone is left at the interface (see Section II, B, 2, b). This method of continuous hot pressing is quite complex but can be justified in terms of the higher production rates for hot pressed products. Future improvements could provide even greater benefits.

Semicontinuous hot pressing systems have been developed, suitable for higher production rates (Zehms and McClelland, 1963; Weiss and Knapp, 1961). Several of these involve multiple dies and transfer mechanisms for handling the preheated components (King, 1967; Alliegro, 1971).

C. Related Hot Pressing Procedures

Several procedures exist, such as hot press welding and forging, and are quite similar to hot pressing and are described elsewhere (Rice, 1970). They are mentioned here because they are conducted on the same kind of equipment as is used for uniaxial pressing. The welding process was discussed in earlier sections in conjunction with special operations and continuous hot pressing. It is entirely similar in principle to the diffusion-bonding techniques used with metals. With ceramics, however, it is usually advantageous to include a small amount of powder between the two solids to be welded. If this is not done, extremely high temperatures (approaching 0.9 T_m) are needed. Such direct bonding has been accomplished with sapphire to form bicrystal elements (Budworth *et al.*, 1963).

The hot forging of ceramics is similar to the technique used with metals and the purpose involves both microstructure control and shape change. In some instances, the preforged billet is not fully densified and the forging technique thus includes both densification and shape change.

The hot forging technique thus in practice would appear to offer the same general advantages in ceramics as in metals. However, except in limited situations, the temperatures required for reasonable plastic deformation in the ceramics are such that recrystallization occurs during forging. However, grain refinement can still be obtained (Anderson *et al.*, 1973). This area is undergoing considerable research and development at present and will undoubtedly find considerably greater application in the future.

References

Alliegro, R. (1971). U.S. Patent 3,557,414.
Amato, I., Columbo, R. L., and Petrucelli Balzari, A. M. (1966). *J. Nucl. Mater.* **21**, 328–336.
Amato, I., Columbo, R. L., and Ravizza, M. (1967). *J. Nucl. Mater.* **22**, 97–99.
Anderson, P. J., Horlock, R. F., and Oliver, J. F. (1965). *Trans. Faraday Soc.* **61**, 2754–2762.
Anderson, R. H., Koepke, B. G., Bemal, E., and Stokes, R. J. (1973). *J. Amer. Ceram. Soc.* **56**, 287.
Barbaras, G. D. (1970). U.S. Patent 3,455,682.
Barnes, E., and Murray, P. (1958). *J. Amer. Ceram. Soc.* **41**, 246–248.
Benecke, M. W., Olson, N. E., and Pask, J. A. (1967). *J. Amer. Ceram. Soc.* **50**, 365–368.
Brandmayr, R. J., Brown, A. E., Di Vita, S., and Fischer, R. J. (1961). U.S. Patent 2,990,602.
Brown, L. M., and Mazdiyasni, K. S. (1970). *J. Amer. Ceram. Soc.* **53**, 590–594.
Buckner, D. A., Hafner, H. C., and Kriedl, N. J. (1962). *J. Amer. Ceram. Soc.* **45**, 435–438.
Budnikov, P. P., and Kharitonov, F. Ya. (1967). *Epitoanyag* **19**, 131–133.
Budworth, D. W., Roberts, E. W., and Scott, W. D. (1963). *Trans. Brit. Ceram. Soc.* **62**, 949–954.
Carnall, E., and Hatch, E. (1967). *Mater. Res. Bull.* **2**, 1075–1086.
Carniglia, S. C., Johnson, R. E., Hott, A. C., and Bentle, G. G. (1964). *J. Nucl. Mater.* **14**, 378–394.

Chaklader, A. C. D., and Baker, V. T. (1965). *Amer. Ceram. Soc., Bull.* **44**, 258–259.
Chaklader, A. C. D., and McKensie, L. G. (1966). *J. Amer. Ceram. Soc.* **49**, 477–483.
Clark, R. E. (1971). U.S. Patent 3,589,880.
Coble, R. L., and Ellis, J. S. (1963). *J. Amer. Ceram. Soc.* **46**, 438–441.
Deeley, G. G., Herbert, J. M., and Moore, W. C. (1961). *Powder Met.* **8**, 145–151.
Dombravo, I. V., Kalinia, A. A., and Kudryavtsev, V. I. (1963). *Sov. Powder Met. Metal Ceram.* **2**, 150–155.
Dutta, S. K., and Gazza, G. E. (1969). *Mater. Res. Bull.* **4**, 791–796.
Dutta, S. K., and Gazza, G. E. (1973). *Amer. Ceram. Soc., Bull.* **52**, 552–554.
Dutta, S. K., and Spriggs, R. M. (1969). *Mater. Res. Bull.* **4**, 797–806.
Egerton, L., and Thompson, J., Jr. (1972). U.S. Patent 3,639,132.
Felten, E. J. (1961). *J. Amer. Ceram. Soc.* **44**, 381–385.
Fischer, J. J. (1964). *Amer. Ceram. Soc., Bull.* **43**, 183–185.
Flügge, W. (1962). "Handbook of Engineering Mechanics," p. 37–13. McGraw-Hill, New York.
Fromm, E., Gebhardt, E., and Roy, V. (1966). *Z. Metallk.* **57**, 808–811.
Gazza, G. E. (1972). *J. Amer. Ceram. Soc.* **55**, 172–173.
Haertling, G. H. (1963). *Amer. Ceram. Soc., Bull.* **42**, 679–684.
Haertling, G. H. (1970). *Amer. Ceram. Soc., Bull.* **49**, 564–567.
Hamano, Y . Kinoshita, M., and Kose, M. (1966). *Yogyo Kyokai Shi* **74**, 295–300.
Hanna, R. (1970). *Amer. Ceram. Soc., Bull.* **49**, 548–549.
Hausner, H. H. (1958). U.S. Patent 3,835,573.
Havel, C. J. (1969). U.S. Patent 3,622,313.
Hendricks, R., Jr. (1970). U.S. Patent 3,529,046.
Hodge, E. S. (1965). *Mater. Des. Eng.* **61**, 92–97.
Hummler, D. R., and Palmour, H., II. (1968). *J. Amer. Ceram. Soc.* **51**, 320–326.
Jaeger, R. E., and Egerton, L. (1962). *J. Amer. Ceram. Soc.* **45**, 209.
Kainarskü, I.S., Alekseenko, L. S., and Degtyareva, E. V. (1967). *Sov. Powder Met. Metal Ceram.* **4**, 273–276.
Kalish, D., and Clougherty, E. V. (1969a). *Amer. Ceram. Soc., Bull.* **48**, 570–578.
Kalish, D., and Clougherty, E. V. (1969b). *J. Amer. Ceram. Soc.* **52**, 26–30.
King, A. G. (1967). U.S. Patents 3,303,533 and 3,340,270.
Kinoshita, M. (1967). *Yogyo Kyokai Shi* **25**, 84–90.
Kinoshita, M. (1969). *Yogyo Kyokai Shi* **77**, 200–207.
Kinoshita, M., Kose, S., and Hamano, N. (1970). *Yogyo Kyokai Shi* **78**, 64–73.
Kodaira, K., and Koizume, M. (1971). *Mater. Res. Bull.* **6**, 261–265.
Kodaira, K., Shimada, M., Kume, S., and Koizumi, M. (1972). *Mater. Res. Bull.* 7, 551–566.
Kose, S., Kinoshita, M., and Hamano, Y. (1967). *Yogyo Kyokai Shi* **75**, 175–183.
Kulkarni, A. K., and Moorthy, V. K. (1965). *Trans. Indian Ceram. Soc.* **24**, 87–95.
Kusnetsova, I. G., and Poluboyarinov. D. N. (1966). *Tr. Mosk. Khim. Tekhnol. Inst.* **50**, 205–209.
Lange, F. F., and Terwilliger, G. R. (1973). *J. Amer. Ceram. Soc.* **52**, 563–565.
Lawless, W. N. (1972). U.S. Patent 3,606,637.
Leipold, M. H. (1966). *J. Amer. Ceram. Soc.* **49**, 498–502.
Leipold, M. H., and Becher, P. F. (1970). *Amer. Ceram. Soc., Bull.* **49**, 647–651.
Leipold, M. H., and Kapadia, C. M. (1973). *J. Amer. Ceram. Soc.* **56**, 200–203.
Leipold, M. H., and Nielsen, T. H. (1964). *J. Amer. Ceram. Soc.* **47**, 419–424.
Leipold, M. H., and Nielsen, T. H. (1966). *J. Amer. Ceram. Soc.* **45**, 281–285.
Leipold, M. H., and Nielsen, T. H. (1968). *J. Amer. Ceram. Soc.* **51**, 94–97.
Levett, P. D. (1963). *Amer. Ceram. Soc., Bull.* **42**, 348–352.
Levey, R. P., Jr., and Smith, A. E. (1968). U.S. Patent 3,363,037.
McClelland, J. D. (1961). *J. Amer. Ceram. Soc.* **44**, 526.

Mangsen, G. E., Lambertson, W. A., and Best, B. (1960). *J. Amer. Ceram. Soc.* **43**, 55–59.
Mannas, D. A., and Smith, J. P. (1962). *J. Metals* **14**, 575–578.
Matsuo, S., Michihiko, H., and Yoshio, J. (1970). *Funtai Oyobi Funmatsuyakin* **17**, 19–24.
Mazdiyasni, K. S., and Brown, L. M. (1972). *J. Amer. Ceram. Soc.* **55**, 548–552.
Moorthy, V. K., Kamath, G. T., and Bahl, J. K. (1967). *Trans. Indian Ceram. Soc.* **26**, 1–8.
Murray, P., Livey, D. T., and Williams, J. (1958). *In* "Ceramic Fabrication Processes" (D. Kingley, ed.). Wiley, New York.
Nakayama, N., Hirota, E., and Nishikawa, T. (1966). *J. Amer. Ceram. Soc.* **49**, 52–53.
Neuroth, N., and Warnach, K. (1969). U.S. Patent 3,465,074.
Nielsen, T. H., and Leipold, M. H. (1966). *J. Amer. Ceram. Soc.* **49**, 626.
Okamato, S., Arase, M., and Okamoto, S. (1969). *J. Amer. Ceram. Soc.* **52**, 110–111.
Oudemans, G. J. (1969). *Proc. Brit. Ceram. Soc.* **12**, 83–98.
Paladino, A. E., and Coble, R. L. (1963). *J. Amer. Ceram. Soc.* **46**, 133–136.
Palmour, H., III, and Johnson, D. R. (1967). *In* "Sintering and Related Phenomena" (G. C. Kuczyski *et al.*, eds.), pp. 779–91. Gordon & Breach, New York.
Poluboyarinov, D. N., and Shal'nov, E. I. (1963). *Zh. Vses. Khim. Obshchestva* **8**, 148–154.
Ramakrishnan, P. (1968). *Trans. Brit. Ceram. Soc.* **67**, 143–145.
Rankin, D. T., Steglich, J. J., Petrak, D. R., and Ruh, R. (1971). *J. Amer. Ceram. Soc.* **45**, 277 281.
Resnick, R., and Siegle, L. (1966). *Trans. AIME* **236**, 1732–1738.
Rice, R. W. (1969a). *J. Amer. Ceram. Soc.* **52**, 420–427.
Rice, R. W. (1969b). *Proc. Brit. Ceram. Soc.* **12**, 99–123.
Rice, R. W. (1970). "Ultrafine-Grain Ceramics. II. Hot Forming of Ceramics." Syracuse Univ. Press, Syracuse, New York.
Rice, R. W. (1971). *J. Amer. Ceram. Soc.* **54**, 205–207
Rossi, R. C., and Fulrath, R. M. (1965). *J. Amer. Ceram. Soc.* **48**, 558–564.
Roy, D. M., Gouda, G. R., and Bobwsky, A. (1972). *Ceram. Concr. Res.* **2**, 349–366.
Roy, D. W., and Parsons, W. F. (1969). U.S. Patent 3,459,503.
Scott, B., and Carruthers, G. G. (1969). *Clay Miner.* **8**, 21–28.
Sheets, H. D., and Duckworth, W. H. (1968). *Amer. Ceram. Soc., Bull.* **47**, 803–805.
Shigetomo, M. (1970). Funtai Oyobi Funnaturakiu **17**[1], 19–24.
Spriggs. R. M., Brissette, L. A., Rissotti, M., and Vasilos, T. (1963). *Amer. Ceram. Soc., Bull.* **42**, 477–479.
Stoops, R. F. (1969). *Amer. Ceram. Soc., Bull.* **48**, 225–227.
Stuart, W. I., Whately, T. L., and Adams, R. B. (1972). *J. Aust. Ceram. Soc.* **8**, 6–9.
Suemune, Y. (1971). *Jap. J. Appl. Phys.* **10**, 454–459.
Toibana, Y., and Hashinioto, H. (1967). *Osaka Kogyo Gijutsu Shikensho Kiho* **18**, 216–223.
Van Asbroeck, P., Mestdagh, G., and Peck, P. (1967). *Energ. Nucl.* **14**, 354–364.
Vasilos, T. (1960). *J. Amer. Ceram. Soc.* **43**, 517–519.
Vasilos, T., and Spriggs, R. M. (1965). *Proc. Brit. Ceram. Soc.* **3**, 195–221.
Vasilos, T., and Spriggs, R. M. (1966). *Progr. Ceram. Sci.* **4**, 95–132.
Weiss, D., and Knapp, W. J. (1961). *Amer. Ceram. Soc., Bull.* **40**, 66–77.
Williams, G. H., and Morris, J. B. (1967). *Proc. Brit. Ceram. Soc.* **7**, 41–60.
Wise, D. C., and Trask, R. B. (1971). "Advanced Materials: Composites and Carbon; Graphite Composites for Use as Hot-Pressing Dies." *Amer. Ceram. Soc.*, Columbus, Ohio.
Zehms, E. H., and McClelland, J. D. (1963). *Amer. Ceram. Soc., Bull.* **42**, 10–12.

Isostatic Pressing

G. F. AUSTIN

Zircoa
Solon, Ohio

and

G. D. MCTAGGART

Zedmark, Inc.
Valencia, Pennsylvania

I. Introduction

Isostatic pressing is a current manufacturing technique representing an application of Pascal's law. That is, when pressure on a liquid in a closed container is increased or decreased, the pressure change takes place throughout the liquid. Hence, powdered material, loaded into a flexible, air-tight container, placed inside a closed vessel filled with liquid to which pressure is applied, will receive the force of the applied pressure uniformly over its surface area. Material compressed in this fashion will be uniformly compacted in all directions and will retain the general shape of the flexible container.

Probably the first successful industrial application in America of Pascal's law, or hydrostatic pressing as it is commonly called, was used by Westinghouse Lamp around 1913 to manufacture billets of metal powders in a process patented under the name of H. D. Madden (Madden, 1913). Re-

portedly, a Frenchman named LeChatelier (Manning, 1967) patented a process using pressure to control synthesis of ammonia from its elements in 1901. This application was unsuccessful because the pressure vessel exploded. Commercial application on a large scale was delayed until technical difficulties in supplying and containing 20,000 to 30,000 pound-per-square-inch (psi) pressures were overcome in the late 1930's. The chemical industry then began to use isostatic pressing in the manufacture of polyethylene. Later the ceramic industry capitalized on the capability of isostatic pressing for the manufacture of spark plug insulators.

Isostatic pressing conditions have been achieved in many different ways. Generally, however, three categories differentiate the usual types: cold, hot, and explosive.

Room temperature or cold isostatic pressing is the process most commonly used in the ceramic industry. In this case pressing is accomplished without applying heat to the process, and the rate of pressure increase is slow relative to the other two processes. Liquids are commonly used to carry the pressure in the vessel and, therefore, it is sometimes referred to as hydrostatic pressing. Pressures commonly experienced in the ceramic industry are in the range of 1000 to 20,000 psi, although much higher pressures are used in special situations.

Explosive isostatic pressing is used primarily in the fabrication of powdered metals and rarely in the ceramic industry. As the name implies, pressure is applied by detonation of an explosive charge, and the resulting, extremely high, pressure is reached in a very short time and maintained only briefly.

Hot isostatic pressing is a process in which pressure and temperatures are increased independently and simultaneously. Pressures are generally lower than 20,000 psi. Gases are used to carry pressure in the vessel.

A wide range of materials are now being processed by this method including titanium, carbides, carbon, zircon, zirconia, alumina, uranium dioxide, magnesia, thoria, beryllia, clays, teflon, nickel, and cermets. Items manufactured by isostatic pressing include refractory bricks and shapes, grinding media, spark plug insulators, radomes, carbide tools, ball check valves, furnace cores, sewer pipes, crucibles, and bearings.

Relatively simple equipment is used to accomplish isostatic pressing: a pressure vessel with a closure that can be opened to allow the insertion of mold or tooling; a pressure-generating system that develops the appropriate pressure; a reservoir sufficiently large to contain the pressure transmitting medium; a safety system to prevent excessive pressure buildup; and a control system that will allow the proper sequencing of operation.

At the end of World War II, laboratory isopresses, built from sections of naval guns, were capable of withstanding 20,000 psi. This was a logical use since large gun barrels must be able to withstand forces of the same magnitude

experienced in isopressing, and there is a breech mechanism by which the vessel can be opened and closed. While the equipment is relatively simple, designing a total system capable of becoming a technical and economic success requires engineering knowledge covering a wide range of disciplines.

II. Presses

Isostatic presses, then, can be as simple as a small block of steel with a hole drilled in it and filled with an appropriately sized closure and seal, or as complex as a huge machined forging that challenges the technical capabilities of major equipment suppliers. The pressure vessel normally will be a forged, thick-walled cylinder. One end will usually be capped with a closure plug having continuous threads mating with threads in the inside vessel walls. The top end of the vessel, which will be the load–unload end will be closed with a plug having interrupted threads similar to a gun breech. The threads will be machined so that the plug can be locked and unlocked with one-eighth of a turn. A hydraulic ram will serve as a hoisting mechanism to lift the lid free of the press. Hydraulic rams may be used to rotate the cover for large presses. The seal is effected with the use of an O-ring as a part of the top plug. See Fig. 1 for typical press construction.

Vessels are usually made by forging a casting of high quality, high strength

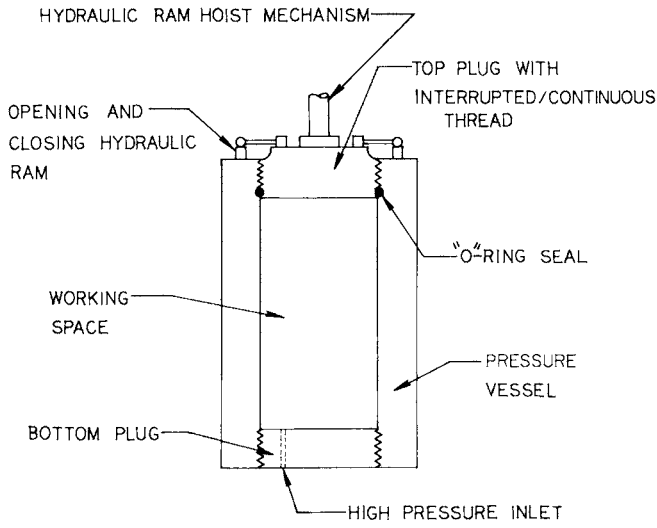

Fig. 1. Isostatic press construction.

steel melted in an electric furnace and subjected to vacuum to insure uniformity throughout. The very stringent requirements that are placed on the press manufacturer to develop extremely high quality metal for the vessel and closure are necessitated by the high stresses generated during the pressing cycle. For example, the total load exerted on a 24 in. closure at 20,000 psi is approximately 4500 tons. The closure can be either the yoke or threaded-type construction. In the case of the threaded type, the specific design of threads is very critical, they must be designed so that the load is distributed as evenly as possible. In extreme cases the closure can be hollowed out so that the closure threads are forced against the vessel threads to compensate for the slight bulging experienced with an unusually long vessel. Threads are normally acme or buttress type, and galling of mating surfaces must be prevented at all costs.

Other important considerations given to the vessel during manufacture include offsetting the pressure inlet hole in the bottom closure of large diameter vessels; honing roots and ends of threads; putting a one-eighth inch radius on the end of threads to eliminate areas of stress concentration cutting coupons at critical areas in casting for property testing; evaluating fatigue properties with strain gauges placed parallel and perpendicular to thread direction; inspecting the surface of the vessel with a dye penetrant, ultrasonic, and magnaflux inspection; and finally pretesting at 125 % of normal use pressure prior to shipment. Prior to shipment, the manufacturer should be required to provide thread protection, to insure against any damage during shipment and erection that could cause catastrophic failure during operation.

Two general types of cold isostatic pressing are employed. These are called wet-bag and dry-bag systems. The remainder of this discussion will

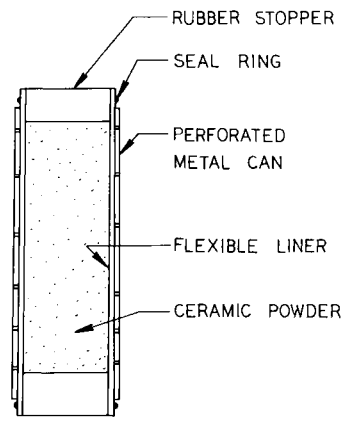

Fig. 2. Simple wet-bag tool.

concern itself with these two systems only since they include most of the isostatic pressing applications in the ceramic industry.

The fundamental difference between wet-bag and dry-bag pressing lies in how the molds are constructed. Wet-bag molds are constructed individually and independent of the press itself. Figure 2 depicts a simple wet-bag tool. After the mold is filled with powder and sealed, it is placed in the vessel and is completely submerged during pressurization and decompression. The mold contents are compacted by the force of the liquid acting directly on the mold surface area. The name, wet-bag, is derived from the fact that the tool is in contact with the liquid during the cycle. Figure 3 illustrates the wet-bag pressing principle.

Dry-bag tooling derives its name from the fact that the mold does not contact the pressure-transmitting liquid during the cycle. As shown in Fig. 4, the tool is a permanent part of the pressure vessel construction. The liquid

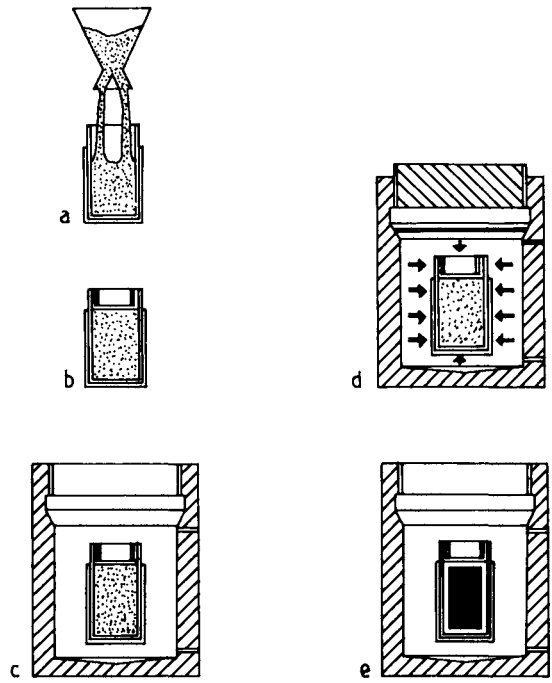

Fig. 3. The wet-bag pressing principle. (a) Fill up flexible bag tooling with material to be compacted. (b) Close and seal bag tooling. (c) Bag tooling in pressure medium and pressure vessel. (d) Pressurize. (e) Resulting compact, after decompression. Courtesy of Loomis Products Company.

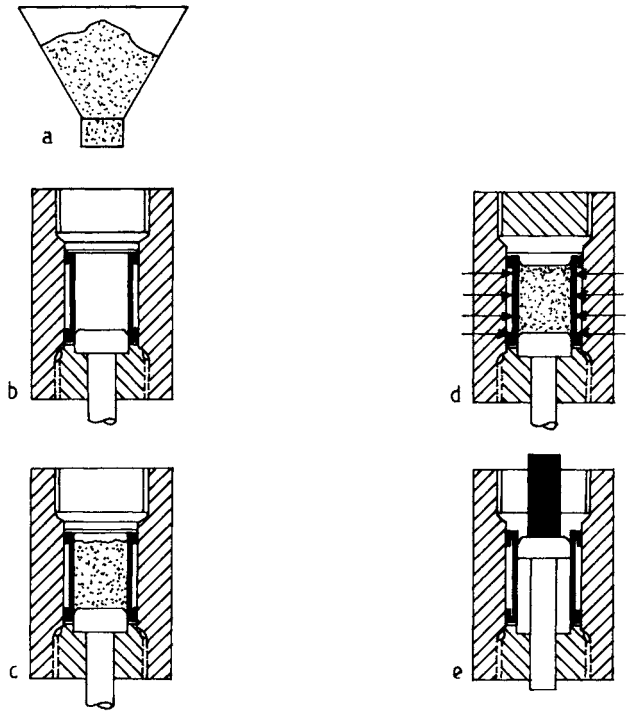

Fig. 4. Dry-bag tool. (a) Material to be compacted. (b) Pressure chamber including dry bag. (c) Pressure chamber filled. (d) Pressurizing. (e) Ejection of compact after decompression. Courtesy of Loomis Products Company.

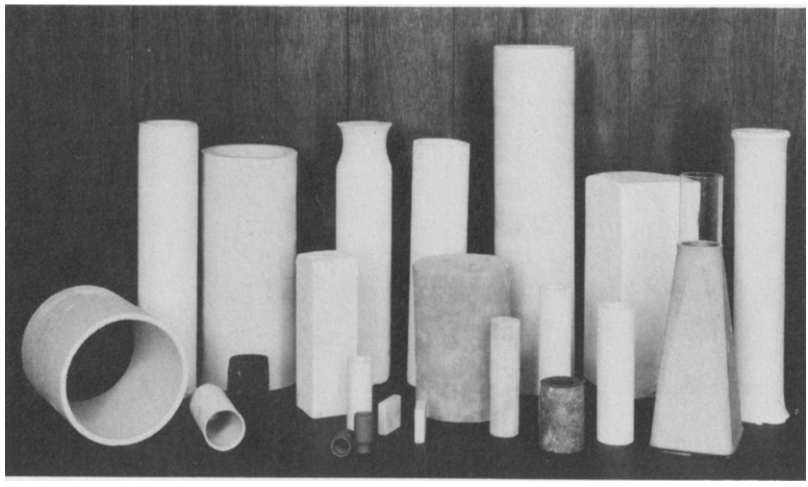

Fig. 5. Various shapes and materials isostatically pressed using both wet- and dry-bag tooling. Courtesy of Loomis Products Company.

is pressurized behind the flexible double liner, forcing it against the mold itself, effecting compaction. Figure 5 shows various shapes and materials isostatically pressed using both wet- and dry-bag tooling.

Molds or tooling for either wet- or dry-bag systems must satisfy certain criteria. Compatibility with both the pressing medium and the material to be compacted is essential. Flexible portions of the mold must be able to change volume as dictated by high pressure application and compaction rate of the material being pressed; yet they must be durable enough to withstand abrasion and repeated cycling. Since each mold is opened and closed once every cycle, the mold material must be able to withstand being resealed many times. While it must be flexible, the mold should be rigid enough to prevent being forced into the powdered material where it would prevent easy removal from the pressed compact. In cases where a very thin material is used to contain the powdered fill, consideration must be given to the entrapped air that can build up pressure in the range of 25–50 psi when it is forced from the compact during compression. The entrapped air will form a bubble at the top of the mold, and the mold must be strong enough to withstand this force.

Molds for wet-bag tooling normally consist of a flexible portion, which is filled with powder, inside a rigid, perforated container that serves as a carrying case as well as to control the shape of the pressed items. The flexible portions can be manufactured from many materials. Some of the more common are natural and synthetic rubber, urethane, polyvinyl chloride (Powell, 1965), silicones, and some plastics. Stainless steel and aluminum are often used for the rigid carrying case, but any metal that is compatible with the chemistry and economics of the particular system can be used.

Dry-bag tooling differs from wet-bag in that a rigid metal carrying case is not used, and the tooling is an integral part of the press construction.

III. Pressure-Generating Systems

Pressure-generating systems can be of two general types. Pressure required for isostatic pressing may be produced with a high-pressure pumping system remote from the pressure vessel or by a piston acting directly on the liquid in the pressure vessel itself. Pumped systems are the more common of the two systems. The direct acting piston system is more expensive, except in the case of a very small pressure vessel. Pumping systems occupy less space, and size of product is dictated by the size of the vessel, rather than by just the diameter and length of stroke as in the piston system.

A pumping system design will be governed largely by required cycle

speed, the compaction characteristics of the ceramic powder, and pressure-transmitting medium and the maximum pressure required. If the maximum pressure is 20,000 psi, serious problems may be encountered. For up to 20,000 psi, reliable equipment is readily available. Pressure can be reached with single, double, or more, pumping stages. For example, in a very large-volume capacity, high-pressure system, it would probably be more economical to consider a three-stage pumping system using a high-volume, low-pressure first stage, a slightly lower volume, higher pressure second stage, and a high pressure, low-volume third stage than to contemplate either a single- or double-stage system. With a three-stage system, all three stages would start pumping at the beginning of the cycle, and each stage would stop pumping automatically when the vessel and pump pressure were equal, until at the highest pressure only one stage would be operative. Generally speaking, cycle time is a function of selecting a larger pump or pumping system, so economics comes into consideration very rapidly with very short cycles.

To prevent entrapped air from destroying the compact, decompression of the system must be considered very carefully including such factors as extremely fine particle size distribution, very large compacts, high moisture content, high binder concentrations, relatively short cycles, or combinations of these parameters. For most applications, decompression can be fairly rapid down to approximately 200 psi pressure due to the compressibility characteristics of air. Air entrapped in the compact will not be disruptive until less than 200 psi, because it is compressed to approximately 85 % of theoretical. Below 200 psi, it is generally recommended that decompression rate requirements be understood rather precisely.

In all systems, fail-safe equipment should be designed to prevent the possibility of failure. Rupture disks, which are calibrated to fail at approximately 10 % over system operating pressure, are universally accepted as one safety device. Barricades are recommended and used where extremely high pressures are encountered. However, there are no universally agreed upon safety standards covering shielding, barricading, instrumentation, maintenance, and operation (Pohto, 1971). Other safety devices and practices that are recommended include operators and maintenance men trained to the extent that they understand the total system completely; an automatic valving arrangement design that allows air to be expelled from the vessel during pressurization; control circuitry design such that the head or closure cannot be opened while the vessel is pressurized; instruments and control systems monitored during each cycle to detect any abnormality when it occurs; instruments and control systems checked and calibrated using qualified maintenance men on a regularly scheduled basis; rupture disks replaced every six months; instrument air filtered routinely; filtering equipment checked for both air and liquid pressure transmitting medium on a

regularly scheduled basis; filter elements replaced on a regularly scheduled basis; and vessel, top and bottom closure, and threads checked by subjecting to ultrasonic, dye penetrant, and strain gauge testing on a regularly scheduled basis using qualified personnel.

Fluids normally used to transmit pressure are glycerin, water, and hydraulic oil. Selection of fluids is determined by their compatibility with bag tooling material, compressibility, compatibility with seals in the vessel and with vessel construction, as well as economics and availability. Compression is an extremely important consideration for wet-bag and pumping systems. High compressibility in wet-bag systems can substantially reduce the available working volume in the vessel. Obviously, high compressibility drastically increases pumping time. Low compressibility liquids, such as water, are considerably less dangerous in the case of failure, since loss of pressure is almost instantaneous in small vessels and very rapid in large vessels.

Consideration must be given to filterability in wet-bag systems to allow for the separation of powder fill in the event of tooling material failure. Since most ceramic powders are extremely abrasive, they must be filtered out prior to the fluid entering the pumping system to ensure economic life and reliability of the pumps. Rust inhibitors must be added to water systems to prevent corrosion and pitting of the inside surface of the vessel. Fortunately, recommending suitable filters and rust inhibitors that are compatible is well within the capabilities of most isostatic press manufacturers.

IV. Equipment Selection

Selection of equipment for an isostatic-pressing process centers around the utilization of the advantages and disadvantages of the system as a fabrication technique.

Advantages are (Teter, 1967):

1. Product uniformity from piece to piece as well as throughout the piece.
2. Shapes and sizes not possible by other methods (Weherenberg *et al.*, 1968).
3. Much faster production rates than slip casting and extrusion because a slow drying process is eliminated.
4. Much less floor space used than slip casting due to elimination of drying.
5. Less sensitive to soluble impurities that hamper slip casting.
6. Green machining possible.

7. Less raw material consumption per piece where subsequent grinding is required.
8. Voids common to slip casting operation eliminated (Weherenberg *et al.*, 1968).
9. Rejects from breakage drastically reduced (Oberschmidt, 1967).

Disadvantages are:

1. Limited information concerning technical details of material preparation and tooling design, necessitating considerable research.
2. Long time necessary to develop and establish a total process.
3. Relative large initial cost of installation.
4. Coarse grains can cause excessive wear on tooling, eliminating them from applications where they might be necessary for control of a product attribute.

V. Parameter Considerations

Once the ceramic designer has reviewed his needs and compared them with the advantages and disadvantages of an isostatic pressing process and decided that he should pursue the isostatic approach, a research and development program will have to be designed to answer questions in several very specific areas: (1) characterization of raw material, (2) methods of preparing raw material for pressing, (3) maximum production rate required, (4) maximum size piece to be manufactured, (5) maximum pressure required for densification, (6) tooling design, (7) exact pressing and decompression cycle, (8) ultimate process flow, (9) what suppliers are capable of meeting the requirement determined by the development program, (10) safety features required, and (11) economic justification.

Characterization of raw material for isostatic pressing should not present a problem to the ceramic designer (except where very coarse grog is required to control a particular product attribute) and, therefore, rather standard procedures should be utilized to determine physical and chemical characteristics that will produce the desired properties when the pressed item is fired.

Material preparation is probably the most important step in the total operation once raw material has been characterized. For the process to be reliable, the material preparation method must be capable of reproducing the ceramic powder fill characteristics day after day. Many characteristics of the powder fill must be controlled during this step of the operation, and these include (1) particle shape, (2) average particle size, (3) particle size distribution, (4) flowability of the powder, (5) apparent density, (6) tap

density, (7) surface area per unit of weight, (8) compressibility, and (9) moisture content.

Many different methods are cited in the literature for preparing raw material for isostatic pressing, but the most commonly used method is spray drying. In spray drying, the ceramic powder is mixed with a combination of binders, a liquid (usually water), dispersing agent, pH control agent, plasticizers, and lubricating agents. It is then pumped through an atomizing unit, forming small spherical droplets, into a drying chamber where evaporation takes place, leaving a free-flowing powder that is very desirable for material handling and mold filling. Spray drying has an advantage over most other granulating systems because of its inherent ability to control the critical powder parameters and at the same time allow the introduction of binder and or other additives easily. Because binders are necessary for the control of particle size distribution, the ceramic designer frequently will find he has to use a combination of binders to get the desired powder characteristics and compact strength in the green state. Binders, then, become extremely important in the isopressing operation and must be selected very carefully (Hoffman, 1972).

Binders must be able to provide control of specific functions from their introduction up to and including burnout during the firing cycle. At the same time they must not have any deleterious impact on any other phase of the manufacturing cycle. For example, the binder must allow the green compact to have sufficient strength for handling or green finishing, but it must not affect the fired characteristics of the compacts with its own burnout characteristics.

As previously discussed, two types of spray dryers are available for use in material preparation. For large outputs, the spinning-disk type is preferred because it tends to be more economical and average particle size tends to be smaller. Where larger average particle size is required, two-fluid nozzle atomization (Wilk, 1965) is preferred.

Very coarse grog may be desired to control a particular product attribute, to decrease the compaction ratio of the powder fill, or simply to reuse rejected material. It can be added to spray-dried material by blending in twin-shell or double-cone type blenders with satisfactory results. Bell (1968) describes a method of mixing up to 60%, 8- to 65-mesh grog, with −100-mesh and −400-mesh Dundas shale by using a rotary drum pelletizer constructed specifically for the project. Material this coarse would be impossible to spray dry. By utilizing the isostatic press, Bell was able to form and fire compacts from materials that are not good candidates for extrusion or slip casting.

Maximum production rate required will be governed largely by economics, as with most fabrication techniques, and it will also play a key role in the decision regarding whether wet-bag or a dry-bag process is utilized. The

dry-bag process is better suited for manufacture of many pieces of the same shapes such as spark plugs, while the wet-bag process is more versatile in that any shape item can be pressed on any given cycle. For laboratory or experimental work, the designer will be wise to select a wet-bag system so he can exploit its versatility. Some companies have purchased the wet-bag type for specialty products, and from the operation developed the necessary information to allow them to justify dry-bag operations.

Maximum piece size to be manufactured determines the size of the pressure vessel. Generally speaking, the larger the vessel the more it will cost. In the case of a wet-bag system, the possibility of using a larger vessel to increase the number of compacts pressed per cycle must be given careful economic consideration because the auxiliary equipment will remain essentially the same in either case.

Maximum pressure required for densification has an impact on size of the vessel, size and type of the pumping system, and type and number of safety measures used. And all of these items will have the effect of increasing the cost of an installation. The designer will have to do considerable research and development in this respect because the literature suggests there is little agreement as to what pressure will be optimum for a given product or raw material. Equipment suppliers are probably the best possible source of recommendations and all are agreeable to cooperative testing programs aimed at determining maximum pressure requirements.

Tool design parameters have been fairly well described (Colthorpe, 1968) but still remain very much an art. This is the weakest area of isostatic pressing and will remain so until there are sufficient quantities of molds designed and manufactured so that engineering data can be accumulated, allowing the tool designer a more scientific approach. Colthorpe (1968) recommends the the following considerations when designing tooling:

1. Final component shape
2. Dimensional accuracy required
3. Surface finish
4. Production rate
5. Ultimate density required
6. Green and/or fired finishing
7. Compaction ratio of the powder
8. Evacuation of tool prior to pressing
9. Vibration of tool prior to pressing
10. Mold tool material

The first six items can be approached in the same fashion as with any other fabrication technique by the ceramic designer. Mold tool material should be established only after consultation with press and tooling manufacturers.

Compaction ratio, which is the ratio of volume change between the pressed and unpressed compact, must be determined experimentally on each material that is to be processed. The compaction ratio is used to determine tooling size as follows:*

1. Dry-Bag Tooling—shapes (radial pressing only)
   a. Determine compaction ratio by measuring the green compact after pressing a blank in a tool of known size. For this exercise use a compaction ratio of 2 : 1.
   b. Shape required will be 6 in. in diameter and 10 in. long.
   c. Tooling size will be:
      desired size × the square root of the compaction ratio.
      $6 \text{ in.} \times \sqrt{2} = 6 \times 1.414 = 8.5 \text{ in. diameter} \times 10 \text{ in. long.}$
2. Wet-Bag
   a. Determine compaction ratio by pressing and measuring blank as above.
   b. Use compaction ratio of 2 : 1 for this example. Shape required: 6-in. diameter by 10-in. long rod.
   c. Tooling size required:
      desired size × the cube root of the compaction ratio.
      $$\sqrt[3]{\text{C.R.}} = \sqrt[3]{2} = 1.26$$
      $$1.26 \times 6 = 7.56 \text{ in. diameter}$$
      $$1.26 \times 10 = 12.6 \text{ in. length}$$
3. Hollow Shapes
   a. These shapes require a slightly different approach than solids. Calculations are made by using areas of shapes, since pressing is radial only. However, compaction ratio is still the basis for calculation. For this example use a compaction ratio of 2 : 1.
   b. Shape required is a hollow rod: (6 in. OD × 3 in. ID × 10 in. long)
   c. Formula used is

$$\begin{aligned} &\text{Area of outside diameter} = 6 \text{ in. } \phi = 28.3 \text{ in.}^2 \\ &\underline{\text{Minus area of mandrel} = 3 \text{ in. } \phi = 7.1 \text{ in.}^2} = 21.2 \text{ in.}^2 \end{aligned}$$

$$21.2 \text{ in.}^2 \times \text{compaction ratio} = 21.2 \times 2 = 42.4 \text{ in.}^2$$

$$\underline{\text{plus area of mandrel} = 3 \text{ in. } \phi = 7.1 \text{ in.}^2} = 49.5 \text{ in.}^2$$

$$49.5 \text{ in.}^2 = \text{area of tooling} = 7\tfrac{15}{16} \text{ in.}$$

Then tooling size is $7\frac{15}{16}$ in. O.D. × 3 in. I.D. × 10 in. long.

The amount of firing shrinkage must be taken into consideration when determining the size of a mold. That is, the difference in size between the fired piece and the mold is the combined result of volume firing shrinkage

*Correspondence with A. Ganss, Loomis Products Company, Levittown, Pa.

and shrinkage due to compaction. Firing shrinkage must be determined experimentally as it is for any other technique. Ultimately, the size vessel needed to accommodate the largest tooling will be determined by adding firing and pressing shrinkage to the appropriate thickness for various mold components. Clearance to facilitate loading must also be added in the case of wet-bag tooling. Also, the designer must remember to use the diagonal for the largest dimension in square or rectangular cross sections when determining the largest mold a vessel will hold. To obtain large size pieces from a given size mold, jolting may be used during the mold-filling operation. This will allow more pounds of fill to be added and will result in a lower compaction ratio. This method is of value in the wet-bag process for rectangular items but is of little value in the dry-bag process.

Exact pressing and decompression cycles can be obtained experimentally in cooperation with most equipment manufacturers and can be very critical in some applications as previously described. To insure the capability of decompressing successfully, evacuation of the tool prior to pressing (Papen, 1968) should be considered. When the tooling is evacuated, positive steps should be taken to prevent the abrasive powder fill from being pulled into the vacuum equipment.

Ultimate process flow will involve the integration of all facets of the operation and the potential combinations will vary as widely as does the application of isostatic pressing. Much more automation is feasible with a spark plug insulator dry-bag operation than with a wet-bag system engaged in the production of specialty refractories for glass tanks. However, there is nothing inherent in isostatic pressing that deters the designer from using fundamental materials-handling principles to establish process flow. At this juncture, the designer will have sufficient experience and knowledge to allow him to make judgments on the capability of potential suppliers to satisfy all the requirements dictated by the experimental data generated during the development program. Review of the isostatic pressing vessel design may well be beyond the capability of the ceramic designer. Consideration should then be given to employing the services of a consultant specializing in this field.

Since there is a limited amount of information available on safety practices, each installation probably varies from all others with regard to safety design. Suppliers will, of course, be familiar with federal and local laws governing the use of high-pressure vessels, and utilizing their experience and knowledge will be of paramount importance to the designer.

Justification for isostatic pressing for some operations may be as straightforward as it is in the spark plug insulator industry or the justification may represent a long-term investment such as it has been in the development of an isostatic press capable of pressing clay sewer pipes. The designer must be aware of current manufacturing costs, as well as projected costs because

the press itself and much of the associated equipment will have a relatively long life. For example, if the press represents a method to reduce the rejection rate in an existing process, there will be a reduction in the amount of fuel required per pound of product yielded by the process. Since fuel costs are predicted to rise at an astronomical rate, the designer must be prepared to put much more emphasis on this portion of the justification then he would have even two years ago.

VI. Operation

A typical isostatic process might be represented by the unit operation shown in Fig. 6. Each of the steps shown can represent a critical operation in most ceramic fabrication processes as far as the final product is concerned.

The plant operator now has the data generated by the ceramic designer and can establish operating parameters that will permit the process to produce a high quality product on a scheduled basis that will satisfy the demands of the market place and allow a reasonable return on investment. The first seven-unit operations shown in Fig. 6 must be controlled precisely if the final product is to be produced with uniform quality from day to day. While the rheology of the wet milling may be fundamentially easier to control than that of a slip-casting operation, rigid adherence to control parameters is mandatory. To exercise the appropriate degree of control, it will be necessary to establish raw material specifications with reliable suppliers and monitor shipments to assure that the material meets specifications as it goes into the batching operation. Batching, wet milling, screening, and magnetic separation are conventional unit operations and are compatible with the isostatic pressing function in all respects. The spray dryer is the granulating mechanism that gives the ceramic raw material its free-flowing characteristic that is so vital for uniform and predictable green densities in the pressed compact. With spray drying, several approaches can be taken based on the specific requirements of the system. If a narrow particle size distribution is desired, only the material generated in the drying chamber can be used. A wider range in distribution can be generated by using a part of the fines collected in the cyclone portion of the spray dryer; or the total chamber and cyclone product can be used. If the cyclone product cannot be used in pressing, it is economically desirable to recycle this material back through the process. Therefore, it is wise to select plasticizers and other additives that will not interfere with the wet-milling operation. If coarse grog is to be used, a blending operation will be necessary to control the homogeneity of the material as it is fed into the tool. Loading or filling the tool may require jolting in the case of wet-bag operations. If this

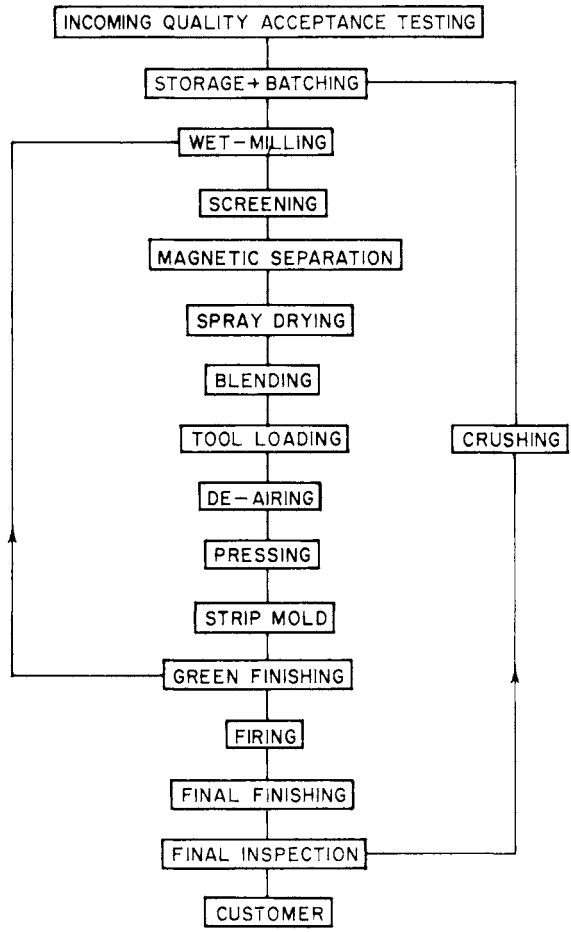

Fig. 6. Isostatic process flow chart.

occurs, care should be taken to guard against the occurrence of laminations. De-airing may be required for either type operation, and a very high vacuum may be necessary in special cases. Conventional equipment can be used to evacuate the tool but a positive method of sealing off the vacuum port must be used.

Specific operation of the isostatic press sequentially is as follows:

1. Fill tooling correctly and seal (evacuate tool if required)
2. Load tooling into vessel (automatic for dry-bag operations)
3. Place closure in vessel

4. Lock closure in place
5. Evacuate tool in dry-bag operation
6. Fill vessel with pressure-transmitting medium
7. Pressurize
8. Depressurize
9. Unlock closure when zero pressure is reached
10. Remove closure
11. Remove mold from press
12. Remove green compact from tooling
13. Repeat the cycle

Mold stripping must be done with some degree of moderation to eliminate any possible danger of destroying the flexible portions of the tooling in a wet-bag operation. Stripping and mold filling can be accomplished while the vessel is running a cycle to utilize manpower efficiently.

Green finishing, firing, final finishing, and inspection will not require special techniques as a result of isostatic processing.

VII. Conclusion

Isostatic pressing is a well-established method of forming that has not yet begun to reach its potential in the ceramic industry. Yet the system has made amazing inroads since its initial large-scale application for spark plug insulators in the early 1950's. As mold design technology improves and press manufacturers learn how to construct smaller units with higher capacities, the use of isostatic pressing in the ceramic industry will accelerate.

References

Bell, K. E. (1968). *J. Can. Ceram. Soc.* **37**, 38–40.
Colthorpe, A. C. (1968). *Ceramics* **71**, 14–18.
Hoffman, E. R. (1972). *Ceram. Bull.* **51**, 24D–242.
Madden, H. D. (1913). U.S. Patent 1,081,681.
Manning, W. R. D. (1967). *Chem. Process Eng.* 51.
Oberschmidt, L. E. (1967). *Brick Clay Rec.* **150**, 34.
Papen, E. L. J. (1968). *Interceram* No. 1, 65–72.
Pohto, H. A. (1971). *U.S. At. Energy Comm., Res. Develop. Rep.* **Y-175B**.
Powell, R. A. (1965). *Int. J. Powder Met.* **1** (3).
Teter, A. R. (1967). *Ceram. Ind.* **88**, 46–48.
Weherenberg, T. M., Begley, E. R., and Patrick, R. F. (1968). *Ceram. Bull.* **47**, 642–645.
Wilk, G. (1965). *Interceram* No. 2, 129–130.

Slip Casting

ROBERT E. COWAN

Los Alamos Scientific Laboratory
University of California
Los Alamos, New Mexico

Slip casting is a unique process that the ceramist has long utilized as one of his basic forming techniques. It is a very versatile process—one that is used both by the ceramic artist and the manufacturer of highly sophisticated technical ceramics. The versatility of the process has led to the development of slip casting techniques for many different materials. It is the intent of this chapter to review some of these new techniques and to guide the reader in his pursuits into similar areas.

I. Basic Slip Casting Process

In essence, slip casting consists of the following steps:

1. Preparation of a mixture of a powdered material and a liquid into a stable suspension, called a slip.
2. Pouring this slip into a porous mold, usually made from plaster of Paris, and allowing the liquid portion of slip to be partially absorbed by the mold. A layer of semihard material is formed against the mold surface as liquid is removed from the slip.
3. Interrupting the casting process when a suitable wall thickness has been formed. This is done simply by pouring the excess slip out of the cavity. This is known as drain casting. Alternatively, a solid object may be made by allowing casting to continue until the entire mold cavity is filled with semihard material. This variation is called solid casting.
4. Drying the material in the mold to provide adequate strength for handling. Some shrinkage usually occurs in this step.
5. Removal of the solid object from the mold.

The slip cast article has sufficient strength to be handled and to permit other operations such as trimming rough surfaces from mold seams. Ware made by slip casting is rarely used in this form but is subsequently fired at a temperature suitable for densifying the particles into a cohesive structure. The firing operation is much like that used in other ceramic processing. Details of firing will not be discussed except as they apply to special problems associated with slip casting.

There are many advantages of slip casting. It is ideally suited for forming thin-walled and complex shapes of uniform wall thickness. The molds, being made from plaster of Paris, are inexpensive. This feature makes slip casting especially attractive for development items or short production runs. The primary disadvantage of the process is its lack of precise dimensional control. Tolerances less than 1 % are possible, but only with well-characterized materials and considerable experience with the process.

II. Theories of Slip Casting

Many theoretical treatments of the slip casting process are found in the literature. These may be roughly divided into three categories. The theories relate to (1) the mechanisms of deflocculation and flocculation of solid particles in liquid media, (2) the rheology or flow characteristics of such suspensions, and (3) the process of forming solid casts from liquid slips.

A. Theories of Deflocculation

There is no single unified theory that accounts for all the observed characteristics of slips. This is unfortunate because such a theory, while being valuable in its own right, would allow the ceramist to choose his deflocculants on a scientific basis rather than by trial-and-error. Most theorists agree that solid particles, when suspended in a liquid medium, become electrically charged. These charges are of like sign and produce forces of electrostatic repulsion between particles. If these forces are sufficient to overcome the attractive van der Waals forces, the system is said to be deflocculated. The state of deflocculation is not unique but varies in degree according to the magnitude of the repulsive forces. This leads to various flow or viscosity characteristics of a slip.

The development of electrically charged particles has been visualized in several ways. Brindley (1958) described the "broken bond" theory in which the particle surfaces show an electrical charge because of unsatisfied chemical bonds. Lewis (1961) pictured the negative charge on alumina being developed by the larger oxygen ions "screening" the positive charges of the smaller aluminum ions. The overall charge on oxide particles is usually negative. However, the charge may not be symmetrically distributed over all surfaces, particularly in the case of clay minerals, which have layered crystal structures.

The electrically charged solid particles are known to attract other charges from the liquid vehicle. In distilled water, H^+ or OH^- ions are attracted to the particles. If an acid such as HCl is added to the liquid, a layer of Cl^- ions

is formed adjacent to the layer of H^+ ions. The exact nature of the layers of ions surrounding the particles is a subject of controversy, probably because the analytical techniques necessary to study such structures are extremely difficult. The classical Helmholtz double layer is one view of the ionic layer structure. Hauth (1950) described the layers as a "diffuse double layer." Worrall (1963) emphasized the importance of "counter ions"—the anions from a deflocculating acid—as a major factor in the structure. Lewis (1961) presented a somewhat different view in which a polar screen is formed around each particle by hydrogen bonding of polar ions or molecules. In general it is found that there is an optimum charge on the particles that will cause proper dispersion. If an excess of electrolyte is added, the layer structure will collapse and allow the particles to flocculate. Less-than-optimum charge fails to overcome the attractive forces and again the system is not fully deflocculated.

The purpose of deflocculating a slip is to make the rheological properties suitable for handling and to allow proper cast formation. Most materials may be deflocculated in either an acid or an alkaline medium. Anderson and Murray (1959) showed that the point of minimum viscosity corresponds closely with the point of maximum zeta potential, a measure of the magnitude of the electrical charge on the particles.

B. Rheology of Slips

It is important not only to have a slip that has minimum viscosity, but one in which the rheological properties are suitable for casting. The flow properties of slips are usually illustrated by graphs showing the shearing stress as a function of the rate of shear. For liquids such a curve is usually a straight line having its origin at zero. Suspensions of solids in liquids, particularly at the concentrations involved in slip casting, rarely show such behavior. Instead, considerable nonlinearity and hysteresis are observed. The three main features of this nonlinearity are yield point, thixotropy, and dilatency.

Yield point is an abrupt change of slope of the curve. Thixotropy is a decrease of viscosity with increasing strain rate. The opposite of this, a decrease of viscosity with increase in strain rate, is called dilatency. All three of these phenomena, singly or in combination, are usually encountered in practical applications of slip casting. The degree to which these occur varies considerably and a good slip is one in which these factors are minimized. A highly dilatent slip cannot be poured nor will it fill small details of a mold. A slip that is thixotropic will have high permeability of the cast layer, which leads to high casting rate and low density (Worrall, 1963). A high yield point will inhibit good draining characteristics. It has been shown by Moore (1959) that yield point is influenced strongly by the amount and type of deflocculating agent. A properly deflocculated slip will exhibit a very low yield point.

Dilatency occurs over relatively narrow ranges of liquid contents. It is accentuated by the presence of a substantial fraction of colloidal particles. Dilatent slips usually have insufficient liquid content. Beazley (1965) described many features of dilatency and how it is formed in china clay suspensions.

Thixotropy is often encountered in casting slips. It is thought to be a characteristic of suspensions of particles having irregular shape. The control of thixotropy is largely a matter of proper liquid content and optimum deflocculation. Moore has emphasized the necessity of making viscosity measurements at very low shear rates. Here the effect of thixotropy is most pronounced and it also approximates the conditions under which slip is poured into a mold. Mehta and Langston (1963) have suggested a control test for casting slips in which shear stress measurements are made at two different shear rates. By calculating the negative shear rate intercept, a measure of the state of deflocculation may be determined. The slope calculated from such data characterizes the state of dilution of a slip. A comparison of these values with those of a known "good" slip allows one to decide whether to add liquid or deflocculant.

C. Mechanism of Cast Formation

Investigations of the mechanism of formation of solid casts from slips have shown that it is a diffusion-controlled process (Hermann and Cutler, 1962) and amounts to a simple dewatering of the slip (Adcock and McDowall, 1957). The driving force for this process is the suction pressure created by the porous plaster mold. When a slip is first poured into a mold a high rate of casting is observed for a few seconds. This is due to the high rate of water diffusion in the plaster. Following this initial stage, the rate of cast formation is determined by the permeability of the solid cast. It has been shown (Adcock and McDowall, 1957) that the rate of cast formation can be quantitatively determined by

$$\frac{L^2}{t} = \frac{2PgE^3}{5\,S_p^2\,\eta\,(y-1)\,(1-E)^2} \tag{1}$$

where L is the thickness of the cast layer, t is time, P is the suction pressure, E is the void fraction, S is the surface area of solid particles, η is the viscosity of fluid, y is the volume of slip containing volume $(1 - E)$ of solids, and g is acceleration due to gravity.

This equation has been experimentally verified and a number of important features of the slip casting process may be predicted from it. These features are as follows.

1. The thickness of the cast layer is proportional to the square root of time.
2. Surface area plays an important role in casting rate because it is a squared term and also because it determines the mode of particle packing and hence the values of E and y.
3. The permeability of the cast, measured by E, strongly influences casting rate. The term $E^3/(1-E)^2$ is very sensitive to small changes in E and therefore strongly affects casting rate.
4. The viscosity of the liquid phase affects casting rate. Temperature changes may cause this term to vary.
5. Casting rate is related directly to the pressure on the slip. This factor is important in techniques such as pressure casting.

III. Molds

A. Plaster

The preparation of plaster molds is an important part of the slip casting process. The reader is referred to the excellent article by Lambe (1958) for a thorough discussion of all aspects of plaster molds.

Most molds are made from pottery plaster using the approximate ratio of 3 parts of water to 4 parts of plaster by weight. The plaster of Paris ($CaSO_4 \cdot \frac{1}{2}H_2O$) rehydrates to form a network of gypsum "needles" which are separated by pores a few tenths of a micron in diameter. These small pores create a suction pressure due to the forces of surface tension and cause liquid to be withdrawn from a slip.

The rate at which casting proceeds is important. High casting rates are difficult to control and may cause premature release of the casting from the mold or other defects. Excessively slow casting rates may result in settling of coarse particles. The casting rate of a slip is partially determined by mold permeability. This is affected by such variables as the plaster–water ratio in the initial mix and the amount of water in the mold from previous use. Plaster molds have different casting properties throughout their lives. Initially, the casting rate is slow but soon becomes faster because of the dissolving action of water on gypsum which increases the permeability (Lambe, 1958; also Harkort and Hoffman, 1971). Deflocculating agents in the slip cause deterioration of the mold by chemical corrosion (Lehmann, 1958). Acid slips are particularly troublesome in this respect. After much use deflocculants block the pores of the mold and the casting rate decreases, often to the point where the mold must be discarded.

B. Mold Release Agents

Despite the best efforts of the ceramist, some materials persist in sticking to the mold surface. Release agents are frequently employed to overcome this problem. These materials must cause minimum interference with the casting process. They usually remain on the cast ware and therefore should burn away harmlessly or cause no deleterious effects during firing. A great variety of mold release agents have been described. These include alginates (Rempes, 1961; also Rempes *et al.*, 1958); graphite (Cowan *et al.*, 1962); oxides and silicates (Williams, 1963); and talc, silicones, and olive oil (St. Pierre, 1958a). It has recently been pointed out to the author that Faultless Spray Starch, made by Faultless Starch Co., Kansas City, Missouri, is an excellent release agent (D. E. Nuckolls, Los Alamos Scientific Laboratory, personal communication, 1973).

C. Nonplaster Molds

Occasional use of nonplaster molds has been made. Adami and Williams (1963) used a perforated metal mold contained in a vacuum vessel and lined with fine macerated paper pulp. Double weight seamless extraction thimbles were successfully used by Greenaway (1952) for casting magnesia. St.Pierre (1958b) used green sand molds similar to those used in foundry practice for casting molybdenum metal.

IV. Constituents of Slips

A. Characteristics of Slips

The characteristics of a good slip may be summarized as follows:

1. *Viscosity.* The slip must pour easily and fill all details of a mold. It must not exhibit pronounced dilatency, thixotropy, or have a significant yield point. It must also allow air bubbles to rise and break.
2. *Settling Rate.* The particles in suspension must not settle appreciably during the time necessary to make a casting. Otherwise tapered walls and thick bottoms will result.
3. *Sensitivity to Mold Conditions.* Some slips may have slow casting rates in areas of the mold containing fingerprints or model release agents. This produces uneven wall thicknesses.
4. *Release.* The dry cast must release from the mold at the proper time.

Premature release causes uneven wall thicknesses. The lack of proper release during drying causes stresses in the ware or may result in fracture during removal.

5. *Shrinkage During Drying.* The cast piece should shrink slightly during drying to allow for proper release.

6. *Drain Properites.* Excess slip, when poured from the mold, should flow freely, allowing the formation of sharp interior corners. Drain marks should not appear inside the cast piece.

7. *Strength of Cast Ware.* The cast object must have sufficient strength to allow handling, trimming, or further shaping operations.

8. *Casting Rate.* The wall must build up at a rate that can be controlled, yet be consistent with reasonable production rates and good properties.

9. *Freedom from Foaming.* A slip that foams often produces poor ware because of entrapped air bubbles.

10. *Low Evaporation Rate of Vehicle.* The liquid must have a low evaporation rate, or a dry film will form on the surface that is exposed to air. This dry material will be difficult to resuspend after the excess slip is drained. These slip characteristics may be attained with the proper blend of solid particles, a liquid, and modifying agents.

B. Solid Phase

The size of the particles constituting the solid phase may vary over a wide range depending upon the density of the material and the desired characteristics of the fired ware. Porous bodies may contain fractions of coarse materials as large as 1 mm. High density materials require submicron particles to avoid settling. Experience has shown that oxide bodies to be fired to vitrification should consist of particles smaller than 20 μm in diameter with at least half the particles being between 1 and 5 μm. Extremely fine particles, such as those smaller than 1 μm may cause problems because they require large amounts of liquid for a useable slip and dilatency is more often encountered.

The surface area of the particles is also an important consideration. This factor is directly related to particle size but is also influenced by particle shape. Powders made by calcination are usually irregular in shape and have higher surface areas than those that are fused and then ground to a fine size. The latter are easier to form into a workable slip, however, their lower surface area may make them more difficult to fire to a high density. Some materials such as magnesia and calcia may react with the suspending liquid. The use of fused material having a low surface area helps minimize this problem.

The proper distribution of particle sizes is also an important factor in slip formulation. The green ware should have a high density to avoid high firing

shrinkage. This can only be attained through proper packing of the particles. A range of sizes is necessary for this to occur. It has been shown (St. Pierre, 1958a) that maximum density is attained using a size distribution which follows

$$P = (x/D)^m \tag{2}$$

where P = percent undersize, x = particle size, D = maximum particle size present, m = a constant between 0.33 and 0.5.

Achieving a particle size distribution such as this is not always easy. Blending several size fractions is possible, but is not always economically feasible. Certain fused silica slips have this distribution and are obtained by wet ball-milling coarse material to the desired size range. These slips cast to green densities greater than 80 % of theoretical (Harris and Welsh, 1973).

C. Liquid Phase

The liquid phase of casting slip should have the following characteristics: (1) relatively low vapor pressure, (2) compatibility with suspended solid, (3) nontoxic and low fire hazard, (4) cheap, (5) low viscosity, and (6) ability to dissolve deflocculating agents. For most materials water is used as the liquid phase. Distilled or deionized water should be used to eliminate the possibility of introducing harmful contaminents. Soluble sulfates are particularly troublesome and have been shown to cause mold deterioration. They also necessitate high deflocculant levels which leads to brittle castings (Merwin, 1955). Organic liquids may be used but they violate most of the requirements listed above. Their use may be imperative when casting materials that react with water. Williams (1963) investigated a number of organic liquids as vehicles for casting calcium oxide and these might be useful for other materials. Lewis (1961) presented one of the few attempts to explain the mechanisms of deflocculation in organic liquids and concluded, as did Williams, that oleic acid is the most effective deflocculant in such media.

D. Deflocculants

The variety of deflocculating agents used in slips seems almost limitless. Each slip caster has his own favorite ingredients and with experience learns to tailor them to the job at hand. In general it is found that monovalent cations are the most effective deflocculants. Acids are frequently used to adjust viscosity, and pH is used as a control test. The concentrations of other cations are not as easily determined and viscosity is the only test of their effectiveness. Michaels (1958) pointed out that the actions of hydrogen ions

and other monovalent cations are fundamentally different. Hydrogen ions affect the charge density by chemically altering the nature of the surface. Other ions alter the forces of repulsion between particles by changing the character of the diffuse ionic atmosphere surrounding the particles. The relative effect of different cations having the same valence is a function of their atomic weight. The deflocculating ability is decreased as the atomic weight increases. Multivalent cations are much less effective. Michaels stated that the flocculating ability of various cations on sodium kaolinite varies directly with the sixth power of cation valence. A number of commercially available deflocculating agents are widely used. Darvan No. 7, made by R. T. Vanderbilt Co., 230 Park Ave., New York, New York, contains sodium and potassium as the major cations. Darvan C is an aqueous solution of ammonium polyacrylate (Fennelly and Reed, 1972a) and is used when the presence of sodium is objectionable. A partial list of other deflocculating agents includes sodium silicate, sodium carbonate, sodium pyrophosphate, lignite (Phelps, 1959), humates (Fedorova, 1959), humic acid plus 10 % sodium hydroxide, ammonium tartrate, and sodium oxalate (Harkort and Herrmann, 1956), gallic acid, oleic acid, tannic acid, silica sol plus a nonionic or cationic surfactant or gelatin (Smith, 1960), carboxymethylcellulose (Stawitz, 1955), and gum acacia (Hepworth and Rutherford, 1964).

E. Binders

Cast ware sometimes has poor green strength and it may be necessary to add a binder to the slip to overcome this problem. It is important that the binder be compatible with the vehicle and the deflocculant. It should not block the capillaries in the mold. Some binder materials are organic and provide only temporary strength. The removal of these during firing is accompanied by the release of gases. This may cause the piece to fracture if too much binder is present or if heating is carried out too rapidly. Other binders are inorganic and may leave a residue after firing. The physical and chemical properties of these residues may be of importance when considering the addition of a binder. Various materials have been used successfully as binders for slip casting. These include polyvinyl alcohol, urea formaldehyde resin (Maĭer, 1956), carboxymethylcellulose (Hoepfner, 1968), silica sol (Smith, 1960), ethyl silicate (Quinn, 1955; also Shaw and Emblem, 1972), and gum tragacanth (Williams, 1963).

F. Antifoaming Agents

Some slips tend to foam and this may be remedied by the addition of small amounts of octyl alcohol. Commercial antifoam agents such as Dow Corning Antifoam A and a series made by Nopco Chemical Company,

Newark, New Jersey are also useful. Judicious use of antifoaming agents is recommended. An excess amount may cause worse foaming, which may be impossible to cure.

V. Novel Casting Processes

A number of variations on the basic slip casting process have been developed. These may be useful in specialized applications.

A. Freeze Casting

This technique makes use of very thick slips which are poured into rigid, nonporous molds such as rubber (Bollman, 1957) and then frozen to retain the shape of the casting. Drying is done by sublimation (Maxwell *et al.*, 1954) or using an absorbent sand (Grala, 1956). This method is especially suitable for coarse-grained materials that cannot be suspended by the usual methods.

B. Pressure Casting

From Eq. (1) it is apparent that the rate of casting can be increased if the pressure on the slip is increased. A modest increase in pressure can be obtained by using a riser made of nonporous material extending above the mold and filled with slip. Higher pressures may be utilized by applying gas pressure to the slip. Fennelly and Reed (1972a,b) examined this process in detail and showed that pressure casting gave increased casting rates with low porosity, small pore sizes, and essentially zero drying shrinkage.

C. Centrifugal Casting

This technique allows the acceleration due to gravity to be increased, thereby increasing casting rate. A cylindrically shaped mold is rotated about its axis and slip is introduced in the ends of the mold. The process is limited to simple shapes and the plaster must be reinforced to withstand the high forces of acceleration. This technique has been described by Parker (1957), Maxwell and Douglas (1960), and Daniel (1960, 1962).

D. Ultrasonic Casting

The application of low amplitude, audio frequency (15–20 kHz) vibrations to plaster molds during casting has been shown to be beneficial in several

respects. Increased green strength, higher density, the ability to cast highly thixotropic slips, rapid gas bubble removal, uniformity in mixed density compositions, and increased rate of water flow through the ceramic were all cited in one study (McKinney *et al.*, 1961). It was demonstrated that cermet and alumina plates measuring 0.06 in. thick by 1 in. wide by 24 in. long could be successfully slip cast using this method.

VI. Slip Casting Oxides

A. Clays

Clay bodies have been slip cast for many years and economically they are the most important of all products made by this process.

When development of processes for casting nonclay materials was accelerated in the early 1950's many workers reported attempts to produce "plastic" properties in various materials. This was an obvious attempt to reproduce the colloidal properties of clays rather than to develop true plasticity. As stated by Rempes *et al.* (1958), "the slip casting process is essentially the only ceramic process wherein no plastic deformation of the ceramic body occurs."

Because of the colloidal properties of clays and their widespread use for many years, a great deal of literature regarding the details of slip casting has appeared. The reader is referred to articles by Magid (1958), Norton (1952), and Newcomb (1947) for reviews of the slip casting of clays.

B. Alumina

This material is used widely in technical ceramics and slip casting is commonly used for its fabrication. Alumina may be cast in either acidic or basic slips. Hydrochloric acid is frequently used to adjust the pH to values between 2.5 and 4. Mold deterioration is a problem with acid slips and some workers prefer to use basic slips to avoid this problem. Polyelectrolytes such as Darvan No. 7 or Darvan C are used in this pH range. In the author's laboratory, a mixture of Darvan No. 7 and gallic acid are used successfully. Lewis (1961) showed that trihydroxybenzoic acid additions to alumina slips made basic with NaOH gave low viscosities that were constant over a wide pH range. A literature review of alumina slip casting was made by Gitzen (1970) and many different deflocculants are mentioned.

C. Silica

The excellent thermal shock properties of silica glass (popularly known as fused quartz) are well known. An extensive program to develop a slip

casting process for it was carried out at the Engineering Experiment Station at Georgia Institute of Technology. These slips usually consist of particles less than 50 μm in diameter, have pH values in the range of 3.5–4, and are characterized by unusually low drying and firing shrinkages. The fired ware is porous and contains a certain fraction of cristobolite, which varies with firing conditions and other processing variables. Very large items such as radomes have been prepared. The reader is referred to an article by Fleming (1961) for a brief summary and to a report by Harris and Welsh (1973) for more complete details and an extensive bibliography.

D. Magnesia

This material is used as a crucible for the preparation of high-purity metals. Crucibles are frequently thin walled and slip casting is an ideal process for their manufacture. Magnesia, in finely divided form, reacts with water to form magnesium hydroxide. This leads to unstable, gelled slips unless special precautions are taken to minimize the effects of the reaction. Greenaway (1952), Whiteway *et al.* (1961), and Schlegel and Schwab (1966) used ethanol as the casting vehicle to avoid hydration. Through proper control of particle size and temperature during milling, magnesia may be cast in aqueous slips. Hydration is minimized by the use of coarse, low surface area material and low temperatures during milling. Several combinations of these may be utilized depending upon the desired characteristics of the fired ware. Stoddard and Allison (1958) and Allison (1959) combined -325 mesh slip aged at 15°C with coarse fractions to obtain porous bodies having low firing shrinkage. Hydrocholoric acid was used as the deflocculant. Garrett and Williams (1960) used magnesium phthalate as a deflocculant for an aqueous slip. Magnesia bodies may be prepared by casting from aqueous slips and fired to vitrification if the particle size of the magnesia is low and reaction with water is minimized. This can be done by ball-milling at a temperature just above freezing (Stoddard and Nuckolls, 1963; also Stoddard *et al.*, 1961). Hydrochloric acid and glycerine or formamide were used as deflocculants.

E. Calcia

The high thermodynamic stability of calcia makes it an ideal container for molten metals. Its reactivity with water, however, makes it imperative that slip casting be done in nonaqueous suspensions. Successful vehicles include isobutyl acetate deflocculated with oleic acid and triethanolamine (Cowan *et al.*, 1962; also Stoddard *et al.*, 1963), high aliphatic hydrocarbons deflocculated with oleic acid (Williams, 1963), and absolute ethyl alcohol (Williams, 1951). A technique for preparing calcia by slip casting calcium

hydroxide in water plus gum acacia followed by firing was described by Hepworth and Rutherford (1964).

F. Zirconia and Zircon

These materials have been successfully cast in aqueous slips as described by St. Pierre (1952) and Smith (1960). Ethanol slips were used by Masson *et al.* (1963).

G. Thoria

The high density of thoria make the use of very fine particles a necessity to avoid settling. St. Pierre (1955) described a low pH slip in which polyvinyl alcohol was used as both a binder and a stabilizing agent. Murray *et al.* (1957) also used acid slips in the pH range of 1–3.5 with the thoria particles being 60 % less than 2 μm. Good results may also be obtained using basic slips in which Darvan No. 7 is used as the deflocculant.

H. Other Oxides

Many other oxides have been slip cast and the reader is referred to the references below for further details. (1) Urania (Murray and Livey, 1956), (2) Tantala (Bieler, 1966), (3) Beryllia (Murry *et al.*, 1954), (4) Lead zirconate-titanate (Wentzel, 1970), (5) Glass (De Clerck and Su, 1966; Seki, 1966), (6) Petalite (Maki and Tashiro, 1964), (7) Basic Refractories (Henry and Miller, 1968; Henry and Scott, 1969), (8) Aluminum Titanate (Morrow *et al.*, 1972).

VII. Slip Casting Fluorides

Fluorine compounds have useful electrical, refractory, and nuclear applications. Calcium fluoride has been slip cast in ethyl alcohol (Masson *et al.*, 1963) to avoid mold erosion problems. Others have used aqueous suspensions with low pH values. Bieler (1966) found that the lowest viscosities were obtained below a pH of 6. A coarse-grained slip was cast at a higher viscosity with a pH of 7.2–7.5 to keep coarse grains in suspension. A basic slip utilizing Darvan No. 7, sodium silicate, and gallic acid is used in the author's laboratory.

VIII. Slip Casting Metals

Some metals are very difficult to form by conventional techniques and slip casting has proved to be a useful forming method for these applications. Complex shapes such as seamless hollow spheres or crucibles with reentrant bottoms may be easier to make by slip casting than by other means. The mechanism of deflocculation of metal powders is probably different from that of oxides. St. Pierre (1959) has discussed many general aspects of metal slip casting.

A. Tungsten

This material presents a unique challenge to one's ability to prepare a workable slip. Its density of 19.3 g/cm^3 is nearly twice that of any oxide, and particle settling is a severe problem. Fortunately, powders of fine particle size are available commercially. It is sometimes advantageous to add organic thickening agents such as alginates to the slip to increase the viscosity. Some feel it necessary to form a thin layer of oxide or carbide on the tungsten particles. This layer is thought to be the factor that allows these slips to be deflocculated (Lewis, 1961). An organic vehicle system of toluene and/or xylene with methylphenyl polysiloxane binder was used by Szymaszek (1961). Water slips are satisfactory and little or no deflocculant is needed (Waldo, 1971). Small amounts of sodium pyrophosphate are sometimes used in well-aged slips in the author's laboratory.

B. Molybdenum

St. Pierre (1958b) described in detail a process for molybdenum slip casting. Water and polyvinyl alcohol were used as the vehicle. Viscosity was shown to be highly dependent on pH. Ammonium hydroxide additions were used to adjust the pH to between 6 and 7.

C. Stainless Steel

Lidman and Rubino (1956) and Hausner (1958) described techniques for casting stainless steel powders. Both techniques utilized alginates, alone, or in combination with polyvinyl alcohol as suspending agents. Slip viscosities were lowest at a pH of approximately 10.

D. Other Metals

The following metals are also used for slip casting:

1. Silicon, titanium, chromium, molybdenum (Rempes *et al.*, 1958).
2. Beryllium (Comstock *et al.*, 1961).
3. Copper (Kimura and Tokuyoshi, 1963).

IX. Slip Casting Intermetallic Compounds

Intermetallic compounds resemble oxides in many respects and similar slip casting techniques have been reported. Further details will be found in the references below.

1. Silicon carbide (Rempes *et al.*, 1958).
2. Titanium carbide (Rempes *et al.*, 1958; Dobrovol'skii and Popichenko, 1965).
3. Titanium nitride (Rempes *et al.*, 1958).
4. Zirconium boride (Rempes *et al.*, 1958).
5. Zirconium carbide (Dobrovol'skii *et al.*, 1966).
6. Niobium carbide (Dobrovol'skii *et al.*, 1967).
7. Molybdenum disilicide (Dobrovol'skii and Nazarchuk, 1966; Tamura, 1963).

X. Slip Casting Cermets

Numerous cermet compositions have been slip cast as reported in the following articles. (1) Tungsten Carbide—Cobalt (Golibersuch, 1954), (2) Titanium Carbide—Nickel (Grala, 1956), (3) Zirconium Carbide— Tungsten (Dobrovol'skii, 1969).

XI. Summary

Slip casting of many materials has been done successfully and it will continue to be a valuable forming technique. The lack of an all-encompassing theory of deflocculation leads to the observation that slip casting is more of an art than a science. It is an art that can be controlled for engineering purposes, and this is the factor which will make it a useful process for many years to come.

ACKNOWLEDGMENTS

The author thanks Donald E. Nuckolls who provided much practical information and Stephen D. Stoddard who provided many valuable references.

References

Adami, A., and Williams, L. S. (1963). *Amer. Ceram. Soc., Bull.* **42**, 391–393.
Adcock, D. S., and McDowall, I. C. (1957). *J. Amer. Ceram. Soc.* **40**, 355–362.
Allison, A. G. (1959). U.S. Patent 2,902,380.
Anderson, P. J., and Murray, P. (1959). *J. Amer. Ceram. Soc.* **42**, 70–74.
Beazley, K. M. (1965). *Trans. Brit. Ceram. Soc.* **64**, 531–548.
Bieler, B. H. (1966). *Amer. Ceram. Soc., Bull.* **45**, 527–529.
Bollman, H. (1957). *Ceram. Age* **70**[1], 36–38.
Brindley, G. W. (1958). *In* "Ceramic Fabrication Processes" (W. D. Kingery, ed.), pp. 7–23. Wiley, New York.
Comstock, G., Guendel, H. W., Kosinski, E. J., and Yoblin, J. A. (1961). Report SCR 306. Sandia Corporation, Livermore, California.
Cowan, R. E., Stoddard, S. D., and Nuckolls, D. E. (1962). *Amer. Ceram. Soc., Bull.* **41**, 102–104.
Daniel, W. A. (1960). U.S. Patent 2,962,790.
Daniel, W. A. (1962). U.S. Patent 3,041,699.
De Clerek, D. H., and Su, G. (1966). *J. Amer. Ceram. Soc.* **49**, 252–256.
Dobrovol'skii, A. G. (1969). *Sov. Powder Met. Metal Ceram.* pp. 156–160; *Ceram. Abstr.* p. 125g (1971).
Dobrovol'skii, A. G., and Nazarchuk, N. V. (1966). *Sov. Powder Met. Metal Ceram.* pp. 349–354; *Ceram. Abstr.* p. 57h (1969).
Dobrovol'skii, A. G., and Popichenko, E. Ya, (1965). *Sov. Powder Met. Metal Ceram.* pp. 731–736; *Ceram. Abstr.* p. 46b (1968).
Dobrovol'skii, A. G., Dobrovol'skii, G. G., Lyudvinskaya, T. A., and Popichenko, E. Ya. (1966). *Izv. Akad. Nauk SSSR, Neorg. Mater.* **2**, 864–869; *Ceram. Abstr.* p. 46d (1968).
Dobrovol'skii, A. G., Palfalvi, A. Yu., and Zyuz, A. P. (1967). *Sov. Powder Met. Metal Ceram.* pp. 536–541; *Ceram. Abstr.* p. 69i (1970).
Fedorova, T. Kh. (1959). *Steklo Keram.* **16**, 27–28; *Ceram. Abstr.* p. 213b (1959).
Fennelly, T. J., and Reed, J. S. (1972a). *J. Amer. Ceram. Soc.* **55**, 264–268.
Fennelly, T. J., and Reed, J. S. (1972b). *J. Amer. Ceram. Soc.* **55**, 381–383.
Fleming, J. D. (1961). *Amer. Ceram. Soc., Bull.* **40**, 748–750.
Garrett, W. G., and Williams, L. S. (1960). *J. Amer. Ceram. Soc.* **43**, 114.
Gitzen, W. H. (1970). "Alumina as a Ceramic Material." *Amer. Ceram. Soc.*, Columbus, Ohio.
Golibersuch, E. W. (1954). U.S. Patent 2,698,232.
Grala, E. M. (1956). *NACA (Nat. Adv. Comm. Aeronaut.) Tech. Notes* **3769**; *Ceram. Abstr.* p. 108i (1957).
Greenaway, H. T. (1952). *Metallurgia* **45**, 159–160; *Ceram. Abstr.* p. 142d (1952).
Harkort, D., and Herrmann, R. (1956). *Ber. Deut. Keram. Ges.* **33**, 18–24; *Ceram. Abstr.* p. 147j (1956).
Harkort, D., and Hoffmann, U. (1971). *Ber. Deut. Keram. Ges.* **48**, 479–483; *Ceram. Abstr.* p. 165c (1972).
Harris, J. N., and Welsh, E. A. (1973). "Fused Silica Design Manual," Vol. 1. Engineering Experiment Station, Georgia Institute of Technology, Atlanta.
Hausner, H. H. (1958). *Powder Met. Bull.* **8**, 53–67.

Hauth, W. E. (1950). *J. Phys. Colloid Chem.* **54**, 142–156.
Henry, G. R., and Miller, E. D. (1968). U.S. Patent 3,418,401.
Henry, G. R., and Scott, R. K. (1969). U.S. Patent 3,449,478.
Hepworth, M. A., and Rutherford, J. (1964). *Amer. Ceram. Soc., Bull.* **43**, 18.
Herrmann, E. R., and Cutler, I. B. (1962). *Trans. Brit. Ceram. Soc.* **61**, 207–211.
Hoepfner, P. (1968). *Ber. Deut. Keram. Ges.* **45**, 103–107; *Ceram. Abstr.* p. 305d (1968).
Kimura, T., and Tokuyoshi, M. (1963). *Funtai Oyobi Funmatsuyakin* **10**, 144–152; *Ceram. Abstr.* p. 217f (1964).
Lambe, C. M. (1958). *In* "Ceramic Fabrication Processes" (W. D. Kingery, ed.), pp. 31–40. Wiley, New York.
Lehmann, L. (1958). *Ber. Deut. Keram. Ges.* **35**, 273–277; *Ceram. Abstr.* p. 89i (1959).
Lewis, A. E. (1961). *J. Amer. Ceram. Soc.* **44**, 208–214.
Lidman, W. G., and Rubino, R. V. (1956). *Precis. Metal Molding* **14** [8], 40–41 and 83; [9], 64–66 and 98.
McKinney, C. D., Jr., Tarpley, W. B., and Gaskins, F. H. (1961). "Ultrasonic Casting of Ceramic and Cermet Slips" Report NYO-9586, Aeroprojects, Inc., West Chester, Pennsylvania.
Magid, H. S. (1958). *In* "Ceramic Fabrication Processes" (W. D. Kingery, ed.), pp. 40–45. Wiley, New York.
Maĭer, A. A. (1956). *Oqneupory* **21**, 139–140; *Ceram. Abstr.* p. 19i (1959).
Maki, T., and Tashiro, M. (1964). *Yogyo Kyokai Shi* **72**, 105–107; *Ceram. Abstr.* p. 125g (1967).
Masson, C. R., Whiteway, S. G., and Collings, C. A. (1963). *Amer. Ceram. Soc., Bull.* **42**, 745–747.
Maxwell, W. A., and Douglas, J. (1960). U.S. Patent 2,944,316.
Maxwell, W. A., Gurnick, R. S., and Francisco, A. C. (1954). *NACA (Nat. Adv. Comm. Aeronaut.), Res. Memo* **E 53L21**.
Mehta, P. K., and Langston, R. B. (1963). *Ceram. Age* **79**[9], 49–50 and 52–56.
Merwin, B. W. (1955). *Amer. Ceram. Soc., Bull.* **34**, 50.
Michaels, A. D. (1958). *In* "Ceramic Fabrication Processes" (W. D. Kingery, ed.), pp. 23–31. Wiley, New York.
Moore, F. (1959). *Trans. Brit. Ceram. Soc.* **58**, 470–494.
Morrow, M. K., Holcombe, C. E., and Cromer, C. A. (1972). Union Carbide Corporation, Nuclear Division. Oak Ridge Y-12 Plant Report Y-1831.
Murray, P., and Livey, D. T. (1956). *Prog. Nucl. Energy, Ser. V* **1**, 448–477; *Ceram. Abstr.* p. 215f (1963).
Murray, P., Denton, I., and Wilkinson, D. (1954). *Silicates Ind.* **19**, 412–417.
Murray, P., Denton, I. E., and Wilkinson, D. (1957). U.S. Patent 2,807,857.
Newcomb, R., Jr. (1947). "Ceramic Whitewares." Pitman, London.
Norton, F. H. (1952). "Elements of Ceramics." Addison-Wesley, Reading, Massachusetts.
Parker, D. E. (1957). *Ceram. Age* **69**[5], 97–98.
Phelps, G. W. (1959). *Amer. Ceram. Soc., Bull.* **38**, 246–250.
Quinn, N. (1955). *Ind. Chem.* **31**, 486–489; *Ceram. Abstr.* p. 117j (1956).
Rempes, P. E. (1961). U.S. Patent 2,990,292.
Rempes, P. E., Weber, B. C., and Schwartz, M. A. (1958). *Amer. Ceram. Soc., Bull.* **37**, 334–339.
St. Pierre, P. D. S. (1952). *Trans. Brit. Ceram. Soc.* **51**, 260–268.
St. Pierre, P. D. S. (1955). *Amer. Ceram. Soc., Bull.* **34**, 231–232.
St. Pierre, P. D. S. (1958a). *In* "Ceramic Fabrication Processes" (W. D. Kingery, ed.), pp. 45–51. Wiley, New York.
St. Pierre, P. D. S. (1958b). Report No. 58-RL-2058. General Electric Co., Schenectady, New York.
St. Pierre, P. D. S. (1959). *Res. App. Ind.* **12**, 460–466.
Schlegel, E., and Schwab, T. (1966). *Silikattechnik* **17**, 10–11; *Ceram. Abstr.* p. 105i (1969).

Seki, Y. (1966). *Osaka Kogyo Gijutsu Shikensho Kiho* **17**, 11–16; *Ceram. Abstr.* p. 7f (1968).
Shaw, R. D., and Emblem, H. G. (1972). *InterCeram* **21**, 105–108.
Smith, E. (1960). U.S. Patent 2,942,991.
Stawitz, J. (1955). *Ber. Deut. Keram. Ges.* **32**, 304–305; *Ceram. Abstr.* p. 43h (1956).
Stoddard, S. D., and Allison, A. G. (1958). *Amer. Ceram. Soc., Bull.* **37**, 409–413.
Stoddard, S. D., and Nuckolls, D. E. (1963). U.S. Patent 3,116,155.
Stoddard, S. D., Nuckolls, D. E., and Cowan, R. E. (1961). *Los Alamos Sci. Lab., Rep.* **LAMS-2639**.
Stoddard, S. D., Nuckolls, D. E., and Cowan, R. E. (1963). U.S. Patent 3,116,350.
Szymaszek, J. W. (1961). U.S. Patent 2,979,401.
Tamura, K. (1963). *Funtai Oyobi Funmatsuyakin* **10**, 44–50; *Ceram. Abstr.* p. 56j (1964).
Waldo, C. T. (1971). U.S. Patent 3,578,478.
Wentzel, J. J. (1970). U.S. Patent 3,517,093.
Whiteway, S. G., Coll-Palagos, M., and Masson, C. R. (1961). *Amer. Ceram. Soc., Bull.* **40**, 432–438.
Williams, A. E. (1951). *Trans. Brit. Ceram. Soc.* **50**, 215–224.
Williams, L. S. (1963). *Amer. Ceram. Soc., Bull.* **42**, 340–343.
Worrall, W. E. (1963). *Trans. Brit. Ceram. Soc.* **62**, 659–672.

Doctor-Blade Process

J. C. WILLIAMS

Bell Laboratories, Inc.
Murray Hill, New Jersey

I. Introduction

The doctor-blade process consists basically of suspending finely divided inorganic powders in aqueous or nonaqueous liquid systems comprised of solvents, plasticizers, and binders to form a slurry that is cast onto a moving carrier surface. The slurry passes beneath the knife edge of a blade that levels

or "doctors" the slurry into a layer of controlled thickness and width as the carrier surface advances along a supporting table. When the solvents evaporate, the fine, solid particles coalesce into a relatively dense, flexible sheet that may be stored on take-up reels or stripped from the carrier in a continuous sequence. The terms tape process, knife coating, tape casting, and sheet casting have been used synonomously with doctor-blading in referring to this process for forming thin, relatively large area sheets of polycrystalline ceramic compositions.

The process has become established as a useful method for manufacturing a variety of electronic ceramics. Typical applications include the preparation of capacitors, piezoactive devices, ferrite memories, electrically insulating substrates for thick and thin film circuitry, and substrates for catalysts. The doctor-blade process has proved to be especially useful in providing an economically feasible technique for the production of high alumina ceramic substrates that meet a combination of stringent requirements for use with thin film circuits. As a basic ceramic forming method it is generally advantageous for preparing relatively large area, thin sheets with uniform and high unfired densities. The usual range of fired thickness of parts made by this process is from 0.001 to 0.045 in. with close dimensional tolerances (fraction of a mil) and areas from 4 to 18 in.^{2}. Complex shapes with intricate hole patterns can be formed directly by punching or stamping the parts from the as-cast sheet.

Although a number of producers of electronic ceramics located throughout the world employ the doctor-blade process among their manufacturing operations, there are relatively few publications that provide many of the details about the process. One of the earliest accounts is by Howatt *et al.* (1947) that discusses the preparation of titanate ceramics for capacitors. The authors of that paper refer to a technique of extruding a ceramic slip onto a moving belt. They also describe an apparatus for casting thin sheets, as well as a slurry formulation that embodies the principles of the method that are still practiced in the early 1970's, including the lamination of multiple sheets which are converted into a monolithic structure during firing. The Park (1961) patent extends the application of the technique to a variety of ceramic compositions and reduces the thickness to the order of 1 mil. Thompson (1963) provides additional information on binder systems and the shaping of parts by stamping on a compound die. Stetson and Gyurk (1972) reported on the preparation of high alumina substrates by the doctor-blade process capable of providing an as-fired surface finish of 2 μin. (CLA). The patent by Stetson and Gyurk (1972, 1973) provides a detailed and explicit description of a high alumina ceramic composition, casting formulation, and firing procedures.

Several publications by Shanefield and Mistler (1971, 1974) and Shanefield

et al. (1974) provide a comprehensive discussion on the investigation of the many phases leading to the development of the ERC-105 process* for the preparation of high alumina substrates. This process is the outgrowth of further investigations by these authors of the original Stetson and Gyurk work with emphasis on surface finish, dimensional control, strength, effects of composition on microstructure, and capability of providing good bond strength for metal leads attached to deposited films by thermocompression

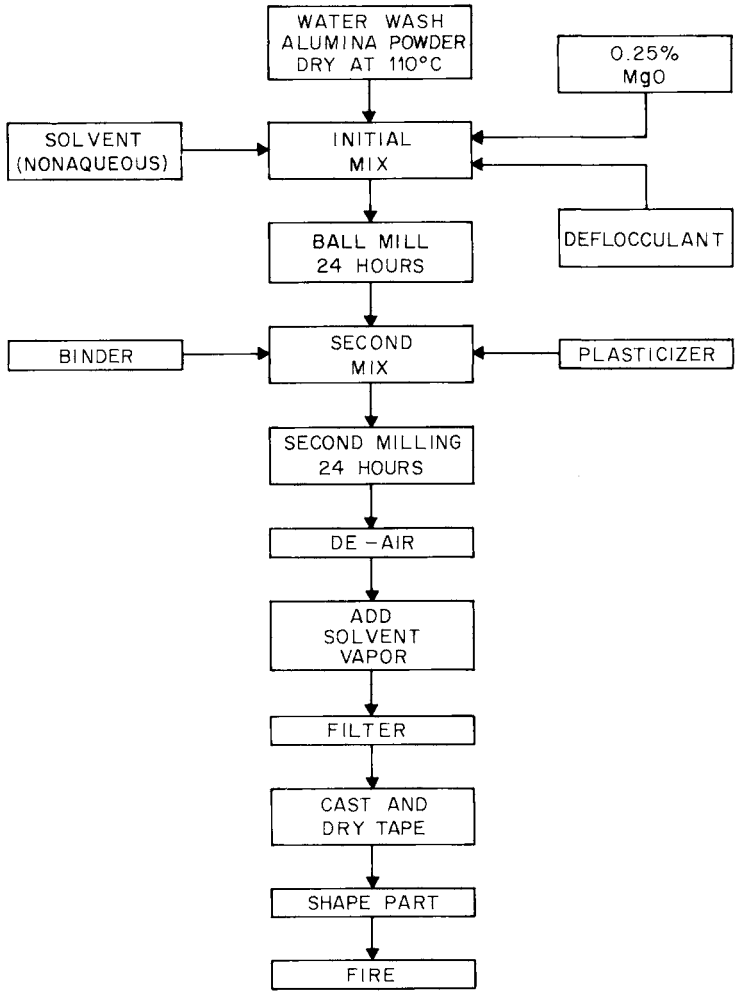

Fig. 1. Flow chart for ERC-105 alumina substrates by the doctor-blade process.

*Engineering Research Center, Western Electric Co., Hopewell, New Jersey.

bonding. Finally, Runk and Andrejco (1975) describe the development of a tape casting machine for fabricating thin tapes (1–10 mils) of organically suspended ceramic powders with thickness tolerances of better than ± 0.3 mil over large areas.

The principles of the doctor-blade process have been studied in more depth and with better understanding for high alumina ceramic substrates than for most other applications. This will provide the basis for illustrating the important parameters of the process in the following discussion. As noted by Shanefield and Mistler (1973), the ERC-105 process needs a balance of many factors for success, hence attention to the control of all phases of the process is essential regardless of the ceramic powder used with the doctor-blade method. In order to meet the requirements of a particular product the preparation of the ceramic powder, liquid vehicle for casting, casting rate and equipment, and firing procedures must be tailored for the occasion. More often the final procedure is attained as a result of a process of evolution, empiricism, and study on the part of the user. The flow chart of a typical doctor-blade process for alumina substrates of the ERC-105 process is shown in Fig. 1, beginning with the preparation of the slurry for casting.

II. Slurry Formulation

Whether the liquid vehicle for forming the casting slurry is categorized as aqueous or nonaqueous the major components usually include a solvent, binder, plasticizer, and deflocculant. As important as each of these is in a given system the nature of their role is mostly transient. Since these forming aids are totally removed during drying and firing, the ultimate success of the process depends upon recognizing the contribution resulting from the proper preparation and characterization of the starting ceramic powder (see Chapters 1 and 3 in this volume). The ingredients and milling procedures for the nonaqueous slurry used in the ERC-105 process of alumina substrates as reported by Shanefield and Mistler (1974) are listed in Table I.

The selection of the doctor-blade process as a method for forming ceramics is usually predicated on the basis of its advantage for providing relatively thin, large area shapes of uniformly high density. There are often other concomitant objectives with a given ceramic composition or application. For instance, electronic properties, surface finish, grain size, fired density and strength, and minimizing heat treatment may be essential requirements also. In addition, high green density in the as-cast tape reduces firing shrinkage that in turn reduces warpage and enhances dimensional control. All of these have become recognized as being strongly dependent upon the characteristics of

TABLE I

NONAQUEOUS DOCTOR-BLADE FORMULATION FOR ERC-105 ALUMINA SUBSTRATES[a]

Process step	Material	Function	Weight (gm)
Mill for 24 hr (first stage)	Alumina powder	Substrate material	3000
	Magnesium oxide	Grain growth inhibitor	7.5
	Menhaden fish oil[b]	Deflocculant	55
	Trichloroethylene	Solvent	1170
	Ethyl alcohol	Solvent	450
Add to above and mill for 24 hr (second stage)	Polyvinyl butyral[c]	Binder	120
	Polyethylene glycol[d]	Plasticizer	128
	Octylphthalate[e]	Plasticizer	108

[a] After Shanefield and Mistler (1974).
[b] Type Z-3 (air treated), Jesse S. Young Co., New York, New York.
[c] Type B-98 (molecular weight approximately 32,000), Monsanto Co., St. Louis, Missouri.
[d] Ucon 2000 — Union Carbide Corp.
[e] 61-P — Allied Chem. Corp.

the starting ceramic powder. A prime objective of alumina substrates for use with thin film circuitry is to provide a smooth surface finish with a ceramic microstructure exibiting an average grain size of < 1 μm.

Much of the progress in the evolution of alumina substrates is the result of technological improvements to the alumina powder by the raw material

TABLE II

EVOLUTION OF ALSIBASE® CERAMIC SUBSTRATES[a]

Parameter	1960	1962	1966	1970	1972	1973
Percent Al_2O_3	96	96 Glazed	99.5	99.5	99.7 +	99.95 +
Density (gm/cm^3)	3.70	3.70	3.88	3.83	3.89	3.96
Crystal size (μm)	6	6	3	1.5	1.2	1.0
Surface finish (μin.)	18	1	8	5	2.5	1
Laser reflectometer	—	—	—	.400	1.300	1.800
Intrinsic pore size (μm)	4	4	1.5	1.5	.5	.3
Flexural strength (kpsi)	60	—	70	85	85	100
Raw Materials						
Purity (% Al_2O_3)	99.6	99.6	99.7	99.7	99.8	99.99
Particle size (μm)	4	4	1.5	1.5	.55	.3
Surface area (m^2/gm)	1	1	3	3	10	12

[a] After Gaddy *et al.* (1973).

producers. An indication of the influence of purity, particle size, and surface area of the powder upon some of the parameters of alumina substrates is shown in Table II from Gaddy *et al.* (1973). Berrin *et al.* (1972) and Johnson *et al.* (1972) have characterized a series of 24 Bayer and non-Bayer processed aluminas in terms of purity, powder density, particle size, and agglomerate content. They determined that the dry ball-milled Bayer-derived products in general have soft agglomerates that are readily dispersed and have an overall higher impurity content. The Bayer processed aluminas provide higher green densities. The non-Bayer products have a higher fraction of hard agglomerates that when present in either type of alumina cause low density areas and surface defects in the finished alumina substrates. The origin of white spots in high alumina bodies has been reported by Francis *et al.* (1972) to be associated with pockets of higher concentration of SiO_2 and Na_2O that cause the formation of porous coarsely crystalline centers. They recommend the use of 99^+ % grinding media and mill linings to minimize introduction of such contaminants into the powders.

A. Powder Consideration

The alumina powder in the ERC-105 process is washed in boiling distilled water and vacuum filtered with a Buchner funnel to reduce the sodium ion concentration. The powder is dried in air at 110°C. The Brunauer-Emmett-Teller (BET) (Brunauer *et al.*, 1938) surface area measurement of the as-received alumina should be about 11 m^2/gm after an outgassing treatment of 300°C. The subsequent milling procedure is effective primarily in deagglomerating and deflocculating the powder. The average particle size after milling is 0.4 μm* equivalent spherical diameter, within a particle size range of 0.1 to 3.0 μm. The resulting particle size distribution or "size-graded" state of commercially available dry-ground aluminas referred to by Stetson and Gyurk (1972) yields a slurry that provides good packing of the powder to about 80 to 90 % by weight of solids in the dried tape after milling and casting. The initial milling of the slurry (Table I) with the deflocculant and solvent disperses the alumina powder.

A slurry system is classified as aqueous or nonaqueous depending upon whether water or an organic liquid serves as the solvent for the binder and other phases exclusive of the alumina in the slurry formulation.

B. Nonaqueous and Aqueous Systems

Most commercial practices of the doctor-blade process use nonaqueous systems. Except for the few references cited in the literature most details

*Model 5000 Sedigraph, Micromeritics Co., Norcross, Georgia.

TABLE III

SOME FUNCTIONAL ADDITIVES IN DOCTOR-BLADE SYSTEMS

Solvent	Binder	Plasticizer	Deflocculant	Wetting agent
Nonaqueous:			Fatty Acids (Glyceryl tri-oleate) (3)[a]	Alkylaryl polyether alcohols (2)[a]
Acetone (2)	Cellulose acetate butyrate resin (2)[a]	Butyl benzyl phthalate (9)[a]	Natural fish oils (Menhaden) (3)	Ethylether of polyethylene glycol (2,4,6)
Ethyl alcohol (2,3,4)	Nitrocellulose (5,6)	Butyl stearate (9)	Synthetic surfactants (Benzene sulfonic acids) (3)	Ethyl phenyl glycol (2)
Benzene (2,6)	Petroleum resins (2)	Dibutyl phthalate (4,6)		Polyoxyethylene acetate (2)
Bromochloromethane (8)	Polyethylene (9)	Dimethyl phthalate (2,3)		Polyoxyethylene ester (2)
Butanol (2)	Polyacrylate esters (2)	Methyl abietate (2,3)		
Diacetone (2)	Poly methylmethacrylate (2,6,7)	Mixed phthalate esters (3) (Hexyl, octyl, decyl alcohols)		
Ethanol (2,6)	Polyvinyl alcohol (5,7,9)	Polyethylene glycol (3,6)		
Isopropanol (2)	Polyvinyl butryal resins (2,3,4,6,7)	Polyalkylene glycol derivatives (Triethylene glycol hexoate) (2,3,6,7)		
Methyl isobutyl ketone (2,6)	Polyvinyl chloride (5,7,9)	Tricresyl phophate (2,3)		
Toluene (1,2,4,6,7)				
Trichloroethylene (3)				
Xylene (6,7)				
Aqueous:				
Water (with defoamers i.e., wax based, silicone based, etc.)	Acrylic polymer (5,10)	Butyl benzyl phthalate (10)	Complex glassy phosphate (10)	Nonionic octyl phenoxyethanol (10)
	Acrylic polymer emulsion (10)	Dibutyl phthalate (4,10)	Condensed arylsulfonic acid (Natural sodium salt) (10)	
	Ethylene oxide polymer (10)	Ethyl toluene sulfonamides (10)		
	Hydroxyethyl cellulose (1)	Glycerine (10)		
	Methyl cellulose (6)	Polyalkylene glycol (10)		
	Polyvinyl alcohol (10)	Triethylene glycol (6)		
	TRIS. Isocyaminate (10)	Tri-*N*-butyl phosphate (10)		
	Wax lubricant (10)			

[a] Key to references: (1) Howatt *et al.* (1947), (2) Park (1961), (3) Stetson and Gyurk (1972), (4) Bennett *et al.* (1970), (5) Callahan and Stark (1970), (6) Thompson (1963), (7) Kappes and Bateson (1973), (8) Shanefield and Mistler (1973), (9) Pauley and Lockwood (1967), (10) G. O. Medowski and R. D. Sutch (personal communication, 1972).

about the vehicle for slurry formulations in commercial use are proprietary. Table III lists some of the types of functional additives that various investigators have indicated as possible constituents in nonaqueous and aqueous systems. These listings are not exhaustive. They are intended only as a guide in the selection of the materials for the various categories of additives. The present doctor-blade technology on casting formulations is based predominantly on the state of the art with little understanding of the fundamental behavior of the constituents in a specific formulation beyond certain general objectives. Shanefield and Mistler (1974) have investigated in detail the mechanism for the effectiveness of menhaden fish oil (mostly polyunsaturated glyceryl esters of fatty acids) and other materials as deflocculants in the alumina slurry for the ERC-105 process. They conclude that steric hindrance is the likely mechanism of deflocculation in the alumina slip with less than a few percent of the oil being adsorbed onto the alumina. Among the other deflocculants considered, they found that the presence of a carbon–carbon double bond, an ester group, and a molecular weight of at least 357 were necessary for satisfactory results. In addition to menhaden oil, corn oil and glyceryl trioleate were also effective as deflocculants.

The following are some of the criteria for the components in most doctor-blade slurries. The solvent should have a low boiling point and viscosity. It should be soluble with the binder, plasticizers, wetting agent and/or deflocculant, but should not dissolve or react with the ceramic powder. A combination of solvents may be advantageous in providing a low viscosity. Azeotropic mixtures of solvents are recommended to avoid preferential volatilization. Nonaqueous solvents offer the advantage of lower boiling points and avoid hydration of the ceramic powder. They require special precautions with respect to toxicity and inflammability. Stetson and Gyurk (1972) chose an azeotropic mixture of trichloroethylene and ethyl alcohol. The alcohol also dissolves any water that may be present and the water is removed with the alcohol during drying. The slip in the ERC-105 process has a flash point of 64°F. Shanefield and Mistler (1973) prepared a nonflammable version (flash point 143°F) by substituting bromochloromethane for about 30 wt. % of the trichloroethylene without altering the normal properties of the substrate. Similarly the substitution of tetrachloroethylene for the alcohol will reduce the flammability hazard.

The purpose of the binder is to provide high strength to the unfired tape after the solvent has evaporated. The binder should enable the tape to have good handling and storage characteristics and not contribute to the formation of cracks, pinholes, and defects in the unfired or fired tape. It should burnout or volatilize completely during firing. The binder should also be compatible with the carrier film. Stetson and Gyurk (1972), for example, noted that the strong adhesion of polyvinyl butyral resins to glass surfaces requires care in

stripping the tape without tearing it. Most binders require the addition of plasticizers to lower their viscosities in order to improve the flexibility and workability of the dried tape. The plasticizer should be soluble in the solvent and not phase separate from the binder. Several investigators refer to the dried tape as having the desired handling properties with terms such as "leather hard" and "oilclothlike."

A deflocculant is essential for keeping the solid powder phases dispersed in the slurry. It should be added periodically during the initial phase of the milling process in order to be uniformly distributed among particles resulting from the deagglomeration. No more than that required for the purpose should be added in total. The menhaden oil in the ERC process also promotes the release of the dried tape from the cellulose acetate carrier film. A deflocculant also aids in developing a castable slurry of high concentration of ceramic powders that reduces shrinkage and cracking during drying.

The use of wetting agents is particularly beneficial in aqueous systems. They promote slip spreading during casting, prevent pinhole formation, and hasten formation of uniform slip viscosity. They should be soluble in the solvent and preferably volatile. Table IV gives an example of an experimental

TABLE IV

EXPERIMENTAL AQUEOUS DOCTOR-BLADE FORMULATION FOR ERC-105 ALUMINA SUBSTRATES[a]

Process step	Material	Function	Weight (gm)
Premix in beaker	Distilled water	Solvent	465.0
	Magnesium oxide	Grain growth inhibitor	3.8
	Polyethylene glycol[b]	Plasticizer	120.0
	Butyl benzyl phthalate[c]	Plasticizer	88.0
	Nonionic octylphenoxyethanol[d]	Wetting agent	5.0
	Condensed arylsulfonic acid[e]	Deflocculant	70.0
Add and ball mill 24 hr	Alumina powder	Substrate material	1900.0
Add, ball mill 1/2 hr	Acrylic polymer emulsion[f]	Binder	200.0
Add, ball mill 3 min	Waxed based emulsion[g]	Defoamer	2.0

[a] After G. O. Medowski, and R. D. Sutch (personal communication, 1972).
[b] Ucon 2000, Union Carbide Corp.
[c] Santicizer 160, Monsanto Corp.
[d] Triton X405, Rohm and Haas.
[e] Tamol 731, Rohm and Haas.
[f] Rhoplex AC33, Rohm and Haas.
[g] Napco NXZ, Diamond Shamrock Co.

slurry formulation and milling procedure by G. O. Medowski and R. D. Sutch (private communication, 1972) for providing the equivalent of the ERC-105 process in an aqueous system prepared in a No. 1 U.S. Stoneware ball mill.

Nonaqueous doctor-blade slurry formulations predominate among users. The state of the art is such that more research is needed to optimize the performance of aqueous systems. The risk of certain constituents hydrating and the slower drying rate accompanying aqueous systems probably account for the dearth of references in which water serves as the solvent in the doctor-blade process. Expediency often favors propagating the use of nonaqueous solvents. It is still too early in the evolution of the doctor-blade process to ignore the use of water in new applications.

C. Milling

Referring to Table I, a 3000 gram charge of alumina powder is wet-milled initially for 24 hr in a 2.3 gallon capacity 85 % alumina ball mill with a 10,000 gram charge of Borundum cylindrical grinding media (13/16 in. × 13/16 in. diam.), the MgO addition, and sufficient solvent to form a slurry of milklike consistency. As noted earlier the deflocculant, Ensign Z3, is added periodically during the milling period. The binder (Butvar 98) and plasticizers (Elastex 61-P and Ucon 2000) are added for an additional 24 hr milling period that results in a slurry with the consistency of heavy cream. The mill is rotated at 60 rpm. Park (1961) and Bennett *et al.* (1970) characterize the viscosity of their slips prior to casting to be in the ranges of 400–1200 and 1000–1500 cp, respectively. A viscosity check prior to casting is recommended for achieving reproducibility in the casting behavior of the slip.

Sufficient impurities from the ball mill become added to the slip during milling in the ERC-105 process to increase the Ca content 3 times and the Si content 21/2 times, to 300 ppm and 1500 ppm, respectively, greater than that present in the initial alumina powder. The presence and concentration of these impurities in the final body composition has been found to have a marked effect upon the ability to obtain fired densities as high as 3.88–3.91 gm/cm^3 when firing to a temperature in the range of 1500°C with a 1.5 hr soak on a 17.5 hr cycle in a tunnel kiln.

D. De-airing

After milling, the dissolved air is removed to eliminate bubbles forming in the tape upon casting. The slip is transferred from the ball mill to a vessel suitable for de-airing the slip under a mechanical forepump vacuum for several minutes. The vessel is backfilled with air presaturated with the solvent to prevent formation of a skin on the surface of the slip.

E. Filtering

Finally, the slip is pumped into the reservoir of the casting machine through two nylon filters with openings of 37 and 10 μm, respectively, to assure removal of agglomerates and coarse particles.

III. Sheet Casting

A. Basic Components

A schematic of a doctor-blade casting system is shown in Fig. 2. The doctor-blade is located at the left end of the machine that has an overall length of about 25 ft by 1 ft wide. The carrier film moves from left to right. Shanefield and Mistler (1971) describe the casting procedure for the ERC-105 process as follows.

> The film is supplied continuously from a spool and enters the slip chamber through a slot in the end of the chamber. The doctor blade at the exit side of the chamber is adjusted by means of a fine screw. To produce the desired final substrate thickness of 0.026 inch, about a 0.063 inch gap between the blade and carrier film is used. The layer of slip passes through the gap with its thickness accurately controlled by the fine screw settings. The thickness of the freshly cast layer of slip (just beyond the doctor-blade) is continuously monitored by a gamma ray back-scatter or x-ray transmission instrument and the gap between the doctor blade and carrier film is adjusted accordingly.

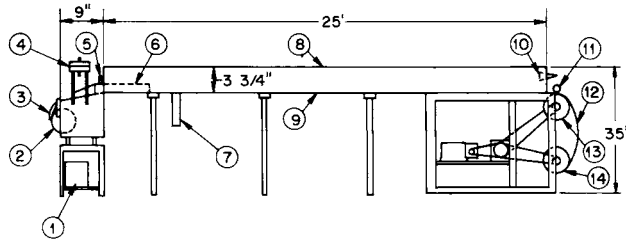

ITEM NO.	DESCRIPTION	ITEM NO.	DESCRIPTION
1	MOTOR CONTROLLER	8	GLASS PLATES
2	ROLL OF CELLULOSE ACETATE	9	ALUMINUM PLATES
3	DUST CLOTH	10	AIR INLET
4	FILTER	11	IDLER WHEEL
5	DOCTOR BLADE AND SLIP RESERVOIR	12	LEADER
6	PLEXIGLASS SHIELD	13	DRIVE ROLLER
7	THICKNESS MONITOR	14	TAKE-UP ROLLER

Fig. 2. Schematic of a doctor-blade casting system. (After Shanefield and Mistler, 1971.)

The layer of slip dries slowly while it is being carried through the machine on the moving plastic film. Filtered air is blown through the machine in a direction opposite to that of the moving slip. This arrangement provides the dry air at the exit end in contact with the almost dry slip. At the other end, in contact with the freshly-cast wet slip, is air saturated with solvent vapor. The difference in solvent content between the slip and the air is slight at any point in the machine. This slows the rate of solvent evaporation, allowing the remaining solvent in the slip slurry to redistribute itself with only a small vertical gradient of concentration. The small gradient of concentration tends to minimize curling and cracking of the slip as it dries.

Heat increases the drying rate. But, its use is limited because the boiling point of the solvent, 71°C, must not be exceeded if controlled, bubble-free drying of the slip is to be achieved. Once the slip becomes semisolid, further drying is controlled by the slowest means; i.e., the diffusion of the remaining solvent through the polymer. This diffusion is a well-known process which follows Fick's laws for thermally activated diffusion.

In its center zone, the electrically heated casting machine has a peak temperature of 60°C. The cellulose acetate carrier and the layer of slip on it move at the rate of 6 inches per minute. At the end of the machine, the polymer-alumina composite layer is dry enough to be cut into easily handled segments and stored. In this form it has the appearance and flexibility of a white leather-like plastic and is commonly called tape.

The reservoir and that portion of the slip prior to the doctor-blade should be covered to prevent formation of a surface skin that can result in the occurrence of lumps in the slurry.

B. Carrier Film

Some of the common materials used as carrier films include Teflon® (polytetrafluorethylene), Mylar® (glycol terephthalic acid polyester), cellophane (regenerated cellulose), and cellulose acetate.* The latter with a thickness of 0.015 in. is preferred for casting alumina substrates by the ERC-105 process. Callahan and Stark (1970) describe the preparation of capacitor chips by casting onto a continuous stainless steel belt treated with a Teflon coating and the use of a parting blade to assist in removing the dry tape from the belt. Carrier films usually have a margin of at least 1 in. on either side of the doctor-blade. Doctor-blades in the range of 4–36 in. in width are used in commercial manufacturing installations.

Carrier films are selected to provide a clean, smooth, impervious, insoluble surface onto which the slurry is cast. The dried tape should not bond to the carrier, but the slurry should have sufficient adherence or interaction during drying according to Park (1961) to effectively control shrinkage during drying to cause it to occur essentially in the thickness direction perpendicular to the tape carrier. Excessive adhesion of the tape to the carrier film may cause difficulties in stripping the tape from the film. Stetson and Gyurk (1972) also

* Kodacel TA-401 from Eastman Chemical Products.

note that the leather-hard tape tends to curl and this condition can persist during firing. They suggest the use of a previously fired substrate as a cover plate resting on the green tape to prevent warpage of this type during firing. Shanefield and Mistler (1974) observe that reactions between the slurry and cellulose acetate cause the carrier film to be 4.7 % thicker and 3.3 % narrower after casting and drying. Films that did not narrow resulted in cracked tapes.

A number of factors such as the thickness of the cast tape, volatility of the solvent, and length of the casting machine determine the casting speed. Alumina substrates having a nominal fired thickness of 0.026 in. have been cast continuously at speeds of 6–24 in./min using laboratory and commercial production tape casting machines. Howatt *et al.* (1947) used a belt speed of 5 ft/min for casting titanate capacitor sheets with a thickness of a few mils and Runk and Andrejco (1975) report forming 1–10 mil fired sheets of a lead zirconium titanate from tape cast at a film carrier speed of 18–30 in./min.

C. Thickness Monitoring

Some of the variables cited for determining the thickness of the dry tape include viscosity of the slurry, height of the doctor-blade opening, speed of the carrier film, and drying shrinkage. The relationship among these parameters should be established for each system. In the ERC-105 process, for example, a doctor-blade opening of 0.063 in. will produce a green tape of about 0.032 in. that in turn provides a fired thickness of 0.026 in. The drying shrinkage in the thickness direction is usually about 50 % of the blade opening. Instruments* are being used commerically for monitoring the as-cast thickness of the ceramic tape. Thicknesses of less than 1 mil become fragile and tedious to handle, while dried tapes in excess of 0.045 in. impose problems of inconvenient drying times and storage on take-up reels.

D. Drying

The slurry is converted into a semirigid yet flexible tape upon removal of the solvent by drying. Callahan and Stark (1970), Park (1961), and Richter (1972) include auxiliary ovens and heat sources to provide a temperature below the boiling point of the solvent to accelerate drying. Although Shanefield (1971) also reports the use of thermally accelerated drying of alumina substrates, the ERC-105 process and other alumina substrate processes nominally use only room temperature air flowing at a rate of 100 ft^3/min counter current

*Such as Model RTA-41, Nucleonics Development Co., Monrovia, California.

to the direction of the carrier film. Covers on the casting machine confine the air flow to a region of several inches above the ceramic tape.

E. Edge Trimming and Tape Storage

After drying, the leather-hard tape may be slit to several desired widths as well as edge trimmed by means of a sharp cutting tool prior to storage on the take-up reel or shaping operation. It is important that all of the solvent be removed before storing the tape on reels.

Ceramic substrates for high density thin film circuit patterns have stringent requirements for the absence of surface defects, particularly "burrs",* of the order of a few microns in size. The overall criteria of these substrates are discussed by Williams (1971) while Sundahl and Berrin (1971) report on the analysis and characterization of the topographical, chemical, and crystallographic properties of many of the surface defects. Special care is taken to minimize the formation of defects as the result of debris and foreign particles settling onto the tape during casting, trimming, storage, and punching. It has proved beneficial to perform these operations in a class 10,000† or better clean room environment.

IV. Forming

Richter (1972) describes a process of stripping and cutting the ceramic tape into pieces for stacking and laminating two pieces to form a thick ceramic part in a subsequent calendering step. Callahan and Stark (1970) strip, slit, and cut the ceramic tape to form a plurality of chips of uniform width and length. Park (1961) describes a procedure for taking tape stored on reels and passing it beneath a gang of wheel knives that cut the ceramic tape, but not the carrier film, into strips and then a transverse cutting edge is synchronized to cut the ceramic tape only into uniform lengths with a tolerance of 0.002 in. The resulting small square or rectangular units of ceramic tape are transferred to refractory setters for firing by inverting the carrier film and stripping it from the ceramic units by peeling it back at 180 degrees over a small diameter rod so as to leave the ceramic units in a precise array on the setter plate.

*See ASTM Designation F-109-69T, "Definition of Surface Imperfections on Ceramics." American Society for Testing Materials.

†A 10,000 class clean room has not more than 10,000 particles of 0.5 μm or larger per cubic foot (see Rott, 1969).

A. Stamping

Thompson (1963) describes the forming of parts by stamping as follows.

> The tape is prepared for stamping by slitting to a width slightly wider than the shape that is to be stamped. The strips of tape are then fed into the stamping die by a mechanism that allows adjustment of the length of tape fed for each stroke of the press. The stamping press employs an eccentric action to drive the die. The speed of the press is variable from 60 to 1000 strokes per minute.
>
> To form a shape that contains no holes, such as a plain disk or rectangle, a simple punch and block die can be used. By this method the shape is punched out of the tape web and falls out the bottom of the die. Shapes that contain one or more holes are stamped on a compound die, similar to one used in the mica industry. The die design grips the tape, simultaneously pierces the holes and stamps the outside configuration, then returns the stamped shape to the tape web to be carried from the stamping zone. No attempt is made to stamp shapes containing holes with centers so close that the wall thickness between holes would be less than one-half the thickness of the tape. The piercing pins that stamp the holes should be less than 0.0005 inch smaller than their matching hole in the die block.

Shanefield and Mistler (1973) in the ERC-105 process have used a punch press such as a Benchmaster 161G to form alumina substrates. The parts are punched oversize to allow for shrinkage (16 %) that occurs during firing. Cleanliness of the punch and die are important to avoid introducing defects into the surface of the substrate. The side of the ceramic tape that was in contact with the cellulose acetate carrier film during casting faces toward the ejector. The punched-out part is removed carefully from the machine to avoid scratching the surface of the tape against the ejector and then wrapped in lint-free paper to await firing.

Piazza and Steele (1972) have determined that the location of holes produced in large substrates by punching and firing is feasible to a tolerance of 175 μm. Hole location to a precision of 25 μm over a 5 in. span in fired substrates has been attained by Longfellow (1971) with the use of CO_2 laser drilling after firing.

B. Scoring

It is convenient and economically advantageous to process multiple arrays of circuit patterns on a single, large substrate and later separate it into discrete circuits. One method for accomplishing this is to score the ceramic tape prior to firing with shallow "V" grooves that divide the area of the larger substrate blank into the desired number of units. After firing and deposition of the circuit pattern these may be separated readily by hand snapping along the grooved path. The objective of the scoring technique is to have the substrate break in a straight path along the score mark. The scoring should retain sufficient strength in the fired substrate to withstand circuit processing without

fracturing prematurely, but at the same time reduce the modulus of rupture along the groove to a value that enables an operator to fracture the part with a snapping action by hand. Kleiner (1969) used the modulus of rupture (MOR) as a measure of the force required for separation as a function of angle of score mark, depth of score mark, and annealing treatment. He found the optimum range of MOR to be 10,000 to 30,000 pounds per square inch. He obtained the best results with a 0.030 in. thick substrate using an included angle on the blade of the forming tool of 30 to 45 degrees and depth of penetration into the substrate at 10 to 30 % of the thickness of the substrate. Annealing the parts had no significant effect upon the MOR value. Similarly, the patent by Pauley and Lockwood (1967) describes the use of a shaping tool for simultaneously stamping and grooving the ceramic tape while still on its carrier film. According to these authors, as illustrated in Fig. 3a, the angle A between the sides of the V-shaped grooves should be 40–75 degrees and the depth D of the groove should be 15–40 % of the thickness T. Usually the grooves are formed on only one surface of the substrate; namely, the side opposite that in contact with the carrier film. For ease in forming grooves and cutting ceramic tape these authors state that the ceramic sheet should have a durometer hardness of 10 to 100 on the Rockwell Shore scale. They further report that a pressing tool (Fig. 3b) can be formed of metal or plastic with hard metal or metal carbide inserts for the cutting and groove-forming edges.

Prior to the availability of prescored substrates, manufacturers of electronic circuits would separate multiple circuit patterns into discrete circuits by sawing the substrate with a diamond cut-off wheel. This technique has the inherent disadvantage of exposing the circuit to debris and contamination

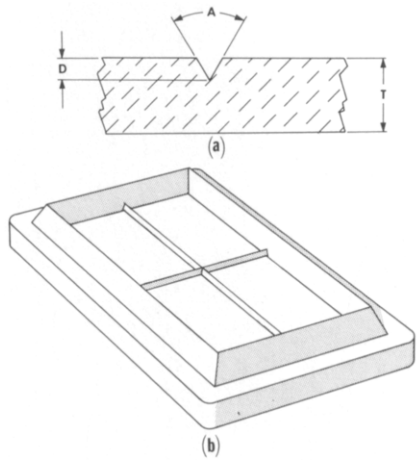

Fig. 3. (a) Score mark profile in unfired ceramic tape. (b) Illustration of groove-forming tool.

from the slicing operation. Manually scribing with a diamond stylus and fracturing by hand along the scribe mark has also been practiced, but frequently the risk of damaging circuits is higher by this method due to the fracture meandering away from the scribe mark.

C. Laser Scribing

When the quantity and variety of patterns are of sufficient volume to justify the investment, circuit manufacturers are using lasers to scribe the substrates after deposition of the pattern. Laser scribing has been used at linear speeds of 120 in./min. In addition, the technique is relatively clean and reduces the need for critical registration of certain circuit patterns as in the case of prescored substrates. Laser scribing consists of drilling a series of blind holes along a line. The basic principles have been described by Longfellow and Oberholzer (1969) and Cohen (1973), while Saifi and Borutta (1975) concluded that the optimum parameters for scribing alumina substrates with a CO_2 laser are an energy pulse of 40 mJ with a pulse length of 0.6–0.8 msec and separation of 100–150 μm between successive holes. The laser was operated in a low order mode at 50 W CW output power.

The laser has also been used in postfiring shaping and forming of alumina substrates prepared by doctor-blading. Lumley (1969) describes the shaping of ceramic substrates with a laser by controlled facture. Intricate shapes have been prepared by laser sawing in a technique described by Longfellow (1973). The 0.024 in. thick alumina detail in Fig. 4 is produced in 28 sec using 120 W of continuous power from a 250 W CO_2 laser. The kerf of this laser cut is 0.002–0.003 in. wide and radii at corners may be as small as 0.010 in. In

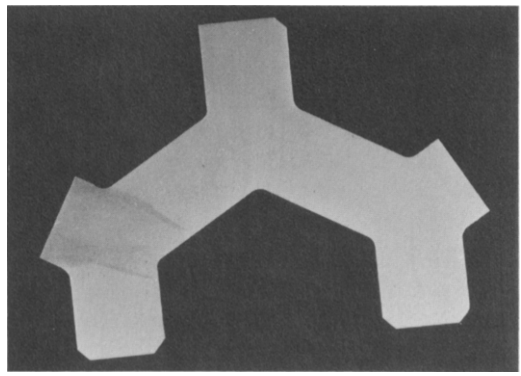

Fig. 4. Complex alumina shape (0.024 in. thick × 15.5 in. linear edge) formed by laser sawing. (From Longfellow, 1973.)

essence, the technique is that of following a pattern contour with a pantograph unit that controls the path of the laser beam. Linear speeds of (1.2 cm/sec) 28 in./min have been achieved.

V. Firing

It is noted in the Introduction that the high packing efficiency and concentration of ceramic powder in the dry tape results in a relatively uniform and high green density for materials that are properly processed by the doctor-blade method. Consequently the method has the distinct advantage of providing close control of dimensional tolerances during firing of large, thin sheets compared to similar parts prepared by other forming processes.

Depending upon composition and specific properties desired, alumina substrates are typically fired in an air atmosphere in the range of 1400°–1700°C. The 99.5 % alumina substrates by the ERC-105 process have an apparent unfired density of 2.9 gm/cm^3. Because of the reactive nature of the alumina powders, fired densities of 3.86 to 3.91 gm/cm^3 have been obtained by sintering at temperatures of 1425°–1500°C in a 7 ft long, pusher-type Pereny kiln equipped with SiC heating elements and hearth plate. The pusher speed is 0.41 ft/min and the hot zone measures 18 in. in length. Parts are fired on a 17 hr schedule of 8 hr heating to 1500°C, 1.5 hr soak, and 7.5 hr cooling. In terms of the pyrometric cone equivalent (PCE), this corresponds to a heat treatment of a Cone 16 at 6 o'clock (1491°C).

Leaver and Mistler (1971) obtained similar densities using a fast cycle of 4.5 hr upon firing to 1532°C using a propane-heated Ipsen roller hearth kiln. They accomplished this after replacing the original rollers with SiC rollers.

A. Dimensional Tolerances

Commercially available tolerances for length, width, and hole location of alumina substrates prepared by doctor-blading were reported by Nordquist (1968) to be within $\pm$ 1/2 %, but not less than $\pm$ .003 in. A tolerance of $\pm$ 1/4 % is obtainable with parts of 3 in.^{2} in area and smaller. He indicated a normal thickness tolerance of $\pm$ 10 % and a flatness (camber) of 0.004 in./in. but not less than 0.002 in.

The standard unfired alumina substrate module of the ERC-105 process tape measures 13.6 cm × 11.3 cm × 0.76 mm (5.4 in. × 4.5 in. × 0.030 in.). Its fired dimensions are 11.43 cm × 9.53 cm × 0.66 mm (4.5 in. × 3.75 in. × 0.026 in.) and correspond to a linear firing shrinkage of 16 %. This nominal shrinkage value can be controlled to $\pm$ 0.1 %. The location of

punched holes are within 0.005 in. or less when separated up to 2 in. from a central reference point. Warpage is regularly controlled to 0.003 in./in. Warpage in excess of these values may cause problems during circuit processing such as variation in scribe lines due to changes in the focus of the laser beam, resolution of circuit geometry during photolithographic processing, and the simultaneous application of multiple leads by thermal compression bonding. Postfiring corrective measures such as grinding and polishing are often precluded for reasons of economy as well as loss of the smooth, defect-free, as-fired surface that is essential in many thin film circuit applications. Procedures for reducing warpage include the use of refractory setters with less than 0.008 in. curvature for the ERC-105 substrates. In addition, the ceramic tapes are fired one high. Three prefired, porous substrates of similar composition except for a coarser alumina (A-14 versus A-16)* and totalling about 100 gm, rest as cover plates on top of the dry ceramic tape. Care is taken to remove all dust, burrs, and particulates adhering to the surface of the cover plate that is in direct contact with the substrate. Substrates are fired with the side that had been in contact with the carrier film facing upward on the setter plate. The cover plates have a life of about 15 cycles after which they become too dense and stick to the substrate during firing. Another practice for reducing warpage has been to stack once-fired substrates about 10 high and refire them to slightly below the initial sintering temperatures.

In applying the doctor-blade process to the fabrication of thin wafers (1–10 mils) of a lead zirconate titanate ceramic, Runk and Andrejco (1975) have

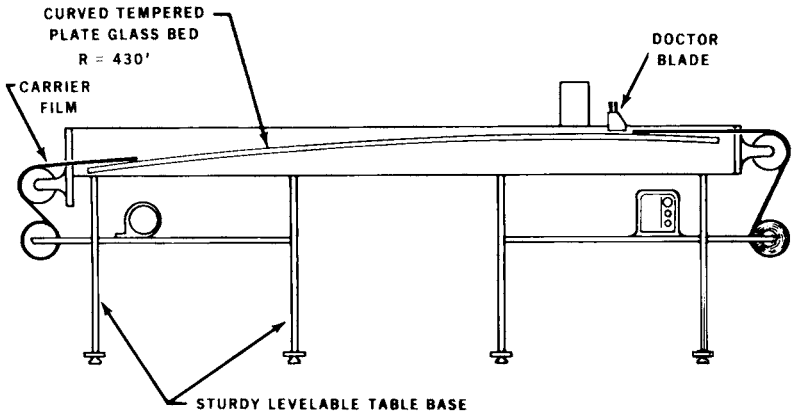

Fig. 5. Schematic of a precision doctor-blade casting machine. Carrier film: Aclar 33, from Allied Chemical Corp. (From Runk and Andrejco, 1975.)

* Aluminum Corp. of America.

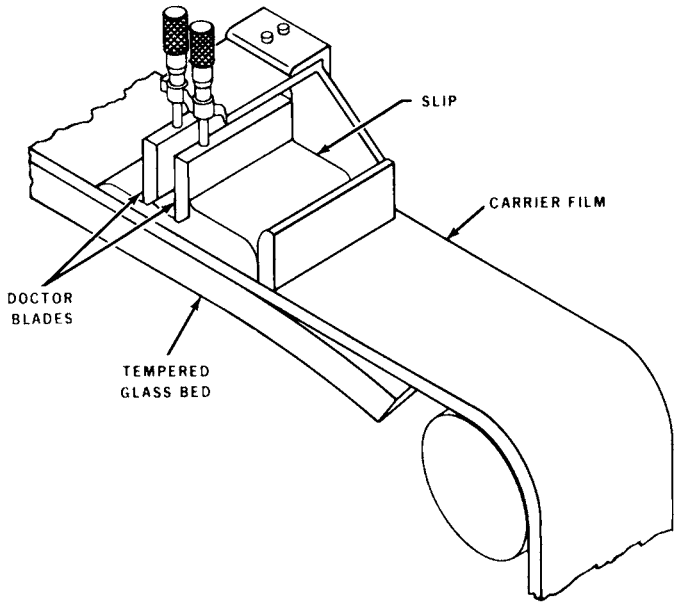

Fig. 6. Dual doctor-blade configuration. (From Runk and Andrejco, 1975.)

designed a precision tape casting machine (Fig. 5) that reduces the nominal thickness tolerance to less than $\pm$ 0.0003 in. In addition to controlling the casting parameters of slurry viscosity, carrier film speed, doctor-blade setting, and drying shrinkage, they have incorporated several improvements into their machine. They include achieving a precise gap between the blade and casting surface, a carrier film of controlled thickness (cellulose acetate 0.003 in.), a blade machined to a fraction of a mil in straightness, and a dual doctor-blade configuration (Fig. 6) that minimizes hydrodynamic and surface tensile forces at the blade. The dual blade provides a constant height to the slurry pool behind the leading blade. The use of a sheet of tempered glass as the film support surface and curved to a radius of 430 ft along the length of the machine, beginning at the blade, provides good contact between the film and bed with a minimum force required to advance the film. The PZT ceramic provides a wafer of 0.0044 $\pm$ 0.0002 in. dry thickness for a blade setting of 0.012 in. Typically the material has a 20 % firing shrinkage when sintered at 1240°C for 2 hr and provides a fired thickness of 0.0035 $\pm$ 0.0002 in.

B. Surface Finish and Microstructure

High alumina substrates prepared by doctor-blading can provide as-fired surface finishes of less than 2 μm (CLA) as reported by Stetson and Gyurk

(1967) and Gaddy *et al.* (1973) (see Table II). Using the firing conditions and composition of the ERC-105 process there is negligible grain growth. The average grain size is 1 μm or less. The as-fired surface finish is similar on both top (A) and bottom (B) surfaces of the substrate versus time at temperature as shown in Fig. 7a. A surface area for the alumina powder of greater than 12 m^2/gm obtained with a 48 hr ball-milling time in Fig. 7b is required to achieve this surface finish.

The size of the internal grains average about 2 μm. This contrast in grain size between the fine grain surface and coarse grain internal regions of high alumina substrates approaches the microstructure proposed by Gutshall and Gross (1968) for optimizing strength in a polycrystalline ceramic. The flexural

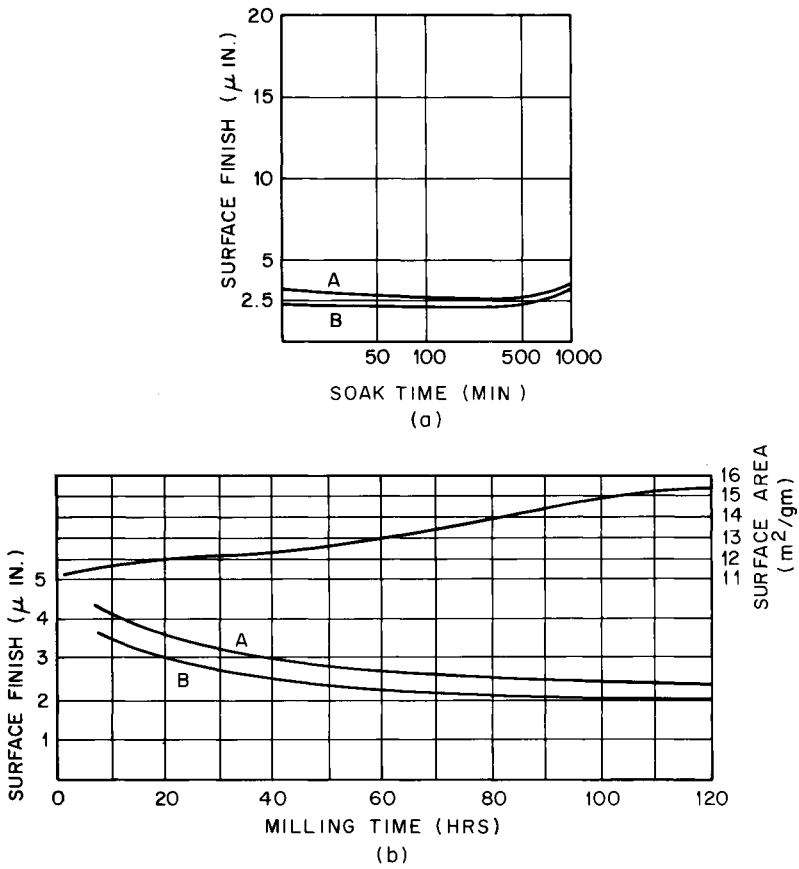

Fig. 7. (a) Surface finish versus time at temperature (1425°C) of ERC-105 alumina substrate. (b) Surface finish and alumina powder surface area vs. ball milling time. (After Stetson and Gyurk, 1972.)

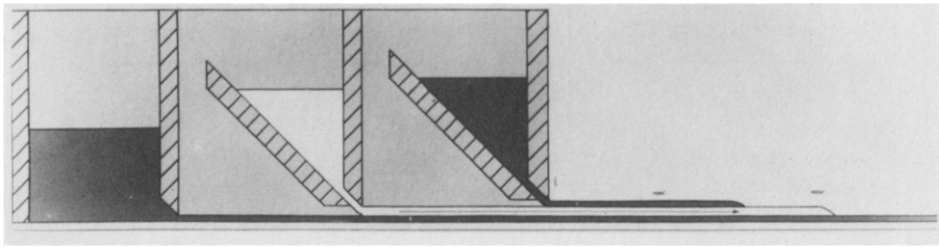

Fig. 8. Schematic of a triple layer doctor-blade casting process. (From Mistler, 1973.)

strength values of the high alumina substrates are in the range of 70,000 pounds per square inch. This observation led Mistler (1973) to further enhance substrate strength by employing a triple doctor-blading process illustrated in Fig. 8. The top and bottom layers contain a few tenths percent MgO addition to the alumina composition as a grain growth inhibitor while the center layer contains 1/2 % of MnO as a grain growth promoter. The three layers are formed into a single sheet by the sequential casting technique. Upon firing, substrates of 0.025 in. thickness prepared in this manner have flexural strengths of 120,000 pounds per square inch. The dependence of flexural strength values upon the presence of flaws and microcracks along the edges of test specimens selected from sheets prepared by doctor-blading is discussed by Lo (1972). Laser scribed specimens of a commercial substrate composition exhibited about 70 % of the strength obtained with specimens prepared by cutting with a diamond wheel. It should not be construed that laser scribing per se is at fault. The resulting edge condition is equally a function of the specific composition and its processing history. Flexural strength specimens with as-fired edges are preferred. Since this is not always practical, the biaxial flexural test that uses disk specimens as described by Wachtman *et al.* (1972) provides a method for determining strength values that are less dependent upon the edge condition of the specimens.

VI. Preferred Orientation

The microstructure of electronic ceramics is known to determine properties other than mechanical strength. Some high alumina substrates formed by doctor-blading were found by DiMarcello *et al.* (1972) to exhibit a preferred orientation among the alumina grains consisting of a fiber texture in which the basal planes are oriented parallel to the surface of the substrate. This condition contributes to an anisotropy of properties and particularly in this

case to the dielectric constant. The dielectric constant measured normal to the surface of the substrate was found to increase 2–9 % over the value for a more randomly oriented microstructure. In the same study little, if any, preferred orientation was detectable in substrates prepared by the ERC-105 process. Differences in the shape of the starting alumina powders and heat treatments with accompanying selective recrystallization, are believed to enhance any preferential alignment among the solid particles that may occur in the slurry during casting.

The increasing use of ceramic substrates for microwave applications in which the substrate becomes an integral part of the circuit has prompted greater interest in controlling the uniformity and nominal value of the dielectric constant Gaddy *et al.* (1973) have studied the effect of processing parameters such as alumina content, density, and selected impurity additives of MgO, CaO, and SiO_2 upon the dielectric constant of alumina substrates at microwave frequencies. They conclude that (1) the presence of minor constituents in the starting alumina powder lowers the dielectric constant, (2) the dielectric constant increases with alumina content and density, and (3) the increase in dielectric constant with density is not linear (Fig. 9). They attribute

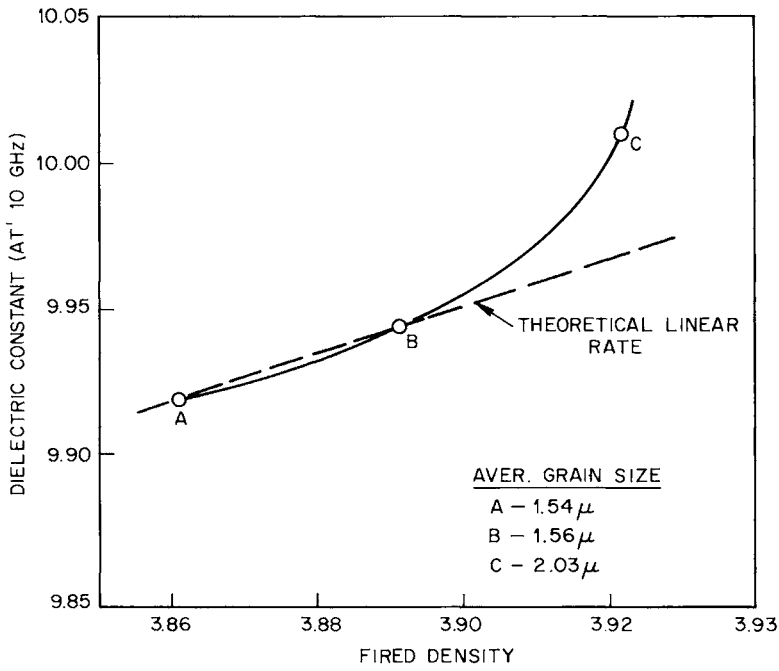

Fig. 9. Dielectric constant vs. fired density for a 99.7% alumina substrate. (After Gaddy *et al.*, 1973.)

the latter to the enhancement of a preferred orientation during the later stages of sintering.

VII. Laminated Structures

The concept of laminating unfired doctor-bladed ceramic sheets has proved to be an important extension of the process for preparing complex, three-dimensional electronic circuits, packages, and components. Stetson and Schwartz (1961) outlined the objectives of the process as follows:

1. Separate formation of individual layers,
2. Lamination of the layers in the green state,
3. Elimination of differential shrinkage, and
4. Single heating cycle.

Schwartz and Wilcox (1967) list the steps for meeting the above objectives, namely,

1. Doctor-blading thermoplastic sheets, heavily loaded with ceramic material,
2. Punching holes,
3. Screening metal electrode patterns,
4. Laminating the separate sheets,
5. Punching the final shapes from the large sheets; and
6. Sintering the monolithic structures.

Most of these steps have been described previously. Metallization is normally done by screen printing. The lamination is performed by stacking several green sheets and applying pressure in the range of 200 to 200,000 pounds per square inch at a temperature that may range from ambient to several hundred degrees fahrenheit. Interconnection among various metallization layers is through holes called "vias". Intricate circuit patterns can be produced relatively cheaply by this process. A major advance by Schwartz and Wilcox (1967) is the combination of forming a coarse, porous refractory metallization pattern that is subsequently infiltrated by a metal of high electrical conductivity such as copper by a capillary filling technique after a densification firing treatment of the ceramic. The advantage is an improved conductivity over standard refractory and noble metals. Chance and Wilcox (1971) discuss the physical compatibility of ceramic and metal combinations for use in developing multilayered laminated ceramics.

Throughout this discussion of the doctor-blade process as a method of forming ceramics, emphasis has been devoted to its application in the preparation of high alumina substrates, particularly by the ERC-105 process. The

reader should not infer that the process is limited to such compositions and applications. It should serve instead to demonstrate that the doctor-blade process is a viable, basic method with the capability of use in manufacturing a variety of ceramic compositions. It is still a relatively new process for the production of ceramics in large quantities that exhibit characteristics not attainable by other processes.

ACKNOWLEDGMENTS

The author wishes to thank D. J. Shanefield and R. B. Runk of the Engineering Research Center, Western Electric Co., for their helpful discussions and M. D. Rigterink of Bell Telephone Laboratories for reviewing the manuscript.

References

Bennett, M., Boyd, W. E., and Nobile, J. C. (1970). U.S. Patent 3,518,756.

Berrin, L., Johnson, D. W., Jr., and Nitti, D. J. (1972). *Amer. Ceram. Soc., Bull.* **51**, 840–844.

Brunauer, S., Emmett, P. H., and Teller, E. (1938). *J. Amer. Chem. Soc.* **60**, 309–316.

Callahan, J. P., and Stark, R. A. (1970). U.S. Patent 3,538,571.

Chance, D. A., and Wilcox, D. L. (1971). *Proc. IEEE* **59**, 1455–1462.

Cohen, M. I. (1973). *In* "Laser Handbook" (F. T. Arecchi and E. O. Schultz-Dubois, eds.), Vol. 2, p. 1577. North-Holland Publ., Amsterdam.

DiMarcello, F. V., Key, P. L., and Williams, J. C. (1972). *J. Amer. Ceram. Soc.* **55**, 509–514.

Francis, T. L., MacZura, G., Marhanka, J. E., and Parker, H. J. (1972). *Amer. Ceram. Soc., Bull.* **51**, 509–514.

Gaddy, J. H., Bailey, J. T., and Olyphant, M. (1973). "Effects of Variation in Alumina Substrates on Dielectric Constant at Microwave Frequencies," *Electron. Mater. Proc. Symp. October 1973* (unpublished).

Gutshall, P. L., and Gross, G. E. (1968). *Ceram. Age* **84**, 22–24.

Howatt, G. N., Breckenridge, R. G., and Brownlow, J. M. (1947). *J. Amer. Ceram. Soc.* **30**, 237–242.

Johnson, D. W., Jr., Nitti, D. J., and Berrin, L. (1972). *Amer. Ceram. Soc., Bull.* **51**, 896–900.

Kappes, K. A., and Bateson, S. (1973). U.S. Patent 3,740,234.

Kleiner, R. N. (1969). *Amer. Ceram. Soc., Bull.* **48**, 1139–1142.

Leaver, N. E., and Mistler, R. E. (1971). *Amer. Ceram. Soc., Bull.* **50**, 710.

Lo, W. C. (1972). *Nat. Bur. Stand. (U.S.), Spec. Publ.* **348**, 399–400.

Longfellow, J. (1971). *Amer. Ceram. Soc., Bull.* **50**, 251–253.

Longfellow, J. (1973). *Amer. Ceram. Soc., Bull.* **52**, 513–515.

Longfellow, J., and Oberholzer, D. J. (1969). *IEEE Int. Conv. Dig.* pp. 146–147.

Lumley, R. M. (1969). *Amer. Ceram. Soc., Bull.* **48**, 580–584.

Mistler, R. E. (1973). *Amer. Ceram. Soc., Bull.* **52**, 850–854.

Nordquist, C. E. (1968). *Hybrid Microelectron. Symp. (Intern. Soc. Hybrid Microelectronics) 1968*, pp. 405–416.

Park, J. L., Jr., (1961). U.S. Patent 2,966,719.

Pauley, D. S., and Lockwood, D. L. (1967). U.S. Patent 3,324, 212.

Piazza, J. R., and Steele, T. G. (1972). *Amer. Ceram. Soc., Bull.* **51**, 516–518.

Richter, F. E. (1972). U.S. Patent 3,695,960.

Rott, C. (1969). *West. Elec. Eng.* **13**, No. 2, 41.

Runk, R. B., and Andrejco, M. J. (1975). *Amer. Ceram. Soc., Bull.* **54**, 199–200.
Saifi, M. A., and Borutta, R. (1975). *Amer. Ceram. Soc., Bull.* **54**, 986–989.
Schwartz, B., and Wilcox, D. L. (1967). *Ceram. Age* **83**, 40–44.
Shanefield, D. J. (1971). *Amer. Ceram. Soc., Bull.* **50**, 462.
Shanefield, D. J. and Mistler, R. E. (1971). *West. Elec. Eng.* **15**, 26–31.
Shanefield, D. J., and Mistler, R. E. (1973). *Amer. Ceram. Soc., Bull.* **52**, 375.
Shanefield, D. J., and Mistler, R. E. (1974). *Amer. Ceram. Soc., Bull.* Part I **53**, 416–420.
Shanefield, D. J., Morzenti, P. T., and Mistler, R. E. (1974). *Amer. Ceram. Soc., Bull.* Part II **53**, 564–568.
Stetson, H. W., and Gyurk, W. J. (1967). *Amer. Ceram. Soc., Bull.* **46**, 387.
Stetson, H. W., and Gyurk, W. J. (1972). U.S. Patent 3,698,923.
Stetson, H. W., and Gyurk, W. J. (1973). U.S. Patent 3,780,150.
Stetson, H. W., and Schwartz, B. (1961). *Amer. Ceram. Soc., Bull.* **40**, 584.
Sundahl, R. C., and Berrin, L. (1971). *In* "Characterization of Ceramics" (L. L. Hench and R. W. Gould, eds.), Part 5, Chapter 20. Dekker, New York.
Thompson, J. J. (1963). *Amer. Ceram. Soc., Bull.* **42**, 480–481.
Wachtman, J. R., Jr., Capps, W., and Mandel, J. (1972). *J. Mater.* **7**, 188–194.
Williams, J. C. (1971). *Proc. Tech. Program, NEPCON, 1971*, pp. 116–126.

Firing

THOMAS REYNOLDS III

Ferroxcube Corporation
Saugerties, New York

I. Introduction

The processing of technical ceramics from a loose physical mixture of discrete particulate phases into a dense homogeneous ceramic involves the application of numerous thermal treatments. Thermal energy is needed to (1) supply the heat of fomation (calcining), (2) supply latent heat of vaporization (drying), (3) provide combustion of organic binders and lubricants, and (4) supply energy for the densification and grain growth of the pressed particulate compact. In addition, the above reactions must take place within a time period that is both practical and economical.

It is only possible to attain precise control over the impurity level and dopant chemistry in the fired ceramic if the control is extended backward in the process to the initial raw materials themselves. This means that in most cases the "ceramic raw materials" are the calcined product of the supplier. As an example, iron (III) oxide, Fe_2O_3, used as a ceramic raw material in the manufacture of ferrites is prepared by the thermal decomposition of ferrous heptahydrate, $FeSO_4 \cdot 7H_2O$. Following the removal of the seven waters of hydration (another thermal process) the sulfate is calcined

and converted into Fe_2O_3. Hancock (1970) has shown that the control of the residence time and peak temperature in the rotary calcining kiln allows particles having a wide range of sizes to be obtained. The reactivity varies with particle size, and this will influence the final properties and microstructures.

The final densification and grain growth takes place in the sintering process. In addition to the normal parameters of time and temperature, many of the transition metal oxides must be fired under controlled atmospheres to establish the proper stoichiometry. Volatilization of components such as lead or zinc must be dealt with and the heating rate and heat flux to the parts should be uniform to prevent warpage and cracking.

II. Compound Formation

The class of reactions covered by the generic name Compound Formation includes those commonly called in the literature *calcining*, *prefiring*, *presintering*, etc. Basically what takes place in this step is the reaction of the physical mixture of oxides to form a homogeneous material that can subsequently be shaped and sintered to yield a high density ceramic with the required electrical and/or magnetic properties. The compound formation process includes several steps: (1) supplying the heat of formation to cause the reaction to take place, (2) supplying the heat of formation at a sufficiently elevated temperature that the reaction kinetics take place in a fashion economically feasible for manufacture of the ceramic, (3) the removal of the products (gaseous) during compound formation—this also includes the removal of any toxic products that may be formed during calcining.

In many cases compound formation is 100 % complete during this step. For example, the mixed titanate ceramics of nominal composition

$$Ba_{1-x}M^{2+}{}_xTiO_3 \quad (M = Sr, Ca, Pb)$$

are usually formed from a mixture of oxides and carbonates according to the reaction

$$(1 - x)\,BaCO_3 + xM^{2+}CO_3 + TiO_2 = Ba_{1-x}M^{2+}{}_xTiO_3 + CO_2(g)$$

and the products are ball milled and processed further for pressing and firing. For many of the magnetic oxides (i.e., ferrites) it has been found that incomplete conversion to the spinel phase during calcining is desirable from a magnetics and processing standpoint. Swallow and Jordan have shown that

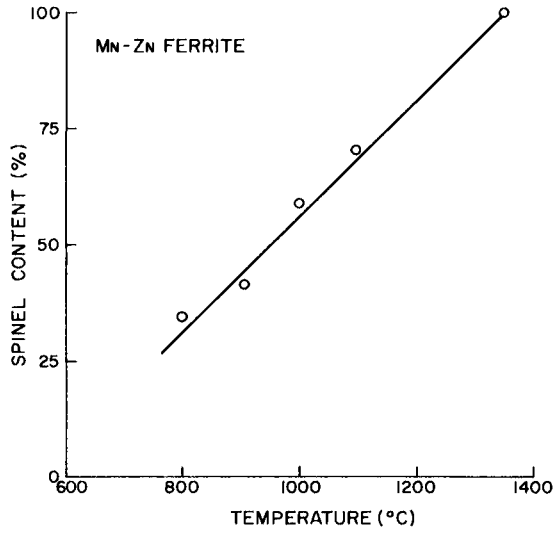

Fig. 1. Effect of calcining temperature on the spinel content of MnZn ferrites. (Swallow and Jordan, 1964).

spinel content, as determined by X-ray diffraction techniques may be controlled by the temperature of the calcining reaction (see Fig. 1).

The compound formation during calcining takes place in the following fashion for the manganese zinc ferrites. As the mixture of oxides and carbonates is brought up to temperature the first reaction that takes place is the formation of zinc ferrite, $ZnFe_2O_4$. This reaction is controlled predominately by the reactivity (particle size and morphology) of the iron oxide but begins at a temperature of approximately 650°C. The reaction proceeds with the subsequent formation of increasing amounts of manganese zinc ferrite and the consequent reduction in zinc ferrite content until a temperature of approximately 800°C at which time no further zinc ferrite lines are observed by X-ray diffraction. At this temperature the conversion to $Mn_{1-x}Zn_xFe_2O_4$ is essentially complete. Further increase in the compound formation temperature results in increasing conversion to the spinel phase.

The reactivity, densification, and grain growth in the sintering process are largely controlled by the conditions of calcining. The particle size, for example, is strongly dependent on the compound formation temperature, and this affects quite dramatically the final grain size in the fired ceramic. Johnson *et al.* (1974), have shown (see Table I) that the average sintered grain size of $LiFe_5O_8$ ceramics prepared from freeze-dried powders (sintered 1055°C; 16 hours) is dependent upon the calcination temperature. This implies that control of the powder in the calcining step is essential. Particle

TABLE I

AVERAGE GRAIN SIZES OF $LiFe_5O_8$ PREPARED BY FREEZE DRYING AND FIRING AT 1055°C FOR 16 HOURS IN AIR[a]

Calcination temperature (°C)	Grain size (μm)
465	4.3
568	4.8
662	5.2
756	5.5
849	10.
943	11.

[a] From Johnson *et al.* (1974).

size and/or surface area are normal and routine control parameters at the end of the calcining step. These may be supplemented by X-ray powder diffraction techniques for phase analysis and analytical chemistry for a check on stoichiometry at this point in the process.

The particle size (μm) or surface area (m^2/g) following the calcining step is also dependent on the method of preparation. As can be seen in Fig. 2, at a given calcining temperature powders prepared by freeze drying or spray drying of solutions have higher surface areas. Precipitated powders have somewhat lower particle size and powders prepared by ball-milling would yield even lower surface areas at corresponding temperatures.

The reason that freeze-dried, spray-dried, and precipitated powders may be fully reacted at low temperatures is that these types of powders are prepared from solution. As a result, each freeze-dried, spray-dried, or precipitated particle is stoichiometric on an atomic scale (to the first approximation). Thus, during calcining, reaction takes place more rapidly because of better homogeneity and shorter diffusion distances for the reactants.

For example, Brown and Mazdiyasni (1972) have used organometallic compounds to form submicron-size lead lanthanum zirconate titanate (PLZT) when calcined at 500°C. By comparison, PLZT prepared by more conventional techniques (i.e., ball-milling of oxides) are calcined at 900°–1000°C (Haertling, 1963, 1966).

A variety of things are accomplished in the presintering reaction.

1. *Decomposition.* The decomposition of the raw materials (i.e., carbonates, organometallic salts, higher oxides, etc.) results in the removal of the gaseous by-products. The evolution of these gases during the sintering cycle would cause internal pressure, stresses, and cracking.

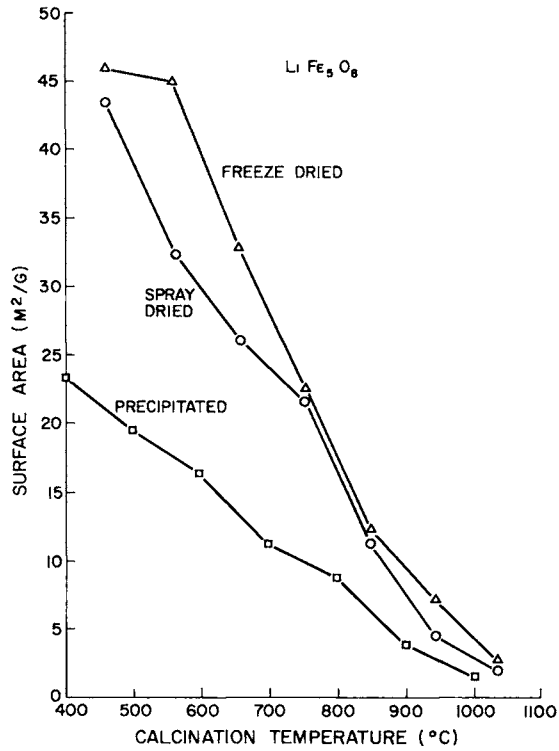

Fig. 2. Surface area versus calcination temperature for $LiFe_5O_8$ prepared by various techniques. (Johnson *et al.*, 1974).

2. *Reaction.* The reaction of a multiphase mixture to form the desired compound. Additional milling after calcining and prior to pressing and sintering stage increases the homogeneity of the ceramic.

3. *Particle Size.* The presintering reaction can be closely controlled and the particle size and/or surface area of the presintered product adjusted so that close shrinkage control is maintained in the sintering operation. This is especially important in technical products which may have a rather complicated sintered shape and require close tolerances and dimensional control.

The calcining reaction itself can take place by a variety of techniques, the simplest of which is simply to place the physically mixed raw materials into a suitable ceramic dish or crucible and to place the crucible in a box-type furnace. Because the temperatures involved are usually of the order of 600°–1200°C one approach is to use an electrically heated furnace having silicon carbide (SiC) heating elements. These types of furnaces are readily available

from commercial suppliers or can be built rather inexpensively from components. If the reaction results in the evolution of CO_2 as a gaseous by-product there should be sufficient venting and gas flow to insure the removal of CO_2 and an adequate supply of oxygen to the reaction so that chemical reduction of the products does not take place.

For ease of reaction the best approach would be to combine raw materials that decompose during the calcining reaction in order to form the desired products. Barium titanate and manganese zinc ferrite are usually prepared by using carbonates or higher oxides as starting materials. During the decomposition of the raw materials, fresh, chemically active, surfaces are generated and this combined with a high surface area of the decomposing phases results in a rapid and uniform conversion to the final product. This is not to say that barium titanate could not be formed by the physical mixture of barium oxide and TiO_2; however, the conversion to barium titanate goes uniformly and at a slightly lower temperature if barium carbonate is used as a starting raw material.

Certain classes of compounds may give off toxic products either during calcining or sintering, specifically the barium lead titanate ceramics and the piezoelectric ceramics lead zirconate titanate, e.g., Pb (Ti, Zr) O_3. Consequently, if these types of materials are to be handled routinely in any quantity, adequate provision should be made for venting the furnaces and the work area.

The technique of calcining in a ceramic boat or tray although simple has some drawbacks in that the portion of the powder at the bottom of the tray will tend to see a different reaction atmosphere than those portions that lie in the surface. For this reason rotary calcining has been employed with a high degree of success in both small and large volume operations.

The mixed dried powders to be reacted are fed into the upper end of a rotating ceramic (or occasionally metallic) tube from a hopper or screw feeder and the calcining reaction takes place as the powders proceed down the tube. The residence time in the hot zone and hence the calcining time can be controlled by varying either the rotational rate of the tube and/or the angular elevation of the tube.

In this fashion all of the powder sees essentially the same atmosphere, it is in effect tumbled as it goes through the rotary calciner, a continuous flow of fresh atmosphere sweeps up the tube and the combustion products are carried away from the upper end of the tube itself. One further advantage of this type of calcining is that the calcined product tends to remain as rather small discrete particles instead of partially sintering into large agglomerated chunks as is the case when batch sintering is used. Far from being just a laboratory method, rotary calcination of titanate ferrites and other ceramics is carried out industrially in units with capacities of 50 kg/hr or greater.

III. Powder for Pressing

Following the calcination reaction the presintered, or calcined, material is again comminuted (i.e., ball milled or vibratory milled) to yield a material having a uniform fine particle size. It then becomes necessary to remove the solvent, usually water, that has been employed in the comminution step. This is done on a laboratory scale by the usual process of filtering and on a commercial scale by spray drying the water/oxide slurry. For most applications where parts are to be pressed from the powder an organic binder is added to the water/oxide slurry. Typical materials that are used are polyvinyl alcohol (PVA) or polyethylene glycol and usual amounts are 1–2 wt % of the oxide.

Pan drying of ceramic may be used for processing small amounts of material. The oxide/water binder slurry is usually placed in an oven and stirred continually to prevent segregation of the binder until it is essentially dry. It is then ground in a mortar and passed through a sieve to obtain a pressable powder. The thermal treatment here is not overly critical except for the fact the temperature should be chosen such that the solvent is removed without volatizing or burning off a binder that will be used in pressing.

An exception is the drying of doctor bladed ceramics in which an organic or aqueous slip is formed into thin sheets. This topic has been adequately covered in an article by Williams elsewhere in this volume.

IV. Sintering

The sintering process is composed of three different steps: (1) binder removal, (2) densification, (3) grain growth. Before densification begins the organic binders and residual moisture contained in the pressed ceramic must be removed slowly from the compact. Rapid heating at this point will result in the creation of pressure at internal voids in the material. This pressure will lead to internal cracks and holes within the material. For very simple shapes such as toroids and disks or other small parts relatively high heating rates ($\leq 500°C/hr$) can be tolerated without much structural difficulty.

The most critical region during heat up is in the range from approximately 60° to 350°C. Within this region most of the moisture and organics are volitalized and burned out. An adequate amount of oxygen or air should be supplied over the ceramic parts to cause complete binder burnout, or the possibility occurs that the binder will be incompletely removed and residual carbon may burn out at higher temperatures with the possibility of warpage

or cracking. It is common practice to force ventilate the binder burnout zone in commercial sintering furnaces to effect rapid and complete elimination of the binder.

A number of workers (Kuczynski *et al.*, 1959; Johnson and Cutler, 1963) have investigated the sintering mechanism in oxide ceramics, and their studies indicate that bulk diffusion of vacancies is the dominant mechanism of material transport during sintering. The driving force for grain growth is the reduction of surface free energy.

A. The Titanates

The PTCR* anomaly in semiconducting barium titanate is caused by the reduction of Ti^{4+} to Ti^{3+} and the adsorption of oxygen ions at grain boundaries to form potential barriers. Consequently, as Tien and Carlson (1966) have shown (see Fig. 3), the resistance anomaly is dependent on the oxygen

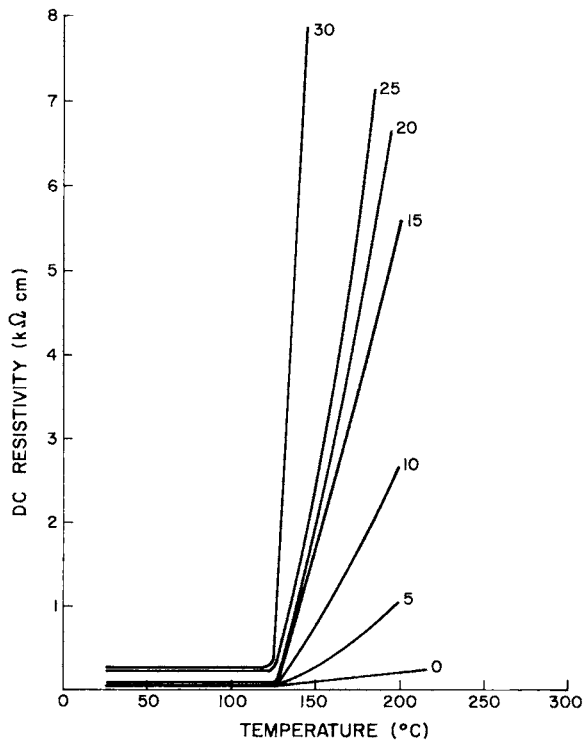

Fig. 3. Effect of P_{O_2} on the resistivity anomaly of doped $BaTiO_3$. The numbers on the curves are volume percent oxygen in the sintering atmosphere. (Tien and Carlson, 1966).

*Positive temperature coefficient of resistance.

content of the firing atmosphere. Data for their samples (sintered 4 hr at 1400°C) are not presented in the more common log ρ vs. T format, but the linear scale shows dramatically the influence of sintering atmosphere. Materials of this class are commonly fired in air in a single zone electrically heated furnace at temperatures of 1350°–1450°C.

The composition of the barium titanate is formulated such that there is an excess of TiO_2, typically

$$Ba_{1-x}M_xTi_{1+y}O_3 : Z\,Re_2O_3$$

$$0 \leq X \leq 0.5 \qquad M = Sr, Pb$$
$$0.005 \leq Y \leq 0.03 \qquad Re_2O_3 = La_2O_3$$
$$0.005 \leq Z \leq 0.0025 \qquad Y_2O_3$$
$$Ce_2O_3$$

This formulation has the beneficial effect that by having a slight excess of TiO_2 the problem of forming the hypostoichiometric compound Ba_2TiO_4, which reacts adversely with atmospheric moisture, is avoided. According to the phase diagram of Rase and Roy (1955) at temperature above 1322°C a liquid phase exists in equilibrium with $BaTiO_3$. This phase enhances the material transport (possibly by a solution-precipitation mechanism) that must take place for sintering and densification to occur.

As a result of liquid phase sintering, sintering times of less than 60 minutes can be used. Such reduced times at elevated temperatures are especially important when firing the higher Curie point barium titanate–lead titanate solid solutions. In this case, volitalization of lead from the sample must be minimized to avoid stoichiometry variation within the ceramic. Temperatures of 1400°–1450°C and times of 0.5–2.0 hours at temperature are common for doped barium titanate ceramics. Doped barium titanate–lead titanate ceramics, however, are fired at lower temperatures (1320°–1350°C) for 0.25–0.50 hours.

The volatilization of lead in this case can also be minimized by several other techniques common to the ceramic art. The pressed parts, with the binder burned off in a previous low temperature firing, are contained in a covered impervious ceramic crucible (e.g., Al_2O_3), which has a low free volume. The low free volume allows the volatile component to establish an equilibrium atmosphere within the container. Once enough volatilization has taken place to reach equilibrium conditions further losses are minimal. However, in this approach, it is essential that there be as little free space as possible.

The pressed parts can also be embedded in and surrounded by a powder of the same or a carefully adjusted composition. Because of its high surface area, the powder loses the volatile component before the pressed parts and hence establishes an equilibrium atmosphere. Some care must be exercised in

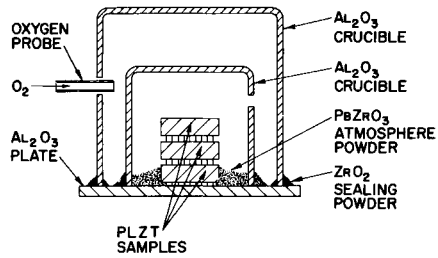

Fig. 4. An atmosphere sintering approach for lead lanthanum zirconium titanate (PLZT). (Snow, 1973a).

picking the composition of the "packing powder." In the case of doped $Ba_{0.8}Pb_{0.2}Ti_{1.015}O_3$ using a packing powder of pure $PbTiO_3$, the present author has observed an increase of the lead content of the pressed parts. The subsequent change in stoichiometry caused the loss of the desired semiconductive properties.

Snow (1973a,b) has successfully adapted this technique for the preparation of transparent lead lanthanum zirconate titanate ceramics in the form of disks as large as 84 mm in diameter by 100 mm thick. His original approach is shown in Fig. 4 and a subsequent simple experimental arrangement in Fig. 5.

One word of caution about the packing powder approach. If one uses an unsintered powder intimately packed around complex shapes, the powder itself may sinter together making it difficult to remove the parts. If, however, the pressed parts are embedded in sintered powder the difference in shrinkage rates between the powder (less shrinkage) and the pressed parts (greater shrinkage) will cause warpage and cracking of the pressed parts.

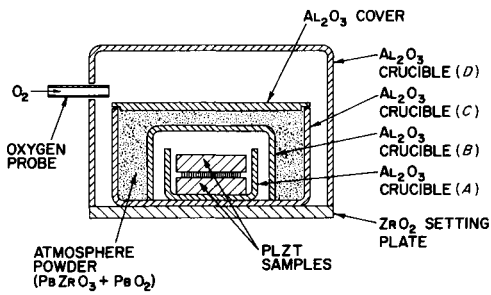

Fig. 5. An atmosphere sintering approach for lead lanthanum zirconium titanate (PLZT). (Snow, 1973b).

B. The Spinel Ferrites

This class of compounds is composed of many components; however, two of the major ones of technical and commercial interest are the manganese zinc and nickel zinc ferrites. The nickel zinc ferrites $Ni_{1-x}Zn_{x+\delta}Fe_{2+\epsilon}O_4$ are formulated with a deficiency of Fe_2O_3 (typically 0.1–0.6 mol %) in order to keep the resistivity high and magnetic losses low.

Because 2+ is the most stable oxidation state for Ni and Zn, the 3+ value of Fe will be the only stable valence state of Fe if there is a slight deficiency of iron. Consequently, nickel zinc ferrites are successfully sintered under a wide variety of oxidizing conditions.

As Reijnen (1968) has pointed out the spinel lattice consists of a close packed anion (i.e., oxygen) sublattice with a cation located in the interstices. It is thought that the rate-limiting step in sintering is the volume diffusion of oxygen vacancies. As a result stoichiometry control or firing atmosphere control will lead to changes in the densification of samples. These data shown in Fig. 6 illustrate the effect of both composition and firing atmosphere on a series of nickel zinc ferrites.

The manganese zinc system introduces an additional degree of complexity to the sintering of spinel ferrites. The spinel phase is only stable over a given atmosphere–temperature domain as demonstrated by several investigators (Blank, 1961; Slick, 1971; Paulus, 1972).

As shown in Fig. 7 there is a relationship between the equilibrium weight of a ferrite sample and the environment in which it is sintered. It is thought that this weight change reflects changes in the anion (oxygen) content of the

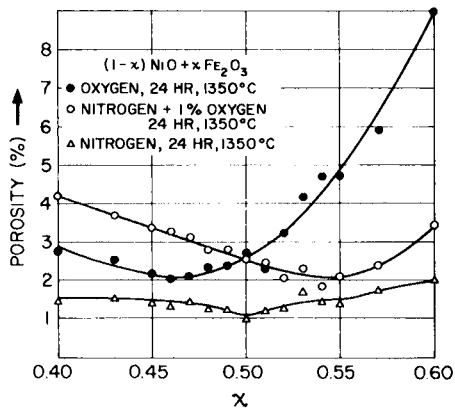

Fig. 6. The effect of firing atmosphere and stoichiometry on the porosity of nickel zinc ferrites. (Reijnen, 1968).

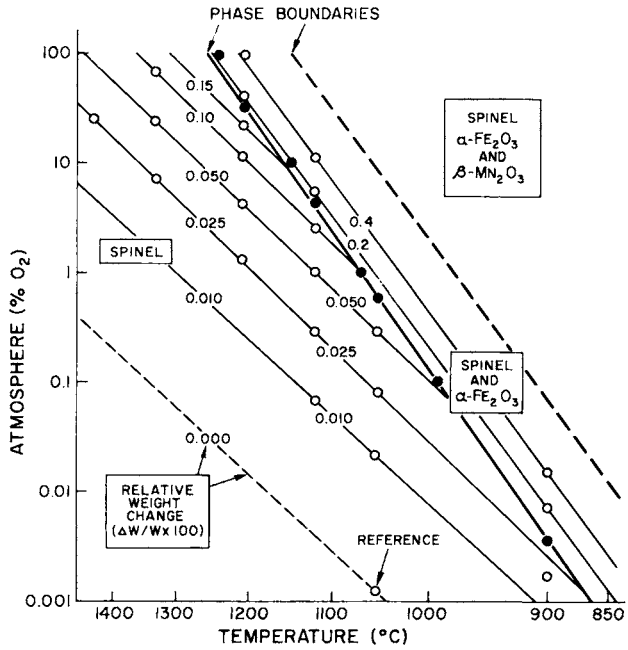

Fig. 7. Equilibrium weight changes as oxygen in the system: $(Fe_2O_3)_{54.9}$–$(MnO)_{26.8}$–$(ZnO)_{18.3}$ (Slick, 1971).

ferrite and hence the valences of the cations. Specifically, since manganese zinc ferrites are formulated with an excess of Fe_2O_3, loss of oxygen would result in the formation of ferrous iron (Fe^{2+}).

The ferrous iron content is critical for the attainment of desired magnetic properties since it provides "anisotropy compensation." Such compensation results in a low value of the magnetic losses and a maximum in the magnetic permeability (van Groenou *et al.*, 1968/1969). It should be noted that such dependence of stoichiometry and phase stability on temperature and atmosphere is by no means unique to the spinel ferrites. It is, in fact, a consequence of the thermodynamic equilibrium between the ambient atmosphere and the solid phase. Eugster and Skippen (1967) and Ernst (1966) have investigated in detail the use of solid state buffers to determine phase stability for a number of geological compounds accurately and these concepts can be adapted and extended for technical ceramics. In the case of transition metal oxides, many of which have several stable valence states, it then becomes quite important to completely control sintering condition (especially atmosphere) to yield the desired properties.

Quite often, to attain proper ferrous iron (Fe^{2+}) content, a two-stage firing approach is employed. The sample is first sintered at a high temperature under a high partial pressure of oxygen (P_{O_2}). The high P_{O_2}(0.3–1.0 atmospheres O_2) is necessary to minimize the volatilization of zinc from the ceramic (a packing powder or shielding technique, as noted for the titanates, may also be used). In this portion of the firing cycle the densification and grain growth are essentially complete. Following this is an anneal step at lower temperature and lower oxygen partial pressure to establish the desired ferrous iron content. Typically, the firing cycle might appear as shown in Fig. 8.

However, if we translate the sintering path to a log P_{O_2} versus temperature graph we see quite different behavior (see Fig. 9). During the sintering portion of the cycle (if equilibrium is reached) the ferrite has a composition that would correspond to point S. At the end of the sintering cycle the temperature and atmosphere are reduced to the conditions corresponding to point A. When equilibrium has been reached, at point A the ferrite will have a different composition (e.g., we have had to cut across the isocomposition lines) which depends on the temperature and oxygen partial pressure. Further

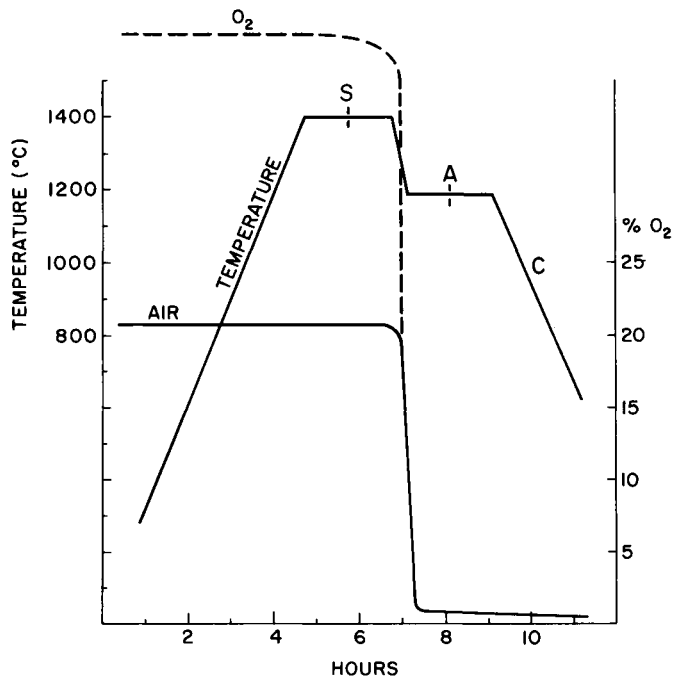

Fig. 8. Schematic firing cycle for manganese zinc ferrites.

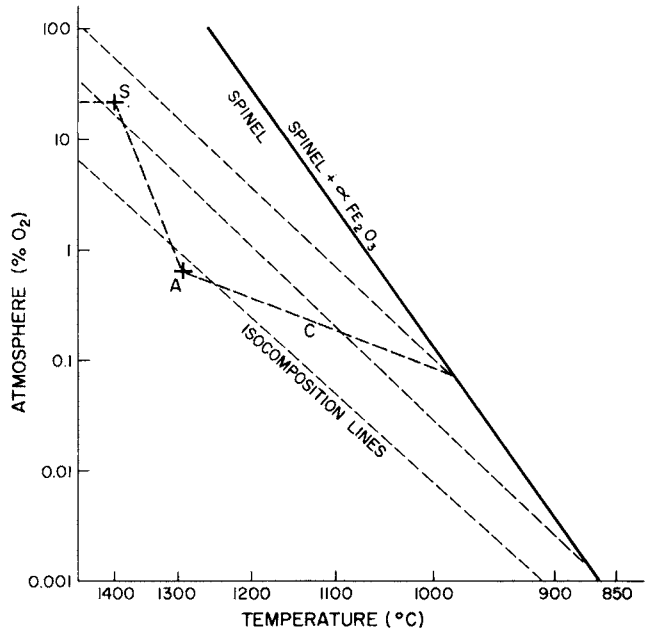

Fig. 9. Schematic representation of the stoichiometry path followed during the firing of manganese zinc ferrite.

cooling along line C results in additional compositional changes (if equilibrium is reached). In practice, however, at the cooling rates normally employed reoxidation of the ferrite is not too severe.

In theory a better approach would be to simultaneously vary the oxygen partial pressure (P_{O_2}) and the temperature to maintain the desired composition (in this example, a composition corresponding to A). Such control is not possible in commercial continuous kilns because a rather abrupt P_{O_2} step is created by blowing air or oxygen in from the front end and nitrogen from the exit and venting the furnace at or near the P_{O_2} discontinuity. It is possible, however, to make such a system work in a closed, periodic kiln or a small tube furnace lined with an impervious ceramic tube. Several techniques for the control of oxygen partial pressure have been reviewed by Paulus.

V. Hot Pressing

A discussion of the firing of electronic ceramics would not be complete without mention of the techniques of hot pressing. This technique employs

an external pressure allowing dense samples to be obtained at lower sintering temperatures (see Vasilos and Spriggs, 1967, for a review). As a consequence of the lower temperature the kinetics of grain growth are slowed and fully dense fine-grain-size materials may be obtained. Such materials are of interest because they have higher strengths (Monforte *et al.* 1971). This greatly improves wear in ferrite magnetic recording heads and enhances transparency in PLZT ceramics, to mention two specific applications.

The major limitation on hot pressing is die strength at elevated temperatures. The materials most commonly used for dies are graphite,* a high density alumina, or hot pressed silicon carbide.†

The ceramic to be hot pressed is often precompacted before being placed in the hot press die to get a reasonable green density. To minimize reaction with the die walls and punches, a layer of ZrO_2 or Al_2O_3 grain is placed around the sample. Typical pressing times are 0.5–4.0 hours at temperatures 1000°–1300°C and pressures of 2000–10,000 psi (138–689 bars).

Recently a novel "moldless" technique for hot pressing has been described by Hardtl (1975). In this approach no die is used and an inert gas is employed as an isostatic pressure medium. Because the working fluid is a gas it is necessary that the ceramic to be hot pressed be sintered first. This first sintering must yield a material having very little open or interconnected porosity. Otherwise the ceramic will be transparent at the working fluid (N_2 or argon) and no force will be transmitted to the part.

Hardtl's technique has been successfully applied to a variety of electronic ceramics including manganese zinc and nickel zinc ferrites, yttrium iron garnet, barium titanate, and others. The conditions were optimized for each specific material but are in the range of 1200°–1300°C, 50–220 bars, and 0.25–20 hours. In the case of barium titanate, theoretically dense ceramics were obtained after 1 hour at 120°C with a pressure of 200 bars (argon).

Although the samples employed were 5 × 5 × 15 mm, the size is only limited by the pressure vessel and the need to diffuse the porosity to an exterior surface. In addition, sample shape is not critical since the pressure is applied isostatically and the pressure vessel itself can be of rather simple construction. An additional benefit is the elimination of unwanted reactions between the sample and the die walls, which can be a problem in uniaxial hot pressing.

Other hot pressing methods investigated have been (1) high pressure isostatic hot pressing (Bush, 1971), (2) semicontinuous hot pressing in ceramic dies (Zehms and McClelland, 1963; Oudemans, 1968), and (3) encapsulation of porous ceramic compacts inside an impervious metal

*Poco Graphite, Inc., P.O. Box 2121, Decatur, Texas 76234.

†Ceralloy 146 Hot Pressing Dies, Ceradyne Inc., Chatsworth, California 91311.

envelope (Egerton and Bieling, 1968), but they involve more difficult engineering and processing problems.

VI. Summary

For general development work quite satisfactory results can be obtained using any of a variety of commercially available furnaces. The calcining reaction can be effectively carried out in a small box kiln in ceramic or platinum dishes. For drying of the powder/water/binder slurry prior to pressing a forced convection hot air oven should be adequate.

For close control of the sintering reaction, the use of a small diameter tube furnace (I.D. $\sim$ 75–100 mm) with an impervious mullite or alumina tube is recommended. If atmosphere control is desired, the tube may be closed at both ends with plates that have inlet and outlet holes. By construction of a suitable gas mixing train or using premixed gases it then becomes possible to maintain a dynamic atmosphere during the firing. If sintering is to be accomplished in air, removal of the end plates and the addition of inlet and outlet extensions and a simple rack and gear arrangement driven by a variable speed motor will allow operation in a semicontinuous fashion (see Fig. 10).

The thermal treatment of electronic ceramics includes not only the final densification but extends all the way back to the preparation of the starting oxides used as raw materials. Removal of the organic binders and lubricants used in dry pressing or tape casting should be controlled to prevent "blow holes" and cracks caused by the too rapid evolution of gases.

The sintering process should be carefully controlled with regard to heating rates, heat flux to the parts, time, temperature, and ambient atmosphere. Such control will allow the materials engineer to design microstructure, density, stoichiometry to suit the application.

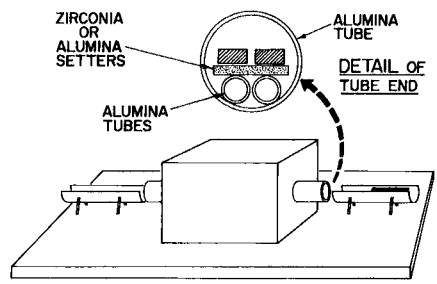

Fig. 10. Laboratory apparatus for semicontinuous sintering of ceramics.

The development of uniaxial and isostatic hot pressing permits the preparation of fully dense, fine grain ceramics. This has resulted in a new degree of freedom in designing specific materials properties and development of new applications for electronic ceramics.

References

Blank, J. M. (1961). *J. Appl. Phys.* **32**, Suppl., 378S.

Brown, L. M., and Mazdiyasni, K. S. (1972). *J. Amer. Ceram. Soc.* **55**, 541.

Bush, E. A. (1971). U.S. Patent 3,562,371.

Egerton, L., and Bieling, C. A. (1968). *Amer. Ceram. Soc., Bull.* **47**, 1151.

Ernst, W. G. (1966). *Amer. J. Sci.* **264**, 37.

Eugster, H. P., and Skippen, G. B. (1967). *Res. Geochem.* **2**, 492.

Haetling, G. H. (1963). *Amer. Ceram. Soc., Bull.* **42**, 679.

Haertling, G. H. (1966). *J. Amer. Ceram. Soc.* **49**, 113.

Hancock, K. R. (1970). *In* "Preparation of Ultra Fine Particles of Metal Oxides in Ultrafine-Grain Ceramics" (J. Burke, N. Reed, and V. Weiss, eds.), p. 39. Syracuse Univ. Press, Syracuse, New York.

Hardtl, K. H. (1975). *Amer. Ceram. Soc., Bull.* **54**, 201.

Johnson, D. L., and Cutler, I. B. (1963). *J. Amer. Ceram. Soc.* **46**, 541.

Johnson, D. W., Jr., Gallagher, P. K., Nitti, D. J., and Schrey, F. (1974). *Amer. Ceram. Soc., Bull.* **53**, 163–167.

Kuczynski, G. C., Abernethy, L., and Allan, J. (1959). *In* "Kinetics of High-Temperature Processes" (W. D. Kingery, ed.), pp. 163–172. MIT Press, Cambridge Massachusetts; *Ceram. Abstr.* p. 246i (1960).

Monforte, F. R., Chen, R., and Baba, P. D. (1971). *IEEE Trans. Magn.* p. 345.

Oudemans, G. J. (1968). *Philips Tech. Rev.* **29**, 25.

Paulus, M. (1972). *In* "Preparative Methods in Solid State Chemistry" (P. Hagenmüller, ed.), p. 487. Academic Press, New York.

Rase, D. E., and Roy, R. (1955). *J. Amer. Ceram. Soc.* **38**, 102–113.

Reijnen, P. L. J. (1968). *Sci. Ceram.* **4**.

Slick, P. I. (1971). *In* "A Thermograumetric Study of the Equilibrium Relations Between a MnZn Ferrite and an O_2–N_2 Atmosphere, in Ferrites," *Proc. Int. Conf.*, 1970, p. 81. Univ. of Tokyo Press, Tokyo.

Snow, G. S. (1973a). *J. Amer. Ceram. Soc.* **56**, 91.

Snow, G. S. (1973b). *J. Amer. Ceram. Soc.* **56**, 479.

Swallow, D., and Jordan, A. K. (1964). *Proc. Brit. Ceram. Soc.* **2**, 80–117.

Tien, T. Y., and Carlson, W. G. (1966). *J. Amer. Ceram. Soc.* **46**, 273.

van Groenou, Broese, A., Bongers, P. F., and Stuyts, A. L. (1968/1969). *Mater. Sci. Eng.* **3**, 317–392.

Vasilos, T., and Spriggs, R. M. (1967). *Proc. Brit. Ceram. Soc.* **3**, 195–221.

Zehms, E. H., and McClelland, J. D. (1963). *Amer. Ceram. Soc., Bull.* **42**, 10.

Ceramic Machining and Surface Finishing

PAUL F. BECHER

U.S. Naval Research Laboratory
Washington, D.C.

The realm of machining and surface finishing of ceramics has received renewed exploration as indicated by the work published in "The Science of Ceramic Machining and Surface Finishing" (Schneider and Rice, 1972). The actual mechanisms by which machining removes material from a ceramic body are not scientific curiosities, but, as will be discussed, have practical significance in the properties of the finished piece. We will review the research work with emphasis on abrasive processes which constitute the bulk of ceramic machining, not with the intent of covering all the studies (an impossibility), but to serve as a starting point for those interested.

I. Grinding

Rice (1975) discusses abrasive machining of ceramics, pointing out that single point diamond grinding experiments have aided in our understanding of how material is removed. Such studies by Imanaka *et al.* (1972) illustrate that chips are thrown out of the ceramic surface in front of, behind, and after the passage of the diamond grinding tool. Grinding force measurements by Gielisse and Stanislao (1972), Koepke and Stokes (1972), and Busch and

Prins (1972) show that the compressive force normal to the surface is much greater than that in the surface. As Gielisse and Stanislao (1972) point out, chip formation after the grinding point passes appears to occur by relaxation of the high compressive stress under the grinding point. This results in putting the ceramic surface in sufficient tension momentarily to cause further fracture.

Heat is generated in the ceramic surface during grinding but actual ceramic surface temperature measurements are difficult to assess. However, Gielisse *et al.* (1972) extimate surface temperature can exceed 1000°C for dry diamond grinding of a variety of hard ceramic bodies. It can be seen from this and the stresses generated that machining can involve not only the brittle fracture but also plastic deformation of the surface. As an example, alumina undergoes detectable plastic deformation in tension and compression tests at temperatures above 800°C and in hydrostatic constraint conditions with very high compressive stresses at room temperature (Bridgman, 1952).

Possible plastic deformation of the ceramic during the cutting action of abrasion are evidenced by the curved or twisted chips observed in rutile (Aghan and McPherson, 1973), sapphire (Ryshkewitch, 1960) and glass (Busch and Prins, 1972). Koepke (1972) also observed smearing of the ceramic along grinding grooves or striations. Direct evidence in the form of slip and twinning of plastic deformation (see Fig. 1) in the ceramic surface as a result of abrasive machining exists in many ceramics, ranging from MgO (Koepke and Stokes, 1970; Rice, 1973) to sapphire (Hockey, 1972a,b;

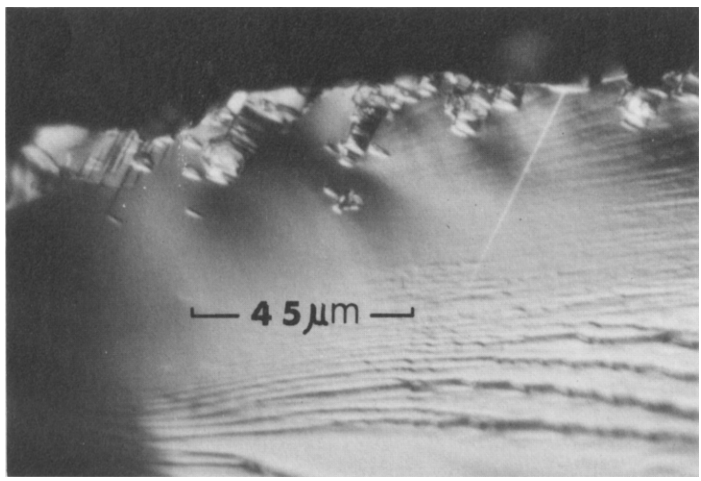

Fig. 1. Slip bands and twins generated in the subsurface of a sapphire crystal during wet surface grinding with a metal-bonded, 180-grit diamond wheel.

Becher, 1973). The depth of this plastically deformed layer increases with the softer (lower hardness) materials (Rice, 1975a), more severe abrasive action (Rice, 1975a; Becher, 1974), and is subject to the anisotropy of plastic deformation (Becher, 1974; Koepke, 1972) similar to wear behavior (Buckley, 1972).

Hockey (1972b) observed that thinning alumina samples containing this deformed layer results in sample bowing, suggesting high residual machining compressive stresses. Bernal and Koepke (1974) measured the residual machining stress on the surfaces of MgO crystals and found a tensile stress in the plastically deformed surface underneath this was a compressive stress (up to 2000–3000 psi) layer which was sometimes followed by another tensile stress region. They indicate that this residual stress pattern results from both heating and plastic deformation effects during grinding and show it is influenced by the type of grinding wheel used.

Besides chip formation, fracture of the ceramic during abrasive action results in cracks which extend into the body of the ceramic. Stickler and Booker (1963) show that the depth of cracks and plastic deformation in silicon crystals increases with coarseness of abrasive. Few such extensive studies exist; however, studies of fracture surfaces are being more frequently used to estimate machining flaw sizes (Rice, 1974). To study surface flaw sizes, artificial flaws can be introduced by microhardness indentations on the tensile surface of machined bend test specimens; here the artificial flaw size is proportional to the indent load. Wachtman (1972) used this technique to estimate surface flaw sizes by noting the indent load necessary to cause a loss in strength (i.e., here the indent flaw is just larger than the largest inherent flaw). Becher (1973) has used this technique, combined with fracture surface observations with sapphire crystals, and has shown that the surface flaw size from machining increases with coarser abrasive grit and severity of machining action. He also noted that annealing causes a decrease in this flaw size for a particular surface finish, indicative of the crack healing observed by Wiederhorn *et al.* (1973). These techniques are not a panacea for determining flaw size but do extend the limit of detection (down to $\sim 10\ \mu m$) of machining flaw sizes over that achieved with dye penetrant, X ray, or ultrasonic techniques.

Examination of machined or polished surfaces by etching is also useful. Holland (1966) points out that glass samples which appear to have flaw-free surfaces actually contain extensive crack patterns revealed by etching. This points out an important fact: although surfaces are given optical polishes and appear free of any flaws, they may still contain remnants of flaws from previous machining processes which are hidden by smeared or plastically deformed surface layers. As noted by Wachtman (1972) further knowledge of flaw sizes generated by various machining processes could serve as a guide to

how much material need be removed in subsequent finishing processes to minimize flaw sizes.

Gielisse *et al.* (1972) observed in single point grinding of alumina that increases in wheel speed decreased both the grinding forces and wear of the diamond cutting tool. They also note that the diamond wear increases with increases in the elastic modulus of the ceramic. Kim *et al.* (1973) showed that wear of alumina tool bits decreases by increasing the tool bit hardness and that wear is associated with plastic deformation of the tool bit. These observations suggest tool wear results when sufficiently high grinding forces are generated (as by decreasing wheel speeds) to cause plastic flow in the ceramic, possibly as a result of high friction forces and local heating.

Gielisse *et al.* (1972) found that both wear of the diamond tool and grinding forces also decreased for wet versus dry grinding of alumina. Westwood *et al.* (1973) observed that the use of alcohols instead of water as a cutting fluid increased the cutting rates during diamond drilling of alumina. The latter is suggested to result because dislocations in the ceramic are more mobile in the presence of alcohols. Buckley (1972) noted that water and other species adsorbed on the surface can decrease the coefficient of friction; but he also shows that they can increase the amount of plastic deformation in the surface during wear. It is seen that reducing friction between the tool and workpiece increases cutting efficiency as well as reducing wear on the tool. The role of increased plastic deformation in the ceramic workpiece in reducing wear of the abrasive or cutting tool and thus increasing machining rates requires further study but it is seen that cutting fluids can play an important role in machining efficiency.

II. Mechanical Polishing

Rice (1975) suggests that abrasive polishing can be thought of as an extension of grinding with a greater degree of plastic deformation occurring in the ceramic. Becher (1974) has shown that polishing has much less effect on surface hardness, indicating that polishing involves a much thinner surface region. As pointed out by Rabinowicz (1965), polishing of metals has been explained by melting of a surface layer or plastic deformation. He also suggests that polishing involves removal of surface molecules to create smooth surfaces. Plastic deformation of the surface during polishing of sapphire is evidenced by Schmidt and Davey (1972) and Hockey (1972a,b). However, as Rabinowicz (1965) notes, polishing of metals involves removal (weight loss) of material and any plastic deformation which only smears material from high to low surface regions would not cause a weight loss. Removal of surface

molecules would create a weight loss; however, the cutting action of abrasive particles may be important. Plastic deformation of the ceramic by the abrasive particles could result in a plowing action and extrusion of material from the ceramic similar to a plow cutting the surface of a field. Subsequent action could cut this "turned" material free, thus resulting in actual material removal. Agahan and McPherson (1973) observed something similar to this in sanding rutiles.

III. Nonabrasive Finishing

Nonabrasive techniques of material removal or polishing do involve a molecular removal mechanism. These include chemical polishing, ion beam, and laser beam techniques, although the latter can also employ melting and fracture or cracking of the ceramic workpiece.

The ease of machining of hard-fired alumina bodies can be enhanced by selective chemical leaching out of the glass phase in the surface; in fact they can be machined with a single point. After being shaped (by extruding, etc.), Vycor is subjected to leaching to remove the borosilicate phase and fired to form a high silica body.

Frechette (1964) noted several chemical and nonchemical techniques for "etching" ceramic microstructure; these also can be employed to obtain a more uniform polish. The use of flame and chemical polishing of ceramics is highlighted by the work of Mallinder and Proctor (1966) to obtain highly polished surfaces on sapphire rods. The development and use of many of these nonabrasive techniques are discussed in "The Science of Ceramic Machining and Surface Finishing" (Schneider and Rice, 1972). As they are rather specialized techniques and find fairly limited application to ceramics, as compared to abrasive machining, the interested reader is referred to the above volume as an excellent starting point.

IV. Surface Topography

The surface topography produced by abrasive finishing is a result of the various mechanisms of surface removal. Smeared or burnished regions are associated with plastic flow, while fracture via chipping and cracking results in a rough, almost lacelike, surface. In unidirectional grinding, grooves or stria can easily be observed also, and in most finer finishing operations (primarily mechanical polishes) these stria or scratches are related to the

abrasive particle size and form the greater portion of the surface roughness in polished surfaces. Characterization of surface topography (or roughness) is, of course, a function of the finishing process and is influential in the application of the ceramic. The latter is particularly evident in thin film substrates where topography affects the sharpness and properties of the thin film. A variety of techniques have been evolved for the purpose of describing surface topography, primarily in the area of substrate applications. Some of these are discussed by Berrin and Sundahl (1971) and Holland (1966).

V. Influence of Surface Finishing on Properties

Why is understanding any machining process important? Aside from the economic benefits that can be derived, the finishing process can influence the ceramic properties. As Stokes (1972) points out, the magnetic properties can be influenced by the surface flaws and residual stresses introduced during machining. He also reiterates the influence of surface finish on semiconductor devices, where surface defects from mechanical finishing are removed by chemical polishes because of their detrimental effects on charge carriers. Holland (1966) shows that the refractive index of the surface of glass can be raised by mechanical polishing. In infrared optics, surface character can increase the optical absorption, and Pastor and Braunstein (1973) indicate this to result from plastic deformation from cleaving new surfaces in alkali halides. Surface cracks and retained abrasives can contribute to scattering and absorption, and Deutsch and Rudko (1973) have shown that surface impurities, presumably introduced during polishing, cause absorption increases. The lowest optical absorption values obtained in these materials are achieved by a combination of chemical and mechanical polishing to minimize both surface contamination and damage (Davisson *et al.*, 1974).

Kirchener *et al.* (1968) and Rice (1974) have shown that fracture often originates from flaws. As illustrated by Griffith (1920), the fracture strength of brittle materials is controlled by the size of flaws. Removal of these flaws by flame polishing results in extremely high room temperature fracture strengths (1–5 % of the elastic modulus), as shown in glass (Holland, 1966) and in sapphire crytals (Mallinder and Proctor, 1966).

However, extension of such strengthening techniques to polycrystalline ceramics is difficult at best. As a result, surface treatments have been studied which would introduce surface compressive stresses, as in tempered glass. Kirchener *et al.* (1968) devised such techniques for polycrystalline alumina ceramics, and thus increased their tensile fracture strength by requiring

higher tensile stresses to cause surface flaws to propagate. As discussed earlier, grinding can result in a surface compressive layer also. Rice (1969, 1973) indicates that the flexure strength of CaO and MgO crystals are raised by extensive plastic deformation in their surfaces as a result of abrasive finishing.

In polycrystalline ceramics, the influence of machining on fracture strength is complex. Sedlacek *et al.* (1972) observed no effect of abrasive grit size of the grinding wheel on the fracture strength of alumina, while McKinney and Herbert (1970) observed a significant effect with lapped samples. This suggests that the type of finishing operation (grinding, which is essentially a unidirectional process, versus lapping, which is not) influences the effect on strength. Also, it is difficult to assess how microstructure (e.g., pores, grain size variations) entered into these conflicting results and points out the need for establishing causes of, or origins of, failure in such studies. Thus in materials where microstructural defects control strength, one would not expect to observe machining effects.

Typical ceramic data of strength versus $(\text{grain size})^{-1/2}$ exhibit an inflection point; one portion having a nonzero intercept, the other passing through zero, and Rice (1974) and Tresseler *et al.* (1974) observe that machining affects this behavior. What Tresseler *et al.* (1974) show is that the level of strength in the nonzero intercept portion of the curve decreases for coarser abrasion. Rice (1974) indicates that the inflection point occurs at a grain size equal to the size of the strength-controlling flaws, which is a constant for a particular material, abrasive process, and grinding direction. These findings indicate that the strength inflection should shift to higher strengths and finer grain sizes with better surface finishes. Thus it appears that machining flaw sizes are not controlled by the grain size of the ceramic, as previously indicated, but by the severity of the abrasive process.

Rice (1972) demonstrates that the grinding direction, as related to the applied tensile stress axis to which the ceramic (both single crystal and polycrystalline) will be subjected influences strength. Thus he found that grinding perpendicular to the tensile axis can lower the fracture strength as compared to grinding parallel to it. Marsh (1960) proposes that surface steps (e.g., grinding grooves) normal to the stress axis act as stress concentrations and lower the strength.

Becher (1976) has shown that the magnitude of this grinding direction–strength loss in sapphire crystals varies with the crystallographic orientation of the surface and the grinding direction. The grinding direction effect on strength appears to be minimized by the ease of plastic deformation occurring in the surface during grinding, which could cause either smearing or rounding of the grooves making them less effective stress concentrators or decrease subsurface cracking.

When plastic deformation occurs under applied stress conditions, the yield strength can be surface-finish sensitive. Stokes (1962) showed that the yield strength MgO crystals was raised by chemical polishing but could be lowered by damaging the surface by sprinkling it with abrasive particles. Polishing removes the easily activated surface dislocation sources, while sprinkling reintroduced them, and these act to supply the dislocations required for yielding. Firestone and Heuer (1973) showed that machining causes similar effects in the high temperature yield strength of sapphire crystals. Bertolotti and Scott (1971) observed also that the mechanical twins which lead to fracture in sapphire crystals appeared to be introduced during machining.

Although many studies are concerned with the effect of surface finish on elevated temperature strength of crystals (particularly filaments or whiskers for use in composites), only a few similar studies of polycrystalline ceramics are reported. From those studies considering machining effects it would appear that surface finish has little influence. However, properties such as the brittle-ductile temperature should be influenced by surface flaws even though crack healing can occur at elevated temperatures. Perhaps just describing the surface finish used in many of these studies would help.

VI. Summary

The processes of abrasive material removal from a ceramic involve local heating, fracture, and plastic deformation of the surface by the high stresses generated by the grinding or polishing action of the abrasive particles. Their relative roles are controlled by the severity of the abrasive process and the mechanical properties of the ceramic. However, much remains to be understood about the influence of grinding parameters before the abrasive machining phenomena can be adequately described. But we can see that the amount and extent of the damage introduced by machining tends to increase with coarser abrasive processes. The influence of machining on the properties of ceramics provides a portion of the necessary information required to its understanding. As discussed, studies of how machining affects fracture strength are beginning to generate information on the size of machining flaws.

ACKNOWLEDGMENTS

The author extends his appreciation to his colleagues, especially to R. W. Rice for making available some of the manuscripts prior to publication and for his many helpful discussions.

References

Aghan, R. L., and McPherson, R. (1973). *J. Amer. Ceram. Soc.* **56**, 46–47.

Becher, P. F. (1973). *Amer. Ceram. Soc., Bull.* **52**, 340 (abstr.)

Becher, P. F. (1974). *J. Amer. Ceram. Soc.* **57**, 108–109.

Becher, P. F. (1976). *J. Amer. Ceram. Soc.* **58** (in press).

Bernal, G. E., and Koepke, B. G. (1974). *J. Amer. Ceram. Soc.* **56**, 634–639.

Berrin, L., and Sundahl, R. C. (1971). *In* "Characterization of Ceramics" (L. L. Hench and R. W. Gould, eds.), pp. 583–624. Dekker, New York.

Bertolotti, R. L., and Scott, W. D. (1971). *J. Amer. Ceram. Soc.* **54**, 286–291.

Bridgman, P. W. (1952). "Studies in Large Plastic Flow and Fracture." McGraw-Hill, New York.

Buckley, D. H. (1972). *Amer. Ceram. Soc., Bull.* **31**, 884–905.

Busch, D. M., and Prins, J. F. (1972). *Nat. Bur. Stand. (U.S.), Spec. Publ.* **348**, 73–87.

Davisson, J. W., Hass, M., Klein, P. H., and Krulfeld, M. (1974). "High Energy Laser Windows," Semi-Ann. Rep. No. 3, ARPA Order 2031. U.S. Naval Research Laboratory, Washington, D.C.

Deutsch, T., and Rudko, R. I. (1973). *In* "High Power Infrared Laser Window Materials" (C. A. Pitha, ed.), Vol. I, pp. 201–221, AFCRL-TR-0372. AFCRL, Hanscom Field, Massachusetts.

Firestone, R. F., and Heuer, A. H. (1973). *J. Amer. Ceram. Soc.* **56**, 136–139.

Frechette, V. D. (1964). *Nat. Bur. Stand. (U.S.), Misc. Publ.* **257**, 15–28.

Gielisse, P. J., and Stanislao, J. (1972). *Nat. Bur. Stand. (U.S.), Spec. Publ.* **348**, 5–35.

Gielisse, P. J., Kim, T. J., Choudry, A., Short, J. F., and Tucker, E. J. (1972). "Force and Wear Analysis in Ceramic Processing," Final Tech. Rep., NASC Contract N00019-72-C-0202. University of Rhode Island, Kingston.

Griffith, A. A. (1920). *Phil. Trans. Roy. Soc. London, Ser. A* **221**, 163–198.

Hockey, B. J. (1972a). *Nat. Bur. Stand. (U.S.), Spec. Publ.* **348**, 333–339.

Hockey, B. J., (1972b). *Proc. Brit. Ceram. Soc.* **20**, 95–115.

Holland, L. (1966). "The Properties of Glass Surfaces." Chapman & Hall, London.

Imanaka, O., Fujino, S., and Mineta, S. (1972). *Nat. Bur. Stand. (U.S.), Spec. Publ.* **348**, 37–44.

Kim, C. H., Smith, W. C., Hasselman, D. P. H., and Kane, G. E. (1973). *J. Appl. Phys.* **44**, 5175–5176.

Kirchener, H. P., Gruver, R. M., and Walker, R. E. (1968). *Amer. Ceram. Soc., Bull.* **47**, 789–802.

Koepke, B. G. (1972). *Nat. Bur. Stand. (U.S.), Spec. Publ.* **348**, 317–332.

Koepke, B. G., and Stokes, R. J. (1970). *J. Mater. Sci.* **5**, 240–247.

Koepke, B. G., and Stokes, R. J. (1972). *J. Mater. Sci.* **7**, 385.

Mallinder, F. P., and Proctor, B. A. (1966). *Proc. Brit. Ceram. Soc.* **6**, 9–16.

McKinney, K. R., and Herbert, C. M. (1970). *J. Amer. Ceram. Soc.* **53**, 513–516.

Marsh, D. M. (1960). *Phil. Mag.* [8] **5**, 1197–1199.

Pastor, R. C., and Braunstein, M. (1973). "Halide Window Material Technology," Vol. II, Tech. Rep. AFWL-TR-72-152, Contract F29601-71-C-0101. Hughes Research Laboratory, Malibu, California.

Rabinowicz, E. (1965). *Sci Amer.* **218**, 91–99.

Rice, R. W. (1972). *Nat. Bur. Stand. (U.S.), Spec. Publ.* **348**, 365–376.

Rice, R. W. (1973). *J. Amer. Ceram. Soc.* **56**, 536–541.

Rice, R. W. (1974). *In* "Fracture Mechanics of Ceramics" (R. C. Bradt, D. P. H. Hasselman, and F. F. Lange, eds.), Vol. 1, pp. 323–345. Plenum, New York.

Rice, R. W. (1975). *In* "Ceramics for High Performance Applications" (L. J. Burke, A. E. Gorum, and R. N. Katz, eds.), pp. 287–343. Brook Hill Publ. Co., Chestnut Hill, Massachusetts.

Ryshkewitch, E. (1960). "Oxide Ceramics." Academic Press, New York.
Schmidt, W. A., and Davey, J. E. (1972). *Nat. Bur. Stand. (U.S.), Spec. Publ.* **348**, 259–264.
Schneider, S. J., and Rice, R. W., eds. (1972). "The Science of Ceramic Machining and Surface Finishing," *Nat. Bur. Stand. (U.S.), Spec. Publ.* No. 348. U.S. Govt. Printing Office, Washington, D.C.
Sedlacek, R., Halden, F. A., and Jorgensen, P. J. (1972). *Nat. Bur. Stand. (U.S.), Spec. Publ.* **348**, 391–398.
Stickler, R., and Booker, G. R. (1963). *Phil. Mag.* [8] **8**, 859–879.
Stokes, R. J. (1962). *Trans. AIME* **224**, 1227–1237.
Stokes, R. J. (1972). *Nat. Bur. Stand. (U.S.), Spec. Publ.* **348**, 343–352.
Tresseler, R. E., Largensiepen, R. A., and Bradt, R. C. (1974). *J. Amer. Ceram. Soc.* **57**, 226–227.
Wachtman, J. B. (1972). *In* "Mechanical Behavior of Materials," Vol. IV, pp. 432–442. *Soc. Mater. Sci.*, Kyoto, Japan.
Westwood, A. R. C., MacMillan, N. H., and Kalyoncu, R. S. (1973). *J. Amer. Ceram. Soc.* **56**, 258–262.
Wiederhorn, S. M., Hockey, B. J., and Roberts, D. E. (1973). *Phil. Mag.* [8] **28**, 783–795.

Surface Treatments

MINORU TOMOZAWA

Materials Division
Rensselaer Polytechnic Institute
Troy, New York

Mechanical strength is one of the most important engineering properties of ceramics, and its improvement would lead to vast expansion of the applicability of ceramics. In general, ceramics fail under tensile stress and the failure originates at a surface flaw. Therefore, the mechanical strength of ceramics can be substantially improved by placing the surface layer under compression. In fact, the modulus of rupture should be equal to the original strength plus the surface compressive stress developed.

There are several methods of producing a surface compression layer. Probably the best known technique is fast quenching or tempering as used in the manufacturing of strengthened glass. In addition, surface compression can be produced by chemical methods such as ion exchange as well as by surface coating. In this chapter, various surface treatments that produce the surface compression layer on ceramics will be reviewed. Strengthening methods of glass and glass-ceramics have previously been reviewed by many authors (Stookey, 1964; Ernsberger, 1966; Schroder and Gliemeroth, 1970; Doreumus, 1973).

I. Chemical Strengthening

The development of surface compression by changing the surface composition of ceramics is called chemical strengthening. It includes (a) ion

stuffing—exchange of large ions for small ions at relatively low temperature and (b) differential expansion—formation of a low thermal expansion layer at relatively high temperature. The latter can be attained by various methods such as surface crystallization and chemical reactions. Most methods were originally developed for glass but were found equally applicable for crystalline ceramics.

A. Ion Stuffing

When a ceramic specimen containing sodium ions is immersed in a fused salt containing potassium ions, some of the sodium ions in the surface layer of the ceramics are replaced by potassium ions. In general, the replacement of the small ions in the surface layer of ceramics with the large ions at relatively low temperature produces compressive stress in the surface. The situation is shown schematically in Fig. 1. This strengthening technique was first applied to glasses (Kistler, 1962; Nordberg *et al.*, 1964; Burggraaf and

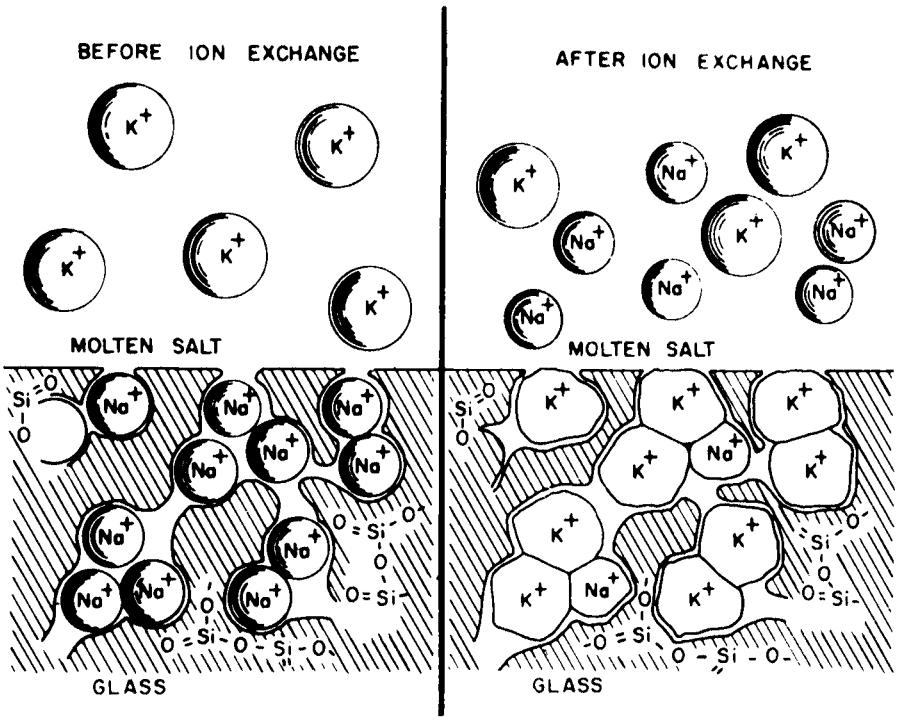

Fig. 1. Schematic representation of ion stuffing. (After Nordberg *et al.*, 1964.)

Cornelissen, 1964; Burggraaf, 1966; Spoor and Burggraaf, 1966; Ward *et al.*, 1965). Subsequently the method was extended to glass-ceramics (Karstetter and Voss, 1967; Duke *et al.*, 1967; Beall *et al.*, 1967). Exchanged ionic species included K^+ for Na^+, K^+ for Li^+, Na^+ for Li^+, as well as $2Li^+$ for Mg^{2+}. Recently the same technique was applied to glazed alumina (Platts *et al.*, 1970).

Application of this technique to conventional ceramics such as pottery does not seem promising since alkali impurities (e.g., K^+) in the main body of a ceramic diffuse into the glaze and smear out the concentration profile produced by surface ion exchange (Ruddesden and Airey, 1967).

One of the requirements in this method is the presence of fast moving ionic species such as alkali ions. The surface compressive stress produced by the ion exchange, and consequently the improvement in mechanical strength by this technique, is controlled by relative ionic size, concentration profile of exchanged ionic species, and stress relaxation.

The kinetics of ion exchange follows Fick's law of diffusion. However, since two exchanging ionic species with different sizes and consequently different diffusion coefficients are involved, the quantity called the interionic diffusion coefficient $\tilde{D}$ is used in diffusion equations. This is defined by

$$\tilde{D} = \frac{D_1 D_2}{N_1 D_1 + N_2 D_2} \tag{1}$$

where D_1, D_2 are the self-diffusion coefficient of the exchanging ions and N_1,N_2 are the corresponding mole fractions (Doremus, 1964).

The concentration profile of exchanged ions has been determined by many investigators and found to follow the solution of the diffusion equation,

$$C(x, t) = C_0 \operatorname{erfc}\left[\frac{x}{2(\tilde{D}t)^{1/2}}\right] \tag{2}$$

with a constant surface concentration C_0, where x is the distance from the surface of the specimen and t is the time of ion exchange treatment at a constant temperature. The interionic diffusion coefficient $\tilde{D}$ was found, in general, to be concentration dependent (Burggraaf and Cornelissen, 1964; Garfinkel, 1967).

Amount of exchanged ion Q is given by

$$Q = 2\, C_0\, (\tilde{D}t/\pi)^{1/2} \tag{3}$$

where $\tilde{D}$ is the value corresponding to C_0. Thus, $t^{1/2}$ dependency is expected even when $\tilde{D}$ is concentration dependent. In Fig. 2 the experimental results are shown, together with the mechanical strength of the specimens (Nordberg *et al.*, 1964).

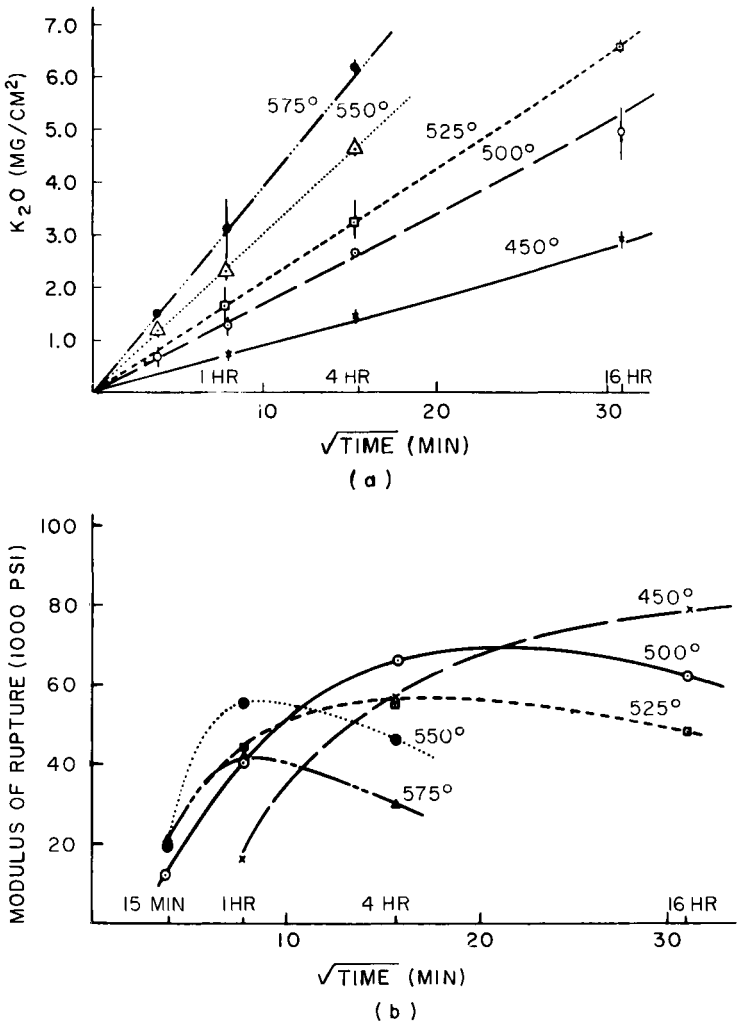

Fig. 2. (a) Rate of ion exchange in glasses with 25% Al_2O_3 and 16% Na_2O. (b) Effect of temperature on strength of a glass containing 25% Al_2O_3 and 16% Na_2O. Treatment: 150-grit abrasion. (After Nordberg *et al.*, 1964.)

The stress can be calculated from the concentration profile using the analogy to the thermal stress (Richmond *et al.*, 1964; Cooper and Krohn, 1969) if stress relaxation is absent. For a slab of thickness l, the stress σ is given, as a function of position and time, by (Timoshenko, 1934; Garfinkel and King, 1970)

$$\sigma(x, t) = -\frac{BEC}{1-\nu} + \frac{BE}{l(1-\nu)}\int_0^l Cdx \tag{4}$$

where E is Young's modulus, ν Poisson's ratio, and B the lattice dilation coefficient. The negative sign indicates the compressive stress. Here E and ν are assumed unaffected by ion exchange. The stress at the surface which controls the mechanical strength is given by

$$\sigma_s(0, t) = -\frac{BEC_0}{1-\nu} + \frac{BE}{l(1-\nu)}\int_0^l Cdx \tag{5}$$

For a thick specimen the second term of Eq. (5) is negligible. It is believed that small flaws exist on a surface of the ceramic specimen. In addition, specimens are often deliberately abraded to reduce the scatter of the mechanical strength data. In these cases, the compressive stress at the depth of flaws determines the amount of strengthening. The mechanical strength of the specimen then is expected to increase with the ion exchange treatment time, finally reaching the value corresponding to $BEC_0/1-\nu$. The time required to attain this value is determined by the interionic diffusion coefficient $\tilde{D}$. Addition of Al_2O_3 component to alkali silicate glasses is known to improve the efficiency of ion exchange strengthening (Nordberg *et al.*, 1964; Grosskupf and Scholze, 1970) and this is caused, at least partly, by the increase of $\tilde{D}$ with Al_2O_3 (Burggraaf and Cornelissen, 1964).

When the specimen is small, the second term of Eq. (5) becomes important, causing the reduction of the surface compressive stress and the corresponding reduction of the mechanical strength of the specimen after longer ion exchange treatment time (Cooper and Krohn, 1969). When the ion exchange treatment temperature is high, the stress relaxation becomes important, causing further reduction of the strength with treatment time (Burggraaf, 1966; Spoor and Burggraaf, 1966; Krohn, 1971).

The maximum strengthening attainable by this method is determined by the quantity $BEC_0/(1-\nu)$, as can be seen from Eq. (5). For a given ion exchange combination (e.g., K^+ for Na^+), B can be regarded as a constant. The only significant variable, therefore, is C_0, the concentration of the exchanged ion on the surface of the specimen.

The concentration of the exchanged ion on the specimen surface is governed by the thermodynamic equilibrium constant (Garfinkel, 1968). The equilibrium can be represented by

$$A^+(\text{fused salt}) + B^+(\text{ceramics}) \rightleftarrows A^+(\text{ceramics}) + B^+(\text{fused salt}).$$

Therefore the equilibrium constant is given by

$$K = \frac{\bar{a}_{A+} a_{B+}}{a_{A+} \bar{a}_{B+}} \tag{6}$$

where a_{A+}, a_{B+} are activities of A^+, B^+ ions in the fused salt, respectively, and $\bar{a}_{A+}$, $\bar{a}_{B+}$ are corresponding quantities in ceramics. The maximum attainable strengthening of the specimen is, therefore, determined by this constant K. Eisenman discussed this equilibrium constant in terms of the field strength of the anion sites in the specimen (Eisenman, 1962), and it is expected that the presence of Al_2O_3 in alkali silicate glasses increases this constant.

There is a possibility that the surface conditions of the specimen, especially hydroxide concentration on the surface, influences the ion exchange (Doremus, 1973). There is an opinion that this equilibrium constant K is primarily determined by the elastic energy which accompanies the ion exchange (Hale, 1968; Urnes, 1973). Application of an electric field is known to accelerate the ion exchange (Weber, 1965).

One drawback of the specimen strengthened by ion stuffing is the phenomenon of thermal fatigue, i.e., a decrease of mechanical strength observed when the strengthened specimen is reheated (Kerper and Scuderi, 1966; Garfinkel, 1967; Garfinkel and King, 1970). This is primarily caused by the rearrangement or interdiffusion of exchanged ions in the specimen. In terms of Eq. (5), the surface compressive stress is lowered by the decrease of the first term. Garfinkel showed that the process is described in terms of the product of the interionic diffusion coefficient and the time of reheat (Garfinkel, 1967). It is possible to suppress this phenomenon of thermal fatigue at a given temperature by selecting the combination of the exchanging ionic species (Ernsberger, 1973). However, in this case, the required time for the strengthening treatment will be longer since the same interionic diffusion coefficient controls both the strengthening and the thermal fatigue processes.

An additional contribution to the decrease of the strength may come from the viscous relaxation of the network (Kerper and Scuderi, 1966; Ernsberger, 1973), especially when the temperature is close to the glass transition temperature.

B. Differential Expansion

The formation of a low thermal expansion surface layer at a relatively high temperature will lead to a surface compressive layer upon cooling.

When a glass is involved, this can be attained by the surface crystallization (Stookey *et al.*, 1962; Olcott, 1963) as well as by chemical reactions (Douglas and Isard, 1949; Mochel *et al.*, 1966). For crystalline ceramics, chemical reactions are primarily used to produce the low thermal expansion layer.

The stress produced by a chemical reaction for a slab of ceramic can be calculated using an equation similar to Eq. (4) used for an ion exchanged specimen, provided Young's modulus and Poisson's ratio remain unchanged by the chemical reaction. In this case, instead of the lattice dilation coefficient B and concentration C, the strain due to the thermal expansion $\Delta T\alpha$ is used, where α is the linear thermal expansion coefficient and ΔT (<0) is the temperature range of cooling after the chemical reaction. When the reacted surface layer is thin compared with the thickness of the specimen, the surface compressive stress becomes

$$\sigma_s = \frac{E\,\Delta T}{1-\nu}\,(\alpha_{\text{original}} - \alpha_{\text{surface}}) \tag{7}$$

Kirchner and associates strengthened various ceramics using this technique. For example an Al_2O_3–Cr_2O_3 solid solution was produced on the surface of alumina by packing specimens in Cr_2O_3 powders and firing at various temperatures (Kirchner and Gruver, 1966; Kirchner *et al.*, 1967, 1968a, 1969). A similar solid solution was formed to strengthen other ceramics, eg., TiO_2–SnO_2 on TiO_2 (Kirchner and Gruver, 1966), and $MgO\cdot Al_2O_3$–$MgO\cdot Cr_2O_3$ on $MgO\cdot Al_2O_3$ (Kirchner *et al.*, 1967).

Al_2O_3–Cr_2O_3 solid solution has a lower thermal expansion coefficient than Al_2O_3 and this difference is believed to be the main factor causing the strengthening. In addition, the change in the thermal expansion anisotropy (difference in expansion coefficients of a and c axes) may contribute to the strengthening. There is a reversal in the sign of expansion anisotropy from the Al_2O_3-rich phase to the Cr_2O_3-rich phase, and a surface layer with little or no thermal expansion anisotropy may be formed by the chemical reaction. This should contribute to the strengthening since the formation of microcracks along grain boundaries is less likely with an isotropic phase (Merz *et al.*, 1962).

The TiO_2–SnO_2 phase has an appreciably lower thermal expansion coefficient than TiO_2 and a substantial strenghtening is expected from this difference in expansion coefficients. In this system, however, there is an miscibility gap that may reverse the trend (Padurow, 1956). In a glass system separation into two phases is known to reduce the mechanical strength, although the exact mechanism for it is not known (Utsumi *et al.*, 1970).

It has been reported that the prior etching of the specimen with hydrofluoric acid or the addition of halides to the packing materials further improves the strength of specimens. Fluoride is believed to remove intergranular material and increase the thickness of the solid solution layer (Kirchner *et al.*, 1967). In addition, it will probably remove hydroxyl ions on the surface of the specimen. On a glass surface a fluoride treatment is known to remove the hydroxyl group and produce the fluorine group, which is hydrophobic

(Elmer *et al.*, 1963; Doremus, 1973). The resulting surface has a drastically different reactivity.

Alumina has been strengthened by chemical reactions with other compounds such as CaO or SiO_2 (Kirchner *et al.*, 1971). In these cases, the volume of the product is greater than that of the alumina and this volume difference, in addition to the differential contraction, can lead to the additional surface compression.

It is possible that numerous other chemical reactions can produce a surface compression layer. However the reacting component has to be selected with the intended use of the specimen in mind. For example, a calcium aluminate surface layer on alumina is not appropriate when it is desired to retain the refractoriness of alumina.

II. Surface Coating

When a ceramic specimen is coated at high temperature with another ceramic (or glass) having a lower thermal expansion coefficient, a compressive stress is produced on the surface layer upon cooling. Glazes commonly used in the manufacturing of conventional ceramics serve this purpose, although glazes in general have various other functions as well: for example, (1) to make the body impermeable to liquid, and (2) to make attractive and readily cleanable surface (Parmelee, 1973). Cladding of glass with glass (Stookey, 1964; Krohn and Cooper, 1969), as well as laminar ceramics (Warshaw, 1957; Brubaker and Russell, 1967) employs the same principle.

In recent years glazing was used to strengthen glass-ceramics (Stookey, 1964; Duke *et al.*, 1968) as well as alumina (Kirchner *et al.*, 1968b, 1969). In addition, this technique has been combined with other techniques, for example, glazing and quenching (Kirchner *et al.*, 1968b) and glazing and ion exchange (Platts *et al.*, 1970) to further improve the mechanical strength of the specimen.

Glazes, that are silicate mixtures similar to silicate glasses, are normally mixed with water and applied on the specimen in the form of a slip. When water-soluble components such as alkali carbonates are involved, glazes are fritted in advance by melting the glass and crushing and milling it. The prime consideration in the glazing of ceramics for strengthening is the thermal expansion characteristic. An example of the adequate combination of the thermal expansion characteristics is shown in Fig. 3. When the thermal expansion coefficient of the glaze is excessively higher than that of the ceramic body, the glaze will develop minute fractures or crazing. On the other hand, if the thermal expansion coefficient of the glaze is excessively low

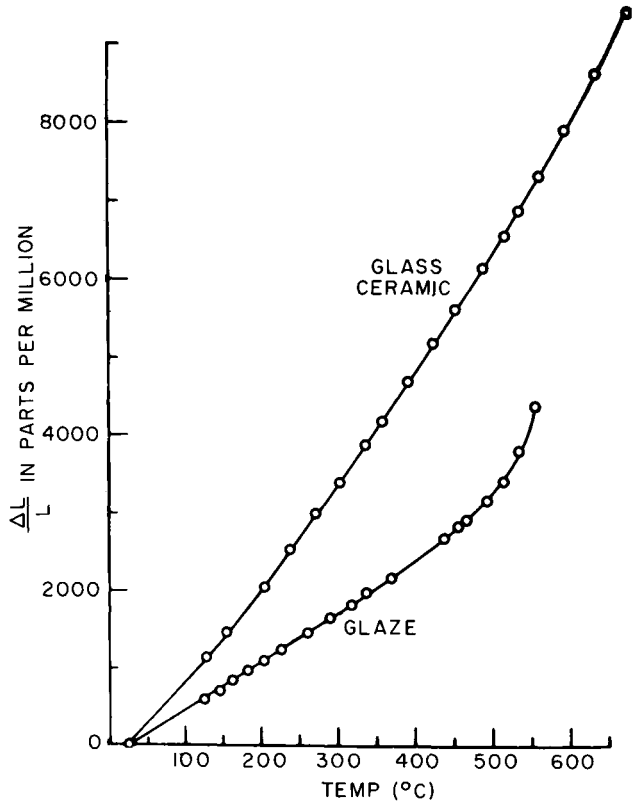

Fig. 3. Expansion curves of a representative glaze and glass-ceramic. (After Duke *et al.*, 1968.)

compared with that of the body a condition called shivering or peeling can take place. These defects are influenced by the reaction conditions of the glaze–body interface which in turn are influenced by the firing conditions. Thus the study of interface reaction is necessary (Scholze *et al.*, 1970; Roberts and Marshall, 1970). A method to produce a strong interlocking intermediate layer was suggested by Bopp *et al.* (1968).

Another important consideration in glazing is the wetting of glaze and body. In strengthening by surface coating it is desirable to have a thin and uniform glaze layer. Often a thin layer of glaze tends to crawl or break up. An expression for a critical thickness t_c below which the layers tend to break up is given by (Budworth, 1971)

$$t_c = \left[\frac{2\gamma_{LV}\,(1 - \cos\theta)}{\rho g}\right]^{1/2} \tag{8}$$

where γ_{LV} is the surface energy of glaze, θ is contact angle, ρ is density of glaze, and g is the acceleration due to gravity.

The surface compressive stress produced by the thin coating can be calculated using the same equation as in the chemical reaction. Namely,

$$\sigma_s = \frac{E \Delta T}{1 - \nu}(\alpha_{\text{body}} - \alpha_{\text{coating}}) \tag{7'}$$

where ΔT is the temperature difference between the setting point of the glaze and the temperature where the stress is measured. When the coating is not thin, a modification is necessary (Brubaker and Russell, 1967; Duke *et al.*, 1968; Krohn and Cooper, 1969).

One new development in this field is the use of the glass ceramics technique. Specifically, glazes are converted to glass ceramics, after application to a ceramic body, by controlled nucleation and growth of crystals (Parmelee, 1973; Kosiorek and Loughman, 1969; Wolf and Kosiorek, 1969; Martin, 1970). In this way the desirable characteristics of glass-ceramics such as high mechanical strength and refractoriness are added to the product. Along this line it would be desirable to develop high temperature glass-ceramics (Beall, 1971) to further improve the refractoriness of the glazed body.

Since most mechanical strength testing is distructive in nature, it is often desirable to be able to detect and measure the surface compressive stress produced. For transparent specimens such as glass or some of the glass-ceramics (e.g., Beall *et al.*, 1967), a convenient optical method based upon birefringence of the specimen is available. This method is not applicable for

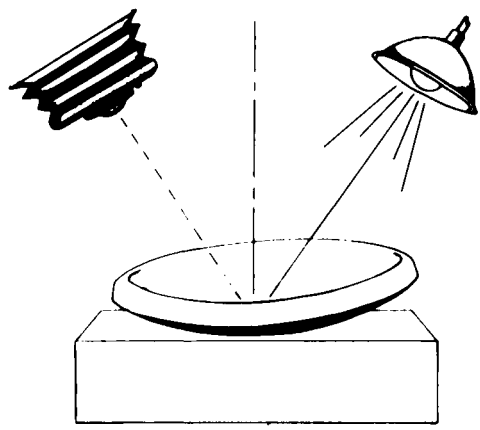

Fig. 4a. Setup for photographing Newton's rings. (After Kistler, 1962.)

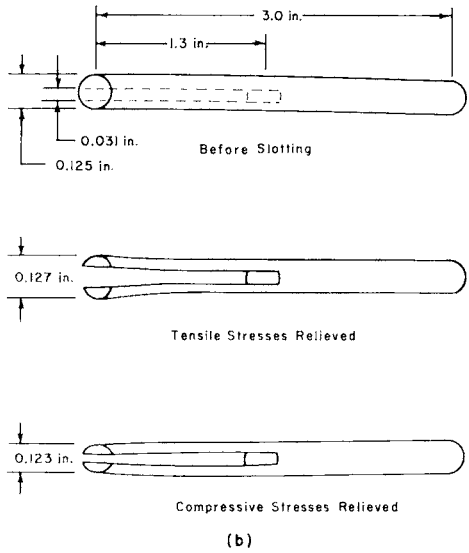

Fig. 4b. Rod test. (After Gruver and Kirchner, 1968.)

most ceramics and other means have to be sought. Methods based upon the deformation of the stressed specimen offer a practical solution. Two such methods are shown in Fig. 4a and b. One (Fig. 4a) shows the disk specimen, one side of which was ion exchanged (Kistler, 1962). The radius of curvature developed is measured by counting the number of Newton rings and is related to the surface stress through bending moment. The other (Fig. 4b)

TABLE I

COMPARISON OF STRENGTHENING BY VARIOUS METHODS

Materials	Process	% Strengthening	Reference
Glass-ceramics	Ion stuffing	500	Beall *et al.*, 1967
Glass-ceramics	Ion stuffing	800 ~ 2500	Duke *et al.*, 1967
Glazed alumina	Ion stuffing	80	Platts *et al.*, 1970
Alumina	Reaction with CaO	65	Kirchner *et al.*, 1971
Alumina	Reaction with Cr_2O_3	5–10	Kirchner *et al.*, 1967
Alumina	Leach and reactions with Cr_2O_3	25	Kirchner *et al.*, 1967
Alumina	Glaze	30	Kirchner *et al.*, 1968b
Alumina	Glaze and quench	75	Kirchner *et al.*, 1968b
Glass-ceramics	Glaze	400	Duke *et al.*, 1968

shows the rod specimen on the surface of which the stressed layer is created (Gruver and Kirchner, 1968). When a slot is cut on one side of the rod the ends will bend and from the direction and the magnitude of the bend, surface stress can be estimated (Gruver and Buessem, 1971).

Finally, various strengthening techniques described in this chapter are compared in Table I, in terms of percent strengthening. In general, the strength measurement shows a wide scattering because of the uncontrolled surface flaws. In addition, the strength of brittle materials is a function of loading time as well as atmosphere. The strengthened specimen is not an exception (Creyke, 1968, 1970). Thus the above table should be regarded as an "order of magnitude" comparison.

References

Beall, G. H. (1971). *In* "High Temperature Oxides" (A. M. Alper, ed.), Part IV, 15–36. Academic Press, New York.

Beall, G. H., Karstetter, B. R., and Ritter, H. L. (1967). *J. Amer. Ceram. Soc.* **50**, 181–190.

Bopp, H. F., Megles, J. E., and Morrisey, J. W. (1968). U.S. Patent 3,384,508.

Brubaker, B. D., and Russell, R., Jr. (1967). *Amer. Ceram. Soc., Bull.* **46**, 1194–1197.

Budworth, D. W. (1971). *Trans. J. Brit. Ceram. Soc.* **70**, 57–59.

Burggraaf, A. J. (1966). *Phys. Chem. Glasses* **7**, 169–172.

Burggraaf, A. J., and Cornelissen, J. (1964). *Phys. Chem. Glasses* **5**, 123–127.

Cooper, A. R., and Krohn, D. A. (1969). *J. Amer. Ceram. Soc.* **52**, 665–669.

Creyke, W. E. C. (1968). *Trans. Brit. Ceram. Soc.* **67**, 339–365.

Creyke, W. E. C. (1970). *Trans. Brit. Ceram. Soc.* **69**, 59–65.

Doremus, R. H. (1964). *J. Phys. Chem.* **68**, 2212–2218.

Doremus, R. H. (1973). "Glass Science." Wiley, New York.

Douglas, R. W., and Isard, J. O. (1949). *J. Soc. Glass Technol.* **33**, 289T–355T.

Duke, D. A., MacDowell, J. F., and Karstetter, B. R. (1967). *J. Amer. Ceram. Soc.* **50**, 67–74.

Duke, D. A., Megles, J. E., Jr., MacDowell, J. F., and Bopp, H. F. (1968). *J. Amer. Ceram. Soc.* **51**, 98–102.

Eisenman, C. (1962). *Biophys. J.* **2**, 259–323.

Elmer, T. H., Chapman, I. D., and Nordberg, M. E. (1963). *J. Phys. Chem.* **67**, 3219–3222.

Ernsberger, F. M. (1966). *Glass Ind.* **47**, 483–487 and 542–545.

Ernsberger, F. M. (1973). *Amer. Ceram. Soc., Bull.* **52**, 240–246.

Garfinkel, H. M. (1967). *In* "Symposium on the Surface of Glass and its Modern Treatments," pp. 165–180. Union Scientifique Continentale du Verre, Charleroiz, Belgium.

Garfinkel, H. M. (1968). *J. Phys. Chem.* **72**, 4175–4181.

Garfinkel, H. M., and King, C. B. (1970). *J. Amer. Ceram. Soc.* **53**, 686–691.

Grosskopf, H., and Scholze, H. (1970). *Ber. Deut. Keram. Ges.* **47**, 556–562.

Gruver, R. M., and Buessem, W. R. (1971). *Amer. Ceram. Soc., Bull.* **50**, 749–751.

Gruver, R. M., and Kirchner, H. P. (1968). *J. Amer. Ceram. Soc.* **51**, 232–233.

Hale, D. K. (1968). *Nature (London)* **217**, 115–118.

Karstetter, B. R., and Voss, R. O. (1967). *J. Amer. Ceram. Soc.* **50**, 133–137.

Kerper, M. J., and Scuderi, T. G. (1966). *J. Amer. Ceram. Soc.* **49**, 613–618.

Kirchner, H. P., and Gruver, R. M. (1966). *J. Amer. Ceram. Soc.* **49**, 330–333.

Kirchner, H. P., Gruver, R. M., and Walker, R. E. (1967). *J. Amer. Ceram. Soc. Soc.* **50**, 169–173.
Kirchner, H. P., Gruver, R. M., and Walker, R. E. (1968a). *J. Amer. Ceram. Soc.* **51**, 251–255.
Kirchner, H. P., Gruver, R. M., and Walker, R. E. (1968b). *Amer. Ceram. Soc., Bull.* **47**, 798–802.
Kirchner, H. P., Gruver, R. M., and Walker, R. E. (1969). *J. Appl. Phys.* **40**, 3445–3452.
Kirchner, H. P., Gruver, R. M., and Walker, R. E. (1971). *Trans. J. Brit. Ceram. Soc.* **70**, 215–219.
Kistler, S.S. (1962). *J. Amer. Ceram. Soc.* **45**, 59–68.
Kosiorek, R., and Loughman, J. I. (1969). U.S. Patent 3,463,647.
Krohn, D. A. (1971). *Glass. Technol.* **12**. 36–41.
Krohn, D. A., and Cooper, A. R. (1969). *J. Amer. Ceram. Soc.* **52**, 661–664.
Martin, F. W. (1970). U.S. Patent 3,488,216.
Merz, K. M., Brown, W. R., and Kirchner, H. P. (1962). *J. Amer. Ceram. Soc.* **45**, 531–536.
Mochel, E. L., Nordberg, M. E., and Elmer, T. H. (1966). *J. Amer. Ceram. Soc.* **49**, 585–589.
Nordberg, M. E., Mochel, E. L., Garfinkel, H. M., and Olcott, J. S. (1964). *J. Amer. Ceram. Soc.* **47**, 215–219.
Olcott, J. S. (1963). *Science* **140**, 1189–1193.
Padurow, N. N. (1956). *Naturwissenschaften* **43**, 395–396.
Parmelee, C. W. (1973). "Ceramic Glazes." Cahners, Boston, Massachusetts.
Platts, D. R., Kirchner, H. P., Gruver, R. M., and Walker, R. E. (1970). *J. Amer. Ceram. Soc.* **53**, 281.
Richmond, O., Leslie, W. C., and Wright, H. A. (1964). *ASM (Amer. Soc. Metals) Trans. Quart.* **57**, 294–300.
Roberts, W., and Marshall, K. (1970). *Trans. Brit. Ceram. Soc.* **69**, 221–241.
Ruddesden, S. N., and Airey, A. C. (1967). *Trans. Brit. Ceram. Soc.* **66**, 607–629.
Scholze, H., Müller, J., and Hildebrandt, U. (1970). *Ber. Deut. Keram. Ges.* **47**, 45–49.
Schroder, H., and Gliemeroth, G. (1970). *Naturwissenschaften* **57**, 533–541.
Spoor, W. J., and Burggraaf, A. J. (1966). *Phys. Chem. Glasses* **7**, 173–177.
Stookey, S. D. (1964). *In* "High-Strength Materials" (V. F. Zackay, ed.), pp. 669–681. Wiley, New York.
Stookey, S. D., Olcott, J. S., Garfinkel, H. M., and Rothermel, D. L. (1962). *Advan. Glass Technol. Tech. Pap. Int. Congr. Glass. 6th, 1962* Vol. 1, pp. 397–411.
Timoshenko, S. (1934). "Theory of Elasticity." McGraw-Hill, New York.
Urnes, S. (1973). *J. Amer. Ceram. Soc.* **56**, 514–517.
Utsumi, Y., Sakka, S., and Tashiro, M. (1970). *Glass. Technol.* **11**, 80–85.
Ward, J. B., Sugarman, B., and Symmers, C. (1965). *Glass Technol.* **6**, 90–97.
Warshaw, S. I. (1957). *Amer. Ceram. Soc., Bull.* **56**, 28–30.
Weber, N. (1965). U.S. Patent 3,218,220.
Wolf, W. F., and Kosiorek, R. (1969). U.S. Patent 3,428,466.

Mechanical Behavior

R. NATHAN KATZ and E. M. LENOE

Army Materials and Mechanics Research Center
Watertown, Massachusetts

I. Introduction

In the past, ceramic materials were chosen for a given application, primarily for their refractory, electronic, or magnetic behavior, with little regard to their mechanical properties. However, the pace of modern technology is such that the traditional utilization of ceramics in these roles is now often mechanical behavior-limited. Thus, the refractoriness which makes ceramics prime candidates for high temperature energy conversion systems (i.e., gas

turbines) is coupled with brittleness so that a rigorous definition of both stress state and mechanical properties are required for successful application. Similar, if less dramatic, examples can be drawn from the electronic (i.e., advanced radomes) or magnetic (i.e., cobalt-rare earth magnets) ceramic areas. Mechanical properties determinations are also important for quality control purposes and for fundamental materials science and process optimization studies.

The central fact of life with respect to the mechanical properties of ceramics is, "they are brittle." This brittleness imposes strict boundary conditions on both designing with and testing of ceramic materials. The brittleness of ceramics is also related to the generally encountered fracture and strength behavior associated with such materials, namely, extreme data scatter, size and surface dependence of strength, and extreme sensitivity to both distribution of stress and stress concentrations.

Since ceramics are often utilized in high temperature applications, it is important to realize that thermal as well as mechanical loading is frequently the cause of failure in ceramics.

The characteristic brittleness, coupled with high temperature service conditions, often in aggressive environments, makes mechanical properties measurements very difficult. Extremely precise and accurate instrumentation and well-constructed fixtures capable of long term survival in severe environments are required for mechanical characterization.

At the outset, it is important to realize that ceramic mechanical characterization methods have not reached the state of development where universal test standards are available. This situation is partly due to inherent scatter in properties, sensitivity to surface finish, and other factors that obstruct comparisons of test procedures and impede precise assessment of utility of the various specimen configurations.

Notwithstanding lack of universally accepted standard test methods, it is necessary to review the common test procedures and discuss their advantages and limitations.

This chapter will deal with the more common methods of mechanical property measurement for brittle materials. It is only a brief introduction to the subject and is certainly not a complete survey. Extensive review of this area has been made by Bortz and Burton (1969), Rudnick *et al.* (1968), and the National Materials Advisory Board (NMAB) (1968).

II. Volume and Surface Finish Effects

There are numerous difficulties in attempting to compare the mechanical behavior of ceramics. One often encountered source of such difficulty is the

presence of surface and volume effects. Even for a standard material such as alumina, these lead to a lack of inherent reproducibility. A study by Pears and Starrett (1966) of 28 tiles of hot pressed alumina revealed that the average strength varied from 22 to 48 ksi (22,000 psi to 48,000 psi) even though processing schedules supposedly remained the same. Different investigators have reported strength variations in hot pressed and fired alumina as much as 10 % from lot to lot. Such results have included data from different types and sizes of specimens, which further exaggerates variability.

One rationale to begin to explain such scatter relies on the observation that the strength of ceramics, as well as other brittle materials, is size or volume dependent.

To explain such effects, Weibull (1939) proposed that the probability of failure

$$P_f = 1 - \exp - \int_{vol} -(\sigma/\sigma_0)^m \, dV \tag{1}$$

where σ is the applied stress, σ_0 is the normalizing stress, and m is known as the Weibull Modulus. Experimental results confirming such a trend are shown in Fig. 1 where tensile strength data for alumina of differing test volumes are compared. The average strength of the smaller-volume specimens (0.031 in.^{3}) was 43 ksi and that of the larger volume (0.63 in.^{3}) was 29,800. In addition to the experimental results, the figure also indicates the predicted strengths based on a Weibull representation for each particular set of data and attempts to estimate the strength of larger or smaller volumes.

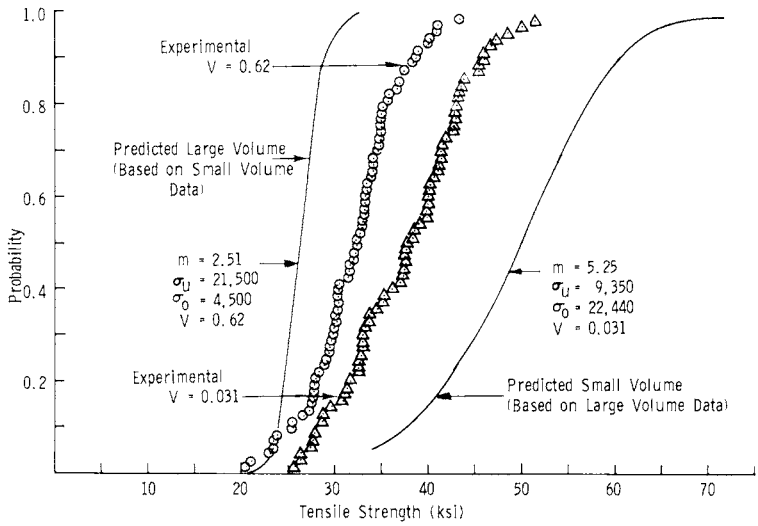

Fig. 1. Probability distributions of strength for different volumes, Al_2O_3. After Pears and Starrett (1966).

It is interesting to observe that the predicted large volume strength distribution function, based on small volume data, is conservative whereas the converse is not true; the small volume distribution predictions based on large volume experiments were overly optimistic. Such conservative predictions based on Weibull statistics predictions have also been observed when comparing predicted burst strength of spinning disks, based on small bend specimens, compared to actual disk burst strength, for hot pressed silicon nitride.

The Weibull theory has limitations since it assumes homogeneous defects, neglects interaction of neighboring flaws, does not otherwise account for their location, and takes a single critical flaw as being sufficient to initiate brittle failure. Current developments seek to account for more accurate description of microstructural details including the nature, orientation, and location of microcracks and voids. The reader is referred to the works of Fisher and Holloman (1947), Freudenthal (1968), McClintock (1974), and Batdorf and Crose (1974). Nothwithstanding limitations of Weibull strength distributions, they are useful in establishing guidelines for the size dependence of the strength of ceramics.

In addition to the size or volume effect the measured strength of ceramics is a function of surface finish. Therefore, when carrying out a mechanical property determination on a ceramic material, extreme care should be exercised in surface preparation. Being brittle materials, they cannot relieve surface stress concentrations due to finishing by plastic deformation. As a result the direction of grinding and lapping can have a large influence on the strength of ceramics. For example, modulus of rupture and tensile bars of silicon nitride have been found to have 50% greater strength when grinding is done parallel rather than perpendicular to the major tensile axis.

The effects of surface finish and condition on strength have been reviewed recently by Rice (1974). Baratta *et al.* (1974) have used a fracture mechanics basis for estimating the upper bound of the surface finish below which there is no stress concentration effect. An important result of this study is that test samples of different geometry may require different surface finishes if one is to be sure that bulk and not surface controlled strength is being measured.

Perhaps the most important concept to keep in mind when comparing strength data from various sources is that the methods of machining and surface preparation can be as important as microstructure and chemistry. Therefore, one should not compare strength data without detailed knowledge of surface preparation. Unfortunately, such data are often not reported.

Both size and surface finish effects must be taken into account to properly interpret the measured mechanical properties of ceramics. From the above discussion it is evident that in any mechanical property determination program it is important to replicate as nearly as possible the volume of the ceramic

under load, the manner of loading, and the surface finish. Since it is not always possible to do extensive tests of large volumes, subscale tests can be assumed to give conservative predictions if Weibull statistics are used. However, it is always prudent to conduct some confirmatory full size testing.

III. Elastic Modulus

For linear elastic materials the stress σ is related to the strain ε by Young's modulus E,

$$\sigma = E\varepsilon \tag{2}$$

Stress along the length of a specimen undergoing elastic deformation, will produce a simultaneous change in the cross section normal to the stress. The relationship between the dimensional changes parallel and normal to the applied stress direction is given by Poisson's ratio v

$$v = \frac{\Delta d/d}{\Delta l/l} \tag{3}$$

where d is the specimen width dimension and l is the length parallel to the applied stress. Typically v ranges from 0.2 to 0.3 for elastic deformation, but is not confined to these values. E is the most commonly measured elastic constant of ceramic materials. For single crystals (even in the cubic system) E is a function of crystal orientation, and the elastic moduli are given as a matrix in terms of crystal orientation (Nye, 1964). Polycrystalline ceramics with random grain orientation or amorphous ceramics (glasses) will be isotropic with respect to Young's modulus. In polycrystalline ceramics with microstructural texturing, E will vary with orientation.

To measure Young's modulus one can use direct measurement of both stress and strain and then obtain E by Eq. (2). Stress is readily obtainable from load and specimen geometry. Strain is more difficult to measure, especially since ceramic test specimens do not readily lend themselves to simple displacement measurements, which are often quite inaccurate over the small deflection range normally encountered in a typical test. For accurate measurement of strain at room temperature to moderate temperatures (the upper temperature is limited by available adhesives) electrical resistance strain gages are commonly used. Such gages are available in the small sizes (less than 1/4 in. square) often required on ceramic test samples, which are themselves often small. Although some literature exists in this area, the best

sources of current information and applications are the strain gage manufacturers or their representatives.

Young's modulus may also be determined by resonance (vibration) tests and ultrasonic techniques (Seaton, 1974; Schreiber and Anderson, 1966). Vibration techniques require determination of the resonant frequencies of rather large (typically 3 in. long by $\frac{1}{4}$ in. $\times$ $\frac{1}{4}$ in. cross section) prisms or rods. If this method is used, care must be taken to be sure the sonic resonance utilized in obtaining E does not result in strength degradation, if one plans to utilize the same specimens for the determination of E and strength. Seaton and Katz (1972, 1973) have demonstrated such "sonic fatigue" in several ceramics. By contrast, ultrasonic techniques can utilize small specimens and require measurement of only the bulk density and the longitudinal and shear sound wave velocities (Schreiber and Anderson, 1966). Poisson's ratio can also be obtained from these data.

Sonic or ultrasonic methods most generally assume an isotropic body, then

$$E = \frac{G}{2(1 + \nu)} \tag{4}$$

where G is the shear modulus. To obtain E, a longitudinal wave is sent the length of a specimen and its velocity (v_l) is measured. The appropriate relationship is:

$$v_l = (E/\rho)^{1/2} \tag{5}$$

where ρ is the materials density. Similarly, to obtain G an appropriately oriented piezoelectric transducer pulses a shear wave through the specimen, then

$$v_s = \sqrt{G/\rho} \tag{6}$$

where v_s is the shear wave velocity. Knowing E and G, one obtains ν from Eq. (4).

IV. Hardness

Hardness is a key parameter in the choice of ceramics for abrasives, tool bits, bearings, wear resistant coatings, and resistance to particulate erosion and ballistic impact. Hardness, generally correlates with melting temperature

(Van Vlack, 1964), with both micro- and macroplastic behavior (Rice, 1971) and with the effect (Rice, 1972) and ease (Westwood and Latanision, 1972) of machining. Although the selection of a material is almost never made on the basis of hardness alone (since most correlations of properties or behavior with hardness are generally qualitative rather than quantitative), the hardness measurement is one of the most useful of all mechanical measurements in ceramic research. The measurement is simple and requires a very small piece of material. Often, the only mechanical property that can be obtained on a small laboratory specimen is hardness.

Hardness can be defined and measured many ways. The two most commonly encountered by ceramists are scratch hardness (Mohs hardness numbers) and indentation hardness (Knoop or Vickers hardness numbers). These numbers are compared in Table I. The determination of the Mohs hardness number is quite simple. One merely determines which substances in Table I will be scratched by the unknown and which will not. For example, if the unknown will scratch topaz but not corundum, its Moh's hardness lies between 8 and 9. Indentation hardness is measured on a microhardness tester equipped with a Knoop elongated diamond pyramidal indentor or a Vickers square cross-sectioned diamond pyramidal indentor. The force required to produce a residual indentation of a given projected area (kg/mm^2) is the hardness. The indentation method of measuring hardness is more precise than the Mohs scale and it can be related to the plastic behavior of the material (Rice, 1971).

TABLE I

HARDNESS SCALES

Material	Mohs hardness number	Knoop hardness (approximate) (kg/mm^2)
Talc $(Mg_3Si_4O_{10})(OH)_2$	1	20
Rock salt (NaCl)	2	35
Calcite ($CaCo_3$)	3	135
Fluorite (CaF_2)	4	180
Apatite ($Ca_5P_3O_{12}F$)	5	450
Feldspar ($KAlSi_3O_8$)	6	600
Quartz (SiO_2)	7	1000
Topaz ($SiAl_2F_2O_4$)	8	1500
Corundum (Al_2O_3)	9	2000
Titanium carbide (TiC)	9 +	2800
Boron carbide (B_4C)	9 +	3500
Diamond (C)	10	7000–8000

V. Tensile Strength

A. Direct Methods

Determination of tensile strength involves subjecting a specimen to a uniform, uniaxial stress state, and gradually increasing the stress until failure occurs. Tensile strength at fracture is defined as

$$\sigma = P/A \tag{7}$$

where σ is the stress, P is the load, and A is the cross-sectional area at the fracture. Load versus deflection behavior is recorded and the local strain across the middle portion of a tapered specimen may also be recorded either via a mechanical extensometer or by means of strain gages. In this way the stress–strain behavior of the ceramic is determined.

There are a number of practical considerations that ought to be mentioned concerning this test method. Due to difficulties in machining ceramics, considerable care is required to achieve concentric specimens. Regardless of the type of grips used to load the specimen, unsymmetrical displacements in the contact zones, as well as stress concentration sensitivity of ceramics, become problematical as far as eliminating extraneous effects which would tend to increase data scatter.

Efforts to cope with such problems include use of strain gages at diametrically opposite positions at the specimen centerline. The strain signals are used to carefully adjust grips so as to minimize parasitic bending stresses. Note the magnitude of stresses arising from uncontrolled eccentricity can be a large percentage of the strength of the material. The increase in stress will be a function of the eccentricity/width ratio. Weil and Daniels (1962) demonstrated that for square cross sections the stress increase is eight times the ratio, and for round configurations it will be six times the ratio.

Notwithstanding the use of strain gage alignment procedures and precision machining of specimens, most experimental data include a high percentage of specimen failure patterns suggestive of eccentricity effects. Checking specimen alignment at temperatures beyond strain gage capabilities becomes an extremely challenging task. A number of test methods have evolved to cope with these problems. The gas bearing system shown in Fig. 2 attempts to minimize eccentricity and provide the necessary well-defined uniaxial stress field. The primary components are large gas bearings at each end of the specimen, the load frame, mechanical drive system, furnace, optical-strain analyzers, and instrumentation for measurement of load and strain. The load-train assembly is statically balanced and fabricated to insure overall alignment within about 0.001 in. throughout the apparatus. Strain measurement consists of optically measuring elongation between two flags or targets which are mounted on the specimen and separated by a predetermined gage length. Image displacements are recorded electromechanically and the

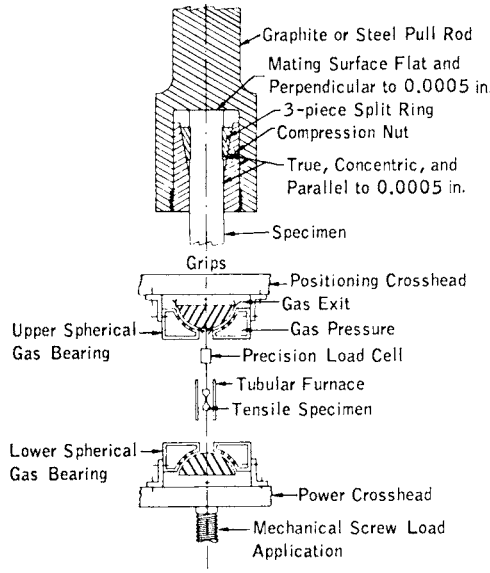

Fig. 2. Schematic of gas bearing apparatus for tension test. After Pears and Starrett (1966).

precision of the strain measurement is to 0.00002 in. Typically the parasitic eccentricity stresses are reduced to about 0.1 % of the strength.

An alternate and inexpensive procedure, suitable for room temperature tests, was developed by Baratta *et al.* (1974). In this scheme a circular, contoured tension specimen is precisely machined to fit within a confining cylinder. The ends of the specimen are sealed with "O"-rings and the interior of the cylinder is pressurized until tensile fracture of the sample is achieved. Since the tension bar rides on the ring seals and is subjected to hydrostatic pressure, the system is largely self-aligning. Proper choice of the ratio of specimen-end area to gage cross-section area minimizes the required hydrostatic pressure and a near-to-uniaxial stress state can be achieved.*

B. Indirect Methods

A number of techniques have evolved wherein the stress state approximates a uniform tension field over portions of the specimen (Bortz and Wade, 1967). In general, these methods rely on more detailed stress analysis of the configuration than do direct methods. As the behavior of the ceramic

*Note Added in Proof: In order to eliminate or reduce specimen eccentricity at elevated temperatures, F. F. Lange (1975, personal communication) has demonstrated the use of appropriate powders such as BN, graphite, WSe_2, etc. in the shoulder bearing portion of the specimen grips. The powder serves to more effectively distribute loads, thereby reducing stress concentrations. Furthermore, the powder flows at high temperatures and approximated hydrostatic pressure to improve concentricity.

tends toward nonlinear stress strain response, these more refined analyses also become inapplicable. Thus the interpretation of the data becomes more unreliable. Therefore, use of these configurations should be restricted to lower temperatures and for materials that retain linear elastic materials characteristics over the range of test conditions. Otherwise even more complex stress analysis techniques must be used in data interpretation.

Ideally tensile strength ought to be measured in a specimen subjected to a simple uniaxial stress state. For the conventional tension test this is approximated by properly contouring the configuration. Indirect tension test methods attempt to achieve this uniform stress condition by other geometric modifications.

1. Thin-Walled Ring

In this experiment a short length, thin-walled ring is subjected to a uniform internal pressure by means of a pressurized balloon, confined within the ring and between massive end plates. Failure stress is ordinarily calculated according to the strength of materials formula

$$\sigma = Pd/t \tag{8}$$

where d is the average diameter in inches, t is the wall thickness in inches, and P is the internal pressure at failure (psi).

This elementary formula is appropriate for thin rings where the radius to wall thickness ratio is ten or greater. Use of strain gage instrumentation on the ring permits measurement of stress–strain behavior and computation of Young's modulus, Poisson's ratio, and ultimate failure strain. This method is obviously ideally suited for ceramic bodies that are naturally produced in cylindrical configurations.

It is worth noting several important features of this test procedure. First, the specimen must be precisely machined to obtain a truly concentric cylinder. Second, since the specimen usually has a relatively high surface area compared to conventional uniaxial tension tests, specimen surface preparation is exceedingly important. Finally, the ring ordinarily shatters into many segments, and it is difficult to systematically investigate fracture features. This difficulty is overcome by surrounding the sample with an energy absorbing material whose purpose is to capture and retain ring fragments to prevent further shattering. For some high strength ceramics, these attempts are not successful and a large percentage of potential fractographic information is lost. An interesting feature of the room temperature experiment is that the expanding balloon often retains an impression of the first crack, and this information can prove useful in reconstructing the ring fracture sequence.

2. Flexure Tests

In this method, a beam of rectangular or circular cross section is subjected to three or four point loads which are gradually increased until fracture occurs. The equations of simple beam flexure are employed to interpret the data. By use of appropriate instrumentation, it is possible to obtain bending strength (commonly termed modulus of rupture) as well as Young's modulus and Poisson's ratio. In principle it is possible to choose a span-to-depth ratio such that the stress state is rather closely approximated by beam theory. In practice, in order to conserve material, or due to lack of billets of sufficient size, relatively small specimens and small span-to-depth ratios are used. Naturally this violates assumptions of the elementary theories that are ordinarily applied. In reality, the material is subjected to complex stress states and gradients. This leads, for instance, to considerable variation in reported properties, depending on specimen dimensions and loading configurations. Different average strengths are observed, for instance, by using three- versus four-point loads (15–20 % higher in three- versus four-point loads). Flexure tests also generally result in considerably higher nominal tensile strengths than can be attained in a true tension test (often by a factor of two for typical geometries). This method should therefore not be used to obtain design information. Furthermore, it should be restricted to use, particularly when using simple beam theories, to temperature ranges where tension and compression modulus are similar, and where small deflections occur at failure.

The simple beam formulas are: (a) For four-point flexure with a beam of length l, width b, and depth h, and for loads at $l/3$, using a linear stress distribution across the specimen, the modulus of rupture (MOR) is:

$$\sigma_B = Pl/bh^2 \tag{9}$$

with P = total load at failure. (b) For center load, and three-point flexure, the modulus of rupture (MOR) is:

$$\sigma_B = 3Pl/2bh^2 \tag{10}$$

3. Theta Ring, Trussed Beam, and Diametral Compression Disk

Motivated by a desire to use compressive forces to induce tensile failures, as well as the necessity to study surface area and volume effects, engineers have devised a number of ingenious indirect tension tests. These include the theta ring (Fig. 3a), the trussed beam (Fig. 3b), and diametral compression disk (Fig. 3c). The methods are plagued by the common problem of precise machining of difficult-to-machine materials.

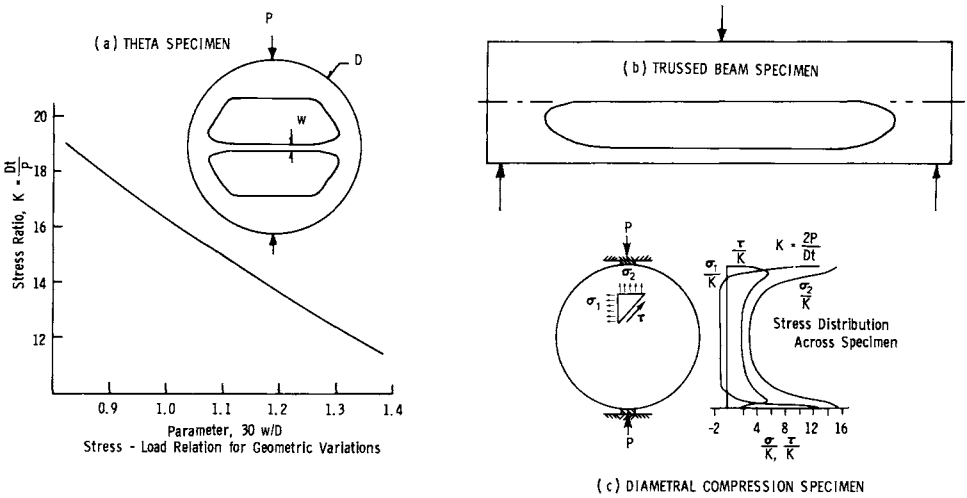

Fig. 3. Typical indirect tension test specimens: (a) theta specimen, (b) trussed beam, and (c) diametral compression.

The theta ring failure stress in the central bar is calculated from the simple formula

$$\sigma = KP/dt \tag{11}$$

where P is the applied load in pounds, d is the diameter in inches, and t is the specimen thickness, and the appropriate value of K is shown in Fig. 3a. The trussed beam uses center-point flexural loading which results in bending stresses through the heavier beam segment and approximates a uniform tensile field throughout most of the length of the thinner segment.

Loading configuration is an important factor in the diametral compression disk (see Fig. 3c). The stress distribution should be independent of length, provided a uniform compression stress is applied. However, friction stress, as well as nonuniform stresses, ordinarily result at contact points.

The simple theory describing the stress distribution under a uniform diametral load on a disk-shaped specimen predicts a uniform tension field at the center of the disk:

$$\sigma = 2P/\pi Dt \tag{12}$$

where P is the applied load in pounds, D is the disk diameter in inches, and t is the thickness of disk in inches. The stress field in the transverse direction is highly dependent on the width of load application and becomes highly

compressive. The disk test has therefore been used to attempt to study biaxial stress failure response.

VI. Other Stress States

A. Compression

In principle the compression test is merely a reversed tension experiment. However, other factors, such as prevention of overall buckling and minimization of parasitic column (eccentricity) stresses, are of prime importance. Compressive strength of ceramics is ordinarily much larger than tensile strength, and therefore a sturdier load train and bearing fixture is required. These factors compound the difficulty of performing an acceptable compression experiment.

Several types of specimens have been used: straight-sided short cylinders or rectangular geometries and tapered or dumbbell-type specimens. The first type is usually confined to low temperatures and efforts are made to reduce end friction by use of grease and/or bearing materials with low coefficients of friction. Needless to say, the efforts are only partially successful with the result that conservative, low compression strengths are measured. In the second type, precision alignment and universal joints are used to minimize eccentric parasitic stresses. The buckling load P_{cr} which determines specimen gage length for the condition of a column free to rotate is

$$P_{cr} = \frac{\pi^2 EI}{l^2} = \text{buckling load}, \tag{13}$$

where I is the moment of inertia of cross section, E is the modulus, and l is the overall length.

Failure must occur by compression rather than at a critical buckling load and a geometry must be selected which insures failure at loads much less than P_{cr}.

B. Shear

The torsion test provides a measure of shear modulus but can be unacceptable for measurement of ultimate shear strength since fracture usually occurs in a tensile mode for this geometry. Various forms of notched tension specimens have been used to attempt to measure shear strength. These notches are made from each side of the specimen so that in theory along the centerline

a segment of the material is subjected to pure shear. Photoelastic and theoretical stress analysis has been applied to choose notch geometries which approximate pure shear; however, these are only grossly correct and become less useful at elevated temperatures as the idealizations of linear elasticity become decreasingly applicable (see Chen, 1966).

C. Combined Stresses

In truth there is no universally accepted procedure to determine failure under combined tension, compression, and shear stresses. No universal failure theory has yet immerged that satisfactorily correlates the available multiaxial stress fracture data. This state of affairs is not for lack of trying—many configurations have been used, including the diametrical compression of disks and flexure of thin circular plates that introduce biaxial stress fields.

One of the most commonly used geometries is a straight-sided thin-walled cylinder that can be subjected to internal or external pressure as well as axial load. A tapered thin-walled tube can be used for axial tension, compression, or torque in conjunction with internal or external pressure. Both detailed analysis and complex specimen preparation are entailed and the study of combined stress behavior is best left to specialists in the field of materials characterization.

VII. Shock Effects

A. Mechanical

Ceramic materials can be exposed to shock loading via the imposition of mechanical or thermal stresses. Mechanical shock loading of sufficient severity to cause shock waves in the material is not normally carried out in the laboratory. Such data which can be important in analyzing ballistic or geologic behavior of brittle materials have recently been reviewed (Burke and Weiss, 1971) and will not be discussed here. Milder shock, or rather impact loading, is of interest for structural uses of ceramics, for example, particulate erosion resistance of gas turbine materials (Metcalfe, 1974). Impact tests are also used to measure the energy required to fracture ceramics (Acquaviva, 1971a). In spite of these examples the interpretation of impact studies on ceramics and their relationship to service performance are not well understood and therefore little used.

B. Thermal

Rapid thermal loading, referred to as thermal shock, is an important failure mechanism in ceramic components such as spark plug insulators,

radomes, turbine components, and refractories. In contrast to the relative lack of an analytic basis for mechanical impact testing, thermal shock testing of ceramics is based on better analytical treatments (Hasselman, 1969; Seaton, 1974; Nakayama, 1974).

Experimental methods for determining the thermal shock resistance of ceramics most frequently utilize quenching techniques to determine (ΔT_c) the critical temperature differential at which a significant reduction in the materials load bearing capability occurs. The severity of the thermal stress determined by such methods depends upon both the quenching medium and the geometry of the test specimen (Kingery, 1955).

Although the curves in Fig. 4 clearly indicate that one should conduct evaluations of the thermal shock behavior of ceramics at the heat transfer condition to be encountered in service, a search of the literature will ascertain that this is rarely done by materials developers in the laboratory. Instead the thermal shock resistance parameters for severe thermal shock R or R' are most commonly measured.

$$\Delta T_c \sim R = S(1 - v)/E\alpha \tag{14}$$

or

$$\Delta T_c \sim R' = KS(1 - v)/E\alpha \tag{15}$$

where S is the bend stress, α the coefficient of thermal expansion, K the thermal conductivity, and E and v have their usual meaning. Figure 5 shows a schematic of such a determination, with the fracture mechanical implications given by Hasselmann (1969) included. This method has gained popularity,

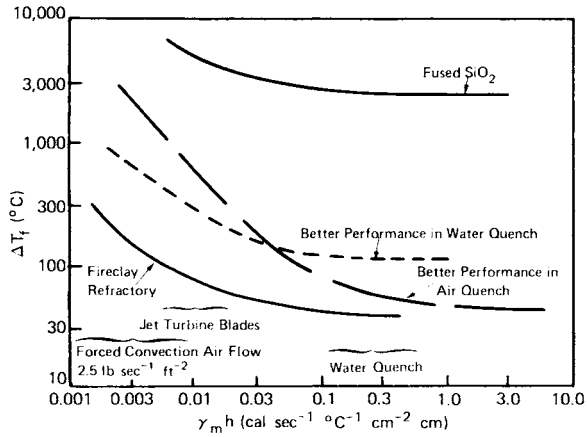

Fig. 4. Variation in maximum quench temperature sufficient to cause fracture initiation (ΔT_f) with different rates of heat transfer ($\gamma_m h$). After Kingery (1955).

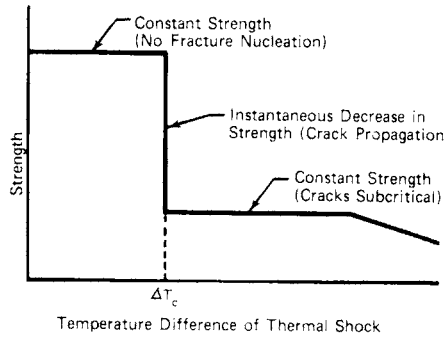

Fig. 5. Typical strength behavior of a thermally shocked ceramic. After Hasselman (1969).

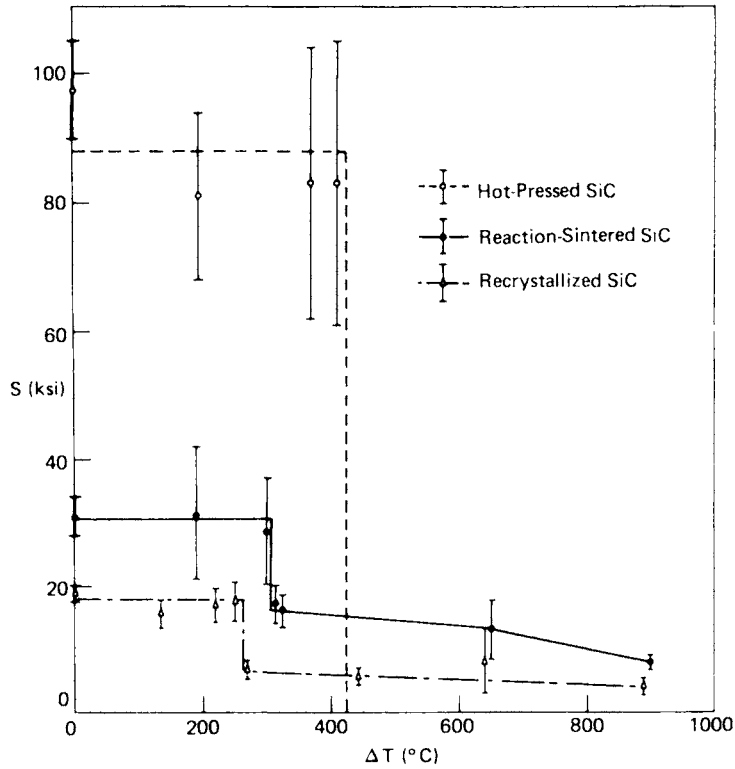

Fig. 6. Strength behavior of thermally shocked SiC. After Seaton (1974).

since the theory as shown in Fig. 5 correlates nicely with experiment as shown in Fig. 6 (Seaton, 1974).

VIII. Fatigue of Ceramics

The term fatigue in ceramic materials is used to describe two quite different phenomena. Stress corrosion, in which the simultaneous action of a stress and a corrosive atmosphere interact to reduce strength, is referred to as *static fatigue*. The reduction in strength suffered by a ceramic material after exposure to cyclic mechanical, thermal, or acoustic stress is also referred to as fatigue. Methods for determining each of these types of fatigue will be discussed below.

A. Static Fatigue

The direct method of measuring static fatigue is to carry out constant load (constant stress) MOR or tensile tests and measure the time to failure as a function of load. This has been done by Acquaviva and Chait (1972) for boron carbide and AD-94 alumina, as shown in Fig. 7. Static fatigue is indicated by the presence of an appreciable strain rate effect in ceramics at temperatures too low for plasticity to be the explanation for such an effect. Glasses or glass-bonded ceramics usually exhibit static fatigue in the presence of water in the atmosphere.

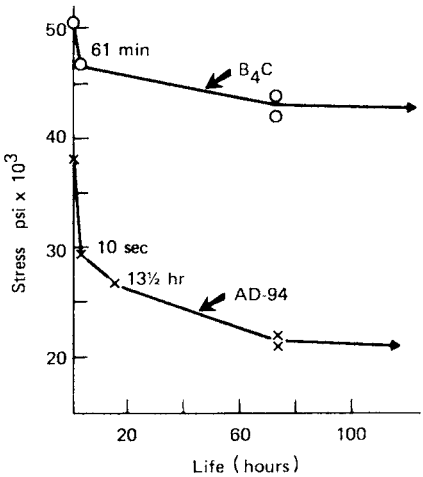

Fig. 7. Static fatigue of ceramic material. After Acquaviva and Chait (1972).

B. Mechanical or Cyclic Fatigue

The sequential loading and unloading of a ceramic member can result in a loss of strength as a function of the number of cycles. This is referred to as mechanical or cyclic fatigue. Because of the great difficulty of conducting tensile tests on ceramics, virtually all test methods devised for studying cyclic fatigue utilize flexural testing. Methods have been described by Acquaviva (1971b) and Kossowsky (1973, 1974). Both methods utilize cantilever loading; however, in order to attain a high temperature coincident with maximum stress, Kossowsky utilized the double-reduced gage section as shown in Fig. 8. The results of Acquaviva and Chait (1972) on boron carbide and AD-94 alumina tested at room temperature and 15 cps are shown in Fig. 9. As can be seen from the results of Kossowsky (1974) (Fig. 10), silicon nitride does not show a cyclic fatigue effect at low temperatures while it is affected by such cycling at high temperatures.

C. Acoustic Fatigue

Resonances produced in a part due to sonic vibrations can lead to a type of cyclic loading called acoustic fatigue. This phenomenon has been little studied in ceramics. However, with the increasing utilization of ceramics in acoustically active environments, it is anticipated that this will be a growing area of concern. Acoustic fatigue in ceramics was studied by Seaton and Katz (1973). They utilized Forster's method (Seaton, 1974) for resonating prisms which were then used as MOR specimens. Comparisons between bars resonated for 10 min. with unresonated bars indicated that TiB_2 lost approximately 35 % of its strength while Si_3N_4 suffered no degradation.

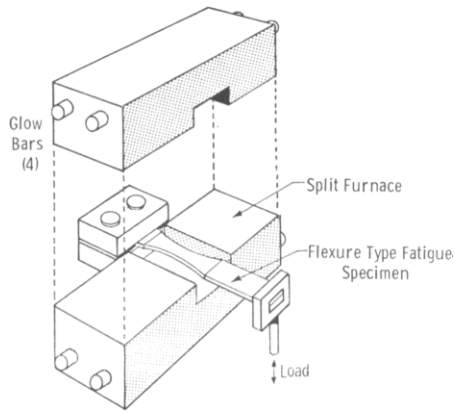

Fig. 8. Flexural fatigue test. After Kossowsky (1974).

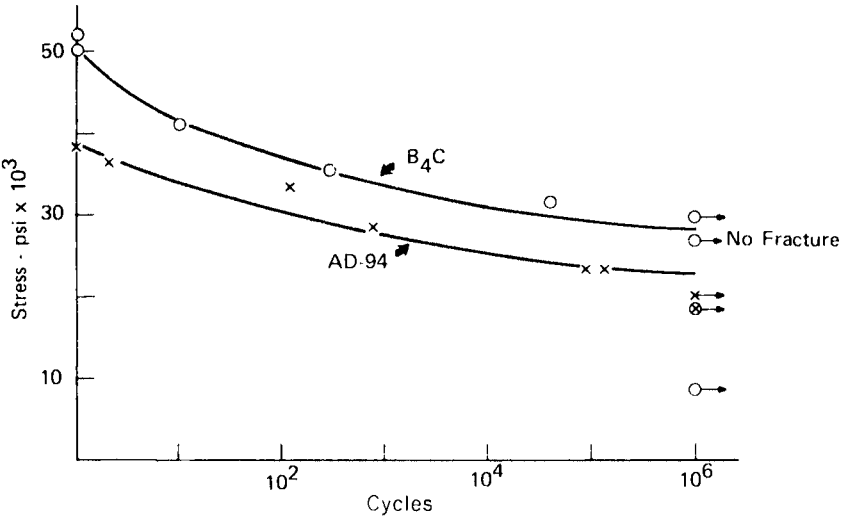

Fig. 9. Room temperature flexural fatigue of boron carbide and alumina. After Acquaviva and Chait (1972).

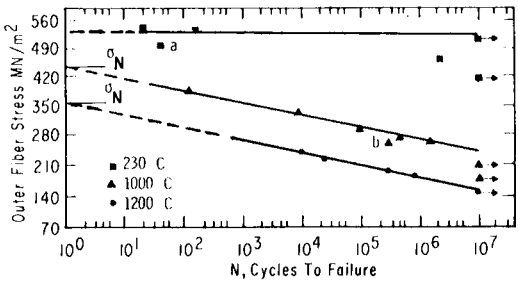

Fig. 10. Cyclic fatigue behavior of hot pressed silicon nitride (HS-110) at 1800 cpm. After Kossowsky (1974).

IX. Time-Dependent Properties

The mechanical properties of ceramics are often found to be a function of time under load or of the rate at which stress or strain are imposed. Strain rate effects have already been discussed as being an indication of static fatigue. A strain rate dependence of strength may also indicate other mechanisms of slow crack growth in the absence of a chemical effect as discussed by Lange and Iskoe (1974). The most frequently studied time-dependent phenomena are creep and stress rupture. Creep is the accumulation of strain as a function of time at constant stress and temperature. Creep tests are designed to measure accumulated strain versus time.

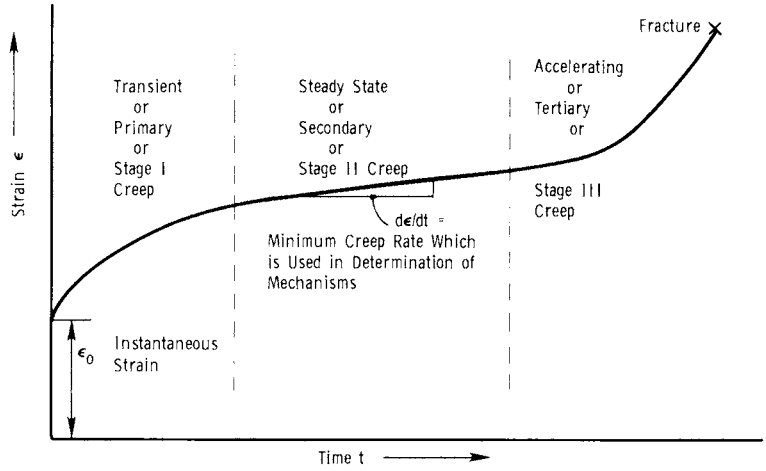

Fig. 11. Typical creep curve.

Figure 11 indicates the three stages encountered in tensile creep and gives the various terminologies associated with those stages. Stress-rupture refers to a specific test rather than a phenomenon. The stress-rupture test measures the time to failure at a constant stress and temperature. This eliminates the necessity for strain measurement (which as discussed in the introduction is a major experimental problem at elevated temperatures) and is consequently easier to perform than an instrumented creep test.

Creep testing of ceramics can be performed in a tensile, flexural, or compressive mode. Lenoe and Quinn (1975) have also developed methods for torsional creep testing. In general, test fixtures used are the same as those used in shorter time, elevated temperature mechanical testing. However, since creep tests can be very extended, it is vital that the test fixtures be able to survive the time, temperature, and environmental conditions of the test with certainty, otherwise hundreds of hours and many dollars of testing will be lost. This condition can make the design of fixtures for a creep test in air at 1500°C and 1000 hr a major experimental task. One aspect of creep testing is simpler than short time testing—namely, dead weight loading can be used. The experimental setup should be capable of operating in several environments, i.e., air, inert gas, or vacuum, since it has often been observed that creep rates vary from one environment to another. These same conditions hold for stress-rupture tests but the times here do not generally exceed 100 hr for a given test.

It is desirable to discuss briefly the mechanisms giving rise to creep in ceramics. There are three main mechanisms: diffusional, dislocation slip,

and grain boundary sliding. Diffusional creep leads to Newtonian flow, i.e., strain rate ε proportional to stress σ. In the case where lattice diffusion controls (Nabarro–Herring creep);

$$\dot{\varepsilon} \propto [D_l/(\text{G.S.})^2]\sigma \tag{16}$$

where D_l is the lattice diffusion coefficient and G.S. is the grain size. In the case where grain boundary diffusion controls (Coble creep);

$$\dot{\varepsilon} \propto [D_b/(\text{G.S.})^3]\sigma \tag{17}$$

where D_b is the grain boundary diffusion coefficient. More detail concerning diffusional creep can be obtained from Heuer *et al.* (1970), Vasilos and Passmore (1966), and Coble (1963).

In non-Newtonian creep, $\dot{\varepsilon} \propto B\,\sigma^n$, where B is a constant and n is a constant greater than 1. If n is 2, than the non-Newtonian creep is usually attributed to grain boundary sliding (Kossowsky, 1974). Dislocation creep, while important in metals is not generally found to be important in ceramics (Heuer *et al.*, 1970).

From a practical standpoint by plotting $\dot{\varepsilon}$ vs. σ or vs. grain size at constant stress, we can determine the controlling mechanism for creep. (Note $\dot{\varepsilon}$ is the steady state creep rate). Since we often wish to modify the existing creep rate, knowledge of the controlling mechanism allows one to choose appropriate schemes to alter it. For example, if we determine creep to be controlled by lattice diffusion, then control of point defects in the lattice becomes important. If, on the other hand $\dot{\varepsilon} \propto \sigma^2$, then grain boundary sliding via a viscous process is implied and modification of a grain boundary phase as described by Kossowsky (1974) becomes important.

X. Fracture Energy

In a qualitative way the concept of fracture energy or fracture toughness can be viewed as a measure of the degree of brittleness of a ceramic material. For example, if one drops tiles of hot pressed Al_2O_3 and hot pressed Si_3N_4 (both of 100,000 psi MOR), very likely the alumina will shatter and the nitride will survive. In this sense the nitride can be said to have more toughness than the alumina, although from an engineering standpoint they are both brittle materials.

At the present time, there is no accepted method for measuring the fracture toughness of ceramics and there is no accepted formulation for utilizing the measured values of fracture toughness or fracture energy in the analytic procedures currently used by designers. Nevertheless, progress is being made

in the areas of applying fracture mechanics concepts and data to service life prediction of ceramic components; most notably the Skylab Orbiting Laboratory windows (Wiederhorn and Evans, 1974), the determination of critical surface finish (Baratta *et al.*, 1974), and advanced failure probability calculations. It is certain that the importance of this area will grow.

The basis of fracture toughness determinations in ceramics lies in the Griffith equation (Griffith, 1920), which very simply states that when the stored elastic energy per unit area due to a stress σ_c in a test piece with a pre-existing crack of length C_0 exceeds twice the energy to create a new surface per unit area γ, a crack will grow with no increase in external driving force and failure will result. Stated analytically

$$\sigma_c \geq \text{Const}_1 (\gamma E / C_0)^{1/2} \tag{18}$$

One can reach the same result via a stress intensity analysis:

$$\sigma_c = \text{Const}_2 (K_c / \sqrt{C_0}) \tag{19}$$

where K_c is the critical stress intensity factor. Thus the effective surface energy γ is related to the critical stress intensity factor K_c by the relation

$$\gamma = K_c^2 / E \, (\text{Const}_2 / \text{Const}_1)^2 \tag{20}$$

Methods for measuring γ and K_c are currently controversial and therefore beyond the scope of the chapter. The interested reader is referred to the *Proceedings of the Symposium on the Fracture Mechanics of Ceramics* (Hasselman *et al.*, 1974) for the most current and thorough review of this area.

References

Acquaviva, S. J. (1971a). *Mater. Res. Stand.* **11**, 21–22.

Acquaviva, S. J. (1971b). *Rev. Sci. Instrum.* **42**, 1858–1859.

Acquaviva, S. J., and Chait, R. (1972). "Static and Cyclic Fatigue of Ceramic Materials." AMMRC TR 72-9, AD 742-210.

Baratta, F., Driscoll, G., and Katz, R. N. (1974). *In* "Ceramics for High Performance Applications" (L. J. Burke, A. E. Gorum, and R. N. Katz, eds.), pp. 445–476. Brook Hill Publ. Co., Chestnut Hill, Massachusetts.

Batdorf, S. B., and Crose, J. G. (1974). *J. Appl. Mech.* **41**.

Bortz, S. A., and Burton, K. T. (1969). "Structural Ceramics and Design," pp. 95–147. Gordon & Breach, New York.

Bortz, S. A., and Wade, T. B. (1967). "Analysis of Mechanical Testing Procedure for Brittle Materials," AMRA CR 67-09/1, AD 658-695.

Burke, J. J., and Weiss, V. (1971). "Shock Waves and the Mechanical Properties of Solids." Syracuse Univ. Press, Syracuse, New York.

Chen, P. E. (1966). *J. Compos. Mater.* **1**, No. 1, 82–90.
Coble, R. L. (1963). *J. Appl. Phys.* **34**, 1679.
Fisher, J. C., and Holloman, J. H. (1947). *Trans. Amer. Inst. Mining Met. Eng.* **171**, 546.
Freudenthal, A. M. (1968). *In* "Fracture" (H. Kiebowitz, ed.), Vol. II, pp. 592–618.
Griffith, A. A. (1920). *Phil. Trans. Roy. Soc. London, Ser. A* **221**, 163.
Hasselman, D. P. H. (1969). *J. Amer. Ceram. Soc.* **52**, 600–604.
Hasselman, D. P. H., Lange, F. F., and Bradt, R. C. (1974). "The Fracture Mechanics of Ceramics." Plenum, New York.
Heuer, A. H., Cannon, R. M., and Tighe, N. J. (1970). *In* "Ultra-Fine Grain Ceramics" (J. J. Burke, N. L. Reed, and V. Weiss, eds.), pp. 339–366. Syracuse Univ. Press, Syracuse, New York.
Kingery, W. D. (1955). *J. Amer. Ceram. Soc.* **38**, 3–15.
Kossowsky, R. (1973). *J. Amer. Ceram. Soc.* **56**, 531–535.
Kossowsky, R. (1974). *In* "Ceramics for High Performance Applications" (L. J. Burke, A. E. Gorum, and R. N. Kata, eds.), pp. 347–371. Brook Hill Publ. Co., Chestnut Hill, Massachusetts.
Lange, F. F., and Iskoe, J. L. (1974). *In* "Ceramics for High Performance Applications" (L. J. Burke, A. E. Gorum, and R. N. Katz. eds.), pp. 223–238. Brook Hill Publ. Co., Chestnut Hill, Massachusetts.
Lenoe, E. M., and Quinn, G. D. (1975). *In* "Deformation of Ceramic Materials," pp. 399–412. Plenum, New York.
McClintock, F. A. (1974). *In* "Fracture Mechanics of Ceramics" (R. C. Bradt, D. P. H. Hasselman, and F. F. Lange, eds.), Vol. 1. Plenum, New York.
Metcalfe, A. G. (1974). *In* "Ceramics for High Performance Applications" (L. J. Burke, A. E. Gorum, and R. N. Katz, eds.), pp. 739–747. Brook Hill Publ. Co., Chestnut Hill, Massachusetts.
Nakayama, J. (1974). *In* "Fracture Mechanics of Ceramics" (R. C. Bradt, D. P. H. Hasselman, and F. F. Lange, eds.), Vol. 1, pp. 759–778. Plenum, New York.
National Materials Advisory Board (NMAB) (1968). *Nat. Acad. Sci.—Nat. Res. Counc., Publ.* **1576**, 175–297.
Nye, J. F. (1964). "Physical Properties of Crystals," pp. 131–149. Oxford Univ. Press, London and New York.
Pears, C. D., and Starrett, H. S. (1966). "An Experimental Study of the Weibull Volume Theory," AFML-TR 66-228, AD 815-390.
Rice, R. W. (1971). "Ceramics in Severe Environments," pp. 195–230. Plenum, New York.
Rice, R. W. (1972). *Nat. Bur. Stand. (U.S.), Spec. Publ.* **348**, 365–376.
Rice, R. W. (1974). *In* "Ceramics for High Performance Applications" (L. J. Burke, A. E. Gorum, and R. N. Katz. eds.), pp. 287–343. Brook Hill Publ. Co., Chestnut Hill, Massachusetts.
Rudnick, A., Marschall, C. W., Duckworth, W. H., and Emrich, B. R. (1968). "The Evaluation and Interpretation of Mechanical Properties of Brittle Materials," DCIC Rep. No. 68-3. Battelle Mem. Inst., Columbus, Ohio.
Schreiber, E., and Anderson, O. L. (1966). *J. Amer. Ceram. Soc.* **49**, 184–190.
Seaton, C. C. (1974). "Thermal and Acoustic Fatigue of Ceramics and their Evaluation," AMMRC MS-74-7, AD 785-547.
Seaton, C. C., and Katz, R. N. (1972). "Ultrasonics Symposium Proceedings," pp. 112–115. IEEE, New York.
Seaton, C. C., and Katz. R. N. (1973). *J. Amer. Ceram. Soc.* **56**, 283.
Van Vlack, L. H. (1964). "Physical Ceramics for Engineers," p. 127. Addison-Wesley, Reading, Massachusetts.
Vasilos, T., and Passmore, E. M. (1966). "Strengthening Mechanisms," pp. 161–179. Syracuse Univ. Press, Syracuse, New York.

Weibull, W. (1939). *Roy. Swed. Inst. Eng. Res., Proc.* No. 151, pp. 1–45.

Weil, N. A., and Daniels, I. M. (1962). "Studies of the Brittle Behavior of Ceramic Materials," ASD Tech. Rep. No. 61-628, Part I, AD-277-659.

Westwood, A. R. C., and Latanision, R. M. (1972). *Nat. Bur. Stand. (U.S.), Spec. Publ.* **348**, 141–153.

Wiederhorn, S. M., Evans, A. G., and Roberts, D. E. (1974). *In* "Fracture Mechanics of Ceramics" (R. C. Bradt, D. P. H. Hasselman, and F. F. Lange, eds.), Vol. 1, pp. 829–841. Plenum, New York.

Methods of Measuring Surface Texture

W. C. LO

Bell Telephone Laboratories, Incorporated
Allentown, Pennsylvania

I. Introduction

Surface texture describes the total topographic features of the surface of solid materials (Reason, 1960). It refers to the geometrical character of the surface irregularities ranging from submicroscopic to macroscopic dimensions. By submicroscopic we mean those with dimensions of 10^2 to 10^4 Å (0.4 to 40 microinch), microscopic, $> 10^4$ to 10^6 Å, and macroscopic, $> 10^6$ Å.* This classification is arbitrarily made for convenience of discussion. The structure and arrangement of atoms and ions on the surface, however, is not included. In this context, roughness (finish), waviness, lay (error of form) defined in American Standard ASA B46.1-1962, as well as random flaws, are all components of surface texture (Fig. 1).

The surface texture of ceramics is determined by the size, shape, arrangement, and distribution of the surface phases. Thus, it is dependent on how the ceramic is made: the raw material used; the forming, drying, and firing method; and the post-firing, machining, or finishing operations that may be required to meet dimensional tolerances.

*1 angstrom (Å) = 10^{-10} meter (m) $\cong$ 0.004 microinch (μin.). 1 microinch (μin.) = 0.0254 microns (μm).

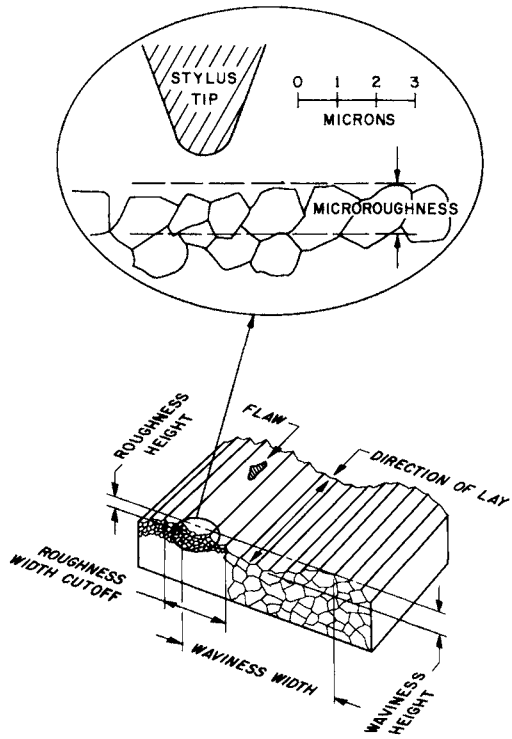

Fig. 1. Surface texture—definition of terms.

Surface texture is functionally significant in many properties and behaviors of ceramics. Zimon and Serebryakov (1971, 1972) have shown that roughness on the atomic and molecular scale is of import in considering the adhesion of particles on a surface. By roughness on the atomic or molecular scale, they mean the asperities on the order of angstroms, due to lattice discontinuities and dislocation outcrops superimposed on the microprojections of the surface. They also attribute the scatter of adhesive forces to this scale of roughness. Wenzel (1936) asserts that the wetting properties of a solid substance are attributable to the roughness of the surface wetted instead of some form of contamination as usually claimed. The effect of surface finish on reflectance has been reported by Torrance and Sparrow (1965), on the breakdown of piezoelectric elements by Radl and Kunc (1970), on the structural failure of alumina ceramics by McKinney and Herbert (1970), and on glass corrosion by Sanders and Hench (1973).

In the electronic industry, the effect of surface texture on the properties of thin films has also been observed. The term "thin film" covers metal and dielectric films that range from a few hundred to tens of thousands of angstroms in thickness. They are deposited on the ceramic substrate normally

by evaporation or sputtering techniques. Usually more than one type of material is deposited on the substrate in sequence such as Ti–Au, Ti–Pd–Au, or TaN–Ti–Pd–Au. Caulton (1971) finds that the conductor loss of a microwave line element used in circuits is a function of the roughness of the metal film which is determined by the roughness of the substrate surface. T. C. Tisone (personal communication, 1971) concludes that the surface topography of substrates can cause shadowing in the deposition of thin metal films by evaporation. This would affect sheet resistivity, adhesion, and stability of thin film devices. His finding is consistent with the observation of Lo (1969, 1970) on the association of ceramic surface texture with pull strenghts of gold-plated copper leads bonded by thermal compression methods to thin film metallized ceramic substrates, and the work of D. O. Melroy (personal communication, 1970) on the sheet resistance of thin films.

More examples of the influence of surface finish on the mechanical, optical, electrical, and magnetic properties of ceramics can be found in the paper by Westbrook (1968) and by Stokes (1972).

Even in the chemical analysis of surfaces, surface texture of the sample cannot be overlooked. With the electron microprobe techniques, Auger electron spectroscopy, and ion microprobe, surface topography can affect the analytical results. Subtle changes in topography change the diffraction pattern in the reflection high energy electron diffraction technique for analyzing the crystallographic structure of the surface phases (Berrin and Sundahl, 1971).

From the foregoing it is apparent that in the application of ceramics, a knowledge of the functional relationship of surface texture with ceramic performance is indeed desirable. It will enable ceramic suppliers to prepare better materials for the job and users to acquire parts without having to overspecify.

Establishing quantitative relationships between surface texture and the performance of the ceramic, however, is no easy task. The difficulty invariably is due to one or more of the following causes.

1. The performance is a function of one or more parameters in addition to surface texture and that these parameters are mutually dependent.
2. The improper choice of the surface texture component.
3. The lack of an available method for measuring the functional component or assigning proper numerical values to describe such a component.

In this article, we attempt to review the methods for assessing the various components of surface texture on different scales of size that are available or have been reported in the literature. Since detail descriptions of these methods are well documented (see references given under the various methods), they will not be repeated here. Only a general discussion on the applicability of the method and its limitations is given.

The main purpose of this article is to provide a stepping stone for those interested in assessing and characterizing surface textures of ceramics and to stimulate interest in the role of surface texture in ceramic applications.

II. Methods

A. General

Methods for assessing surface texture fall into two main categories: the indirect and the direct methods. By indirect methods we mean those which measure the properties of the material that have been found experimentally to relate to surface texture or some of its components. This relationship is usually developed from a model based on known theories with stipulations that certain assumptions must be met. Calibration with standards is required with these methods. Direct methods are those that can produce a visible image or a two-dimensional profile of the actual surface. Understandably, the direct methods are more dependable for accurate information. Tools used in these methods include the tactile trace instruments, the optical light microscope, the transmission electron microscope and the scanning electron microscope.

There is no single method that can be used effectively to assess surface features on all scales of size. Some are more suitable than others for certain features of interest. In the following, we will discuss these methods.

B. Indirect Methods

1. As examples of indirect methods, one may first cite the BET (Brunauer–Emmett–Teller) method for measuring surface area of powdered solids. This method utilizes the BET equation that describes the relationship of the amount of physically adsorbed gas on a solid to its surface area. The basis and background of the method are treated in Brunauer and Emmett (1937), Orr and DallaValle (1959), and Gregg and Sing (1967). Ross and Wiltshire (1966) extended the technique for measuring surface roughness of powdered solids.

2. The thermal comparator of Sherif and Mahmound (1966) for measuring surface finish is based on its effect on thermal conductivity.

3. Many indirect methods for measuring surface finish are based on its effect on the optical properties of light incident on the material. The Fotonic Sensor marketed by MTI Instruments Division, Mechanical Technology Inc., Lantham, New York, the reflectometer of Bennett (1964), and the laser specular reflectometer of Hensler *et al.* (1973) are examples. Both Bennett's and Hensler's methods measure the intensity of the specularly reflected light

from the specimen's surface, differing only in the light source used. In using the laser reflectometer for measuring the average roughness of ceramics, one should note that the validity of the theory on which the method is based assumes that an isotropic random roughness exists on the ceramic surface (Hensler, 1972). If this condition is not met, which can happen when the raw materials or the method of manufacture is changed, the functional relationship between the intensity of the specularly reflected light and the average roughness expressed by a center-line-average (CLA) value may not hold. Furthermore, the laser reflectance value should not be directly related to the grain size of an as-fired substrate surface when it is specified by an average intercept value obtained by counting the number of intercepts of the grain boundary with a test figure (circle or line) laid over a photomicrograph of the surface. Obviously this grain size parameter would not differentiate grains with different dimensions in the direction normal to the

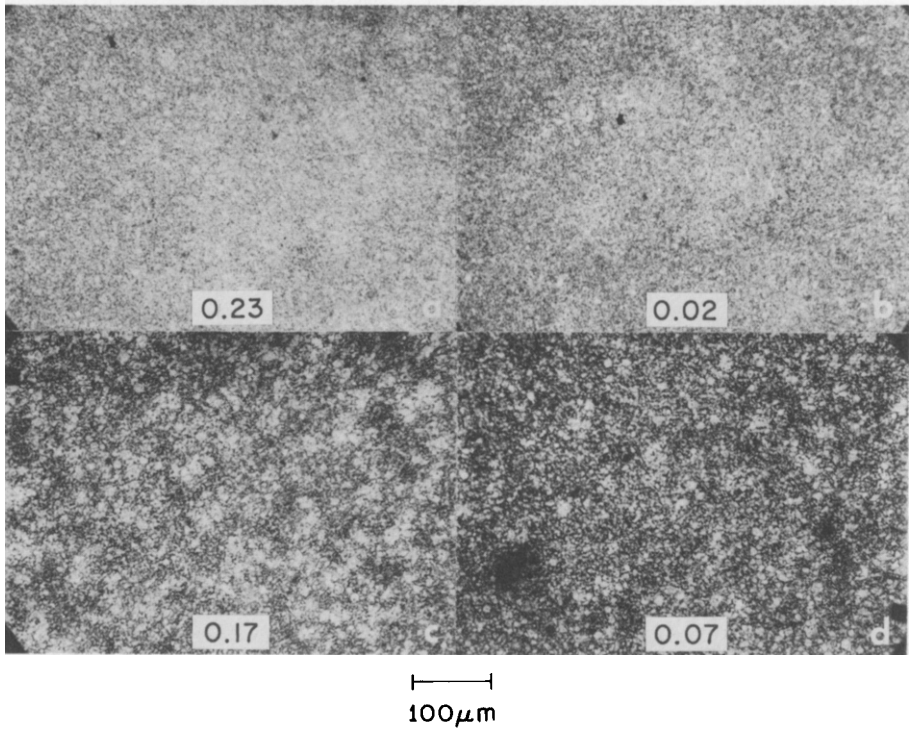

Fig. 2. Surface texture (by reflective replica technique) vs. laser reflectance in arbitrary units shown in center of picture. (a, c, and d) A-side of same type of alumina substrates from different lots. (b) B-side of substrate of (a).

substrate surface. Thus, it is possible to have substrates with the same grain size parameter (average intercept value) but significantly different surface roughness as defined by CLA values, if their grains are of a different geometry. This is illustrated later in the paper. The large difference in laser reflectance values for substrates of similar grain size as observed in Fig. 2 might be explained on this basis.

The reflected intensity of a laser beam has also been successfully used by Tester and Herrick (1972) for measuring the changing surface morphology of a growing crystal, which in this case, is characterized by triangular etch pits in sizes ranging from 1 to 200 μm.

4. The dye penetrant tests according to American Society for Testing and Materials (ASTM) method E165 which are normally used for detecting fine cracks in a component or leaks in a sealed assembly may be considered as another indirect method for assessing surface texture. In a dye penetrant test, the ceramic is first immersed in the dye for a period of time. Following removal of the ceramic from the dye and rinsing off the excess from the surface of the ceramic, one will get different amounts of dye retained by the crevices on the surface. Based on the study of McCauley and Van Winkle (1962–1964) on dye penetrants, one might assume that most of these crevices have dimensions in the micron range. Fluorescent dye such as ZL22 (product of Magnaflux Corporation, New York), can penetrate crevices with openings less than a micron wide. The remanent fluorescent dye trapped in the crevices is made visible by illuminating the surface with an ultraviolet light. Figure 3 shows the difference in dye retention characteristic of ceramic substrates taken from different lots shipped by the same supplier. One must bear in mind that the actual size of the crevice is much smaller than the area represented by the light spot in the figure. The quality of the substrate with respect to fine crevices may be evaluated by comparison with visual standards or by quatifying the intensity of the light emitted by the fluorescent dye using a microphotometer arrangement. The dye test is highly vulnerable to improper testing procedures. Strict adherence to a cleaning and testing procedure is required to obtain valid comparative results. In the interpretation of the test results, one should be aware of the fact that other surface features such as porous foreign particles can also entrap dye and the affinity of the dye to the surface is affected by the surface chemistry. Cleanliness prior to penetrant testing can have a very significant influence on the test results.

Both the laser reflectometer and the dye tests are useful for evaluating and rating substrates for thin film hybrid integrated circuit applications in the electronic industry. Hensler *et al.* (1973) show that a relationship exists between the peel strength of lead terminals bonded by thermal compression to thin film metallized substrate and the laser reflectivity of the substrate for a given type of ceramic. Substrates with higher specular reflectivity values give higher peel strengths. This could be explained by the substrates

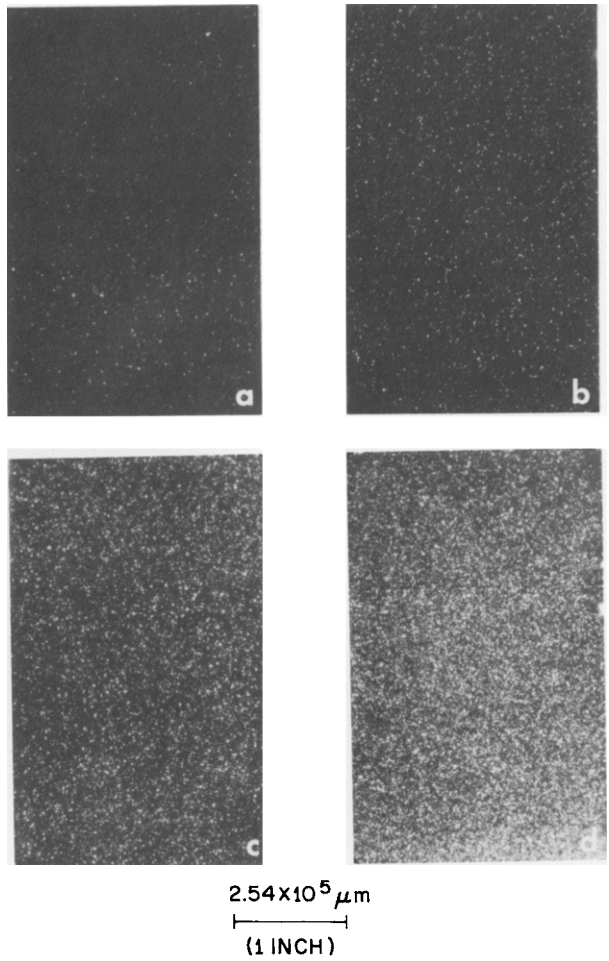

Fig. 3. Fluorescent dye test results.

with the smoother surface and hence higher reflectivity having larger true surface* areas. This is possible since CLA and true surface area are not functionally related (Marian, 1962).

The usefulness of the dye test is based on the premise that fine surface crevices of micron and submicron sizes, while not critical for thick† film

*The difference between true surface area and nominal surface area will be made clear later in the text.

†The term thick film metallization is generally used to refer to the metal film deposited on the ceramic substrate by a process involving screen printing and firing. The thickness of the resulting metal film is on the order of tens of microns.

metallization, can be detrimental for thin film applications. The same crevices that retain dye would tend to entrap contaminants which can cause degradation of the thin film deposited over such surfaces. This can jeopardize the reliability of thin film devices and cause loss of film adherence resulting in low lead-pull strengths. Another aspect is the creation of discontinuities in the base metallizing film in direct contact with the substrate. Discontinuities are possible because of shadowing (T. C. Tisone, personal communication, 1971). Their occurrence is more likely when the thickness of the metallizing film is of the same order of magnitude as the dimension of the crevices. Figure 4 shows an example of such a discontinuity. In this case, the thickness of the metal film was increased by plating to many times its normal thickness. It is obvious that such an approach for bridging the gap would not be satisfactory. Discontinuities are also undesirable since they serve as stress raisers. Unless the cohesive strength of the surface phases are high, low lead-pull strength can result. Failure due to weaknesses in the surface layer have been observed. Figure 5 consists of enlarged views of the surfaces of a gold-plated copper lead (Fig. 5a and c) and the metallized pad (Fig. 5b and d) on a ceramic substrate from which it was separated in a lead-pull test. The force required to separate this lead was way below normal, and yet one might observe that ceramic grains are present on both of these surfaces, suggesting that ceramic-to-ceramic failure did occur. More evidence of ceramic-to-ceramic failures with leads of low pull strengths are shown in Fig. 6. Here, the presence of ceramics on the surfaces of low pull strength leads separated

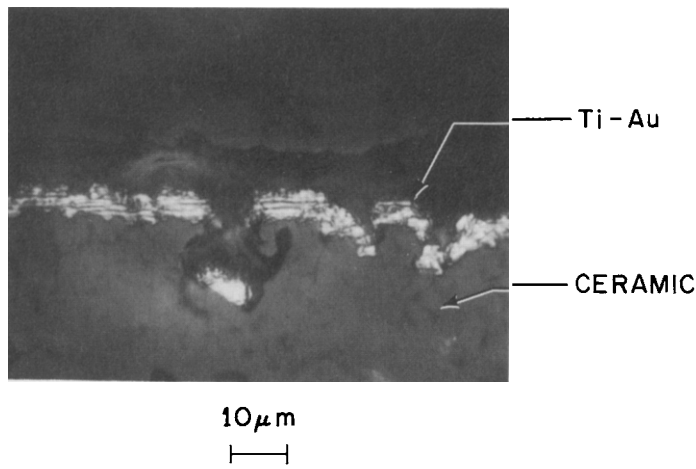

Fig. 4. Discontinuity of thin film metallizing layer observed on a dry-pressed 94% alumina substrate with as-fired surface. Note that the film thickness $\simeq 5$ μm. Normally, film thickness $\simeq 1\mu$m or less is used.

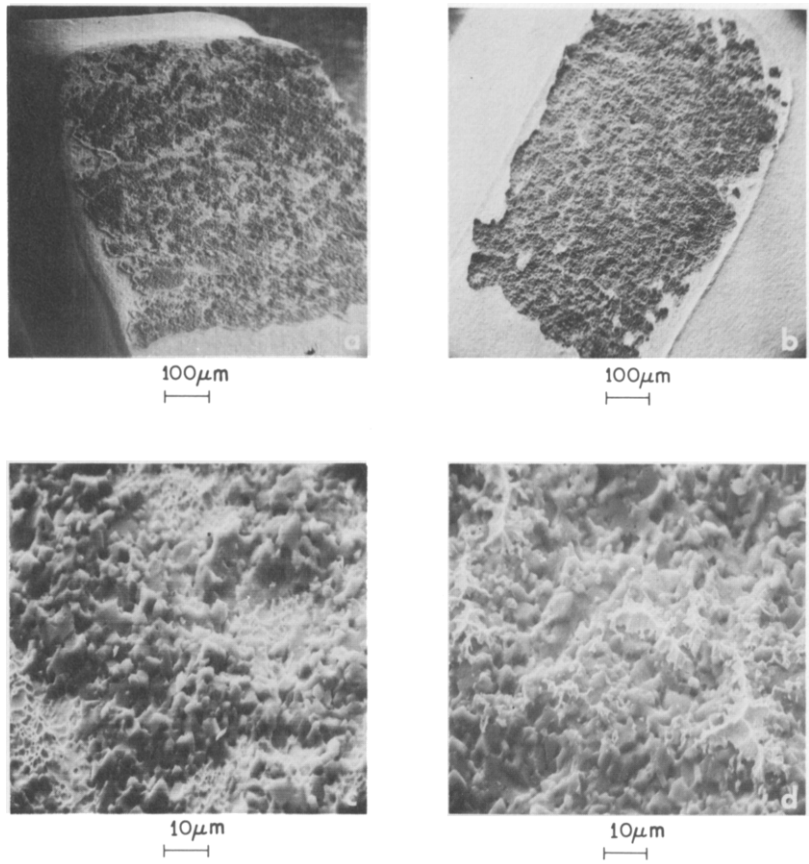

Fig. 5. SEM of the surfaces of a gold-plated copper lead (a) and the metallized pad (b) on a ceramic substrate separated in a pull test. (c) and (d) Views of the respective areas at 1000 × showing that the layer of ceramic pulled off is approximately one grain thick.

from various types of thin film metallized alumina substrates is indicated by the presence of aluminum in a microprobe analysis.

C. Direct Methods

1. Optical Light Microscopes

The optical light microscope (OLM)* is most useful for observing macroscopic to microscopic surface features. Practical magnification can go from

* For references on the principle and use of the microscope, see Chamot and Mason (1958), Allen (1958), Shenk and Kistler (1962), Hartley (1962), Barron (1965), and Richardson (1971).

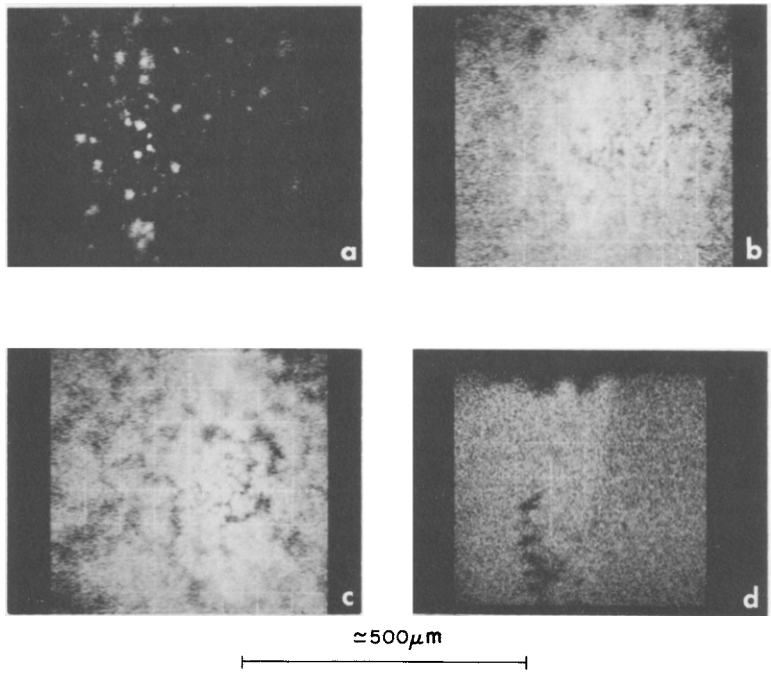

Fig. 6. Microprobe analyses of surfaces of gold-plated copper leads separated from various thin film metallized ceramic substrates with low pull strengths. These are photographs of AL X-ray. Light areas indicate presence of aluminum: (a) Ground sapphire metallized with TaN–Ti–Pd Au, pull strength, 0 lb; (b) isopressed high alumina substrate metallized with TaN–Ti–Pd–Au, pull strength, 1.8 lb; (c) same material as (b) except annealed before metallization, pull strength, 3.2 lb; (d) tape-cast high alumina substrate metallized with Ti–Pd–Au, pull strength, 1.0 lb. Normally, pull strength of 5–6 lb is expected with this type of lead.

1 × up to 2000 ×. With the OLM, lateral resolution is limited to half a light wavelength. This means details separated by a distance of 2500 Å (~ 10 μin.) can be seen distinctly using green light. Using ultraviolet would increase the resolution, but making the image visible would require special instrumentation. The limit of resolution is governed by many factors. Other than the wavelength of light, λ, the more important ones are the numerical aperture (light collecting aperture) of the objective lens and the contrast that can be obtained with the optical system. For surfaces with good reflectivity, the quality of the image is enhanced with the Nomarski differential interference-contrast system (Lang, 1968, 1969, 1970).

The low reflectivity of most polycrystalline ceramic substrate surfaces makes it difficult to obtain adequate contrast with an ordinary OLM. However, this can be remedied by using the transparent replica technique (Allen and Friedberg, 1948) or the reflective replica technique (Lo, 1972). In the latter

technique a replica of the surface is made with a plastic film having a reflective aluminum backing. To prepare the replica, a drop of solvent is placed on the area to be replicated. The plastic film is immediately pressed tight against this surface and held there until the solvent has dried; this takes one or two minutes. The dried replica is then peeled off and viewed under the OLM with incident illumination. Examples of ceramic substrates with different surface textures delineated by this technique are shown in Fig. 7. Figures 7a, b, c, d, e, and f show the variety of surface texture of as-fired high alumina substrates one may get from different sources. Figures 7g and h are the surface texture of ground alumina substrates. Grinding marks and pull-outs are evident on these surfaces.

Another simple technique for enhancing the image of polycrystalline ceramic surfaces is by wiping the surface with a colored ink. The water soluble ink from a Flair felt-tipped pen, for example, will work well with alumina substrates (see Fig. 8). For surfaces with coarser features, rubbing the surface with fine graphite powder will achieve similar results.

The depth of focus (or depth of field) of the OLM is small [viz. 0.5 μm at 1000 $\times$ using an objective of 1.4 numerical aperture (N.A.)]. It is inversely proportional to the magnification and the numerical aperture of the objective. But this small depth of focus is not always a disadvantage. Quantitative measurements of surface asperities of tens to hundreds of microns can be measured with an accuracy of 1 μm or better using a high quality microscope by focusing the asperities at different levels with an objective that has a small depth of focus.

The OLM can be used to reveal and measure extremely small height deviations with special set-ups. With a multiple-beam interference attachment, interference fringes representing height deviations of half a wavelength apart may be created on the image of the surface. Thus, outcrops of dislocations, slip bands, etch pits with height differences on the order of angstrom units can be observed and quantified. However, this method is not generally applicable to ceramics. The surface under study must have high reflectivity or the deposition of a thin reflective coating is required. Physical contact of the specimen with a reference plane with comparable reflectivity is another prerequisite. It is important to point out that this fine resolution in the order of angstroms only applies to the direction normal to the surface and not the lateral directions. Height changes of features with small lateral dimensions cannot be revealed by this technique. A lateral extension of 10 μm is usually required (Tolansky, 1955, 1960, 1968).

Attachments based on the two-beam interference principle are more convenient for measuring height deviations in the range of 0.025 to 1 or 2 μm. The limiting value depends on the type of irregularities and the reflectivity of the surface. With these attachments, one need not contact the surface

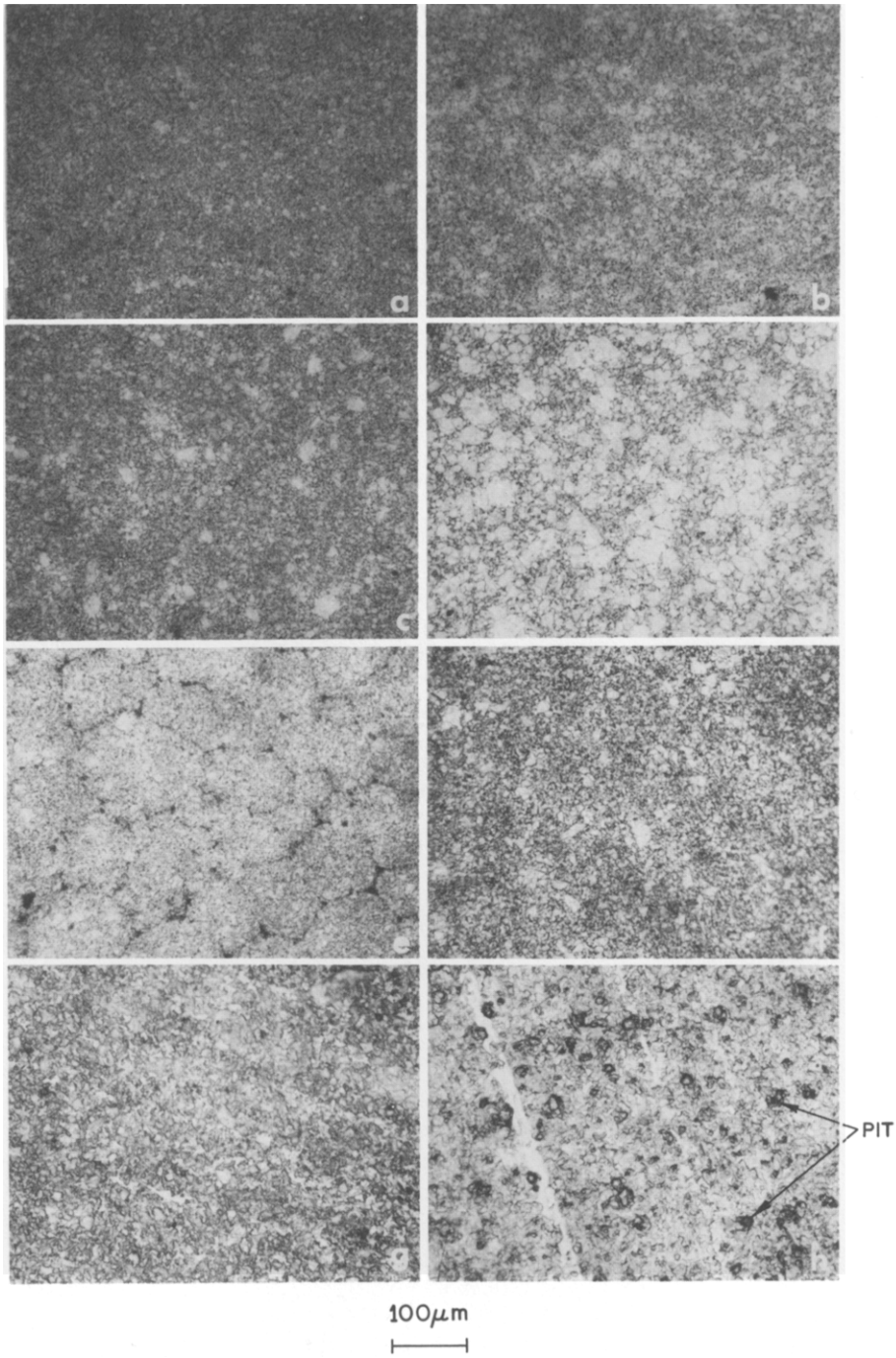

Fig. 7. Surface texture of high alumina substrates from different sources using reflective replica technique: (a, b, c, d, e, and f) as-fired surfaces, (g and h) ground surfaces.

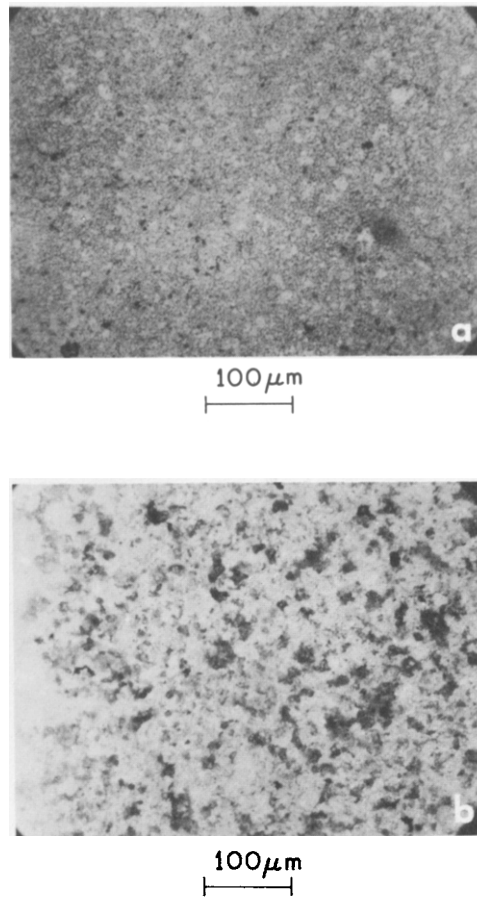

Fig. 8. Surface texture of ceramic substrates by the inking technique: (a) as-fired surface, (b) ground surface.

of the specimen. There are also commercial units known as microinterferometers specifically designed for such applications. An object field of 1200 μm diameter may be viewed at 162 $\times$ and 250 μm at 750 $\times$ with these instruments.

The OLM is more convenient for use in applications where an overall view of the surface is more important than a highly magnified view. An example of such a need may be found in the use of ceramic substrates for the manufacture of microelectronic circuits where the ceramic surface texture may affect the performance of the substrate. Consider for example the surface texture of a substrate shown in Fig. 7h. Such a surface would be undesirable in applications where beam leads of silicon chips or integrated circuits are to be bonded thereon. The area of the pit or open pore on the

substrate surface is about 25 % of the bonding area of a beam lead which is between 50 μm (0.002 in.) to 100 μm (0.004 in.) square. Unacceptable lead bond strengths would result even if there were no problem with the adherence of the metallization with the substrate. The large pit, which is a component of the substrate surface texture, would have easily escaped notice if only a small area of the surface were used in assessing the surface quality of the substrate. This would be the case if the transmission electron microscope, described later in this text, were used. At a magnification of 4000 × the field of view in a TEM is about 25 μm^2. Unless a large number of fields were inspected, the difference in surface textures between Fig. 7a and 7c may not be detected. One would expect more variation in the pull strength of beam leads bonded on surface of Fig. 7c or 7d than on that of Fig. 7a.

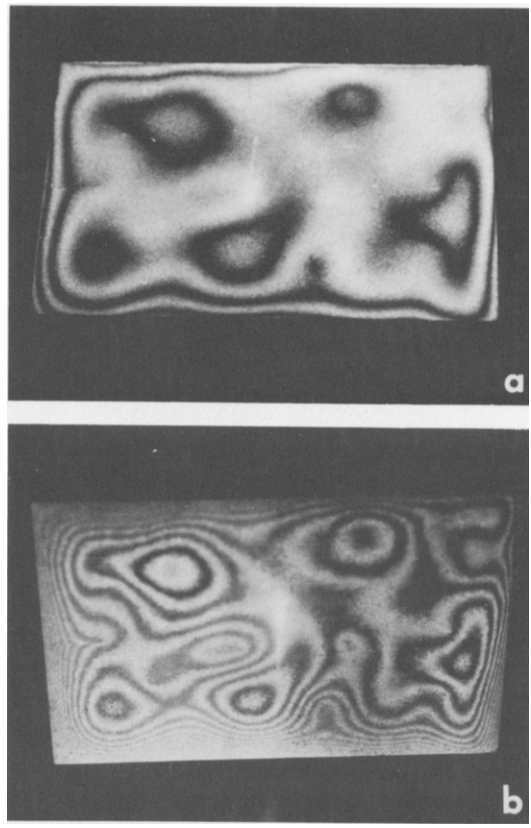

Fig. 9. Surface waviness delineated by Moire fringes: (a) fringe spacing = 0.002 in., (b) fringe spacing = 0.0005 in.

It is difficult as well as costly and time consuming to gather sufficient quantitative data with the OLM to provide statistical confidence for studying the functional relationship of surface texture and performance. Application of the digital computer and scanning devices in the analyses of images* by virtue of their differences in optical density (light intensity) may be the solution but would take much effort. The varying optical density of the image of a surface can be due to surface composition and parameters other than surface texture. Furthermore, the computer cannot distinguish the different types of features that will produce the same level of optical density.

For the detection of random flaws—burrs, pits, scratches, etc.—visual examination with oblique illumination of the surface is quite effective. Burrs less than 25 μm (0.001 in.) high but with lateral dimensions of 25 μm may be detected. It has the advantage over a laser scanning device of being able to differentiate the type of defects.

Although surface flatness or waviness on the macroscopic scale may be beyond the scope of surface texture, one might mention that visual methods utilizing Moire fringes are available. Figure 9 depicts the variation of height deviation of an alumina substrate from a reference plane observed with the Flatscope made by Accumet Engineering Corp., Massachusetts. The contour lines (Moire fringes) are 50.8 μm (2000 μin.) apart in Fig. 9a and 12.7 μm (500 μin.) in Fig. 9b. The spacing of the contour lines depends on the pitch of the gratings on the reference flat used. It should be noted that the contours observed by this technique could be due to either surface undulations or the wrinkling of the substrate as a whole.

2. Electron Microscopes

For studying surface features on the submicroscopic and microscopic scales, one may use the electron microscopes: the conventional transmission electron microscope (TEM) and the scanning electron microscope (SEM). A comparison of the operation of these instruments with the OLM is shown in Fig. 10.

With the TEM, an image of the object is formed by the transmission of electron beams, analogous to the light beam in an OLM operating with transmitted light illumination. The contrast of the image is primarily due to differential scattering of the electrons by different parts of the specimen with different mass density. For surface studies, a replica of the specimen surface must first be made. Techniques for making replicas are described by Philips *et al.* (1965). The contrast of the image can be enhanced by using shadowed replicas, and if the shadowing angle is known, quantitative information on the elevation of the surface asperities may also be obtained.

* Examples of commercial image and analyzers are the Quantimet 720 by Imanco, New York, the Micro-Videomat by Zeiss, and the QMS by Bausch & Lomb.

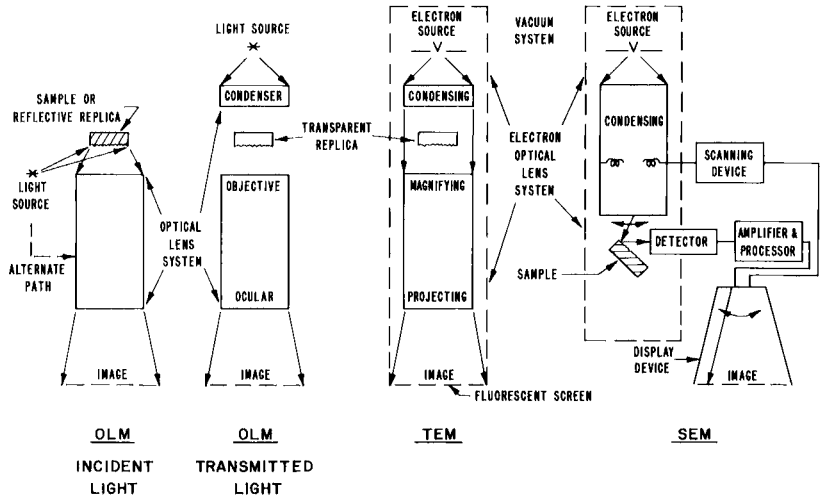

Fig. 10. Schematic diagram showing the operation of the optical light microscope (OLM), the transmission electron microscope (TEM), and the scanning electron microscope (SEM).

Under optimum conditions, resolution attainable with the TEM is 6.5 Å. Commercial units like the Elektros* ETEM, which uses electrostatic lenses, claim to give 10 Å resolution. The high resolution may be seen by considering that fast-moving electrons are optically equivalent to extremely short wavelength, λ, of light. Electrons moving with 90 eV has an equivalent λ of 1.3 Å. Resolution is inversely proportional to λ. Thus, resolution of the electron microscope is several hundred times better than the OLM which uses light of $\lambda = 5000$ Å. Magnification available starts from 300 × and goes as high as 300,000 ×, although practical magnification lies somewhere in between.

Image formation by the SEM is done by rastering the surface of the specimen with a focused beam of high energy electrons (usually about 5 to 30 keV) with a beam diameter of about 100 Å or less (Fig. 10). This motion is synchronized with the raster of the displaying screen unit, which may be a cathode ray tube or a TV screen, to form the image of the surface. The contrast of the image is controlled by the intensity of the secondary electrons, the back-scattered electrons, or whatever type of emission chosen that is generated by the scanning electron beam from the specimen surface. Better contrast is obtained with the higher energy back-scattered electrons, although the secondary electrons can reveal surfaces with reentrant cavities better since its path to the detector is curved in contrast to the case of back-scattered electron (Johari, 1968a).

* For references on electron microscopy, see Fischer (1953), Hall, (1966), Wischnitzer, (1970), Johari (1968), Thornton (1968), Kimoto (1973), Oatley (1972), and Hearle *et al.* (1972).

Change in magnification of the SEM is achieved by varying the traverse of the scanning electron beam on the specimen surface while maintaining the same raster on the display screen. If the area covered by the scanning beam is 10×10 μm and the size of the display screen is 10 mm $\times$ 10 mm, a linear magnification of 1000 $\times$ is obtained. One should be aware that the magnification is not the same in all directions in an SEM micrograph, if the specimen surface is tilted from the axis of the scanning electron beam, which is commonly done to obtain optimum contrast with secondary electrons. With some instruments, this difference in magnification is compensated by changing the traverse distance of the scanning beam on the specimen that is affected by the tilt. Figure 11 are SEM micrographs taken with such an instrument. From these micrographs, one may recognize that a large variance in the analyses of grain size by the intercept method would be expected if SEM micrographs were obtained with the specimen surface tilted from the axis of the scanning beam.

The highest practical magnification with the SEM is limited to 100,000 $\times$ and resolution to 250 Å (0.025 μm) or between 150 and 300 Å, depending on the instrument. In spite of these limitations, the SEM has many advantages over the TEM for the assessment of surface texture.

a. The specimen surface can be viewed directly, except for nonconductive materials where a thin ($\leq$ 500 Å) coating of conductive material such as carbon has to be applied over the surface to avoid charging of the surface when the SEM is operating at high voltages.
b. Much larger sizes of specimen can be accommodated in the SEM chamber. Some commercial units, e.g., CWIKSCAN/100 made by Coates & Welter Instrument Corp., California, can hold up to 3 in. specimens. Sampling of the surface is facilitated.
c. It has a large depth of field. At a magnification of 10^4, the depth of field is 1 μm under typical operating conditions (Oatley, 1972).
d. Stereograms can be easily obtained to provide a three-dimensional visual picture of a complex surface and which may also be used for quantitative measurements of elevation. For simple surface features, depth measurements can be made by introducing calibration lines (Hoover, 1971).
e. SEM signals are more adaptable for computer processing, which may ease the acquisition of quantitative data on the surface texture of the specimen under study. Work in this area has been reported by White *et al.* (1968, 1972).

In recent years, the cost of an SEM such as the Mini-Rapid Scan model made by International Scientific Instruments, Inc., with a capability of 50 to 12,000 $\times$, has come down to that of a fully equipped high power OLM. Only a few feet of bench space is required for its installation. The operation of some SEM is no more difficult than that of a high performance OLM.

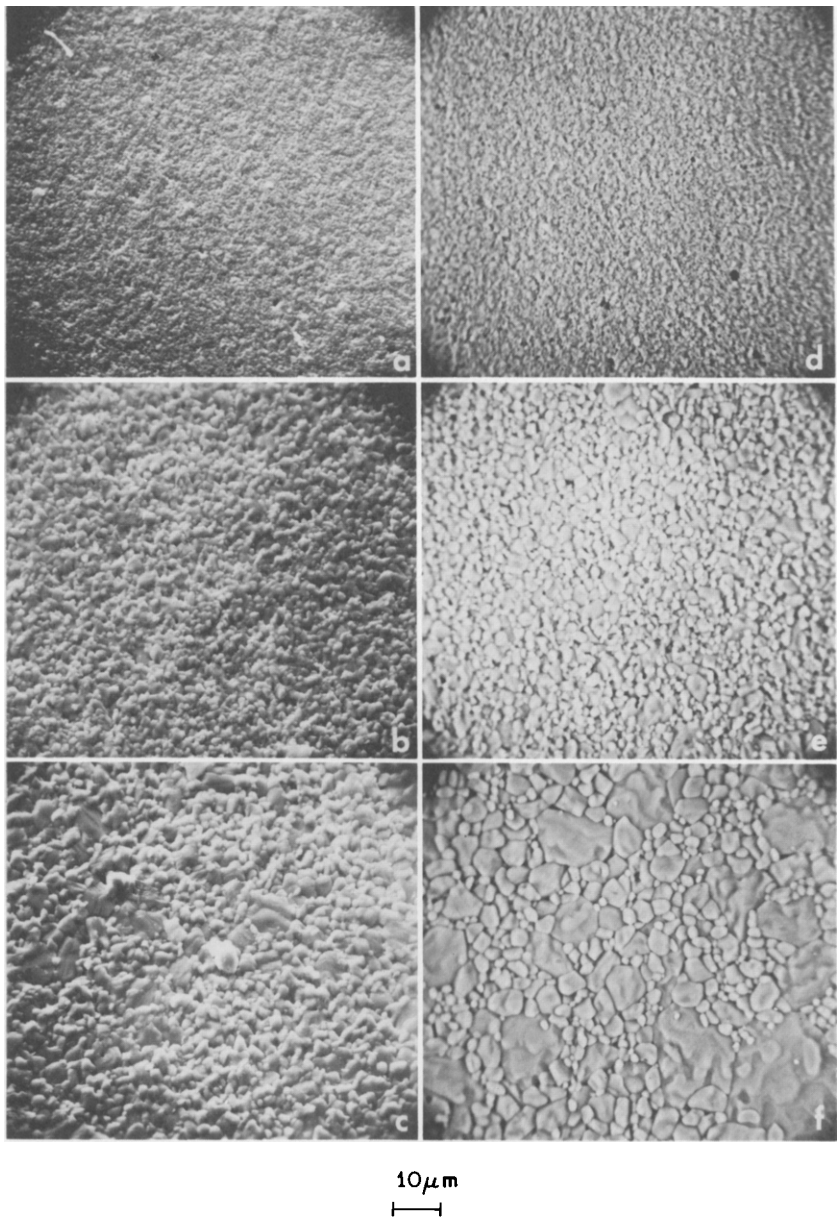

Fig. 11. SEM view of ceramic surfaces at 1000 × magnification: (a, b, and c) secondary electrons and 45° tilt; (d, e, and f) back-scattered electrons and 0° tilt.

3. *Tactile Trace Instruments*

Other than the light and electron microscopes, there are the tactile trace instruments for assessing surface texture on the microscopic to the submicroscopic scale. These instruments measure the surface irregularities by probing them with a mechanical stylus. They are capable of measuring vertical deviations in the range of 0.001 μm (0.04 μin.) to 100 μm. However, the fine resolution at the low end of the scale only holds for the case when the deviation is extended over a large lateral distance. Depending on the stylus size and geometry relative to those of the feature being measured, this distance may be 1000 to 10,000 times that in the vertical direction. This is somewhat analogous to the case with the interference microscope. Depth of submicroscopic crevices cannot be measured (Fig. 12). The standard diamond stylus of the Talysurf 4 instrument distributed by the Engis Equipment Co., Illinois, has a nominal 2.5 μm (0.0001 in.) tip. The shape of this tip is not spherical but may be likened to the truncated end of a rectangular based pyramid which has been rounded (Jungles and Whitehouse, 1970).

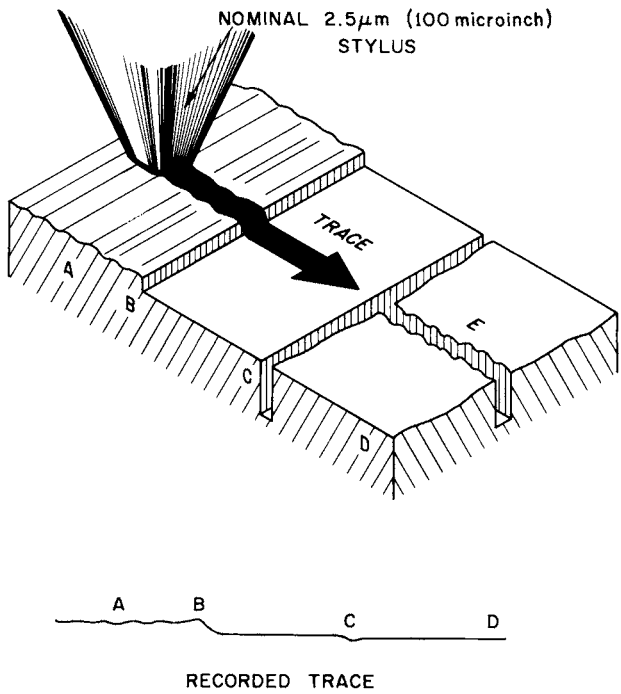

Fig. 12. Schematic diagram of a stylus traversing over a solid surface showing its limitation in representing the true surface topography.

One should also note that the graphical record of the surface irregularities obtained with these instruments is usually distorted due to the greater magnification used in the vertical direction than in the lateral direction. Their ratio is normally 10 : 1 and can be as high as 5000 : 1.

To have a proper conception of the representation of the surface texture produced by these instruments, one needs to be familiar with the workings of these instruments.* All stylus instruments convert the vertical motions of the stylus into electrical signals which are fed to a chart recorder to generate a graph of the surface undulation or to an average meter that gives an average

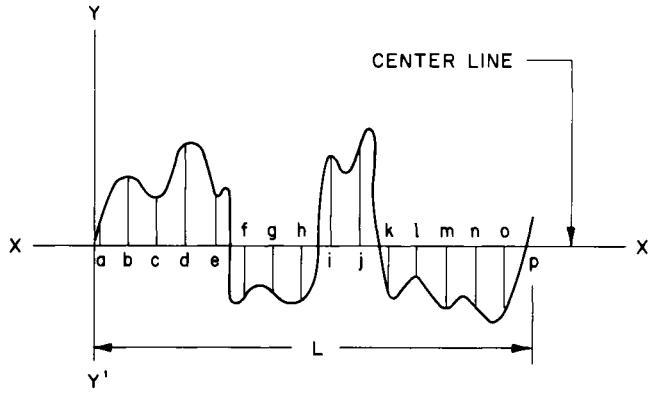

$$\text{CENTER-LINE-AVERAGE (CLA)} = \frac{1}{L}\int_{X=0}^{X=L} |y|\, dx$$

L = LENGTH OVER WHICH THE AVERAGE IS TAKEN

y = ORDINATE OF THE CURVE OF THE PROFILE

$$\text{CLA (APPROXIMATE VALUE)} = \frac{y_a + y_b + y_c + y_d \ldots + y_n}{n}$$

Fig. 13. Definition of center-line-average (CLA).

* For more information on stylus instruments, see Reason (1954, 1957, 1960), Miller (1964), Collart (1957), Eberhardt (1965), and Khol (1972).

roughness value. The most widely accepted roughness value in this country is the center-line-average, which is known in Europe as the arithmetic average (AA). The meaning of CLA is illustrated in Fig. 13. Some instruments also provide information on the maximum peak height or maximum depth of valley about the center line of the modified profile, as well as the total height from the highest peak to the lowest valley.

The major difference between these instruments is in the device used for converting the mechanical motion of the stylus into electrical signals. Some use a carrier modulating device. A carrier current is modulated by the position of the stylus with respect to the datum generated by the instrument through the use of a skid or shoe mounted in front of the stylus. The datum may also be generated by a probe mounted on the opposite side of the stylus such that it glides on a replaceable optical flat which may be set parallel to a plane containing a point on the specimen surface at the beginning and at the end of the stylus traverse. The response of this type of device is independent of frequency which in this context is the speed of the stylus traverse divided by the crest-to-crest spacing or the wavelength of the surface undulations.

If skids or shoes are used, distortion in the representation of the surface can result if the radius of curvature of the skid, its size, or its mounting position relative to the stylus, is improperly chosen. Waviness or crest-to-crest distance of the surface undulation greater than the skid dimension would not be detected. Correct choice of skid requires a prior knowledge of the surface texture to be measured. There is also the possibility of disturbing or ploughing the surface by the skid due to its weight. This may not be problematic with hard surfaces but can cause poor reproducibility of results with soft surfaces. For estimating the maximum pressure $\hat{P}$ of the stylus on the surface, one might use the following expression (Shigley, 1956):

$$\hat{P} = 2P/\pi BL \tag{1}$$

where P = applied load (lb), L = effective length of the stylus (in.), $B = \frac{1}{2}$ the contact area of the stylus with the surface (in.^{2}) expressed by the hertzian formula for the condition of a roller in contact with a plane surface. $B = [4PD(1-\mu^2)/\pi LE]^{1/2}$ in which D = mean diameter of roller (stylus) in inches, μ = Poisson's ratio, and E = Young's modulus of the substrate material in psi. In ASA B46.1-1962, the standard for surface finish measurements with stylus instruments, the recommended stylus force is given by the following relationship:

$$\text{Maximum force (grams)} = 0.00001\ [\text{tip radius (microinches)}]^2 \tag{2}$$

Thus, based on Eq. (1), the maximum pressure exerted by a stylus with a tip of 2.5 μm (100 μin.) diameter and 2.5 μm long using a force obeying the

relationship of Eq. (2) is approximately 300,000 psi in compression on an alumina substrate with $E = 50 \times 10^6$ psi and $\mu = 0.25$.

The carrier-modulating type of instrument when used with a stylus that generates the datum by the optical flat described, is useful for assessing the roughness and profile of flat, as well as curved surfaces. The Talysurf 4, the Hommel Analyzer, and the Proficorder are examples of such instruments.

Other types of stylus instruments use devices that will generate a current or voltage by the vertical motions of the stylus. The response of these devices are frequency dependent and are not suitable for measuring profiles, since they are not sensitive to long range waviness or surface undulations with large crest-to-crest spacings. Then there are the instruments which relate the average velocity of the vertical motions of the stylus to the average roughness height. This representation is only valid for surface undulations of pure sinusoidal waves.

With all stylus instruments using electrical devices, the electrical frequency f of the readout instrument is related to the wavelength λ of the surface irregularities by the following expression:

$$f = \text{traverse speed of the stylus}/\lambda \tag{3}$$

The output depends on the response curve of the instrument with respect to the frequency spectrum as shown in Fig. 14. The dropoff at the high frequency end is the consequence of the size of the stylus. At the lower end of the spectrum, the attenuation is inherent to the device or purposely introduced by a wave filter to separate the short range undulations (roughness) from the long range undulations which one may choose to exclude in the readout of the instrument. The crest-to-crest distance of this long range undulation is known as the cutoff wavelength λ or roughness width cutoff. It is effectively the sampling length L shown in Fig. 13. Thus, the roughness of the surface indicated by a stylus instrument will depend on the chosen cutoff value

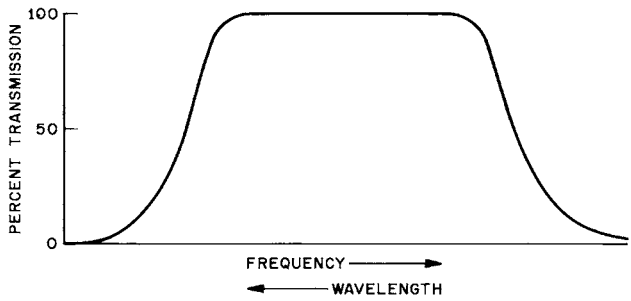

Fig. 14. Response curve.

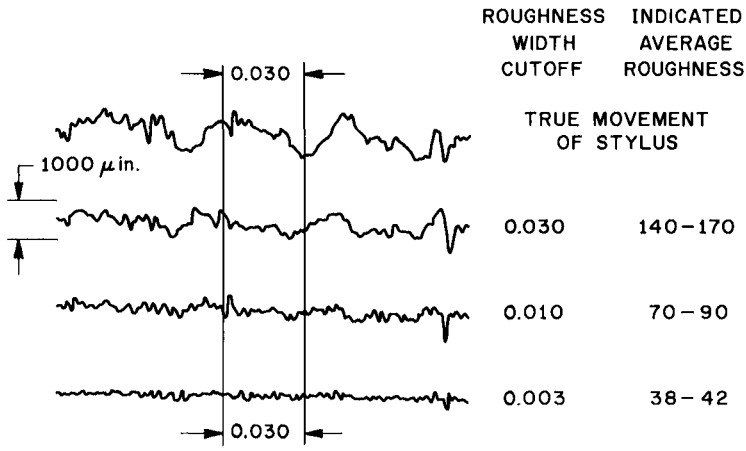

Fig. 15. Effect of cutoff wavelength on CLA values. Extracted from "Surface Texture" Rep. No. ASA B46.1-1962) with the permission of the publisher, The American Society of Mechanical Engineers.

(Fig. 15). It is apparent that the roughness cutoff value is a parameter that must be specified in order to obtain valid data for comparative purposes.

Concerning precision of CLA values, von Weingraber (1969) shows that values measured on a specimen can have a scatter of ± 13 % around their mean using the same instrument. The mean values for the same specimen obtained with different instruments can deviate from the overall mean by as much as ± 15 % in some cases. He attributes the scatter largely to the uncertainty of the calibration operation and peculiarities of the individual instrument. The results of his study indicate that agreement in CLA values on the same specimen by different laboratories is only possible to within ± 8 %.

Since one is often tempted to use CLA to represent the physical surface characteristic of ceramics in studying its relationship to ceramic behavior and performance, it is pertinent to point out that CLA measures only one of the many facets of the physical character of the surface. As shown by Lo (1972), CLA does not totally distinguish the surface texture of ceramics (Fig. 16). Comparing the surface textures of the samples with their recorded traces in Fig. 16, one may further note that the CLA of the samples indicated quantifies only the undulations within the sampling length chosen, i.e., 0.030 in. Waviness on a larger size scale, i.e., $\lambda > 0.030$ in. present in the sample of Fig. 16b is not included in the CLA readout. Because of stylus size limitations, crevices of micron and submicron sizes would also contribute little to the CLA values. This would preclude the establishing of a relationship of CLA with dye retention characteristics and the fracture strengths of ceramics if

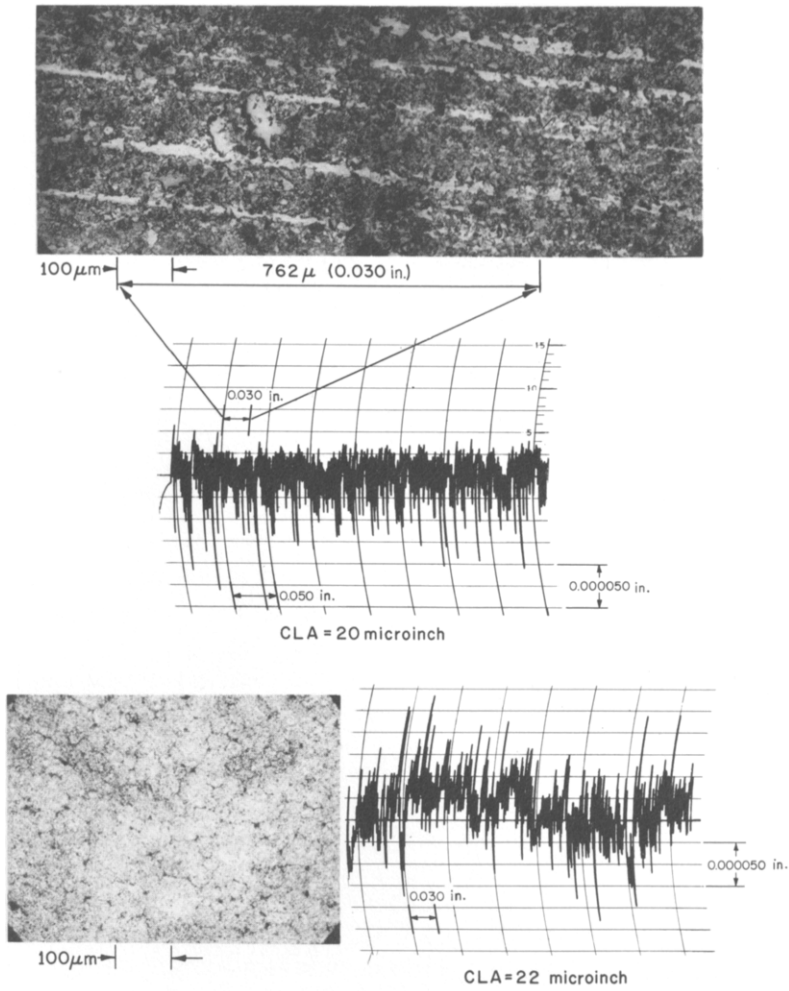

Fig. 16. Surface texture vs. CLA values. The trace is recorded by a Proficorder with a stylus of 500 μin. (12.7 μm) radius. Each vertical division = 25 μin. (0.64 μm) and each horizontal division = 50,000 μin. (1270 μm). The ratio of vertical magnification/horizontal magnification is 1000/1.

these properties were controlled by the geometry and amount of these small crevices. Correlating CLA with ceramic behavior or performance that is dependent on the true surface area A_t of the ceramic will also be futile because CLA is not functionally related to A_t (Marian, 1962). It is interesting to note that A_t of ceramic substrates can be greatly influenced by its surface grain shape rather than its grain size under certain conditions.

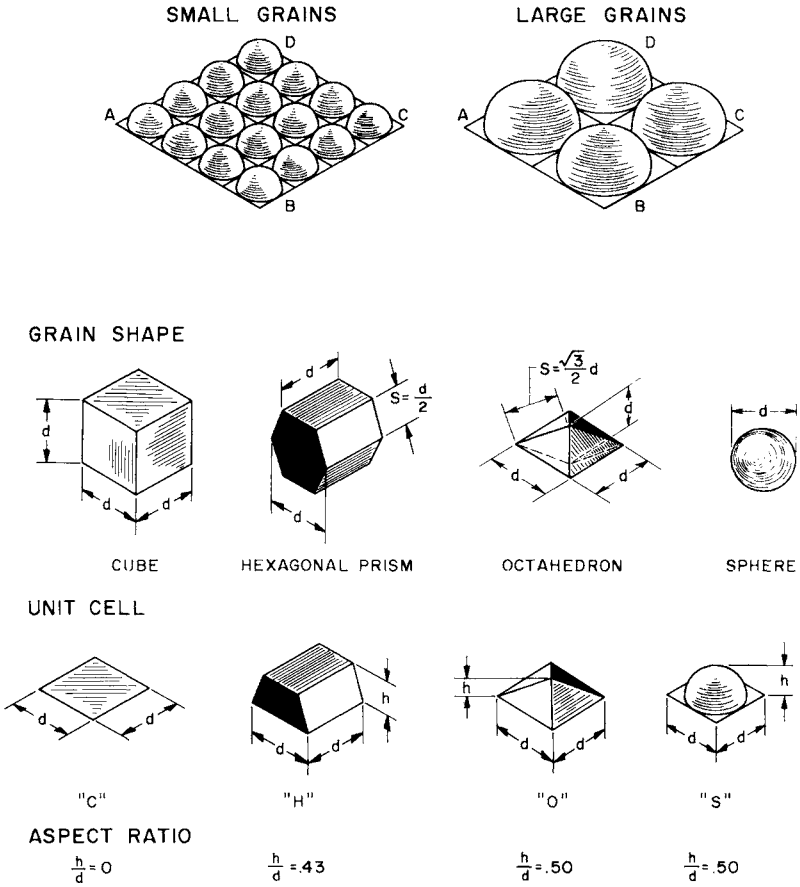

Fig. 17. Grains of "equal" size but different geometry.

To illustrate the effect of grain shape on A_t, let us consider four simple grain shapes, a cube, a hexagonal prism, an octahedron, and a sphere (Fig. 17). It is difficult to speak of equal grain size when we have grains of different geometry. But let us take equal size to mean that the dimension d of the four different grains shown in Fig. 17 to have the same value. Corresponding to these grain shapes, we can create four different unit cells, "C", "H", "O", and "S", which may be used to fill an area on the surface bounded by the line ABCD. The surface area of the unit cell is Kd^2, where K is a constant whose value depends on the goemetry of the grain. The true surface area of ABCD will be expressed by

$$A_t = NKd^2 \tag{4}$$

where N is the number of unit cells that can fit into the nominal area A of ABCD. Since $N = A/d^2$, Eq. (4) may be written as

$$A_t = KA \tag{5}$$

which shows that A_t is only dependent on the grain shape and not the grain size. This means that A_t of the area ABCD filled with small grains is equal to that filled with large grains of the same geometry (Fig. 17). Notice, however, that the volume of material above the base plane ABCD in the two cases is not the same. In practice, this condition may be realized if raw materials having grains of the same shape but different sizes were used to produce these substrates. If the difference in surface grain size of substrates is achieved by difference in sintering schedules, the geometry of the large grains would not be the same as that of the small grains. But the volume above the base plane would remain practically constant. In this case, A_t of the surface with the large grains could be smaller than that with the small grains.

From Fig. 18, it is apparent that the effect of grain shape on A_t is by no means trivial, and that a wide range of A_t values can be obtained by combin-

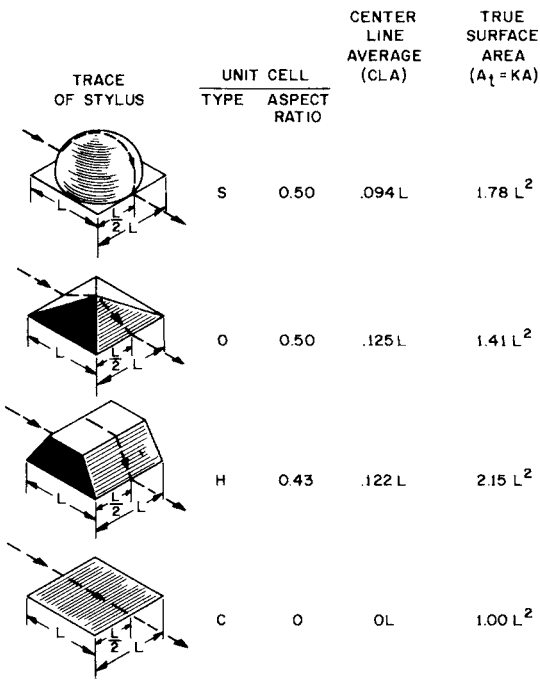

Fig. 18. Effect of grain shape on true surface area A_t and center-line-average values. L, sampling length; A, nominal area of surface; K, geometric factor.

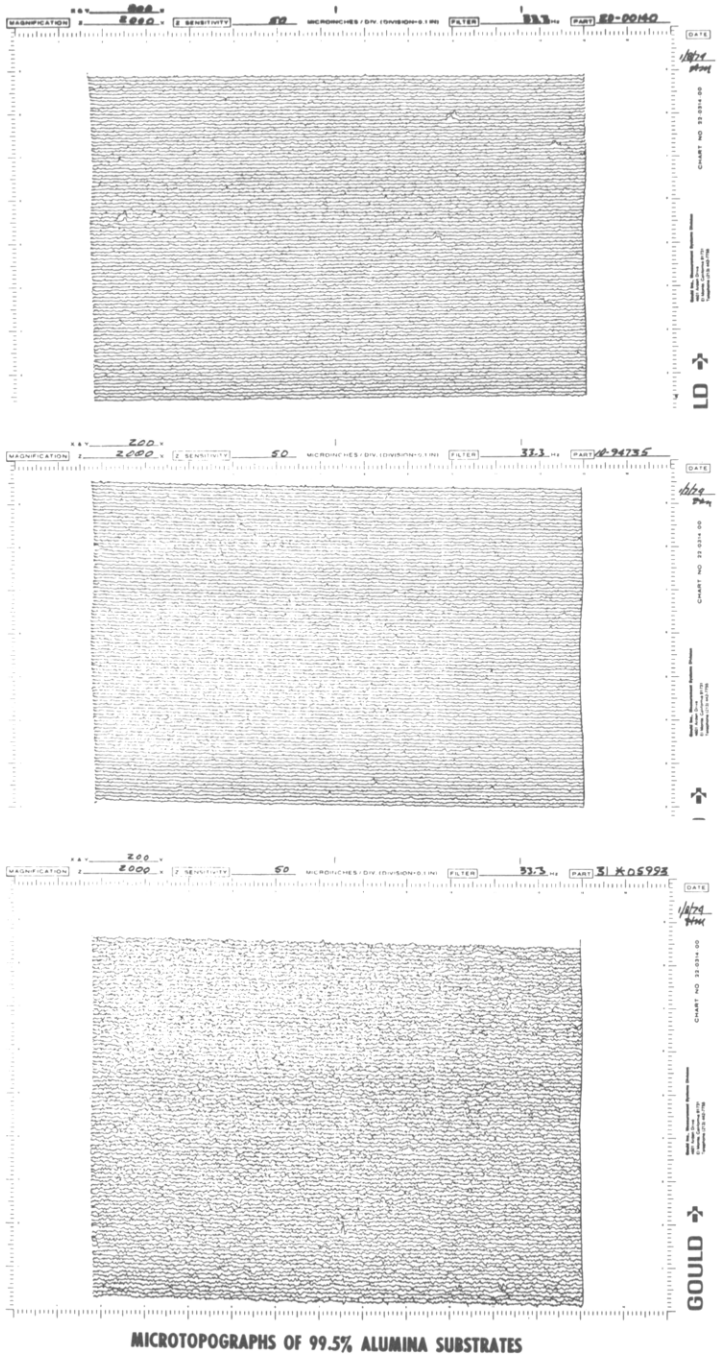

Fig. 19. Microtopographs of ceramic surfaces obtained by a stylus instrument.

ing different unit cells. It appears that differences in A_t could be used as a logical basis for explaining observed variations in sheet resistance of thin films and lead-pull strength of terminals bonded on thin films deposited on substrates with different surface textures (Melroy, 1970; Lo, 1970; Lo and Menzel, 1970).

Finally, one might mention that a stylus type instrument (the Microtopographer MT-200 made by Gould Inc., California) is also available for measuring surface texture or mapping the surface geometry in three dimensions of a specimen as large as 2 in. × 2 in. The map is a series of parallel profiles of the surface made on an X-Y recorder chart and stacked vertically (Fig. 19). Obviously the limitations of stylus instruments discussed earlier also apply to this instrument.

III. Summary

Besides advancing our knowledge, the study of the functional relationship of surface texture or its components with performance in the application of ceramics has important economic justifications.

After reviewing the various indirect and direct methods currently available for assessing surface texture and the significance and limitations of these methods, one may conclude that much remains to be done to arrive at the stage where meaningful quantitative data sufficient to establish statistical confidence for studying the role of surface texture can be easily acquired.

ACKNOWLEDGMENTS

The author wishes to thank A. C. Dumbri for providing the SEM pictures, D. R. Wonsidler for the microprobe analyses, D. T. Hawkins for his aid in the literature search, Y. S. Kim, R. C. Sundahl, J. C. Williams, and many of his colleagues for reviewing the manuscript. He is also grateful to W. B. Grupen and B. E. Nevis for their encouragement and critical comments.

References

Allen, A. W., and Friedberg, A. L. (1948). *J. Amer. Ceram. Soc.* **31**, 83–88.
Allen, R. M. (1958). "Photomicrography." Van Nostrand-Reinhold, Princeton, New Jersey.
Barron, A. L. E. (1965). "Using the Microscope." Chapman & Hall, London.
Bennett, H. E. (1964). U.S. Patent 3,160,752.
Berrin, L., and Sundahl, R. C. (1971). In "Characterization of Ceramics" (L. I. Hench and R. W. Gould, eds.), pp. 583–624. Dekker, New York.
Brunauer, S., and Emmett, P. H. (1973). *J. Amer. Chem. Soc.* **59**, 2682–2689.
Caulton, M. (1971). *Proc. IEEE* **59**, 1481–1489.

Chamot, E. M., and Mason, C. W. (1958). "Handbook of Chemical Microscopy." Wiley, New York.
Collart, K. S. (1957). *Prod. Eng.* **28**, 82–83.
Eberhardt, H. W. (1965). *Prod. Eng.* **36**, 105–107.
Fisher, R. B. (1953). "Applied Electron Microscopy." Indiana Univ. Press, Bloomington.
Gregg, S. J., and Sing, K. S. W. (1967). "Adsorption, Surface Area and Porosity." Academic Press. New York.
Hall, C. E. (1966). "Introduction to Electron Microscope." McGraw-Hill, New York.
Hartley, W. G. (1962). "Microscopy." English Universities Press Ltd., London; American edition by J. J. Lee and B. Friedman, Natur. Hist. Press, New York, 1964.
Hearle, J. W. S., Sparrow, J. T., and Cross, P. M. (1972). "Use of the Scanning Electron Microscope." Pergamon, Elmsford.
Hensler, D. (1972). *Appl. Opt.* **11**, 2522–2528.
Hensler, D., Soos, N. A., Haas, E. H., Frankson, R. W., and Rott, D. A. (1973). *Amer. Ceram. Soc., Bull.* **52**, 191–194.
Hoover, R. A. (1971). *J. Phys. E.* **4**, 474–479.
Johari, O. (1968a). *J. Metals* **20**, 26–32.
Johari, O. (1968b). *Metal Progr.* **94**, 147–150.
Jungles, J., and Whitehouse, D. J. (1970). *J. Phys. E.: Sci. Instr.* **3**, 437–440.
Khol, R. (1972). *Mach. Des.* **44**, 86–91.
Kimoto, S. (1972). *JOEL News* **10**, No. 2, 1–31 (published by JEOL Ltd., Tokyo, Japan).
Lang, W. (1969a). *Zeiss Inform.* **16**, No. 70, 114–120.
Lang, W. (1969b). *Zeiss Inform.* **17**, No. 71, 12–16.
Lang, W. (1970). *Amer. Lab.* **2**, 45–51.
Lo, W. C. (1969). Bell Lab. Tech. Rpt. (unpublished).
Lo, W. C. (1970). Bell Lab. Tech. Rpt. (unpublished).
Lo, W. C. (1972). *Nat. Bur. Stand. (U.S.), Spec. Publ.* **348**, 301–307.
Lo, W. C., and Menzel, P. (1970). Bell Lab. Tech. Rpt. (unpublished).
McCauley, R. M., and Van Winkle, Q. (1962). WADD-TR-60-520 Part I, Ohio State Univ. Res. Foundation, Columbus, Ohio; available from National Technical Information Service, AD275617.
McCauley, R. M., and Van Winkle, Q. (1963a). WADD-TR-60-520 Part II, Ohio State Univ. Res. Foundation, Columbus; available from NTIS, AD401499.
McCauley, R. M., and Van Winkle, Q. (1963b). WADD-TR-60-520 Part III, Ohio State Univ. Res. Foundation, Columbus; available from NTIS, AD426833.
McCauley, R. M., and Van Winkle, Q. (1964). WADD-TR-60-520 Part IV, Ohio State Univ. Res. Foundation, Columbus; available from NTIS, AD606217.
McKinney, K. R., and Herbert, C. M. (1970). *J. Amer. Ceram. Soc.* **53**, 513–516.
Marian, T. E. (1962). *ASTM Spec. Publ.* **340**.
Miller, B. S. (1964). *Metalworking* **20**, 39–45.
Oatley, C. W. (1972). "The Scanning Electron Microscope." Cambridge Univ. Press, London and New York.
Orr, C., Jr., and DallaValle, T. M. (1959). "Fine Particle Measurement Size, Surface, and Pore Volume." Macmillan, New York.
Philips, A., Kerlins, V., and Whiteson, B. V. (1965). ML-TR-64-416, Douglas Aircraft Co.; available from NTIS, AD612912.
Radl, Z., and Kunc, B. (1970). *Tesla Electron* **3**, 24–25.
Reason, R. E. (1954). *J. Inst. Prod. Eng.* **33**, 263–276.
Reason, R. E. (1957). *Prod. Eng.* **28**, 77–81.
Reason, R. E. (1960). "The Measurement of Surface Texture." Cleaver-Hume, London.
Richardson, J. H. (1971). "Optical Microscopy for the Material Sciences." Dekker, New York.

Ross, S., and Wiltshire, I. J. (1966). *J. Phys. Chem.* **70**, 2107–2111.
Sanders, D. M., and Hench, L. L. (1973). *Amer. Ceram. Soc., Bull.* **52**, 666–669.
Shenk, R., and Kistler, G. (1962). "An Introduction to the Principles of the Microscope and its Application to the Practice of Photomicrography." Chapman Hall, London.
Sherif, I. I., and Mahmound, N. S. (1966). *J. Appl. Phys.* **37**, 2193–2194.
Shigley, J. E. (1956). "Machine Design," pp. 31–32. McGraw-Hill, New York.
Stokes, R. J. (1972). *Nat. Bur. Stand. (U.S.), Spec. Publ.* **348**, 344–352.
Tester, T. W., and Herrick, C. C. (1972). *Rev. Sci. Instrum.* **43**, 530–535.
Thornton, P. R. (1968). "Scanning Electron Microscopy." Chapman & Hall, London.
Tolansky, S. (1955). "An Introduction to Interferometry." Longmans, Green, New York.
Tolansky, S. (1960). "Surface Microtopography." Wiley (Interscience), New York.
Tolansky, S. (1968). "Microstructure of Surfaces." Amer. Elsevier, New York.
Torrance, K. E., and Sparrow, E. M. (1965). *J. Heat Transfer* **87**, 283–292.
von Weingraber, H. (1969). UCRL-Trans-10398, Lawrence Radiation Lab., Livermore, available from NTIS, PB 188141T; CIRP Annelen **18**, 63–76, 1970.
Wenzel, R. N. (1936). *J. Ind. Eng. Chem.* **8**, 988–994.
Westbrook, J. H. (1968). *Surface and Interfaces; Proc. Sagemore Army Mater. Res. Conf., 14th, 1967* pp. 95–138.
White, E. W., McKinstry, H. A., and Johnson, G. G., Jr. (1968). *Proc. Scanning Electron Microsc. Symp., 1968* pp. 95–103.
White, E. W., McKinstry, H. A., and Diness, A. (1972). *Nat. Bur. Stand. (U.S.), Spec. Publ.* **348**, 309–316.
Wischnitzer, S. (1970). "Introduction to Electron Microscopy." 2nd. Edition. Pergamon, Oxford.
Zimon, A. D., and Serebryakov, G. A. (1971). *Russ. J. Phys. Chem.* **45**, 163–165 and 249–250.
Zimon, A. D., and Serebryakov, G. A. (1972). *Russ. J. Phys. Chem.* **46**, 1, 126–130.

Crystal Growth

CHANDRA P. KHATTAK

Brookhaven National Laboratory
Upton, New York

I. Introduction

A treatise on ceramic processing would not be complete without the mention of crystal growth. This article is not intended to deal extensively with this subject but, rather, to give an overview of the various growth processes.

Natural crystals have been recognized and valued since prehistoric times when their principal use was in decorative jewelry. The demand on materials in modern times has made it necessary to grow "artificial" crystals for use in research and various optical and electronic devices.

Although many material properties may be obtained from polycrystalline samples, in most cases single crystals are needed for more detailed studies. Polycrystals contain grain boundaries and these may greatly affect the measurement of certain bulk properties. For example, the electrical conductivity of semiconductors is a very sensitive function of impurity content, and foreign atoms tend to segregate at the grain boundaries. Therefore, single crystals are necessary for these measurements of the intrinsic properties of semiconductors. Moreover, many of the electrical and mechanical properties of polycrystalline materials are directly related to both grain size and orientation and measured values will vary depending on the method of preparation. Therefore, for studies of anisotropic properties, property tensors, complex structure, etc., single crystals are essential. In recent years, single crystals have

been found to be a prerequisite for important studies in solid state physics and chemistry.

Because large natural crystals are scarce and expensive, much research has been applied to producing both those crystals found in nature and crystals tailored for many applications, especially in electronics and optics.

Large scale commercial production of crystals was first undertaken when the transistor industry came into being, although earlier large sapphire and quartz crystals were grown and marketed. Today single crystals have found important practical applications in a number of devices. These applications include tunnel diodes (GaAs), filters and oscillators (quartz, YIG), lasers ($CaWo_4$, YAG, InP, ruby), laser modulators (KDP, $LiNbO_3$, $LiTaO_3$), and radiation detectors (KCl, Si, GaAs).

Preparation of single crystals is essentially a nucleation and growth process. It is imperative to keep the number of nucleating sites at a minimum but, at the same time, encourage the growth of favorably situated nuclei. This involves having conditions for the formation of the proper phase, transportation to the nucleating site, and coherent growth of the new material onto the existing mass. It is always desirable to grow crystals at the lowest possible temperature. Besides being experimentally convenient, low defect density, more perfect, less contaminated crystals are formed under these conditions. Moreover, certain undesirable phase changes and evaporation losses can also be avoided. In some cases certain materials, called dopants, are purposely added. Whether the impurity has been deliberately added or already existed in the starting material, the system can still be considered as monocomponent. Polycomponent growth may be as simple as the synthesis of quartz (Si–O system) or as complex as the growth of Ba_2CoWO_6 (Ba–Co–W–O system). In some cases it is possible to reduce the temperature at which growth takes place by the selection of a suitable solvent, called a flux. As was pointed out earlier, this technique allows the growth of refractory single crystals to take place under experimentally more favorable conditions.

Single crystals may be grown from the vapor, liquid, or solid phases.

II. Crystal Growth by the Vapor–Solid Process

This technique of crystal growth has found wide applications for epitaxial films. An excellent review of this process has been given by Ellis (1968). Monocomponent or polycomponent systems can utilize this process. It involves the sublimation and condensation of the desired material. This can be done in closed tubes, in the presence of a carrier gas, or by evaporation in vacuum (Fig. 1). This technique has been utilized for metals (Brenner, 1963),

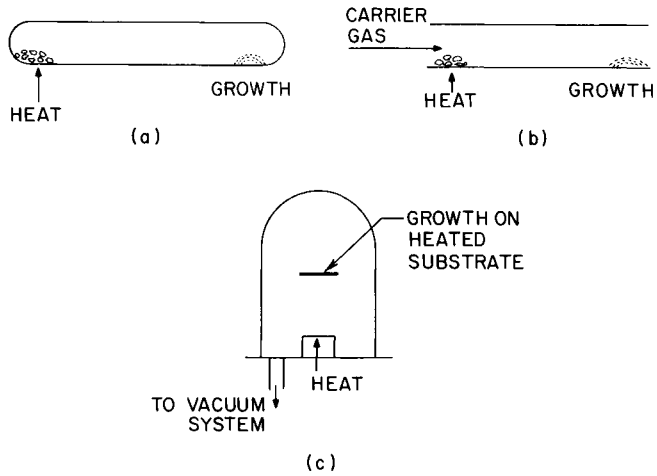

Fig. 1. Crystal growth by vapor transport: (a) sublimation and condensation, (b) using a carrier gas, (c) vacuum evaporation.

organic compounds (Bradley, 1963), sulfides (Reynolds, 1963), silicon (Glang and Wajda, 1963), silicon carbide (O'Connor, 1963), and ice (Mason, 1963).

Sometimes volatilization of materials is brought about at lower temperatures by the application of an electric field. This process is called sputtering. Although polycrystalline or amorphous films are generally obtained, it is possible to make single crystal films. In the case of a multicomponent system simultaneous sputtering (co-sputtering) of different materials is carried out (Theuerer and Hauser, 1964, 1965).

Single crystals have been grown by the reduction of halides. In such instances it is also referred to as a chemical vapor transport process. This process has been adopted for metals (Brenner, 1963), oxides (Fonstad *et al.*, 1969), and intermetallic compounds like Nb_3Sn (Hanak *et al.*, 1964).

III. Crystal Growth by the Liquid–Solid Process

The most useful method of growing large crystals falls under this category. This method and later modifications was first used by Bridgman (1925) and later modified by Stockbarger (1936). This technique produces nucleation on a single solid–liquid interface. It is achieved by holding the molten material in a crucible with a pointed tip and passing it through a furnace with a suitable gradient (Fig. 2). Modified versions of this method moved the furnace instead of the crucible. Detail reviews of this technique have been reported

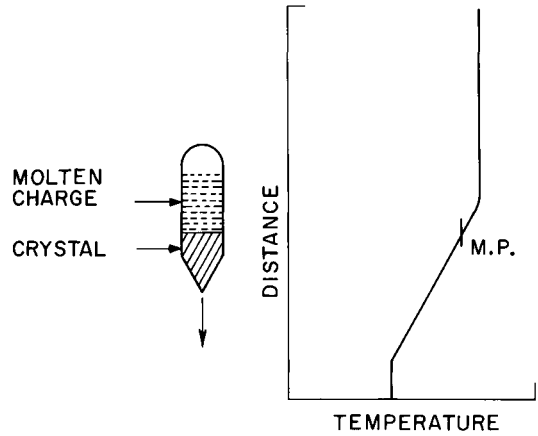

Fig. 2. Directional solidification from the melt (Bridgman growth).

(Buckley, 1951; Lawson and Nielson, 1958; Tanenbaum, 1959; Schadler, 1963). This technique is generally utilized for monocomponent systems in sealed crucibles. One of the problems encountered in this method is the establishment of the optimum thermal gradient—too big a gradient may lead to the formation of a number of nuclei and too small a gradient supercools the melt. Both cases would lead to the formation of small crystals.

A technique of pulling a crystal from the melt was first practiced by Czochralski (1917). At first this method was applied to low melting metals. Recently it has been utilized for the growth of semiconductors and laser host materials (Nassau and Van Uitert, 1960; Johnson and Nassau, 1961; Nassau and

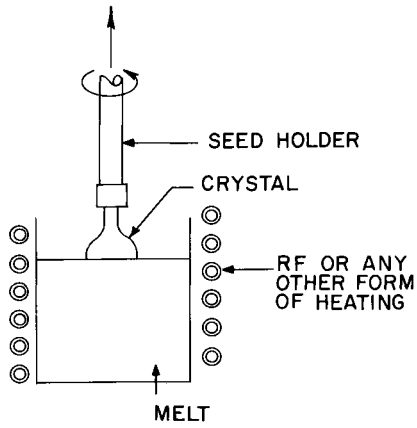

Fig. 3. Drawing crystal from the melt (Czochralski growth).

Broyer, 1962a,b). This technique involves heating the material to a molten state, immersing a small oriented single crystal of the host material, called a "seed," in the melt and withdrawing it slowly (Fig. 3). The rate of pulling should be compatible with the growth rate of the material.

A number of ceramic materials have high melting points or are incongruently melting. Such materials are commonly grown by the flux method. The most common fluxes or solvents are halides or low melting oxides like KF, PbO, PbF_2, B_2O_3 or mixtures of these. The choice of the solvent plays a major part in the flux growth processes. It should have high solute solubility, low solubility in the growing crystal, low viscosity, low volatility, and should not react with the crucible. In most cases the choice of the flux is guided by intuition or by analogy with other known systems.

The technique of flux growth involves the heating of the flux and material until molten, thereafter controlling the nucleation and growth to yield single crystals. This could be achieved by evaporation of the flux or slowly cooling of the melt. The flux may be solidified with the material or drained from the crucible prior to its freezing. In certain cases the crystal is pulled out of solution. A number of fluxed-growth techniques have been developed and described in literature (Laudise, 1963, 1970; White, 1965; Anthony and Collongues, 1972; Brice, 1973).

A variation of the Czochralski method is the Kyropoulos technique, which utilizes a flux. Growth is achieved by cooling the seed holder or by slowly cooling the melt. In this process there is no pulling involved (Fig. 4).

Of the various methods known for the fluxed growth of single crystals a process of particular interest is the top-seeded solution (TSS) growth technique (Linz, 1965; Hurst and Linz, 1971). This is a very versatile technique and adaptable to a variety of systems.

The material is taken up in solution in the hot zone of a furnace and a seed crystal attached to a platinum tube is dipped into the melt which forms the nucleation site. Air cooling of the platinum tube makes the seed a preferred

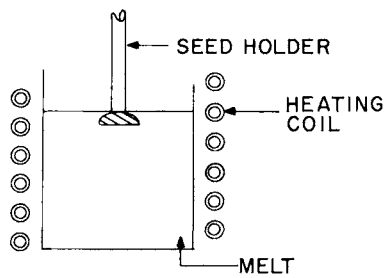

Fig. 4. Growth on a "seed" (Kyropoulos method).

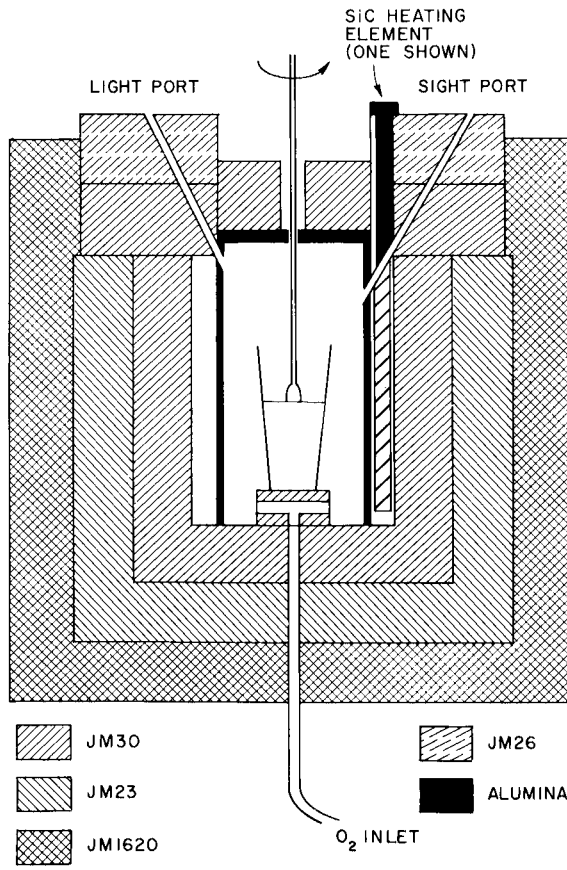

Fig. 5. Top-seeded solution growth. [From J. J. Hurst and A. Linz, *Mater Res. Bull.* **6**, 163–168 (1971), by permission of Pergamon Press.]

nucleation site. A schematic diagram for this process is shown in Fig. 5. This technique has been utilized for the growth of crystals of complex systems (Khattak, 1973; Khattak and Hurst, 1973). It provides an advantage over the flux method in that the liquid–solid interface can be viewed during the growth process, and it is also possible to control the process so that there is one nucleating site.

Other processes falling under this general category utilize high pressure and temperature to increase the solubility of the desired phase. This technique is generally referred to as hydrothermal crystal growth. Two commercially important materials are grown by variations of this technique. Synthetic quartz (Laudise and Sullivan, 1959) and diamond (Bundy *et al.*, 1955) are synthesized at high temperatures and pressures.

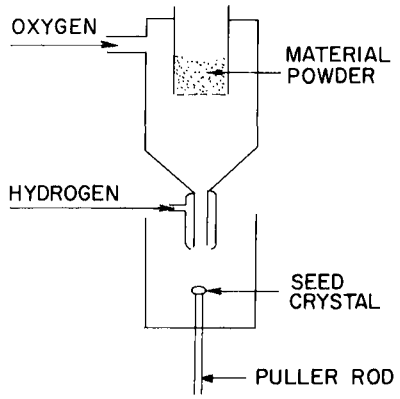

Fig. 6. Crucibless growth (Verneuil process).

In most crystal growth methods, the reaction is carried out in a crucible, which could be a source of impurities. Therefore, techniques not using crucibles were developed in which the liquid phase of the material is held to the solid by surface tension. Two such methods are the Verneuil named after its inventor (Verneuil, 1902) and the floating-zone technique developed by Keck and Golay (1953).

In the Verneuil process, historically an old technique, the material is shaken as a powder through a flame where it melts and the liquid drops on top of the seed crystal. A simple diagram of the apparatus used for this technique is shown in Fig. 6. This process has been used for the growth of ruby (Silnichenko and Gritsenko, 1965), emerald (Gentile *et al.*, 1963), and

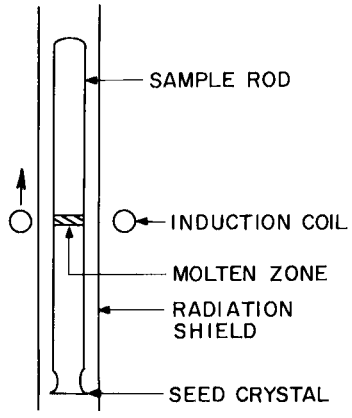

Fig. 7. Zone fusion process (float-zone technique).

other oxides (Gillette, 1950; Merker, 1955; Lefever and Chase, 1962; Haldane and Sedlacek, 1963; Gambino, 1965).

The float-zone technique involves the principle of zone refining. Here the liquid is held between two columns of solid by surface tension. The apparatus is a single turn induction coil or electron gun which moves slowly up the solid rod. This is illustrated in Fig. 7. This technique has been applied to high surface tension metals (Keck *et al.*, 1954; Cunnell and Wickham, 1960; Brilliantov *et al.*, 1961; Zhimskaya, 1963) as well as oxides (Brown and Todt, 1964; Class, 1968; Okada *et al.*, 1971; Falckenberg, 1972; Takahashi *et al.*, 1972).

IV. Crystal Growth by the Solid–Solid Process

This process is essentially secondary crystallization of the material. It is a low temperature process but there is no control on the shape, size, and orientation of the crystal produced. The main disadvantage is that since the growth takes place in the solid the number of the nucleating sites is very high and results in the formation of a number of crystals. This method is often limited to metallic systems. Cold-worked metals have a fine grained structure and strain annealing can result in the formation of larger grains, as shown in Fig. 8. Large grains can also be achieved by passing the solid through a phase transformation. Under these circumstances the fine grained material is replaced by larger grains of the low temperature form. A review of these processes is given by Aust (1963).

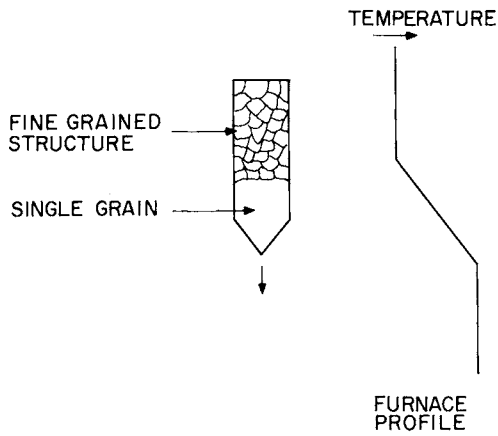

Fig. 8. Growth from the solid (strain annealing method).

ACKNOWLEDGMENT

The author wishes to gratefully acknowledge the helpful discussions with J. J. Hurst, Jr.

References

Anthony, A. M., and Collongues, R. (1972). *In* "Preparative Methods in Solid State Chemistry" (P. Hagenmüller, ed.), pp. 147–249. Academic Press, New York.

Aust, K. T. (1963). *In* "The Art and Science of Growing Crystals" (J. J. Gilman, ed.), pp. 452–478. Wiley, New York,

Bradley, R. S. (1963). *In* "The Art and Science of Growing Crystals" (J. J. Gilman, ed.), pp. 55–61. Wiley, New York.

Brenner, S. S. (1963). *In* "The Art and Science of Growing Crystals" (J. J. Gilman, ed.), pp. 30–54. Wiley, New York.

Brice, J. C. (1973). "Growth of Crystals from Liquids." Amer. Elsevier, New York.

Bridgman, P. W. (1925). *Proc. Amer. Acad. Arts Sci.* **60**, 303.

Brilliantov, N. A., Starostina, L. S., and Fedorov, O. P. (1961). *Sov. Phys.—Crystallog.* **6**, 202.

Brown, F., and Todt, W. H. (1964). *J. Appl. Phys.* **35**, 1594.

Buckley, H. E. (1951). "Crystal Growth," pp. 71 and 99. Wiley, New York.

Bundy, F. P., Hall, H. T., Strong, H. M., and Wentorf, R. H. (1955). *Nature (London)* **176**, 51.

Class, W. (1968). *J. Cryst. Growth* **3–4**, 241.

Cunnell, F. A., and Wickham, R. (1960). *J. Sci. Instrum.* **37**, 410.

Czochralski, J. (1917). *Z. Phys. Chem. (Leipzig)* **92**, 219.

Ellis, W. C. (1968). *In* "Techniques of Metals Research" (R. F. Bunshah, ed.), Vol. I, Part 2. Wiley (Interscience), New York.

Falckenberg, R. (1972). *J. Cryst. Growth* **13–14**, 723.

Fonstad, C. G., Linz, A., and Rediker, R. H. (1969). *J. Electrochem. Soc.* **116**, 1269.

Gambino, R. J. (1965). *J. Appl. Phys.* **36**, 656.

Gentile, A. L., Cripe, D. M., and Andres, F. H. (1963). *Amer. Mineral.* **48**, 940.

Gillette, R. H. (1950). *Rev. Sci. Instrum.* **21**, 294.

Glang, R., and Wajda, E. S. (1963). *In* "The Art and Science of Growing Crystals" (J. J. Gilman, ed.), pp. 80–92. Wiley, New York.

Haldane, F. A., and Sedlacek, R. (1963). *Rev. Sci. Instrum.* **34**, 622.

Hanak, J. J., Strater, K., and Cullen, G. W. (1964). *RCA Rev.* **25**, 342.

Hurst, J. J., and Linz, A. (1971). *Mater. Res. Bull.* **6**, 163.

Johnson, L. F., and Nassau, K. (1961). *Proc. IRE* **49**, 1704.

Keck, P. H., and Golay, M. J. E. (1953). *Phys. Rev.* **89**, 1297.

Keck, P. H., Van Horne, W., Soled, J., and MacDonald, A. (1954). *Rev. Sci. Instrum.* **25**, 331.

Khattak, C. P. (1973). Ph.D. Thesis, SUNY at Stony Brook, Stony Brook, New York.

Khattak, C. P., and Hurst, J. J. (1973). *Amer. Ceram. Soc., Bull.* **52**, 635.

Laudise, R. A. (1963). *In* "The Art and Science of Growing Crystals" (J. J. Gilman, ed.), pp. 252–273. Wiley, New York.

Laudise, R. A. (1970). "The Growth of Single Crystals." p. 257. Prentice-Hall, Englewood Cliffs, New Jersey.

Laudise, R. A., and Sullivan, R. A. (1959). *Chem. Eng. Progr.* **55**, 55.

Lawson, W. D., and Nielsen, S. (1958). "Preparation of Single Crystals," p. 14. Butterworth, London.

Lefever, R. A., and Chase, A. B. (1962). *J. Amer. Ceram. Soc.* **45**, 32.

Linz, A. (1965). *J. Electrochem. Soc.* **112**, 60C.
Mason, B. J. (1963). *In* "The Art and Science of Growing Crystals" (J. J. Gilman, ed.), pp. 119–150. Wiley, New York.
Merker, L. (1955). *Trans. AIME* **202**, 645.
Nassau, K., and Broyer, A. M. (1962a). *J. Appl. Phys.* **33**, 3064.
Nassau, K., and Broyer, A. M. (1962b). *J. Amer. Ceram. Soc.* **45**, 474.
Nassau, K., and Van Uitert, L. G. (1960). *J. Appl. Phys.* **31**, 1508.
O'Connor, J. R. (1963). *In* "The Art and Science of Growing Crystals" (J. J. Gilman, ed.), pp. 93–118. Wiley, New York.
Okada, T., Matsumi, K., and Makino, H. (1971). *Solid State Phys. (Japan)* **6**, 170.
Reynolds, D. C. (1963). *In* "The Art and Science of Growing Crystals" (J. J. Gilman, ed.), pp. 62–79. Wiley, New York.
Schadler, H. W. (1963). *In* "The Art and Science of Growing Crystals" (J. J. Gilman, ed.), pp. 343–364. Wiley, New York.
Silnichenko, V. G., and Gritsenko, M. M. (1965). *Sov. Phys.—Crystallog.* **9**, 647.
Stockbarger, D. C. (1936). *Rev. Sci. Instrum.* **7**, 133.
Takahashi, A., Namatsu, S., and Kimura, M. (1972). *J. Cryst. Growth* **13–14**, 681.
Tanenbaum, M. (1959). *Solid State Phys.* **6**, Part A, 86.
Theuerer, H. C., and Hauser, J. J. (1964). *J. Appl. Phys.* **35**, 554.
Theuerer, H. C., and Hauser, J. J. (1965). *Trans. AIME* **233**, 588.
Verneuil, A. (1902). *C. R. Acad. Sci.* **135**, 791.
White, E. A. D. (1965). "Techniques in Inorganic Chemistry." Wiley (Interscience), New York.
Zhimskaya, N. V. (1963). *Sov. Phys.—Crystallog.* **8**, 340.

Controlled Solidification in Ceramic Eutectic Systems

KEDAR P. GUPTA

Monsanto Company
St. Peters, Missouri

I. Introduction

Over the last twenty years there has been a rapidly increasing need for special purpose materials useful at very high temperatures. Most widely developed and accepted in high temperature technology has been the wide variety of ceramic coatings, metal fibers in ceramic matrix, ceramic filaments, etc., that have been described in many review articles and books (Davis and Bradstreet, 1970; Levitt, 1970; Rauch *et al.*, 1968; Scala, 1965; Stokes, 1966; Vasilos and Wolff, 1966; Zimmer and Palmour, 1973). Many number of techniques involved in fabrication of these special materials include hot-press sintering, slip casting, control vapor deposit, and plasma spraying (Ault, 1957; Kern *et al.*, 1968; Kingery, 1958).

A recent development in high temperature and high strength materials is related to eutectic composites. In a eutectic composition two or more phases are solidified simultaneously from the fully liquid state to the solid state under control conditions. The aligned eutectic microstructure may have unusual material properties including a high degree of anisotropy and the

capacity to combine the properties of various components in one body. So far, the bulk of research on eutectic composites has been limited to metallic systems; they have been reported in many fine review articles (Chadwick, 1963; Hogan *et al.*, 1971; Tiller, 1958).

Ceramic eutectic systems have potential for structural applications at high temperatures since they are not as susceptible to thermal shock as single component systems (Schmid and Viechnicki, 1973). The large boundary area inherent in fine grain directionally solidified eutectics may deflect crack propagation. This is specially true if there is a large mismatch of the crystallographic planes at the eutectic phase boundary (Schmid and Viechnicki, 1973).

Although very little work has been done on nonmetallic systems, mainly due to their complex nature, there has been a rapidly growing interest in the past few years. The fracture behavior of many oxide systems is currently being studied by many workers (Hulse and Batt, 1969–1973; Hulse and Batt, 1973a; Kennard *et al.*, 1974). Loxham and Hellawell (1964) have reported extensive work on many alkali halide eutectics. Some other systems that have been studied are Al_2O_3/Y_2O_3 (Viechnicki and Schmid, 1969), Al_2O_3/ZrO_2 (Schmid and Viechnicki, 1970), $BaF_{12}O_{19}/BaFe_2O_6$ (Galasso *et al.*, 1967), NaF/NaCl (Batt *et al.*, 1968), $MgO/MgAl_2O_4$ (Kennard *et al.*, 1972, 1973), and $Al_6Si_2O_{13}$–Al_2O_3 (Kennard *et al.*, 1972, 1973).

The aim of this paper is to describe the controlled solidification of ceramic eutectics. It covers various fabrication methods and observed eutectic microstructures. The microstructures in solidified ingots are controlled by many parameters, for example, growth rate, temperature gradient at the liquid–solid interface, impurity content, crystallographic orientations. (Gupta, 1973). This article also explains the correlation between these parameters and the observed microstructures. One eutectic system, $BaNb_2O_6/SrNb_2O_6$, is covered extensively along with reference of many other systems.

II. Experimental Details

The controlled solidification of oxides or halides is different from that of metallic systems in many ways. The high melting temperatures of oxides impose many problems in the selection of crucible materials. The crucible should not react chemically with the molten charge and should be able to stand high temperatures and thermal shocks. Another problem is that it is absolutely necessary to use a susceptor if induction heating is required for melting the charge. Sometimes, the crucible itself is used as a container as well as a susceptor (Kennard *et al.*, 1972, 1973; Schmid and Viech-

nicki, 1970; Viechnicki and Schmid, 1969). Tungsten and graphite are two commonly used susceptors, but both need some shielding atmospheric conditions to avoid any oxidation. These conditions may be suitable for some systems, but are not suitable in most cases (Gupta, 1973; Viechnicki and Schmid, 1969). The excess reduction of oxides in reducing atmosphere may produce metallic forms, thus changing the basic melt characteristics of the system.

The exact experimental set-up for controlled solidification depends on the nature of the molten material and the related requirements. Two distinct ways used for directional solidification of oxide systems are (a) the gradient furnace method, and (b) the float zone method. The gradient furnace is some modification of Bridgman-type crystal growing furnace in which a temperature gradient is exerted at the liquid–solid interface. Figure 1 shows a schematic diagram of the equipment used for controlled solidification of the system $Al_2O_3/Y_3Al_5O_{12}$ (Viechnicki and Schmid, 1969). Cylindrical vapor-deposited tungsten crucibles are used as susceptors for induction heating. The charge is in form of sintered powder of the eutectic composition. Directional solidification is accomplished by passing the crucible down through the heating induction coils. A typical temperature gradient G attained by this method is about 200°C/cm.

For the system $BaNb_2O_6/SrNb_2O_6$, a platinum-resistance furnace is used (Gupta, 1973). A desired temperature gradient is established by varying the temperature profile inside the furnace. This is done by short-circuiting some of the heating coil taps and by positioning the crucible. Temperature gradient attained by this method did not exceed over 50°C/cm. Controlled solidification is achieved by withdrawing the molten charge to lower temperature regions at a desired speed. The convection in the melt is minimized by withdrawal of the crucible in a way as to always have the solidifying material at the bottom. Accurate temperature gradient measurements were made by placing several thermocouples at different locations on the crucible.

A slightly modified set was used for the system Al_2O_3/ZrO_2 (Schmid and Viechnicki, 1970). After the initial melting but prior to the controlled solidification, the bottom of the tungsten crucible is cut off. The crucible is then put into a furnace where a graphite susceptor is used for heating. The bottom of the crucible with exposed ingot is positioned at 1–3 cm below the graphite susceptor. The gradient attained by such experimental set-up was about 200°C/cm.

In the floating zone method, developed by Hulse and Batt (1973a), a molten zone of ceramic eutectic is slowly traversed along a rod of the material of interest by moving a heater along the axis of the rod. With refractory materials, the rod is usually vertical and the molten zone is kept short enough

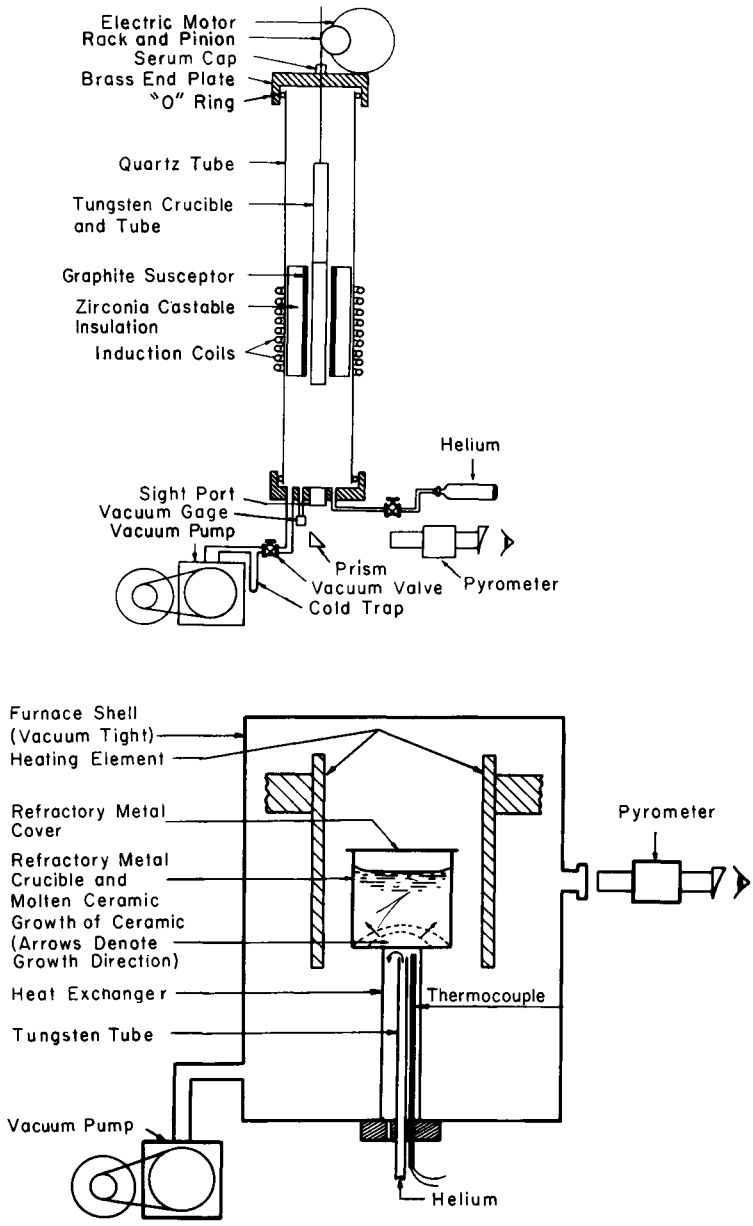

Fig. 1. A schematic diagram of the equipment used for controlled solidification of the system $Al_2O_3/Y_3Al_5O_{12}$. From Viechnicki and Schmid (1969).

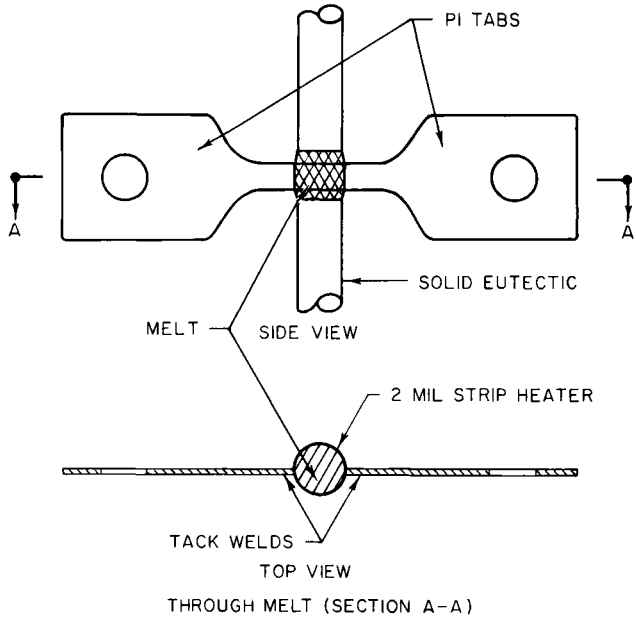

Fig. 2. Schematic view of platinum or iridium strip heater for float zone eutectics. From Hulse and Batt (1973a).

to be held in place by surface tension. This kind of arrangement is very similar to the one used by semiconductor industries to produce large scale silicon crystals by float-zone technique (Matlock, 1973).

Figure 2 shows one of the most suitable heating systems developed for the float zone method. Two strips of platinum or iridium are tack welded together to form a circular heater appropriate for the size of the charge rod. The melt wets the heater so that heater and melt temperature essentially are identical. The heater also functions as a container to hold the melt. Surface tension forces also help in containing the melt and, thus, a large molten pool is allowed to move from one end of the rod to the other. The wide molten zone also gives good mixing of the component phases before solidifying. In contrast to the gradient furnace, the temperature gradient in the float zone method is almost one order higher. Careful measurements on some systems reported the liquid–solid thermal gradient near 2000°C/cm (Hulse and Batt, 1973a).

In both the methods, preparation of a satisfactory charge is an important step in the production of good eutectic ingots. It is important that the purity of the raw materials not be diminished during the charge preparation and that the composition be homogeneous. If a charge is required in rod form,

as is the case in the float zone method, it must be dense and straight as possible. The removal of the pores during the solidification process is very important for good quality ingots and depends a great deal on the condition of the charge.

There are many methods of charge preparation. One commonly used is the conventional sintering of the components by thorough mixing and multifiring at 50°–100°C below the melting temperature (Gupta, 1973; Viechnicki and Schmid, 1969). Charge rods are prepared by pressing the calcined powders and by sintering to attain high density (Hulse and Batt, 1973). There are other methods employed for charge preparation, for example, pouring the molten eutectic in the crucible or sucking the melt into a tube used as a crucible (Hulse and Batt, 1973). These techniques are suitable mostly for low melting systems.

III. Heat Transfer in the Solidifying Ingot

The nature of heat transfer in the solidifying ingot is very important since it governs the solidification characteristics (temperature gradient, growth rate, etc.) which influence the microstructures. At a low temperature gradient, about 10°C/cm, the melt ahead of the liquid–solid interface may be constitutionally supercooled, resulting in a nonplanar interface. This is especially of interest in ceramic materials which have lower thermal conductivities than metallic systems. For example, at 500°C, the thermal conductivity of alumina, $K_{Al_2O_3} = 0.07$ W/°C cm, is about two orders less than that of aluminum metal, $K_{Al} = 2.2$ W/°C cm. The heat transfer, through conduction, in aluminum rods is much faster than the heat transfer in an alumina ingot of the same dimension. The high thermal conductivity of metals makes it easy to have an unidirectional heat flow in a metallic ingot. When the heat transfer is primarily in the longitudinal direction, it is considered to be unidirectional. It is assumed that the radial heat transfer (in transverse directions of the ingot) through the ingot surface is negligible compared to the longitudinal heat transfer. A unidirectional heat flow in ceramic ingot, such as barium niobate–strontium niobate, is difficult to attain unless an extremely high temperature gradient is exerted along the length of the ingot. Since the temperature gradient applied in the longitudinal direction is only about 40°C/cm, it can be assumed that on withdrawal of the sample, the heat transfer is not completely unidirectional (Gupta, 1973). A rigorous analysis of the heat transfer of the moving boundary condition in this study is given by (Carslaw and Jaeger, 1959)

$$DT/Dt - \kappa \nabla^2 T - v[T - T_p(Z)] = 0 \tag{1}$$

where $\kappa = K/\rho c$, $v = Hp/\rho cw$, D/Dt is convective derivative, ∇^2 is the Laplacian operator, T is the temperature profile inside the ingot, T_p is the temperature profile of the furnace, K is the thermal conductivity of the material in question, ρ is the density of the ingot, c is the specific heat, H is the surface conductance, w, the area of the ingot, and p is the perimeter of the ingot.

With suitable initial and boundary conditions, a solution of Eq. (1) will yield the exact temperature inside the sample as a function of time as well as location. However, this study is aimed only at understanding the solidification process in ceramic eutectics, and a complex solution of the Eq. (1) is not necessary. A simplified approach to heat transfer would be sufficient to understand the microstructures of the solidified phases. Figure 3 describes a schematic presentation of the temperature gradient inside the ingot as a function of withdrawal rates R. The temperature profile is constructed assuming that heat flow in the ingot is through conduction as well as radiation. If conductivity of the material is very large, and the thermal gradient applied in the longitudinal direction is extremely high, the heat flow through the surface radiation is negligible. Then a constant temperature gradient across the sample is possible. This is the case for

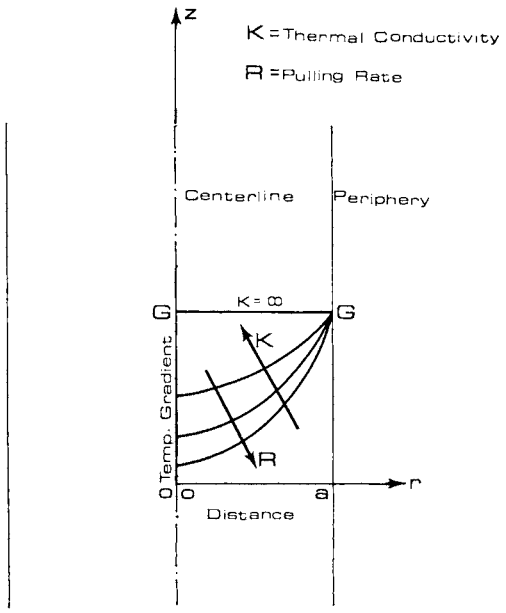

Fig. 3. A schematic diagram showing the variation of thermal gradient in a longitudinal section of an ingot.

metallic systems. For oxides, because of low thermal conductivity, heat flow through the surface radiation is not negligible. It is comparable to the heat flow through conduction in the longitudinal direction. This results in lowering of the temperature gradient from the periphery to the center of the sample. In other words, the liquid–solid interface near the center of the ingot experiences a lower temperature gradient than the actual temperature gradient G applied in the furnace. As the withdrawal rate is increased, the drop in the temperature gradient is more pronounced. A low temperature gradient at the interface is favorable for producing a nonplanar interface, and, thus, leads to a dendritic structure. It is also apparent that constitutional supercooling, which is produced when the temperature gradient at the interface is low, is greater as we approach the area nearer to the center line. Experimental observations are in agreement with such predictions (Gupta, 1973).

IV. Eutectic Microstructures

A typical and simplified eutectic phase diagram can be represented as shown in Fig. 4. Eutectic solidification occurs when a completely miscible

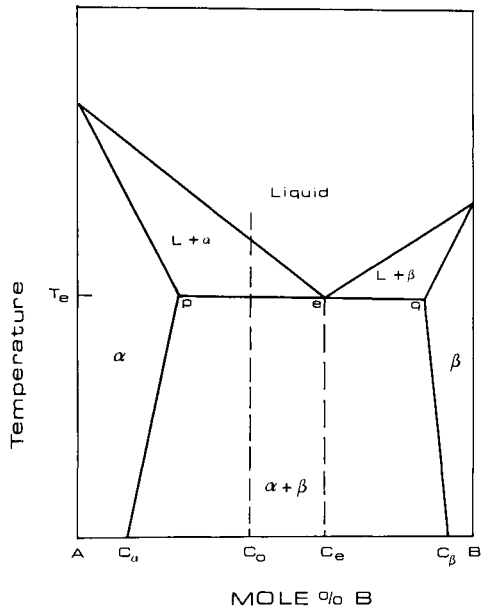

Fig. 4. A typical eutectic type phase diagram.

liquid of composition C_0 is cooled through the eutectic temperature T_e. Solidification starts with the simultaneous crystallization of both α and β phases of composition p and q, respectively. The different arrangements of these two solidifying phases can give rise to different microstructures. They are dependent on many solidification parameters, such as growth rate, temperature gradient, entropy of fusion of each phase (Hogan, 1962; Kofler, 1965; Mollard and Flemings, 1967; Tiller, 1958). Two major categories of the phase arrangements are described below.

A. Normal Eutectic Structures

A normal eutectic structure is typically lamellar in form. The two separating phases on solidification are arranged in alternate parallel sheets or lamellae, in a structure comparable to that of pearlite in steels. A diagrammatic representation of steady state growth of a lamellar eutectic is shown in Fig. 5. The essential feature of a normal or continuous eutectic structure is that the two phases can be traced along some unbroken path from the beginning of the solidification process to the region of its completion, i.e., both phases crystallize simultaneously by the advance of a common interface into the melt (Fig. 5) (Chadwick, 1963; Hogan, 1961).

A frequent variation is rodlike structure in which one phase crystallizes as a series of parallel rods embedded in a continuous matrix of the other phase. Another commonly observed variation of normal eutectic structure is colony formation (Grogan, 1926). A colony structure is a subgrain structure whose unit contains several dozen particles of each phase arranged in a characteristic pattern. It is important to note that the colonies are distinguished by phase particle arrangements and not by crystallographic orientations as in the case of eutectic grains [a grain structure is analogous to the

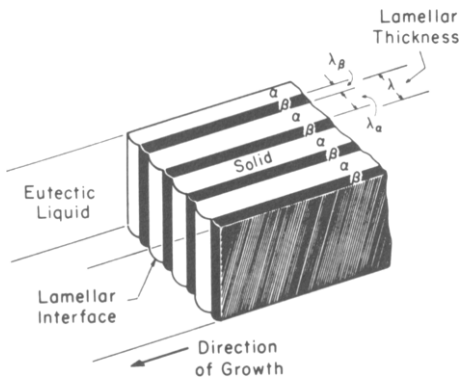

Fig. 5. Diagrammatic representation of steady state growth of a lamellar eutectic.

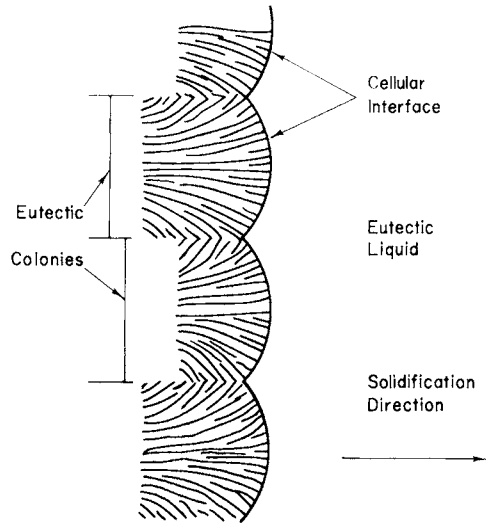

Fig. 6. Schematic presentation of colony structure.

polycrystalline structure of a single phase alloy in that each grain grows from a single nucleus (Grogan, 1926)]. However, a somewhat broader interpretation is needed here because of the presence of two phases in each grain. Since in most eutectics, particles of one phase are dispersed in the matrix of the other, a grain may be taken as a region in which the matrix is monocrystalline.) In one grain there may be many colony boundaries, depending on the characteristics of the phase structure. The colony boundaries are present only by virtue of the phase particle arrangements. Figure 6 is a schematic presentation of colony structure.

B. Anomalous Eutectic Structures

The structure is typified as one of the phases of the alloy dispersed in the second phase in any direction (Chadwick, 1963; Hogan, 1961). The growth of two phases is much less closely coupled than in the case of a normal eutectic. This permits a greater diversity of form. The outstanding example of this type of structure is the Al–Si eutectic system, in which Si is finely dispersed in the Al matrix.

Other anomalous structures having varied microscopic features are dendritic and spiral structures (Weart and Mack, 1958). Breakdown of the planar solid–liquid interface during growth may lead to a dendritic or cellular structure as in single phase alloys (Mullins and Sekerka, 1964; Sekerka, 1965). In single phase alloys, the concept of constitutional super-

cooling may explain the dendritic behavior (Sekerka, 1965). A similar theory can be advanced for the eutectic alloys. Only a few examples of eutectic spirals have been reported (Chadwick, 1963; Dippenaar *et al.*, 1971; Fullman and Wood, 1954; Hunt and Chilton, 1966). The theory for the development of the spiral structure, given by Fullman and Wood, is based on an argument of anisotropy of the growth rates in different crystallographic directions of the component phases (Fullman and Wood, 1954).

Eutectic microstructures may be classified according to growth characteristics of the component phases involved. Hunt and Jackson (Jackson and Hunt, 1966) have suggested that this classification can be based on the entropy of fusion of the component phases. Based on thermodynamic considerations, Jackson showed that the type of growth depended on a factor α [$\alpha = \xi(\Delta S_f/R)$, where ΔS_f is the entropy of fusion, R is the gas constant, and ξ is the crystallographic factor which is less than but nearly equal to 1 for close packed planes], which is almost entropy of melting (Jackson, 1958a,b). In general, metals have low entropy of fusion. Their crystal

TABLE I

VALUES OF ENTROPY OF MELTING FOR VARIOUS NONMETALLIC INORGANIC COMPOUNDS

	T_E (°K)	L (kcal/mol)	S_f (kcal/°K mol)	Crystal structure
ThO_2	3225	291.1	90.3	Cubic
SeO_2	603	24.3	40.3	Monoclinic
Ta_2O_5	2150	48.0	22.3	Rhombic
Fe_3O_4	1869	33.0	17.7	Cubic
Sb_2O_3	928	14.74	15.9	Cubic
Nb_2O_5	1783	24.2	13.6	Rhombic
Al_2O_3	2318	26	11.2	Trigonal
Y_2O_3	2500	25	10	Cubic
Cr_2O_3	2533	25	9.9	Rhombic
B_2O_3	723	5.74	7.9	Rhombic
WO_3	1743	13.94	8	Rhombic
TiO_2	2098	16	7.6	Tetragonal
ZrO_2	2988	20.8	7.0	Monoclinic
NaCl	1073	7.22	6.7	Cubic
MgO	2915	18.5	6.3	Cubic
Bi_2O_3	1090	6.8	6.2	Rhombic
BeO	2823	17	6.0	Hexagonal
KF	1148	6.5	5.7	Cubic
FeO	1653	7.5	4.6	Cubic
PbO	1163	2.82	2.4	Tetragonal
SiO_2 (quartz)	1743	3.4	2.0	Hexagonal

faces are rough, corresponding to interfaces of nearly half-filled or half-vacant sites. In most cases, nonmetals, especially oxides, have high values of ΔS_f. But a list of ΔS_f values for various nonmetallic inorganic compounds, as shown in Table I, revealed that they cover a wide range of ΔS *values.*

The three classified groups of eutectic structures are those in which both phases have low entropy of fusion (nonfaceted/nonfaceted), those in which one phase has low and other phase has high entropy of melting (nonfaceted/faceted), and those in which both phases have high entropy of melting (faceted/faceted) (Hogan *et al.*, 1971). Normal lamellar or rodlike structures are found in the first group. Most metallic systems, Pb–Sn (Mollard and Flemings, 1967), Al–Al_3Ni (Lemkey *et al.*, 1965), etc., fall under this category. Abnormal (irregular) or complex structures are formed in the second group. In the third group, each phase grows with a faceted solid–liquid interface. Oxides in general fall in the last two categories. But in many instances, regular lamellar have been observed in oxides, especially at high temperature gradients (Gupta, 1973; Hulse and Batt, 1973a; Kennard *et al.*,

TABLE II

OBSERVED MICROSTRUCTURES IN SOME NONMETALLIC EUTECTIC SYSTEMS[a]

System $\alpha + \beta$	Wt % α	Microstructure	Crystallographic relationship
LiF–NaF	48.7–60	Lamellar	Interface $\parallel (111)_{LiF} \parallel (111)_{NaF}$ Growth dir. $\parallel [1\bar{1}0]_{LiF} \parallel [1\bar{1}0]_{NaF}$ Growth dir. $\parallel [100]_{LiF} \parallel [100]_{NaF}$
NaF–NaCl	22–23.1	Rectangular rod	Interface $\parallel (110)_{NaCl} \parallel (110)_{NaF}$ Growth dir. $\parallel [001]_{NaCl} \parallel [001]_{NaF}$
NaBr–NaF	83.4	Rectangular rod	Interface $\parallel (110)_{NaBr} \parallel (110)_{NaF}$ Growth dir. $\parallel [1\bar{1}1]_{NaBr} \parallel [1\bar{1}1]_{NaF}$
LiF–NaCl		Rod	Unknown
NaF–CaF_2		Lamellar	Unknown
NaF–MgF_2	~ 20	Rod	Unknown
NaF–PbF_2	~ 20	Rod	Unknown
MnO–MnS	43.5	Lamellar	Interface $\parallel (111)_{MnS} \parallel (111)_{MnO}$ Growth dir. $\parallel [11\bar{2}]_{MnS} \parallel [11\bar{2}]_{MnO}$
FeO–FeS	36.1	Rectangular rod	Interface $\parallel (100)_{FeO} \parallel (0001)_{FeS}$ Growth dir. $\parallel [011]_{FeO} \parallel [10\bar{1}0]_{FeS}$
$Zn_3B_4O_{11}$–ZnB_2O_{11}	50	Lamellar	Unknown
$BaFe_{12}O_{19}$–$BaFe_2O_4$	28.6	Abnormal	Growth dir. $\parallel (0001)_{BaFe_{12}O_{19}}$
$PbMoO_4$–PbO		Rods of $PbMoO_4$	Unknown
$Al_6Si_2O_{13}$–Al_2O_3 (77.5 wt % Al_2O_3)		Lamellar (metastable)	Unknown
MgO–$MgAl_2O_4$ (55 wt % Al_2O_3)		Oriented whiskers	Interface $(hkl)MgO \parallel (hkl)MgAl_2O_4$ Growth dir. $[hkl]MgO \parallel [hkl]MgAl_2O_4$
Al_2O_3–ZrO_2 (57.7 wt % Al_2O_3)		Colony, rod	Unknown

[a] Samples prepared by gradient furnace method (Hogan *et al.*, 1971; Kennard *et al.*, 1972, 1973; Schmid and Viechnicki, 1970, 1973).

1974; Schmid and Viechnicki, 1970). Chadwick (1967) has given examples of several exceptions in this method of classification.

V. Eutectic System, $BaNb_2O_6/SrNb_2O_6$

Most of the ceramic systems might be expected to solidify from the melt in a faceted manner because of their complex crystal structures and high

TABLE III

OBSERVED MICROSTRUCTURES IN SOME CERAMIC EUTECTIC SYSTEMS[a]

System	Eutectic temp. (°C)	Growth rate (cm/hr)	Comments
PbO–$Pb_2Fe_2O_4$ (12.8 wt % Fe_2O_3)	730	0.5–2	Broken lamellar, 2-phase matrix
PbO–$Pb_3Nb_2O_8$ (6.85 wt % Nb_2O_5)	835	2	Lamellar
V_2O_5–$Pb_2V_2O_7$ (5.7 wt % V_2O_5)	760	Cast	Lamellar
Pb_4GeO_6–$Pb_3Ge_2O_7$ (15.0 wt % GeO_2)	707	1.45	Circular rod
WO_3–$BaWO_4$ (18.5 wt % BaO)	935	Cast	Water soluble
V_2O_5–BaV_2O_6 (32.2 wt % BaO)	550	Cast	Glassy
$Bi_4Ge_3O_{12}$–$Bi_{14}GeO_{24}$ (10.3 wt % GeO_2)	880	Cast	Unbranched dendrites
V_2O_5–ZnV_2O_6 (14.2 wt % ZnO)	640	Cast	Coarse unbranched dendrites
V_2O_5–NiV_2O_6 (9.2 wt % NiO)	650	Cast	Coarse unbranched dendrites
V_2O_5–MnV_2O_6 (9.10 wt % $MnCO_3$)	660	2	Coarse unbranched dendrites
PbO–Pb_2WO_5 (17.6 wt % WO_3)	725	Cast	No fine 2-phase areas seen
Bi_2O_3–$Bi_{26}Zn_2O_{38}$ (1.24 wt % ZnO)	750	2	Circular rod, spheroidized
$BiFeO_3$–$Bi_{40}Fe_2O_{63}$ (1.14 wt % Fe_2O_3)	790	0.5–2.5	Circular rod, matrix may be faceted
Li_2WO_4–WO_3 (18.1 wt % WO_3)	695	Cast	Porous, very soluble in water
V_2O_5–CuV_2O_6 (12.7 wt % CuO)	620	Cast	No fine 2-phase areas seen
V_2O_5–CaV_2O_6 (2.74 wt % CaO)	618	Cast	No fine 2-phase areas seen
Bi_2O_3–$Bi_2Mn_2O_9$ (12.2 wt % Mn_2O_3)	790	Cast	Lamellar
Bi_2O_3–Bi_8TiO_4 (0.53 wt % TiO_2)	835	Cast	Lamellar
WO_3–$CaWO_4$ (7.46 wt % CaO)	1135	Cast	Triangular rods
WO_3–$SrWO_4$ (17.1 wt % $SrCO_3$)	1075	Cast	Triangular rods
WO_3–$MgWO_4$ (12.6 wt % $MgCO_3$)	1120	2	Lamellar "Chinese script"
La_2O_3–$LaFeO_3$ (28.5 wt % La_2O_3)	1430	~ 2	Triangular rods
Fe_2O_3–$YFeO_3$ (15.9 wt % Y_2O_3)	1455	Coil	Lamellar/rod, matrix forms 3-pronged webs
Gd_2O_3–$GdFeO_3$ (15.0 wt % Gd_2O_3)	1500	Cast	Lamellar/rod, matrix forms 3-pronged webs
$BaTiO_3$–$BaTiSiO_5$ (9.9 wt % SiO_2, 90.1 wt % $BaTiO_2$)	1260	2	Rodlike
$BaTiO_3$–$BaTiO_4$ (41.9 wt % TiO_2)	1563	2	Lamellar and rod
Zn_2TiO_4–TiO^2 (43.0 wt % ZnO)	1418	2	Lamellar
Al_2O_3–$ZrO_2(Y_2O_3)$ (55 wt % Al_2O_3, 38.3 wt % ZnO_2)	1890	0.5–10	Circular rod, matrix may be faceted

[a] Samples prepared by float-zone method (Hulse and Batt, 1973).

TABLE IV

CHEMICAL COMPOSITIONS AND GROWTH PARAMETERS OF THE EUTECTIC SAMPLES OF $BaNb_2O_6/SrNb_2O_6$

Sample No.	Designation	Composition	G (°C/cm)	R (μm/sec)
1	EU-40-04	88 mole % $BaNb_2O_6$	40	4
2	EU-40-40	88 mole % $BaNb_2O_6$	40	40
3	EU-15-02	88 mole % $BaNb_2O_6$	15	2
4	EU-15-07	88 mole % $BaNb_2O_6$	15	7
5	EU-15-16	88 mole % $BaNb_2O_6$	15	16
6	OEU-40-04	80 mole % $BaNb_2O_6$	40	4
7	OEU-40-40	80 mole % $BaNb_2O_6$	40	40

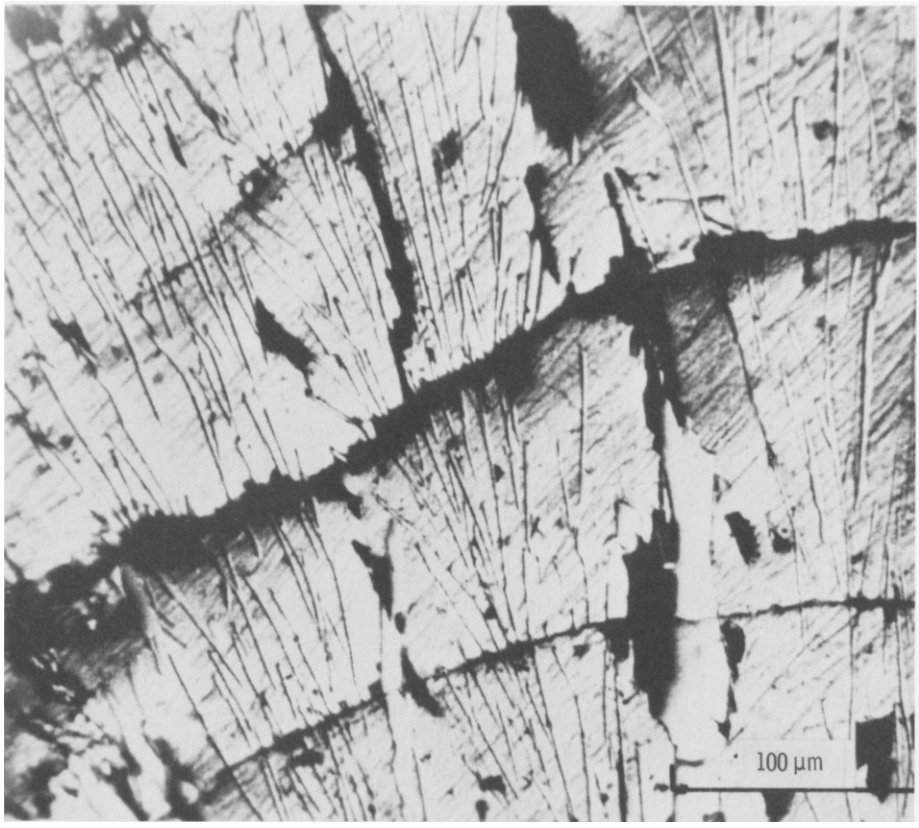

Fig. 7. Reflected photomicrograph of longitudinal section of Sample EU-40-04, showing lamellar structure.

entropies of fusion. Tables II and III list the observed microstructures in many ceramic eutectic systems. A complete discussion on the microstructures and their correlation with the growth parameters are now discussed for the eutectic system, $BaNb_2O_6/SrNb_2O_6$.

A total of seven samples were prepared at different temperature gradients and growth rates (Table IV). The chemical compositions chosen were 88 mole % $BaNb_2O_6$–12 mole % $SrNb_2O_6$, corresponding to the eutectic composition, and 80 mole % $BaNb_2O_6$–20 mole % $SrNb_2O_6$ an off-eutectic composition. The phase diagram for the system is reported by Carruthers and Grasso (1970).

In sample EU-40-04, which was solidified at temperature gradient $G = 40°C/cm$, and pulling rate, $R = 4$ μm/sec, a "coupled" or normal structure

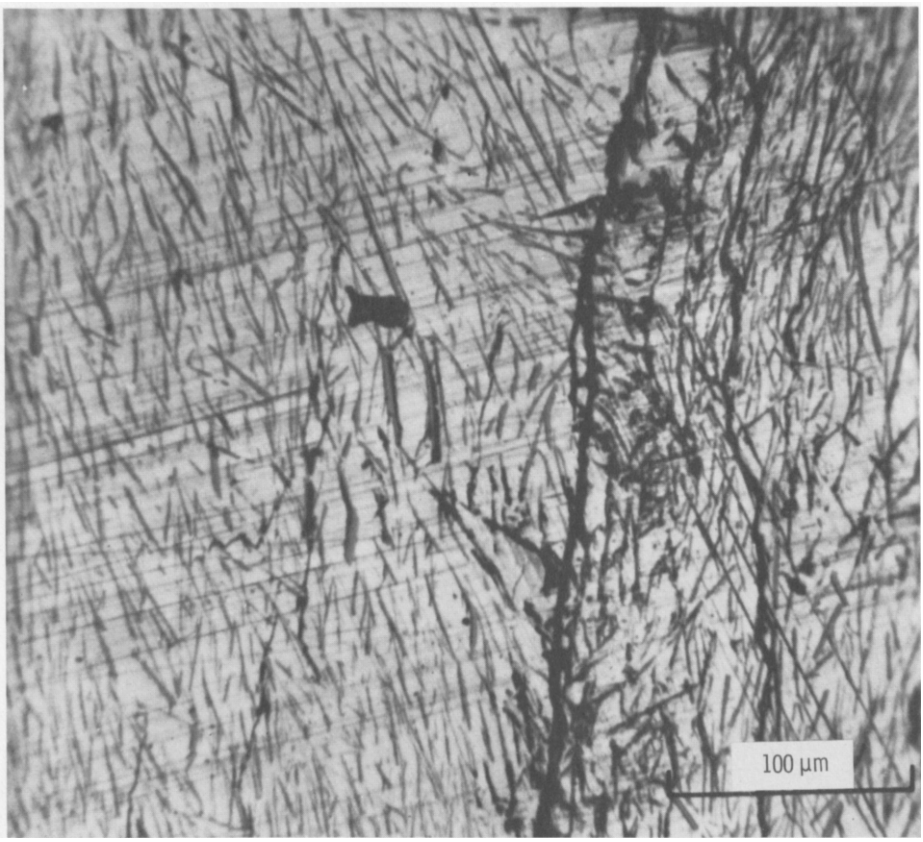

Fig. 8. Longitudinal section of specimen EU-40-40.

was observed (Fig. 7). At the same temperature gradient but at a higher pulling rate, a less coupled eutectic structure was seen, as shown in Fig. 8. In this micrograph, lamellae are discontinuous and shorter than those in the micrograph of Fig. 7. Microstructures observed in the samples solidified at

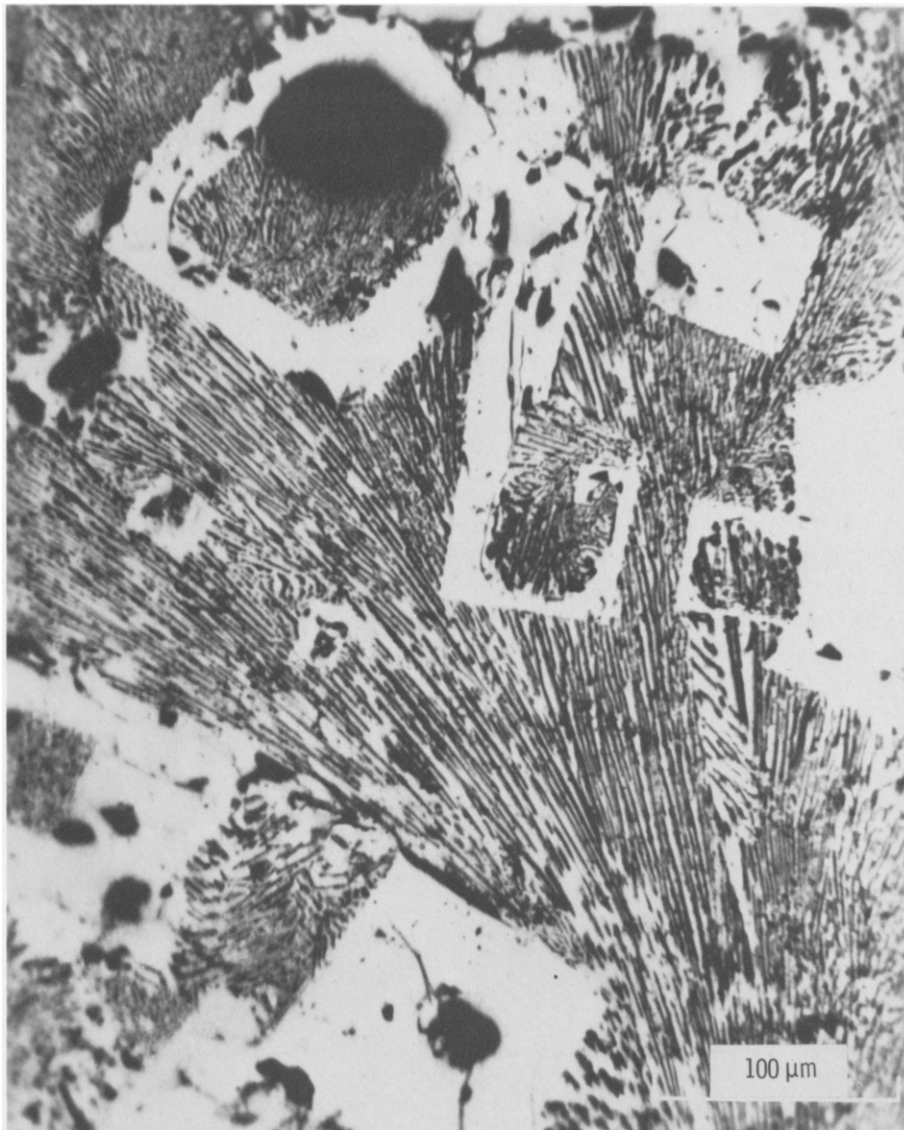

Fig. 9. Prismatic and spiral growth morphologies with the normal eutectic structures were found in sample EU-15-07 (Gupta, 1973).

a lower temperature gradient, $G = 15°C/cm$, were markedly different from the microstructures of the samples EU-40-04 and EU-40-40, which were solidified at a high temperature gradient, $G = 40°C/cm$. In the former, a distinct growth morphology of one of the eutectic phases was seen, along with the lamellar structures. Prismatic and spiral growth morphologies with the normal eutectic structures were found in sample EU-15-07 (Fig. 9). The microstructures of the transverse section of sample EU-15-07 changed gradually from the periphery to the core. Near the periphery, a lamellar structure was resolved. In between the core and the periphery, distinct growth morphologies (prismatic and spiral structures) and lamellar structures were present in different proportions.

Although growth spirals were present in sample EU-15-07, they were mainly found in the eutectic melt solidified at $G = 15°C/cm$ and $R = 16$ $\mu m/sec$. Figure 10 shows one of these spirals, found in the sample EU-15-16. When measured from the outermost segments toward the center, pairs of

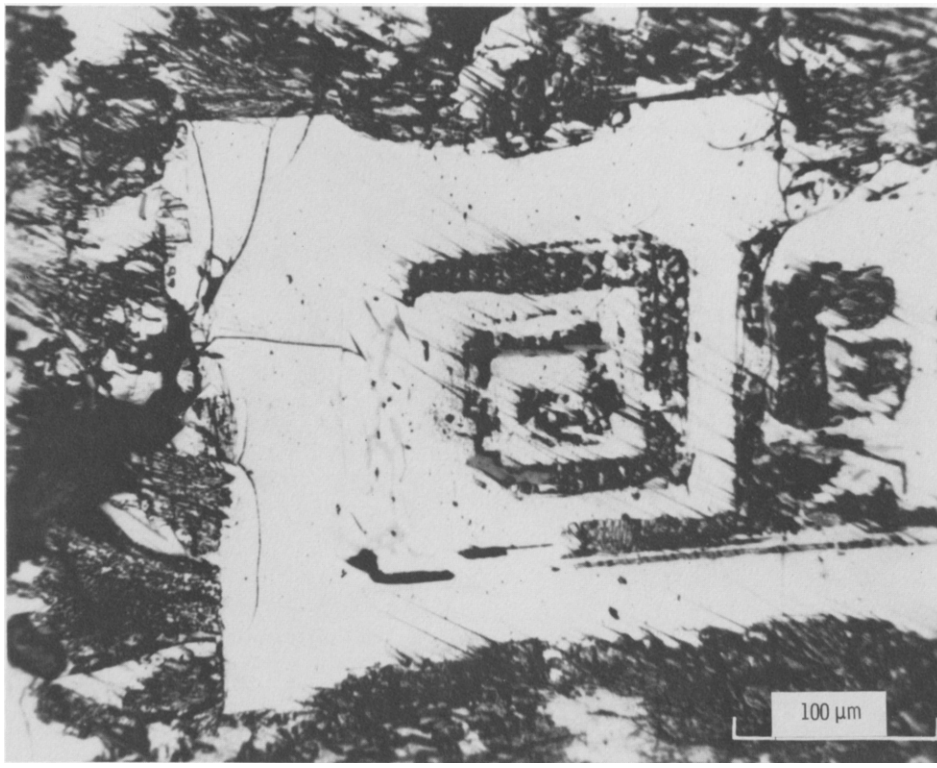

Fig. 10. Growth spiral in the transverse section of specimen EU-15-16 (Gupta, 1973).

perpendicular arms were shorter than those preceding them, and the arms of each pair were of nearly the same length and width. The length of the arm changed from 340 μm, at the outermost segment to 14 μm in the center. The change in width was from 84 to 8 μm. This was not as systematic a change as in the lengths. In some cases, spirals only had a few turns. The largest size spiral had more than 15 turns and had an area larger than $10^5 \mu m^2$. The spiral boundaries were dendritic, but planar at many places.

In off-eutectic samples OEU-40-04 and OEU-40-40, many complex

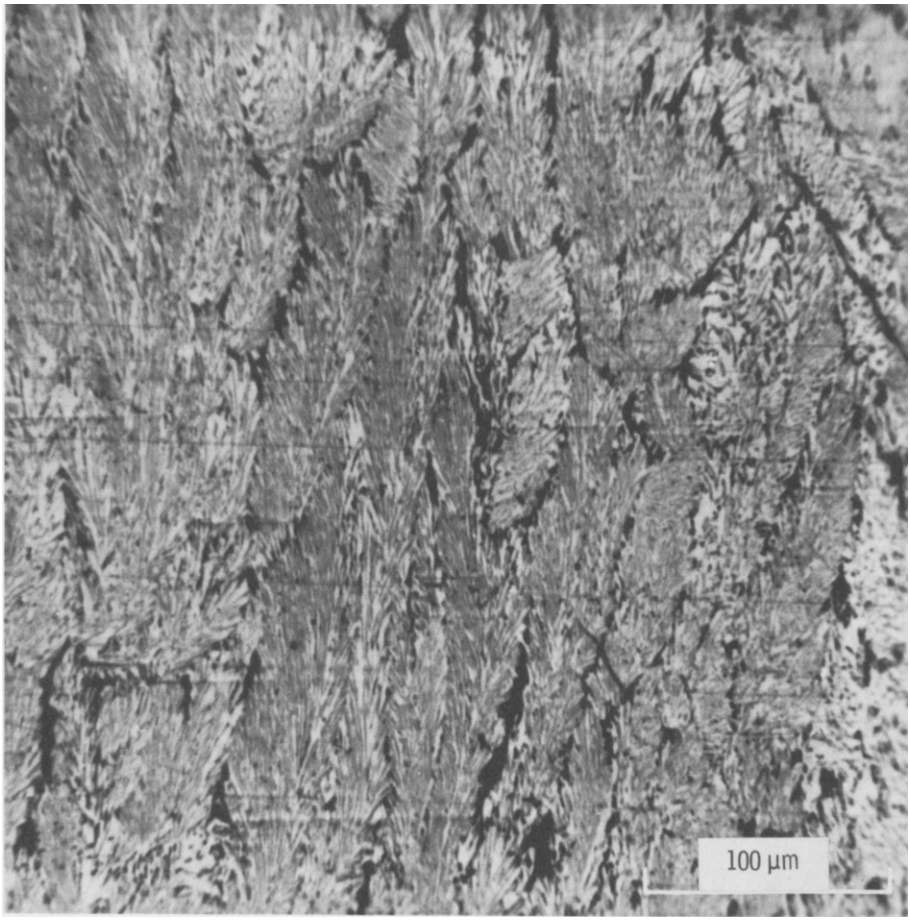

Fig. 11. Slightly modified microstructure (colonies) was observed in the noneutectic sample. Specimen OEU-40-04 (Gupta, 1973).

microstructures were observed, depending on the growth rates and the location in the sample. Normal eutectic structure was observed as a colony structure, shown in Figure 11. Most of the other microstructures were very complex and included some partial and complete spirals (Gupta, 1973; Gupta *et al.*, 1975).

The effects of the temperature gradient and pulling rate are discussed below to correlate the solidification phenomena and the observed eutectic microstructures.

The effects of the temperature gradient on the growth characteristics of the solidifying melt is interconnected with the pulling rates, as discussed earlier. The temperature gradient influences the supercooling of the melt just ahead of the interface. The freezing temperature of the boundary layer with respect to one of the phases is shown in Fig. 12. Since the average liquid composition at the interface is approximately at the eutectic temperature, the curve starts at equilibrium temperature, T_e. The eutectic interface will be at some temperature below T_e, say T_1. G_1, G_2, G_3 lines represent the temperature gradients applied at the interface ($G_1 > G_2 > G_3$). Regions of varying amounts of constitutional undercooling exist for different temperature gradients. An extensive discussion of the effects of temperature

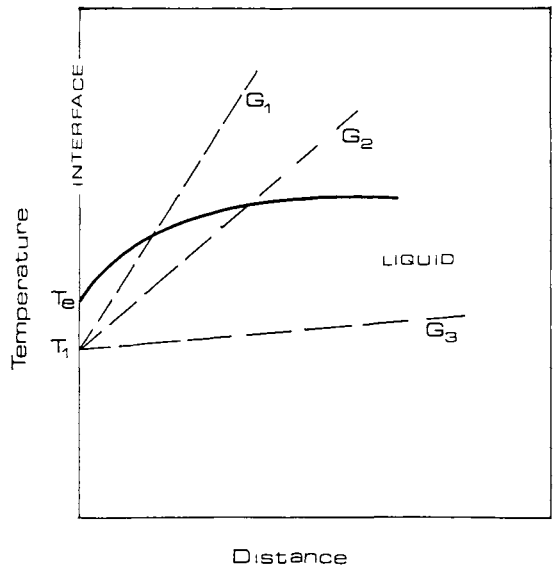

Fig. 12. Schematic drawing of the freezing temperature (with respect to one phase) as a function of distance from the interface. G_1,G_2, and G_3 are different temperature gradients ($G_1 > G_2 > G_3$). Solid line represents the equilibrium liquidus temperature.

gradient on the microstructure of the solidified phases is reported by Chalmers (1970) and Li (1973). The change in the growth morphology depends on the amount of supercooling (ΔT_s) and on the boundary layer.

When the maximum supercooling is small, and when it occurs close to the interface, a lamellar or a cellular structure is predicted. This requires, of course, that a lamellar interface is stable, which in turn depends on the pulling rate R. Samples EU-40-04 and EU-40-40 (Fig. 7 and 8), which were solidified at 40°C/cm show the presence of lamellar structures. A slightly modified microstructure (colonies) was observed in the noneutectic samples solidified at the same temperature gradient (Fig. 11). The colony microstructure in eutectic alloys was first recognized by Weart and Mack (1958) from experiments in which eutectic ingot melts were decanted. They also established a relationship between the colony structure and the cellular formation. The formation of colonies is explained by the long range diffusion patterns in the liquid ahead of the interface. The short range diffusion between lamellae explains the formation of lamellar structure. With an excess of one of the constituents (which is the case in off-eutectic melts), a long range solute distribution will exist ahead of the advancing interface. This is similar to the case where a cellular interface is formed in a slightly impure single phase material. Since the growth fluctuations allow certain portions of the interface to grow out from the original planar interface, the projections extend into the constitutionally cooled zone, resulting in a dome-shaped cellular structure. The impurities are then rejected more toward the cell boundaries than ahead of the cell caps, lowering the equilibrium temperature in the region of the cell walls, and consequently stabilizing the cellular or colony structure. The lamellar formation inside the colonies is formed in the same way as the normal eutectic and follows the direction of the applied temperature gradient. The direction of the lamellar near the cell boundary is nearly normal to the interface.

The amount of supercooling ahead of the interface is greater for a lower temperature gradient. Also the region of the constitutionally supercooled liquid is substantial. Nonlamellar, or dendritic, structures observed in the samples solidified at lower temperature gradients (samples EU-15-07 and EU-15-16, Fig. 9 and 10) are thus in accordance with the theoretical predictions for dendritic structures.

The difference in the morphologies among the samples of low temperature gradients arises mainly from the growth rates, which depend on the pulling rate of the samples. The temperature profile inside the sample changes with increasing withdrawal rate (Fig. 3). The temperature profile leads to changes in the growth pattern of the solidifying phases. From experimental observations, it was established that the total percent area of nonlamellar structures in the samples with $G = 15$°C/cm increased with the increasing pulling rate

(Gupta, 1973). At $R = 16$ μm/cm, more than half of the transverse section of sample EU-15-16 was dendritic.

For the samples with $G = 40°C/cm$, the effect of withdrawal rate was reflected in the lamellar spacings. As R was increased, branching of the lamellae was more evident (Fig. 8, sample EU-40-40). Also, the lamellar spacing λ and the aspect ratio (length-to-breadth ratio of lamellae) decreased with increasing pulling rate. Tiller (1958) and Jackson and Hunt (1966) predicted a relationship between growth rate and lamellar spacing for eutectic solidification controlled by the diffusion of solute species to the growing interface. As the interface velocity increases, the solute piles up ahead of the interface, resulting in a decrease of lamellar spacing. A smaller diffusion distance is needed for the eutectic phases to have coupled growth, as the pulling rate is increased. In most of the metallic systems, lamellar spacing has been found to be related to growth rate by $\lambda^2 R = \text{constant}$ (Hogan *et al.*, 1971). In the present study, an exact relation between the pulling rate and lamellar spacing was not established because of the large variation in the measured lamellar spacing from various locations in the same sample. This situation was further complicated due to crystallographic dependence of the lamellar spacing. Figure 13a is a photomicrograph of a transverse section of sample EU-15-16, near the periphery. The three adjacent grains, A, B, and C, have different microstructures. Grain A has lamellae, grain B has rodlike structure, and grain C has a structure somewhere between the lamellae and rods. A magnified micrograph of a rodlike structure is shown in Fig. 13b. The rods were less than 0.5 μm in diameter with the average separation between rods being 1.78 ± 0.4 μm. Some very short (3–10 μm) lamellae were also present in the matrix. This clearly indicates that the formation of lamellae or rod-type structure is dependent on crystallographic orientation. In the metallic systems, where $\alpha > 2$ $[\alpha = \xi(\Delta S_f/R)]$ for both the phases, the solid surface in contact with the melt will be "rough" and will provide many sites for attachment of atoms. This will happen irrespective of the crystallographic plane which lies parallel to the liquid–solid interface. In the present study, where $\alpha > 2$ for both the phases (commonly observed case for oxides), the solid surface in contact with the melt tends to consist of high density crystallographic planes forming "smooth" facets. A large kinetic cooling is needed for the lamellar structure, and the amount is dependent on the crystallographic orientations of both phases (interfacial energy term). This may explain the difficulty in having stable lamellar structure in $BaNb_2O_6/SrNb_2O_6$ and crystallographic dependence of the structure. In a highly supercooled melt, the interface tends to become nonisothermal, leading to abnormal structures.

In the samples with $G = 15°C/cm$, the growth characteristics of nonlamellar structures have been found to vary with the pulling rate. At a 2 μm/sec

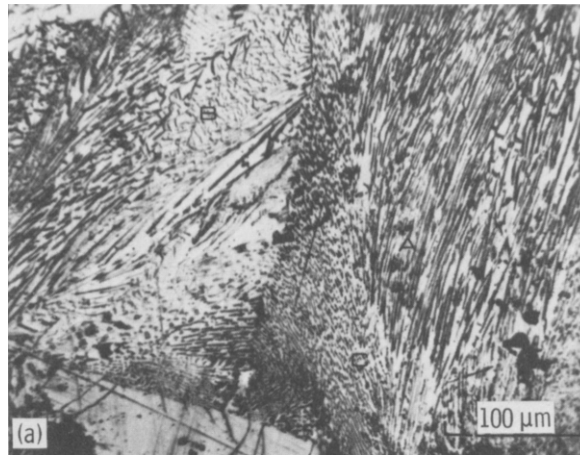

Fig. 13a. A photomicrograph of a transverse section of sample EU-15-16 (Gupta, 1973).

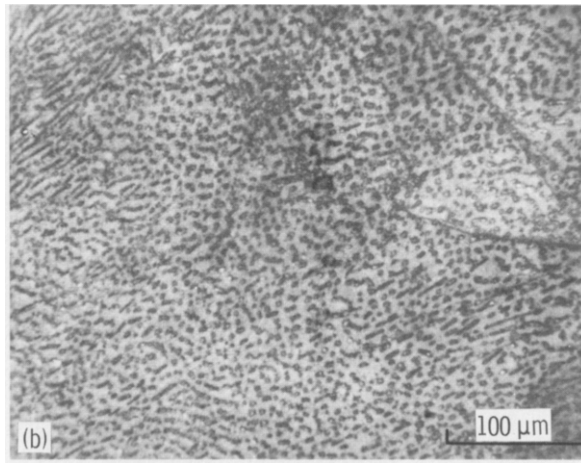

Fig. 13b. A magnified micrograph of a rodlike structure that has crystallographic orientation dependence (Gupta, 1973).

withdrawal rate, the white phase (phase with higher strontium concentration) grows mostly as long thin plates. As the pulling rate is increased, it becomes as a cylinder with a square cross section at $R = 7$ μm/sec (Fig. 9, sample EU-15-07), and finally, as an orthogonal spiral at 16 μm/sec (Fig. 10, sample EU-15-16). It was also found experimentally that the spiral axis was along $<001>$. The development of well-defined crystallographic surfaces

during the growth implies that the ordinary continuous growth mechanism is not operative. This mechanism is found to be operative in the solidification of metallic systems where no faceting is observed. In other words, growth of barium strontium niobate crystals must have occurred by a layer spreading mechanism (lateral growth mechanism) (Cahn *et al.*, 1964; Chalmers, 1970). A cylindrical whisker with a square cross section is apparently bounded by low index lateral faces. A sharp boundary between the solidifying phases also supports this theory. Since the whisker maintains a constant cross section while growing axially, there must be a barrier to the growth of the lateral faces. Similar conclusions can be drawn for other morphologies.

Li (1973) has shown that as the pulling rate is increased, the supercooling of the melt ahead of the interface increases. The degree of supercooling (ΔT_s) directly affects the growth rate of the solidifying phases (Bennema, 1967; Hunt and Chilton, 1964).

In general, growth rate normal to the surface is given by (Cahn *et al.*, 1964):

$$V = \text{growth rate (cm/sec)} = k(\Delta T_s)^n \tag{2}$$

where k is a constant and is temperature dependent; ΔT_s is the amount of supercooling. It is important to mention that pulling rate R is related to velocity of the interface but not that of the component phases which is given by V. The value of n in Eq. (2) changes depending on the growth mechanism (Cahn *et al.*, 1964).

However, over a wider range of cooling, especially for viscous materials like barium strontium niobate, the growth rate should be corrected for its temperature dependence. This is done adequately by multiplying the growth rate (at each temperature) times the ratio of the liquid diffusion at the melting temperature to its value at the growth temperature. This ratio is also expressed as the fluidity of the liquid (a/η), where η is the viscosity of the melt. The corrected V then reveals the mechanistic aspects of its dependence even under large undercooling. The growth rate goes to a maximum and decreases at large undercooling. The solidification rates in molten metals are usually high and do not need any viscosity correction. The fluidities of metallic melts are usually temperature insensitive (Cahn *et al.*, 1964).

The morphological changes in the samples with $G = 15°C/cm$ are easily explained by the growth anisotropy and dependence of the growth rate on the degree of supercooling. The lateral layer spreading mechanism of the growth shows a "go/no-go" type of growth behavior. A slight increase in ΔT_s creates a marked effect on mechanical damage of perfect habit faces. This situation is shown in Fig. 9. A similar situation is encountered when growth rate is increased from 7 μm/sec to 16 μm/sec. The boundaries in

sample EU-15-16 are much less sharp than those in sample EU-15-07 (Figs. 10 and 9). Evidence of a layer growth mechanism is found in *p*-toluidine crystal growth. At small undercoolings, *p*-toluidine platelets grow from the melt at nearly constant thickness giving lateral diameter to thickness ratios of 1000:1 (Chalmers, 1970). Thickening of the platelet was instantaneous with a slight increase in the undercooling.

References

Ault, N. N. (1957). *J. Amer. Ceram. Soc.* **40**, 69.

Batt, J. A., Douglas, F. C., and Galasso, F. S. (1968). *Amer. Ceram. Soc., Bull.* **48**, 623.

Bennema, P. (1967). *J. Cryst. Growth* **1**, 287.

Cahn, J. W., Hillig, W. B., and Sears, G. W. (1964). *Acta Met.* **12**, 1421.

Carruthers, J. R., and Grasso, M. (1970). *J. Electrochem. Soc.* **117**, 1426.

Carslaw, H. S., and Jaeger, J. C. (1959). "Conduction of Heat in Solids," pp. 148 and 388. Oxford Univ. Press, London and New York.

Chadwick, G. A. (1963). *Prog. Mater. Sci.* **12**, 97.

Chadwick, G. A. (1967). *Proc. Joint Conf. Solidification, Brighton, U.K.*

Chalmers, B. (1970). *In* "Solidification" (T. J. Hughel and R. F. Bolling, eds.), p. 295. Amer. Soc. Metals, Metals Park, Ohio.

Davis, L. W., and Bradstreet, S. W. (1970). "Metal and Ceramic Matrix Composites," p. 101. Cohners Book Div.

Dippenaar, A., Bridgman, H. D. W., and Chadwick, G. A. (1971). *J. Inst. Metals* **99**, 137.

Fullman, R. L., and Wood, D. L. (1954). *Acta. Met.* **2**, 188.

Galasso, F., Darby, W. L., Douglas, F. C., and Batt, J. A. (1967). *J. Amer. Ceram. Soc., Bull.* **50**, 333.

Grogan, J. D. (1926). *J. Inst. Metals* **36**, 269.

Gupta, K. P. (1973). Ph.D. Thesis. Materials Science Department, SUNY at Stony Brook, Stony Brook, New York.

Gupta, K. P., Wang, F. F. Y., and Li, C. H. (1975). *J. Cryst. Growth* **29**, 203.

Hogan, L. M. (1961). *J. Aust. Inst. Metals* **6**, 279.

Hogan, L. M. (1962). *J. Aust. Inst. Metals* **7**, 188.

Hogan, L. M., Kraft, R. W., and Lemkey, F. D. (1971). *Advan. Mater. Res.* **5**, 83.

Hulse, C. O., and Batt, J. A. (1969–1973). "The Effect of Eutectic Microstructures of the Mechanical Properties of Ceramic Oxides," Uni. Aircraft Res. Lab., Connecticut.

Hulse, C. O., and Batt, J. A. (1973a). *In* "Advanced Materials: Comp. and Carb." (J. D. Buckley, ed.), p. 132. *Amer. Ceram. Soc.*, Columbus, Ohio.

Hulse, C. O., and Batt, J. A. (1973b). *In* "Fracture Mechanics of Ceramics" (R. C. Bradt, D. P. M. Hasselman, and F. F. Lange, eds.), Vol. 2, p. 483. Plenum, New York.

Hunt, J. D., and Chilton, J. P. (1964). *J. Inst. Metals* **92**, 21.

Hunt, J. D., and Chilton, J. P. (1966). *J. Inst. Metals* **94**, 146.

Jackson, K. A. (1958a). *In* "Growth and Perfection of Crystals" (R. H. Doremus, ed.), p. 319. Wiley, New York.

Jackson, K. A. (1958b). "Liquid Metals and Solidification," p. 174. Amer. Soc. Metals, Metals Park, Ohio.

Jackson, K. A., and Hunt, J. D. (1966). *Trans. AIME* **236**, 1129.

Kennard, F. L., Bradt, R. C., and Stubican, V. S. (1972). *J. Amer. Ceram. Soc.* **56**, 566.
Kennard, F. L., Bradt, R. C., and Stubican, V. S. (1973). "Reactivity of Solids," 7th Int. Symp., p. 580. Chapman & Hall, London.
Kennard, F. L., Bradt, R. C., and Stubican, V. S. (1974). *Amer. Ceram. Soc., Bull.* **53**, 313.
Kern, E. L., Hamill, D. W., and Jacobson, K. A. (1968). *Advan. Tech. Mater. Invest. Fabric, 1968* Vol. 14, p. 2-B-3.
Kingery, W. D. (1958). "Ceramic Fabrication Processes." pp. 45 and 147. MIT Press, Cambridge, Massachusetts.
Kofler, A. (1965). *J. Aust. Inst. Metals* **10**, 169.
Lemkey, F. D., Hertzberg, R. W., and Ford, J. A. (1965). *Trans. AIME* **233**, 334.
Levitt, A. P. (1970). "Whisker Technology," pp. 3, 303, and 343. Wiley (Interscience), New York.
Li, C. H. (1973). Report RE-458. Grumman Aerospace Corp., New York.
Loxham, J. G., and Hellawell, A. (1964). *J. Amer. Ceram. Soc.* **47**, 184.
Matlock, J. H. (1973). "Electronic Materials—from Substrate to Thin Film Devices," Trans. M R C, 1-1.
Mollard, F. R., and Flemings, M. C. (1967). *Trans. AIME* **239**, 1526 and 1534.
Mullins, W. W., and Sekerka, R. F. (1964). *J. Appl. Phys.* **35**, 444.
Rauch, H. W., Sr., Sutton, W. H., and McCreight, L. R. (1968). "Ceramic Fibers and Fibrous Composite Materials," pp. 49 and 101. Academic Press, New York.
Scala, E. (1965). *In* "Ceramic for Advanced Techniques" (J. E. Hove and W. C. Riely, eds.), p. 286. Wiley, New York.
Schmid, F., and Viechnicki, D. (1970). *J. Mater. Sci.* **5**, 470.
Schmid, F., and Viechnicki, D. J. (1973). *In* "Advanced Materials: Compo. and Carb." (J. D. Buckley, ed.), p. 132. Amer. Ceram. Soc. Columbus, Ohio.
Sekerka, R. F. (1965). *J. Appl. Phys.* **36**, 264.
Stokes, R. J. (1966). *Proc. Brit. Ceram. Soc.* **6**, 189.
Tiller, W. A. (1958). "Liquid Metals and Solidification," p. 276. Amer. Soc. Metals, Metals Park, Ohio.
Vasilos, T., and Wolff, E. G. (1966). *J. Metals* **18**, 583.
Viechnicki, D., and Schmid, F. (1969). *J. Mater. Sci.* **4**, 84.
Weart, W. H., and Mack, J. D. (1958). *Trans. AIME* **212**, 664.
Zimmer, C. E., and Palmour, H. (1973). *In* "Advanced Materials: Compo. and Carb." (J. D. Buckley, ed.), p. 84. Amer. Ceram. Soc., Columbus, Ohio.

Controlled Grain Growth

R. J. BROOK

Department of Ceramics
The University of Leeds
Leeds, United Kingdom

I. Introduction

The interest in controlling grain growth in ceramic fabrication processes arises from two main causes. It may be a direct end in itself insofar as the grain size of the finished article is one of the major factors determining its properties; alternatively it may be a means to the end of preparing articles of close to theoretical density. As a consequence, the justification for efforts to control grain size is sought in the advantages brought either by a specific grain size or by high density.

The process which is to be controlled or, as is the usual case, restricted is that of grain boundary migration. The techniques available therefore lie either in adjusting the nature of the grain boundary (and with this its mobility) or in so accelerating the other processes being undertaken (most commonly densification) that the time available for the grain growth process is severely cut down.

By employing such methods, a range of ceramic materials has now been prepared either with close control on final grain size or with densities approaching the single crystal value.

A. The Importance of Grain Size

Grain size can affect the properties of the finished article either because it fixes the length over which some parameter accumulates (for example, the extent of the mismatch between grains arising from anisotropic thermal expansion) or because it fixes the frequency with which grain boundaries and their different properties, for example, in mass transport, are encountered. While few properties of ceramics are completely independent of grain size, most attention has been drawn to those mechanical and dielectric/magnetic properties where the structure–property relationship is very clear. The most striking of these are treated briefly in the following paragraphs.

1. Fracture

The effect of grain size on fracture strength has been generally interpreted (Carniglia, 1972; Davidge and Evans, 1970) in terms of a dependence

$$\sigma = f(G^{-1/2}) \tag{1}$$

where σ is the fracture strength and G the grain size. This relation can arise where fracture results from the presence of an inherent flaw in the material (Griffith, 1920) and where the flaw size is related to the grain size (Davidge, 1972). It can also arise where fracture arises from stress concentrations caused by dislocation pile-up, the length of the pile-up being limited by the grain size. Since observation of the second mechanism is dependent on the absence of the first, the strength grain size variation can be idealized as in Fig. 1. This dependence has been the driving force for the study of ultrafine grain size materials in the quest for high strengths (Burke *et al.*, 1970).

2. Creep

A second area where mechanical properties have been observed to depend closely on grain size is that of high temperature creep deformation. This is

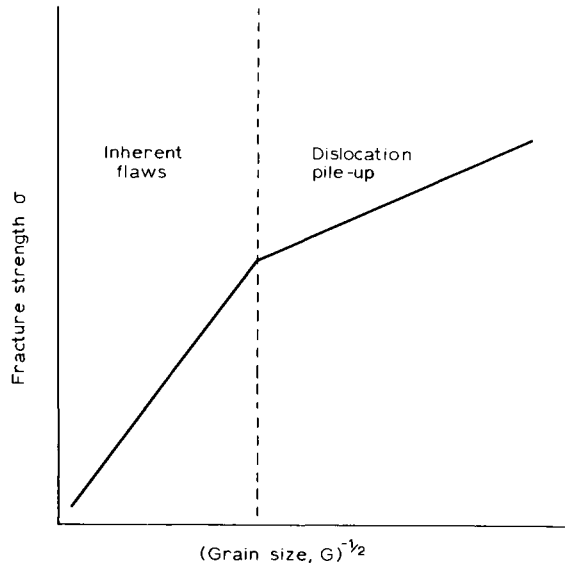

Fig. 1. An idealized representation of the dependence of strength on grain size (Davidge and Evans, 1970).

generally analyzed in terms of an equation of the form (Spriggs and Dutta, 1974)

$$\dot{\varepsilon} = f(G^{-m}) \tag{2}$$

where $\dot{\varepsilon}$ is the strain rate and m is a constant whose value depends on the creep mechanism (Table I). The predominant mechanism can involve

TABLE I

CREEP/GRAIN-SIZE DEPENDENCE FOR DIFFUSION CONTROLLED PROCESSES[a]

Mechanism	m
Diffusional creep	
Lattice diffusion	2
Grain boundary diffusion	3
Grain boundary sliding	
Grain elongation	1
No grain elongation	3

[a] From Gifkins (1968).

diffusional creep or grain boundary sliding processes (Heuer, 1970), and, as may be seen from Table I, these can obey similar grain size dependences. It has been claimed, however (Heuer *et al.*, 1970) that the importance of the sliding processes becomes greater as the grain size is decreased.

3. Electrical and Magnetic Properties

A wide range of electrical and magnetic parameters are affected by grain size, and it is in this area that the most deliberate manipulation of microstructural variables has been used to prepare materials with properties suitable for specific applications. The subject has been covered by a number of reviews (Graham and Tallan, 1971; Jonker and Stuijts, 1971; Broese van Groenen *et al.*, 1968/1969; Jaffe *et al.*, 1971; Standley, 1972).

Generally, for properties where hysteresis loops are observed, as in ferrimagnets and ferroelectrics, the importance of grain size can be interpreted in terms of the existence of domain walls and the effect of interactions with grain boundaries on the ease of wall migration. Below a certain grain size (which depends on the nature of the material) domains cannot form, and hard magnetic properties in ferrites (high coercive field and high remanent magnetization) and high dielectric constants in ferroelectrics are observed. When grain sizes are sufficient for domain formation to occur, the grain boundaries are best regarded as impediments to domain wall movement, and a direct relation between permeability and grain size has been observed (Perduijn and Peloschek, 1968).

Grain boundaries can have a pronounced effect on electrical conductivity in ceramics since they can adjust more readily to changing conditions (equilibration in terms of either temperature or composition) than can the interior of the grains. This effect is perhaps most pronounced in semiconducting $BaTiO_3$, where the occurrence of oxygen adsorption at the grain boundaries introduces a very high resistance barrier to electrical conduction (Heywang, 1971). Control of the grain size can then be used as a means of increasing the concentration of such barriers, thus making the system more resistant to electrical breakdown (Hirose and Sasaki, 1971).

In the case of ion conduction, the degree of disorder and the relatively open structure associated with grain boundaries can cause them to act as relatively conducting regions (particularly for the anion), and control of grain size can be used to enhance conduction; this approach has been employed in the search for improved ceramic electrolytes (Steele, 1973).

The fact that other microstructural features such as porosity or solid second phases comprising either glassy or crystalline material are frequently associated with the grain boundary serves to emphasize the isolation of grains from one another with respect to the passage of charge carriers or of domain walls. While in this case it is difficult to separate effects arising from

grain size per se, the role of boundaries as sweepers of other microstructural features and hence the use of controlled grain growth as a means of preparing pore-free grains should be noted (Reijnen, 1968).

B. Sintering to Complete Densification

The second reason for controlling grain growth has been found in the search for high density in sintering (Coble and Burke, 1963). The recognition that densification can only proceed at a reasonable rate as long as the sources and sinks for the associated diffusion process are kept close together and, more particularly, the identification of the grain boundary and the pore as the sources and sinks for the diffusing atoms, have suggested that ultimate density is only to be expected where pores remain attached to grain boundaries (Burke, 1957) (Fig. 2). The interaction of pores and grain boundaries will be considered more fully later. At this point, it may be noted that the recognition of this effect means that the abnormal grain growth process, in which boundaries become separated from pores, and which is a regular phenomenon encountered in prolonged sintering experiments (Fig. 3), must be suppressed in the quest for high density ceramics. This suppression has generally been achieved by the use of additives (Table II). The mode of operation of these additives has frequently become clear only some time after their discovery, and this, coupled with the fact that different mechanisms may be

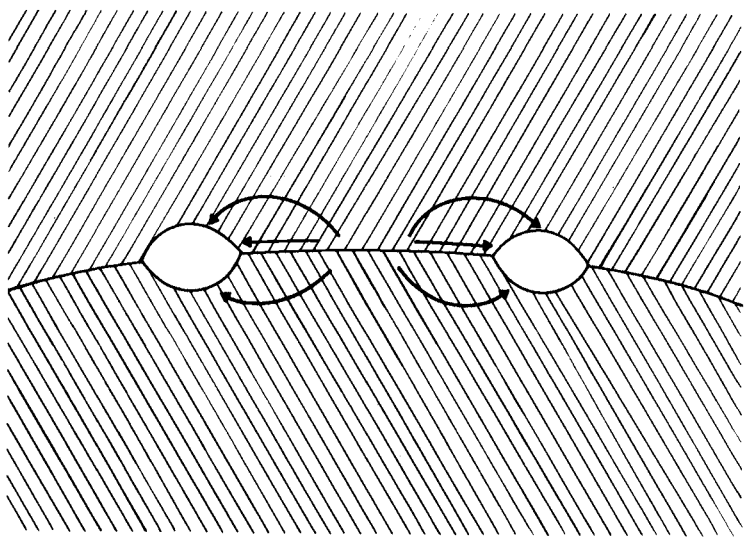

Fig. 2. Densification mechanisms for porosity attached to a grain boundary. The arrows indicate pathways for atom migration.

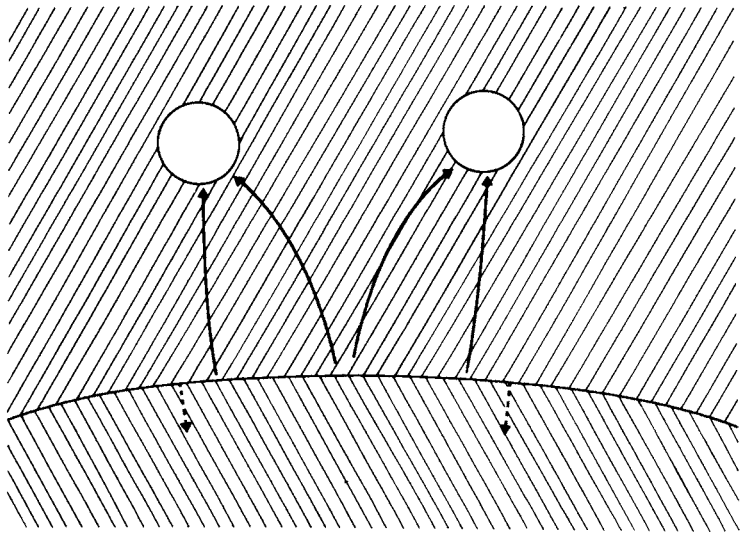

Fig. 3. Densification mechanism for porosity separated from a grain boundary. The solid arrows indicate pathways for atom migration, and the dashed arrows the direction of boundary migration.

TABLE II

HIGH DENSITY SINTERING OF OXIDES

Host	Additive	Reference[a]
Al_2O_3	MgO	(1)
	NiO	(2)
Y_2O_3	ThO_2	(3)
ThO_2	CaO, Y_2O_3	(4),(5)
Cr_2O_3	MgO	(6)
MgO	NaF	(7)
$PbLa(ZrTi)O_3$	PbO	(8)
MFe_2O_4	MO	(9)
$MgAl_2O_4$	CaO	(10)

[a] Key to references:

(1) Coble (1961).
(2) Jorgensen and Westbrook (1964).
(3) Jorgensen and Anderson (1967); Greskovich and Woods (1973).
(4) Jorgensen and Schmidt (1970).
(5) Greskovich *et al.* (1972).
(6) Ownby and Jungquist (1972).
(7) Banerjee and Budworth (1972).
(8) Snow (1973).
(9) Kooy (1962).
(10) Bratton (1974).

operative in the different systems, has made it difficult to predict with confidence the choice of additive for any new system.

The objective in the search for theoretical density has been the improvement that results in certain properties from the absence of pores. For example, pores act as stress concentrators with adverse effects on mechanical properties; they act as pinning agents for domains with adverse effects on permeability; the most extreme instance, and the one most exploited, lies in the effect of pores on optical properties and in particular on light transmission (Peelen and Metselaar, 1974). In this last example, the elimination of pores, which act as efficient scattering centers for light, has allowed the use of completely dense polycrystalline ceramics in envelopes for high intensity vapor lamps.

C. Grain Boundary Migration

The control of grain growth is achieved by controlling the responsible process, which is that of grain boundary migration. Consequently, in seeking

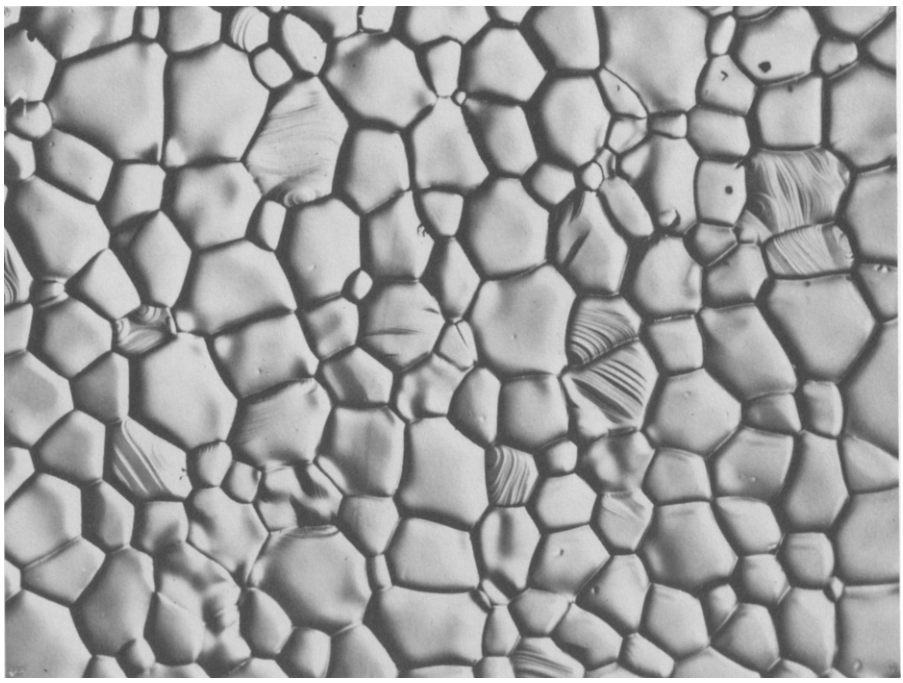

Fig. 4. A normal grain size distribution in an alumina ceramic (courtesy E. W. Roberts).

ways of encouraging or restraining grain growth, one is attempting to affect the mechanisms involved in boundary migration, and it will be necessary as a preliminary to consider these. There are a number of different mechanisms that can determine the migration rate, the particular one encountered in any situation being dependent on such factors as the purity of the material, its density, and the instantaneous distribution of the porosity, the impurities, and the boundaries with respect to one another.

Very little information on boundary migration has resulted from direct measurement (Simpson and Aust, 1972) so that the determination of the controlling factors has usually been attempted by the analysis of grain growth kinetics. For this purpose, microstructures have been divided into two categories depending on whether the distribution of grain sizes is relatively narrow (Fig. 4) and of fixed form throughout growth (normal) or whether the distribution becomes progressively wider (Fig. 5) with pronounced growth of a small fraction of the grains (abnormal). A number of analyses have attempted to show the stability of normal growth in a situation where pores and second phases are absent (Hillert, 1965; Louat, 1974). The criterion

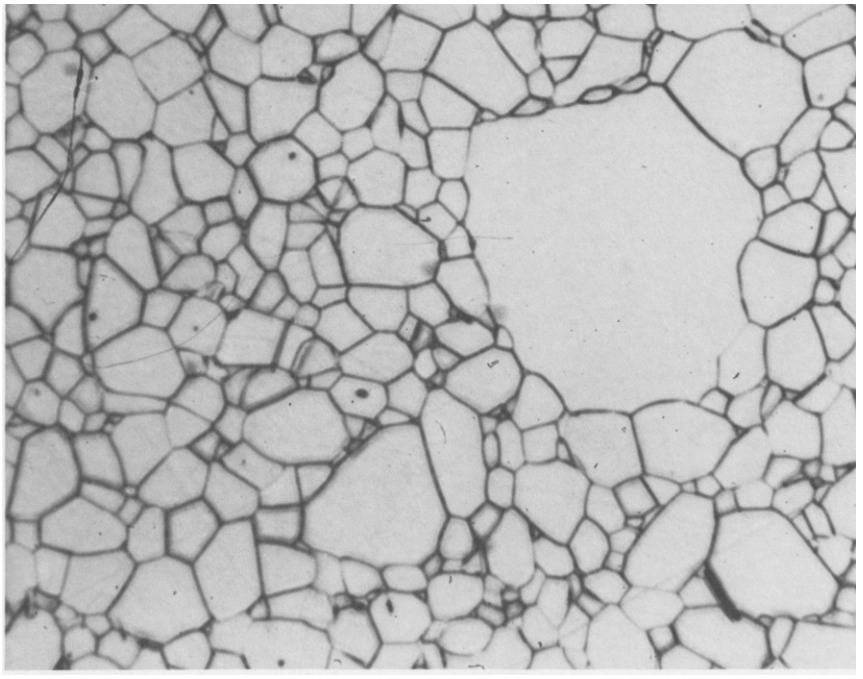

Fig. 5. Initiation of abnormal grain growth in an alumina ceramic (courtesy E. W. Roberts).

commonly taken for the existence of the normal state is that the largest grain should be smaller than twice the mean size (Hillert, 1965).

II. Normal Grain Growth Kinetics

This subject has been widely discussed and studied in the hope that the knowledge of the growth law obeyed by a particular system will allow detection of the rate-controlling process. This may then be describable in terms of a diffusion coefficient which can be compared with those from other diffusion processes, such as sintering, creep, or ionic conductivity. Once the controlling process is known, then steps may be taken to design a particular grain size into a specimen in the light of an intended application or to limit growth to benefit sintering to high density.

Growth kinetics can be complicated insofar as a wide variety of possible mechanisms has been recognized. In the summary that follows, these mechanisms are treated initially as separate phenomena; the more likely progressions from one mechanism to another during a process such as sintering will be considered subsequently.

The various growth processes are distinguished by the mechanisms of grain boundary motion, it being assumed (i) that the instantaneous rate of growth is directly proportional to the instantaneous average rate $\bar{v}$ of grain boundary migration in the structure (Burke and Turnbull, 1952). Thus

$$d\bar{G}/dt \sim \bar{v} \tag{3}$$

where $\bar{G}$ is the average grain size. The term $\bar{v}$ can in turn be represented in terms of a force-mobility product

$$\bar{v} = M\bar{F} \tag{4}$$

so that factors arising from the mechanism of migration can be isolated in the mobility term M. The driving force for boundary migration in ceramics is most commonly derived from the pressure gradient ΔP across the boundary arising from its curvature given by

$$\Delta P = S\,(1/r_1 + 1/r_2) \tag{5}$$

where S is the grain boundary energy, and r_1 and r_2 are the two radii of curvature of the boundary surface.

Assuming (ii) that the distribution of grains remains constant during normal growth, so that the change of appearance of a structure is analogous

to the progressive enlargement of a single pattern,

$$(1/r_1 + 1/r_2) = 1/K\bar{G} \tag{6}$$

where K is a constant. From this point to reach an expression for the time dependence of $\bar{G}$, the dependence of the mobility of the boundary M on $\bar{G}$ is required, so that substitution in Eq. (3) and integration of the resulting growth law can be effected. The different mechanisms are most easily identified in terms of the different boundary mobilities that apply.

A. Pure Single-Phase Systems

The process involved in the simplest case is the transfer of atoms from the edge of a shrinking grain across the grain boundary onto the edge of the neighboring growing grain (Burke and Turnbull, 1952). The driving force $\bar{F}$ for this atom migration is the chemical potential gradient caused by the pressure difference across the boundary

$$\bar{F} = \frac{d\mu}{dx} = \frac{d(V\Delta P)}{dx} = \frac{a^3 S}{K\bar{G}} \frac{1}{w} \tag{7}$$

where V is the atom volume ($\sim a^3$) and w is the boundary thickness. The flux of atoms is then

$$J = \frac{1}{a_*^3} M_a \frac{d\mu}{dx} = \frac{1}{a_*^3} \frac{D_a}{kT} \frac{a^3 S}{K\bar{G}} \frac{1}{w} \tag{8}$$

where D_a is the diffusion coefficient for atoms at the boundary; the boundary velocity becomes

$$\bar{v} = a^3 \frac{D_a}{kT} \frac{S}{w\bar{G}K} \sim \frac{d\bar{G}}{dt} \tag{9}$$

On integration

$$\bar{G}^2 - \bar{G}_0^2 = K' \frac{a^3}{w} \frac{D_a}{kT} S\, t = K'' t \tag{10}$$

the so-called parabolic growth law with G_0 the starting grain size.

Several features may be noted. First, the driving force is held to arise from the curvature of the boundary alone; energy differences arising from any difference in the crystallographic situation of the atom on the shrinking and

growing grains have not been considered. Second, the term w for the boundary width has been assumed to remain constant during growth because the absence of impurities and of second phases implies that the detailed structure of the boundary is independent of grain size. It is to be expected that w will depend on orientation. Third, for boundary migration in ionic compounds, the term a_*^3 in Eq. (8) will represent the volume of material transferred along with each ion of the slower moving species while the diffusion coefficient D_a will also be that for the slower species.

B. Impure Single-Phase Systems

Impurities present in solid solution can give rise to an impurity drag effect which impedes boundary motion (Cahn, 1962). The effect arises from any preferred segregation of the impurity either to or from the grain boundary area. If, for example, because of size or charge differences, the impurity can occupy energetically favorable sites at the grain boundary, boundary motion implies either that the impurities must diffuse along with the boundary or that their energy is raised as they are left behind.

Analysis of the drag effect leads to a distinction between low and high velocity situations. Experimental observations (Sun and Bauer, 1970) indicate that the former is more likely for normal grain growth in ceramic systems, and, as a consequence, the following discussion is limited to this low velocity situation. The expression for boundary velocity in this regime is given by

$$v = P/(L + \alpha C_0) \tag{11}$$

where P is a driving pressure ($= F/a^2$) and L is the intrinsic drag coefficient ($= 1/Ma^2$). In present notation then

$$v = F\left(\frac{M}{1 + M\,\alpha C_0\, a^2}\right) \tag{12}$$

Here C_0 is the bulk impurity concentration and α is a function of the energy profile for solute atoms at the boundary. For situations where segregation is toward the boundary region and where the center of the boundary contributes most to the drag effect

$$\alpha = \frac{4\Phi kTwQ}{D_b} \tag{13}$$

where Φ is the volume concentration of atoms and Q is the partition coef-

ficient for the impurity between the boundary region and the bulk. Substituting, and making the approximation that D_b, the diffusion coefficient for the impurity in the boundary region, is similar to D_a,

$$v = F\frac{M}{1 + 4\Phi wQ\, C_0 a^2} \tag{14}$$

The reciprocal of the velocity is from Eq. (11) a linear function of the impurity concentration.

From Eq. (14), it is seen that whenever the impurity concentration or degree of segregation is pronounced, the rate of boundary migration and hence of grain growth is reduced. The growth law can also be altered from the form given in Eq. (10), since C_0, the bulk impurity concentration, is a function of the grain size (Brook, 1968)

$$C_0 = \frac{C_T}{1 + f(S/G)\,(Q - 1)} \tag{15}$$

where C_T is the total impurity concentration which remains constant. Under conditions of large Q and small G, and large C_T, a law of the form

$$dG/dt \sim 1/G^2; \qquad G^3 - G_0^3 = Kt \tag{16}$$

is expected.

It may be noted that in the solid solution drag effect, the boundary thickness w is the width of the zone over which impurities interact with the boundary. This is taken as independent of the grain size. The diffusion coefficients D_a and D_b of the host and impurity species in the boundary region will depend upon the nature of the boundary structure. An important point is that impurities, in affecting the boundary velocity in an ionic solid, may act either through the C_0 term in Eq. (14) or through the effect of introduced point defects (for example, vacancies) on the diffusion coefficient terms in M. The relative importance of these factors must, in the absence of detailed knowledge of grain boundary structure in ceramics, await experimental determination.

C. Systems Containing a Continuous Second Phase

The effect of a liquid phase in the grain boundary is most easily considered in terms of the idealized case where the liquid completely wets the grains (dihedral angle = 0). Then growth occurs by migration of atoms from the shrinking grain through the liquid to the growing grain. For a constant total volume of liquid, the growth law takes the form of Eq. (16).

Cases of varying dihedral angle, and of substantial quantities of liquid phase, where the treatment is analogous to that of Ostwald ripening (Lifschitz and Slezov, 1961) have been described quantitatively (White, 1973); the form of the law obtained is unchanged.

D. Systems Containing Fixed Second-Phase Inclusions

Second-phase inclusions act as pinning agents to grain boundaries since the attachment of an inclusion reduces the total boundary energy by an amount equal to the specific surface energy times the area occupied by the inclusion particle. If the inclusions are relatively immobile (Ashby, 1969), a boundary pinned at an inclusion can only move by breaking free. To pull the boundary away from a spherical particle in this way requires a force πrS, where r is the particle radius. When this retarding force is equal to the driving force arising from the curvature of the boundary, boundary migration ceases and the system reaches a limiting grain size. For randomly distributed inclusions (C. Zener, 1949, private communication to Smith, 1948), the two forces cancel at a size given by

$$G_{\text{limit}} \sim r/V_f \tag{17}$$

where V_f is the volume fraction of inclusions. Similar expressions have been derived for a variety of distributions of the inclusion phase (K. T. Harrison, private communication, 1972, but see Woolfrey, 1967).

The significance of this effect is that a grain size can be stabilized by the presence of inclusions. Thereafter further growth can only occur (i) if the inclusions coalesce, i.e., the large ones grow by diffusion of atoms from the small ones through the host matrix (Ostwald ripening); (ii) if the inclusions gradually go into solution in the host lattice; (iii) if abnormal growth is seeded.

The rate of coalescence has been treated by a number of authors. If the inclusions coalesce by atom migration through the bulk of the matrix (Greenwood, 1956) then $r^3 \sim t$, and if by atom migration along the grain boundary (Speight, 1968) then $r^4 = t$. Since V_f remains constant in Eq. (17), these expressions mean that for coalescence by matrix diffusion,

$$G_{\text{limit}}{}^3 \sim t \tag{18}$$

which is a growth law analogous to Eq. (16) in form.

For the situation where the inclusions are soluble, control of the solution rate by an interface reaction leads to a constant rate of reduction in the radius of the inclusions. Assuming that the number of particles is unchanged, this

leads to a growth equation

$$G \sim (r_0 - Kt)^{-2} \tag{19}$$

where r_0 is the inclusion radius at time zero. Since the rate of dissolution must have been small relative to the rate of grain growth prior to the attainment of the limiting size, K may be taken as small, and, to an approximation,

$$G - G_0 \sim 2Kt/r_0^3 \tag{20}$$

The case of seeding of abnormal growth is considered in a later section.

E. Systems Containing Mobile Second-Phase Inclusions

This is both the most frequent and the most technologically important of the grain growth situations encountered in ceramic materials, since it includes the case of porosity and its effect on grain growth. The type of growth that occurs during sintering is therefore included in this category.

As before, the important consideration is the type of interaction that can occur between the boundaries and the second phase. As in the case of immobile inclusions, grain growth can occur until the stage is reached where boundaries are pinned by the inclusions. The present case is then complicated by the fact that the second phase can coalesce, or go into solution (or, in the case of porosity, disappear as densification occurs), or, as a new alternative, migrate along with the boundaries, in some circumstances giving a boundary migration rate controlled by the movement of the second-phase particles. This third alternative can most usefully be discussed in terms of porosity.

It is important first to decide under what circumstances the pores and the boundaries remain attached at a particular stage during the processing. For this, the parameters of interest are v_p and v_b, the velocities at which the pores and boundaries, respectively, are capable of moving under the forces acting on them. To introduce microstructural variables, these velocities can be treated as force–mobility products

$$v_p = M_p F_p \tag{21}$$

$$v_b = M_b F_b' \tag{22}$$

Separation of pores from the boundaries then occurs when $v_b > v_{p\,max}$ (Speight and Greenwood, 1964). Noting that F_b', the force on the boundary consists

of two parts: F_b, the force arising from the curvature of the boundary, and NF_p, the drag force of the N attached pores (Nichols, 1968), the condition for attachment can be written

$$v_p = F_p M_p = v_b = (F_b - NF_p)M_b \tag{23}$$

from which

$$v_b = F_b \frac{M_p M_b}{NM_b + M_p} \tag{24}$$

When $NM_b \gg M_p$,

$$v_b = F_b(M_p/N) \tag{25}$$

and pore parameters control boundary movement. When $NM_b \ll M_p$,

$$v_b = F_b M_b \tag{26}$$

and boundary parameters control boundary movement.

The kinetics for the various boundary-controlled processes have been discussed in earlier sections. Those for the pore-controlled situation may be considered by way of the terms in Eq. (25). To do this, it will be necessary to make assumptions about microstructural parameters such as pore shape and pore distribution. This greatly reduces the generality of the argument and requires a degree of approximation that has called into question the value of this approach (Mocellin and Kingery, 1973). However, faced with the very wide range of microstructural situations that are encountered in ceramics processing, it is probable that any theory which closely matches one particular system will necessarily be inapplicable to a wide range of others. Consequently, the basis for using average microstructures with idealized features is that a qualitative picture may emerge which has widespread, if approximate, validity. The hope is that qualitative explanations for observed behavior may be provided which will allow the interpretation of experiments, and therefore provide a basis for predicting the effects of deliberate changes in conditions on microstructure development. More exact work can then follow, either by refinements in the model to meet particular structures (J. White, private communication, 1972) or by choice of those structures which most closely match the features of the idealized model.

Proceeding to the model, the mobility of pores M_p has been described (Shewmon, 1964) for the idealized case of the spherical pore. If, for example, such a pore moves by surface diffusion of atoms from the front wall to the

back, the net atom flux is

$$J_s A_s = \frac{D_s}{a^3 kT} F_a 2\pi rw \tag{27}$$

where the subscripts s denote surface diffusion round a pore, radius r, in a surface zone, depth w, under a driving force of F_a per atom. For the pore to move distance dx, a volume $\pi r^2 dx$ flows around the pore. Hence

$$\frac{dx}{dt} = \frac{-J_s A_s a^3}{\pi r^2}$$

$$= \frac{-2 D_s w}{kTr} F \tag{28}$$

The work done in moving the pore a distance dx is the same as that to move $\pi r^2 dx/a^3$ atoms a distance $2r$, so that

$$F_p dx = -F_a 2r \frac{\pi r^2 dx}{a^3} \tag{29}$$

and

$$v_p = F_p \frac{D_s w a^3}{kT \pi r^4} \tag{30}$$

The various possibilities for the mobility by different diffusion mechanisms are collected in Table III.

Evaluation of grain growth kinetics from M_p and Eq. (25) requires two further assumptions:

(i) that in the later stages of sintering, grain growth is relatively faster than densification so that the pore fraction remains essentially consistent. Under these conditions, as grains are removed in the growth process, pores migrating with the boundaries are brought together, and pore growth occurs together with grain growth (Kingery and François, 1965), so one may put $r \sim G$. Experimental evidence for this assumption is not unambiguous (Kapadia and Leipold, 1973).

(ii) that N can be expressed in terms of its grain size dependence. The particular value of N taken for any system must depend on observation. For the particular situation where pores are located at grain corners, their separation is of the order of G, so that the density on the boundary

$$N \sim a^2/G^2 \tag{31}$$

TABLE III

A. Mobilities[a]		
M_p	Mobility of spherical pore: migration by the faster of:	
	(a) Surface diffusion	$\frac{D_s\, wa^3}{kT\,\pi r^4}$
	(b) Lattice diffusion	$\frac{D_l\, a^3}{fkT\,\pi r^3}$
	(c) Gas phase diffusion	$\frac{D_g\, \rho_g\, a^3}{kT\,\rho_s\, 2\,\pi r^3}$
M_b	Mobility of boundary:	
	Pure system	D_a/kT
	Impurity drag	$\frac{1}{kT}\left(\frac{1}{D_a}+\frac{4\Phi rwQ\, C_0 a^2}{D_b}\right)^{-1}$
B. Forces		
F_p	Maximum drag force of pore	πrS
F_b	Force on pore-free curved boundary	$2Sa^2/KG$

[a] f, correlation factor for diffusion.
ρ_g, density in the gas phase of the rate controlling species.
ρ_s, density in the solid phase of the rate controlling species.

A relation similar to Eq. (31) holds wherever the distribution of pores relative to grains remains constant during growth. With these assumptions, the kinetics of growth can be evaluated. As an example, for control of boundary motion by pore migration involving surface diffusion of atoms as the operative mechanism

$$\begin{aligned} dG/dt \sim v_b &= F_b M_p (1/N) \\ &\sim (1/G)\,(1/G^4)\,(G^2) \sim 1/G^3 \\ G^4 - G_0{}^4 &= Kt \end{aligned} \tag{32}$$

A tabulation of the various growth laws together with the possible responsible mechanisms is given in Table IV, both for the pore-controlled processes and for the boundary processes described earlier.

F. Discussion

Measurements of normal grain growth kinetics have generally concentrated on the following items: (i) demonstration that normal growth is

TABLE IV

KINETICS OF GRAIN GROWTH FOR VARIOUS MECHANISMS

	n in $G \sim t^{1/n}$
Pore control	
Surface diffusion	4
Lattice diffusion	3
Vapor transport ($P = \text{const}$)	3
Vapor transport ($P = 2S/r$)	2
Boundary control	
Pure system	2
Impure system	
coalescence of second phase by lattice diffusion	3
coalescence of second phase by grain boundary diffusion	4
solution of second phase	1
diffusion through continuous second phase	3
impurity drag (low solubility)	3
impurity drag (high solubility)	2

Note: The pore control kinetics are given for the situation where the pore separation is related to the grain size, i.e., $N \sim 1/G^2$. Changes in distribution during growth would change the kinetics.

occurring, (ii) measurement of the growth exponent n, and (iii) measurement of an activation energy E_a. In isolation, these three parameters are not capable of giving an unambiguous explanation of the growth behavior. The parameter n, even if a constant value is observed over a wide temperature and grain size range, does not indicate a specific mechanism—the most commonly observed value, 3, can for example be indicative of one of five separate processes.

Similarly the activation energy has rarely been identified with a definite atom migration process. In addition to D_s, D_l, D_g, D_a, and D_b referred to in Table III, there are possible diffusion coefficients for the coalescence of second-phase inclusions, porosity included, any one of which in a given set of experiments may be responsible for the temperature dependence of the growth process.

Because of this dilemma there has been a tendency in more recent studies of grain growth to follow the procedure noted earlier and to observe closely the microstructural and compositional parameters (pore size, pore distribution, extent of solid second phases, level of dopants, nonstoichiometry) so that these, in conjunction with measurements of n and E_a, will afford an identification of the rate-controlling process and will allow comparison of grain growth kinetics with other mass transport processes. The rewards from

such studies in the form of an improved ability to prepare ceramics with controlled microstructures are potentially considerable.

III. Abnormal Grain Growth

Control of grain growth in practice has usually been considered in the context of suppressing abnormal grain growth. This process, where a small number of grains in the population grow rapidly to very large size (on occasion to several orders times the size of the average in the population) is of importance first because of the extreme sizes reached and second because the walls of the large grains can pull away from any restraining second phase during the growth process. The second phase is, as a consequence of this latter factor, trapped within the grains. Where the second phase is porosity, this trapping sets a limit to densification in reasonable times.

Once growth of this type has begun, it follows linear kinetics as may be readily seen from structural considerations. Where all grains are of comparable size, the boundary curvature required to attain three-boundary intersections of 120° is small. Direct observations (Haroun and Budworth, 1968) have indicated $G \approx r/10$. However, for an abnormal grain of size such that its unrelaxed surface is planar in comparison with the faces of surrounding grains, the attainment of 120° intersections requires local curvatures with radii close to the matrix grain radius. From Eqs. (5) and (26), assuming that the atomic structure of the boundary at the abnormal grain is unchanged, one has

$$v_b^{\text{abnormal grain}} = M_b(2a^2S/G) \tag{33}$$

where the boundary velocity has increased owing to the enhanced driving force.

The assumption is commonly made that the difference in driving force is sufficient that the rate of change of the matrix grain size G can be considered negligible. Then Eq. (33) is relatively constant, and the abnormal grain increases in size linearly with time as $G - G_0 = Kt$. This argument is more convincing where the matrix grain structure has reached a limiting size owing to the presence of inclusions. The linear growth rate means that once abnormal growth has begun, the growing centers can rapidly consume the original grain structure to the point where only large grains remain. It is possible that a number of the observations of rapid normal grain growth in the literature (Table V) are the result of an abnormal intermediate stage rather than of a truly accelerated normal growth.

TABLE V

EFFECT OF ADDITIVES ON GRAIN BOUNDARY MIGRATION

Host	Additive	
	Enhancement[a]	Suppression[a]
Al_2O_3	H_2,[1] Ti, Mn[2]	Mg,[3,4] Zn, Ni,[4] Cr, Mo, Ni, W, BN, ZrB_2[2]
BeO		Graphite[5]
Cr_2O_3		Mg[6]
HfO_2	Mn, ZrB_2[2]	Cr, Mo, W, Ni, Ti, BN[2]
MgO	Mn,[2] B[7]	MgFe,[8] Fe,[9] Cr, Mo, Ni, Ti, V, BN, ZrB_2[2]
ThO_2		Ca[10]
UO_2	Ti[11]	V,[12] H_2[13]
Y_2O_3		Th[14]
ZnO		O_2,[15] K[16]
ZrO_2		H_2,[17] Cr, Mo, W, Mn, Ni, Ti, BN, ZrO_2[2]
$BaTiO_3$		Ta,[18] Nb,[19] Ti,[20] Al/Si/Ti[21]
TIG	O_2[22]	
YIG		Y[23]
$Pb(ZrTi)O_3$		Al, Nb,[24] Fe,[25] Ta,[26] Bi,[27] La[26,28]
$MgCr_2O_4$		O[29]
CoO		Li[30]

[a] Superscript numbers are references as follows:

[1] Hamanu *et al.* (1964).
[2] Arias (1966).
[3] Coble (1961); Bruch (1962); Jorgensen (1965); Mocellin and Kingery (1973).
[4] Haroun and Budworth (1970).
[5] Langrod (1965).
[6] Ownby and Jungquist (1972).
[7] Miyagawa *et al.* (1972).
[8] Van Vlack and Iuadden (1964).
[9] Gordon *et al.* (1970).
[10] Jorgensen and Schmidt (1970).
[11] Amato *et al.* (1966a).
[12] Amato *et al.* (1967b).
[13] Kostic and Petrovic (1968).
[14] Jorgensen and Anderson (1967).
[15] Gupta and Coble (1968); Dutta and Spriggs (1970).
[16] Gupta (1971).
[17] Tien and Subbarao (1963).
[18] Inarkulich *et al.* (1966).
[19] Kahn (1971).
[20] Jonker and Noorlander (1962).
[21] Matsuo *et al.* (1968).
[22] Low (1970).
[23] Paladino and Maguire (1970).
[24] Atkin and Fulrath (1971).
[25] Weston *et al.* (1969).
[26] Kulcsar (1959).
[27] Haertling (1964).
[28] Langman *et al.* (1973).
[29] Anderson (1974).
[30] Kumar and Johnson (1974).

Since the abnormal process is rapid once begun, the effort to control it must be made at the initiation stage. From this point of view, two factors have been recognized as leading to abnormal growth. The first is that the original distribution of grain sizes in the starting material may contain grains larger than are stable in terms of the Hillert criterion. In this respect, wide initial particle size distributions have been recognized as predisposing toward abnormal growth (Chol, 1971).

The second situation arises in systems undergoing normal grain growth where a mobile second phase is attached to the boundary (Brook, 1969). If one takes the case of porosity, then since the maximum pore velocities are more strongly dependent on pore size than the boundary velocities are on grain size, the observation that pore size increases in step with grain size means (Fig. 6) that pores eventually become separated from grain boundaries as normal growth proceeds. This situation, which has been noted as symptomatic of abnormal growth, can be expressed in the earlier notation as

$$v_p^{\max} = F_p^{\max} M_p < v_b = (F_b - NF_p^{\max}) M_b \tag{34}$$

or

$$F_b > NF_p^{\max} + \frac{M_p F_p^{\max}}{M_b} \tag{35}$$

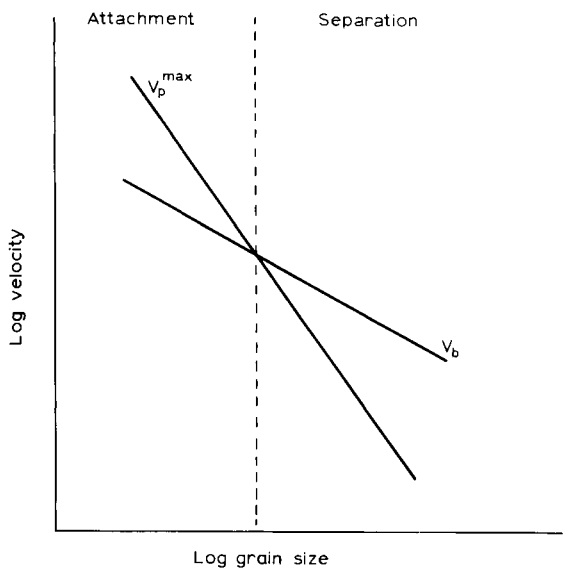

Fig. 6. The dependence of pore velocity $V_p^{\max}$ and boundary velocity V_b on grain size for the situation where pores move by a surface diffusion mechanism and where the boundary is unaffected by impurity. Under these conditions, $V_p^{\max} \sim G^{-3}$; $V_b \sim G^{-1}$.

TABLE VI

TERMINOLOGY AND PORE–BOUNDARY INTERACTIONS

Pore–boundary interaction	Type of growth	Controlling process	Conditions
Attachment	Normal	Pore migration	$1 > B > Y - 1$
Attachment	Normal	Boundary migration	$1 < B > Y - 1$
Separation	Abnormal	Boundary migration	$B < Y - 1$

Mobility ratio $B = M_p/NM_b$ where M_p = pore mobility, M_b = boundary mobility, N = pore density at boundary.

Force ratio $Y = F_b/NF_p$ where F_p = force exerted on pore by boundary, F_b = force on boundary arising from curvature.

which defines the circumstances for pore–boundary separation. Defining a mobility ratio, $B = M_p/NM_b$, and a force ratio, $Y = F_b/NF_p$, the possible pore–boundary interactions can then be categorized as shown in Table VI.

In sum, normal growth proceeds to the point where local variations in microstructure first bring the inequality [Eq. (35)] into effect; thereafter, abnormal growth occurs until the abnormally growing grains impinge. The situation is then that of a normal grain distribution with the grains having large size. By the earlier arguments, the term F_b is then greatly reduced, attachment of inclusions to the boundary is restored, and depending on the value of M_p, zero growth, or growth controlled by Eqs. (25) or (26) follows. Microstructures showing these features have been recently observed (Rossi and Burke, 1973).

IV. Direct Control of Grain Growth

The technique employed for direct control of the growth processes has involved the use of additives which, because of their most common objective, namely the suppression of abnormal growth to enhance sintering, are commonly termed sintering additives. The mechanisms for growth have been outlined in an earlier section, and it is apparent that the situation is sufficiently complicated and ambiguous, that the role played by such additives can rarely be pinned down to an exact process. However, the general mode of operation has become clear and this is now outlined prior to a brief consideration of specific systems.

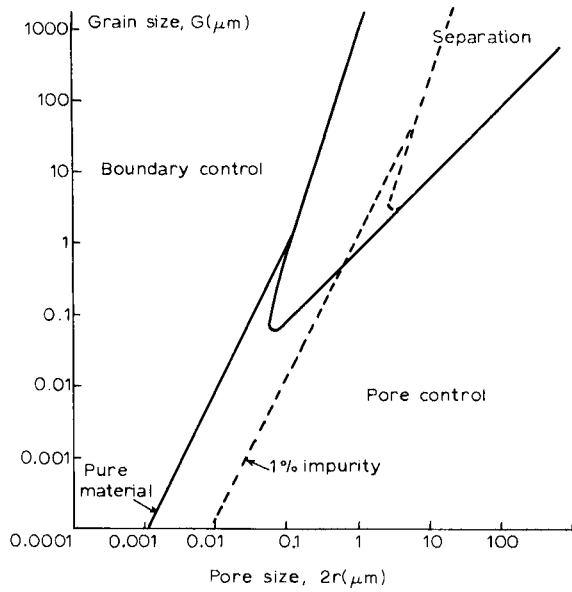

Fig. 7. The dependence of the type of pore–boundary interaction on microstructural parameters when pores migrate by a surface diffusion mechanism. The interpore spacing is assumed equal to the grain size (Brook, 1969).

A. Solid Solution Additives

For suppression of abnormal growth, it can be seen by reference to Fig. 6 that a delay in the onset of the process can be achieved either by lowering v_b or raising v_p^{max}, thus shifting the crossover point to the right, that is, to a later stage in the firing process. For a given microstructural configuration this is the same as raising M_p or lowering M_b.

For slowing of normal growth one can either lower M_b [Eq. (26)] or M_p [Eq. (25)], though the latter approach may accelerate any tendency toward the onset of abnormal growth [Eq. (35)]. Consequently, on both counts the desired effect is achieved by a suppression of the grain boundary mobility.

The effect may be shown graphically. Considering idealized microstructures which incorporate spherical and regularly spaced pores, it may be seen that expressions for M_p, M_b (Table III), F_p, F_b, and N are available, so that substitution of these terms in the conditions listed in Table VI allows construction of a diagram showing the types of boundary–pore interaction that occur under different conditions of pore size and grain size.

An example of this technique is shown in Fig. 7 where it has been assumed that (i) pores move by surface diffusion, and (ii) the interpore spacing is equal

to the grain size, this being an approximation to the situation in the final stage of sintering.

The figure can be used to trace qualitatively the progress of a firing cycle or sintering process for which these assumptions are valid, since the overall microstructural changes can be represented as combinations of sintering (reduction in pore size) and grain growth.

Thus, for example, the initial conditions of grain size and pore size can be located on the diagram and the early stages of sintering, in which the pores shrink but grain growth is small, can be represented by a line running to the left of the original position. At later stages, grain growth occurs and the line turns upward. And in the final stages, for normal grain growth where sintering is slow and where the pore size as a result is proportional to the grain size, the line moves diagonally toward the upper right-hand portion of the diagram.

As far as sintering to high density is concerned, the aim is to avoid the separation region in Fig. 7, and the approach suggested has been that of lowering M_b. As indicated earlier in Eq. (14), this can be achieved by adding an impurity which forms a solid solution with the host but which segregates to the grain boundary, giving rise to an impurity drag effect. Using Eq. (14), and introducing 1 % bulk concentration of impurity, C_0, the effect is as

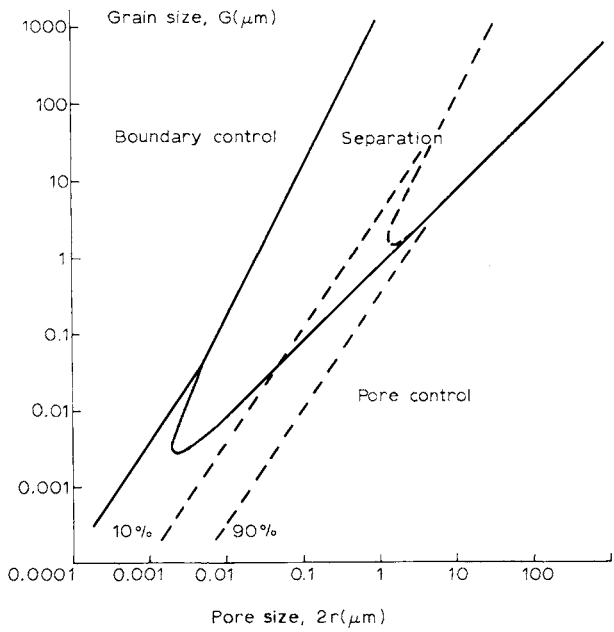

Fig. 8. Pore–boundary interactions when pores migrate by a lattice diffusion process.

shown in Fig. 7. It can be seen that the impurity increases the possibility that a given starting microstructure can be sintered without the onset of separation.

If the pores move by different mechanisms, M_p can show a different pore-size dependence, and the form of the diagram will then change (Table III). Figures 8, 9, and 10 are drawn for pore migration, respectively, by lattice diffusion, vapor transport with pore interior pressure $= 2S/r$ in a pure system, and vapor transport ($P = 2S/r$) in a system containing impurities, where [Eqs. (14), (15)] $M_b \sim 1/G$.

In Fig. 8, the effect of 1 % impurity addition is again shown. The 10 and 90 % lines represent points where boundary migration is 10 and 90 % controlled by pore migration kinetics. In all the other figures, the solid line dividing the boundary control and pore control regions is the 10 % line ($B = 10$). In Figs. 7 and 8, the values for diffusion coefficients and other parameters can be approximated (Brook, 1969) so that the values on the axes give semiquantitative information. Figures 9 and 10, however, are constructed with the relevant size dependencies and a value of B selected to match that of Fig. 7 for $G = 1$ μm and $2r = 0.1$ μm. This is done to allow better comparison between the three diagrams and because the choice of

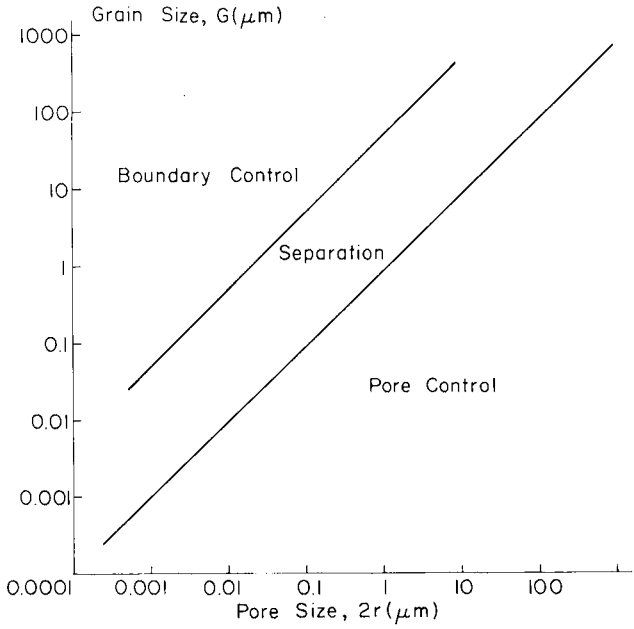

Fig. 9. Pore–boundary interactions when pores migrate by a vapor transport process with pore interior pressure $= 2S/r$.

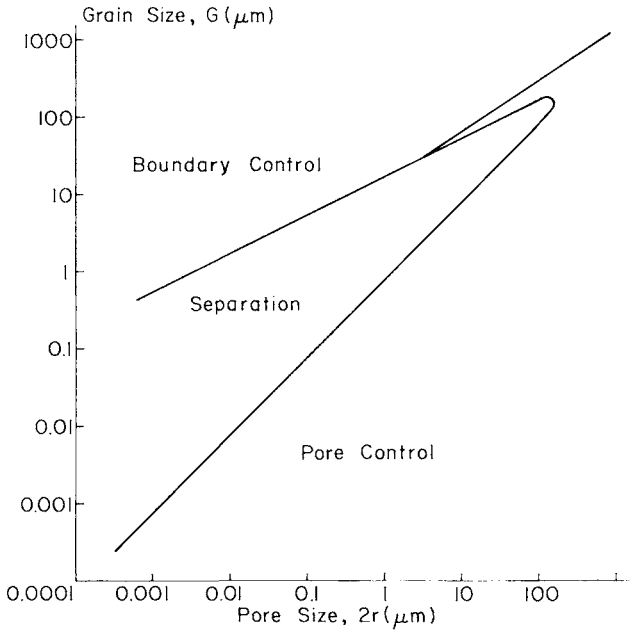

Fig. 10. Pore–boundary interactions when pores migrate by a vapor transport process with pore interior pressure $= 2S/r$ and when $M_p \sim G^{-1}$ as a result of the presence of impurities.

values for the vapor processes is distinctly arbitrary. There is consequently little significance in stating relative magnitudes for the B terms.

It may be noted in passing that, of these mechanisms, surface diffusion is favored under the microstructural conditions common in ceramic sintering, namely, fine grain and pore size, since the mobility of the pore by the surface diffusion mechanism is larger than the mobility by other mechanisms at small pore sizes. As growth proceeds, however, and particularly if an intermediate abnormal stage has led to a generation of large grains, the conditions appropriate to one diagram may change to those appropriate to another. It may not therefore be possible to trace a complete sintering cycle on any single diagram.

Working on the basis that the role of the additive in suppressing abnormal grain growth by restricting the separation region of Fig. 7 lies by way of the impurity drag effect, the choice of additives for a given system may be made by observing (Table III) that optimum results will be achieved with an additive that is highly soluble (C_0 large) but preferentially attracted to the grain boundaries (Q large). Aside from this, since the desired end result is a single-phase material, the additive should preferably not form a second phase.

The requirements on C_0 and Q are to an extent contradictory in that the high C_0 explicitly requires a high bulk solubility for the additive, whereas the high Q implies an additive with high solubility at the boundary and low solubility in the bulk. Consideration of the examples in Table II suggests that a compromise has commonly been reached whereby use has been made of an additive with (i) similar cation size to that of the host, and (ii) different cation valence from that of the host. It may be that other compromise solutions would be equally effective. The segregation of impurities to grain boundaries has recently been reviewed by Kingery (1974).

A further item (where the surface diffusion mechanism for pore migration applies) is that the mobility ratio B increases as the temperature is lowered, since the activation energy for surface diffusion is generally less than that for diffusion across the boundary. Accordingly, the lowest practicable sintering temperature should be employed when aiming for high density results.

Accounts of the operation of sintering additives based on effects other than impurity drag have also been presented (Jorgensen, 1967; Budworth, 1970). A common feature in these accounts is the action of the additive in slowing the mobility of the grain boundary M_p. The accounts differ in proposing mechanisms for the retarding effect which involve, respectively, second-phase inclusions at the boundaries or an impurity film at the boundary in a form intermediate between solid solution and second phase. A complicating factor in all accounts is that for ionic compounds, a major effect of the additive may be in its interaction with the defect chemistry of the host. Generally, such effects are less important for diffusion at the grain boundary (atom migration from one crystallite to the next) than they are in bulk processes (where diffusion occurs by point defect migration). However, in such mechanisms as impurity drag, where the diffusion of the added impurity in the region close to the boundary is involved, any interaction between the impurity and the host imperfection chemistry may affect the value of the impurity diffusion coefficient. Then, for instance, when a cation of higher charge than the host cation is added and cation vacancies are created as charge compensation, D_b may be increased even to the extent that M_b is little different for the impure case than for the pure case. Separation of pores from the boundary is then encouraged for a wider range of microstructural conditions than would be expected from the simpler analysis (Fig. 7). Similarly, for additives which suppress the concentration of defects responsible for diffusion, D_b is reduced and the additive is expected to be more effective than predicted in the simpler analysis.

Generally, the situation for alivalent additives can become extremely complicated and the analysis of any particular experiment requires a detailed understanding of the defect chemistry which, in ceramic systems, is usually

unavailable. Accordingly, the simpler models must act as starting points for the analysis of current experimental data.

B. Second-Phase Additives

The existence of a second phase in the grain boundary can affect grain growth in a number of ways, and a reliable interpretation of the mechanisms involved has rarely been possible. Some of the situations that can arise are briefly noted in the following.

The second phase may exist as a solid or as a liquid at the processing temperature and its effect on boundary migration will depend strongly on its distribution in the boundary, which in turn will depend on the various interfacial energies or more precisely on the ratio of the clean boundary energy and the interfacial energy between the two phases (Smith, 1948). Where this ratio is small, the second phase will, at small concentrations, form isolated spheres in the host matrix. In this configuration, the behavior will be similar to that for porosity as treated earlier, and while the boundary velocity is reduced when the phase is attached to the boundary, the conditions are such as will lead to the initiation of abnormal growth. Both solid and liquid should behave in this way with solid inclusions perhaps having more effect because of a lower mobility.

Where the energy ratio is high, the second phase will exist as plates or films in the grain boundaries. In addition to the effect on the driving force for growth arising from change in the boundary energy, the film will alter the kinetics for growth since migration now requires diffusion of atoms from the shrinking grain through the boundary phase to the growing grain. This reduction in mobility of the boundary then has a similar effect to the solid solution situation in suppressing abnormal growth and slowing normal growth (Budworth, 1970). It has been observed in some of the examples of sintering to complete densification (Jorgensen, 1967).

A problem encountered with liquid second phases is that diffusion coefficients for the matrix atoms in the second phase may be relatively high. Thus although the boundary migration rate is slowed with respect to that of the pure material, the rate may be enhanced when compared with a material in which solid solution drag effects have been operating. With the level of purity normally available in ceramics such effects must normally be expected. Consequently, the observed migration rate in such a system is increased by dopants which give a continuous liquid grain boundary phase, and any tendency toward abnormal growth is enhanced. This situation is fairly common in ceramics, resulting in microstructures showing abnormal growth in which the large grains have pronounced development of favored crystallographic faces.

The variety of effects that can result from the presence of second phases and the fact that the influence on grain growth rates can be of either type, makes it particularly difficult to predict what the influence of a specific additive will be. Although the various factors that can be of importance have been recognized, this aspect of grain growth control remains almost entirely empirical.

C. Adjustment of Nonstoichiometry

In addition to the use of impurities as dopants for the control of grain growth, it is possible, particularly in systems which display a wide range of nonstoichiometry, to adjust the proportions of the host atoms and thereby affect kinetic processes. In binary oxides this is usually achieved by control of the oxygen partial pressure in equilibrium with the system during processing (Kroger, 1964; Kofstad, 1972). In ternary oxides the same results can be brought about by adjusting the ratios of the constituent binary oxides (Schmalzried, 1965).

The effect of, for example, variation in oxygen activity over a binary oxide is in the most simple situation to vary the concentration of native point defects in the oxide. Regarding boundary migration as the diffusion of atoms from a shrinking to a growing grain across a narrow boundary zone, it is not clear that native point defects need be involved in a proposed mechanism. However, since in most ceramic examples second phases (pores) and impurities are present, point defects become of significance in the processes whereby these second phases or impurities are moved. In short, the various diffusion coefficients listed earlier as possibly rate controlling in the practical situation are affected by defect concentrations.

To take an example, if migration is controlled by movement of second-phase pinning agents by lattice diffusion of the host atoms around the second phase, then the overall process would be controlled by the diffusion of the slower of the two host species. Since this is commonly oxygen in the case of oxides, the process would be slowed by a reduction in the number of point defects responsible for oxygen transport. If these were known to be oxygen vacancies then the use of high oxygen activities during processing should suppress growth.

Although such factors are real in the sense that they do affect rates of processes, the level of uncertainty in ceramic systems is such that any interpretation of grain growth data in these terms must be considered speculative. One would need to know something of the defect chemistry of the system in question, the relative importance of lattice and boundary diffusion pathways for the species in question, and the controlling mechanism for boundary migration.

It has long been an ambition for those concerned with the processing of ceramics to use control of point defect concentrations as a deliberate technique for desired microstructural development in a full range of materials. The first stage in the realization of this hope, which is the understanding of the defect chemistry of single crystal systems, has made substantial progress. However, a number of intervening stages and in particular the establishment of firm data for mass transport and defect chemistry in the grain boundary regions of polycrystals remain before the selection of processing conditions including atmosphere control can become widespread.

D. Examples of the Use of Additives

Instances where additives have been observed to affect grain growth are assembled in Table V. The concentrations used have ranged from fractions of a percent to several percent. Generally the role of the additive has been to suppress the growth rate, the mechanism being that of slowing boundary migration either by solid solution drag or second phase pinning. This preponderance of suppression in the observations is not unexpected in that additives to pure materials suppress normal growth in both mechanisms.

The observations of growth enhancement may arise (i) from observations following an intervening abnormal growth stage in a system where normal growth has been slowed, (ii) from impure systems in which further additives had formed a liquid phase, or (iii) from compositional enhancement of the native diffusion coefficients.

Clear identification of the mechanism of operation in any set of experiments has usually not been available. In a few instances, subsequent close examination of the microstructure has allowed identification of the controlling process. As more instances of this type are described, it is to be hoped that the ability to predict additives for specific systems can be developed.

V. Avoidance of Grain Growth

The second major technique in achieving desired grain sizes is to accelerate the other desired microstructural changes so that relatively little grain growth takes place. This has been achieved in the case of densification, which is the usual desired process, either by increasing the driving force (by applied pressure) or by increasing diffusion coefficients (by raising the temperature).

The first of these (hot pressing or pressure sintering) has been the subject of recent reviews (Spriggs and Dutta, 1974) and is described in an earlier chapter in the present volume. A tabulation of some oxide systems that have been

TABLE VII

SOME EXAMPLES OF HOT PRESSING IN OXIDES

Al_2O_3	Rossi *et al.* (1970)
$Al_6Si_2O_{13}$	Penty *et al.* (1973)
$BaTiO_3$	Graham *et al.* (1971)
BeO	Kodairi *et al.* (1972)
CaO	Gupta *et al.* (1973)
CoO	Urick and Notis (1973)
CrO_2	Nakayama *et al.* (1966)
$(KNa)NbO_3$	Perduijn *et al.* (1970)
$LiAl_5O_8$	Gazza (1972)
$Li_{0.5}Fe_{2.5}O_4$	West and Blankenship (1967)
$MgAl_2O_4$	Chay *et al.* (1968)
MgO	Rice (1971)
NiO	Notis *et al.* (1973)
$(NiZn)Fe_2O_4$	Suemune (1971)
$Pb(ZrTi)O_3$	Ishitobi *et al.* (1974)
$(PbLa)(ZrTi)O_3$	Haertling (1971)
Sc_2O_3	Gazza *et al.* (1971)
SiO_2	Vasilos (1960)
ThO_2	Kulkarni and Moorthy (1965)
TiO_2	Egerton and Thomson (1971)
UO_2	Amato *et al.* (1966b)
$Y_3Fe_5O_{12}$ (YIG)	Nicolas and Hildebrandt (1973)
Y_2O_3	Lefever and Matsko (1967)
ZrO_2	Amato *et al.* (1967a)

studied is given in Table VII. It may be noted that the process is often conducted in conjunction with the use of additives.

The second process uses very high temperatures as in the zone sintering process where the firing cycle duration can be reduced to the order of 5 min. This process has been found particularly effective (Wynn Jones and Miles, 1971) for the preparation of dense β-Al_2O_3. The use of high temperature tends to encourage the initiation of abnormal growth processes, but the overall process time is so short that the finished grain size remains small. Considering its potential, this process has, in comparison with hot pressing, received very little attention.

VI. Conclusions

Although the use of additives, controlled atmospheres, and fast firing processes is widespread in the preparation of ceramics with controlled grain sizes, and although the various mechanisms by which such factors can effect the grain growth rate have been identified, it remains true that links between these two areas—that is, between the technological application and the scientific understanding—are mainly qualitative and that the approach to any system must still be largely empirical. This situation is not an unusual one in the area of ceramics, and, as understanding of the processes involved increases and data on a wider variety of different systems become available, it is to be hoped that the grounds for a quantitative approach will become more firm in the near future.

ACKNOWLEDGMENTS

The assistance of Mr. K. T. Harrison and Mr. A. Tompkins in the preparation of Table V is gratefully acknowledged.

References

Amato, I., Colombo, R. L., Balzari, A., and Petruccioli, J. (1966a). *J. Nucl. Mater.* **18**, 252.
Amato, I., Colombo, R. L., and Balzari, A. M. P. (1966b). *J. Nucl. Mater.* **20**, 210.
Amato, I., Colombo, R. L., and Ravizza, M. (1967a). *J. Nucl. Mater.* **22**, 97.
Amato, I., Ravizza, M., and Colombo, R. L. (1967b). *J. Nucl. Mater.* **23**, 103.
Anderson, H. U. (1974). *J. Amer. Ceram. Soc.* **57**, 34.
Arias, A. (1966). *J. Amer. Ceram. Soc.* **49**, 621.
Ashby, M. F. (1969). *Scr. Met.* **3**, 843.
Atkin, R. B., and Fulrath, R. M. (1971). *J. Amer. Ceram. Soc.* **54**, 265.
Banerjee, M., and Budworth, D. W. (1972). *Trans. Brit. Ceram. Soc.* **71**, 51.
Bratton, R. J. (1974). *J. Amer. Ceram. Soc.* **57**, 283.
Broese van Groenen, A., Bongers, P. J., and Stuijts, A. L. (1968/1969). *Mater. Sci. Eng.* **3**, 317.
Brook, R. J. (1968). *Scr. Met.* **2**, 375.
Brook, R. J. (1969). *J. Amer. Ceram. Soc.* **52**, 56.
Bruch, C. A. (1962). *Amer. Ceram. Soc., Bull.* **41**, 799.
Budworth, D. W. (1970). *Mineral. Mag.* **37**, 833.
Burke, J. E. (1957). *J. Amer. Ceram. Soc.* **40**, 80.
Burke, J. E., and Turnbull, D. (1952). *Progr. Metal Phys.* **3**, 220.
Burke, J. J., Reed, N. L., and Weiss, V., eds. (1970). "Ultra-fine Grain Ceramics." Syracuse Univ. Press, Syracuse, New York.
Cahn, J. W. (1962). *Acta Met.* **10**, 789.
Carniglia, S. C. (1972). *J. Amer. Ceram. Soc.* **55**, 243.
Chay, D. M., Palmour, H., III, and Kriegel, W. W. (1968). *J. Amer. Soc.* **51**, 320.
Chol, G. R. (1971). *J. Amer. Ceram. Soc.* **54**, 34.
Coble, R. L. (1961). *J. Appl. Phys.* **32**, 793.
Coble, R. L., and Burke, J. E. (1963). *Progr. Ceram. Sci.* **3**, 197.
Davidge, R. W. (1972). *Proc. Brit. Ceram. Soc.* **20**, 364.

Davidge, R. W., and Evans, A. G. (1970). *Mater. Sci. Eng.* **6**, 281.
Dutta, S. K., and Spriggs, R. M. (1970). *J. Amer. Ceram. Soc.* **53**, 61.
Egerton, L., and Thomson, J., Jr. (1971). *Amer. Ceram. Soc., Bull.* **50**, 924.
Gazza, G. E. (1972). *J. Amer. Ceram. Soc.* **55**, 172.
Gazza, G. E., Roderick, D., and Levine, B. (1971). *J. Mater. Sci.* **6**, 1137.
Gifkins, R. G. (1968). *J. Amer. Ceram. Soc.* **51**, 69.
Gordon, R. S., Inarchant, D. D., and Hollenberg, G. W. (1970). *J. Amer. Ceram. Soc.* **53**, 339.
Graham, H. C., and Tallan, N. M. (1971). *In* "Physics of Electronic Ceramics A" (L. L. Hench and D. B. Dore, eds.), p. 491. Dekker, New York.
Graham, H. C., Tallan, N. M., and Mazdiyasni, K. S. (1971). *J. Amer. Ceram. Soc.* **54**, 548.
Greenwood, G. W. (1956). *Acta Met.* **4**, 243.
Greskovich, C., and Woods, K. N. (1973). *Amer. Ceram. Soc., Bull.* **52**, 473.
Greskovich, C., O'Clair, C. R., and Curran, M. J. (1972). *J. Amer. Ceram. Soc.* **55**, 324.
Griffith, A. A. (1920). *Phil. Trans. Roy. Soc. London, Ser. A* **221**, 163.
Gupta, T. K. (1971). *J. Amer. Ceram. Soc.* **54**, 413.
Gupta, T. K., and Coble, R. L. (1968). *J. Amer. Ceram. Soc.* **51**, 525.
Gupta, T. K., Rossing, B. R., and Straub, W. D. (1973). *J. Amer. Ceram. Soc.* **56**, 339.
Haertling, G. H. (1964). *Amer. Ceram. Soc., Bull.* **43**, 875.
Haertling, G. H. (1971). *J. Amer. Ceram. Soc.* **54**, 303.
Hamanu, Y., Kinoshita, M., and Oishi, Y. (1964). *Ceram. Abstr.* 263c.
Haroun, N. A., and Budworth, D. W. (1968). *J. Mater. Sci.* **3**, 326.
Haroun, N. A., and Budworth, D. W. (1970). *Trans. Brit. Ceram. Soc.* **69**, 73.
Heuer, A. H. (1970). *Proc. Brit. Ceram. Soc.* **15**, 173.
Heuer, A. H., Cannon, R. M., and Tighe, N. J. (1970). *In* "Ultra-fine Grain Ceramics" (J. J. Burke, N. L. Reed, and V. Weiss, eds.), p. 339. Syracuse Univ. Press, Syracuse, New York.
Heywang, W. (1971). *J. Mater. Sci.* **6**, 1214.
Hillert, M. (1965). *Acta Met.* **13**, 227.
Hirose, N., and Sasaki, H. (1971). *J. Amer. Ceram. Soc.* **54**, 320.
Inarkulich, T. M., Inagder, J., Vukasovich, M. S., and Lockhart, R. J. (1966). *J. Amer. Ceram. Soc.* **49**, 295.
Ishitobi, Y., Shimada, M., and Koizumi, M. (1974). *J. Amer. Ceram. Soc.* **57**, 458.
Jaffe, B., Cook, W. R., Jr., and Jaffe, H. (1971). "Piezoelectric Ceramics." Academic Press, New York.
Jonker, G. H., and Noorlander, W. (1962). *Sci. Ceram.* **1**, 255.
Jonker, G. H., and Stuijts, A. L. (1971). *Philips Tech. Rev.* **32**, 79.
Jorgensen, P. J. (1965). *J. Amer. Ceram. Soc.* **48**, 207.
Jorgensen, P. J. (1967). *Amer. Ceram. Soc., Bull.* **46**, 902.
Jorgensen, P. J., and Anderson, R. C. (1967). *J. Amer. Ceram. Soc.* **50**, 553.
Jorgensen, P. J., and Schmidt, W. G. (1970). *J. Amer. Ceram. Soc.* **53**, 24.
Jorgensen, P. J., and Westbrook, J. H. (1964). *J. Amer. Ceram. Soc.* **47**, 332.
Kahn, M. (1971). *J. Amer. Ceram. Soc.* **54**, 452.
Kapadia, C. M., and Leipold, M. H. (1973). *J. Amer. Ceram. Soc.* **56**, 289.
Kingery, W. D. (1974). *J. Amer. Ceram. Soc.* **57**, 74.
Kingery, W. D., and Fançois, B. (1965). *J. Amer. Ceram. Soc.* **48**, 546.
Kodairi, K., Shimada, M., Kume, S., and Koizumi, M. (1972). *Mater. Res. Bull.* **7**, 551.
Kofstad, P. (1972). "Nonstoichiometry, Diffusion, and Electrical Conductivity in Binary Metal Oxides." Wiley (Interscience), New York.
Kooy, C. (1962). *Sci. Ceram.* **1**, 21.
Kostic, E., and Petrovic, V. (1968). *Bull. Boris Kidric Inst. Nucl. Sci.* **19**, 440.
Kroger, F. A. (1964). "The Chemistry of Imperfect Crystals." Wiley (Interscience), New York.
Kulcsar, F. (1959). *J. Amer. Ceram. Soc.* **42**, 343.
Kulkarni, A. K., and Moorthy, V. K. (1965). *Trans. Indian Ceram. Soc.* **24**, 87.

Kumar, P., and Johnson, D. L. (1974). *J. Amer. Ceram. Soc.* **57**, 65.
Langman, R. A., Runk, R. B., and Butler, S. R. (1973). *J. Amer. Ceram. Soc.* **56**, 486.
Langrod, K. (1965). *J. Amer. Ceram. Soc.* **48**, 110.
Lefever, R. A., and Matsko, J. (1967). *Mater. Res. Bull.* **2**, 865.
Lifschitz, J. M., and Slezov, V. V. (1961). *J. Phys. Chem. Solids* **19**, 35.
Louat, N. P. (1974). *Acta Met.* **22**, 721.
Low, N. M. P. (1970). *J. Can. Ceram. Soc.* **39**, 1.
Matsuo, Y., Fujimara, M., Sasaki, H., Nagase, K., and Hayakowa, S. (1968). *Amer. Ceram. Soc., Bull.* **47**, 292.
Miyagawa, S., Hirano, S., and Somiya, S. (1972). *Yogyo Kyokai Shi* **80**, 53.
Mocellin, A., and Kingery, W. D. (1973). *J. Amer. Ceram. Soc.* **56**, 309.
Nakayama, N., Hirota, E., and Nishikawa, T. (1966). *J. Amer. Ceram. Soc.* **49**, 52.
Nichols, F. A. (1968). *J. Amer. Ceram. Soc.* **51**, 468.
Nicolas, T., and Hildebrandt, M. (1973). *Sci. Ceram.* **6**, XXX (1–16).
Notis, M. R., Urick, P. A., and Spriggs, R. M. (1973). "Sintering and Related Phenomena" (G. C. Kuczynski, ed.), p. 409. Plenum, New York.
Ownby, P. D., and Jungquist, G. E. (1972). *J. Amer. Ceram. Soc.* **55**, 433.
Paladino, A. E., and Maguire, E. A. (1970). *J. Amer. Ceram. Soc.* **53**, 98.
Peelen, J. G. J., and Metselaar, R. (1974). *J. Appl. Phys.* **45**, 216.
Penty, R. A., Hasselman, D. P. H., and Spriggs, R. M. (1973). *Amer. Ceram. Soc., Bull.* **52**, 692.
Perduijn, D. J., and Peloschek, H. P. (1968). *Proc. Brit. Ceram. Soc.* **10**, 263.
Perduijn, D. J., Varekamp, R. R. P., and Verjans, H. C. (1970). *Proc. Brit. Ceram. Soc.* **18**, 239.
Reijnen, P. J. L. (1968). *Sci. Ceram.* **4**, 169.
Rice, R. W. (1971). *J. Amer. Ceram. Soc.* **54**, 205.
Rossi, G., and Burke, J. E. (1973). *J. Amer. Ceram. Soc.* **56**, 654.
Rossi, R. C., Buch, J. D., and Fulrath, R. M. (1970). *J. Amer. Ceram. Soc.* **53**, 629.
Schmalzried, H. (1965). *Prog. Solid State Chem.* **2**, 265.
Shewmon, P. G. (1964). *Trans. AIME* **230**, 1134.
Simpson, C. J., and Aust, K. T. (1972). *Surface Sci.* **31**, 479.
Smith, C. S. (1948). *Trans. AIME* **175**, 15.
Snow, G. S. (1973). *J. Amer. Ceram. Soc.* **56**, 91.
Speight, M. V. (1968). *Acta Met.* **16**, 133.
Speight, M. V., and Greenwood, G. W. (1964). *Phil. Mag.* [8] **9**, 683.
Spriggs, R. M., and Dutta, S. K. (1974). *Sci. Sintering* **6**, 1.
Standley, K. J. (1972). "Oxide Magnetic Materials." Oxford Univ. Press, London and New York.
Steele, B. C. H. (1973). *In* "Fast Ion Transport in Solids" (W. van Gool, ed.), p. 545. North-Holland Publ., Amsterdam.
Suemune, Y. (1971). *Jap. J. Appl. Phys.* **10**, 454.
Sun, R. C., and Bauer, C. L. (1970). *Acta Met.* **18**, 635 and 639.
Tien, T. Y., and Subbarao, E. C. (1963). *J. Amer. Ceram. Soc.* **46**, 489.
Urick, P. A., and Notis, M. R. (1973). *J. Amer. Ceram. Soc.* **56**, 570.
Van Vlack, L. H., and Iuadden, G. I. (1964). *Trans. AIME* **230**, 1200.
Vasilos, T. (1960). *J. Amer. Ceram. Soc.* **43**, 517.
West, R. G., and Blankenship, A. C. (1967). *J. Amer. Ceram. Soc.* **50**, 343.
Weston, T. B., Webster, A. H., and McNamara, V. M. (1969). *J. Amer. Ceram. Soc.* **52**, 253.
White, J. (1973). *In* "Sintering and Related Phenomena" (G. C. Kuczynski, ed.), p. 81. Plenum, New York.
Woolfrey, J. L. (1967). AAEC/E-170. Australian AEC Report.
Wynn Jones, I., and Miles, L. J. (1971). *Proc. Brit. Ceram. Soc.* **19**, 161.

Subject Index

T